

UC San Diego

UC San Diego Electronic Theses and Dissertations

Title

The Synthesis and Structure-Activity Relationship of Covalent Inhibitors Targeting SCP1 and GNAS

Permalink

<https://escholarship.org/uc/item/4b17z6nc>

Author

schweer, joshua

Publication Date

2024

Peer reviewed|Thesis/dissertation

UNIVERSITY OF CALIFORNIA SAN DIEGO

The Synthesis and Structure-Activity Relationship of Covalent Inhibitors Targeting SCP1
and GNAS

A dissertation submitted in partial satisfaction of the
requirements for the degree Doctor of Philosophy

in

Chemistry

By

Joshua Vance Schweer

Committee in charge:

Professor Dionicio Siegel, Chair
Professor Carlo Ballatore
Professor Thomas Bussey
Professor Fleur Ferguson
Professor Nathan Romero

2024

Copyright

Joshua Vance Schweer, 2024

All rights reserved

The dissertation of Joshua Vance Schweer is approved, and it is acceptable in quality and form for publication on microfilm and electronically.

University of California San Diego

2024

Table of Contents

Dissertation Approval Page.....	iii
Table of Contents.....	iv
List of Figures.....	vi
List of Schemes.....	ix
List of Tables.....	xi
List of Spectra.....	xii
List of Abbreviations.....	xxii
Vita.....	xxv
Abstract of the Dissertation.....	xxvi
Chapter 1: Synthesis and Structure-Activity Relationship of Covalent Inhibitors Targeting the SCP1 Phosphatase	
Introduction	
Glioblastoma.....	1
Addressing GBM Through RE-1 Silencing Transcription Factor.....	2
Small C-terminal Domain Phosphatase 1 Modulates REST.....	3
Identification and Anatomy of a Lead Compound.....	4
Covalent Bond Formation with SCP1.....	7
Results	
Docking Model.....	9
Kinetics of Covalent Inhibitors.....	11
Optimization of the Hydrophobic Region.....	12
Optimization of the Warhead Region.....	17
Reactivity Study.....	32
Conclusion.....	41
Experimental Section.....	42
References.....	263
Chapter 2: Covalent Guanosine GNAS Inhibitors	
Introduction	
Natural Nucleosides.....	274
Mechanism of Action of Nucleoside Analogues.....	276
Anticancer Nucleoside Analogues.....	278
Nucleoside and Nucleotide Analogues as Therapeutics.....	283
Prodrug Strategy.....	285
G-Protein Coupled Receptors.....	297

Gas ^{R201C} as a Target to Modulate Tumorigenesis.....	300
Results	
Synthesis of Guanosine-Epoxyde and its Prodrug.....	304
Covalent Acyclic Guanosine Inhibitors.....	307
Updated Covalent Guanosine Phosphoamidates.....	317
Conclusion.....	320
Experimental Section.....	321
References.....	381

List of Figures

Figure 1.1 Depiction of how REST can be modulated by SCP1.....	3
Figure 1.2 Lead compounds towards the inhibition of SCP1.....	4
Figure 1.3 Anatomy of lead compound 1c	5
Figure 1.4 Surface representation of SCP1 showing cysteine residues proximal to the catalytic site.....	7
Figure 1.5 Docking model of 1c and SCP1 WT.....	10
Figure 1.6 A visual illustration explaining the kinetic parameters K_I and k_{inact}	11
Figure 1.7 Library of inhibitors (1j-1ab) designed to increase π - π stacking interactions.....	12
Figure 1.8 Derivatization of the biphenyl moiety leading to compounds 1ac-1al	13
Figure 1.9 Docking model of 1aj and SCP1 WT.....	14
Figure 1.10 Compounds 1.72-1.86 designed to test the effects of derivatization at the ortho position of the terminal phenyl ring.....	16
Figure 1.11 Examples of FDA approved drugs containing acrylamides.....	18
Figure 1.12 SCP1 inhibitors 1.1-1.9	19
Figure 1.13 SCP1 inhibitors containing acrylamides and biphenyl scaffold.....	20
Figure 1.14 SCP1 inhibitors with varied warheads.....	21
Figure 1.15 SCP1 inhibitors containing reversible covalent warhead.....	22
Figure 1.16 SCP1 inhibitor analogs containing a vinyl sulfone.....	23
Figure 1.17 Benzothiophenes containing electron withdrawing halides.....	24
Figure 1.18 SCP1 activity for compounds 1.53-1.63	25
Figure 1.19 Benzothiophene derivatives containing electron donating groups.....	26

Figure 1.20 Synthesis and proposed mechanism of substituted benzothiophenes.....	27
Figure 1.21 SCP1 inhibitors 1aj , 1.96 , and 1.97	28
Figure 1.22 Tunable reversibility of α -heteroaromatic acrylonitriles.....	32
Figure 1.23 Resonance between the sulfone and amide.....	37
Figure 2.1 General structure of nucleosides and nucleotides.....	274
Figure 2.2 DNA and RNA nitrogenous bases.....	275
Figure 2.3 Nucleoside analogues mechanism of action.....	277
Figure 2.4 Anticancer purine nucleobases and nucleosides.....	278
Figure 2.5 Anticancer pyrimidine nucleobases and nucleosides.....	280
Figure 2.6 Modifications to the nucleobase, carbohydrate, and phosphate group.....	283
Figure 2.7 Endogenous decarboxylation of levodopa to dopamine.....	285
Figure 2.8 General depiction of the prodrug strategy.....	286
Figure 2.9 The pronucleotide “ProTide” strategy.....	287
Figure 2.10 Generic structure of bis(POM) (A) and bis(POC) (B) pronucleotides.....	287
Figure 2.11 FDA approved POM and POC nucleotide prodrugs.....	288
Figure 2.12 Common routes to access carbonyloxymethyl phosphate nucleoside prodrugs.....	290
Figure 2.13 Generic phosphoramidate structure and FDA-approved nucleoside protides.....	292
Figure 2.14 Extracellular activation and signal transduction through a G-protein coupled receptor.....	297
Figure 2.15 Interaction of $G\alpha_s$ and adenylate cyclase leading to intracellular signal transduction as well as conversion of ATP to cAMP.....	298

Figure 2.16 GDP and guanosine-epoxide bound to the GNAS ^{R201C} active site.....	301
Figure 2.17 Deprotection of isobutryl amide (2.6) failed.....	306
Figure 2.18 Esterification of phosphoric acid intermediates with POM-Cl.....	310
Figure 2.19 Comparing the structural similarity of guanosine and ganciclovir.....	311

List of Schemes

Scheme 1.1 Synthesis of the lead compound 1c	6
Scheme 1.2 Reversible covalent bond formation between Cys181 and 1c	8
Scheme 1.3 Improved synthesis of 1c	17
Scheme 1.4 Initial route towards SCP1 inhibitor 1.98	30
Scheme 1.5 Synthetic route that affords SCP1 inhibitor 1.98	31
Scheme 1.6 Pfizer's reaction with standard NMR conditions used to generate rate information ($k_{psuedo1st}$ and $t_{1/2}$).....	34
Scheme 1.7 General reaction scheme used to generate rate information ($k_{psuedo1st}$ and $t_{1/2}$).....	34
Scheme 1.8 General reaction scheme and conditions used to generate rate information ($k_{psuedo1st}$ and $t_{1/2}$).....	35
Scheme 1.9 Synthetic pathway used to generate thioether adducts used in kinetic study.....	37
Scheme 2.1 The endogenous activation mechanism of bis(POM) (A) and bis(POC) (B) pronucleotides.....	289
Scheme 2.2 Hwang and Cole's route to bis(POM)-phosphochloridate.....	291
Scheme 2.3 The endogenous activation mechanism of aryloxyphosphoramidates pronucleotides.....	293
Scheme 2.4 Main pathways to conjugate phosphochloridates and nucleosides.....	294
Scheme 2.5 Competitive O ⁶ -phosphorylation and hydrolysis.....	295
Scheme 2.6 Masking the competitive 2-NH ₂ with the dimethylforamidine group.....	296
Scheme 2.7 Traditional route to generate epoxide on carbohydrate of nucleoside.....	301

Scheme 2.8 Proposed mechanism through which the abnormal Mattocks reaction proceeds.....	303
Scheme 2.9 Reaction path to guanosine-epoxide and its prodrug.....	305
Scheme 2.10 Route towards acyclic guanosine prodrugs.....	307
Scheme 2.11 Mechanism through which the McKenna reaction proceeds.....	308
Scheme 2.12 Continuation of the route towards acyclic guanosine prodrugs.....	309
Scheme 2.13 Alternate route towards acyclic guanosine prodrugs.....	311
Scheme 2.14 Route towards acyclic guanosine analogs starting with ganciclovir.....	312
Scheme 2.15 Route towards acyclic guanosine prodrug using less bulky protecting groups.....	314
Scheme 2.16 Synthetic approach towards covalent guanosine prodrugs.....	319

List of Tables

Tables 1.1 Optimization conditions for the generation of rate information ($k_{\text{psuedo1st}}$ and $t_{1/2}$).....	35
Table 1.2 Experimental rate information ($k_{\text{psuedo1st}}$ and $t_{1/2}$).....	39
Table 2.1 Optimization conditions for the conjugation of nucleoside and masked phosphate.....	316

List of Spectra

Spectra 1.1 ¹ H NMR Spectrum of compound 1.2	177
Spectra 1.2 ¹ H NMR Spectrum of compound 1.3	177
Spectra 1.3 ¹ H NMR Spectrum of compound 1.5	178
Spectra 1.4 ¹ H NMR Spectrum of compound 1.6	178
Spectra 1.5 ¹ H NMR Spectrum of compound 1.7	179
Spectra 1.6 ¹ H NMR Spectrum of compound 1.8	179
Spectra 1.7 ¹ H NMR Spectrum of compound 1.9	180
Spectra 1.8 ¹ H NMR Spectrum of compound 1.10	180
Spectra 1.9 ¹ H NMR Spectrum of compound 1.11	181
Spectra 1.10 ¹ H NMR Spectrum of compound 1.12	181
Spectra 1.11 ¹ H NMR Spectrum of compound 1.13	182
Spectra 1.12 ¹ H NMR Spectrum of compound 1.14	182
Spectra 1.13 ¹ H NMR Spectrum of compound 1.15	183
Spectra 1.14 ¹ H NMR Spectrum of compound 1.16	183
Spectra 1.15 ¹ H NMR Spectrum of compound 1.17	184
Spectra 1.16 ¹ H NMR Spectrum of compound 1.16	184
Spectra 1.17 ¹ H NMR Spectrum of compound 1.19	185
Spectra 1.18 ¹ H NMR Spectrum of compound 1.20	185
Spectra 1.19 ¹ H NMR Spectrum of compound 1.21	186
Spectra 1.20 ¹ H NMR Spectrum of compound 1.22	186
Spectra 1.21 ¹ H NMR Spectrum of compound 1.23	187
Spectra 1.22 ¹ H NMR Spectrum of compound 1.24	187

Spectra 1.23 ¹ H NMR Spectrum of compound 1.25	188
Spectra 1.24 ¹ H NMR Spectrum of compound 1.26	188
Spectra 1.25 ¹ H NMR Spectrum of compound 1.27	189
Spectra 1.26 ¹ H NMR Spectrum of compound 1.28	189
Spectra 1.27 ¹ H NMR Spectrum of compound 1.29	190
Spectra 1.28 ¹ H NMR Spectrum of compound 1.30	190
Spectra 1.29 ¹ H NMR Spectrum of compound 1.31	191
Spectra 1.30 ¹ H NMR Spectrum of compound 1.33	191
Spectra 1.31 ¹ H NMR Spectrum of compound 1.34	192
Spectra 1.32 ¹ H NMR Spectrum of compound 1.35	192
Spectra 1.33 ¹ H NMR Spectrum of compound 1.36	193
Spectra 1.34 ¹ H NMR Spectrum of compound 1.37	194
Spectra 1.35 ¹ H NMR Spectrum of compound 1.38	194
Spectra 1.36 ¹ H NMR Spectrum of compound 1.39	195
Spectra 1.37 ¹ H NMR Spectrum of compound 1.40	195
Spectra 1.38 ¹ H NMR Spectrum of compound 1.41	196
Spectra 1.39 ¹ H NMR Spectrum of compound 1.42	196
Spectra 1.40 ¹ H NMR Spectrum of compound 1.43	197
Spectra 1.41 ¹ H NMR Spectrum of compound 1.44	197
Spectra 1.42 ¹ H NMR Spectrum of compound 1.45	198
Spectra 1.43 ¹ H NMR Spectrum of compound 1.46	198
Spectra 1.44 ¹ H NMR Spectrum of compound 1.53	199
Spectra 1.45 ¹ H NMR Spectrum of compound 1.54	199

Spectra 1.46	¹ H NMR Spectrum of compound 1.55	200
Spectra 1.47	¹ H NMR Spectrum of compound 1.56	200
Spectra 1.48	¹ H NMR Spectrum of compound 1.57	201
Spectra 1.49	¹ H NMR Spectrum of compound 1.58	201
Spectra 1.50	¹ H NMR Spectrum of compound 1.59	202
Spectra 1.51	¹ H NMR Spectrum of compound 1.60	202
Spectra 1.52	¹ H NMR Spectrum of compound 1.61	203
Spectra 1.53	¹ H NMR Spectrum of compound 1.62	203
Spectra 1.54	¹ H NMR Spectrum of compound 1.63	204
Spectra 1.55	¹ H NMR Spectrum of compound 1.64	204
Spectra 1.56	¹ H NMR Spectrum of compound 1.65	205
Spectra 1.57	¹ H NMR Spectrum of compound 1.66	205
Spectra 1.58	¹ H NMR Spectrum of compound 1.67	206
Spectra 1.59	¹ H NMR Spectrum of compound 1.68	206
Spectra 1.60	¹ H NMR Spectrum of compound 1.69	207
Spectra 1.61	¹ H NMR Spectrum of compound 1.71	207
Spectra 1.62	¹ H NMR Spectrum of compound 1.72	208
Spectra 1.63	¹ H NMR Spectrum of compound 1.73	208
Spectra 1.64	¹ H NMR Spectrum of compound 1.74	209
Spectra 1.65	¹ H NMR Spectrum of compound 1.75	209
Spectra 1.66	¹ H NMR Spectrum of compound 1.77	210
Spectra 1.67	¹ H NMR Spectrum of compound 1.78	210
Spectra 1.68	¹ H NMR Spectrum of compound 1.79	211

Spectra 1.69	¹ H NMR Spectrum of compound 1.80	211
Spectra 1.70	¹³ C NMR Spectrum of compound 1.80	212
Spectra 1.71	¹ H NMR Spectrum of compound 1.81	212
Spectra 1.72	¹³ C NMR Spectrum of compound 1.81	213
Spectra 1.73	¹ H NMR Spectrum of compound 1.82	213
Spectra 1.74	¹ H NMR Spectrum of compound 1.83	214
Spectra 1.75	¹ H NMR Spectrum of compound 1.84	214
Spectra 1.76	¹³ C NMR Spectrum of compound 1.85	215
Spectra 1.77	¹ H NMR Spectrum of compound 1.86	215
Spectra 1.78	¹ H NMR Spectrum of compound 1.87	216
Spectra 1.79	¹ H NMR Spectrum of compound 1.88	216
Spectra 1.80	¹ H NMR Spectrum of compound 1.89	217
Spectra 1.81	¹ H NMR Spectrum of compound 1.90	217
Spectra 1.82	¹ H NMR Spectrum of compound 1.91	218
Spectra 1.83	¹ H NMR Spectrum of compound 1.94	218
Spectra 1.84	¹ H NMR Spectrum of compound 1.95	219
Spectra 1.85	¹ H NMR Spectrum of compound 1.96	219
Spectra 1.86	¹ H NMR Spectrum of compound 1.97	220
Spectra 1.87	¹ H NMR Spectrum of compound 1.98	220
Spectra 1.88	¹ H NMR Spectrum of compound 1.99	221
Spectra 1.89	¹ H NMR Spectrum of compound 1.101	221
Spectra 1.90	¹ H NMR Spectrum of compound 1.100	222
Spectra 1.91	¹ H NMR Spectrum of compound 1.102	222

Spectra 1.92	¹ H NMR Spectrum of compound 1.103	223
Spectra 1.93	¹ H NMR Spectrum of compound 1.104	223
Spectra 1.94	¹³ C NMR Spectrum of compound 1.104	224
Spectra 1.95	¹ H NMR Spectrum of compound 1.105	224
Spectra 1.95	¹³ C NMR Spectrum of compound 1.105	225
Spectra 1.96	¹ H NMR Spectrum of compound 1.106	225
Spectra 1.97	¹³ C NMR Spectrum of compound 1.106	226
Spectra 1.98	¹ H NMR Spectrum of compound 1.107	226
Spectra 1.99	¹³ C NMR Spectrum of compound 1.107	227
Spectra 1.100	¹ H NMR Spectrum of compound 1.108	227
Spectra 1.101	¹³ C NMR Spectrum of compound 1.108	228
Spectra 1.102	¹ H NMR Spectrum of compound 1.109	228
Spectra 1.103	¹³ C NMR Spectrum of compound 1.109	229
Spectra 1.104	¹ H NMR Spectrum of compound 1.110	229
Spectra 1.105	¹³ C NMR Spectrum of compound 1.110	230
Spectra 1.106	¹ H NMR Spectrum of compound 1.111	230
Spectra 1.107	¹³ C NMR Spectrum of compound 1.111	231
Spectra 1.108	¹ H NMR Spectrum of compound 1.112	231
Spectra 1.109	¹³ C NMR Spectrum of compound 1.112	231
Spectra 1.110	¹ H NMR Spectrum of compound 1.113	232
Spectra 1.111	¹³ C NMR Spectrum of compound 1.113	232
Spectra 1.112	¹ H NMR Spectrum of compound 1.114	233
Spectra 1.113	¹³ C NMR Spectrum of compound 1.114	233

Spectra 1.114	¹ H NMR Spectrum of compound 1.115	234
Spectra 1.115	¹³ C NMR Spectrum of compound 1.115	234
Spectra 1.116	¹ H NMR Spectrum of compound 1.116	235
Spectra 1.117	¹³ C NMR Spectrum of compound 1.116	235
Spectra 1.118	¹ H NMR Spectrum of compound 1.117	236
Spectra 1.119	¹³ C NMR Spectrum of compound 1.117	236
Spectra 1.120	¹ H NMR Spectrum of compound 1.118	237
Spectra 1.121	¹³ C NMR Spectrum of compound 1.118	237
Spectra 1.122	¹ H NMR Spectrum of compound 1.119	238
Spectra 1.123	¹³ C NMR Spectrum of compound 1.119	238
Spectra 1.124	¹ H NMR Spectrum of compound 1.120	239
Spectra 1.125	¹ H NMR Spectrum of compound 1.121	239
Spectra 1.126	¹³ C NMR Spectrum of compound 1.121	240
Spectra 1.127	¹ H NMR Spectrum of compound 1.122	240
Spectra 1.128	¹³ C NMR Spectrum of compound 1.122	241
Spectra 1.129	¹ H NMR Spectrum of compound 1.123	241
Spectra 1.130	¹³ C NMR Spectrum of compound 1.123	242
Spectra 1.131	¹ H NMR Spectrum of compound 1.124	242
Spectra 1.132	¹³ C NMR Spectrum of compound 1.124	243
Spectra 1.133	¹ H NMR Spectrum of compound 1.125	243
Spectra 1.134	¹³ C NMR Spectrum of compound 1.125	244
Spectra 1.135	¹ H NMR Spectrum of compound 1.126	244
Spectra 1.136	¹³ C NMR Spectrum of compound 1.126	245

Spectra 1.137	¹ H NMR Spectrum of compound 1.127	245
Spectra 1.138	¹³ C NMR Spectrum of compound 1.127	246
Spectra 1.139	¹ H NMR Spectrum of compound 1.128	246
Spectra 1.140	¹³ C NMR Spectrum of compound 1.128	247
Spectra 1.141	¹ H NMR Spectrum of compound 1.129	247
Spectra 1.142	¹³ C NMR Spectrum of compound 1.129	248
Spectra 1.143	¹ H NMR Spectrum of compound 1.130	248
Spectra 1.144	¹³ C NMR Spectrum of compound 1.130	249
Spectra 1.145	¹ H NMR Spectrum of compound 1.131	249
Spectra 1.146	¹³ C NMR Spectrum of compound 1.131	250
Spectra 1.147	¹ H NMR Spectrum of compound 1.132	250
Spectra 1.148	¹³ C NMR Spectrum of compound 1.132	251
Spectra 1.149	¹ H NMR Spectrum of compound 1.133	251
Spectra 1.150	¹³ C NMR Spectrum of compound 1.133	252
Spectra 1.151	¹ H NMR Spectrum of compound 1.134	252
Spectra 1.152	¹³ C NMR Spectrum of compound 1.134	253
Spectra 1.153	¹ H NMR Spectrum of compound 1.135	253
Spectra 1.154	¹³ C NMR Spectrum of compound 1.135	254
Spectra 1.155	¹ H NMR Spectrum of compound 1.136	254
Spectra 1.156	¹³ C NMR Spectrum of compound 1.136	255
Spectra 1.157	¹ H NMR Spectrum of compound 1.137	255
Spectra 1.158	¹³ C NMR Spectrum of compound 1.137	256
Spectra 1.159	¹ H NMR Spectrum of compound 1.138	256

Spectra 1.160	¹³ C NMR Spectrum of compound 1.138	257
Spectra 1.161	¹ H NMR Spectrum of compound 1.139	257
Spectra 1.162	¹³ C NMR Spectrum of compound 1.139	258
Spectra 1.163	¹ H NMR Spectrum of compound 1.140	258
Spectra 1.164	¹³ C NMR Spectrum of compound 1.140	259
Spectra 1.165	¹ H NMR Spectrum of compound 1.141	259
Spectra 1.166	¹³ C NMR Spectrum of compound 1.141	260
Spectra 1.167	¹ H NMR Spectrum of compound 1.142	260
Spectra 1.168	¹³ C NMR Spectrum of compound 1.142	261
Spectra 1.169	¹ H NMR Spectrum of compound 1.143	261
Spectra 1.170	¹³ C NMR Spectrum of compound 1.143	262
Spectra 2.1	¹ H NMR Spectrum of compound 2.2	362
Spectra 2.2	¹ H NMR Spectrum of compound 2.3	362
Spectra 2.3	¹ H NMR Spectrum of compound 2.4	363
Spectra 2.4	¹ H NMR Spectrum of compound 2.5	363
Spectra 2.5	¹ H NMR Spectrum of compound 2.6	364
Spectra 2.6	¹ H NMR Spectrum of compound 2.12	364
Spectra 2.7	¹ H NMR Spectrum of compound 2.13	365
Spectra 2.8	¹ H NMR Spectrum of compound 2.14	365
Spectra 2.9	¹ H NMR Spectrum of compound 2.15	366
Spectra 2.10	¹ H NMR Spectrum of compound 2.16	366
Spectra 2.11	¹ H NMR Spectrum of compound 2.17	367
Spectra 2.12	¹ H NMR Spectrum of compound 2.18	367

Spectra 2.13	¹ H NMR Spectrum of compound 2.19	368
Spectra 2.14	¹ H NMR Spectrum of compound 2.20	368
Spectra 2.15	¹ H NMR Spectrum of compound 2.21	369
Spectra 2.16	¹ H NMR Spectrum of compound 2.22	369
Spectra 2.17	¹ H NMR Spectrum of compound 2.23	370
Spectra 2.18	¹ H NMR Spectrum of compound 2.24	370
Spectra 2.19	¹ H NMR Spectrum of compound 2.25	371
Spectra 2.20	¹ H NMR Spectrum of compound 2.26	371
Spectra 2.21	¹ H NMR Spectrum of compound 2.27	372
Spectra 2.22	¹ H NMR Spectrum of compound 2.28	372
Spectra 2.23	¹ H NMR Spectrum of compound 2.29	373
Spectra 2.24	¹ H NMR Spectrum of compound 2.30	373
Spectra 2.25	¹ H NMR Spectrum of compound 2.31	374
Spectra 2.26	¹ H NMR Spectrum of compound 2.32	374
Spectra 2.27	¹ H NMR Spectrum of compound 2.33	375
Spectra 2.28	¹ H NMR Spectrum of compound 2.34	375
Spectra 2.29	¹ H NMR Spectrum of compound 2.35	376
Spectra 2.30	¹ H NMR Spectrum of compound 2.36	376
Spectra 2.31	¹ H NMR Spectrum of compound 2.37	377
Spectra 2.32	¹ H NMR Spectrum of compound 2.38	377
Spectra 2.33	¹ H NMR Spectrum of compound 2.39	378
Spectra 2.34	¹ H NMR Spectrum of compound 2.40	378
Spectra 2.35	¹ H NMR Spectrum of compound 2.41	379

Spectra 2.36 ^1H NMR Spectrum of compound 2.42	379
Spectra 2.37 ^1H NMR Spectrum of compound 2.43	380

List of Abbreviations

2Cda - cladribine	cAMP - cyclic AMP
5-AC - azacytidine	Cbz – carboxybenzyl
5-FU - 5-fluorouracil	CO ₂ – <i>carbon dioxide</i>
5'-NT - 5'-nucleosidases	CRG - covalent reactive group
6-MP - 6-mercaptapurine	Cs ₂ CO ₃ – cesium carbonate
6-TG - thioguanine	<i>CTP - cytidine triphosphate</i>
AA - appendiceal adenocarcinoma	CTP - cytidine triphosphate
ACN – acetonitrile	Cyd – cytidine
Ade – adenine	Cys - cysteine
Ado – adenosine	Cyt – cytosine
Ado – adenosine	DAC - decitabine
AgTFA – silver trifluoroacetate	dAdo - deoxyadenosine
<i>AMP - adenosine diphosphate</i>	dAdo - deoxyadenosine
<i>AMP - adenosine monophosphate</i>	dCF – deoxycoformycin
Ara-G – arabinosylguanine	DCM - dichloromethane
ATP - adenosine triphosphate	dCyt - deoxycytidine
BBB - blood-brain barrier	dGuo - deoxyguanosine
BnBr – benzyl bromide	DIPEA – <i>N,N-diisopropylethylamine</i>
Boc - <i>tert</i> -butylcarbonate	DMA – dimethylacetamide
Boc ₂ O – di- <i>tert</i> -butyl decarbonate	DMAP - 4-dimethylaminopyridine
BOP-Cl - bis(2-oxo-3-oxazolidinyl)phosphinic chloride	DMDO - dimethyl dioxirane
BSA - bis(trimethylsilyl)acetamide	DMF - dimethylformamide
Bz ₂ O – benzoic anhydride	DMSO – dimethylsulfoxide
CAFdA – clofarabine	DNA - deoxyribonucleic acid
CAM - ceric ammonium molybdate	DPTBS-Cl - <i>tert</i> -butyldiphenylsilyl chloride

EDC - N-ethyl-N'-(3-dimethylaminopropyl)carbodiimide hydrochloride
Et₂O - diethyl ether
EtOH – ethanol
FA – fludarabine
FUdR – floxuridine
G α s - G α subunit
GDP - guanosine diphosphate
GMB - glioblastoma
GPCR - G-protein coupled receptors
GSH - glutathione
GTP - guanosine triphosphate
Gua – guanine
Guo – guanosine
H₂ – hydrogen
H₂O – water
H₂SO₄ – sulfuric acid
HATU - 1-[bis(dimethylamino)methylene]-1H-1,2,3-triazolo[4,5-b]pyridinium 3-oxid hexafluorophosphate
HCl - hydrochloric acid
HCl – hydrochloric acid
HFIP – *hexafluoroisopropanol*
HOAc – acetic acid
HOBt - hydroxybenzotriazole
HPLC/MS - high pressure liquid chromatography / mass spectrometry

IC₅₀ - half-maximal inhibitory concentration
iPro – isopropanol
KMnO₄ - potassium permanganate
KOH – potassium hydroxide
mCPBA - m-chloroperoxybenzoic acid
MeOH - methanol
MLSMR - molecular libraries small molecule repository
MMt - monomethoxy trityl group
MsCl – mesyl chloride
N₂H₄ - hydrazine
NaBH₄ – sodium borohydride
NaCO₃ - sodium carbonate
NaH – sodium hydride
NaHCO₃ – sodium bicarbonate
Nal – sodium iodide
NaN₃ – sodium azide
NAs - nucleoside analogs
nBuLi – n-butyl lithium
NH₃Cl – ammonium chloride
NMI - 1-methylimidazole
NMP - 1-methylpyrrolidone
NMR - nuclear magnetic resonance
NRSF - neuron-restrictive silencer factor
PBS - phosphate buffered solution
Pd(OAc)₂ – palladium acetate
Pd/C – palladium on carbon

PheMe – toluene
 PIDA - (diacetoxyiodo)benzene
 PMP - pseudomyxoma peritonei
 pNPP - *p*-nitrophenyl phosphate
 POC – propargyloxycarbonyl
 POM – *polyoxymethylene*
 POM-Cl - chloromethyl pivalate
PPA – *polyphosphoric acid*
 ppm - parts per million
 PyBOP - benzotriazol-1-
 yloxytripyrrolidinophosphonium
 hexafluorophosphate
 Pyr - pyridine
 REST - repressor element-1 silencing
 transcription factor
 RNA - ribonucleic acid
 RR - ribonucleotide reductase
 SCP1 - C-terminal domain phosphatase
 1
S_NAR - nucleophilic aromatic
 substitution
t-BuMgCl - *tert-butylmagnesium chloride*
 TBAF - tetra-*n*-butylammonium fluoride
 TBEV - tick-borne encephalitis virus
 TEA – triethylamine
 TEMPO - (2,2,6,6-tetramethylpiperidin-
 1-yl)oxyl
 TFA – trifluoroacetic acid
 Thd – thymidine
THF – *tetrahydrofuran*
 Thy – thymine
 TLC - thin-layer chromatography
 TMS-Br – bromotrimethylsilane
 TMS-Cl – trimethylchlorosilane
 TMSOTf - trifluoromethanesulfonic *acid*
 trimethylsilylester
 TMZ - temozolomide
Tol – *toluene*
 TS - thymidylate synthase
 TsCl - tosyl chloride
 Urd - uridine
 Uta – uracil
 WHO - world health organization
 WT - wild type

Vita

2018 Bachelor of Science, University of California San Diego
2019-2024 Teaching Assistant, University of California San Diego
2019-2024 Research Assistant, University of California San Diego
2021 Master of Science, University of California San Diego
2024 Doctor of Philosophy, University of California San Deigo

Publications

S, Konduri; J, Schweer; D, Siegel. Short synthesis of a broadly reactive, cell permeable serine hydrolase fluorophosphate-alkyne probe. *Bioorganic & Medicinal Chemistry Letters*. **2023**, 19,129434.

I, Mohanty; H, Mannocho-Russo; J, Schweer; Y, El Abiead; W, Bittremieux; S, Xing; R, Scmid; S, Simone; F, Vasquez; B, Valentina; J, Zemlin; O, Tovar-Herrera; S, Moraïs; D, Desai; S, Amin; I, Koo; C, Turck; I, Mizrah; T, Huan; A, Patterson; D, Siegel; H, Lee; M, Wang; A, Allegra; P, Dorrstein. The Underappreciated Diversity of Bile Acid Modifications. *Cell*. **2024**, 187, 1801-1818.

S, Panina; J, Schweer; Q, Zhang; W, Yang; G, Raina; H, Hardtke; D, Siegel; J, Zhang. Targeting of REST with rationally-designed small molecule compounds exhibits synergetic therapeutic potential in human glioblastoma cells. *BMC Biology*. **2024**, 22(83).

Patents

D. Siegel, J.P. Shen, R. Abagayan, J. Schweer. 2023. Small molecule for treatment of cancer of the appendix. U.S. Provisional Patent Application No.: 63/389,793. Filed July 14, 2023. Provisional Patent

D. Siegel, A. Saghatelian, J. Schweer, S. Konduri, G. Raina. 2023. Illuminating the dynamic 3D protein complexes, DNA, and RNA interactions that determine global gene expression and cell fate in living cells. Filed October 13, 2023. Patent Pending

Abstract of the Dissertation

The Synthesis and Structure-Activity Relationship of Covalent Inhibitors Targeting SCP1 and GNAS

by

Joshua Vance Schweer

Doctor of Philosophy in Chemistry

University of California San Diego, 2024

Professor Dionicio Siegel, Chair

Glioblastoma (GBM) represents the most prevalent malignant tumor affecting the central nervous system. The current treatment regime consisting of surgery, chemotherapy, and radiation has remained the same for over two decades even though patients rarely live three years past treatment. Post-translational regulation of the repressor element-1 silencing transcription factor (REST) has been shown to be a successful method in reducing GBM derived tumors. Inhibition of REST's regulatory protein small C-terminal domain phosphatase 1 (SCP1) is an effective strategy to modulate REST levels and therefore GBM. Guided by a structure-based drug design

approach over 220 final compounds were synthesized and tested generating a broad understanding of their structure-activity relationship. To better understand the kinetics of the dually activated benzo[*b*]thiophene 1,1-dioxide warhead, an NMR based kinetic study was performed to generate half-life ($t_{1/2}$) data and find the target zone of reactivity.

The GNAS gene, responsible for encoding the G α s subunit of heterotrimeric G proteins, exhibits the second highest mutation frequency in mucinous appendiceal adenocarcinoma. Despite being a druggable target, there are currently no commercially available inhibitors specifically targeting G α s. Additionally, GNAS^{R201C} stands out as a target because it is the most cancer-causing mutation of all heterotrimeric G-proteins. As guanosine-5'-triphosphate (GTP) is the G α s's endogenous substrate the strategy was to synthesize GTP derivatives that covalently bind the GNAS^{R201C} mutation allowing selectivity of the cancerous cells. Guanosine-epoxide (**2.4**) and a diastereomeric pair of its phosphoramidate prodrugs were synthesized and tested showing a proof of concept. Synthetic routes affording cyclic and acyclic covalent guanosine analogues were bottlenecked by a phosphorylation step. Although optimization efforts resulted in parameters generating the desired product, reaction yields were insufficient to allow the generation of a diverse library.

Synthesis and Structure-Activity Relationship of Covalent Inhibitors Targeting the SCP1 Phosphatase

Glioblastoma

Glioblastoma (GBM) represents the most prevalent malignant tumor affecting the central nervous system, with a worldwide incidence rate up to 3.69 per 100,000 individuals¹. Associated with poor prognosis the median patient survives between 1-1.5 years from diagnosis²⁻³ and only 3-5% of those diagnosed live to 3 years or more⁴⁻⁵. The current treatment strategy for GBM patients has remained the same for over two decades and includes surgery, adjuvant radiotherapy and temozolomide (TMZ) chemotherapy. While surgery can remove a large section of tissue, it fails to remove all cancerous cells and usually leads to adverse side effects like pain, infections, other illnesses, and blood clots⁶. Radiation therapy does slow and kill the growth of cancer cells however it is not specific and affects healthy cells as well causing downstream side effects that vary depending on the location of body being treated⁷⁻⁸. Chemotherapy treatment through TMZ, an alkylating agent, slows the growth of cancer cells however it fails to eradicate all malignant cells and remaining cells can form resistance. TMZ may also increase the risk to the development of other types of cancer⁹. Three years is considered a long-term survival rate despite the aggressive combinatorial therapy¹⁰. Given the high mortality rate of GBM patients, it is essential to explore new therapeutic avenues to improve patient prognosis and work towards finding a cure for this deadly disease¹¹⁻¹².

Addressing GBM Through RE-1 Silencing Transcription Factor

Discovered to be overexpressed in some medulloblastoma cell lines¹⁵, the repressor element-1 silencing transcription factor (REST)¹³, also known as neuron-restrictive silencer factor (NRSF)¹⁴, plays a critical role in the transcription of neuronal genes. As a silencing transcription factor, it interacts with transcriptional co-regulators at the promoter region of targeted genes to prevent transcription¹³. The imbalance of REST expression has been shown to correlate with a broad range of diseases¹⁶⁻¹⁷, commonly seen in neuronal diseases like epilepsy¹⁸⁻²⁰, Parkinson's²¹⁻²⁴, and Huntington's²⁵⁻³⁰. Not only are REST levels overexpressed in GBM³¹⁻³⁴, but REST aids cancerous cells in their pluripotency and self-renewal leading to resistance^{16,32}. As REST has been identified as a driving force in tumor formation³¹⁻³² and its elimination from the nucleus in animal models reduces tumor size³², treatment of GBM through the modulation of REST is an attractive approach. Unfortunately, because transcription factors' activity depends on association with proteins over large surfaces, they lack active catalytic sites as seen in enzymes³⁵. The largely disorder structure of transcription factors are challenging to inhibit through small molecules³⁶ and are traditionally viewed as "undruggable." With no obvious binding site or small molecules known to bind REST, the strategy was to modulate REST levels through its regulatory proteins.

Small C-terminal Domain Phosphatase 1 Modulates REST

Post-translational regulation of REST levels through phosphorylation has been shown to be an effective method to induce protein turnover³⁸⁻³⁹. **Figure 1.1** shows how REST is modulated through the key phosphorylation sites of Ser-861 and Ser-864. Following phosphorylation, REST translocates to the cytosol and is degraded by the ubiquitin ligase SCF^{β-TrCP} 38-39. REST's regulatory protein, small C-terminal domain phosphatase 1 (SCP1), is responsible for the dephosphorylation of Ser-861 and Ser-864 which prevents the translocation and therefore the degradation of REST. It has already been shown that REST levels can be decreased with the loss of SCP1 activity⁴⁰⁻⁴¹. As protein phosphatases contain an active site that can be modified by small molecules⁴²⁻⁵⁰ this regulatory protein is a promising strategy to control REST's transcriptional functionality.

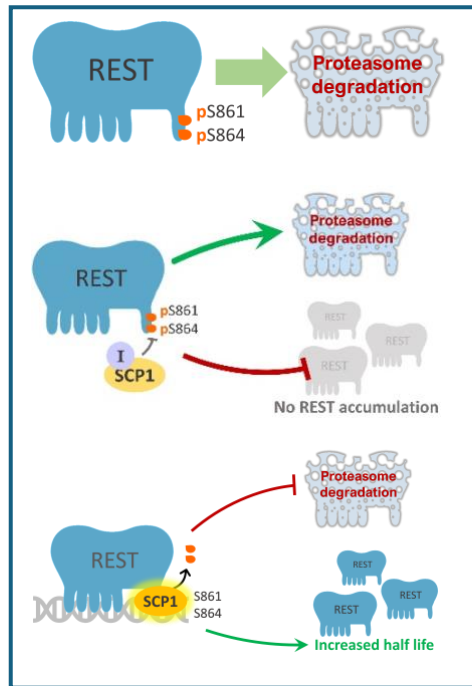


Figure 1.1 Depiction of how REST can be modulated by SCP1

Identification and Anatomy of a Lead Compound

To find a lead compound a high-throughput screening of the molecular libraries small molecule repository (MLSMR) library was performed at the Chemical Genomics Center in La Jolla and the Burnham Institute. Twenty four of the 350,478 compounds were hits based on their inhibition of IC₅₀ greater than 50 μ M. As false positives when targeting phosphatases are common the more sensitive p-nitrophenyl phosphatase (pNPP) assay was conducted on the freshly synthesized 24 hits. Interestingly no inhibition was detected. Observation of the 24 hit's structure showed a common structural trend. The compounds shared a phenyl sulfonamide and thiophene bridged by piperazine. As sulfides are prone to oxidation over time⁵¹⁻⁵³ potentially the oxidized chemicals were responsible to inhibition in the high-throughput screening. Compound **1a** showed an IC₅₀ of 797 \pm 4 μ M when incubated with SCP1 for 2hours. Oxidation of **1a** with *m*-chloroperoxybenzoic acid (mCPBA) led to a mixture of products of which contained **1b**. This mixture led to the increased inhibition of 219.9 \pm 0.2 μ M.

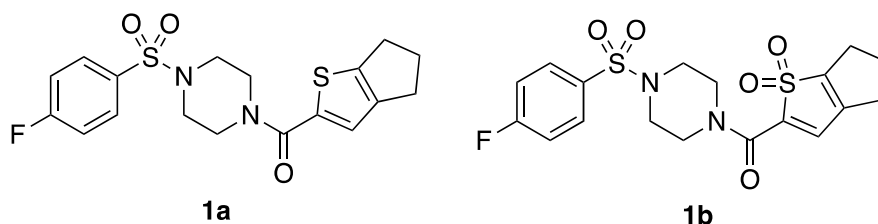


Figure 1.2 Lead compounds towards the inhibition of SCP1

An initial optimization program utilizing **1b** as the lead compound led to compound **1c**⁵⁴. **Figure 1.3** shows the 3 segments that compose the lead compound. The compound is composed of an electron-deficient hydrophobic region depicted in

blue, an electrophilic covalent bonding group in red, connected by linker shown in green.

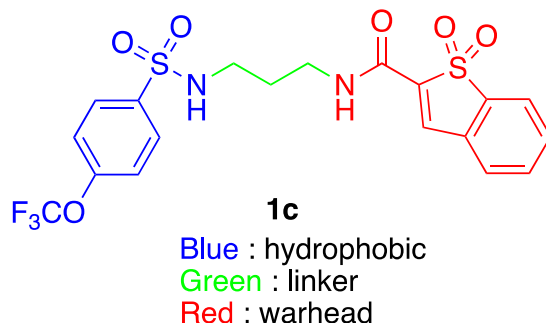
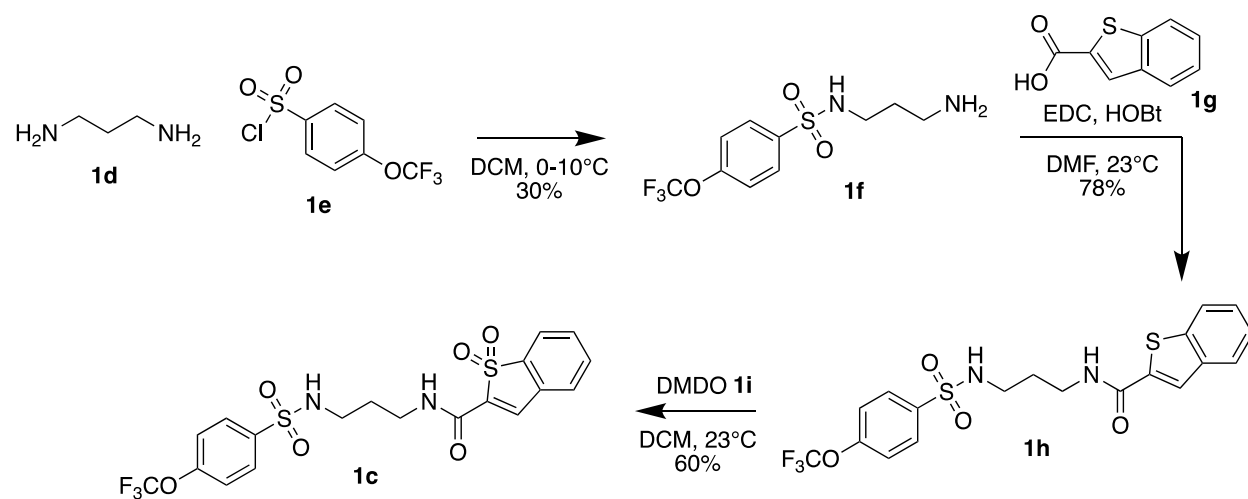


Figure 1.3 Anatomy of lead compound **1c**

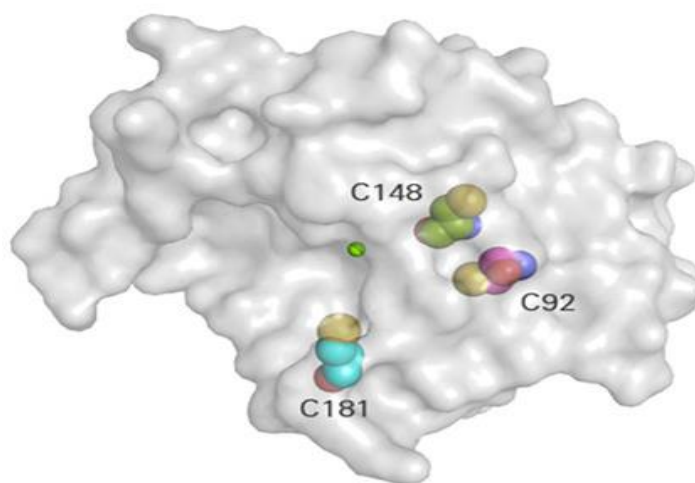
Derivatization of one segment while keeping the other two constant drove the optimization program forward and led to focused library of 100 compounds. Synthesis of **1c** starts with an excess of linker **1d**, propane-1,3-diamine, and the sulfonyl chloride **1e** which undergoes an addition-elimination reaction to yield the free amine **1f** in a 30% yield. Linkers varying carbon chain length, rigidity, and stereochemistry were introduced at this stage to better understand the ideal linker. Shifting piperazine to propane-1,3-diamine increase flexibility and distance between the warhead and hydrophobic region leading to increased activity. Subsequent amide formation with **1g**, benzo[*b*]thiophene-2-carboxylic acid, introduces the thiophene moiety. Various covalent scaffolds were introduced in attempts to balance reactivity to bind SCP1, but not react promiscuously. Substituting the cyclopentane for a phenyl group on the thiophene resulted a better reactivity profile. Oxidation of the sulfide intermediate **1h** with dimethyl dioxirane (**1i**, DMDO) produced the vinyl sulfone **1c** in a 60% yield.



Scheme 1.1 Synthesis of the lead compound **1c**

Covalent Bond Formation with SCP1

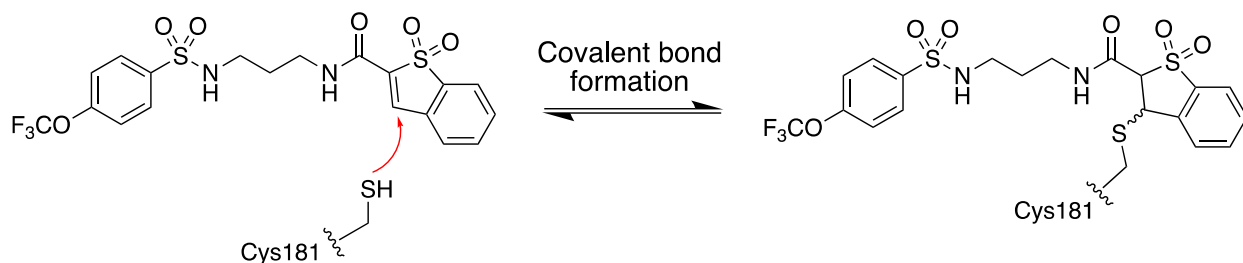
The pNPP assay generated IC_{50} data used to design iterative generations of lead compounds. Interestingly it was observed that increasing incubation time led to additional activity, which is indicative of covalent bond formation. To test this hypothesis the Zhang lab incubated SCP1 with the inhibitor **1c** and measured the protein's molecular weight by MALDI-TOF. Appearance of a peak with an additional 490 Da supports that the inhibitor covalently bonded to SCP1. Additionally when **1c**, SCP1, and β -mercaptoethanol (BME) were incubated together no phosphatase-inhibitor adduct was observed. As BME was able to prevent the protein-ligand adduct formation then a cysteine residue may be involved in the covalent linkage. Figure 1.4 shows the cysteine residues near SCP1's catalytic site which are likely the thiols participating in the covalent bond with **1c**.



54

Figure 1.4 Surface representation of SCP1 showing cysteine residues proximal to the catalytic site. Single point mutation of SCP1 generated variants at C148, C92, and C181, converting cysteine to alanine. Each variant was tested for activity after incubation with **1c**. Variant

C181A was no longer inhibited by **1c** showing C181 is participating in the protein-ligand interaction.



Scheme 1.2 Reversible covalent bond formation between Cys181 and **1c**

Covalent bond formation between cysteine residues and acrylamides⁵⁵⁻⁷³ as well as vinyl sulfones⁷⁴⁻⁹³ are well documented. A Thia-Michael reaction is proposed to be the mechanism by which the protein-inhibitor bond is formed. The lone pair on Cys181's thiol can add into the dually-activated β -carbon of the **1c**. Interestingly dually activated alkenes have been shown participate in Michael addition, but also contain intrinsic reversibility⁹⁴.

Docking Model

A docking model showing **1c** covalently bound to SCP1's Cys181 gave explanation to why the structural changes from **1b** to **1c** generated a more potent inhibitor. **Figure 1.5** shows the structural model of **1c** and SCP1 WT. Two aromatic residues, F106 and Y158, provides a molecular recognition through reversible π - π stacking interactions with the inhibitor's electron deficient aromatic section. To test the impact of these two residues each was mutated, and the variant was tested for phosphatase activity by the pNPP assay after being incubated with **1c**. Variant Y158I's activity diminished by 10-times ($IC_{50} > 100 \mu\text{M}$) while F106A showed 5-fold loss of activity ($IC_{50} = 54 \mu\text{M}$) as compared to the wild type ($IC_{50} = 10.6 \mu\text{M}$). Such results support the hypothesis that these π - π stacking interactions are crucial to the inhibitor's potency and molecular recognition. Inhibitor analogs utilizing cyclic or aromatic linker regions decreased binding affinity around 1000-times. The rigidity and steric clash is likely the culprit for loss of inhibition. These bulky linkers may disrupt hydrogen bonding between the flanking amines of the linker and the proximal D98 and T152 residues. In the case of the warhead switching from **1b**'s cyclopentane ring to **1c**'s phenyl ring allowed for the additional cation- π interaction. K190's hydrogen bonding and cation-- π interactions hold the benzothiophene-[b]-1,1-dioxide warhead in proximity to Cys181 allowing more optimal interaction with the electrophilic β -carbon. Observation from the docking analysis provided crucial information used in the design of more SCP1 inhibitors. Inhibitor optimization and elucidation of mechanism of action thus far led to the J. Med. Chem publication, *Target covalent Inhibition of small CTD phosphatase 1 to Promote the degradation of the REST transcription factor in human cells*⁵⁴.

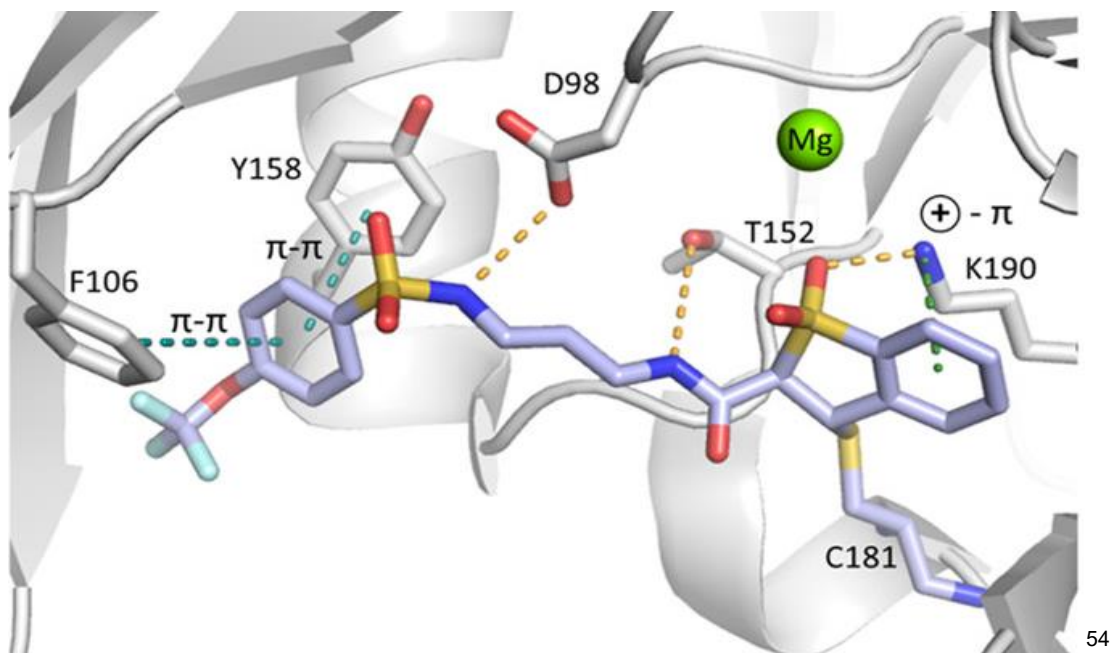


Figure 1.5 Docking model of **1c** and SCP1 WT

Kinetics of Covalent Inhibitors

As covalent inhibitors have seen tremendous success in the clinical and commercial setting the way to describe and characterize their efficacy needs updating. Traditionally the half-maximal inhibitory concentration (IC_{50}) has been the metric to measure a drug's efficacy. Not only are IC_{50} measurements impacted by time and the concentration of the target protein in the assay, they fail to account for a binding equilibrium. A more comprehensive method to describe the kinetics of covalent inhibitors is visually illustrated in **Figure 1.6**

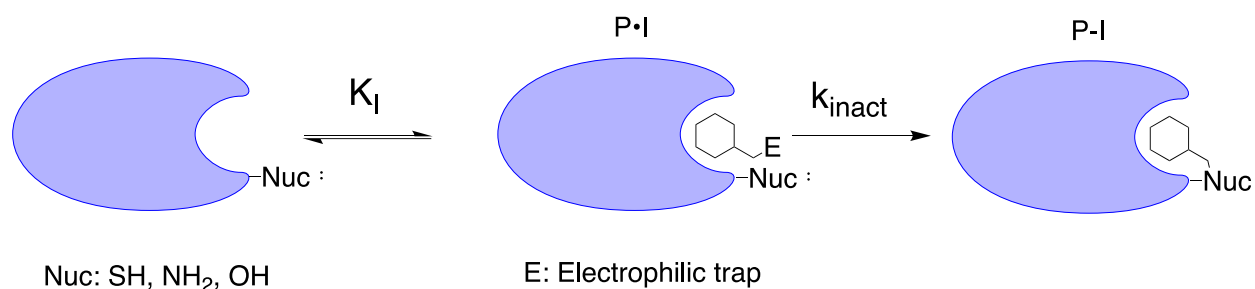


Figure 1.6 A visual illustration explaining the kinetic parameters K_I and k_{inact}

The first step shows a reversible process where unbound protein (P) and inhibitor (I) interact to form a protein-inhibitor complex (P•I). K_I describes the potency of the first reversible binding event. K_I is defined as the concentration of the inhibitor required for half of the maximum potential rate of covalent bond formation. In the second step a covalent bond forming event takes place resulting in a covalent protein-inhibitor complex (P-I). k_{inact} describes this event and is the maximum potential rate of inactivation. Taken together the ratio of $\frac{k_{inact}}{K_I}$ is a second order rate equation describing the over all efficiency of the conversion of free protein (P) to protein-inhibitor complex

(P-I). This method of describing covalent inhibitors gives information on both the affinity a n inhibitor has for its target as well as the rate at which the covalent bond forms.

Optimization of the Hydrophobic Region

Continued efforts towards optimization focused on the hydrophobic section of the inhibitor. The docking model showed two aromatic residues, F106 and Y158, utilizing reversible π - π stacking interactions as a molecular recognition functionality. Variants which contained mutation at these residues further validated this hypothesis. The strategy to increase inhibitor potency came by maximizing the π - π stacking interactions.

Figure 1.7 shows the library compounds **1j-1ab** which were designed to increased interactions with residues F106 and Y158.

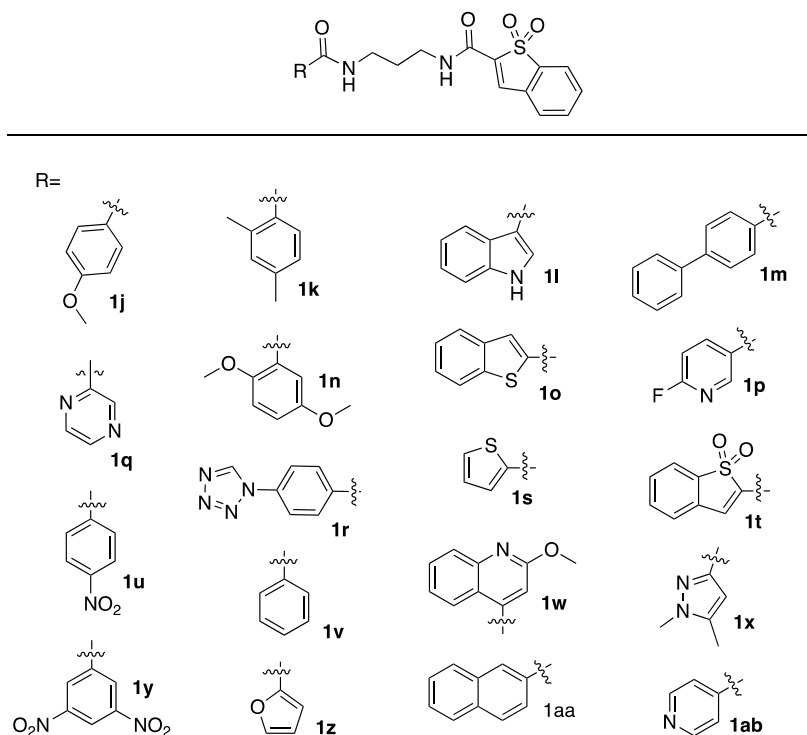


Figure 1.7 Library of inhibitors (**1j-1ab**) designed to increase π - π stacking interactions

Inhibitors **1m**, **1o**, **1t**, and **1aa** were shown the most desirable properties of this initial round of compounds. Although **1t** showed the lowest IC₅₀ (5.3 μM) and contained the best covalent modification effects ($\frac{k_{inact}}{K_i} = 1525 \text{min}^{-1} \text{M}^{-1}$), incorporation of two covalently binding motifs is risky and not ideal. The runner up, **1m**, incorporates a biphenyl structure in the inhibitor. **1m**'s IC₅₀ was 7.7 μM and contained a $\frac{k_{inact}}{K_i}$ of $393 \text{min}^{-1} \text{M}^{-1}$. This became the new lead compound used as a starting point for further investigation.

After the biphenyl scaffold was determined to produce increased inhibition of SCP1, the next step was the derivatization the second phenyl ring. Altering electron density as well as incorporation of groups that increase the number of reversible interactions can play an effect on potency. To test the hypothesis if incorporation of additional functional groups to the biphenyl system will increase SCP1 inhibition compounds **1ac-1al**, shown in **Figure 1.8**, were synthesized.

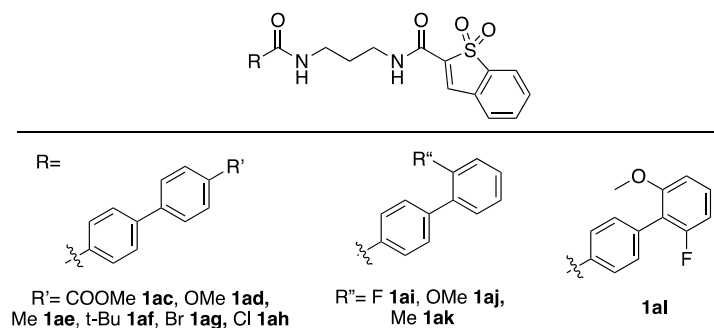
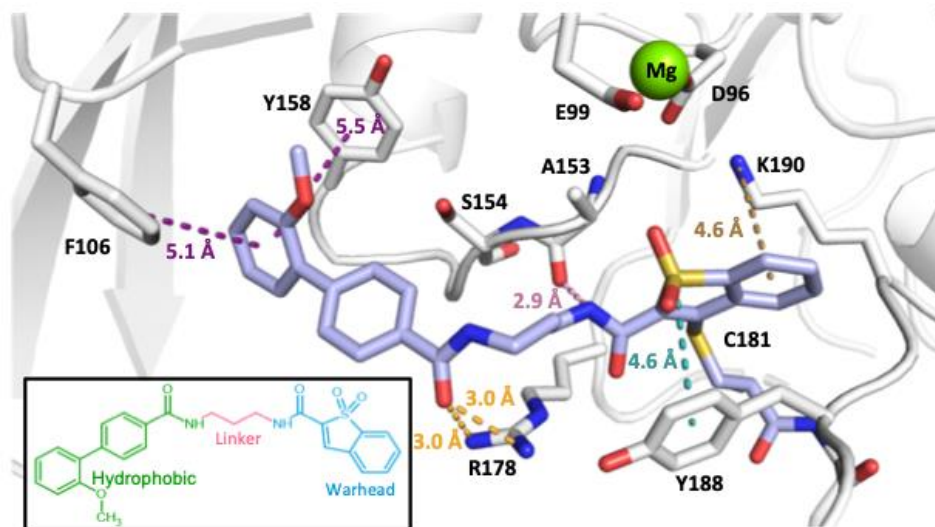


Figure 1.8 Derivatization of the biphenyl moiety leading to compounds **1ac-1al**

From this subset of compounds **1ai**, **1aj**, and **1al** led to the least SCP1 activity in the pNPP assay. From these top three performers compound **1aj** contained the best kinetic

properties. The ortho methyl ether, **1aj**, contained a $\frac{k_{inact}}{K_i}$ of $1383 \text{min}^{-1} \text{M}^{-1}$. As K_i represents the potency of the initial reversible binding event the decreased K_i of **1aj** ($K_i = 0.6 \mu\text{M}$) from the previously published lead compound **1c** ($K_i = 4.8 \mu\text{M}$) suggests increased specificity and better binding of SCP1.

Molecular docking was used to show the new lead compound **1aj** bound to the active of SCP1, seen in **Figure 1.9**. Again, residues F106 and Y158 play key roles in interacting with the hydrophobic region. Residues F106 and Y158 sandwich the terminal phenyl ring participating in π - π stacking interactions. The aryl methyl ether is positioned towards the phosphatase active site in a proximal pocket. While the internal phenyl ring does not show interactions with the protein its rigidity reduces the entropic cost for binding. Residue R178 is positioned to hydrogen bond with the carbonyl oxygen of the amide.



95

Figure 1.9 Docking model of **1aj** and SCP1 WT

Comparing the substitutions of compounds **1ai**, **1aj**, and **1al**, points to the importance of substitution at the ortho position of the terminal phenyl ring. To test effects

of substitution of at the ortho position on the potency compounds **1.72-1.86**, seen in **Figure 1.10**, were synthesized and tested for potency and kinetic characteristics. In designing these compounds variation of 3-dimensional space as well as electron altering characteristics were included. Strategically methyl, ethyl, and benzyl substitutions were included for the sulfonate, carbonate, and ester groups. Interestingly the ethyl sulfonate (**1.85**) and ethyl carbonate (**1.82**) generated the best kinetic properties with $\frac{k_{inact}}{K_i}$ of 683 and $637 \text{min}^{-1} \text{M}^{-1}$ respectively. Unfortunately, these results are less desirable than compound **1aj**. Optimization efforts towards the hydrophobic region up to this point in addition to the biochemical work by the Zhang lab led to the BMC Biology publication, *Targeting of rest with rationally-designed small molecule compounds exhibit synergistic therapeutic potential in human glioblastoma cells*⁹⁵.

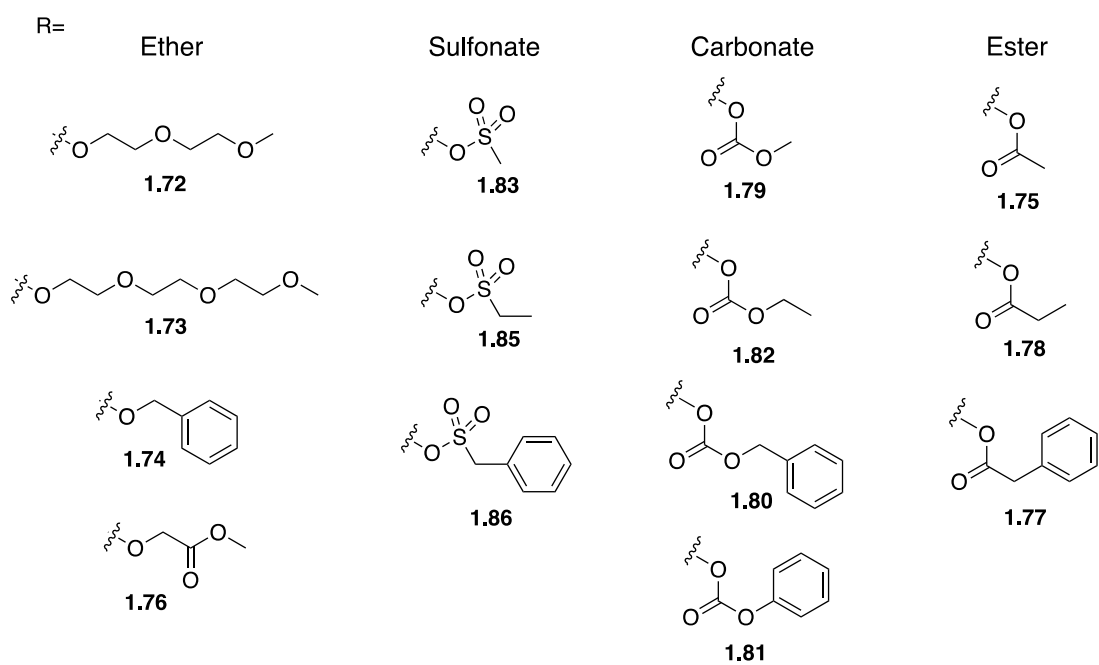
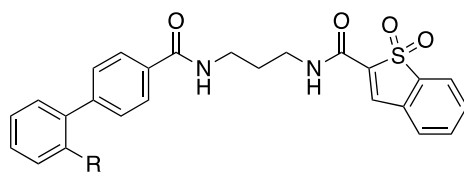
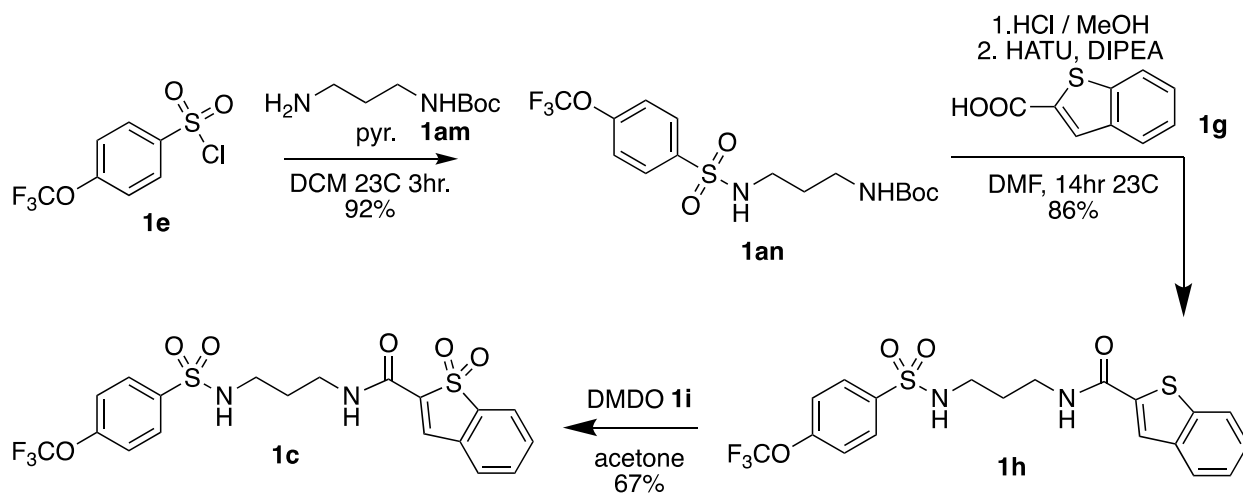


Figure 1.10 Compounds **1.72-1.86** designed to test the effects of derivatization at the ortho position of the terminal phenyl ring

Optimization of the Warhead Region

Improvement of the overall reaction scheme, depicted in **Scheme 1.3**, was the first step towards the optimization of the warhead region. Synthesis of **1c** utilizing the optimized reaction scheme starts with the same sulfonyl chloride **1e**. Use of *tert*-butyl (3-aminopropyl)carbamate, **1am**, eliminates the necessity for high equivalents of the linker. The addition-elimination reaction is subjected to room temperature conditions for 3 hours in the presence of pyridine in DCM. Not only is the yield increased from 30 to 92%, but purification of the boc-protected intermediate **1an** is easier than the analogous free amine intermediate **1f**. Deprotection of the boc-protection group in methanolic hydrochloric acid yields quantitative yields of the free amine (**1f**) which is used directly in the amide coupling reaction without purification. Switching from the carboxyl activating carbodiimide reagent EDC to HATU increased the yield of intermediate **1h** by 8%. The last improvement came from switch the reaction solvent in the oxidation step from DCM to acetone. Changing the solvent increased the yield of **1c** from 60 to 67%. The overall synthetic yield was increased from 14 to 53%.



Scheme 1.3 Improved synthesis of **1c**

While drug discovery programs used to exclude covalent drugs due to the potential toxicity, arising from promiscuous labeling, hapternization, and idiosyncratic drug reactions they recently have become more widely accepted⁹⁶. Acceptance of this strategy is supported by the many publications⁹⁷⁻¹⁰¹ and widespread utilization in FDA approved drugs. **Figure 1.11** shows three examples of covalent inhibitors which contain the acrylamide warhead. Not only are acrylamides the most researched of the cysteine selective covalent electrophiles, but they are also the most widely used¹⁰².

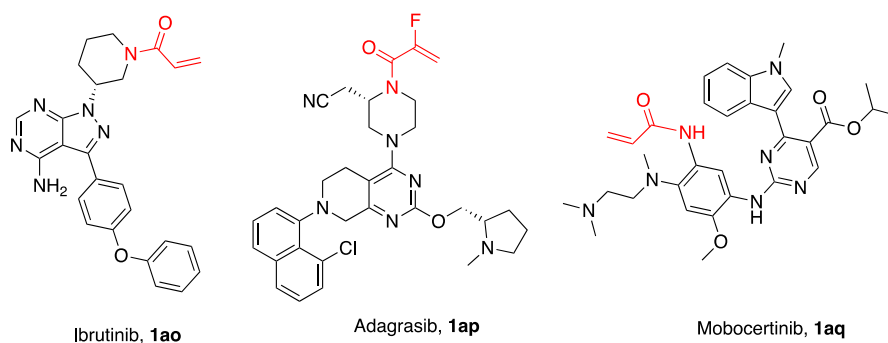


Figure 1.11 Examples of FDA approved drugs containing acrylamides

Due to the proven success of acrylamides, they were the first cysteine selective electrophile to be evaluated. **Figure 1.12** shows the first SCP1 inhibitors (**1.1-1.9**), which contain the parent and substituted acrylamides as well the trifluoromethoxy aryl ether fragment. Compound activity was measured with the Para-nitrophenyl phosphate (pNPP) assay. In this assay SCP1 dephosphorylates the chromogenic substrate pNPP yielding para-nitrophenol which is an intensely yellow product whose fluorescence can be measure on a spectrophotometer. First an inhibitor is incubated with SCP1 and then pNPP is added, generating a solution of varying fluorescence based on the ability of inhibitor to deactivate SCP1. Results were depicted through the remaining activity of SCP1. The positive control, where no inhibitor is incubated with enzyme, leads to full

SCP1 remaining activity. Low remaining enzyme activity shows the inhibitor has a high ability to inhibit SCP1. From this subset of compounds **1.1** and **1.2** showed best inhibition effects on SCP1. In a positive control where no inhibitor is incubated with phosphatase, SCP1 contains full activity. Compounds **1c**, **1.1**, and **1.2** generated relative activity values of 0.15, 0.34, and 0.69 respectively showing this subset of compounds did not lead to a more potent lead compound.

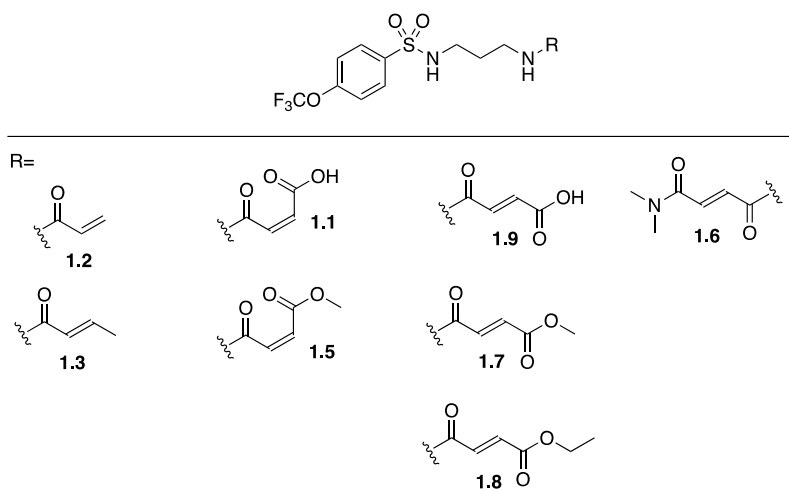


Figure 1.12 SCP1 inhibitors **1.1-1.9**

It has been shown that acrylamides reactivity can be altered through steric and inductive effects¹⁰³⁻¹¹². A subset of compounds diversifying the acrylamide's substitution led to the inhibitors seen in **Figure 1.13**. Compounds **1.17**, **1.24**, and **1.34** show the parent acrylamide as well as a methyl group at the α , and β positions. Determining effects of incorporating even bulkier groups including electron altering functional groups was generated by compounds **1.15**, **1.30**, and **1.31**. The remaining compounds incorporated fumaric acid esters and amides which show low cysteine reactivity¹¹³ and would eventually hydrolyze to the acid. In comparison to the current lead compound **1c**, this subset of acrylamide containing SCP1 inhibitors were less potent. Since a diverse

set of acrylamides was tested leading to less desirable result the search for a more ideal warhead continued.

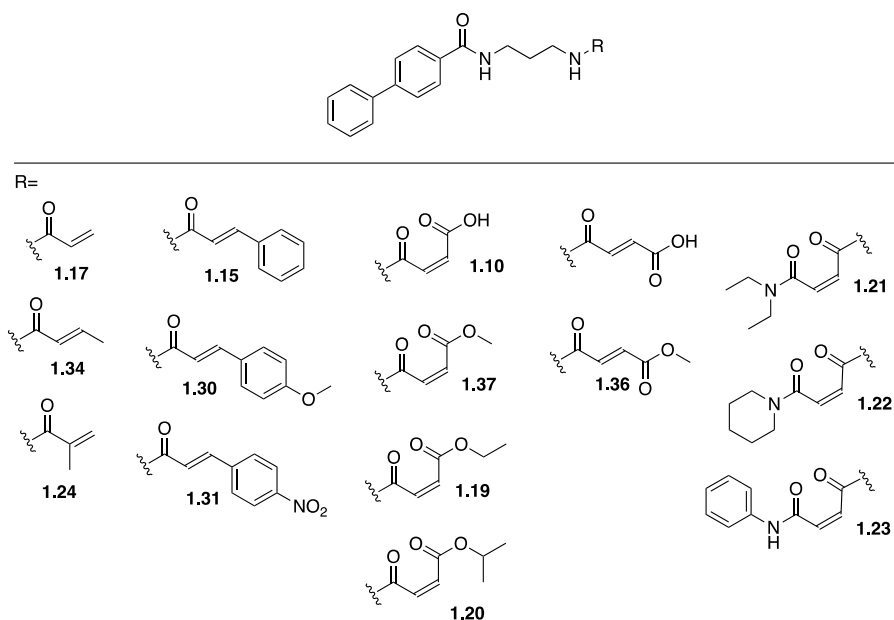


Figure 1.13 SCP1 inhibitors containing acrylamides and biphenyl scaffold

While the most incorporated warhead when targeting cysteine residues is the acrylamide, many other electrophiles have been used with success. A variety of warheads are reported to react preferentially with cysteine and are susceptible to changes in reactivity by steric and inductive effects. Discovered independently by Huib Ovaa¹¹⁴ and Henning Moots¹¹⁵ nonactivated terminal alkynes were found to react with cysteine residues contradicting the assumption of biological inertness. Aryl halides, that undergo nucleophilic aromatic substitution ($S_{\text{N}}\text{AR}$) proceed through a concerted mechanism¹¹⁶⁻¹¹⁷ involving a Meisenheimer transition state have long history in covalent protein history¹¹⁸. Positioning the leaving group ortho or para to the heteroatom increases reactivity. This type of warhead can be incorporated anywhere in the drug due to the many points of attachment of the aromatic ring. Compounds depicted in **Figure**

1.14 were synthesized to find a covalent scaffold which contains improved inhibiting properties to SCP1. No depicted compounds led to improved potency.

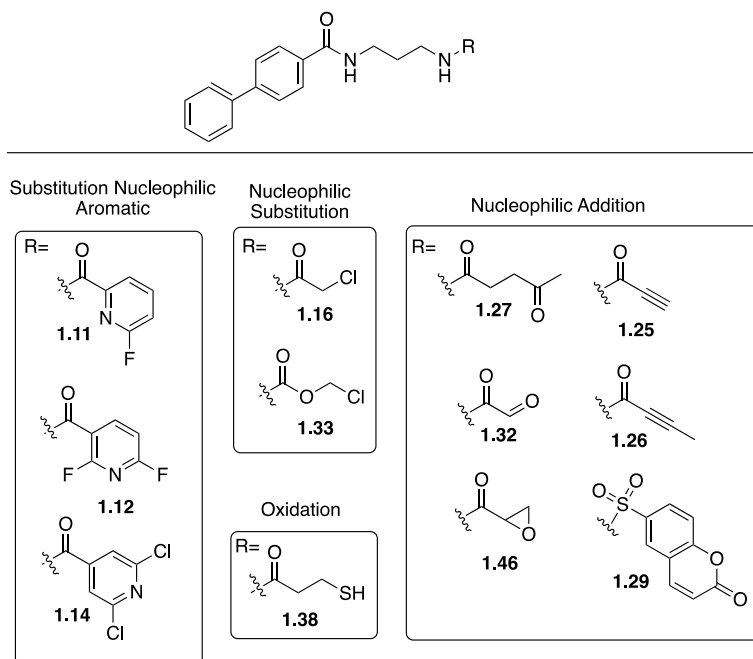


Figure 1.14 SCP1 inhibitors with varied warheads

While covalent inhibitors contain the advantages of enhanced potency, selectivity, and prolonged duration of action¹¹⁹ over their reversible counterparts, they contain the risk of off-target modification leading to idiosyncratic toxicity and haptization¹²⁰. Jack Taunton was the first to describe a warhead which can covalently bind and undergo the reverse reaction, dissociating from off target binding partners¹²¹. The α -cyanoacrylamides contain the advantages of covalent warheads and overcome the potential for toxicity cause by off target interactions. Incorporation of bulky groups to the β -position¹²² and replacement of the amide for a more electron withdrawing functional groups¹²³ can modulate the intrinsic reactivity and dissociation rates of the reversible covalent inhibitor¹²⁴. While relatively inert, nitriles will react with cysteines to form

thioimide especially when activated by electron-withdrawing groups like heteroaromatic rings. Both the α -cyanoacrylamides and nitrile covalent reversible groups incorporated into the SCP1 inhibitor. A variety of bulky groups at the β -position of the α -cyanoacrylamides were included to elucidate the necessary reactivity to bind the targeted cysteine residue. Additionally, a variety of reactivity altering groups was applied to the nitrile containing SCP1 inhibitors. Unfortunately, these covalent reversible inhibitors failed to yield a potency which surpasses the lead compound **1c**.

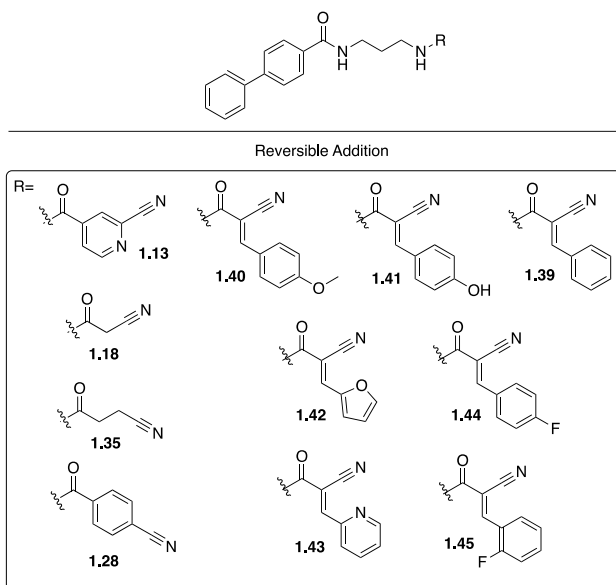


Figure 1.15 SCP1 inhibitors containing reversible covalent warhead

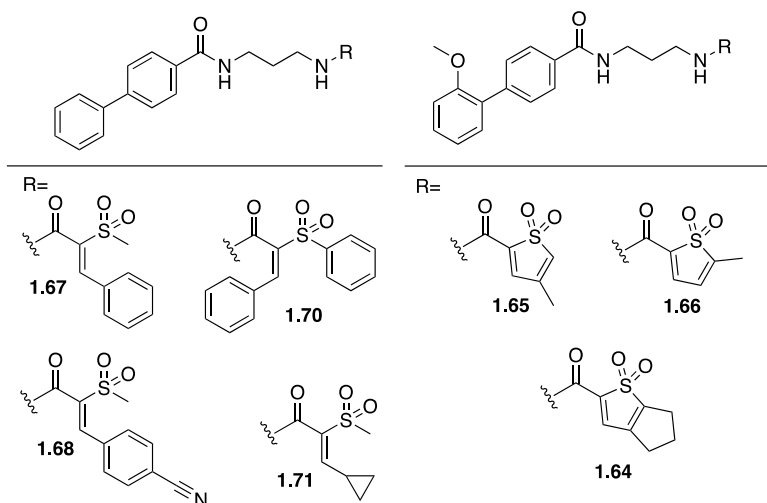


Figure 1.16 SCP1 inhibitor analogs containing a vinyl sulfone

The warhead utilized in the lead compound **1c** contains an alkene dually activated by an amide and sulfone. In attempts to move towards an electrophile with suitable activity and reversibility, it was chosen to incorporate a sulfone into the warhead. **Figure 1.16** shows the next subset of SCP1 inhibitors which contain both an acrylamide and vinyl sulfone to compose a dually activated alkene. After pre-incubating compounds **1.67**, **1.68**, **1.70**, and **1.71** SCP1 for 3 hours and then running the pNPP assay, SCP1 still contained full activity showing these compounds contained low reactivity or high reversibility. From the next subset of compounds **1.65**, and **1.66** decreased SCP1 activity the most with .11 and .12 activity remaining after 18 hours pre-incubation. Both **1.65** and **1.66** showed signs of one-step irreversible inhibition which was determined by the non-saturating behavior and rapid inhibition rates in the kinetic analysis. **1.65** and **1.66** resulted in a $\frac{k_{inact}}{K_i}$ of 1444 ± 45 and $907 \pm 51 \text{ min}^{-1}\text{M}^{-1}$ respectively as well as IC_{50} measurements of 6.4 and 7.5 μM . As reversible covalent inhibition is the goal, these methyl thiophenes were not used as lead compounds.

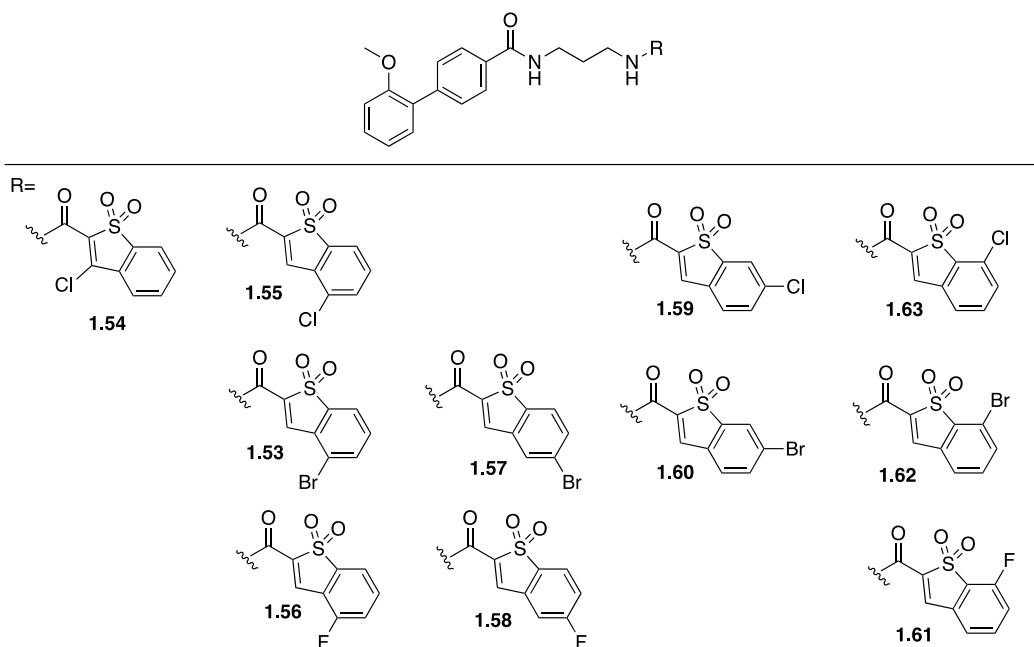


Figure 1.17 Benzothiophenes containing electron withdrawing halides

Thus far attempts to find a warhead which yields a higher potency and better kinetic properties than the benzothiophene has been futile. The docking study depicted in **Figure 1.9** shows a cation- π interaction that could be integral to the desirable potency and kinetic activity. Although previous warheads with have contained an aromatic ring in the warhead region, the flexibility fails to lock the orientation of the β -position proximal to Cys181. The benzothiophene contains inherent rigidity and has been shown to place the dually activated electrophile proximal to the target residue. Since this warhead has been shown to work, alteration of the electron density could alter reactivity. **Figure 1.17** shows the next subset of SCP1 inhibitors which contain a halide at the various position of the benzothiophene's aromatic ring. **Figure 1.18** shows the SCP1 activity for compounds **1.53-1.63**. The general trend shows that the positions meta and para to the sulfone show highest inhibiting activity on SCP1. Compound **1.51** is the major exception and the most potent of this set of compounds. **1.51** produced a k_{inact} of 0.0060 min^{-1} ,

K_i of 9.69 μ M, and $\frac{k_{inact}}{K_i}$ of 619 $min^{-1}M^{-1}$. As potency and kinetic properties are less

ideal than the parent compound, the logical direction was to incorporate electron

donating groups on the benzothiophene.

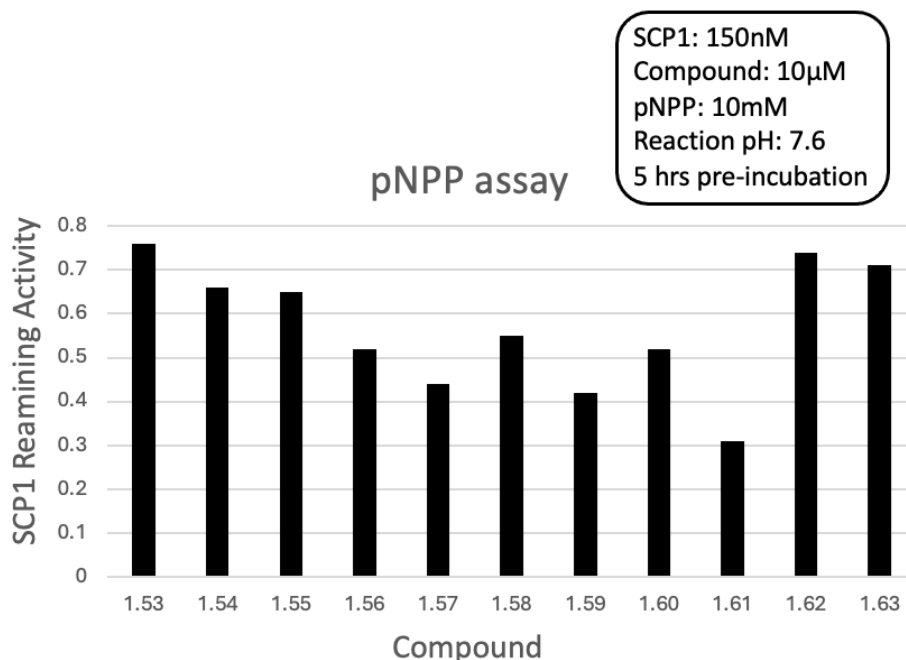


Figure 1.18 SCP1 activity for compounds 1.53-1.63

The next subset of SCP1 inhibitors synthesized contained electron donating groups positioned around the phenyl ring of the benzothiophene. Both methyl and methoxy groups were chosen as the electron donating groups incorporated in

compounds **1.87-1.95**, which are depicted in **Figure 1.19**. As many of the substituted benzothiophenes were not commercially available many of them were synthesized.

Figure 1.20 shows the reaction and proposed mechanism which yielded the necessary benzothiophene derivatives. The starting materials needed to generate the benzothiophene methyl ester is 2-fluorobenzaldehyde and methyl 2-mercaptoacetate. In the first step of the mechanism carbonate deprotonates methyl 2-mercaptoacetate's α -

proton to generate an ester enolate. The enolate adds into the aldehyde and after a subsequent protonation a β -hydroxyketone. Deprotonation of the acidic proton and elimination of a hydroxide ion leads to the $\alpha\beta$ -unsaturated ester. The thiolate generated after a deprotonation step adds into the aromatic carbon containing the fluorine. Electrons flow through the aromatic ring and form an extended Meisenheimer complex which reverts back to eliminate the fluorine ion and subsequently forms the 5-member ring.

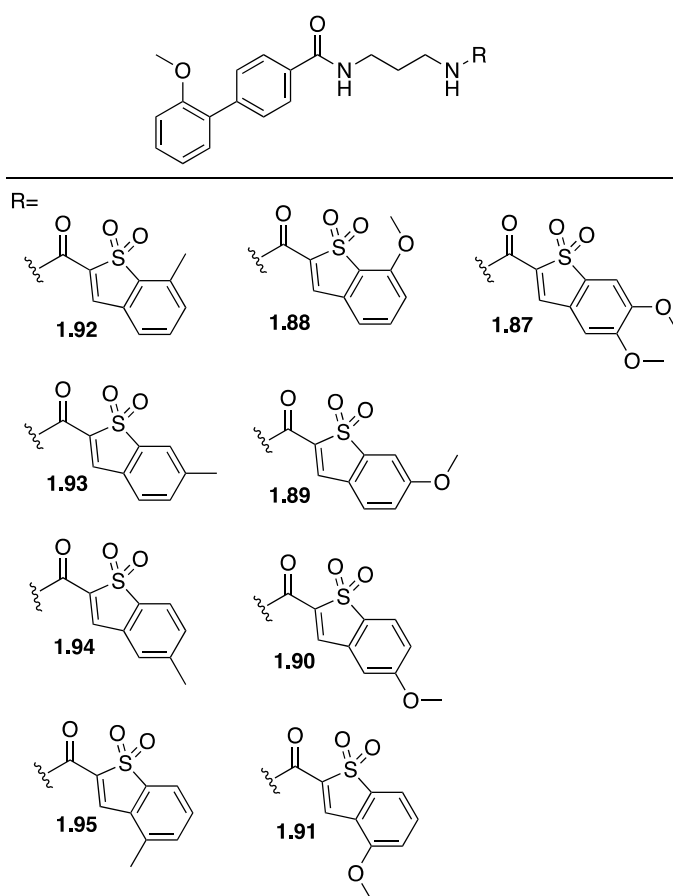


Figure 1.19 Benzothiophene derivatives containing electron donating groups

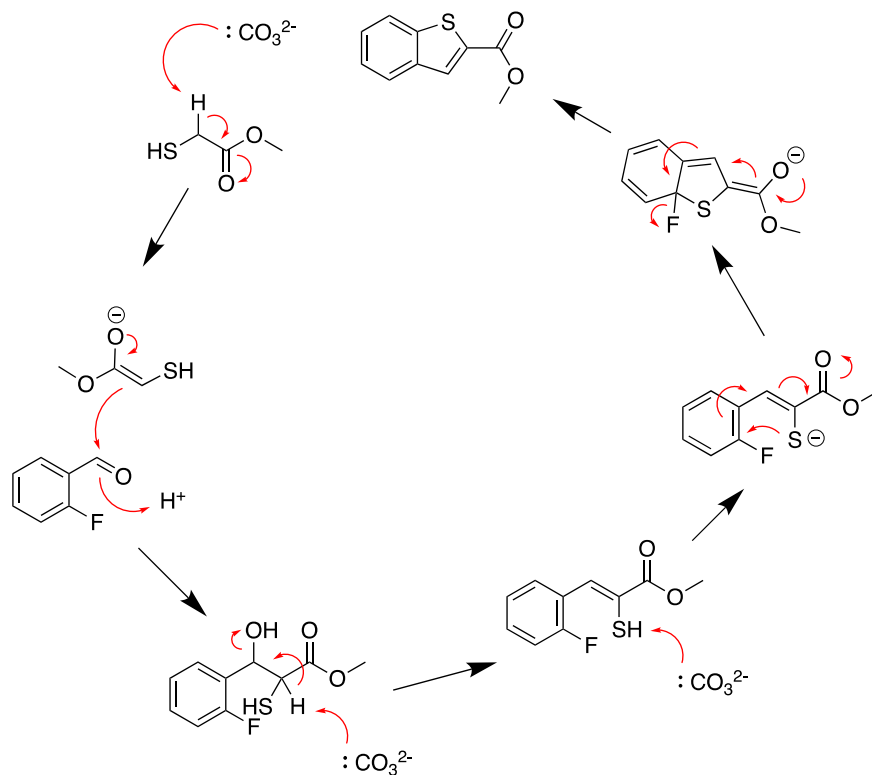
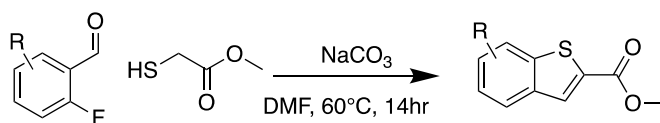


Figure 1.20 Synthesis and proposed mechanism of substituted benzothiophenes

Again, phosphatase activity was tested by the pNPP assay. A control where no compound was preincubated with SCP1 led to full SCP1 activity whereas the GR16 preincubated with SCP1 led to 0.61 remaining SCP1 activity. Of this set of electron-donating SCP1 derivatives the best performing were **1.88**, **1.93**, and **1.94** where SCP1 remaining activity was 0.90, 0.81, and 0.80 respectively. As **1.94** showed the best

results in the pNPP assay it was tested further for kinetic parameters. With $\frac{k_{inact}}{K_i}$ of 191 $min^{-1}M^{-1}$ it shows less ideal kinetic parameters compared to the lead compound **1aj**.

The next question to answer was if maintaining the benzothiophene can replacing the amide with more electron withdrawing functional groups increase potency towards SCP1. To answer this question compounds **1.96** and **1.97** were synthesized. Interestingly both compounds **1.96**, and **1.97** either have negligible activity against SCP1 or contain high reversibility. When these compounds were preincubated 5hrs. with SCP1 and then the pNPP assay was conducted, SCP1 retained all activity.

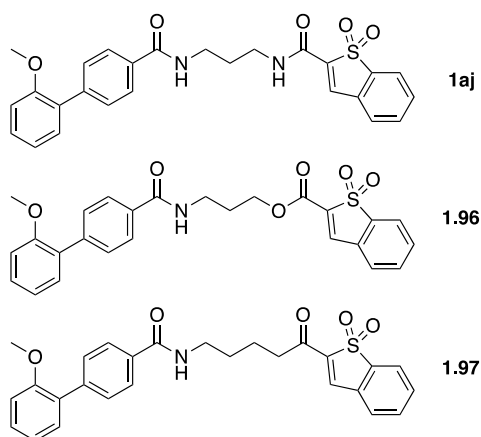
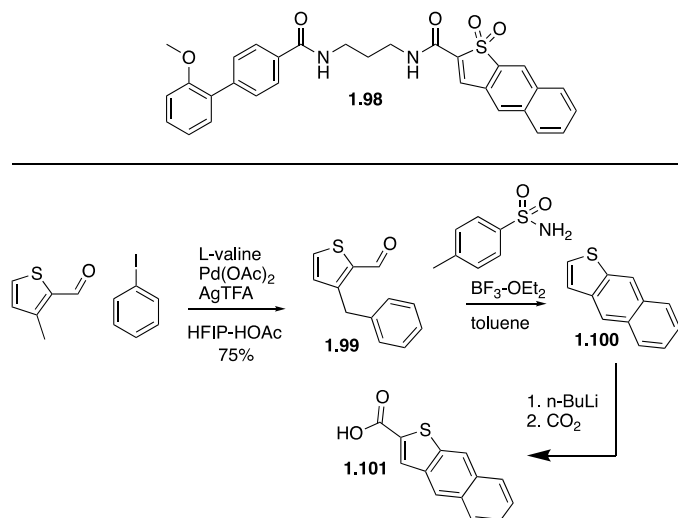


Figure 1.21 SCP1 inhibitors **1aj**, **1.96**, and **1.97**

The docking study seen in **Figure 1.5** shows a cation-pie interaction between the cationic lysine K190 and the phenyl ring of the benzothiophene. As cation-pie interaction are known for molecular recognition, the question if increasing the strength of the cation-pie interaction would result in increased potency or desirable kinetic properties arose. Mecozzi et al. released calculated data which is useful for predicting the strength of interaction between biologically relevant heterocycles and cationic residues¹²⁵. Consistent with previous understanding, the general trend shows more electron rich the

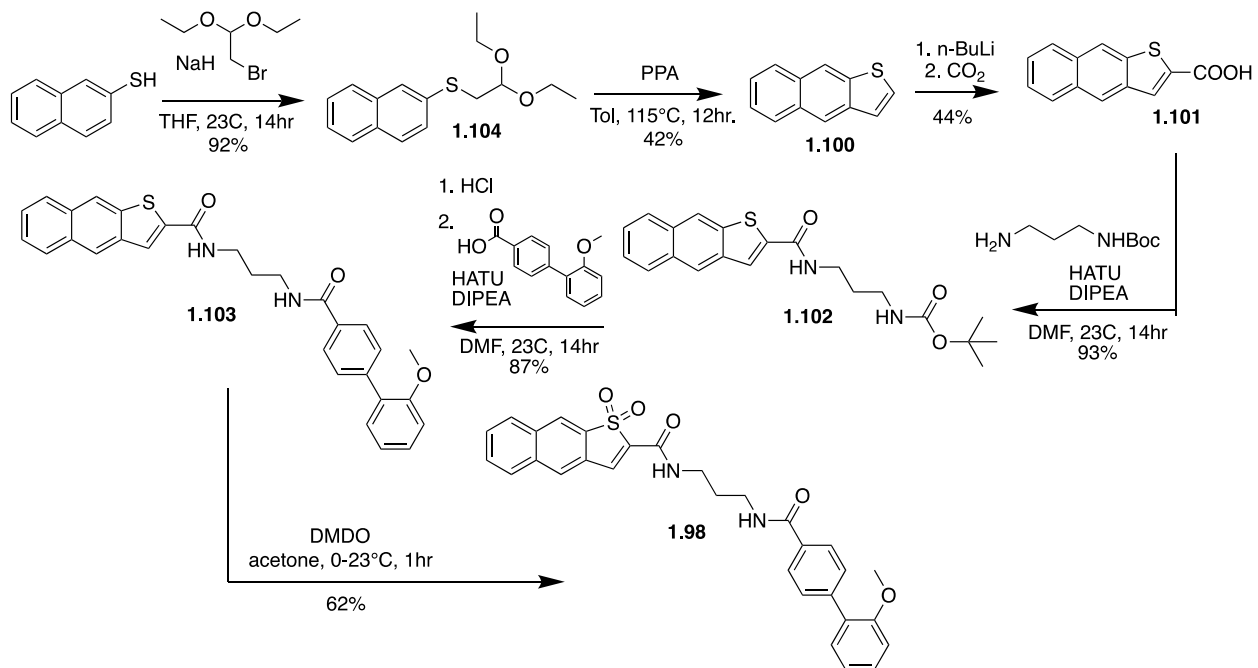
aromatic rings interact stronger with the electron deficient residue. Their data shows a simple benzene ring contains a binding energy of $27.1 \frac{kcal}{mol}$, while a naphthalene ring has an increased binding energy of $28.7 \frac{kcal}{mol}$. Using this information as guidance towards strengthening the cation-pi interaction, the SCP1 inhibitor **1.98** was synthesized. As the naphtho[2,3-*b*]thiophene-2-carboxylic acid (**1.101**) intermediate was not commercially available it was synthesized. **Scheme 1.4** shows the initial synthetic route which would yield the necessary carboxylic acid (**1.101**). This route was modeled after published literature¹²⁶ led by Chennakesava Reddy. The initial step proceeds through a γ -C(sp³)-H arylation of 3-methylthiophene-2-carbaldehyde utilizing L-valine as a transient ligand directing group to generate **1.99** in 75% yields. Attempts to cyclize and produce naphtho[2,3-*b*]thiophene (**1.100**) were modeled after Yu's paper published in *Advanced Synthesis & Catalysis*¹²⁷. The reaction utilizes boron trifluoride etherate (BF₃·Et₂O) as a catalyst in an aza-Friedel-Crafts. Unfortunately, published conditions failed to yield the desired product **1.100**. Additional efforts of altering solvent, time, catalyst, and Lewis acid were fruitless.



Scheme 1.4 Initial route towards SCP1 inhibitor **1.98**

The previous approach failed to produce naphtho[2,3-*b*]thiophene (**1.100**) due to cyclization of the internal phenyl ring. The revised synthetic scheme depicted in **Scheme 1.5** circumvents this by starting with naphthalene-2-thiol and focusing on the formation of the thiophene. An S_N2 reaction between naphthalene-2-thiol and 2-bromo-1,1-diethoxyethane generates the thioether **1.104** in 92% yields. Subsequent acid catalyzed acetal deprotection and intermolecular cyclization generates naphtho[2,3-*b*]thiophene (**1.100**). Introduction of CO₂ to the lithiated naphtho[2,3-*b*]thiophene generates a carboxylic acid ortho to the thioether producing **1.101** in 44% yield. Activation of the carboxylic acid by HATU and subsequent amide formation with *tert*-butyl (3-aminopropyl)carbamate generates intermediate **1.102**. Cleavage of the carbamate followed by amide coupling with 2'-methoxy-[1,1'-biphenyl]-4-carboxylic acid yields **1.103**. Oxidation of the sulfide to sulfone by DMDO completes the synthesis of the SCP1 inhibitor **1.98**. Unfortunately, SCP1 retained full activity after incubation with **1.98** for 5 hours. Thus far attachment of any substituents along the phenyl ring of the benzothiophene has reduced potency compared to the lead compound **1aj**. It is

possible that SCP1's binding site cannot accommodate substitutions on the benzothiophene warhead due to steric clash.



Scheme 1.5 Synthetic route that affords SCP1 inhibitor **1.98**

Reactivity Study

While covalent inhibitors can offer advantageous properties compared to reversible inhibitors like an increased biochemical efficiency, lower dose sizes potentially leading to increased therapeutic index, potential to overcome drug resistance, and longer duration of action there are risks¹²⁸. Off target modification resulting from high reactivity or lack of specificity can lead to immunotoxicity and idiosyncratic hypersensitivity¹²⁹⁻¹³¹. To mitigate these risks, it is imperative to balance the chemical reactivity and specificity to the intended target. A second strategy to avoid liabilities associated with covalent modification is to incorporate reversible covalent electrophile into the inhibitor.

Dually activated Michael acceptors have received much attention and development for their reversible covalent properties. The α -cyanoacrylamide is one of the first cysteine selective reversible warheads to receive research efforts toward illuminating kinetic reactivity and reversibility. A study conducted by Jack Taunton and coworkers¹³² shows that altering steric mass of the β -position and electron withdrawing groups at the α -position of acrylonitriles allows the capability to tune reversibility.

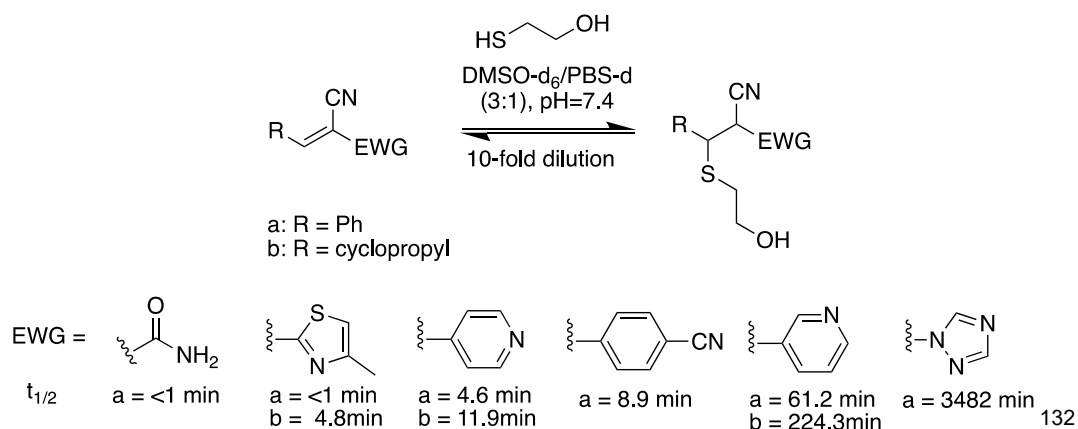


Figure 1.22 Tunable reversibility of α -heteroaromatic acrylonitriles

Illuminating the electrophilic reactivity and reversibility of reversible covalent warheads is an essential step in the optimization process. While kinetic measurements give insight on general reactivity trends, they do not always transfer as expected when applied in biological settings.

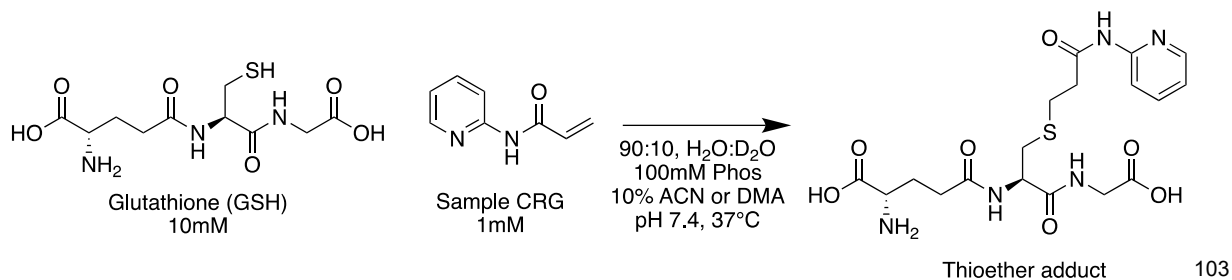
Literature¹⁰³ produced by Pfizer describes two convenient methods to measure the reactivity of covalent reactive groups. The first method uses the ReactArray automated reaction system in combination with high pressure liquid chromatography / mass spectrometry (HPLC/MS) while the second method utilizes nuclear magnetic resonance (NMR) to monitor the reaction progress. Plotting the natural log of the consumption of starting material as a function of time generates the rate information $k_{pseudo1st}$ which can be used to calculate half-life ($t_{1/2}$)¹³³.

$$\ln([electrophile]) = -k_{pseudo1st} \times t + \ln([electrophile_0])$$

$$t_{1/2} = \frac{\ln(2)}{k_{pseudo1st}}$$

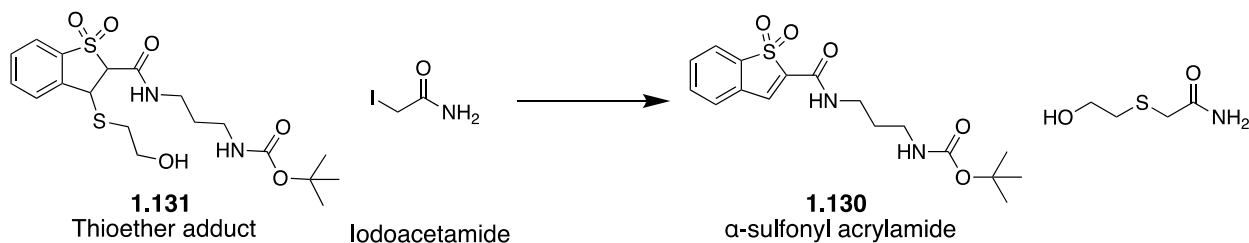
Scheme 1.6 shows an example reaction between glutathione (GSH) and a sample covalent reactive group (CRG) as well as the reaction conditions used to determine kinetic data by NMR. Reaction conditions as close to physiological conditions were used. Glutathione (GSH) is the model nucleophile because it is a biologically relevant thiol containing compound. A phosphate buffered solution (PBS) maintained the physiological pH (7.4) within the aqueous environment. Noteworthy is the necessity for

a cosolvent and elevated temperature to aid in solubility. Manipulation of initial concentration of reactants allows the use of pseudo 1st order kinetics.



Scheme 1.6 Pfizer's reaction with standard NMR conditions used to generate rate information ($k_{\text{psuedo1st}}$ and $t_{1/2}$)

To better understand the reactivity and reversibility of the benzothiophene CRG, a reactivity study was conducted based on Taunton and Pfizer's NMR based kinetic studies. **Scheme 1.7** shows the general reaction used to generate the pseudo first order rate constant and half-life data. The exact reaction conditions and procedure used in the Pfizer study was attempted however failed to produce reproducible data due to solubility issues.



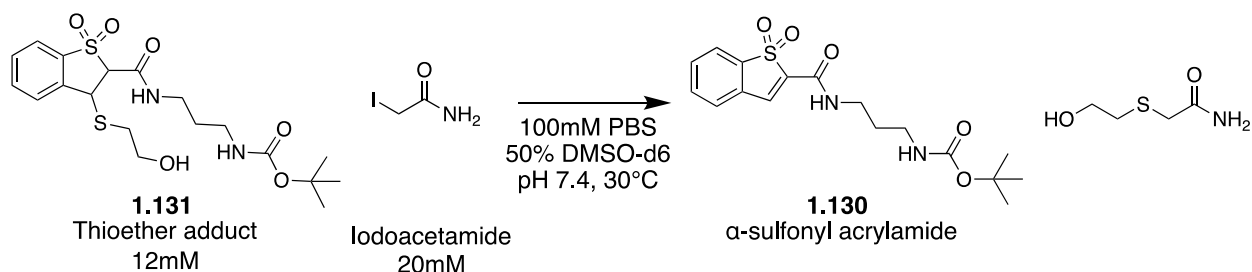
Scheme 1.7 General reaction scheme used to generate rate information ($k_{\text{psuedo1st}}$ and $t_{1/2}$)

As the aqueous solubility of the benzothiophene compounds is less than Pfizer's compounds, alteration of the reaction conditions were necessary to generate reliable data. **Table 1.1** shows the evolution of reaction parameters leading to the optimized conditions used to generate kinetic data. In conditions **1** and **2** high equivalents of

DMSO-d₆ were used to ensure the solubility of the reactants however caused the phosphate salts to precipitate. Additionally, the amount of phosphate buffered solution (PBS) used does not fit pseudo first order kinetic parameters. Conditions **3** and **4** used less equivalents of DMSO-d₆ solving the PBS precipitation issue and brings reaction conditions closer to physiological conditions however these sample failed to lock in the NMR. Conditions **5** and **6** solved locking problems however led to the precipitation of reactants. Decreasing D₂O, seen in conditions **7** and **8**, allowed reactants to remain soluble however led to locking problems. Using equal volume of DMSO and PBS shows ideal solubility properties to solubilize both reactants and phosphate salts. Conditions **9** show the optimized parameters allowing the generation of kinetic data. Equal volume of DMSO-d₆ and 0.2M PBS made with H₂O contained sufficient buffer capacity and solubility properties.

Table 1.1 Optimization conditions for the generation of rate information ($k_{\text{psuedo1st}}$ and $t_{1/2}$)

Condition	DMSO-d6	DMSO	D2O- 0.2M PBS	H2O- 0.2M PBS	Issue
1	4		1		buffer capacity & precipitation
2	3		1		buffer capacity & precipitation
3	2		1		NMR locking
4	1		1		NMR locking
5		1	4		precipitation
6		1	3		precipitation
7		1	2		NMR locking
8		1	1		NMR locking
9	1			1	



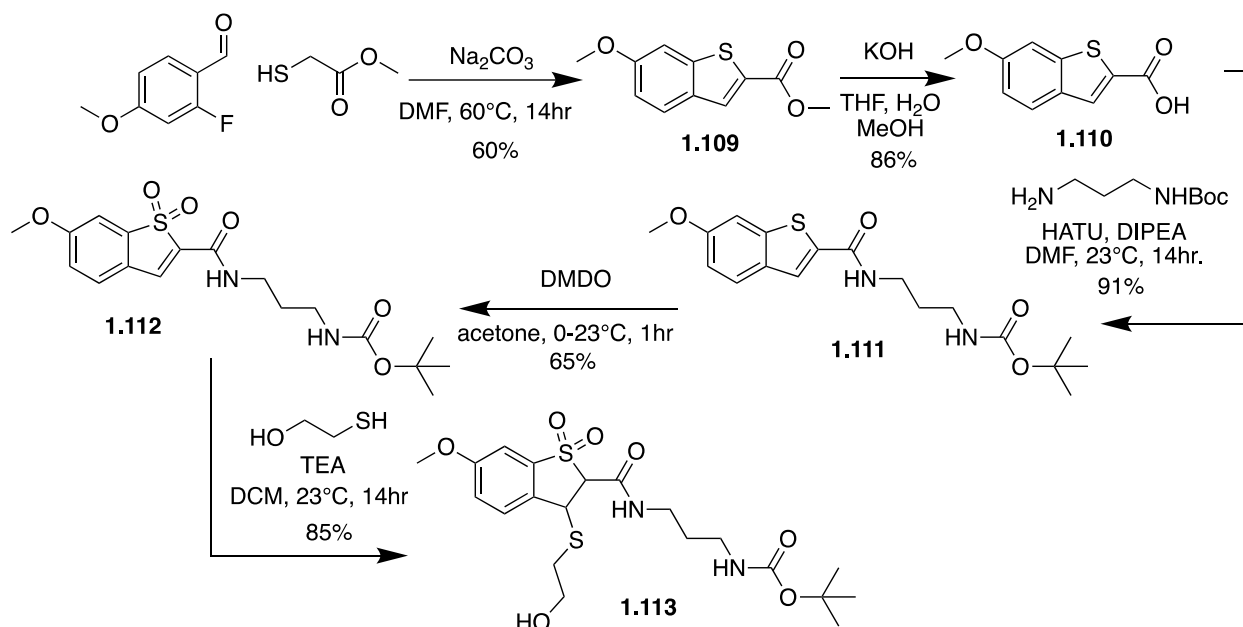
Scheme 1.8 General reaction scheme and conditions used to generate rate information ($k_{\text{psuedo1st}}$ and $t_{1/2}$)

The example reaction with standard conditions are displayed in **Scheme 1.8**. A final concentration of 12mM of thioether adduct was chosen to ensure the conditions fall under pseudo-first-order kinetics. Excess iodoacetamide was included as a thiol trap ensuring the eliminated 2-hydroxyethane-1-thiolate did not undergo a thia-Michael reaction. A final concentration of 100mM PBS is significantly higher than the thioether to ensure the conditions fall under pseudo-first-order-kinetics. The PBS was made to pH 7.4 mimicking physiological conditions. A 1:1 volume ratio of DMSO-d₆ and PBS ensured sufficient solubility for all reaction components allowing reaction temperatures to be lowered to 30°C.

A thioether adduct stock was initially prepared as a 200mM solution in DMSO-d₆. A iodoacetamide stock was initially prepared as a 500mM solution in DMSO-d₆. A 30μL aliquot of the concentrated thioether stock and 20μL aliquot of the concentrated iodoacetamide stock was pipetted into a 5mm outside diameter NMR tube. To this was added 200μL DMSO-d₆ and 250μL of 200mM potassium phosphate buffer (pH = 7.4). The reaction mixture was vortexed thoroughly and placed in a Bruker 600 MHz NMR spectrometer (Bruker BioSpin Corporation, Billerica, MA) controlled with Topspin V3.6.5 equipped with a 5mm Broadband inverse detection probe. The probe temperature was set to 30°C. 1D spectra were recorded employing water suppression by using excitation sculpting (zgpg30) with a sweep width of 7184 and a total recycle time of 3.3 s. The resulting time-averaged free induction decays were transformed using an exponential line broadening of 0.3 Hz to enhance signal-to-noise. The water signal at 4.45 ppm was placed on resonance. Each acquisition consisted of 8 dummy scans followed by 64 scans for a total acquisition time of 3 min and 49 s. Most analyses consisted of 10

successive acquisitions every 10 min over 1.5 h. Pseudo-first-order rate constants were determined by plotting the natural log of the consumption of thioether adduct, as defined by area of given resonance from a thioether adduct vs time.

In order to characterize and better understand the reversibility of the thioether adduct a subset of compounds incorporating electron altering substituents on the aromatic ring were synthesized. **Scheme 1.9** shows the synthetic pathway used to generate the compounds used in the NMR based kinetic experiments.

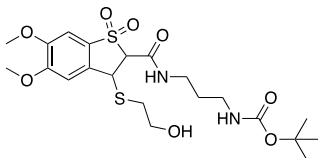
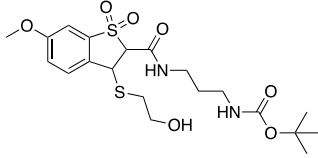
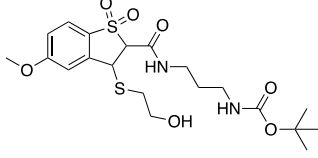
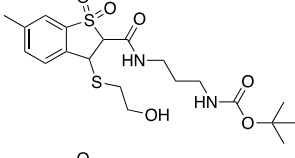
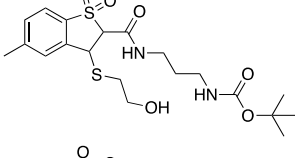
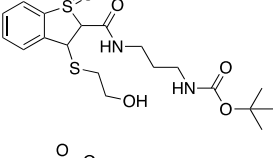
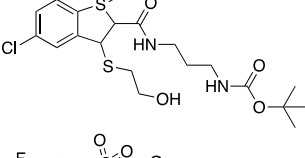
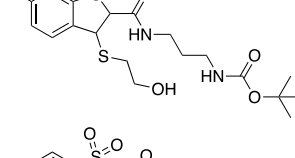
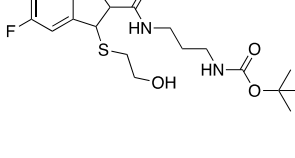


Scheme 1.9 Synthetic pathway used to generate thioether adducts used in kinetic study

To form the benzothiophene scaffold a domino Aldol-S_NAR reaction takes place between a 2-fluoroaldehyde and methyl 2-mercaptoacetate. The newly formed substituted benzothiophene, like **1.109**, is saponified resulting in a carboxylic acid (**1.110**). Amide formation using HATU and *tert*-butyl (3-aminopropyl)carbamate forms the carbamate containing compound (**1.111**) in high yields. Sulfide oxidation with DMSO

quickly produces the sulfone intermediate (**1.112**). A thia-Micheal reaction using 2-mercaptoethanol as the thiol source results in a thioether adduct (**1.113**).

Table 1.2 Experimental rate information ($k_{\text{psuedo1st}}$ and $t_{1/2}$)

Compound	Structure	$t_{1/2}$ (min)	$k_{\text{psuedo1st}}$ ($\text{min}^{-1} \times 10^{-3}$)
1.108		248	2.8
1.113		288	2.4
1.118		223	3.1
1.123		247	2.8
1.128		223	3.1
1.131		385	1.8
1.137		239	2.9
1.140		433	1.6
1.143		346	2.0

Utilizing the previously described experimental procedure yielded the rate information displayed in **Table 1.2**. Consistent trends are seen not only with respect to the electron altering nature of the substituent, but also its position on the aromatic ring. Half-life data shows that strong electron donating groups, such as the methoxy and methyl groups, decrease the half-life and speed up the elimination of 2-hydroxyethane-1-thiolate when compared to the parent compound **1.131**. **Figure 1.23** helps visually explain the experimental trend. After a base deprotonates the acidic proton, electron density is spread between the sulfone and amide. Incorporation of electron withdrawing substituents would help stabilize this resonance while electron donating substituents would destabilize resonance and increase the rate of elimination.

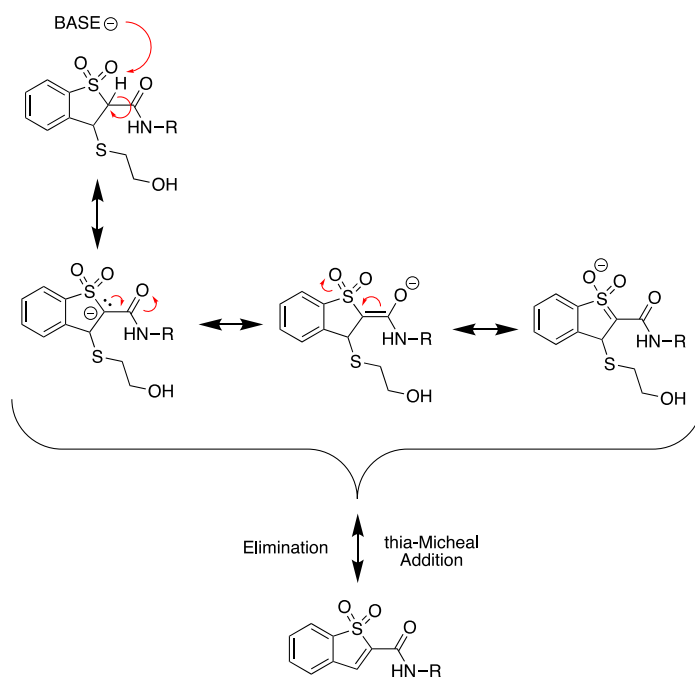


Figure 1.23 Resonance between the sulfone and amide

Conclusion

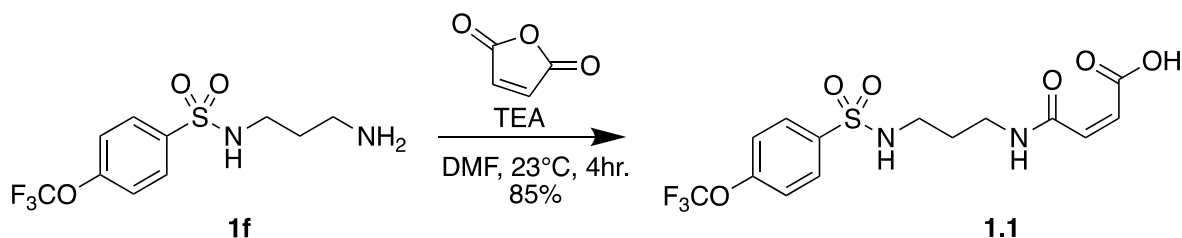
Described herein is the synthesis of nonreversible and reversible covalent inhibitors targeting the SCP1 phosphatase. Control of this regulatory enzyme enables the modulation of the transcription factor REST and therefore glioblastoma. Guided by a structure-based drug design approach over 220 final compounds were synthesized and tested generating a broad understanding of their structure-activity relationship. Incorporation of an additional electron-rich aromatic ring to the hydrophobic region of the molecule, determination of the optimal linker chain length, and use of a reversible covalent dually activated benzo[*b*]thiophene 1,1-dioxide warhead led to compound **1aj** whose K_I is 0.6 μM and $\frac{k_{inact}}{K_i}$ is 1383 $\text{min}^{-1}\text{M}^{-1}$. An NMR based kinetic study on a thia-Micheal reaction using a benzo[*b*]thiophene 1,1-dioxide warhead showed that incorporation of electron-donating substituents promotes the reverse reaction (elimination) faster than electron-withdrawing substituents supported by half-life data.

Experimental Section

General Information

All reactions were performed in flame- or oven-dried glassware sealed with rubber septa and under a nitrogen atmosphere unless otherwise indicated. Air- and/or moisture-sensitive liquids or solutions were transferred by cannula or syringe. Organic solutions were concentrated by rotary evaporator at 30 millibars with the water bath heated to not more than 40°C unless specified otherwise. Tetrahydrofuran (THF), dichloromethane (DCM), toluene (PheMe), diethyl ether (Et₂O) was purified with a Pure-Solve MD-5 Solvent Purification System (Innovative Technology). Acetonitrile (ACN, 99.9%, anhydrous) was purchased from FisherScientific. N,N,-Dimethylformamide (DMF, 99.8%, anhydrous) was purchased from Acros. Ethanol (EtOH, 200 proof, absolute) and methanol (MeOH, 99.8%, anhydrous) were purchased from Sigma-Aldrich. Analytical thin-layer chromatography (TLC) was carried out using commercial silica plates (silica gel 60, F254, Sigma-Aldrich) and was visualized by UV lamp, ceric ammonium molybdate (CAM), aqueous potassium permanganate (KMnO₄), or in an iodine (I₂) chamber. Nuclear Magnetic Resonance (NMR) spectra were collected at 298 K on a Bruker Avance III spectrometer (¹H NMR at 600 MHz; ¹³C NMR 151 MHz) fitted with a 1.7 mm or 5 mm triple resonance cryoprobe with z-axis gradients. All spectra were taken in Methanol-d₄ with shifts reported in parts per million (ppm) referenced to the proton or carbon of the solvent (3.31 or 49.00, respectively). All spectra were taken in Chloroform-d with shifts reported in parts per million (ppm) referenced to the proton or carbon of the solvent (7.26 or 77.0, respectively). All spectra were taken in Dimethyl

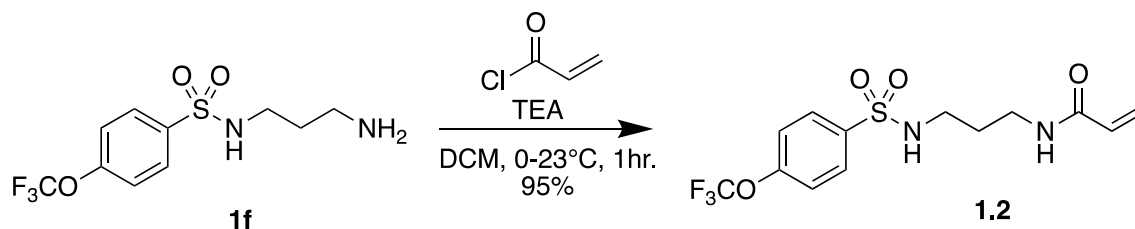
sulfoxide-d6 with shifts reported in parts per million (ppm) referenced to the proton or carbon of the solvent (2.50 or 39.5, respectively). All spectra were taken in Benzene-d6 with shifts reported in parts per million (ppm) referenced to the proton or carbon of the solvent (7.16 or 128.1, respectively). Coupling constants are reported in Hertz (Hz). Data for $^1\text{H-NMR}$ are reported as follows: chemical shift (ppm, reference to protium; s = single, d = doublet, t = triplet, q = quartet, dd = doublet of doublets, m = multiplet, coupling constant (Hz), and integration).



(Z)-4-oxo-4-((3-((4-(trifluoromethoxy)phenyl)sulfonamido)propyl)amino)but-2-enoic acid (1.1)

To a stirring solution of N-(3-aminopropyl)-4-(trifluoromethoxy)benzenesulfonamide (600 mg, 1 Eq, 2.01 mmol)(1f) and triethylamine (611 mg, 841 μL , 3 Eq, 6.03 mmol) in DMF (4 mL) at 23 $^\circ\text{C}$ was added solid furan-2,5-dione (986 mg, 5 Eq, 10.1 mmol) and stirred for 4 hour. Upon completion the reaction was diluted with EtOAc (20mL), washed with DI water (4x20mL), brine (20mL), dried by Na_2SO_4 , filtered, and concentrated under reduced pressure. The residue was purified by silica gel chromatography (DCM:MeOH (0-20%)) to yield 1.1 (0.68 g, 1.7 mmol, 85 %).

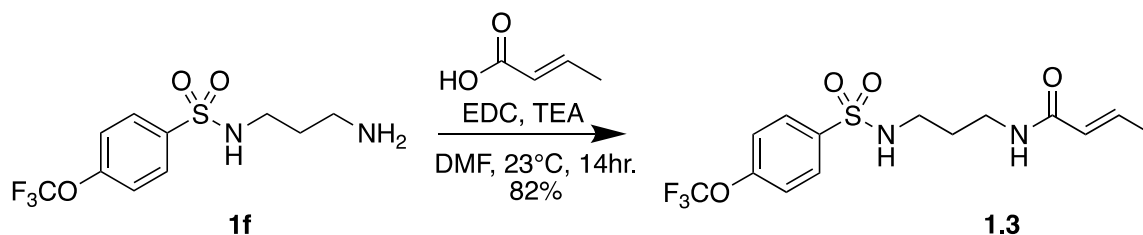
$R_f = 0.07$ (DCM:MeOH (8:2)) $^1\text{H NMR}$ (599 MHz, MeOD) δ 7.96 (d, $J = 8.8$ Hz, 2H), 7.48 (d, $J = 8.5$ Hz, 2H), 2.94 (t, $J = 6.8$ Hz, 2H), 1.73 (p, $J = 6.9$ Hz, 2H).



N-(3-((4-(trifluoromethoxy)phenyl)sulfonamido)propyl)acrylamide (1.2)

To a stirring solution of N-(3-aminopropyl)-4-(trifluoromethoxy)benzenesulfonamide (100 mg, 1 Eq, 335 μmol)(**1f**) and triethylamine (170 mg, 234 μL , 5 Eq, 1.68 mmol) in DCM (5 mL) at 0 °C was added neat acryloyl chloride (36.4 mg, 32.5 μL , 1.2 Eq, 402 μmol) dropwise. The reaction was allowed to come to 23 °C and stir for 1 hour after which time the reactants had been consumed as seen by TLC. The reaction was quenched by the addition of DI water (5mL), washed with brine (5mL), dried by MgSO_4 , filtered, and concentrated under reduced pressure. The residue was purified by silica gel chromatography (DCM:MeOH (0-5%)) to yield **1.2** (0.11 g, 0.32 mmol, 95 %).

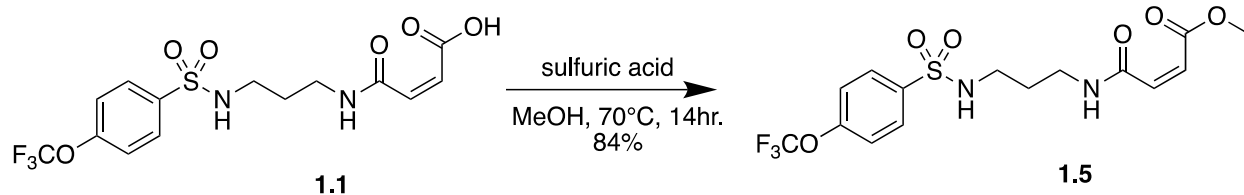
$R_f = 0.72$ (DCM:MeOH (9:1)) $^1\text{H NMR}$ (599 MHz, CDCl_3) 7.92 (d, $J = 8.8$ Hz, 2H), 7.31 (d, $J = 8.3$ Hz, 2H), 6.26 (d, $J = 16.0$ Hz, 1H), 6.04 (dd, $J = 16.9, 10.3$ Hz, 1H), 5.92 (t, $J = 6.2$ Hz, 1H), 5.79 (s, 1H), 5.67 (d, $J = 11.2$ Hz, 1H), 3.45 (dd, $J = 12.2, 6.5$ Hz, 2H), 2.95 (dd, $J = 12.2, 6.4$ Hz, 2H), 1.74 – 1.68 (m, 2H).



(E)-N-(3-((4-(trifluoromethoxy)phenyl)sulfonamido)propyl)but-2-enamide (1.3)

A solution of (E)-but-2-enoic acid (6.9 mg, 1.2 Eq, 80 μmol), 3-(((ethylimino)methylene)amino)-N,N-dimethylpropan-1-amine, HCl (18 mg, 1.4 Eq, 94 μmol), and triethylamine (20 mg, 28 μL , 3 Eq, 0.20 mmol) was stirred in DMF (3 mL) for 15 min after which time N-(3-aminopropyl)-4-(trifluoromethoxy)benzenesulfonamide (**1f**) (20 mg, 1 Eq, 67 μmol) was added and allowed to react for 14 hour at 23 $^\circ\text{C}$. Upon completion the reaction was diluted with EtOAc (15mL), washed with DI water (4x15mL), brine (15mL), dried by Na_2SO_4 , filtered, and concentrated under reduced pressure. The residue was purified by silica gel chromatography (DCM:MeOH (0-4%)) to yield **1.3** (20 mg, 55 μmol , 82 %).

$R_f = 0.30$ (DCM:MeOH (9:1)) $^1\text{H NMR}$ (599 MHz, CDCl_3) δ 7.93 (d, $J = 8.8$ Hz, 2H), 7.31 (d, $J = 8.5$ Hz, 2H), 6.82 (dq, $J = 13.8, 6.9$ Hz, 1H), 6.05 (t, $J = 6.7$ Hz, 1H), 5.73 (dd, $J = 15.1, 1.6$ Hz, 1H), 5.57 (s, 1H), 3.42 (dd, $J = 12.2, 6.5$ Hz, 2H), 2.93 (dd, $J = 12.1, 6.5$ Hz, 2H), 1.85 (dd, $J = 6.9, 1.5$ Hz, 3H), 1.69 (dt, $J = 11.9, 6.0$ Hz, 2H).

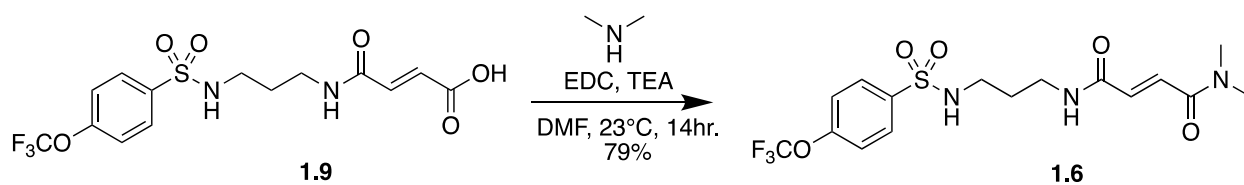


methyl (Z)-4-oxo-4-((3-((4-(trifluoromethoxy)phenyl)sulfonamido)propyl)amino)but-2-enoate (1.5)

General Procedure A: Fischer Esterification

To RBF was added **1.1** (17 mg, 1 Eq, 43 μmol), MeOH (4 mL), and a catalytic amount of sulfuric acid. The RBF was fitted with a reflux condenser and the stirring reaction was heated to 70 $^\circ\text{C}$ for 14 hour. After which time the reaction was evaporated to dryness, redissolved in EtOAc (5mL), washed with 1M NaHCO_3 (5mL), brine (5mL), dried with Na_2SO_4 , filtered, and concentrated under reduced pressure. The residue was purified by silica gel chromatography (DCM:MeOH (0-4%)) to yield **1.15** (15 mg, 36 μmol , 84 %).

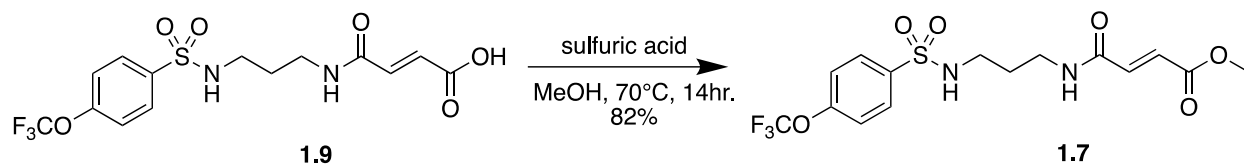
$^1\text{H NMR}$ (599 MHz, MeOD) δ 7.97 (d, $J = 8.8$ Hz, 2H), 7.48 (d, $J = 8.3$ Hz, 2H), 6.37 (d, $J = 12.0$ Hz, 1H), 6.16 (d, $J = 12.0$ Hz, 1H), 3.72 (s, 3H), 3.27 (t, $J = 6.7$ Hz, 2H), 2.96 (t, $J = 6.9$ Hz, 2H), 1.72 (h, $J = 7.0$ Hz, 2H).



N1,N1-dimethyl-N4-(3-((4-(trifluoromethoxy)phenyl)sulfonamido)propyl)fumaramide (1.6)

A solution of **1.9** (15 mg, 1 Eq, 38 μmol), EDC (10 mg, 1.4 Eq, 53 μmol), and triethylamine (11 mg, 16 μL , 3 Eq, 0.11 mmol) was stirred in DMF (3 mL) for 15 min after which time dimethylamine (3.4 mg, 38 μL , 2 molar, 2 Eq, 76 μmol) was added and allowed to react for 14 hours at 23 $^\circ\text{C}$. Upon completion the reaction was diluted with EtOAc (15 mL), washed with DI water (4x15 mL), brine (15 mL), dried by Na_2SO_4 , filtered, and concentrated under reduced pressure. The residue was purified by silica gel chromatography (DCM:MeOH (0-10%)) to yield **1.6** (13 mg, 30 μmol , 79 %).

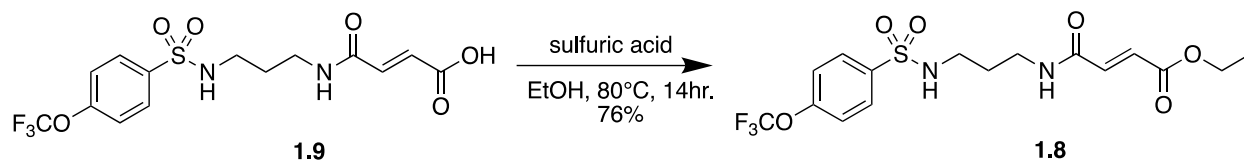
$^1\text{H NMR}$ (599 MHz, CDCl_3) δ 7.92 (d, $J = 8.7$ Hz, 2H), 7.37 (d, $J = 14.6$ Hz, 1H), 7.32 (d, $J = 8.3$ Hz, 2H), 6.85 (d, $J = 14.9$ Hz, 1H), 6.42 (s, 1H), 5.83 (s, 1H), 3.46 (dd, $J = 12.5, 6.3$ Hz, 2H), 3.15 (s, 3H), 3.04 (s, 3H), 2.98 (dd, $J = 12.1, 6.1$ Hz, 2H), 1.76 – 1.68 (m, 2H).



methyl (E)-4-oxo-4-((3-((4-(trifluoromethoxy)phenyl)sulfonamido)propyl)amino)but-2-enoate (1.7)

General Procedure A: Fischer Esterification

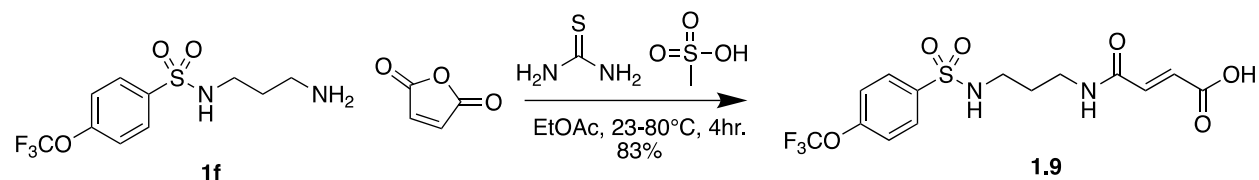
¹H NMR (599 MHz, CDCl₃) δ 7.92 (d, *J* = 8.8 Hz, 2H), 7.33 (d, *J* = 8.5 Hz, 2H), 6.86 (d, *J* = 15.3 Hz, 1H), 6.79 (d, *J* = 15.3 Hz, 1H), 6.23 (s, 1H), 5.68 (t, *J* = 6.6 Hz, 1H), 3.80 (s, 3H), 3.48 (dd, *J* = 12.4, 6.4 Hz, 2H), 2.96 (dd, *J* = 12.3, 6.4 Hz, 2H), 1.78 – 1.72 (m, 2H).



ethyl (E)-4-oxo-4-((3-((4-(trifluoromethoxy)phenyl)sulfonamido)propyl)amino)but-2-enoate (1.8)

General Procedure A: Fischer Esterification

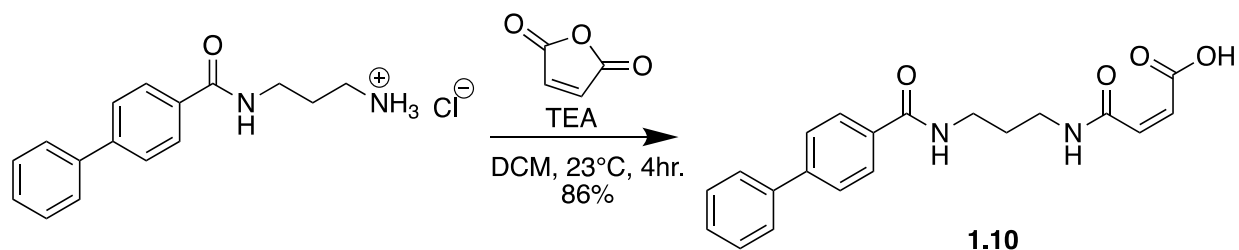
¹H NMR (599 MHz, CDCl₃) δ 7.92 (d, *J* = 8.7 Hz, 2H), 7.33 (d, *J* = 8.5 Hz, 2H), 6.84 (d, *J* = 15.3 Hz, 1H), 6.78 (d, *J* = 15.3 Hz, 1H), 6.11 (t, *J* = 5.7 Hz, 1H), 5.66 (t, *J* = 6.6 Hz, 1H), 4.26 (q, *J* = 7.1 Hz, 2H), 3.48 (dd, *J* = 12.3, 6.4 Hz, 2H), 2.96 (dd, *J* = 12.2, 6.4 Hz, 2H), 1.78 – 1.71 (m, 2H), 1.32 (t, *J* = 7.1 Hz, 3H).



(E)-4-oxo-4-((3-((4-(trifluoromethoxy)phenyl)sulfonamido)propyl)amino)but-2-enoic acid (1.9)

Furan-2,5-dione (0.7 g, 1 Eq, 7 mmol) and **1f** (2 g, 1 Eq, 7 mmol) were dissolved in EtOAc (100 mL) and were vigorously stirred for 2 hours. Then thiourea (0.04 g, .08 Eq, 0.5 mmol), and methanesulfonic acid (0.05 g, 0.03 mL, .07 Eq, 0.5 mmol) were added and the reaction was refluxed for 2 hours. The mixture was cooled, washed with brine (100 mL), dried by Na₂SO₄, and concentrated in vacuo. The residue was purified by silica gel chromatography (DCM:MeOH (0-20%)) to yield **1.9** (2 g, 6 mmol, 83 %).

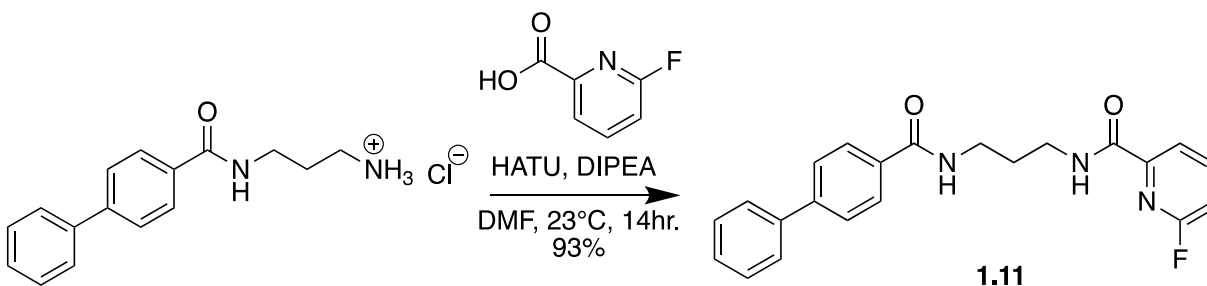
R_f= 0.72 (DCM:MeOH (9:1)) **¹H NMR** (599 MHz, MeOD) δ 7.97 (d, *J* = 8.8 Hz, 2H), 7.49 (d, *J* = 8.3 Hz, 2H), 6.94 (d, *J* = 15.5 Hz, 1H), 6.68 (d, *J* = 15.5 Hz, 1H), 3.32 – 3.30 (m, 2H), 2.93 (t, *J* = 6.9 Hz, 2H), 1.73 (p, *J* = 6.9 Hz, 2H).



(Z)-4-((3-([1,1'-biphenyl]-4-carboxamido)propyl)amino)-4-oxobut-2-enoic acid (1.10)

To a stirring solution of N-(3-aminopropyl)-[1,1'-biphenyl]-4-carboxamide, HCl (550 mg, 1 Eq, 1.89 mmol) and triethylamine (574 mg, 791 μ L, 3 Eq, 5.67 mmol) in DCM (10 mL) at 23 $^{\circ}$ C was added solid furan-2,5-dione (371 mg, 2 Eq, 3.78 mmol) and stirred for 4 hours. Upon completion the reaction was washed with DI water (10mL), brine (10mL), dried by $MgSO_4$, filtered, and concentrated under reduced pressure. The residue was purified by silica gel chromatography (DCM:MeOH (0-20%)) to yield **1.10** (0.57 g, 1.6 mmol, 86 %).

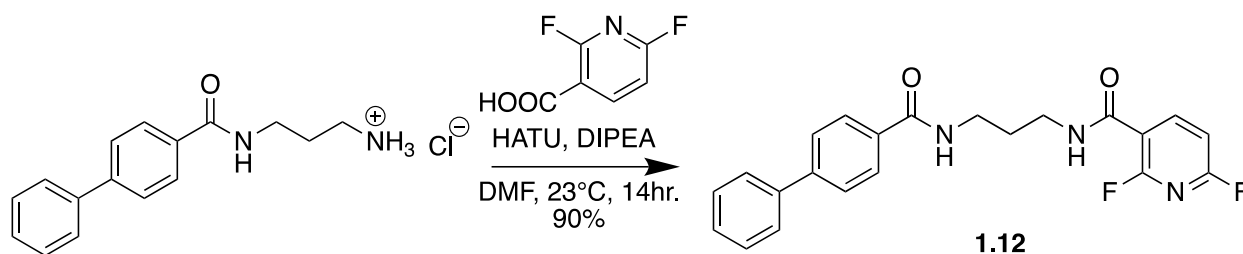
1H NMR (599 MHz, MeOD) δ 7.91 (d, J = 8.4 Hz, 2H), 7.72 (d, J = 8.4 Hz, 2H), 7.66 (d, J = 7.4 Hz, 2H), 7.46 (t, J = 7.7 Hz, 2H), 7.38 (t, J = 7.4 Hz, 1H), 6.42 (d, J = 12.6 Hz, 1H), 6.25 (d, J = 12.6 Hz, 1H), 3.48 (t, J = 6.8 Hz, 2H), 3.41 (t, J = 6.8 Hz, 2H), 1.90 (p, J = 6.8 Hz, 2H).



N-(3-([1,1'-biphenyl]-4-carboxamido)propyl)-6-fluoropicolinamide (1.11)

A solution of 2-fluoronicotinic acid (36 mg, 1.5 Eq, 0.26 mmol), HATU (0.13 g, 2 Eq, 0.34 mmol), and DIPEA (89 mg, 0.12 mL, 4 Eq, 0.69 mmol) were stirred in DMF (3 mL) for 15 minutes before adding N-(3-aminopropyl)-[1,1'-biphenyl]-4-carboxamide, HCl (50 mg, 1 Eq, 0.17 mmol) which was stirred at 23 °C for 14 hour. Upon completion the reaction was diluted with EtOAc (15mL), washed with DI water (4x15mL), brine (15mL), dried by Na₂SO₄, filtered, and concentrated under reduced pressure. The residue was purified by silica gel chromatography (Hex:EtOAc (75-25%)) to yield **1.11** (60 mg, 0.16 mmol, 93 %).

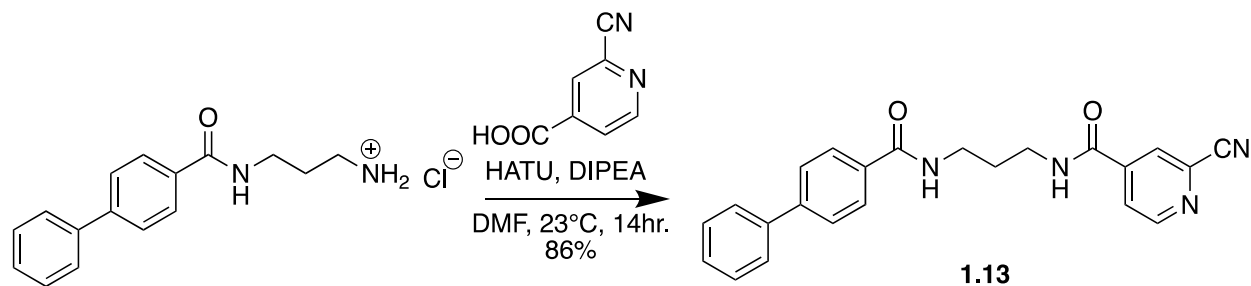
$R_f = 0.53$ (DCM:MeOH (9:1)) **¹H NMR** (599 MHz, CDCl₃) δ 8.58 (ddd, $J = 9.7, 7.6, 2.0$ Hz, 1H), 8.35 (dd, $J = 3.2, 1.4$ Hz, 1H), 7.95 (d, $J = 8.3$ Hz, 2H), 7.68 (d, $J = 8.3$ Hz, 2H), 7.62 (dd, $J = 8.1, 0.9$ Hz, 2H), 7.47 (t, $J = 7.7$ Hz, 2H), 7.41 – 7.35 (m, 3H), 7.25 (s, 1H), 3.65 (dd, $J = 12.0, 6.1$ Hz, 2H), 3.57 (dd, $J = 12.2, 6.2$ Hz, 2H), 1.93 – 1.87 (m, 2H). **LRMS**: m/z : [M+H]⁺ Calcd for [C₂₂H₂₁FN₃O₂]⁺ Theo mass: 378.16 ; Found: 378.30



N-(3-([1,1'-biphenyl]-4-carboxamido)propyl)-2,6-difluoronicotinamide (1.12)

A solution of 2,6-difluoronicotinic acid (29 mg, 1.5 Eq, 0.18 mmol), HATU (92 mg, 2 Eq, 0.24 mmol), and DIPEA (62 mg, 84 μ L, 4 Eq, 0.48 mmol) were stirred in DMF (3 mL) for 15 minutes before adding N-(3-aminopropyl)-[1,1'-biphenyl]-4-carboxamide, HCl (35 mg, 1 Eq, 0.12 mmol) which was stirred at 23 °C for 14 hour. Upon completion the reaction was diluted with EtOAc (15mL), washed with DI water (4x15mL), brine (15mL), dried by Na₂SO₄, filtered, and concentrated under reduced pressure. The residue was purified by silica gel chromatography (Hex:EtOAc (75-25%)) to yield **1.12** (43 mg, 0.11 mmol, 90 %).

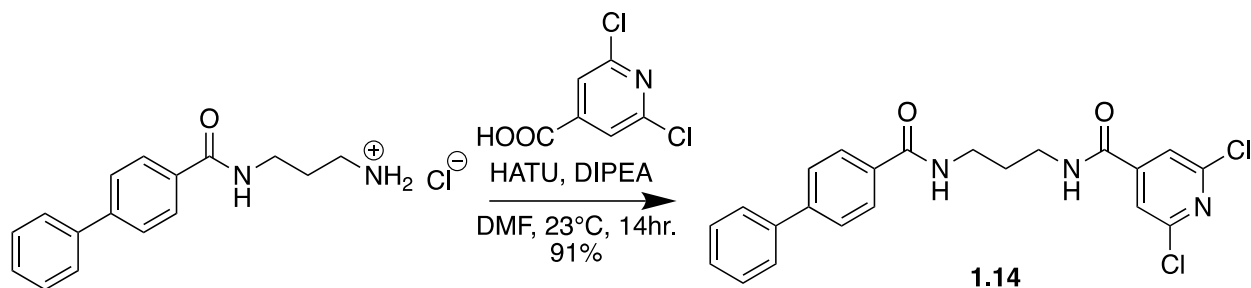
¹H NMR (599 MHz, CDCl₃) δ 8.68 (dd, J = 17.2, 8.1 Hz, 1H), 7.93 (d, J = 8.3 Hz, 2H), 7.68 (d, J = 8.3 Hz, 2H), 7.62 (d, J = 7.5 Hz, 2H), 7.47 (t, J = 7.6 Hz, 2H), 7.39 (t, J = 7.4 Hz, 1H), 7.36 (s, 1H), 7.12 (s, 1H), 6.98 (dd, J = 8.2, 2.6 Hz, 1H), 3.63 (dd, J = 12.0, 6.1 Hz, 2H), 3.58 (dd, J = 12.1, 6.2 Hz, 2H), 1.92 – 1.87 (m, 2H).



N-(3-([1,1'-biphenyl]-4-carboxamido)propyl)-2-cyanoisonicotinamide (**1.13**)

A solution of 2-cyanoisonicotinic acid (38 mg, 1.5 Eq, 0.26 mmol), HATU (0.13 g, 2 Eq, 0.34 mmol) undefined, and DIPEA (89 mg, 0.12 mL, 4 Eq, 0.69 mmol) undefined were stirred in DMF (5 mL) for 15 minutes before adding N-(3-aminopropyl)-[1,1'-biphenyl]-4-carboxamide, HCl (50 mg, 1 Eq, 0.17 mmol) undefined which was stirred at 23 °C for 14 hour. Upon completion the reaction was diluted with EtOAc (20mL), washed with DI water (4x20mL), brine (20mL), dried by Na₂SO₄, filtered, and concentrated under reduced pressure. The residue was purified by silica gel chromatography (DCM:MeOH (0-2%)) to yield **1.13** (57 mg, 0.15 mmol, 86 %)

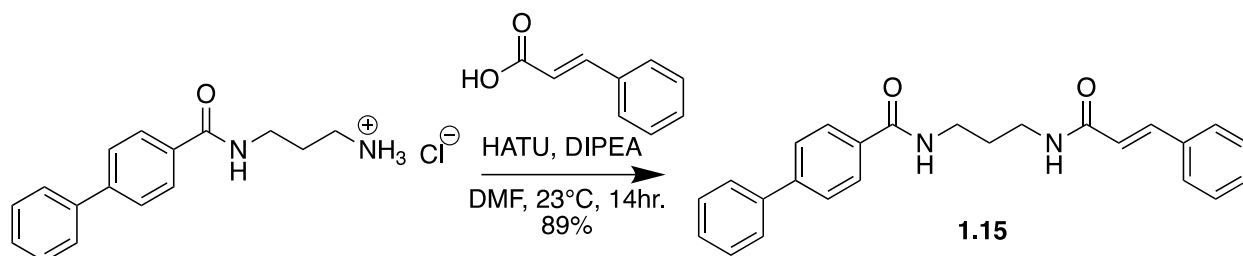
$R_f = 0.31$ (DCM:MeOH (9.5:0.5)) **¹H NMR** (599 MHz, CDCl₃) δ 8.88 (d, $J = 5.0$ Hz, 1H), 8.44 (s, 1H), 8.28 (s, 1H), 8.06 (dd, $J = 5.0, 1.5$ Hz, 1H), 7.89 (d, $J = 8.3$ Hz, 2H), 7.71 (d, $J = 8.3$ Hz, 2H), 7.62 (d, $J = 7.5$ Hz, 2H), 7.48 (t, $J = 7.6$ Hz, 2H), 7.41 (t, $J = 7.4$ Hz, 1H), 6.64 (t, $J = 6.2$ Hz, 1H), 3.65 (dd, $J = 12.0, 6.4$ Hz, 2H), 3.56 (dd, $J = 11.8, 6.1$ Hz, 2H), 1.91 – 1.85 (m, 2H).



N-(3-([1,1'-biphenyl]-4-carboxamido)propyl)-2,6-dichloroisonicotinamide (1.14)

A solution of 2,6-dichloroisonicotinic acid (50 mg, 1.5 Eq, 0.26 mmol), HATU (0.13 g, 2 Eq, 0.34 mmol), and DIPEA (89 mg, 0.12 mL, 4 Eq, 0.69 mmol) were stirred in DMF (5 mL) for 15 minutes before adding N-(3-aminopropyl)-[1,1'-biphenyl]-4-carboxamide, HCl (50 mg, 1 Eq, 0.17 mmol) which was stirred at 23 °C for 14 hour. Upon completion the reaction was diluted with EtOAc (20mL), washed with DI water (4x20mL), brine (20mL), dried by Na₂SO₄, filtered, and concentrated under reduced pressure. The residue was purified by silica gel chromatography (DCM:MeOH (0-2%)) to yield **1.14** (67 mg, 0.16 mmol, 91 %).

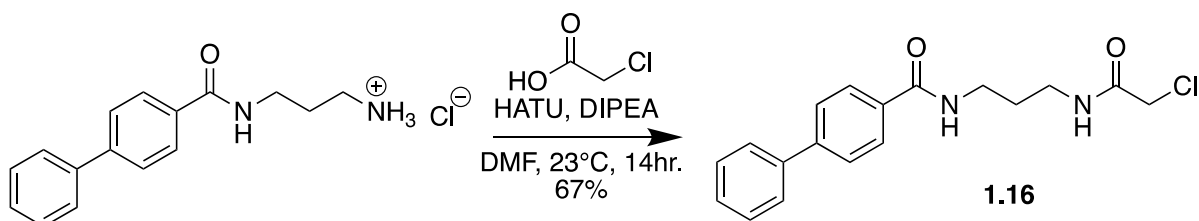
¹H NMR (599 MHz, CDCl₃) δ 8.27 (t, *J* = 5.4 Hz, 1H), 7.90 (d, *J* = 8.3 Hz, 2H), 7.79 (s, 2H), 7.68 (d, *J* = 8.2 Hz, 2H), 7.61 (d, *J* = 7.4 Hz, 2H), 7.47 (t, *J* = 7.6 Hz, 2H), 7.40 (t, *J* = 7.3 Hz, 1H), 6.90 (t, *J* = 6.3 Hz, 1H), 3.61 (dd, *J* = 12.0, 6.3 Hz, 2H), 3.54 (dd, *J* = 11.8, 6.1 Hz, 2H), 1.89 – 1.83 (m, 2H).



N-(3-cinnamamidopropyl)-[1,1'-biphenyl]-4-carboxamide (**1.15**)

A solution of cinnamic acid (38 mg, 1.5 Eq, 0.26 mmol), HATU (0.13 g, 2 Eq, 0.34 mmol), and DIPEA (89 mg, 0.12 mL, 4 Eq, 0.69 mmol) were stirred in DMF (5 mL) for 15 minutes before adding N-(3-aminopropyl)-[1,1'-biphenyl]-4-carboxamide, HCl (50 mg, 1 Eq, 0.17 mmol) which was stirred at 23 °C for 14 hour. Upon completion the reaction was diluted with EtOAc (20mL), washed with DI water (4x20mL), brine (20mL), dried by Na₂SO₄, filtered, and concentrated under reduced pressure. The residue was purified by silica gel chromatography (DCM:MeOH (0-2%)) to yield **1.15** (59 mg, 0.15 mmol, 89 %).

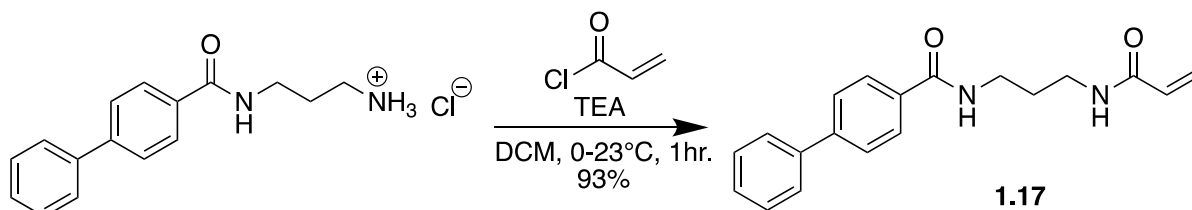
¹H NMR (599 MHz, CDCl₃) δ 7.97 (d, *J* = 8.3 Hz, 2H), 7.70 – 7.64 (m, 3H), 7.61 (d, *J* = 7.2 Hz, 2H), 7.52 (dd, *J* = 7.5, 1.7 Hz, 2H), 7.46 (t, *J* = 7.7 Hz, 2H), 7.40 – 7.34 (m, 4H), 6.46 (d, *J* = 15.6 Hz, 1H), 6.39 (t, *J* = 6.1 Hz, 1H), 3.57 (dd, *J* = 11.9, 6.2 Hz, 2H), 3.53 (dd, *J* = 11.9, 6.3 Hz, 2H), 1.85 – 1.79 (m, 2H).



N-(3-(2-chloroacetamido)propyl)-[1,1'-biphenyl]-4-carboxamide (1.16)

A solution of 2-chloroacetic acid (24 mg, 1.5 Eq, 0.26 mmol), HATU (0.13 g, 2 Eq, 0.34 mmol), and DIPEA (89 mg, 0.12 mL, 4 Eq, 0.69 mmol) were stirred in DMF (5 mL) for 15 minutes before adding N-(3-aminopropyl)-[1,1'-biphenyl]-4-carboxamide, HCl (50 mg, 1 Eq, 0.17 mmol) which was stirred at 23 °C for 14 hour. Upon completion the reaction was diluted with EtOAc (20mL), washed with DI water (4x20mL), brine (20mL), dried by Na₂SO₄, filtered, and concentrated under reduced pressure. The residue was purified by silica gel chromatography (DCM:MeOH (0-2%)) to yield **1.16** (38 mg, 0.12 mmol, 67 %).

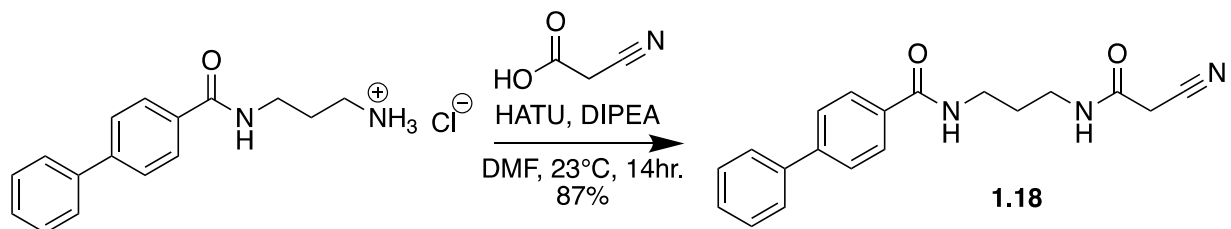
¹H NMR (599 MHz, CDCl₃) δ 7.85 (d, *J* = 8.3 Hz, 2H), 7.61 (d, *J* = 8.3 Hz, 2H), 7.55 (d, *J* = 7.3 Hz, 2H), 7.40 (t, *J* = 7.7 Hz, 2H), 7.32 (t, *J* = 7.3 Hz, 1H), 7.14 (s, 1H), 6.99 (s, H), 4.04 (s, 2H), 3.47 (dd, *J* = 12.2, 6.2 Hz, 2H), 3.40 (dd, *J* = 12.3, 6.4 Hz, 2H), 1.77 – 1.72 (m, 2H).



N-(3-acrylamidopropyl)-[1,1'-biphenyl]-4-carboxamide (1.17)

To a stirring solution of N-(3-aminopropyl)-[1,1'-biphenyl]-4-carboxamide, HCl (100 mg, 1 Eq, 344 μmol) and triethylamine (104 mg, 144 μL , 3 Eq, 1.03 mmol) in DCM (10 mL) at 0 °C was added neat acryloyl chloride (46.7 mg, 41.7 μL , 1.5 Eq, 516 μmol) dropwise. The reaction was allowed to come to 23 °C and stir for 1 hour after which time the reactants had been consumed as seen by TLC. The reaction was quenched by the addition of DI water (10mL), washed with brine (10mL), dried by MgSO_4 , filtered, and concentrated under reduced pressure. The residue was purified by silica gel chromatography (DCM:MeOH (0-3%)) to yield **1.17** (99 mg, 0.32 mmol, 93 %).

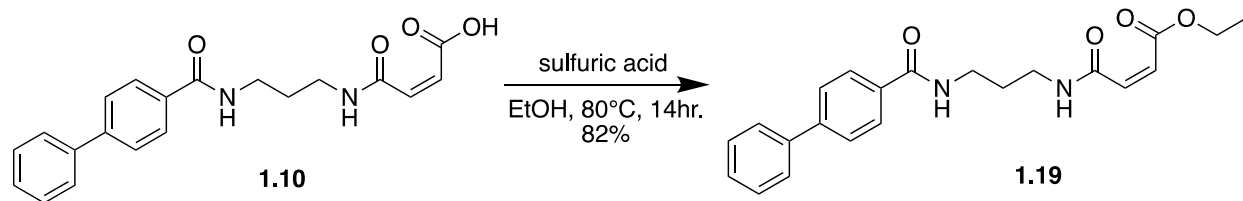
^1H NMR (599 MHz, CDCl_3) δ 7.95 (d, $J = 8.3$ Hz, 2H), 7.68 (d, $J = 8.3$ Hz, 2H), 7.62 (d, $J = 7.6$ Hz, 1H), 7.47 (t, $J = 7.7$ Hz, 2H), 7.39 (t, $J = 7.4$ Hz, 2H), 7.29 (s, 1H), 6.34 (dd, $J = 17.0, 1.1$ Hz, 1H), 6.17 (dd, $J = 17.0, 10.3$ Hz, 1H), 5.69 (dd, $J = 10.4, 1.1$ Hz, 1H), 3.53 (dd, $J = 12.1, 6.2$ Hz, 2H), 3.47 (dd, $J = 12.3, 6.6$ Hz, 2H), 1.83 – 1.74 (m, 2H).



N-(3-(2-cyanoacetamido)propyl)-[1,1'-biphenyl]-4-carboxamide (1.18)

A solution of 2-cyanoacetic acid (329 mg, 1.5 Eq, 3.87 mmol), HATU (1.96 g, 2 Eq, 5.16 mmol), and DIPEA (1.33 g, 1.80 mL, 4 Eq, 10.3 mmol) were stirred in DMF (20 mL) for 15 minutes before adding N-(3-aminopropyl)-[1,1'-biphenyl]-4-carboxamide, HCl (750 mg, 1 Eq, 2.58 mmol) which was stirred at 23 °C for 14 hour. Upon completion the reaction was diluted with EtOAc (80mL), washed with DI water (4x80mL), brine (80mL), dried by Na₂SO₄, filtered, and concentrated under reduced pressure. The residue was purified by silica gel chromatography (DCM:MeOH (0-4%)) to yield **1.18** (0.72 g, 2.2 mmol, 87 %).

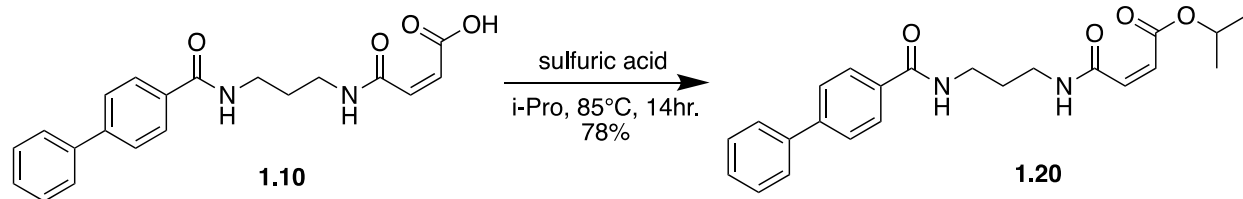
¹H NMR (599 MHz, CDCl₃) δ 7.88 (d, *J* = 8.3 Hz, 2H), 7.68 (d, *J* = 8.3 Hz, 2H), 7.62 (d, *J* = 7.2 Hz, 2H), 7.47 (t, *J* = 7.6 Hz, 2H), 7.40 (t, *J* = 7.3 Hz, 1H), 7.17 (s, 1H), 6.74 (s, 2H), 3.57 (dd, *J* = 12.2, 6.3 Hz, 2H), 3.45 – 3.39 (m, 2H), 1.84 – 1.76 (m, 2H).



ethyl (Z)-4-((3-([1,1'-biphenyl]-4-carboxamido)propyl)amino)-4-oxobut-2-enoate (1.19)

General Procedure A: Fischer Esterification

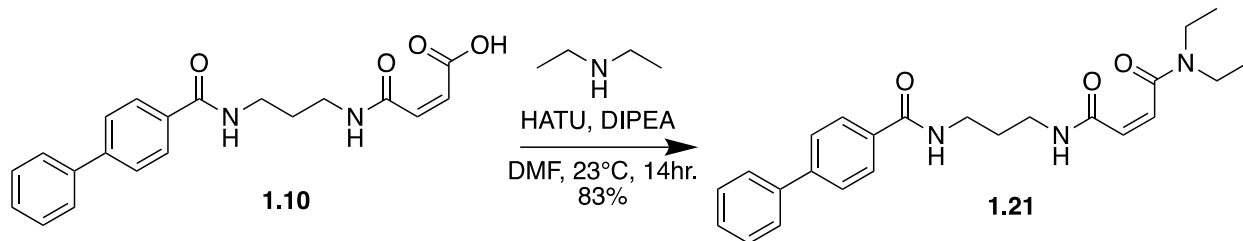
¹H NMR (599 MHz, CDCl₃) δ 8.37 (s, 1H), 7.95 (d, *J* = 8.3 Hz, 2H), 7.66 (d, *J* = 8.3 Hz, 2H), 7.61 (d, *J* = 7.2 Hz, 2H), 7.46 (t, *J* = 7.6 Hz, 3H), 7.38 (t, *J* = 7.4 Hz, 1H), 6.37 (d, *J* = 12.9 Hz, 1H), 6.16 (d, *J* = 12.9 Hz, 1H), 4.24 (q, *J* = 7.1 Hz, 2H), 3.54 (dd, *J* = 12.1, 6.2 Hz, 2H), 3.49 (dd, *J* = 12.3, 6.3 Hz, 2H), 1.86 – 1.81 (m, 2H), 1.31 (t, *J* = 7.1 Hz, 3H).



isopropyl (Z)-4-((3-([1,1'-biphenyl]-4-carboxamido)propyl)amino)-4-oxobut-2-enoate (1.20)

General Procedure A: Fischer Esterification

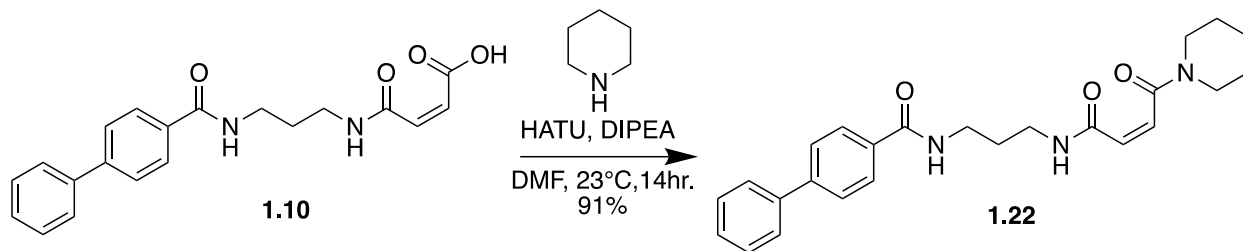
¹H NMR (599 MHz, CDCl₃) δ 8.48 (s, 1H), 7.96 (d, *J* = 8.3 Hz, 2H), 7.66 (d, *J* = 8.3 Hz, 2H), 7.61 (d, *J* = 7.3 Hz, 2H), 7.50 (s, 1H), 7.46 (t, *J* = 7.6 Hz, 2H), 7.38 (t, *J* = 7.4 Hz, 1H), 6.35 (d, *J* = 13.0 Hz, 1H), 6.14 (d, *J* = 13.0 Hz, 1H), 5.12 – 5.04 (m, 1H), 3.54 (dd, *J* = 12.1, 6.1 Hz, 2H), 3.49 (dd, *J* = 12.2, 6.3 Hz, 2H), 1.87 – 1.80 (m, 2H), 1.30 (d, *J* = 6.3 Hz, 6H).



N1-(3-([1,1'-biphenyl]-4-carboxamido)propyl)-N4,N4-diethylmaleamide (1.21)

A solution of **1.10** (23.2 mg, 1 Eq, 65.8 μmol), HATU (37.6 mg, 1.5 Eq, 98.8 μmol), and DIPEA (25.5 mg, 34.4 μL , 3 Eq, 198 μmol) were stirred in DMF (5 mL) for 15 minutes before adding neat diethylamine (5.78 mg, 8.17 μL , 1.2 Eq, 79.0 μmol) which was stirred at 23 $^{\circ}\text{C}$ for 14 hour. Upon completion the reaction was diluted with EtOAc (20mL), washed with DI water (4x20mL), brine (20mL), dried by Na_2SO_4 , filtered, and concentrated under reduced pressure. The residue was purified by silica gel chromatography (DCM:MeOH (0-10%)) to yield **1.21** (22 mg, 55 μmol , 83 %).

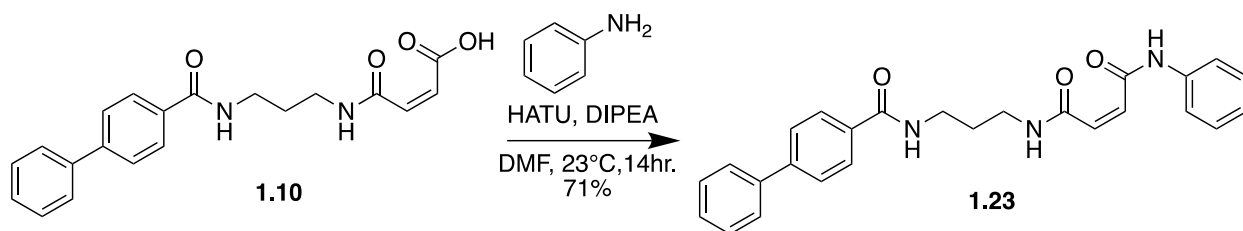
$^1\text{H NMR}$ (599 MHz, CDCl_3) δ 8.72 (s, 1H), 7.98 (d, $J = 8.3$ Hz, 2H), 7.66 (d, $J = 8.3$ Hz, 2H), 7.61 (d, $J = 7.2$ Hz, 2H), 7.46 (t, $J = 7.6$ Hz, 2H), 7.37 (t, $J = 7.7$ Hz, 1H), 6.44 (d, $J = 13.0$ Hz, 1H), 6.18 (d, $J = 13.0$ Hz, 1H), 3.48 (dd, $J = 12.2, 5.9$ Hz, 2H), 3.36 (q, $J = 7.1$ Hz, 4H), 1.84 – 1.75 (m, 2H), 1.19 (t, $J = 13.2, 7.0$ Hz, 6H).



(Z)-N-(3-(4-oxo-4-(piperidin-1-yl)but-2-enamido)propyl)-[1,1'-biphenyl]-4-carboxamide (1.22)

A solution of **1.10** (22.9 mg, 1 Eq, 65.0 μmol), HATU (37.1 mg, 1.5 Eq, 97.5 μmol), and DIPEA (25.2 mg, 34.0 μL , 3 Eq, 195 μmol) were stirred in DMF (5 mL) for 15 minutes before adding neat piperidine (6.09 mg, 7.06 μL , 1.1 Eq, 71.5 μmol) which was stirred at 23 °C for 14 hour. Upon completion the reaction was diluted with EtOAc (20mL), washed with DI water (4x20mL), brine (20mL), dried by Na_2SO_4 , filtered, and concentrated under reduced pressure. The residue was purified by silica gel chromatography (DCM:MeOH (0-10%)) to yield **1.22** (25 mg, 59 μmol , 91 %).

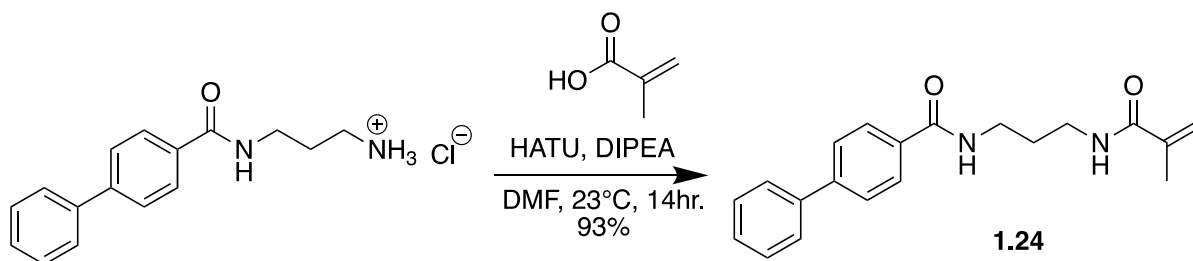
$^1\text{H NMR}$ (599 MHz, CDCl_3) δ 8.20 (s, 1H), 7.97 (d, $J = 8.2$ Hz, 2H), 7.65 (d, $J = 8.3$ Hz, 5H), 7.63 (s, 2H), 7.60 (d, $J = 7.7$ Hz, 2H), 7.45 (t, $J = 7.6$ Hz, 2H), 7.37 (t, $J = 7.3$ Hz, 1H), 6.43 (d, $J = 12.8$ Hz, 1H), 6.13 (d, $J = 12.8$ Hz, 1H), 3.63 – 3.57 (m, 2H), 3.48 (dd, $J = 12.0, 6.1$ Hz, 2H), 3.43 (dt, $J = 11.0, 5.9$ Hz, 4H), 1.78 (dt, $J = 11.9, 6.1$ Hz, 2H), 1.64 (d, $J = 4.9$ Hz, 2H), 1.61 – 1.53 (m, 4H).



N1-(3-([1,1'-biphenyl]-4-carboxamido)propyl)-N4-phenylmaleamide (1.23)

A solution of **1.10** (14.7 mg, 1 Eq, 41.7 μmol), HATU (23.8 mg, 1.5 Eq, 62.6 μmol), and DIPEA (16.2 mg, 21.8 μL , 3 Eq, 125 μmol) were stirred in DMF (3 mL) for 15 minutes before adding neat aniline (3.88 mg, 3.81 μL , 1 Eq, 41.7 μmol) which was stirred at 23 °C for 14 hour. Upon completion the reaction was diluted with EtOAc (15mL), washed with DI water (4x15mL), brine (15mL), dried by Na_2SO_4 , filtered, and concentrated under reduced pressure. The residue was purified by silica gel chromatography (DCM:MeOH (0-10%)) to yield **1.23** (13 mg, 30 μmol , 71 %).

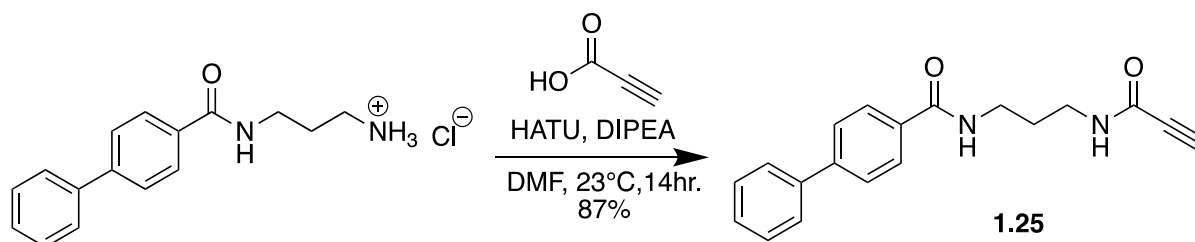
$^1\text{H NMR}$ (599 MHz, CDCl_3) δ 7.98 (s, 1H), 7.89 (d, $J = 8.3$ Hz, 2H), 7.68 (t, $J = 7.3$ Hz, 4H), 7.61 (d, $J = 7.3$ Hz, 2H), 7.47 (t, $J = 7.6$ Hz, 2H), 7.40 (t, $J = 7.4$ Hz, 1H), 7.31 (t, $J = 7.9$ Hz, 2H), 7.10 (t, $J = 7.4$ Hz, 1H), 6.94 (t, $J = 6.2$ Hz, 1H), 6.28 (d, $J = 13.4$ Hz, 1H), 6.23 (d, $J = 13.4$ Hz, 1H), 3.58 (dd, $J = 12.1, 6.3$ Hz, 2H), 3.47 (dd, $J = 12.0, 6.2$ Hz, 2H), 1.85 (dt, $J = 11.8, 6.1$ Hz, 2H).



N-(3-methacrylamidopropyl)-[1,1'-biphenyl]-4-carboxamide (1.24)

A solution of methacrylic acid (22 mg, 22 μL , 1.5 Eq, 0.26 mmol), HATU (98 mg, 1.5 Eq, 0.26 mmol), and DIPEA (89 mg, 0.12 mL, 4 Eq, 0.69 mmol) were stirred in DMF (5 mL) for 15 minutes before adding N-(3-aminopropyl)-[1,1'-biphenyl]-4-carboxamide, HCl (50 mg, 1 Eq, 0.17 mmol) which was stirred at 23 $^\circ\text{C}$ for 14 hour. Upon completion the reaction was diluted with EtOAc (15mL), washed with DI water (4x15mL), brine (15mL), dried by Na_2SO_4 , filtered, and concentrated under reduced pressure. The residue was purified by silica gel chromatography (DCM:MeOH (0-5%)) to yield **1.24** (52 mg, 0.16 mmol, 93 %).

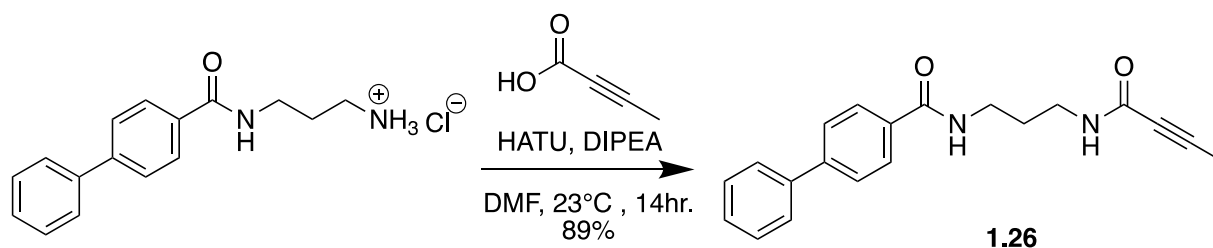
$^1\text{H NMR}$ (599 MHz, CDCl_3) δ 7.94 (d, $J = 8.3$ Hz, 2H), 7.67 (d, $J = 8.3$ Hz, 2H), 7.61 (d, $J = 7.3$ Hz, 2H), 7.46 (t, $J = 7.6$ Hz, 2H), 7.38 (t, $J = 7.4$ Hz, 1H), 7.34 (t, $J = 5.4$ Hz, 1H), 6.68 (s, 1H), 5.81 (s, 1H), 5.38 (s, 1H), 3.53 (dd, $J = 12.0, 6.2$ Hz, 2H), 3.45 (dd, $J = 12.0, 6.3$ Hz, 2H), 2.02 (s, 3H), 1.78 (dt, $J = 11.8, 6.0$ Hz, 2H).



N-(3-propionamidopropyl)-[1,1'-biphenyl]-4-carboxamide (**1.25**)

A solution of propiolic acid (18 mg, 16 μL , 1.5 Eq, 0.26 mmol), HATU (0.13 g, 2 Eq, 0.34 mmol), and DIPEA (89 mg, 0.12 mL, 4 Eq, 0.69 mmol) were stirred in DMF (5 mL) for 15 minutes before adding N-(3-aminopropyl)-[1,1'-biphenyl]-4-carboxamide, HCl (50 mg, 1 Eq, 0.17 mmol) which was stirred at 23 °C for 14 hour. Upon completion the reaction was diluted with EtOAc (15mL), washed with DI water (4x15mL), brine (15mL), dried by Na_2SO_4 , filtered, and concentrated under reduced pressure. The residue was purified by silica gel chromatography (DCM:MeOH (0-3%)) to yield **1.25** (46 mg, 0.15 mmol, 87 %).

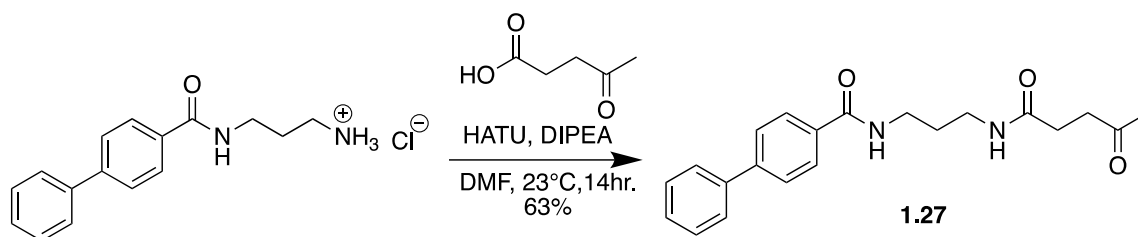
$^1\text{H NMR}$ (599 MHz, CDCl_3) δ 7.83 (d, $J = 8.3$ Hz, 2H), 7.58 (d, $J = 8.3$ Hz, 2H), 7.53 (d, $J = 7.4$ Hz, 2H), 7.39 (t, $J = 7.6$ Hz, 1H), 7.31 (t, $J = 7.4$ Hz, 1H), 7.05 (s, 1H), 6.87 (s, 1H), 3.48 (dd, $J = 12.1, 6.2$ Hz, 2H), 3.35 (dd, $J = 12.2, 6.4$ Hz, 2H), 2.77 (s, 1H), 1.75 – 1.69 (m, 2H).



N-(3-(but-2-ynamido)propyl)-[1,1'-biphenyl]-4-carboxamide (1.26)

A solution of but-2-ynoic acid (22 mg, 22 μ L, 1.5 Eq, 0.26 mmol), HATU (0.13 g, 2 Eq, 0.34 mmol), and DIPEA (89 mg, 0.12 mL, 4 Eq, 0.69 mmol) were stirred in DMF (5 mL) for 15 minutes before adding NN-(3-aminopropyl)-[1,1'-biphenyl]-4-carboxamide, HCl (50 mg, 1 Eq, 0.17 mmol) which was stirred at 23 °C for 14 hour. Upon completion the reaction was diluted with EtOAc (15mL), washed with DI water (4x15mL), brine (15mL), dried by Na₂SO₄, filtered, and concentrated under reduced pressure. The residue was purified by silica gel chromatography (DCM:MeOH (0-3%)) to yield **1.26** (49 mg, 0.15 mmol, 89 %).

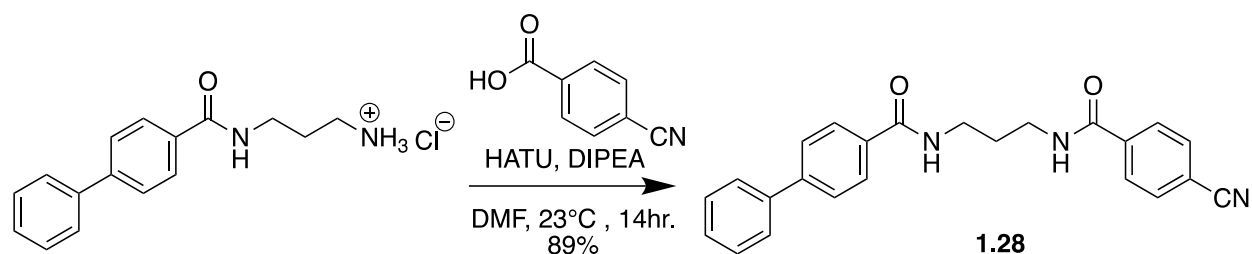
¹H NMR (599 MHz, CDCl₃) δ 7.93 (d, J = 8.2 Hz, 2H), 7.67 (d, J = 8.2 Hz, 2H), 7.61 (d, J = 7.5 Hz, 2H), 7.46 (t, J = 7.6 Hz, 2H), 7.39 (t, J = 7.3 Hz, 1H), 7.14 (s, 1H), 6.40 (s, 1H), 3.54 (dd, J = 12.0, 6.2 Hz, 2H), 3.42 (dd, J = 12.1, 6.4 Hz, 2H), 1.96 (s, 3H), 1.80 – 1.74 (m, 2H).



N-(3-(4-oxopentanamido)propyl)-[1,1'-biphenyl]-4-carboxamide (1.27)

A solution of 4-oxopentanoic acid (30 mg, 26 μ L, 1.5 Eq, 0.26 mmol), HATU (0.13 g, 2 Eq, 0.34 mmol), and DIPEA (89 mg, 0.12 mL, 4 Eq, 0.69 mmol) were stirred in DMF (5 mL) for 15 minutes before adding N-(3-aminopropyl)-[1,1'-biphenyl]-4-carboxamide, HCl (50 mg, 1 Eq, 0.17 mmol) which was stirred at 23 °C for 14 hour. Upon completion the reaction was diluted with EtOAc (15mL), washed with DI water (4x15mL), brine (15mL), dried by Na₂SO₄, filtered, and concentrated under reduced pressure. The residue was purified by silica gel chromatography (DCM:MeOH (0-5%)) to yield **1.27** (38 mg, 0.11 mmol, 63%).

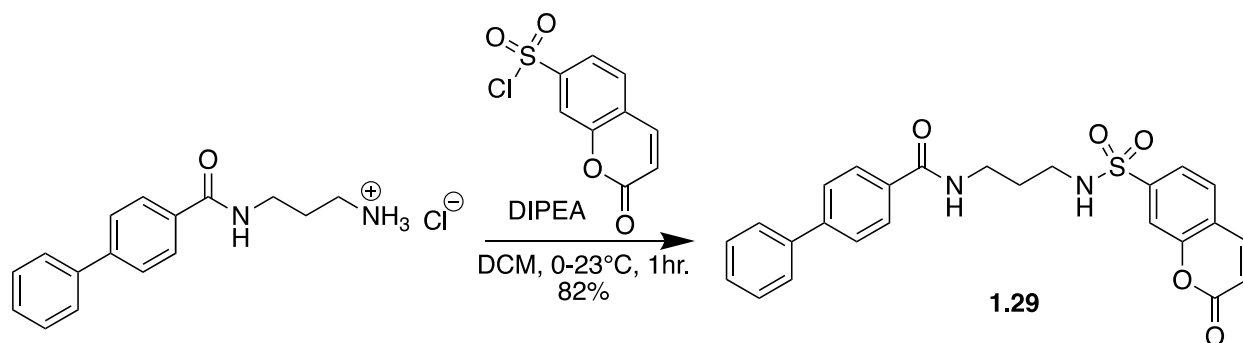
¹H NMR (599 MHz, CDCl₃) δ 7.93 (d, J = 8.3 Hz, 2H), 7.66 (d, J = 8.3 Hz, 2H), 7.61 (d, J = 7.3 Hz, 2H), 7.46 (t, J = 7.6 Hz, 2H), 7.38 (t, J = 7.4 Hz, 1H), 7.34 (s, 1H), 6.27 (s, 1H), 3.50 (dd, J = 12.1, 6.2 Hz, 2H), 3.38 (dd, J = 12.1, 6.3 Hz, 2H), 2.84 (t, J = 6.4 Hz, 2H), 2.48 (t, J = 6.4 Hz, 2H), 2.19 (s, 3H), 1.74 (dt, J = 11.9, 6.0 Hz, 2H).



N-(3-(4-cyanobenzamido)propyl)-[1,1'-biphenyl]-4-carboxamide (1.28)

A solution of 4-cyanobenzoic acid (38 mg, 1.5 Eq, 0.26 mmol), HATU (0.13 g, 2 Eq, 0.34 mmol), and DIPEA (89 mg, 0.12 mL, 4 Eq, 0.69 mmol) were stirred in DMF (5 mL) for 15 minutes before adding N-(3-aminopropyl)-[1,1'-biphenyl]-4-carboxamide, HCl (50 mg, 1 Eq, 0.17 mmol) which was stirred at 23 °C for 14 hour. Upon completion the reaction was diluted with EtOAc (15mL), washed with DI water (4x15mL), brine (15mL), dried by Na₂SO₄, filtered, and concentrated under reduced pressure. The residue was purified by silica gel chromatography (DCM:MeOH (0-5%)) to yield **1.28** (59 mg, 0.15 mmol, 89 %).

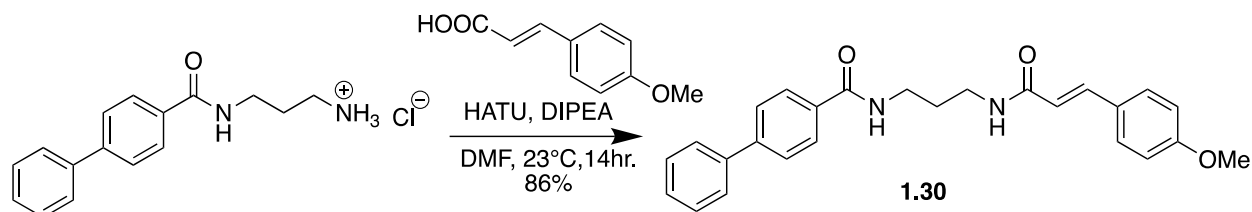
¹H NMR (599 MHz, CDCl₃) δ 8.05 (d, *J* = 8.3 Hz, 2H), 7.90 (d, *J* = 8.3 Hz, 2H), 7.86 (s, 1H), 7.76 (d, *J* = 8.3 Hz, 2H), 7.69 (d, *J* = 8.3 Hz, 2H), 7.62 (d, *J* = 7.4 Hz, 2H), 7.48 (t, *J* = 7.6 Hz, 2H), 7.40 (t, *J* = 7.3 Hz, 1H), 6.81 (s, 1H), 3.63 (dd, *J* = 12.0, 6.3 Hz, 2H), 3.57 (dd, *J* = 11.8, 6.1 Hz, 2H), 1.89 – 1.83 (m, 2H).



N-(3-((2-oxo-2H-chromene)-6-sulfonamido)propyl)-[1,1'-biphenyl]-4-carboxamide (1.29)

To a stirring solution of N-(3-aminopropyl)-[1,1'-biphenyl]-4-carboxamide, HCl (50 mg, 1 Eq, 0.17 mmol) and DIPEA (67 mg, 90 μ L, 3 Eq, 0.52 mmol) in DCM (5 mL) at 0 $^{\circ}$ C was added 2-oxo-2H-chromene-6-sulfonyl chloride (63 mg, 1.5 Eq, 0.26 mmol) portion wise. After allowing the reaction to come to 23 $^{\circ}$ C slowly over 1 hour and monitoring for the consumption of reactants by TLC, the reaction was quenched with DI water (5mL), washed with brine (5mL), dried by $MgSO_4$, filtered, and concentrated under reduced pressure. The residue was purified by silica gel chromatography (DCM:MeOH (0-5%)) to yield **1.29** (65 mg, 0.14 mmol, 82 %).

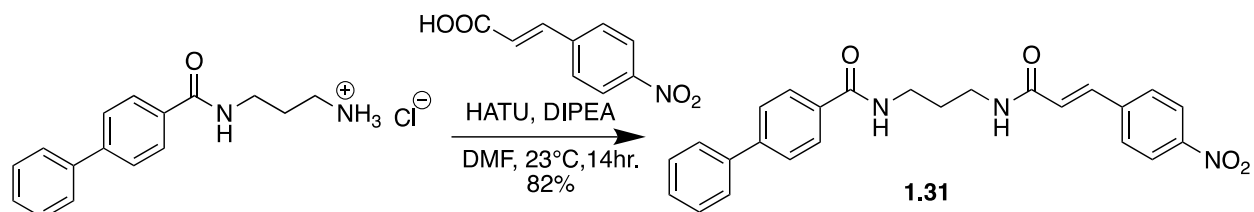
1H NMR (599 MHz, $CDCl_3$) δ 8.05 (d, $J = 2.1$ Hz, 1H), 8.02 (dd, $J = 8.7, 2.1$ Hz, 1H), 7.77 (d, $J = 8.3$ Hz, 2H), 7.67 (d, $J = 9.6$ Hz, 2H), 7.64 (d, $J = 8.3$ Hz, 2H), 7.59 (d, $J = 7.3$ Hz, 2H), 7.47 (t, $J = 7.6$ Hz, 2H), 7.42 – 7.37 (m, 2H), 6.51 (t, $J = 6.3$ Hz, 1H), 6.47 (d, $J = 9.6$ Hz, 1H), 6.17 (t, $J = 6.6$ Hz, 1H), 3.61 (dd, $J = 12.1, 6.4$ Hz, 2H), 3.01 (dd, $J = 12.0, 6.4$ Hz, 2H), 1.84 – 1.78 (m, 2H).



(E)-N-(3-(3-(4-methoxyphenyl)acrylamido)propyl)-[1,1'-biphenyl]-4-carboxamide (1.30)

A solution of (E)-3-(4-methoxyphenyl)acrylic acid (46 mg, 1.5 Eq, 0.26 mmol), HATU (0.13 g, 2 Eq, 0.34 mmol), and DIPEA (89 mg, 0.12 mL, 4 Eq, 0.69 mmol) were stirred in DMF (5 mL) for 15 minutes before adding N-(3-aminopropyl)-[1,1'-biphenyl]-4-carboxamide, HCl (50 mg, 1 Eq, 0.17 mmol) which was stirred at 23 °C for 14 hour. Upon completion the reaction was diluted with EtOAc (15mL), washed with DI water (4x15mL), brine (15mL), dried by Na₂SO₄, filtered, and concentrated under reduced pressure. The residue was purified by silica gel chromatography (DCM:MeOH (0-5%)) to yield **1.30** (61 mg, 0.15 mmol, 86 %).

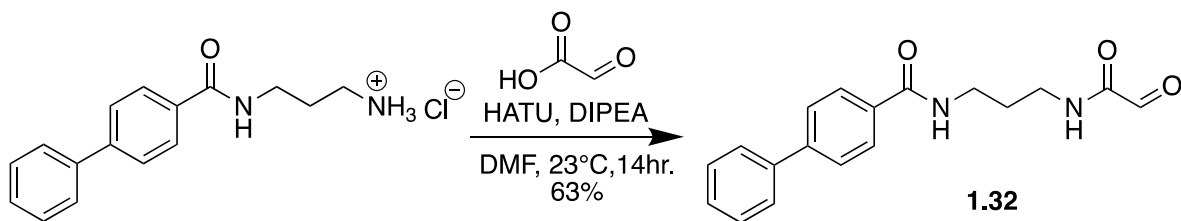
¹H NMR (599 MHz, CDCl₃) δ 7.98 (d, *J* = 8.2 Hz, 2H), 7.68 (d, *J* = 8.2 Hz, 2H), 7.61 (d, *J* = 7.4 Hz, 2H), 7.49 – 7.43 (m, 5H), 7.39 (t, *J* = 7.3 Hz, 1H), 6.89 (d, *J* = 8.6 Hz, 2H), 6.33 (d, *J* = 15.6 Hz, 1H), 6.27 (s, 1H), 3.83 (s, 3H), 3.56 (dd, *J* = 11.8, 6.2 Hz, 2H), 3.53 (dd, *J* = 11.9, 6.4 Hz, 2H), 1.84 – 1.77 (m, 2H).



(E)-N-(3-(3-(4-nitrophenyl)acrylamido)propyl)-[1,1'-biphenyl]-4-carboxamide (1.31)

A solution of (E)-3-(4-nitrophenyl)acrylic acid (50 mg, 1.5 Eq, 0.26 mmol), HATU (0.13 g, 2 Eq, 0.34 mmol), and DIPEA (89 mg, 0.12 mL, 4 Eq, 0.69 mmol) were stirred in DMF (5 mL) for 15 minutes before adding N-(3-aminopropyl)-[1,1'-biphenyl]-4-carboxamide, HCl (50 mg, 1 Eq, 0.17 mmol) which was stirred at 23 °C for 14 hour. Upon completion the reaction was diluted with EtOAc (15mL), washed with DI water (4x15mL), brine (15mL), dried by Na₂SO₄, filtered, and concentrated under reduced pressure. The residue was purified by silica gel chromatography (DCM:MeOH (0-5%)) to yield **1.31** (61 mg, 0.14 mmol, 82 %).

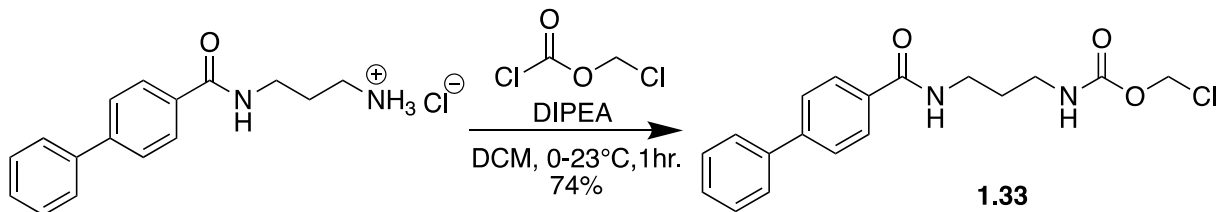
¹H NMR (599 MHz, CDCl₃) δ 8.22 (d, *J* = 8.7 Hz, 2H), 7.93 (d, *J* = 8.2 Hz, 2H), 7.71 – 7.66 (m, 3H), 7.64 (d, *J* = 8.7 Hz, 2H), 7.60 (d, *J* = 7.4 Hz, 2H), 7.46 (t, *J* = 7.6 Hz, 2H), 7.39 (t, *J* = 7.3 Hz, 1H), 7.08 (s, 1H), 6.84 (s, 1H), 6.60 (d, *J* = 15.6 Hz, 1H), 3.59 (dd, *J* = 11.7, 6.1 Hz, 2H), 3.52 (dd, *J* = 11.6, 6.1 Hz, 2H), 1.83 (s, 2H).



N-(3-(2-oxoacetamido)propyl)-[1,1'-biphenyl]-4-carboxamide (**1.32**)

A solution of 2-oxoacetic acid (38 mg, 29 μ L, 50% Wt, 1.5 Eq, 0.26 mmol), HATU (0.13 g, 2 Eq, 0.34 mmol), and DIPEA (89 mg, 0.12 mL, 4 Eq, 0.69 mmol) were stirred in DMF (5 mL) for 15 minutes before adding N-(3-aminopropyl)-[1,1'-biphenyl]-4-carboxamide, HCl (50 mg, 1 Eq, 0.17 mmol) which was stirred at 23 °C for 14 hour. Upon completion the reaction was diluted with EtOAc (15mL), washed with DI water (4x15mL), brine (15mL), dried by Na₂SO₄, filtered, and concentrated under reduced pressure. The residue was purified by silica gel chromatography (DCM:MeOH (0-7%)) to yield **1.32** (34 mg, 0.11 mmol, 63 %).

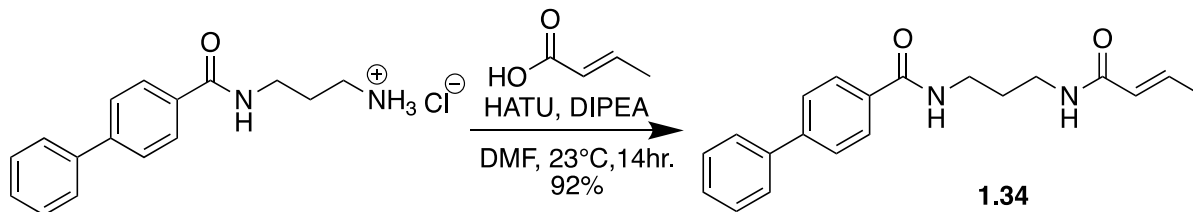
¹H NMR (599 MHz, CDCl₃) δ 9.29 (s, 1H), 7.85 (d, J = 8.3 Hz, 2H), 7.61 (d, J = 8.2 Hz, 2H), 7.55 (d, J = 7.3 Hz, 2H), 7.40 (t, J = 7.6 Hz, 3H), 7.33 (t, J = 6.2 Hz, 2H), 3.46 (dd, J = 12.3, 6.3 Hz, 2H), 3.42 (dd, J = 11.5, 5.6 Hz, 2H), 1.79 (dt, J = 12.2, 6.1 Hz, 2H).



chloromethyl (3-([1,1'-biphenyl]-4-carboxamido)propyl)carbamate (**1.33**)

To a stirring solution of chloromethyl carbonochloridate (76 mg, 52 μ L, 3 Eq, 0.59 mmol) and DIPEA (0.13 g, 0.17 mL, 5 Eq, 0.98 mmol) in DCM (5mL) at 0 °C was added N-(3-aminopropyl)-[1,1'-biphenyl]-4-carboxamide (50 mg, 1 Eq, 0.20 mmol) portionwise. The reaction was allowed to warm to 23 °C and was stirred for 1 hour until all starting material had been consumed. The reaction was quenched with DI water (10mL), washed with brine (10mL), dried by $MgSO_4$, filtered, and concentrated under reduced pressure. The residue was purified by silica gel chromatography (DCM:MeOH (0-3%)) to yield chloromethyl **1.33** (50 mg, 0.15 mmol, 74 %).

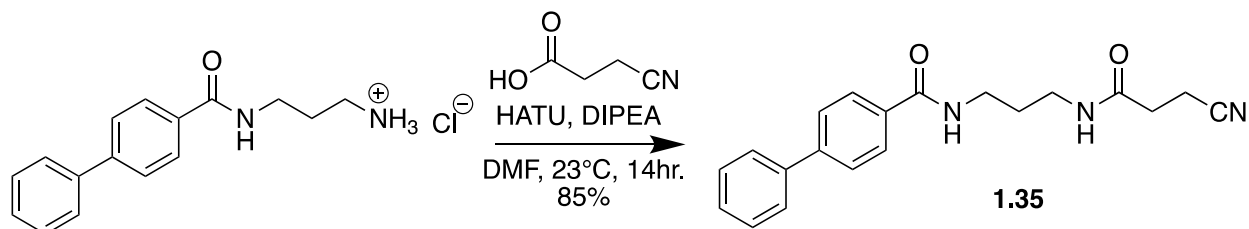
1H NMR (599 MHz, $CDCl_3$) δ 7.89 (d, $J = 8.3$ Hz, 2H), 7.68 (d, $J = 8.3$ Hz, 2H), 7.62 (d, $J = 7.3$ Hz, 2H), 7.47 (t, $J = 7.6$ Hz, 2H), 7.39 (t, $J = 7.3$ Hz, 1H), 6.78 (s, 1H), 5.78 (s, 2H), 5.69 (s, 1H), 3.57 (dd, $J = 12.2, 6.2$ Hz, 2H), 3.36 (dd, $J = 12.2, 6.3$ Hz, 2H), 1.83 – 1.76 (m, 2H).



(E)-N-(3-(but-2-enamido)propyl)-[1,1'-biphenyl]-4-carboxamide (1.34)

A solution of (E)-but-2-enoic acid (22 mg, 1.5 Eq, 0.26 mmol), HATU (0.13 g, 2 Eq, 0.34 mmol), and DIPEA (89 mg, 0.12 mL, 4 Eq, 0.69 mmol) were stirred in DMF (3 mL) for 15 minutes before adding N-(3-aminopropyl)-[1,1'-biphenyl]-4-carboxamide, HCl (50 mg, 1 Eq, 0.17 mmol) which was stirred at 23 °C for 14 hour. Upon completion the reaction was diluted with EtOAc (9mL), washed with DI water (4x9mL), brine (9mL), dried by Na₂SO₄, filtered, and concentrated under reduced pressure. The residue was purified by silica gel chromatography (DCM:MeOH (0-3%)) to yield **1.34** (51 mg, 0.16 mmol, 92 %).

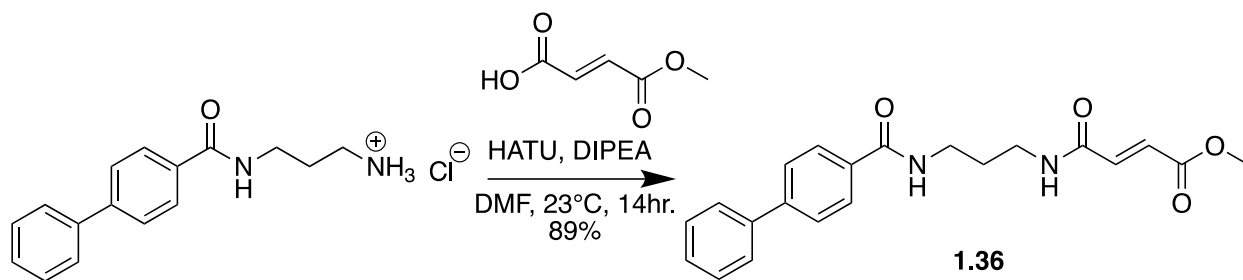
¹H NMR (599 MHz, CDCl₃) δ 7.89 (d, *J* = 8.3 Hz, 2H), 7.60 (d, *J* = 8.3 Hz, 2H), 7.54 (d, *J* = 7.2 Hz, 2H), 7.39 (t, *J* = 7.7 Hz, 3H), 7.31 (t, *J* = 7.4 Hz, 1H), 6.82 (dq, *J* = 13.8, 6.9 Hz, 1H), 6.09 (s, 1H), 5.80 (dd, *J* = 15.2, 1.6 Hz, 1H), 3.45 (dd, *J* = 12.0, 6.2 Hz, 2H), 3.38 (dd, *J* = 12.0, 6.4 Hz, 2H), 1.80 (dd, *J* = 6.8, 1.5 Hz, 3H), 1.72 – 1.66 (m, 2H).



N-(3-(3-cyanopropanamido)propyl)-[1,1'-biphenyl]-4-carboxamide (1.35)

A solution of 3-cyanopropanoic acid (26 mg, 1.5 Eq, 0.26 mmol), HATU (0.13 g, 2 Eq, 0.34 mmol), and DIPEA (89 mg, 0.12 mL, 4 Eq, 0.69 mmol) were stirred in DMF (3 mL) for 15 minutes before adding N-(3-aminopropyl)-[1,1'-biphenyl]-4-carboxamide, HCl (50 mg, 1 Eq, 0.17 mmol) which was stirred at 23 °C for 14 hour. Upon completion the reaction was diluted with EtOAc (9mL), washed with DI water (4x9mL), brine (9mL), dried by Na₂SO₄, filtered, and concentrated under reduced pressure. The residue was purified by silica gel chromatography (DCM:MeOH (0-4%)) to yield **1.35** (49 mg, 0.15 mmol, 85 %).

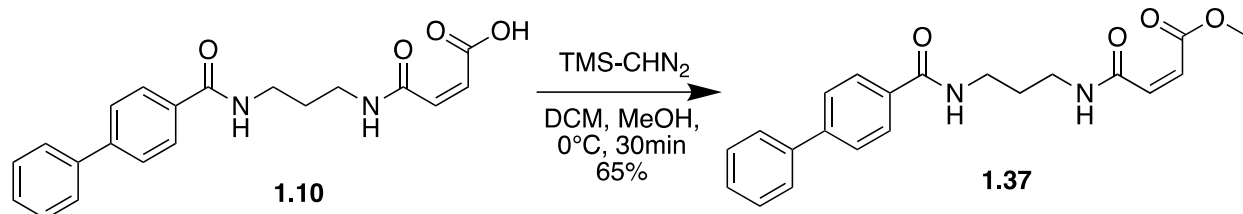
¹H NMR (599 MHz, CDCl₃) δ 7.89 (d, *J* = 8.3 Hz, 2H), 7.68 (d, *J* = 8.3 Hz, 2H), 7.62 (d, *J* = 7.2 Hz, 2H), 7.47 (t, *J* = 7.6 Hz, 2H), 7.39 (t, *J* = 7.3 Hz, 1H), 6.88 (s, 1H), 6.65 (s, 1H), 3.55 (dd, *J* = 12.2, 6.3 Hz, 2H), 3.39 (dd, *J* = 12.0, 6.2 Hz, 2H), 2.72 (t, *J* = 7.3 Hz, 2H), 2.60 (t, *J* = 7.3 Hz, 2H), 1.81 – 1.74 (m, 2H).



methyl (E)-4-((3-([1,1'-biphenyl]-4-carboxamido)propyl)amino)-4-oxobut-2-enoate (1.36)

A solution of (E)-4-methoxy-4-oxobut-2-enoic acid (336 mg, 1.5 Eq, 2.58 mmol), HATU (1.31 g, 2 Eq, 3.44 mmol), and DIPEA (889 mg, 1.20 mL, 4 Eq, 6.88 mmol) were stirred in DMF (15 mL) for 15 minutes before adding N-(3-aminopropyl)-[1,1'-biphenyl]-4-carboxamide, HCl (500 mg, 1 Eq, 1.72 mmol) which was stirred at 23 °C for 14 hour. Upon completion the reaction was diluted with EtOAc (45mL), washed with DI water (4x45mL), brine (45mL), dried by Na₂SO₄, filtered, and concentrated under reduced pressure. The residue was purified by silica gel chromatography (DCM:MeOH (0-4%)) to yield **1.36** (0.56 g, 1.5 mmol, 89 %).

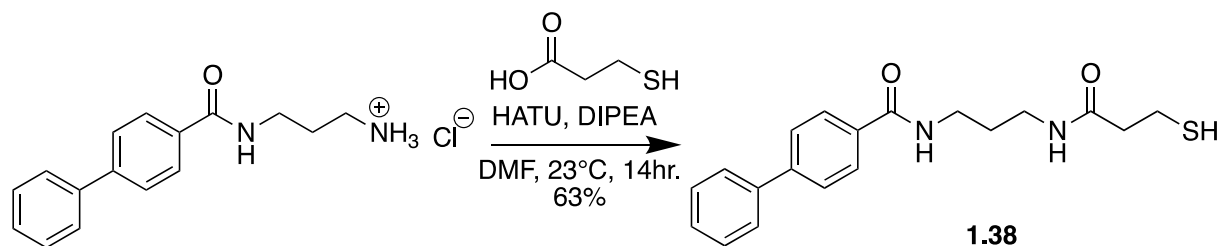
¹H NMR (599 MHz, CDCl₃) δ 7.91 (d, *J* = 8.3 Hz, 2H), 7.68 (d, *J* = 8.3 Hz, 2H), 7.62 (d, *J* = 7.3 Hz, 2H), 7.47 (t, *J* = 7.6 Hz, 2H), 7.39 (t, *J* = 7.3 Hz, 1H), 6.98 (d, *J* = 15.4 Hz, 2H), 6.86 (d, *J* = 15.4 Hz, 2H), 3.80 (s, 3H), 3.55 (dd, *J* = 12.0, 6.2 Hz, 2H), 3.48 (dd, *J* = 12.0, 6.2 Hz, 2H), 1.81 (dt, *J* = 11.7, 6.0 Hz, 2H).



methyl (Z)-4-((3-([1,1'-biphenyl]-4-carboxamido)propyl)amino)-4-oxobut-2-enoate (1.37)

To a stirring solution of **1.10** (22.5 mg, 1 Eq, 63.8 μmol) in DCM (5 mL) and MeOH (1 mL) at 0 °C was added TMS-diazomethane (43.8 mg, 192 μL , 2 molar, 6 Eq, 383 μmol) dropwise. After 30 minutes the reaction was concentrated under reduced pressure. The residue was purified by silica gel chromatography (DCM:MeOH (0-4%)) to yield **1.37** (15 mg, 42 μmol , 65 %).

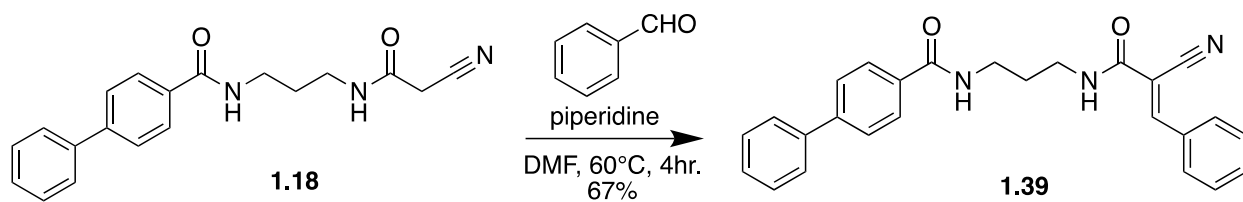
¹H NMR (599 MHz, CDCl₃) δ 8.22 (s, 1H), 7.95 (d, J = 8.3 Hz, 2H), 7.66 (d, J = 8.3 Hz, 2H), 7.61 (d, J = 7.4 Hz, 2H), 7.45 (t, J = 7.6 Hz, 3H), 7.38 (t, J = 7.4 Hz, 1H), 6.39 (d, J = 12.8 Hz, 1H), 6.16 (d, J = 12.8 Hz, 1H), 3.79 (s, 3H), 3.55 (dd, J = 12.1, 6.1 Hz, 2H), 3.49 (dd, J = 12.1, 6.3 Hz, 2H), 1.88 – 1.80 (m, 2H).



***N*-(3-(3-mercaptopropanamido)propyl)-[1,1'-biphenyl]-4-carboxamide (1.38)**

A solution of 3-mercaptopropanoic acid (27 mg, 22 μL , 1.5 Eq, 0.26 mmol), HATU (0.13 g, 2 Eq, 0.34 mmol), and DIPEA (89 mg, 0.12 mL, 4 Eq, 0.69 mmol) were stirred in DMF (5 mL) for 15 minutes before adding *N*-(3-aminopropyl)-[1,1'-biphenyl]-4-carboxamide, HCl (50 mg, 1 Eq, 0.17 mmol) which was stirred at 23 $^\circ\text{C}$ for 14 hour. Upon completion the reaction was diluted with EtOAc (15mL), washed with DI water (4x15mL), brine (15mL), dried by Na_2SO_4 , filtered, and concentrated under reduced pressure. The residue was purified by silica gel chromatography (DCM:MeOH (0-5%)) to yield **1.38** (37 mg, 0.11 mmol, 63 %).

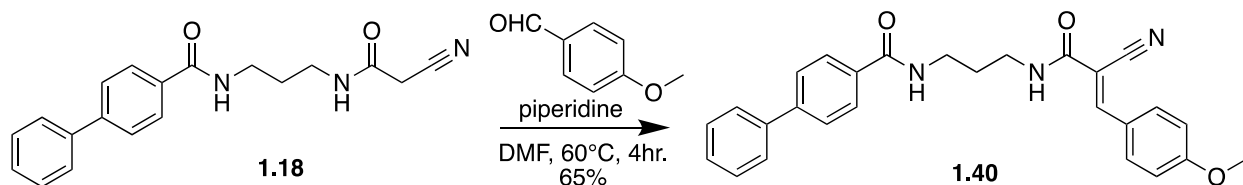
$^1\text{H NMR}$ (599 MHz, CDCl_3) δ 7.93 (d, $J = 8.3$ Hz, 2H), 7.66 (d, $J = 8.2$ Hz, 2H), 7.61 (d, $J = 7.3$ Hz, 2H), 7.46 (t, $J = 7.6$ Hz, 2H), 7.38 (t, $J = 7.4$ Hz, 1H), 7.16 (s, 1H), 6.69 (s, 1H), 3.50 (q, $J = 6.1$ Hz, 2H), 3.39 (dd, $J = 11.9, 6.1$ Hz, 2H), 3.27 (t, $J = 6.5$ Hz, 2H), 2.70 (t, $J = 6.6$ Hz, 2H), 1.86 – 1.78 (m, 2H).



(E)-N-(3-(2-cyano-3-phenylacrylamido)propyl)-[1,1'-biphenyl]-4-carboxamide (1.39)

A solution of **1.18** (50 mg, 1 Eq, 0.16 mmol), benzaldehyde (17 mg, 16 μ L, 1 Eq, 0.16 mmol), and piperidine (1.3 mg, 1.5 μ L, 0.1 Eq, 16 μ mol) was stirred in DMF (3 mL) at 60 °C for 4 hour. After which time the reaction was diluted with EtOAc (15mL), washed with DI water (4x15mL), brine (15mL), dried with Na₂SO₄, filtered, and concentrated in vacuo. The residue was purified by silica gel chromatography (DCM:MeOH (0-5%)) to yield **1.39** (43 mg, 0.10 mmol, 67 %).

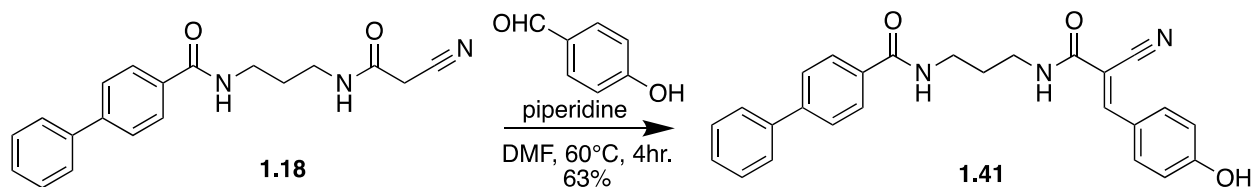
¹H NMR (599 MHz, CDCl₃) δ 8.36 (s, 1H), 7.96 (d, *J* = 8.2 Hz, 4H), 7.68 (d, *J* = 8.3 Hz, 2H), 7.61 (d, *J* = 7.3 Hz, 2H), 7.55 (t, *J* = 7.3 Hz, 1H), 7.50 (t, *J* = 7.4 Hz, 2H), 7.46 (t, *J* = 7.6 Hz, 2H), 7.39 (t, *J* = 7.3 Hz, 1H), 7.15 (s, 1H), 7.04 (s, 1H), 3.58 (td, *J* = 12.5, 6.2 Hz, 4H), 1.92 – 1.85 (m, 2H).



(E)-N-(3-(2-cyano-3-(4-methoxyphenyl)acrylamido)propyl)-[1,1'-biphenyl]-4-carboxamide (1.40)

A solution of **1.18** (50 mg, 1 Eq, 0.16 mmol), 4-methoxybenzaldehyde (21 mg, 19 μ L, 1 Eq, 0.16 mmol), and piperidine (0.13 mg, 0.01 Eq, 1.6 μ mol) was stirred in DMF (3 mL) at 60 °C for 4 hour. After which time the reaction was diluted with EtOAc (15mL), washed with DI water (4x15mL), brine (15mL), dried with Na₂SO₄, filtered, and concentrated in vacuo. The residue was purified by silica gel chromatography (DCM:MeOH (0-5%)) to yield **1.40** (44 mg, 0.10 mmol, 65 %).

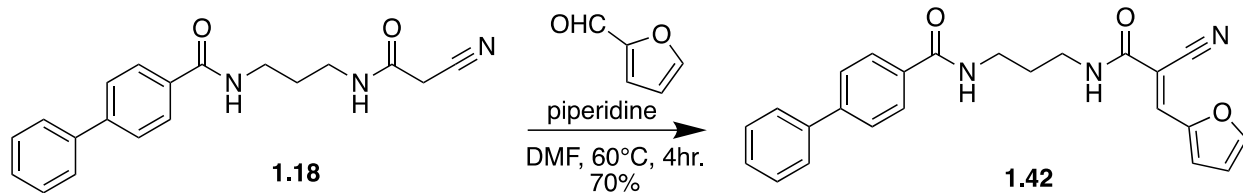
¹H NMR (599 MHz, CDCl₃) δ 8.27 (s, 1H), 7.96 (d, J = 7.1 Hz, 4H), 7.68 (d, J = 8.3 Hz, 2H), 7.61 (d, J = 7.3 Hz, 2H), 7.46 (t, J = 7.6 Hz, 2H), 7.39 (t, J = 7.4 Hz, 1H), 7.24 (s, 1H), 6.99 (d, J = 8.8 Hz, 2H), 6.87 (s, 1H), 3.89 (s, 3H), 3.57 (ddd, J = 18.2, 12.1, 6.2 Hz, 4H), 1.90 – 1.83 (m, 2H).



(E)-N-(3-(2-cyano-3-(4-hydroxyphenyl)acrylamido)propyl)-[1,1'-biphenyl]-4-carboxamide (1.41)

A solution of **1.18** (50 mg, 1 Eq, 0.16 mmol), 4-hydroxybenzaldehyde (19 mg, 1 Eq, 0.16 mmol), and piperidine (0.13 mg, 0.01 Eq, 1.6 μ mol) was stirred in DMF (3 mL) at 60 °C for 4 hour. After which time the reaction was diluted with EtOAc (15mL), washed with DI water (4x15mL), brine (15mL), dried with Na₂SO₄, filtered, and concentrated in vacuo. The residue was purified by silica gel chromatography (DCM:MeOH (0-7%)) to yield **1.41** (42 mg, 98 μ mol, 63 %).

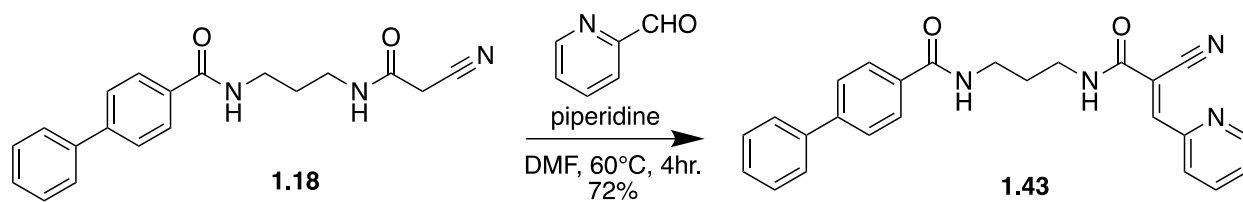
¹H NMR (599 MHz, MeOD) δ 7.99 (s, 1H), 7.83 (d, J = 8.3 Hz, 2H), 7.80 (d, J = 8.8 Hz, 2H), 7.61 (d, J = 8.3 Hz, 2H), 7.54 (d, J = 7.4 Hz, 2H), 7.36 (t, J = 7.8 Hz, 2H), 7.28 (t, J = 7.4 Hz, 1H), 6.80 (d, J = 8.7 Hz, 1H), 3.39 (t, J = 6.7 Hz, 2H), 3.36 (t, J = 6.7 Hz, 2H), 1.84 – 1.78 (m, 2H).



(E)-N-(3-(2-cyano-3-(furan-2-yl)acrylamido)propyl)-[1,1'-biphenyl]-4-carboxamide (1.42)

A solution of **1.18** (50 mg, 1 Eq, 0.16 mmol), furan-2-carbaldehyde (15 mg, 13 μ L, 1 Eq, 0.16 mmol), and piperidine (0.13 mg, 0.01 Eq, 1.6 μ mol) was stirred in DMF (3 mL) at 60 °C for 4 hour. After which time the reaction was diluted with EtOAc (15mL), washed with DI water (4x15mL), brine (15mL), dried with Na₂SO₄, filtered, and concentrated in vacuo. The residue was purified by silica gel chromatography (DCM:MeOH (0-5%)) to yield **1.42** (44 mg, 0.11 mmol, 70 %).

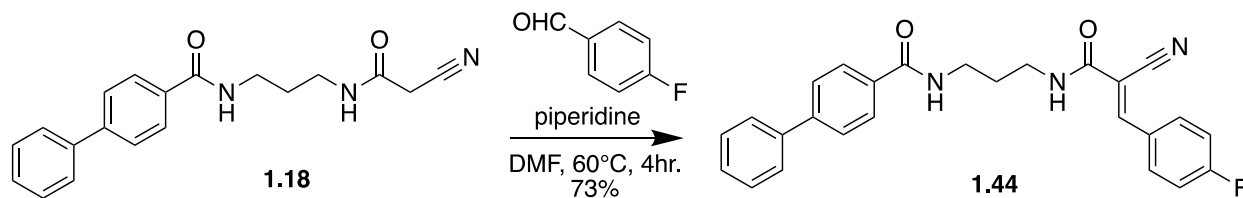
¹H NMR (599 MHz, CDCl₃) δ 8.09 (s, 1H), 7.95 (d, *J* = 8.3 Hz, 2H), 7.72 (d, *J* = 1.2 Hz, 1H), 7.67 (d, *J* = 8.3 Hz, 2H), 7.61 (d, *J* = 7.2 Hz, 2H), 7.46 (t, *J* = 7.6 Hz, 2H), 7.38 (t, *J* = 7.4 Hz, 1H), 7.24 (s, 1H), 7.22 (d, *J* = 3.5 Hz, 1H), 6.94 (s, 1H), 6.63 (dd, *J* = 3.5, 1.7 Hz, 1H), 3.57 (dd, *J* = 11.0, 5.0 Hz, 2H), 3.54 (dd, *J* = 10.8, 4.9 Hz, 2H), 1.89 – 1.83 (m, 2H).



(E)-N-(3-(2-cyano-3-(pyridin-2-yl)acrylamido)propyl)-[1,1'-biphenyl]-4-carboxamide (1.43)

A solution **1.18** (50 mg, 1 Eq, 0.16 mmol), picolinaldehyde (17 mg, 15 μ L, 1 Eq, 0.16 mmol), and piperidine (0.13 mg, 0.01 Eq, 1.6 μ mol) was stirred in DMF (3 mL) at 60 $^{\circ}$ C for 4 hour. After which time the reaction was diluted with EtOAc (15mL), washed with DI water (4x15mL), brine (15mL), dried with Na_2SO_4 , filtered, and concentrated in vacuo. The residue was purified by silica gel chromatography (DCM:MeOH (0-5%)) to yield **1.43** (46 mg, 0.11 mmol, 72 %).

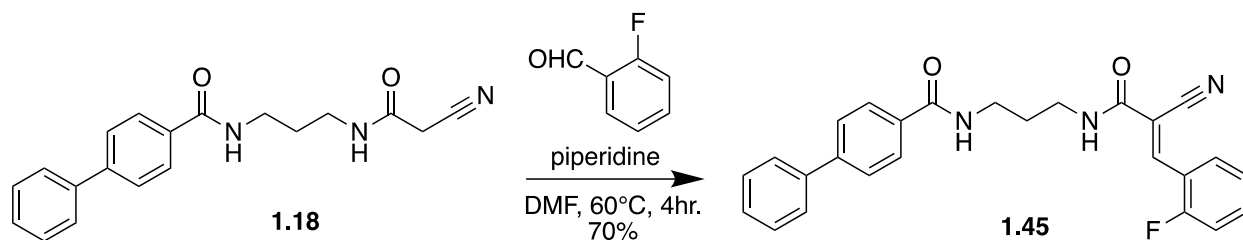
$^1\text{H NMR}$ (599 MHz, CDCl_3) δ 8.82 (d, $J = 4.1$ Hz, 1H), 8.34 (s, 1H), 7.96 (d, $J = 8.3$ Hz, 2H), 7.82 (td, $J = 7.7, 1.7$ Hz, 1H), 7.67 (t, $J = 8.4$ Hz, 3H), 7.61 (d, $J = 7.2$ Hz, 2H), 7.46 (t, $J = 7.7$ Hz, 2H), 7.43 – 7.35 (m, 2H), 7.20 (s, 1H), 7.12 (s, 1H), 3.61 (dd, $J = 12.3, 6.3$ Hz, 2H), 3.56 (dd, $J = 12.1, 6.2$ Hz, 2H), 1.94 – 1.85 (m, 2H).



(E)-N-(3-(2-cyano-3-(4-fluorophenyl)acrylamido)propyl)-[1,1'-biphenyl]-4-carboxamide (1.44)

A solution **1.18** (50 mg, 1 Eq, 0.16 mmol), 4-fluorobenzaldehyde (19 mg, 17 μ L, 1 Eq, 0.16 mmol), and piperidine (0.13 mg, 0.01 Eq, 1.6 μ mol) was stirred in DMF (3 mL) at 60 $^{\circ}$ C for 4 hour. After which time the reaction was diluted with EtOAc (15mL), washed with DI water (4x15mL), brine (15mL), dried with Na₂SO₄, filtered, and concentrated in vacuo. The residue was purified by silica gel chromatography (DCM:MeOH (0-3%)) to yield **1.44** (49 mg, 0.11 mmol, 73 %).

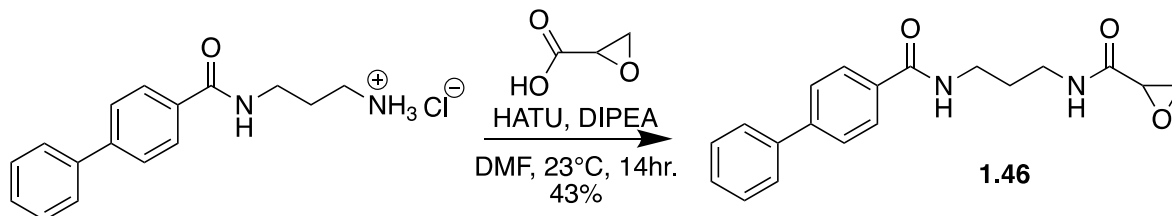
¹H NMR (599 MHz, CDCl₃) δ 8.29 (s, 1H), 7.97 (dd, *J* = 8.7, 5.2 Hz, 2H), 7.94 (d, *J* = 8.3 Hz, 2H), 7.67 (d, *J* = 8.3 Hz, 2H), 7.60 (d, *J* = 7.3 Hz, 2H), 7.46 (t, *J* = 7.6 Hz, 2H), 7.39 (t, *J* = 7.4 Hz, 1H), 7.18 (t, *J* = 8.5 Hz, 2H), 7.16 – 7.09 (m, 2H), 3.57 (dt, *J* = 12.9, 6.7 Hz, 4H), 1.87 (dt, *J* = 12.0, 6.2 Hz, 2H).



(E)-N-(3-(2-cyano-3-(2-fluorophenyl)acrylamido)propyl)-[1,1'-biphenyl]-4-carboxamide (1.45)

A solution **1.18** (50 mg, 1 Eq, 0.16 mmol), 2-fluorobenzaldehyde (19 mg, 16 μ L, 1 Eq, 0.16 mmol), and piperidine (0.13 mg, 0.01 Eq, 1.6 μ mol) was stirred in DMF (5 mL) at 60 °C for 4 hour. After which time the reaction was diluted with EtOAc (20mL), washed with DI water (4x20mL), brine (20mL), dried with Na₂SO₄, filtered, and concentrated in vacuo. The residue was purified by silica gel chromatography (DCM:MeOH (0-3%)) to yield **1.45** (47 mg, 0.11 mmol, 70 %).

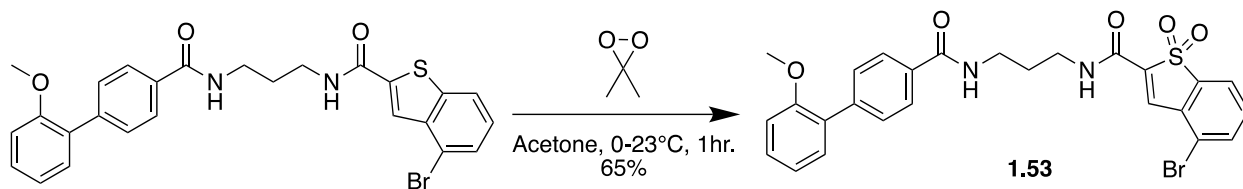
¹H NMR (599 MHz, CDCl₃) δ 8.63 (s, 1H), 8.25 (t, *J* = 7.0 Hz, 1H), 7.95 (d, *J* = 8.3 Hz, 2H), 7.68 (d, *J* = 8.3 Hz, 2H), 7.61 (d, *J* = 7.5 Hz, 2H), 7.55 – 7.50 (m, 1H), 7.46 (t, *J* = 7.6 Hz, 2H), 7.38 (t, *J* = 7.3 Hz, 1H), 7.28 (t, *J* = 7.7 Hz, 1H), 7.20 – 7.15 (m, 1H), 7.13 (d, *J* = 2.5 Hz, 2H), 3.58 (td, *J* = 12.6, 6.5 Hz, 4H), 1.93 – 1.84 (m, 2H).



N-(3-([1,1'-biphenyl]-4-carboxamido)propyl)oxirane-2-carboxamide (**1.46**)

A solution of oxirane-2-carboxylic acid (27 mg, 1.2 Eq, 0.31 mmol), HATU (0.20 g, 2 Eq, 0.52 mmol), and DIPEA (0.10 g, 0.13 mL, 3 Eq, 0.77 mmol) were stirred in DMF (3 mL) for 15 minutes before adding N-(3-aminopropyl)-[1,1'-biphenyl]-4-carboxamide, HCl (75 mg, 1 Eq, 0.26 mmol) which was stirred at 23 °C for 14 hour. Upon completion the reaction was diluted with EtOAc (15mL), washed with DI water (4x15mL), brine (15mL), dried by Na₂SO₄, filtered, and concentrated under reduced pressure. The residue was purified by silica gel chromatography (DCM:MeOH (0-3%)) to yield **1.46** (36 mg, 0.11 mmol, 43 %).

¹H NMR (599 MHz, MeOD) δ 7.81 (d, *J* = 8.3 Hz, 2H), 7.62 (d, *J* = 8.3 Hz, 2H), 7.56 (d, *J* = 8.3 Hz, 2H), 7.36 (t, *J* = 7.7 Hz, 2H), 7.28 (t, *J* = 7.4 Hz, 1H), 3.33 (t, *J* = 6.8 Hz, 3H), 3.29 (dd, *J* = 4.4, 2.4 Hz, 1H), 3.22 (t, *J* = 4.7 Hz, 2H), 2.86 (dd, *J* = 5.9, 4.6 Hz, 2H), 2.72 (dd, *J* = 6.0, 2.4 Hz, 2H), 1.71 (p, *J* = 6.8 Hz, 2H).

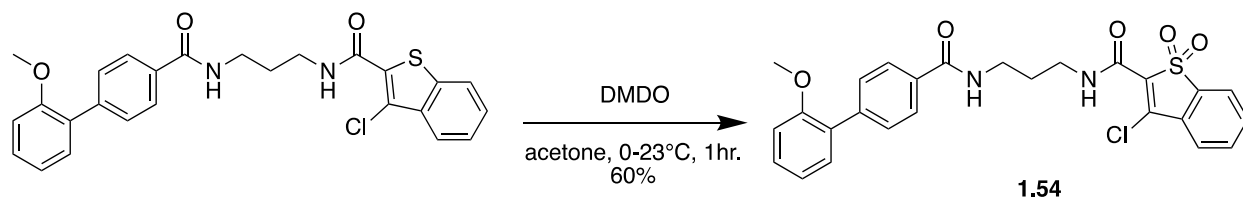


4-bromo-N-(3-(2'-methoxy-[1,1'-biphenyl]-4-carboxamido)propyl)cinnamamide 1,1-dioxide (1.53)

General Procedure B: DMDO oxidation

To a stirring solution of 4-bromo-N-(3-(2'-methoxy-[1,1'-biphenyl]-4-carboxamido)propyl)benzo[b]thiophene-2-carboxamide (27 mg, 1 Eq, 52 μ mol) in 0 °C Acetone (3 mL) was added dimethyldioxirane (11 mg, 1.5 mL, 0.1 molar, 3 Eq, 0.15 mmol) and the reaction was allowed to warm to 23 °C over 1 hour. After which time the starting material had been consumed (visualized by TLC) and the reaction was concentrated in vacuo. The residue was purified by silica gel chromatography (Hex: EtOAc (80-33%)) to yield 4-bromo-N-(3-(2'-methoxy-[1,1'-biphenyl]-4-carboxamido)propyl)cinnamamide 1,1-dioxide (19 mg, 34 μ mol, 65 %).

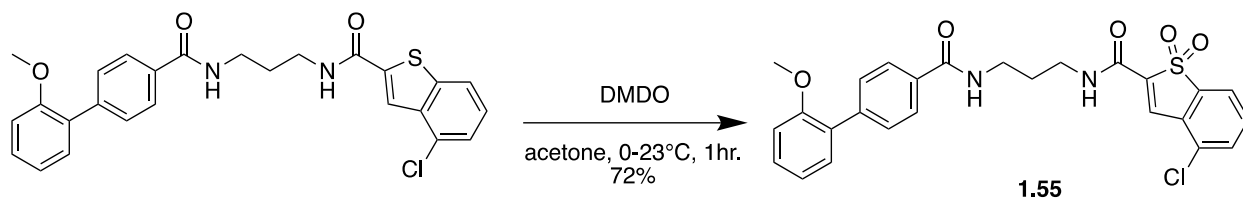
$^1\text{H NMR}$ (599 MHz, MeOD) δ 8.11 (s, 1H), 7.91 (d, J = 8.1 Hz, 1H), 7.88 (d, J = 8.2 Hz, 2H), 7.80 (d, J = 7.5 Hz, 1H), 7.62 (t, J = 7.8 Hz, 1H), 7.59 (d, J = 8.3 Hz, 2H), 7.37 (t, J = 7.9 Hz, 1H), 7.30 (d, J = 7.6 Hz, 1H), 7.10 (d, J = 8.2 Hz, 1H), 7.04 (t, J = 7.4 Hz, 1H), 3.82 (s, 3H), 3.56 – 3.47 (m, 4H), 1.99 – 1.94 (m, 2H).



3-chloro-N-(3-(2'-methoxy-[1,1'-biphenyl]-4-carboxamido)propyl)cinnamamide 1,1-dioxide (1.54)

General Procedure B: DMSO oxidation

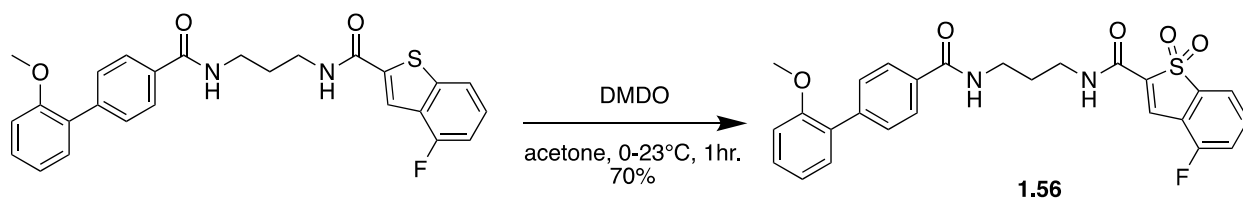
$R_f = 0.05$ (Hex:EtOAc (1:1)) $^1\text{H NMR}$ (599 MHz, CDCl_3) δ 7.89 (d, $J = 8.2$ Hz, 2H), 7.80 (d, $J = 6.9$ Hz, 2H), 7.77 – 7.71 (m, 2H), 7.61 (d, $J = 8.2$ Hz, 2H), 7.35 (t, $J = 7.8$ Hz, 1H), 7.32 (dd, $J = 7.5, 1.4$ Hz, 1H), 7.04 (t, $J = 7.4$ Hz, 1H), 7.00 (d, $J = 8.1$ Hz, 1H), 3.82 (s, 3H), 3.59 (dd, $J = 12.3, 6.4$ Hz, 4H), 1.93 – 1.86 (m, 2H).



4-chloro-N-(3-(2'-methoxy-[1,1'-biphenyl]-4-carboxamido)propyl)cinnamamide 1,1-dioxide (1.55)

General Procedure B: DMSO oxidation

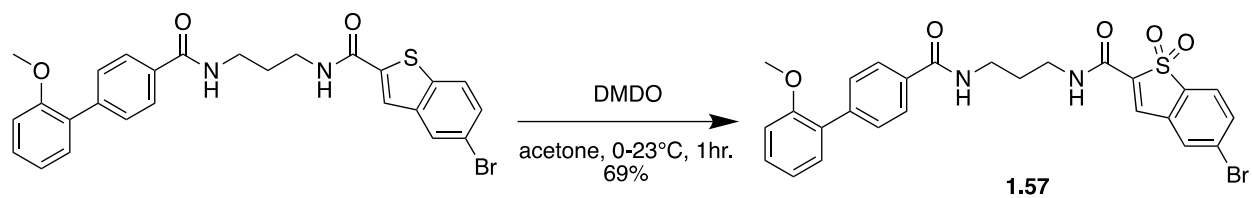
$R_f = 0.05$ (Hex:EtOAc (1:1)) $^1\text{H NMR}$ (599 MHz, CDCl_3) δ 8.10 (s, 1H), 7.90 (d, $J = 8.2$ Hz, 2H), 7.65 (d, $J = 7.3$ Hz, 1H), 7.61 (d, $J = 8.1$ Hz, 3H), 7.59 – 7.53 (m, 1H), 7.35 (t, $J = 7.8$ Hz, 1H), 7.34 – 7.31 (m, 1H), 7.14 – 7.08 (m, 2H), 7.04 (t, $J = 7.4$ Hz, 1H), 7.00 (d, $J = 8.2$ Hz, 1H), 3.81 (s, 3H), 3.58 (td, $J = 12.6, 6.2$ Hz, 4H), 1.92 – 1.85 (m, 2H).



4-fluoro-N-(3-(2'-methoxy-[1,1'-biphenyl]-4-carboxamido)propyl)cinnamamide 1,1-dioxide (1.56)

General Procedure B: DMSO oxidation

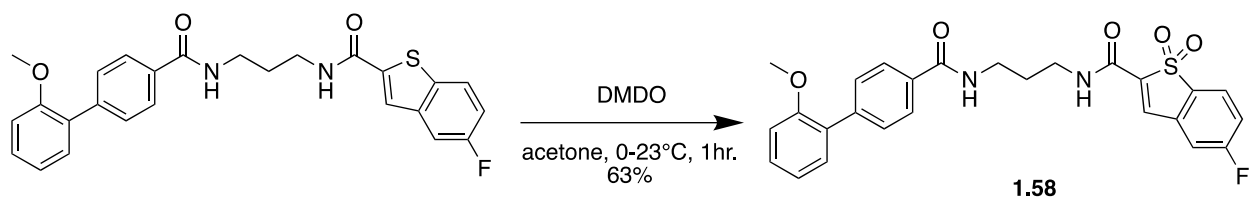
$R_f = 0.05$ (Hex:EtOAc (1:1)) $^1\text{H NMR}$ (599 MHz, CDCl_3) δ 8.03 (s, 1H), 7.90 (d, $J = 8.2$ Hz, 2H), 7.68 – 7.63 (m, 1H), 7.62 (d, $J = 8.2$ Hz, 2H), 7.57 (d, $J = 7.5$ Hz, 1H), 7.36 (t, $J = 9.1$ Hz, 2H), 7.33 (dd, $J = 7.5, 1.4$ Hz, 1H), 7.05 (t, $J = 7.4$ Hz, 2H), 7.00 (d, $J = 8.2$ Hz, 1H), 3.82 (s, 3H), 3.58 (dt, $J = 21.2, 6.2$ Hz, 4H), 1.92 – 1.87 (m, 2H).



5-bromo-N-(3-(2'-methoxy-[1,1'-biphenyl]-4-carboxamido)propyl)cinnamamide 1,1-dioxide (1.57)

General Procedure B: DMDO oxidation

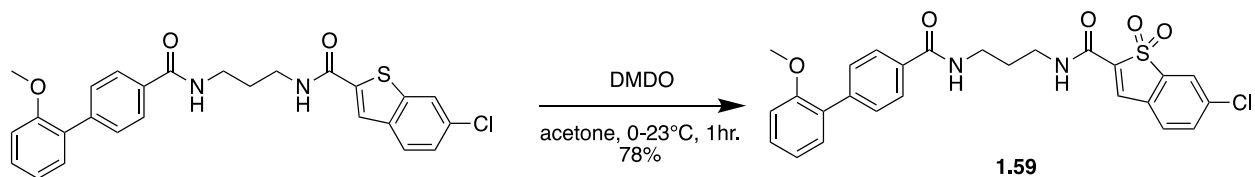
$R_f = 0.05$ (Hex:EtOAc (1:1)) **$^1\text{H NMR}$** (599 MHz, CDCl_3) δ 7.89 (d, $J = 8.1$ Hz, 2H), 7.78 (t, $J = 3.8$ Hz, 2H), 7.66 (s, 1H), 7.62 (dd, $J = 8.2, 3.2$ Hz, 3H), 7.36 (t, $J = 7.8$ Hz, 1H), 7.33 (d, $J = 7.5$ Hz, 1H), 7.10 – 7.02 (m, 1H), 7.01 (d, $J = 8.2$ Hz, 2H), 3.82 (s, 3H), 3.58 (td, $J = 11.4, 5.7$ Hz, 4H), 1.92 – 1.86 (m, 2H).



5-fluoro-N-(3-(2'-methoxy-[1,1'-biphenyl]-4-carboxamido)propyl)cinnamamide 1,1-dioxide (1.58)

General Procedure B: DMDO oxidation

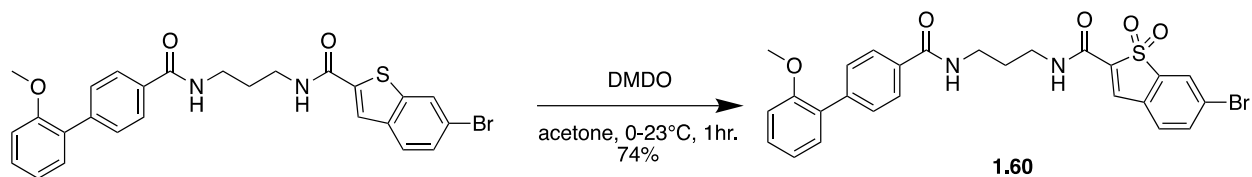
$R_f = 0.05$ (Hex:EtOAc (1:1)) $^1\text{H NMR}$ (599 MHz, CDCl_3) δ 7.83 (d, $J = 8.2$ Hz, 2H), 7.71 (s, 1H), 7.69 (dd, $J = 8.4, 4.6$ Hz, 1H), 7.55 (d, $J = 8.2$ Hz, 2H), 7.31 – 7.27 (m, 1H), 7.27 – 7.22 (m, 2H), 7.15 (dd, $J = 7.7, 1.8$ Hz, 1H), 6.97 (dd, $J = 14.2, 6.7$ Hz, 2H), 6.94 (t, $J = 8.1$ Hz, 2H), 3.75 (s, 3H), 3.51 (td, $J = 12.6, 6.3$ Hz, 4H), 1.87 – 1.79 (m, 2H).



6-chloro-N-(3-(2'-methoxy-[1,1'-biphenyl]-4-carboxamido)propyl)cinnamamide 1,1-dioxide (1.59)

General Procedure B: DMSO oxidation

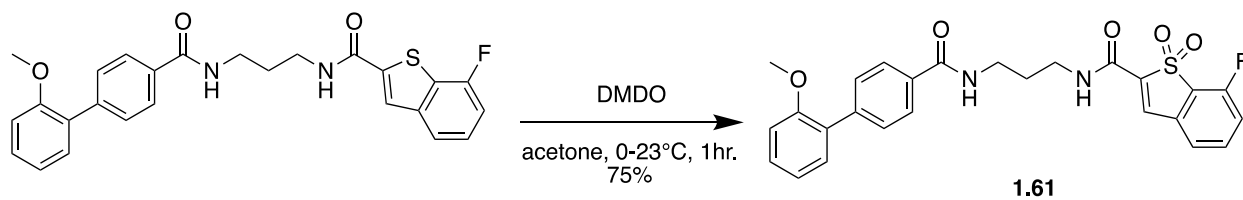
$R_f = 0.05$ (Hex:EtOAc (1:1)) $^1\text{H NMR}$ (599 MHz, CDCl_3) δ 7.89 (d, $J = 8.3$ Hz, 2H), 7.81 (s, 1H), 7.74 (s, 1H), 7.63 – 7.59 (m, 3H), 7.45 (d, $J = 8.0$ Hz, 1H), 7.36 (t, $J = 7.7$ Hz, 1H), 7.33 (dd, $J = 7.5, 1.6$ Hz, 1H), 7.05 (t, $J = 7.4$ Hz, 2H), 7.00 (dd, $J = 13.2, 5.2$ Hz, 2H), 3.82 (s, 3H), 3.58 (td, $J = 12.1, 6.3$ Hz, 4H), 1.92 – 1.86 (m, 2H).



6-bromo-N-(3-(2'-methoxy-[1,1'-biphenyl]-4-carboxamido)propyl)cinnamamide 1,1-dioxide (1.60)

General Procedure B: DMSO oxidation

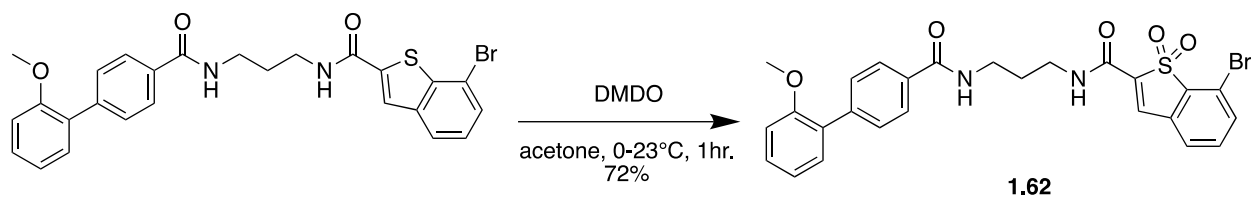
$R_f = 0.05$ (Hex:EtOAc (1:1)) $^1\text{H NMR}$ (599 MHz, CDCl_3) δ 7.89 (d, $J = 8.5$ Hz, 3H), 7.80 (s, 1H), 7.76 (d, $J = 7.5$ Hz, 1H), 7.61 (d, $J = 8.1$ Hz, 2H), 7.34 (ddd, $J = 22.3, 15.3, 7.5$ Hz, 3H), 7.05 (t, $J = 7.3$ Hz, 2H), 7.00 (d, $J = 8.3$ Hz, 2H), 3.82 (s, 3H), 3.61 – 3.52 (m, 4H), 1.91 – 1.85 (m, 2H).



7-fluoro-N-(3-(2'-methoxy-[1,1'-biphenyl]-4-carboxamido)propyl)cinnamamide 1,1-dioxide (1.61)

General Procedure B: DMDO oxidation

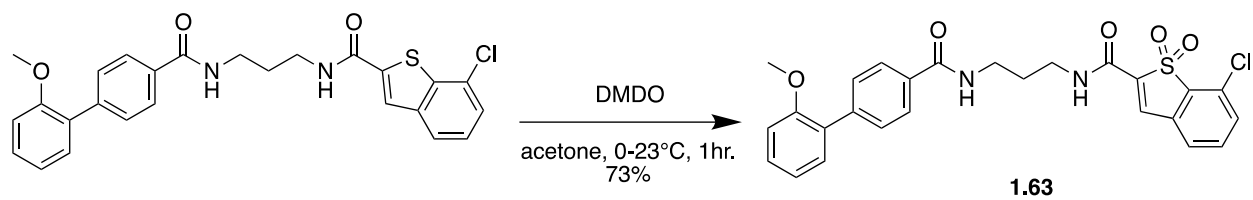
¹H NMR (599 MHz, CDCl₃) δ 7.90 (d, *J* = 8.2 Hz, 2H), 7.81 (s, 1H), 7.62 (d, *J* = 8.2 Hz, 3H), 7.36 (t, *J* = 8.0 Hz, 2H), 7.34 – 7.29 (m, 2H), 7.05 (t, *J* = 7.3 Hz, 2H), 7.01 (d, *J* = 8.2 Hz, 2H), 3.82 (s, 3H), 3.58 (td, *J* = 12.6, 6.0 Hz, 4H), 1.93 – 1.86 (m, 2H).



7-bromo-N-(3-(2'-methoxy-[1,1'-biphenyl]-4-carboxamido)propyl)cinnamamide 1,1-dioxide (1.62)

General Procedure B: DMSO oxidation

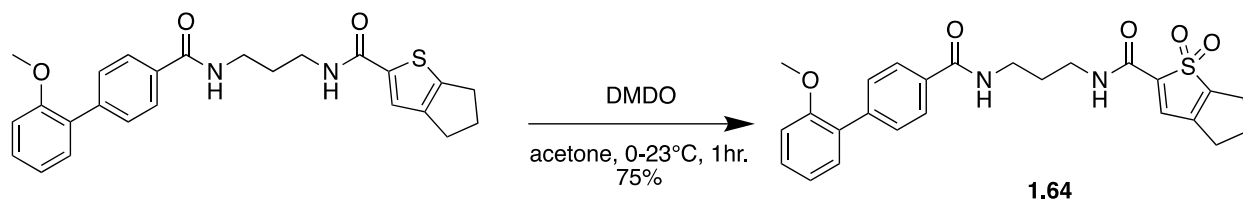
¹H NMR (599 MHz, DMSO) δ 8.74 (t, $J = 5.7$ Hz, 1H), 8.59 (t, $J = 5.4$ Hz, 1H), 7.94 (s, 1H), 7.85 (d, $J = 8.0$ Hz, 1H), 7.82 (d, $J = 8.3$ Hz, 2H), 7.68 (d, $J = 7.7$ Hz, 1H), 7.61 (t, $J = 7.7$ Hz, 1H), 7.53 (d, $J = 8.2$ Hz, 2H), 7.36 (t, $J = 7.1$ Hz, 1H), 7.28 (dd, $J = 7.4, 1.3$ Hz, 1H), 7.10 (d, $J = 8.8$ Hz, 1H), 7.04 (t, $J = 7.1$ Hz, 1H), 3.73 (s, 6H), 3.34 (q, $J = 5.9$ Hz, 2H), 3.29 (q, $J = 6.1$ Hz, 1H), 1.84 – 1.74 (m, 2H).



7-chloro-N-(3-(2'-methoxy-[1,1'-biphenyl]-4-carboxamido)propyl)cinnamamide 1,1-dioxide (1.63)

General Procedure B: DMSO oxidation

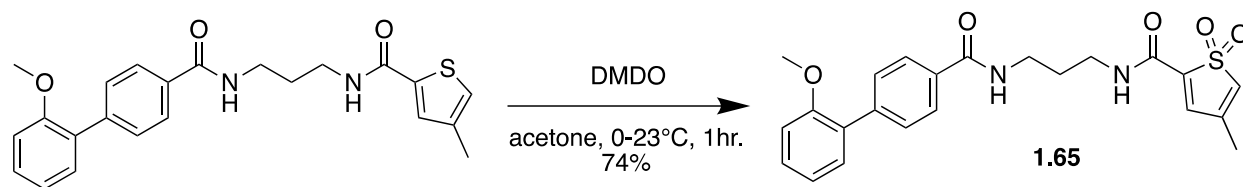
$^1\text{H NMR}$ (599 MHz, CDCl_3) δ 7.89 (d, $J = 7.6$ Hz, 2H), 7.79 (s, 1H), 7.61 (d, $J = 7.9$ Hz, 1H), 7.59 – 7.49 (m, 3H), 7.39 (d, $J = 6.9$ Hz, 1H), 7.37 – 7.28 (m, 2H), 7.14 – 6.88 (m, 4H), 3.82 (s, 3H), 3.58 (dd, $J = 13.3, 6.3$ Hz, 4H), 1.93 – 1.86 (m, 2H).



N-(3-(2'-methoxy-[1,1'-biphenyl]-4-carboxamido)propyl)-5,6-dihydro-4H-cyclopenta[b]thiophene-2-carboxamide 1,1-dioxide (1.64)

General Procedure B: DMSO oxidation

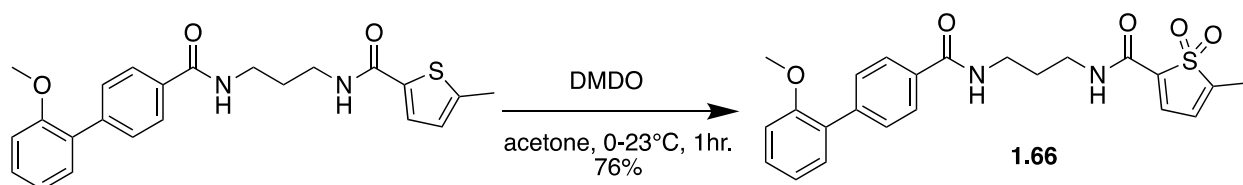
¹H NMR (599 MHz, CDCl₃) δ 7.89 (d, *J* = 8.2 Hz, 2H), 7.61 (d, *J* = 8.2 Hz, 2H), 7.38 – 7.30 (m, 3H), 7.37 – 7.31 (m, 1H), 7.14 (t, *J* = 6.0 Hz, 1H), 7.04 (t, *J* = 7.4 Hz, 1H), 7.00 (d, *J* = 8.2 Hz, 1H), 6.76 (t, *J* = 5.9 Hz, 1H), 3.82 (s, 3H), 3.54 (td, *J* = 12.2, 6.3 Hz, 4H), 2.81 – 2.76 (m, 2H), 2.67 – 2.62 (m, 2H), 2.46 (p, *J* = 7.5 Hz, 2H), 1.91 – 1.80 (m, 2H).



N-(3-(2'-methoxy-[1,1'-biphenyl]-4-carboxamido)propyl)-4-methylthiophene-2-carboxamide 1,1-dioxide (1.65)

General Procedure B: DMDO oxidation

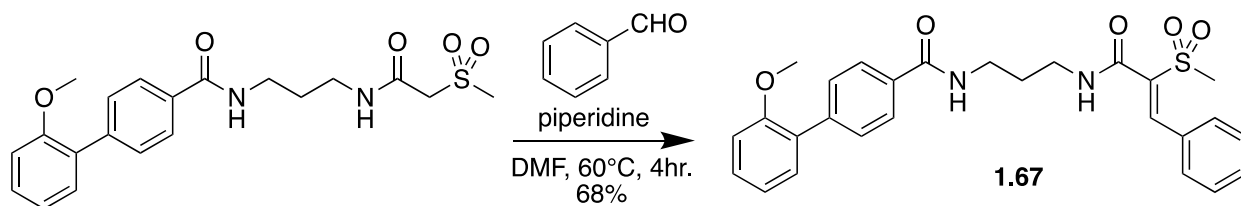
$R_f = 0.5$ (EtOAc) $^1\text{H NMR}$ (599 MHz, CDCl_3) δ 7.89 (d, $J = 8.1$ Hz, 2H), 7.61 (d, $J = 8.1$ Hz, 2H), 7.34 (dd, $J = 18.8, 7.8$ Hz, 2H), 7.22 (s, 1H), 7.08 (s, 1H), 7.05 (t, $J = 7.5$ Hz, 1H), 7.00 (d, $J = 8.2$ Hz, 1H), 6.81 (s, 1H), 6.38 (s, 1H), 3.82 (s, 3H), 3.54 (td, $J = 12.4, 6.2$ Hz, 4H), 2.16 (s, 3H), 1.90 – 1.80 (m, 2H).



N-(3-(2'-methoxy-[1,1'-biphenyl]-4-carboxamido)propyl)-5-methylthiophene-2-carboxamide 1,1-dioxide (1.66)

General Procedure B: DMSO oxidation

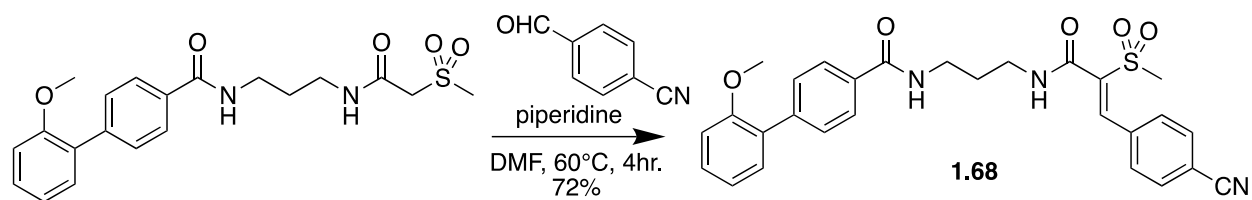
¹H NMR (599 MHz, CDCl₃) δ 7.88 (d, *J* = 7.3 Hz, 2H), 7.63 (d, *J* = 7.5 Hz, 2H), 7.43 (d, *J* = 4.1 Hz, 1H), 7.41 (s, 1H), 7.36 (t, *J* = 7.8 Hz, 1H), 7.33 (d, *J* = 7.5 Hz, 1H), 7.05 (t, *J* = 7.4 Hz, 1H), 7.00 (d, *J* = 8.2 Hz, 1H), 6.82 (s, 1H), 6.49 (d, *J* = 1.8 Hz, 1H), 3.82 (s, 3H), 3.59 – 3.52 (m, 4H), 2.21 (s, 3H), 1.92 – 1.84 (m, 2H).



(Z)-2'-methoxy-N-(3-(2-(methanesulfonyl)-3-phenylacrylamido)propyl)-[1,1'-biphenyl]-4-carboxamide (1.67)

A solution 2'-methoxy-N-(3-(2-(methanesulfonyl)acetamido)propyl)-[1,1'-biphenyl]-4-carboxamide (45 mg, 1 Eq, 0.11 mmol), benzaldehyde (12 mg, 11 μ L, 1 Eq, 0.11 mmol), and piperidine (0.95 mg, 1.1 μ L, 0.1 Eq, 11 μ mol) was stirred in DMF (3 mL) at 60 °C for 4 hour. After which time the reaction was diluted with EtOAc (15mL), washed with DI water (4x15mL), brine (15mL), dried with Na₂SO₄, filtered, and concentrated in vacuo. The residue was purified by silica gel chromatography (Hex:EtOAc (80-33%)) to yield **1.67** (37 mg, 76 μ mol, 68 %).

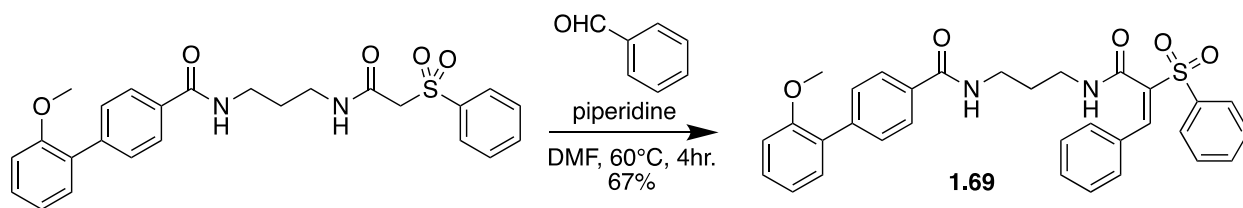
¹H NMR (599 MHz, CDCl₃) δ 7.82 (d, *J* = 8.2 Hz, 2H), 7.70 (s, 1H), 7.60 (d, *J* = 8.2 Hz, 2H), 7.55 (d, *J* = 7.3 Hz, 2H), 7.47 – 7.39 (m, 3H), 7.35 (t, *J* = 7.8 Hz, 1H), 7.32 (d, *J* = 7.5 Hz, 1H), 7.04 (t, *J* = 7.5 Hz, 1H), 7.00 (d, *J* = 8.2 Hz, 1H), 6.84 (s, 1H), 6.75 (s, 1H), 3.81 (s, 3H), 3.46 (p, *J* = 6.3 Hz, 4H), 3.24 (s, 3H), 1.83 – 1.76 (m, 2H).



(Z)-N-(3-(3-(4-cyanophenyl)-2-(methylsulfonyl)acrylamido)propyl)-2'-methoxy-[1,1'-biphenyl]-4-carboxamide (1.68)

A solution 2'-methoxy-N-(3-(2-(methylsulfonyl)acetamido)propyl)-[1,1'-biphenyl]-4-carboxamide (45 mg, 1 Eq, 0.11 mmol), 4-formylbenzonitrile (18 mg, 1.2 Eq, 0.13 mmol), and piperidine (95 μ g, 0.01 Eq, 1.1 μ mol) was stirred in DMF (3 mL) at 60 $^{\circ}$ C for 4 hour. After which time the reaction was diluted with EtOAc (15mL), washed with DI water (4x15mL), brine (15mL), dried with Na₂SO₄, filtered, and concentrated in vacuo. The residue was purified by silica gel chromatography (Hex:EtOAc (80-33%)) to yield **1.68** (41 mg, 80 μ mol, 72 %).

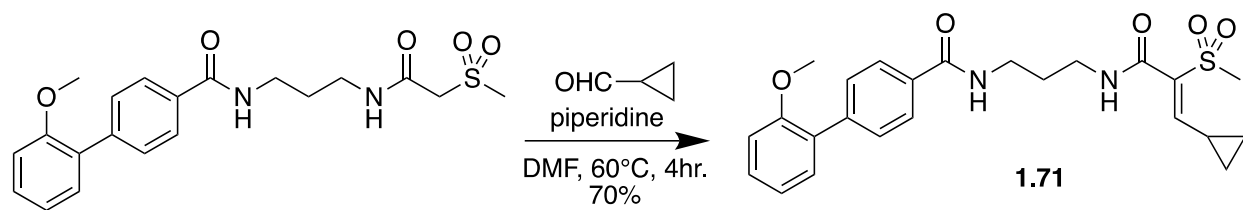
¹H NMR (599 MHz, CDCl₃) δ 7.74 (d, J = 8.1 Hz, 2H), 7.71 – 7.67 (m, 3H), 7.65 (d, J = 8.2 Hz, 2H), 7.36 (t, J = 7.8 Hz, 2H), 7.33 – 7.27 (m, 1H), 7.05 (t, J = 7.4 Hz, 1H), 7.00 (d, J = 8.2 Hz, 1H), 6.56 (s, 1H), 3.82 (s, 3H), 3.46 – 3.37 (m, 4H), 3.25 (s, 3H), 1.80 – 1.75 (m, 2H).



(Z)-2'-methoxy-N-(3-(3-phenyl-2-(phenylsulfonyl)acrylamido)propyl)-[1,1'-biphenyl]-4-carboxamide (1.69)

A solution 2'-methoxy-N-(3-(2-(phenylsulfonyl)acetamido)propyl)-[1,1'-biphenyl]-4-carboxamide (40 mg, 1 Eq, 86 μ mol), benzaldehyde (11 mg, 10 μ L, 1.2 Eq, 0.10 mmol), and piperidine (73 μ g, 85 nL, 0.01 Eq, 0.86 μ mol) was stirred in DMF (3 mL) at 60 °C for 4 hour. After which time the reaction was diluted with EtOAc (15mL), washed with DI water (4x15mL), brine (15mL), dried with Na₂SO₄, filtered, and concentrated in vacuo. The residue was purified by silica gel chromatography (Hex:EtOAc (80-33%)) to yield **1.69** (32 mg, 57 μ mol, 67 %).

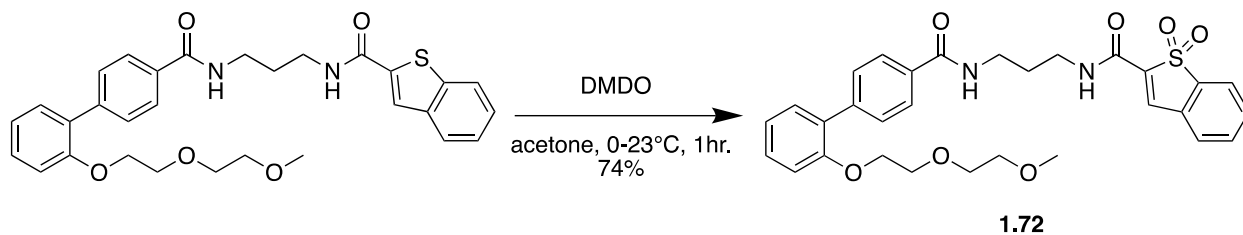
¹H NMR (599 MHz, CDCl₃) δ 7.95 (d, *J* = 7.8 Hz, 2H), 7.88 (s, 1H), 7.79 (d, *J* = 8.1 Hz, 2H), 7.60 (dd, *J* = 20.5, 13.2 Hz, 1H), 7.55 (dt, *J* = 15.6, 7.7 Hz, 6H), 7.44 – 7.33 (m, 4H), 7.31 (d, *J* = 7.4 Hz, 1H), 7.04 (t, *J* = 7.4 Hz, 1H), 7.00 (d, *J* = 8.2 Hz, 1H), 6.97 (s, 1H), 6.80 (s, 1H), 3.81 (s, 3H), 3.41 (ddd, *J* = 18.4, 11.9, 6.1 Hz, 4H), 1.78 – 1.71 (m, 2H).



(Z)-N-(3-(3-cyclopropyl-2-(methylsulfonyl)acrylamido)propyl)-2'-methoxy-[1,1'-biphenyl]-4-carboxamide (1.71)

A solution 2'-methoxy-N-(3-(2-(methylsulfonyl)acetamido)propyl)-[1,1'-biphenyl]-4-carboxamide (37 mg, 1 Eq, 91 μmol), cyclopropanecarboxaldehyde (7.7 mg, 8.2 μL , 1.2 Eq, 0.11 mmol), and piperidine (78 μg , 0.01 Eq, 0.91 μmol) was stirred in DMF (3 mL) at 60 °C for 4 hour. After which time the reaction was diluted with EtOAc (15mL), washed with DI water (4x15mL), brine (15mL), dried with Na_2SO_4 , filtered, and concentrated in vacuo. The residue was purified by silica gel chromatography (Hex:EtOAc (80-33%)) to yield **1.71** (29 mg, 64 μmol , 70 %).

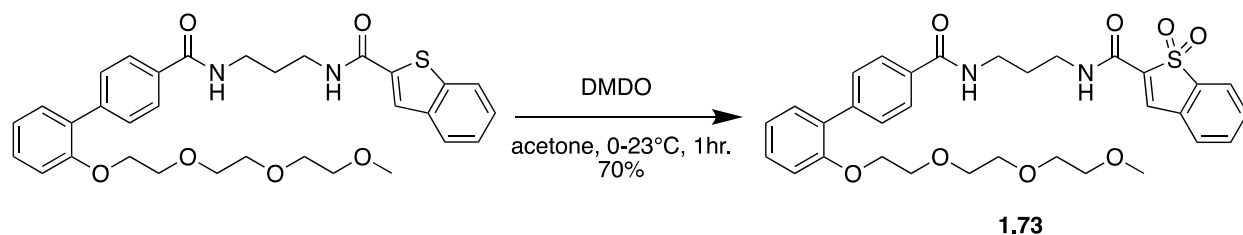
$^1\text{H NMR}$ (599 MHz, CDCl_3) δ 7.88 (d, $J = 8.1$ Hz, 2H), 7.61 (d, $J = 8.1$ Hz, 2H), 7.35 (t, $J = 7.4$ Hz, 2H), 7.32 (d, $J = 7.5$ Hz, 1H), 7.12 (s, 1H), 7.04 (t, $J = 7.4$ Hz, 1H), 7.00 (d, $J = 8.2$ Hz, 1H), 6.44 (d, $J = 11.2$ Hz, 1H), 3.81 (s, 3H), 3.54 (td, $J = 12.2, 6.2$ Hz, 4H), 3.08 (s, 3H), 2.29 (pd, $J = 8.1, 4.3$ Hz, 1H), 1.91 – 1.80 (m, 2H), 1.24 – 1.19 (m, 2H), 0.89 – 0.84 (m, 2H).



N-(3-(2'-(2-(2-methoxyethoxy)ethoxy)-[1,1'-biphenyl]-4-carboxamido)propyl)cinnamamide 1,1-dioxide (1.72)

General Procedure B: DMSO oxidation

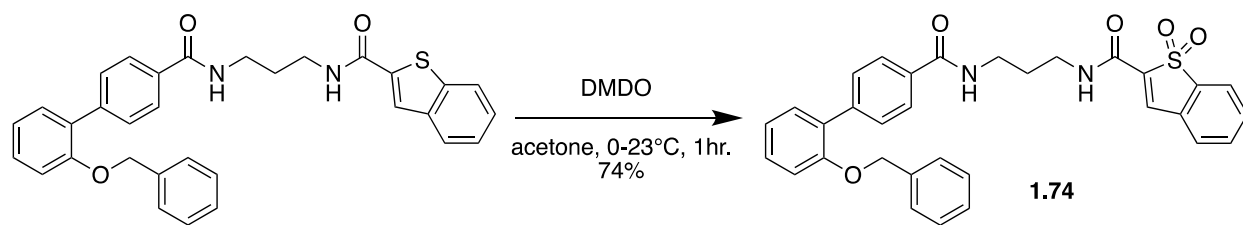
¹H NMR (599 MHz, CDCl₃) δ 7.91 (dt, *J* = 15.0, 6.2 Hz, 3H), 7.85 (s, 1H), 7.78 – 7.75 (m, 1H), 7.67 – 7.60 (m, 5H), 7.52 (t, *J* = 6.5 Hz, 1H), 7.30 (d, *J* = 2.0 Hz, 1H), 7.17 (s, 1H), 6.92 (d, *J* = 8.7 Hz, 2H), 3.77 – 3.74 (m, 2H), 3.57 (ddd, *J* = 19.8, 12.7, 6.0 Hz, 8H), 3.52 – 3.46 (m, 2H), 3.36 (s, 3H), 1.92 – 1.88 (m, 2H).



N-(3-(2'-(2-(2-(2-methoxyethoxy)ethoxy)ethoxy)-[1,1'-biphenyl]-4-carboxamido)propyl)cinnamamide 1,1-dioxide (1.73)

General Procedure B: DMSO oxidation

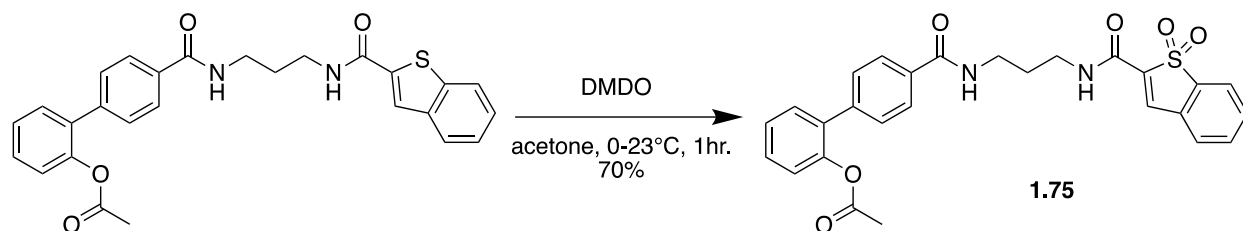
¹H NMR (599 MHz, CDCl₃) δ 7.90 (dd, *J* = 7.7, 5.2 Hz, 2H), 7.86 (s, 1H), 7.79 – 7.74 (m, 1H), 7.67 (d, *J* = 8.1 Hz, 1H), 7.66 – 7.61 (m, 3H), 7.53 (dd, *J* = 8.1, 4.9 Hz, 1H), 7.33 (dd, *J* = 16.4, 8.4 Hz, 2H), 7.19 (t, *J* = 5.9 Hz, 1H), 7.06 (dd, *J* = 16.8, 9.3 Hz, 1H), 7.02 – 6.97 (m, 2H), 4.14 (t, *J* = 4.7 Hz, 1H), 4.14 (t, *J* = 4.7 Hz, 1H), 4.12 – 4.09 (m, 1H), 4.12 – 4.09 (m, 1H), 3.79 – 3.73 (m, 3H), 3.80 – 3.74 (m, 3H), 3.63 (d, *J* = 11.5 Hz, 4H), 3.60 – 3.54 (m, 3H), 3.55 – 3.51 (m, 2H), 3.36 (s, 3H), 1.94 – 1.87 (m, 2H).



N-(3-(2-(benzyloxy)-[1,1'-biphenyl]-4-carboxamido)propyl)cinnamamide 1,1-dioxide (1.74)

General Procedure B: DMSO oxidation

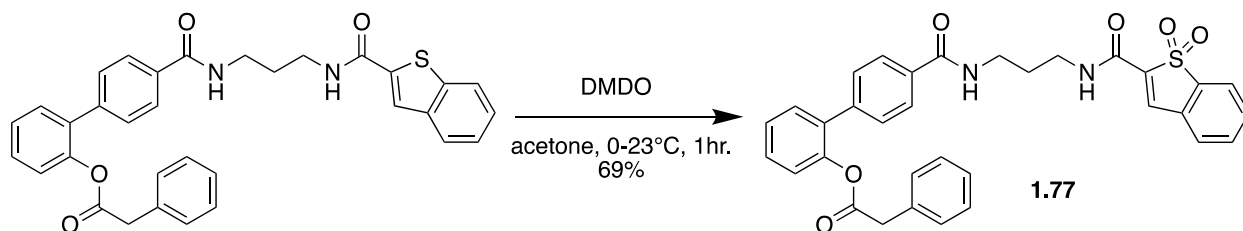
¹H NMR (599 MHz, MeOD) δ 8.56 (s, 1H), 7.92 (s, 1H), 7.86 (d, $J = 8.3$ Hz, 2H), 7.80 – 7.74 (m, 1H), 7.69 (dd, $J = 4.7, 3.8$ Hz, 2H), 7.63 (d, $J = 8.3$ Hz, 3H), 7.37 – 7.28 (m, 6H), 7.25 (t, $J = 5.8$ Hz, 1H), 7.16 (d, $J = 8.4$ Hz, 1H), 7.05 (t, $J = 7.5$ Hz, 1H), 5.09 (s, 2H), 3.49 (dt, $J = 13.8, 6.3$ Hz, 4H), 1.92 (p, $J = 6.7$ Hz, 2H).



**4'-((3-(1,1-dioxidocinnamamido)propyl)carbamoyle)-[1,1'-biphenyl]-2-yl
acetate (1.75)**

General Procedure B: DMSO oxidation

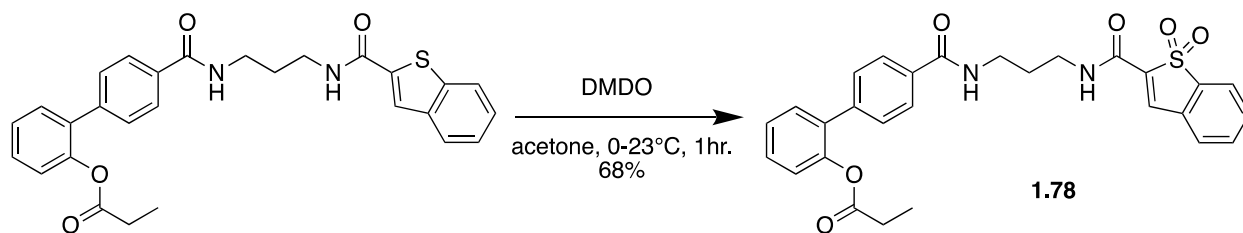
¹H NMR (300 MHz, CDCl₃) δ 7.92 (d, *J* = 8.4 Hz, 2H), 7.87 (s, 1H), 7.81 – 7.74 (m, 2H), 7.69 – 7.60 (m, 2H), 7.52 (dd, *J* = 8.4, 4.8 Hz, 3H), 7.45 – 7.37 (m, 2H), 7.35 (dd, *J* = 7.0, 1.4 Hz, 1H), 7.21 (t, *J* = 5.1 Hz, 1H), 7.15 (d, *J* = 9.3 Hz, 1H), 6.93 (t, *J* = 5.2 Hz, 1H), 3.59 (td, *J* = 12.3, 6.2 Hz, 4H), 2.10 (s, 3H), 1.96 – 1.84 (m, 2H).



4'-((3-(1,1-dioxidocinnamamido)propyl)carbamoyle)-[1,1'-biphenyl]-2-yl 2-phenylacetate (1.77)

General Procedure B: DMSO oxidation

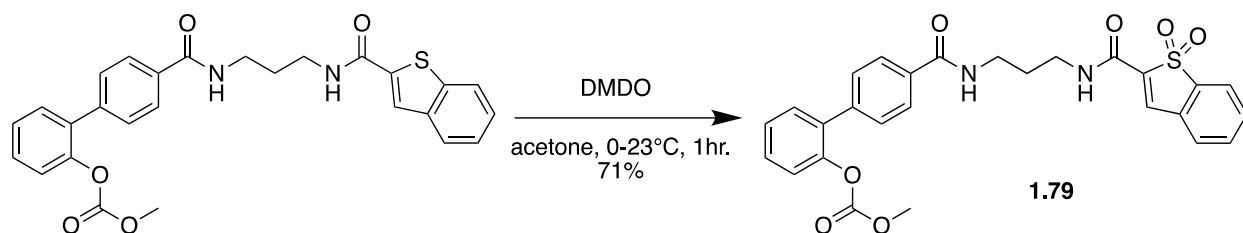
¹H NMR (300 MHz, CDCl₃) δ 7.88 (s, 1H), 7.82 (d, *J* = 8.3 Hz, 2H), 7.78 (dd, *J* = 6.5, 3.1 Hz, 1H), 7.66 (dd, *J* = 5.5, 3.1 Hz, 2H), 7.53 (dd, *J* = 5.5, 2.9 Hz, 1H), 7.44 – 7.38 (m, 4H), 7.37 – 7.29 (m, 4H), 7.23 – 7.10 (m, 4H), 7.00 (t, *J* = 5.8 Hz, 1H), 3.65 (s, 2H), 3.62 (dt, *J* = 11.4, 6.6 Hz, 4H), 1.99 – 1.87 (m, 2H).



**4'-((3-(1,1-dioxidocinnamamido)propyl)carbamoyle)-[1,1'-biphenyl]-2-yl
propionate (1.78)**

General Procedure B: DMSO oxidation

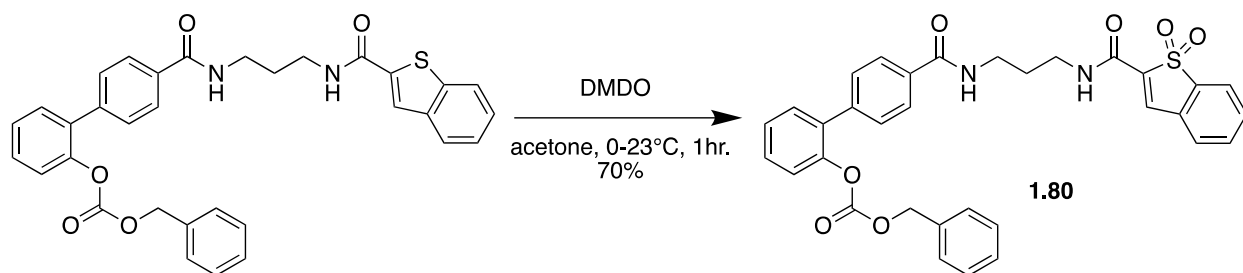
¹H NMR (300 MHz, CDCl₃) δ 7.94 (d, *J* = 8.3 Hz, 2H), 7.89 (s, 1H), 7.79 (dd, *J* = 5.2, 3.5 Hz, 1H), 7.71 – 7.63 (m, 2H), 7.59 – 7.54 (m, 1H), 7.52 (d, *J* = 8.3 Hz, 2H), 7.43 (ddd, *J* = 6.7, 4.0, 1.9 Hz, 2H), 7.38 – 7.31 (m, 1H), 7.23 (t, *J* = 5.9 Hz, 1H), 7.17 (d, *J* = 7.8 Hz, 1H), 6.97 (t, *J* = 5.9 Hz, 1H), 3.60 (td, *J* = 11.9, 6.3 Hz, 4H), 2.41 (q, *J* = 7.6 Hz, 2H), 2.01 – 1.81 (m, 2H), 1.09 (t, *J* = 7.6 Hz, 3H).



4'-((3-(1,1-dioxidocinnamamido)propyl)carbamoyl)-[1,1'-biphenyl]-2-yl methyl carbonate (1.79)

General Procedure B: DMSO oxidation

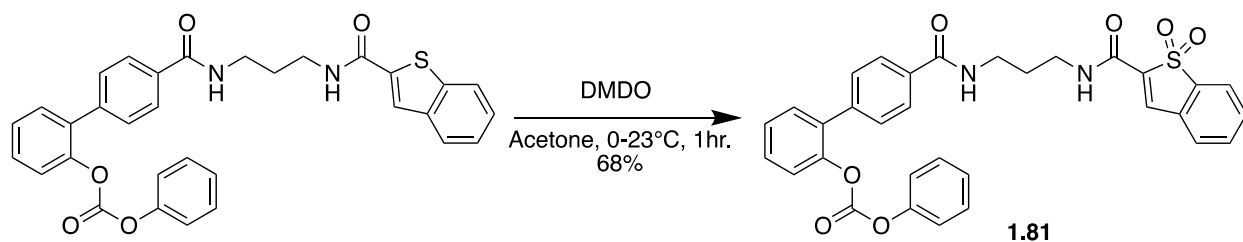
¹H NMR (599 MHz, CDCl₃) δ 7.86 (d, *J* = 8.3 Hz, 2H), 7.80 (s, 1H), 7.70 (dd, *J* = 5.2, 3.4 Hz, 1H), 7.66 – 7.62 (m, 2H), 7.61 – 7.56 (m, 2H), 7.48 (d, *J* = 8.9 Hz, 2H), 7.47 – 7.44 (m, 2H), 7.35 (t, *J* = 7.6 Hz, 2H), 7.29 (t, *J* = 6.9 Hz, 1H), 7.13 (s, 1H), 6.87 (s, 1H), 3.66 (s, 3H), 3.54 (dd, *J* = 12.1, 6.5 Hz, 2H), 3.50 (dd, *J* = 12.2, 6.3 Hz, 2H), 1.64 – 1.58 (m, 2H).



benzyl (4'-((3-(1,1-dioxidocinnamamido)propyl)carbamoyl)-[1,1'-biphenyl]-2-yl) carbonate (1.80)

General Procedure B: DMSO oxidation

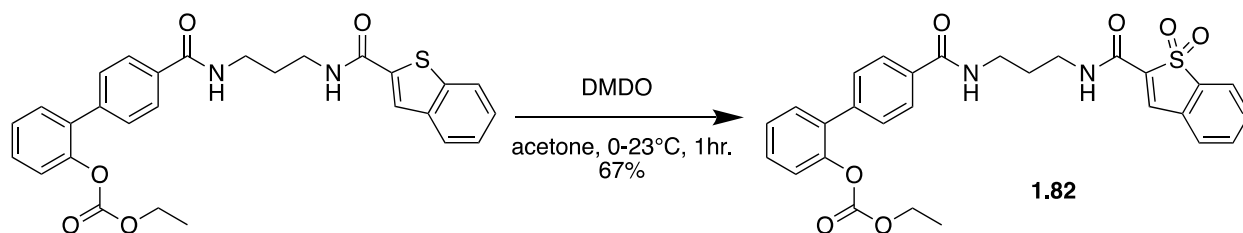
¹H NMR (599 MHz, CDCl₃) δ 7.87 (s, 1H), 7.86 (d, *J* = 5.3 Hz, 2H), 7.79 – 7.73 (m, 1H), 7.66 – 7.61 (m, 2H), 7.53 – 7.48 (m, 3H), 7.43 – 7.38 (m, 2H), 7.37 – 7.29 (m, 4H), 7.25 – 7.22 (m, 3H), 7.20 (s, 1H), 6.98 (s, 1H), 5.09 (s, 2H), 3.62 – 3.55 (m, 4H), 1.94 – 1.87 (m, 2H). **¹³C NMR** (151 MHz, CDCl₃) δ 167.3, 158.1, 153.3, 148.0, 140.2, 137.0, 136.9, 136.5, 134.7, 134.3, 133.8, 133.4, 132.4, 130.9, 129.2, 129.2, 129.1, 128.6, 128.6, 128.3, 127.2, 127.1, 126.8, 122.5, 122.0, 70.3, 36.8, 36.2, 29.6.



4'-((3-(1,1-dioxidocinnamamido)propyl)carbonyl)-[1,1'-biphenyl]-2-yl phenyl carbonate (1.81)

General Procedure B: DMSO oxidation

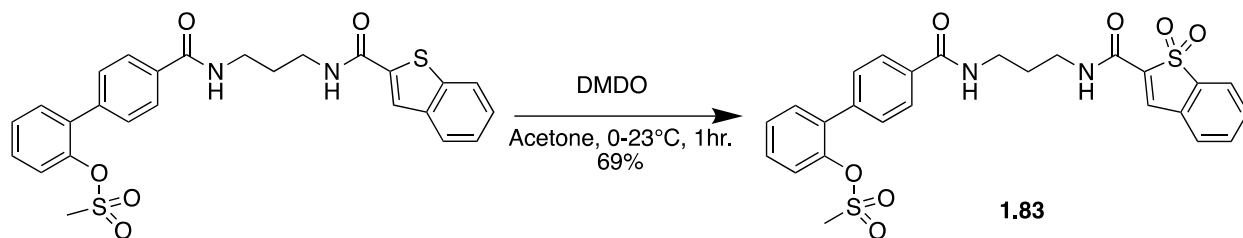
¹H NMR (599 MHz, CDCl₃) δ 7.96 (d, *J* = 8.3 Hz, 1H), 7.84 (s, 1H), 7.75 – 7.69 (m, 1H), 7.59 (dd, *J* = 5.6, 3.0 Hz, 1H), 7.57 (d, *J* = 8.3 Hz, 1H), 7.46 (dd, *J* = 5.7, 2.7 Hz, 1H), 7.44 – 7.39 (m, 2H), 7.37 (d, *J* = 6.9 Hz, 1H), 7.35 – 7.32 (m, 1H), 7.29 (t, *J* = 8.0 Hz, 1H), 7.16 (dd, *J* = 14.0, 6.8 Hz, 1H), 6.95 (d, *J* = 7.8 Hz, 1H), 3.61 – 3.50 (m, 4H), 1.89 – 1.80 (m, 2H). **¹³C NMR** (151 MHz, CDCl₃) δ 167.5, 158.2, 151.7, 150.9, 148.0, 140.2, 137.1, 136.9, 136.2, 134.3, 133.8, 133.6, 132.5, 131.0, 129.6, 129.4, 129.3, 129.1, 127.4, 127.2, 127.2, 126.4, 122.4, 122.0, 120.8, 53.6, 36.8, 36.4, 29.6.



4'-((3-(1,1-dioxidocinnamamido)propyl)carbamoxy)-[1,1'-biphenyl]-2-yl ethyl carbonate (1.82)

General Procedure B: DMSO oxidation

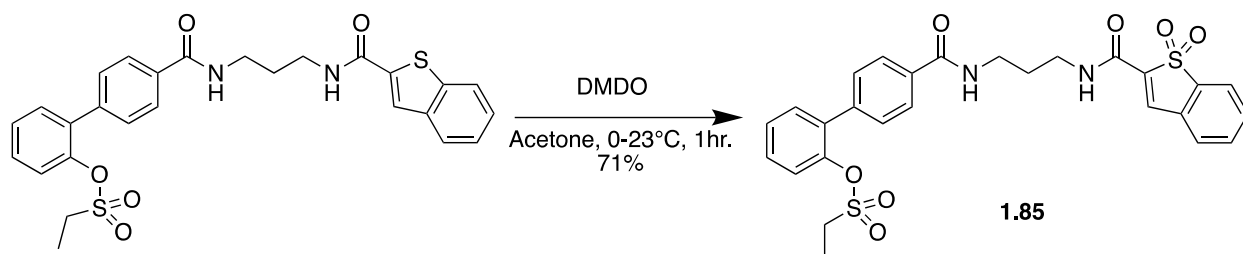
¹H NMR (599 MHz, CDCl₃) δ 7.93 (d, *J* = 8.3 Hz, 2H), 7.86 (s, 1H), 7.76 (dt, *J* = 7.8, 3.8 Hz, 1H), 7.68 – 7.62 (m, 2H), 7.54 (d, *J* = 8.3 Hz, 2H), 7.53 – 7.50 (m, 2H), 7.41 (t, *J* = 7.6 Hz, 2H), 7.37 – 7.33 (m, 1H), 7.25 (d, *J* = 8.1 Hz, 1H), 7.22 (t, *J* = 6.2 Hz, 1H), 6.95 (t, *J* = 6.1 Hz, 1H), 4.12 (q, *J* = 7.1 Hz, 2H), 3.60 (dd, *J* = 12.4, 6.3 Hz, 2H), 3.56 (dd, *J* = 12.2, 6.2 Hz, 2H), 1.92 – 1.86 (m, 2H), 1.20 (t, *J* = 7.1 Hz, 3H).



**4'-((3-(1,1-dioxidocinnamamido)propyl)carbamoyl)-[1,1'-biphenyl]-2-yl
methanesulfonate (1.83)**

General Procedure B: DMSO oxidation

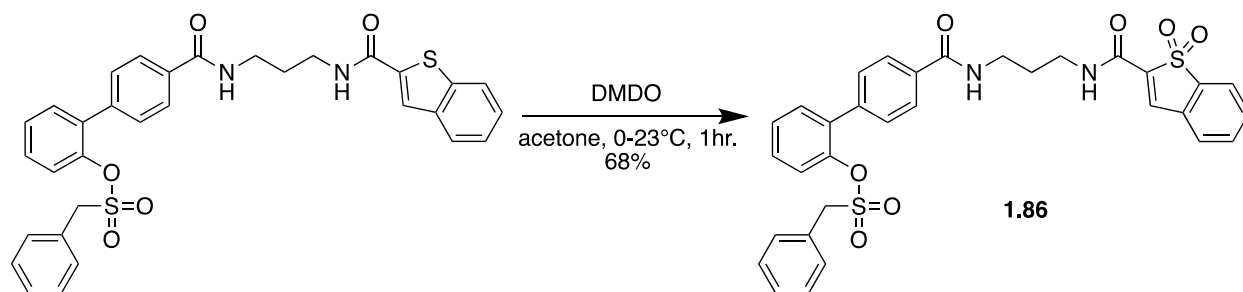
¹H NMR (599 MHz, CDCl₃) δ 7.92 (d, *J* = 7.9 Hz, 2H), 7.82 (s, 1H), 7.73 – 7.68 (m, 1H), 7.61 – 7.57 (m, 2H), 7.55 (d, *J* = 8.0 Hz, 2H), 7.48 – 7.45 (m, 1H), 7.43 (d, *J* = 7.4 Hz, 1H), 7.38 (t, *J* = 8.3 Hz, 3H), 7.37 – 7.32 (m, 1H), 7.28 – 7.24 (m, 1H), 6.85 (t, *J* = 6.7 Hz, 1H), 3.55 (dd, *J* = 11.9, 6.3 Hz, 2H), 3.51 (dd, *J* = 11.3, 5.7 Hz, 2H), 2.54 (s, 3H), 1.88 – 1.80 (m, 2H).



**4'-((3-(1,1-dioxidocinnamamido)propyl)carbamoyl)-[1,1'-biphenyl]-2-yl
ethanesulfonate (1.85)**

General Procedure B: DMDO oxidation

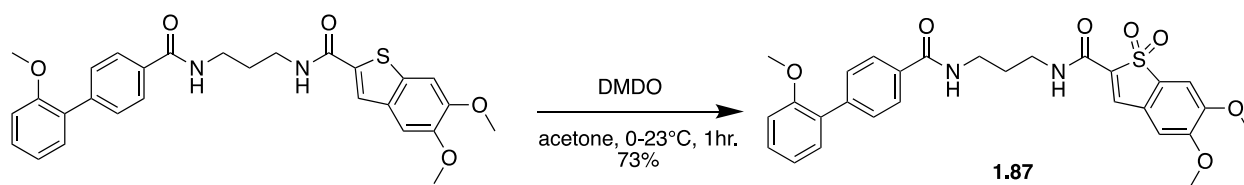
¹H NMR (599 MHz, CDCl₃) δ 7.96 (d, *J* = 8.2 Hz, 2H), 7.88 (s, 1H), 7.78 – 7.73 (m, 1H), 7.66 – 7.62 (m, 2H), 7.58 (d, *J* = 8.2 Hz, 2H), 7.53 (dd, *J* = 5.6, 2.5 Hz, 1H), 7.51 (d, *J* = 7.3 Hz, 1H), 7.41 (ddd, *J* = 17.1, 8.0, 4.1 Hz, 3H), 7.36 (dd, *J* = 11.6, 5.5 Hz, 1H), 7.03 (t, *J* = 5.9 Hz, 1H), 3.57 (tt, *J* = 12.0, 6.1 Hz, 4H), 2.82 (q, *J* = 7.4 Hz, 2H), 1.92 – 1.86 (m, 2H), 1.15 (t, *J* = 7.4 Hz, 3H). **¹³C NMR** (151 MHz, CDCl₃) δ 167.2, 158.1, 146.1, 140.1, 137.0, 136.8, 136.5, 134.3, 134.2, 133.7, 132.5, 131.3, 129.7, 129.4, 129.1, 127.5, 127.2, 127.2, 123.5, 122.0, 45.9, 36.8, 36.3, 29.5, 7.8.



**4'-((3-(1,1-dioxidocinnamamido)propyl)carbamoyle)-[1,1'-biphenyl]-2-yl
phenylmethanesulfonate (1.86)**

General Procedure B: DMDO oxidation

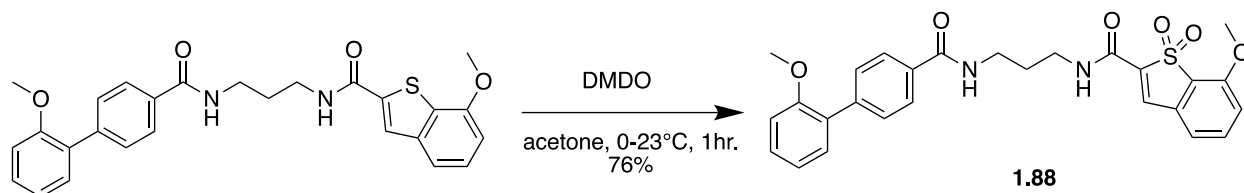
¹H NMR (599 MHz, CDCl₃) δ 7.95 (d, *J* = 8.3 Hz, 2H), 7.86 (s, 1H), 7.76 (dt, *J* = 7.8, 3.8 Hz, 1H), 7.66 – 7.62 (m, 2H), 7.58 (d, *J* = 8.3 Hz, 2H), 7.54 – 7.50 (m, 1H), 7.42 (dt, *J* = 9.8, 3.0 Hz, 1H), 7.41 – 7.36 (m, 3H), 7.33 (ddd, *J* = 14.4, 7.1, 2.1 Hz, 4H), 7.23 (d, *J* = 7.1 Hz, 2H), 6.97 (t, *J* = 6.0 Hz, 1H), 4.04 (s, 2H), 3.60 (dd, *J* = 12.9, 6.9 Hz, 2H), 3.56 (dd, *J* = 12.3, 6.4 Hz, 2H), 1.93 – 1.86 (m, 2H).



5,6-dimethoxy-N-(3-(2'-methoxy-[1,1'-biphenyl]-4-carboxamido)propyl)cinnamamide 1,1-dioxide (1.87)

General Procedure B: DMSO oxidation

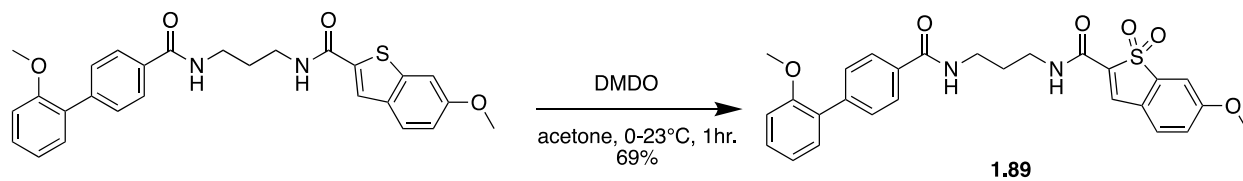
¹H NMR (599 MHz, CDCl₃) δ 7.90 (d, *J* = 8.2 Hz, 2H), 7.73 (s, 1H), 7.60 (d, *J* = 8.2 Hz, 2H), 7.34 (t, *J* = 7.8 Hz, 1H), 7.29 (dd, *J* = 17.0, 6.8 Hz, 2H), 7.22 (s, 1H), 7.03 (t, *J* = 7.4 Hz, 1H), 6.98 (dd, *J* = 13.0, 7.2 Hz, 2H), 6.91 (s, 1H), 3.97 (s, 3H), 3.92 (s, 3H), 3.80 (s, 3H), 3.60 – 3.51 (m, 4H), 1.87 (dd, *J* = 12.0, 6.2 Hz, 2H).



**7-methoxy-N-(3-(2'-methoxy-[1,1'-biphenyl]-4-carboxamido)propyl)cinnamamide
1,1-dioxide (1.88)**

General Procedure B: DMSO oxidation

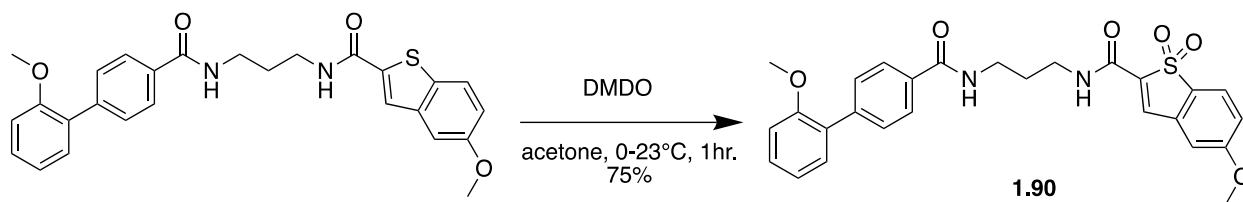
¹H NMR (599 MHz, CDCl₃) δ 7.91 (d, *J* = 8.2 Hz, 2H), 7.76 (s, 1H), 7.61 (d, *J* = 8.2 Hz, 2H), 7.58 – 7.54 (m, 1H), 7.34 (dd, *J* = 16.7, 7.8 Hz, 2H), 7.22 (s, 1H), 7.11 (d, *J* = 8.5 Hz, 1H), 7.05 (t, *J* = 8.1 Hz, 2H), 7.00 (d, *J* = 8.2 Hz, 1H), 6.89 (s, 1H), 4.02 (s, 3H), 3.82 (s, 3H), 3.60 (dd, *J* = 12.4, 6.3 Hz, 2H), 3.55 (dd, *J* = 12.1, 6.2 Hz, 2H), 1.91 – 1.86 (m, 2H).



**6-methoxy-N-(3-(2'-methoxy-[1,1'-biphenyl]-4-carboxamido)propyl)cinnamamide
1,1-dioxide (1.89)**

General Procedure B: DMSO oxidation

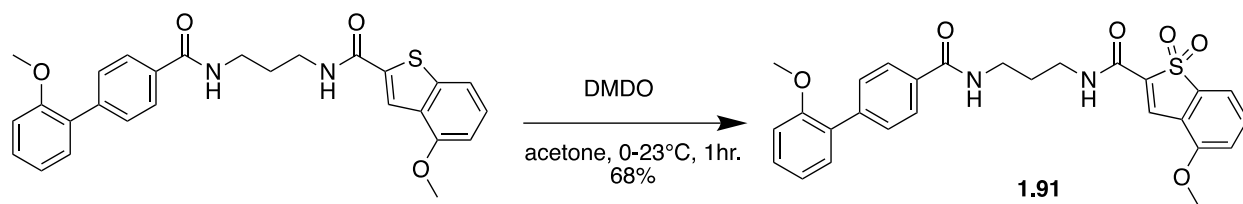
¹H NMR (599 MHz, CDCl₃) δ 7.83 (d, *J* = 8.2 Hz, 2H), 7.75 (s, 1H), 7.53 (d, *J* = 8.2 Hz, 2H), 7.33 (d, *J* = 8.4 Hz, 1H), 7.30 – 7.25 (m, 1H), 7.25 – 7.20 (m, 2H), 7.20 (d, *J* = 1.7 Hz, 1H), 6.99 (dd, *J* = 8.4, 2.2 Hz, 1H), 6.97 (t, *J* = 7.4 Hz, 2H), 6.91 (t, *J* = 8.4 Hz, 1H), 3.83 (s, 3H), 3.73 (s, 3H), 3.53 – 3.45 (m, 4H), 1.84 – 1.77 (m, 2H).



**5-methoxy-N-(3-(2'-methoxy-[1,1'-biphenyl]-4-carboxamido)propyl)cinnamamide
1,1-dioxide (1.90)**

General Procedure B: DMSO oxidation

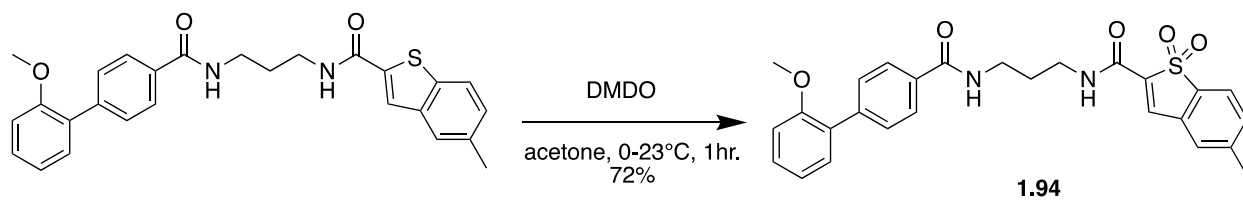
¹H NMR (599 MHz, CDCl₃) δ 7.89 (d, *J* = 8.2 Hz, 2H), 7.75 (s, 1H), 7.64 (d, *J* = 8.5 Hz, 1H), 7.59 (d, *J* = 8.2 Hz, 2H), 7.34 (t, *J* = 7.8 Hz, 1H), 7.29 (dd, *J* = 13.8, 7.3 Hz, 2H), 7.09 (t, *J* = 6.0 Hz, 1H), 7.05 – 7.01 (m, 2H), 6.99 (d, *J* = 8.2 Hz, 1H), 6.96 (d, *J* = 2.0 Hz, 1H), 3.86 (s, 3H), 3.80 (s, 3H), 3.55 (td, *J* = 11.9, 6.2 Hz, 4H), 1.90 – 1.84 (m, 2H).



**4-methoxy-N-(3-(2'-methoxy-[1,1'-biphenyl]-4-carboxamido)propyl)cinnamamide
1,1-dioxide (1.91)**

General Procedure B: DMSO oxidation

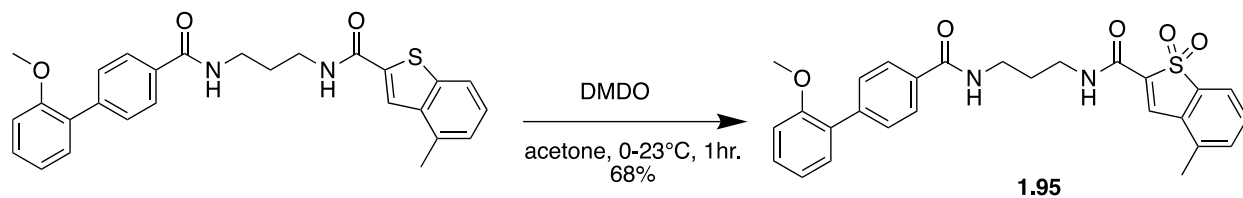
¹H NMR (599 MHz, CDCl₃) δ 8.10 (s, 1H), 7.91 (d, *J* = 8.0 Hz, 2H), 7.65 – 7.52 (m, 3H), 7.37 – 7.28 (m, 4H), 7.11 (d, *J* = 8.4 Hz, 1H), 7.04 (t, *J* = 7.4 Hz, 1H), 6.99 (d, *J* = 8.2 Hz, 1H), 6.92 (s, 1H), 3.93 (s, 3H), 3.81 (s, 3H), 3.60 – 3.52 (m, 4H), 1.92 – 1.84 (m, 2H).



N-(3-(2'-methoxy-[1,1'-biphenyl]-4-carboxamido)propyl)-5-methylcinnamamide 1,1-dioxide (1.94)

General Procedure B: DMSO oxidation

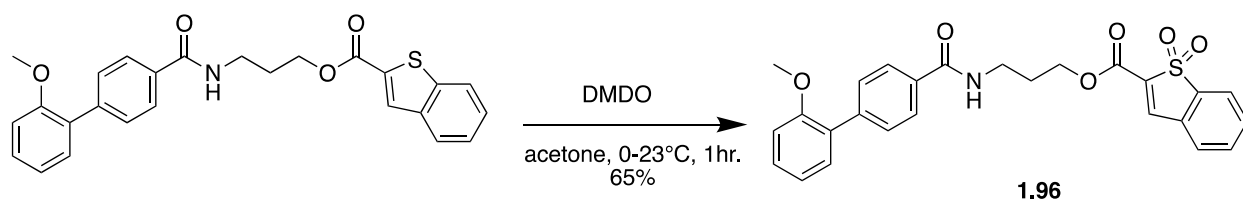
¹H NMR (599 MHz, CDCl₃) δ 7.91 (d, *J* = 8.2 Hz, 2H), 7.80 (s, 1H), 7.64 (d, *J* = 7.8 Hz, 1H), 7.61 (d, *J* = 8.2 Hz, 2H), 7.42 (d, *J* = 7.8 Hz, 1H), 7.35 (t, *J* = 8.6 Hz, 1H), 7.34 – 7.32 (m, 1H), 7.30 (s, 1H), 7.18 (t, *J* = 6.0 Hz, 1H), 7.05 (t, *J* = 7.4 Hz, 1H), 7.00 (d, *J* = 8.2 Hz, 1H), 6.92 (t, *J* = 6.1 Hz, 1H), 3.82 (s, 3H), 3.59 (q, *J* = 6.4 Hz, 2H), 3.56 (dd, *J* = 13.0, 7.1 Hz, 2H), 2.46 (s, 3H), 1.92 – 1.86 (m, 2H).



N-(3-(2'-methoxy-[1,1'-biphenyl]-4-carboxamido)propyl)-4-methylcinnamamide 1,1-dioxide (1.95)

General Procedure B: DMDO oxidation

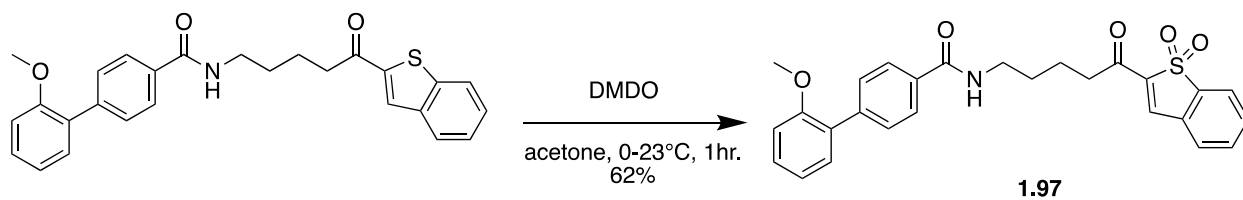
¹H NMR (599 MHz, CDCl₃) δ 8.04 (s, 1H), 7.91 (d, *J* = 8.2 Hz, 2H), 7.60 (d, *J* = 8.2 Hz, 2H), 7.56 (d, *J* = 7.5 Hz, 1H), 7.50 (t, *J* = 7.6 Hz, 1H), 7.42 (d, *J* = 7.7 Hz, 1H), 7.34 (t, *J* = 7.8 Hz, 1H), 7.31 (d, *J* = 7.0 Hz, 2H), 7.04 (q, *J* = 7.5 Hz, 2H), 6.99 (d, *J* = 8.2 Hz, 1H), 3.80 (s, 3H), 3.58 (dd, *J* = 12.3, 6.2 Hz, 2H), 3.55 (dd, *J* = 12.0, 6.1 Hz, 2H), 2.47 (s, 3H), 1.90 – 1.84 (m, 2H).



3-(2'-methoxy-[1,1'-biphenyl]-4-carboxamido)propyl cinnamate 1,1-dioxide (1.96)

General Procedure B: DMDO oxidation

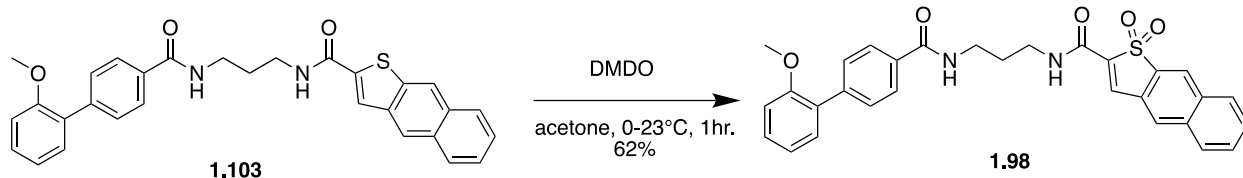
¹H NMR (599 MHz, CDCl₃) δ 7.95 (s, 1H), 7.85 (d, *J* = 8.3 Hz, 2H), 7.75 (d, *J* = 7.5 Hz, 1H), 7.66 (t, *J* = 7.4 Hz, 1H), 7.60 (t, *J* = 7.4 Hz, 1H), 7.56 (d, *J* = 8.3 Hz, 2H), 7.48 (d, *J* = 7.4 Hz, 1H), 7.36 – 7.31 (m, 1H), 7.28 (dd, *J* = 7.5, 1.7 Hz, 1H), 7.02 (d, *J* = 7.4 Hz, 1H), 6.98 (d, *J* = 8.2 Hz, 1H), 6.86 (t, *J* = 5.7 Hz, 1H), 4.50 (t, *J* = 6.0 Hz, 2H), 3.79 (s, 3H), 3.66 (q, *J* = 6.2 Hz, 2H), 2.14 (p, *J* = 6.2 Hz, 2H).



N-(5-(1,1-dioxidobenzo[b]thiophen-2-yl)-5-oxopentyl)-2'-methoxy-[1,1'-biphenyl]-4-carboxamide (1.97)

General Procedure B: DMDO oxidation

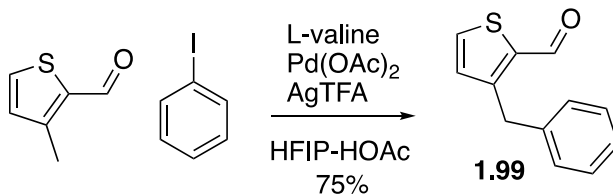
¹H NMR (599 MHz, CDCl₃) δ 7.92 (s, 1H), 7.82 (d, *J* = 8.2 Hz, 2H), 7.75 (d, *J* = 7.4 Hz, 1H), 7.66 (t, *J* = 7.5 Hz, 1H), 7.62 (t, *J* = 7.4 Hz, 1H), 7.58 (d, *J* = 8.2 Hz, 2H), 7.54 (d, *J* = 7.4 Hz, 1H), 7.37 – 7.32 (m, 1H), 7.31 (d, *J* = 7.5 Hz, 1H), 7.03 (t, *J* = 7.4 Hz, 1H), 6.99 (d, *J* = 8.2 Hz, 1H), 3.80 (s, 3H), 3.52 (q, *J* = 6.5 Hz, 2H), 2.97 (t, *J* = 7.1 Hz, 2H), 1.90 – 1.79 (m, 2H), 1.73 (p, *J* = 6.9 Hz, 2H).



N-(3-(2'-methoxy-[1,1'-biphenyl]-4-carboxamido)propyl)naphtho[2,3-b]thiophene-2-carboxamide 1,1-dioxide (1.98)

General Procedure B: DMSO oxidation

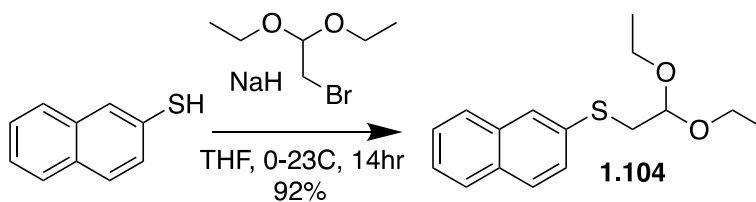
¹H NMR (599 MHz, CDCl₃) δ 8.51 (s, 1H), 8.16 (t, *J* = 7.5 Hz, 2H), 7.99 (d, *J* = 8.0 Hz, 1H), 7.94 (d, *J* = 8.2 Hz, 2H), 7.80 (d, *J* = 8.4 Hz, 1H), 7.75 (t, *J* = 7.1 Hz, 1H), 7.72 (dd, *J* = 13.3, 6.0 Hz, 1H), 7.63 (d, *J* = 8.2 Hz, 2H), 7.38 – 7.34 (m, 1H), 7.33 (dd, *J* = 7.5, 1.4 Hz, 1H), 7.20 (t, *J* = 5.9 Hz, 1H), 7.05 (t, *J* = 7.4 Hz, 1H), 7.00 (d, *J* = 8.3 Hz, 1H), 6.98 (s, 1H), 3.82 (s, 3H), 3.65 (dd, *J* = 12.4, 6.3 Hz, 2H), 3.60 (dd, *J* = 12.1, 6.2 Hz, 2H), 1.96 – 1.89 (m, 2H).



3-benzylthiophene-2-carbaldehyde (1.99)

To a 50mL pressure flask with a stir bar was added 3-methylthiophene-2-carbaldehyde (500 mg, 1 Eq, 3.96 mmol), iodobenzene (1.21 g, 665 μ L, 1.5 Eq, 5.94 mmol), palladium(II) acetate (89.0 mg, 0.1 Eq, 396 μ mol), and silver trifluoroacetate (1.31 g, 1.5 Eq, 5.94 mmol), followed by a mixture of 1,1,1,3,3,3-Hexafluoroisopropanol (20 mL) and Acetic Acid (2.2 mL) at 23 °C. The reaction was degassed by bubbling argon through the solvent for around 2 minutes while vigorously stirring, after which the reaction flask was sealed and stirred for 15 minutes at 23 °C. The reaction was then heated to 110 °C for 14 hour, upon completion the reaction was cooled and diluted with EtOAc (150mL). The diluted reaction mixture was passed through celite and concentrated under reduced pressure. The residue was purified by silica gel chromatography (Hex:EtOAc (100-95%)) to yield **1.99** (0.60 g, 3.0 mmol, 75 %) as a yellow oil.

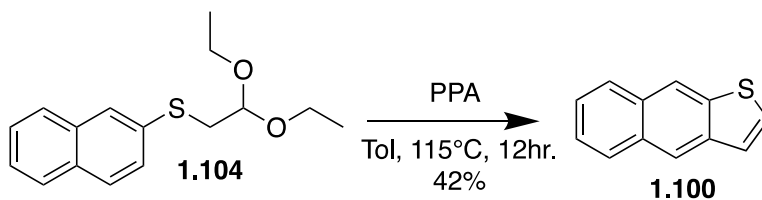
$R_f = 0.5$ (Hex:EtOAc (9:1)) $^1\text{H NMR}$ (599 MHz, CDCl_3) δ 10.09 (s, 1H), 7.64 (d, $J = 4.8$ Hz, 1H), 7.31 (t, $J = 7.7$ Hz, 2H), 7.23 (t, $J = 7.2$ Hz, 1H), 7.19 (d, $J = 7.5$ Hz, 2H), 6.94 (d, $J = 4.8$ Hz, 1H), 4.34 (s, 2H).



(2,2-diethoxyethyl)(naphthalen-2-yl)sulfane (1.104)

To a stirring solution of naphthalene-2-thiol (2150 mg, 1 Eq, 13.42 mmol) in THF (100 mL) at 0 °C was added sodium hydride (697.7 mg, 60% Wt, 1.3 Eq, 17.44 mmol) portionwise. The reaction was allowed to come to 23 °C and was stirred until no more hydrogen gas bubble could be detected (30 min). To the reaction was added 2-bromo-1,1-diethoxyethane (3.966 g, 3.1 mL, 1.5 Eq, 20.13 mmol) and stirred 14 hour. Upon completion the excess hydride was quenched with the slow addition of DI water (100mL). The organic layer was separated, washed with brine (100mL), dried by Na₂SO₄, filtered, and concentrated under reduced pressure. The residue was purified by silica gel chromatography (Hex:EtOAc (100-94%)) to yield **1.104** (3.4 g, 12 mmol, 92 %).

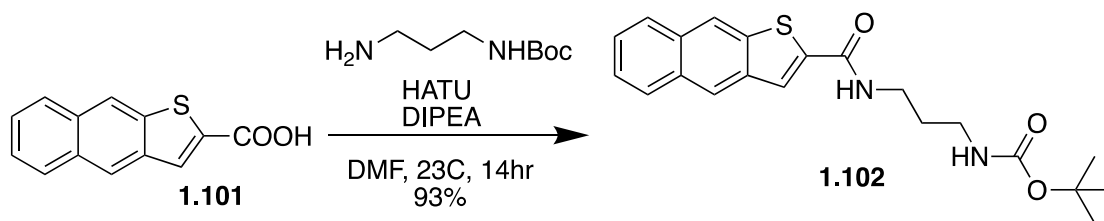
¹H NMR (599 MHz, CDCl₃) δ 7.81 (s, 1H), 7.78 (d, *J* = 8.3 Hz, 1H), 7.74 (dd, *J* = 8.6, 4.2 Hz, 2H), 7.47 (t, *J* = 7.2 Hz, 2H), 7.43 (t, *J* = 6.8 Hz, 1H), 4.71 (t, *J* = 5.7 Hz, 1H), 3.70 (dq, *J* = 9.2, 7.0 Hz, 2H), 3.57 (dq, *J* = 9.6, 7.0 Hz, 2H), 3.25 (d, *J* = 5.7 Hz, 2H), 1.21 (t, *J* = 7.0 Hz, 6H).



naphtho[2,3-*b*]thiophene (**1.100**)

A mixture of **1.104** (3.4 g, 1 Eq, 12 mmol) and polyphosphoric acid (1.3 g, 0.64 mL, 0.6 Eq, 7.4 mmol) in Toluene (40 mL) was heated to 110 °C for 12 hour. Upon completion the reaction was diluted with EtOAc (40mL), washed with brine (80mL), dried with Na₂SO₄, filtered, and concentrated in vacuo. The residue was purified by silica gel chromatography (Hex (100%)) to yield **1.100** (0.95 g, 5.2 mmol, 42 %).

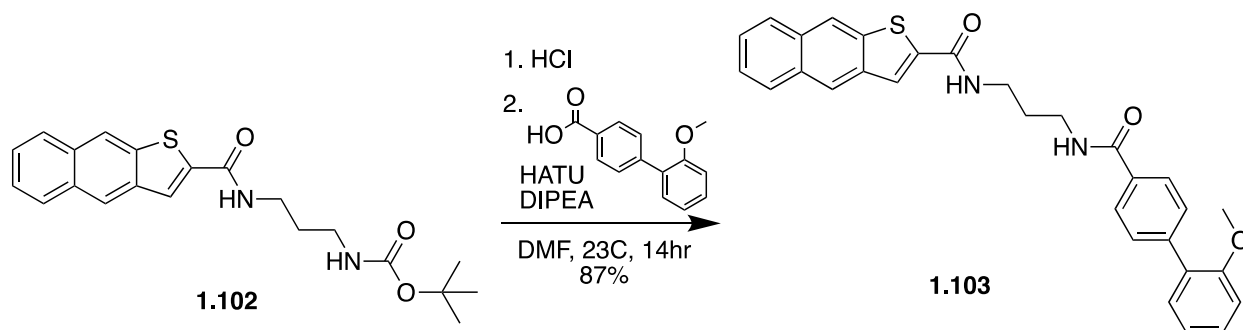
¹H NMR (599 MHz, CDCl₃) δ 8.36 (d, *J* = 8.3 Hz, 1H), 8.01 (d, *J* = 5.7 Hz, 1H), 7.97 (d, *J* = 7.9 Hz, 1H), 7.91 (d, *J* = 8.8 Hz, 1H), 7.76 (d, *J* = 8.8 Hz, 1H), 7.63 (t, *J* = 7.0 Hz, 1H), 7.60 (d, *J* = 5.3 Hz, 1H), 7.56 (t, *J* = 7.5 Hz, 1H).



***tert*-butyl (3-(naphtho[2,3-*b*]thiophene-2-carboxamido)propyl)carbamate (1.102)**

A solution of 1.101 (200 mg, 1 Eq, 876 μ mol), HATU (500 mg, 1.5 Eq, 1.31 mmol), and DIPEA (340 mg, 458 μ L, 3 Eq, 2.63 mmol) were stirred in DMF (15 mL) for 15 minutes before adding *tert*-butyl (3-aminopropyl)carbamate (198 mg, 1.3 Eq, 1.14 mmol) which was stirred at 23 °C for 14 hour. Upon completion the reaction was diluted with EtOAc (45mL), washed with DI water (4x45mL), brine (45mL), dried by Na₂SO₄, filtered, and concentrated under reduced pressure. The residue was purified by silica gel chromatography (DCM:MeOH (100-97%)) to yield **1.102** (0.31 g, 0.81 mmol, 93 %).

¹H NMR (599 MHz, CDCl₃) δ 8.54 (s, 1H), 8.29 (d, *J* = 7.9 Hz, 1H), 7.90 (d, *J* = 7.9 Hz, 1H), 7.80 (d, *J* = 8.8 Hz, 2H), 7.76 (d, *J* = 8.8 Hz, 1H), 7.71 (t, *J* = 6.4 Hz, 1H), 7.57 (d, *J* = 7.9 Hz, 1H), 7.52 (t, *J* = 7.5 Hz, 1H), 5.07 (t, *J* = 6.8 Hz, 1H), 3.56 (q, *J* = 6.4 Hz, 2H), 3.30 (q, *J* = 6.6 Hz, 2H), 1.76 (p, *J* = 6.6 Hz, 2H), 1.49 (s, 9H).

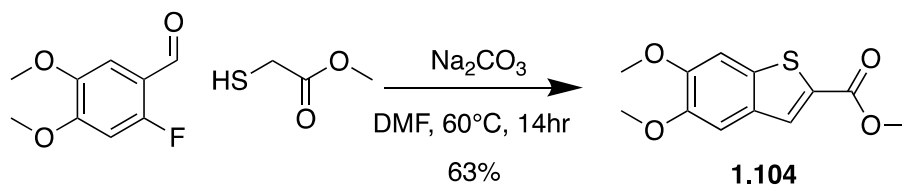


***N*-(3-(2'-methoxy-[1,1'-biphenyl]-4-carboxamido)propyl)naphtho[2,3-*b*]thiophene-2-carboxamide (1.103)**

To a stirring solution of HCl (4M in dioxane, 5mL) at 0 °C was added **1.102** (136.6 mg, 1 Eq, 355.3 μ mol). The reaction was allowed to come to 23 °C and consumption of starting material was monitored by TLC. Upon completion (15 min) the reaction was rotovaped to dryness. A separate flask of 2'-methoxy-[1,1'-biphenyl]-4-carboxylic acid (105.4 mg, 1.3 Eq, 461.9 μ mol), HATU (405.3 mg, 3 Eq, 1.066 mmol), and DIPEA (91.84 mg, 124 μ L, 2 Eq, 710.6 μ mol) were stirred in DMF (10 mL) for 15 minutes before adding the newly formed amine salt which was stirred at 23 °C for 14 hour. Upon completion the reaction was diluted with EtOAc (30mL), washed with DI water (4x30mL), brine (30mL), dried by Na₂SO₄, filtered, and concentrated under reduced pressure. The residue was purified by silica gel chromatography (DCM:MeOH (100-97%)) to yield **1.103** (0.15 g, 0.31 mmol, 87 %).

¹H NMR (599 MHz, CDCl₃) δ 8.60 (s, 1H), 8.32 (d, *J* = 7.9 Hz, 1H), 7.94 (d, *J* = 7.9 Hz, 2H), 7.92 (d, *J* = 7.9 Hz, 1H), 7.85 – 7.77 (m, 2H), 7.74 (t, *J* = 6.4 Hz, 1H), 7.61 (d, *J* = 8.3 Hz, 2H), 7.59 (d, *J* = 7.5 Hz, 1H), 7.53 (t, *J* = 7.5 Hz, 1H), 7.35 (t, *J* = 8.8 Hz, 1H), 7.28 (d, *J* = 7.5 Hz, 0H), 7.24 (t, *J* = 6.6 Hz, 1H), 7.03 (t, *J* = 7.5 Hz, 1H), 6.99 (d, *J* = 8.3

Hz, 1H), 3.79 (s, 3H), 3.65 (q, $J = 6.4$ Hz, 2H), 3.61 (q, $J = 6.4$ Hz, 2H), 1.88 (q, $J = 5.5$ Hz, 2H).

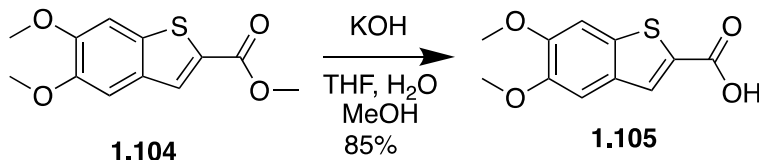


UTA148: methyl 5,6-dimethoxybenzo[b]thiophene-2-carboxylate (1.104)

General Procedure C: Domino Aldol-S_NAR

To a stirring mixture of 2-fluoro-4,5-dimethoxybenzaldehyde (1000 mg, 1 Eq, 5.430 mmol) and 2-fluoro-4,5-dimethoxybenzaldehyde (1000 mg, 1 Eq, 5.430 mmol) in DMF (15 mL) at 23 °C was added neat methyl 2-mercaptoacetate (633.9 mg, 533 μL, 1.1 Eq, 5.973 mmol) dropwise. After the reaction was heated to 60 °C for 14 hour, it was cooled to 23 °C, and then ice cold DI water (60mL) was poured in. The mixture was vigorously stirred for 15 minutes before filtering. The filtrate was washed with water and dried on high vac. The residue was purified by silica gel chromatography (Hex:EtOAc (90-50%)) to yield **1.104** (0.86 g, 3.4 mmol, 63 %).

¹H NMR (599 MHz, CDCl₃) δ 7.92 (s, 1H), 7.23 (s, 1H), 7.22 (s, 1H), 3.96 (s, 3H), 3.94 (s, 3H), 3.91 (s, 3H). **¹³C NMR** (151 MHz, CDCl₃) δ 163.4, 150.7, 148.9, 136.2, 132.4, 131.0, 130.5, 105.7, 103.5, 56.3, 56.2, 52.4. **HRMS**: m/z: [M+H]⁺ Calcd for [C₁₂H₁₃O₄S]⁺ Theo mass: 253.0529; Found: 253.0531

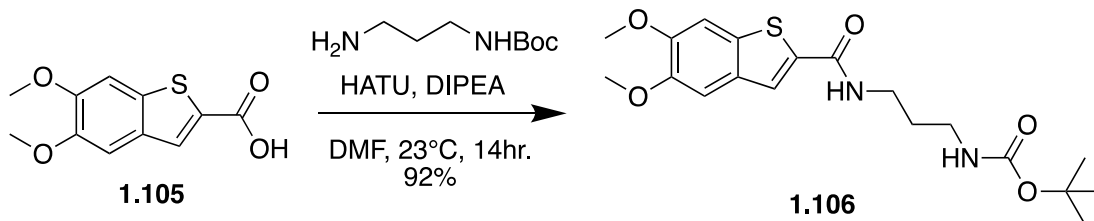


UTA166: 5,6-dimethoxybenzo[b]thiophene-2-carboxylic acid

General Procedure D: Saponification

To a solution of methyl 5,6-dimethoxybenzo[b]thiophene-2-carboxylate (605 mg, 1 Eq, 2.40 mmol) in a Methanol (5 mL)/THF (5 mL)/Water (5 mL) solvent mixture was added KOH (404 mg, 3 Eq, 7.19 mmol) and heated to 60 °C for 1 hour. Upon completion the reaction was cooled and concentrated to remove methanol. The reaction mixture was wash with diethyl ether (2x5 mL), brought to pH 3 with dilute HCl, and extracted with EtOAc (3x 5mL). The organic solution washed with brine (15mL), dried by Na₂SO₄, filtered, and concentrated under reduced pressure. The residue was purified by silica gel chromatography (DCM:MeOH (100-97%)) to yield 5,6-dimethoxybenzo[b]thiophene-2-carboxylic acid (0.49 g, 2.0 mmol, 85 %).

R_f = 0.15 (DCM:MeOH (9:1)) **¹H NMR** (599 MHz, MeOD) δ 7.93 (s, 1H), 7.43 (s, 1H), 7.40 (s, 1H), 3.92 (s, 3H), 3.90 (s, 3H). **¹³C NMR** (151 MHz, MeOD) δ 166.1, 152.1, 150.2, 137.7, 134.0, 131.5, 56.6, 56.5 **HRMS:** m/z: [M-H]⁻ Calcd for [C₁₁H₉O₄S]⁻ Theo mass: 237.0227; Found: 237.0227

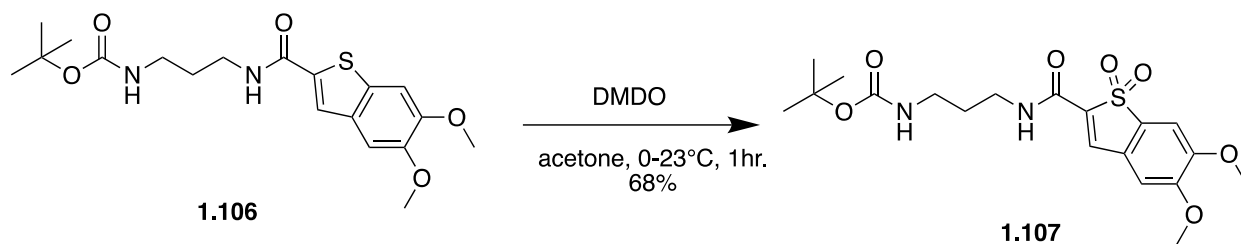


UTA237: tert-butyl (3-(5,6-dimethoxybenzo[b]thiophene-2-carboxamido)propyl)carbamate (1.106)

General Procedure E: HATU Amide Coupling

A solution of **1.105** (290 mg, 1 Eq, 1.22 mmol), HATU (694 mg, 1.5 Eq, 1.83 mmol), and DIPEA (472 mg, 636 μL , 3 Eq, 3.65 mmol) were stirred in DMF (15 mL) for 15 minutes before adding tert-butyl (3-aminopropyl)carbamate (276 mg, 1.3 Eq, 1.58 mmol) which was stirred at 23 $^\circ\text{C}$ for 14 hour. Upon completion the reaction was diluted with EtOAc (45mL), washed with DI water (4x45mL), brine (45mL), dried by Na_2SO_4 , filtered, and concentrated under reduced pressure. The residue was purified by silica gel chromatography (DCM:MeOH (100-97%)) to yield **1.106** (0.44 g, 1.1 mmol, 92 %).

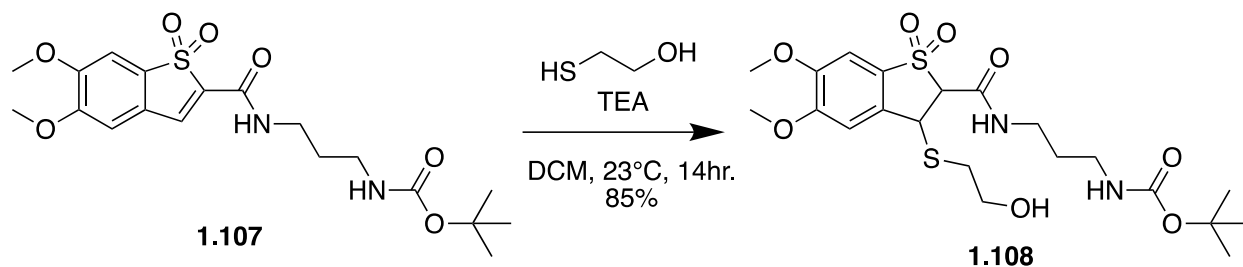
$^1\text{H NMR}$ (599 MHz, CDCl_3) δ 7.69 (s, 1H), 7.43 (s, 1H), 7.22 (s, 1H), 7.16 (s, 1H), 5.05 (s, 1H), 3.93 (s, 3H), 3.89 (s, 3H), 3.48 (dd, $J = 12.2, 6.2$ Hz, 2H), 3.24 (d, $J = 4.7$ Hz, 2H), 1.74 – 1.65 (m, 2H), 1.44 (s, 9H). **$^{13}\text{C NMR}$** (151 MHz, CDCl_3) δ 161.7, 156.1, 148.8, 147.5, 135.8, 133.5, 131.7, 123.6, 104.4, 102.6, 78.6, 55.1, 55.0, 36.0, 35.1, 29.2, 27.4 **HRMS**: m/z : $[\text{M}+\text{H}]^+$ Calcd for $[\text{C}_{19}\text{H}_{26}\text{O}_5\text{SNa}]^+$ Theo mass: 417.1455; Found: 417.1456



UTA239: tert-butyl (3-(5,6-dimethoxy-1,1-dioxidocinnamamido)propyl)carbamate (1.107)

General Procedure B: DMSO oxidation

¹H NMR (599 MHz, CDCl₃) δ 7.74 (s, 1H), 7.23 (s, 1H), 6.93 (s, 1H), 6.72 (s, 1H), 4.96 (s, 1H), 3.98 (s, 3H), 3.97 (s, 3H), 3.50 (dd, *J* = 6.4 Hz, 2H), 3.21 (d, *J* = 5.8 Hz, 2H), 1.77 (p, *J* = 6.5 Hz, 2H), 1.45 (s, 9H). **¹³C NMR** (151 MHz, CDCl₃) δ 157.7, 156.4, 153.5, 152.6, 136.3, 129.4, 122.5, 109.0, 104.8, 56.8, 56.7, 37.4, 37.0, 30.1, 28.5. **HRMS:** *m/z*: [M+MeOH+Na]⁺ Calcd for [C₂₀H₃₀N₂O₈SNa]⁺ Theo mass: 481.1615; Found: 481.1616

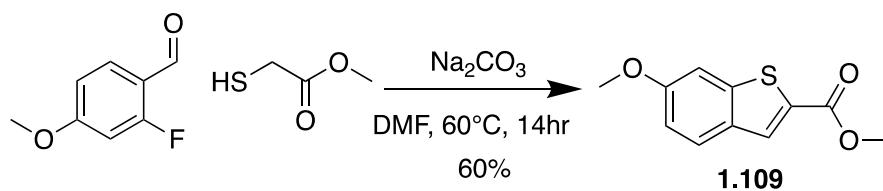


UTA252: tert-butyl (3-(3-((2-hydroxyethyl)thio)-5,6-dimethoxy-1,1-dioxido-2,3-dihydrobenzo[b]thiophene-2-carboxamido)propyl)carbamate (1.108)

General Procedure E: Thia-Micheal Addition

To a stirring solution of 2-mercaptoethan-1-ol (35 mg, 31 μ L, 2 Eq, 0.45 mmol) and triethylamine (45 mg, 62 μ L, 2 Eq, 0.45 mmol) in DCM (3 mL) was added **1.107** (95 mg, 1 Eq, 0.22 mmol). The reaction was left to stir at 23 °C for 14 hour. Upon completion to the reaction was washed with DI water (3x 5mL), brine (5mL), dried with MgSO₄, filtered. and concentrated under reduced pressure. The residue was purified by silica gel chromatography (DCM:MeOH (100-97%)) to yield **1.108** (96 mg, 0.19 mmol, 85 %).

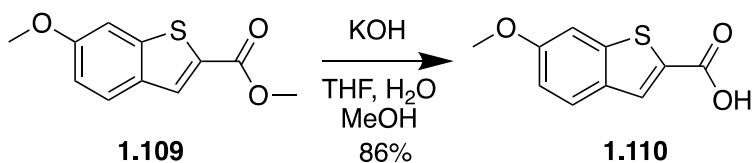
¹H NMR (599 MHz, CDCl₃) δ 7.43 (s, 1H), 7.12 (s, 1H), 7.06 (s, 1H), 5.08 (d, J = 6.1 Hz, 1H), 5.04 (s, 1H), 4.59 (d, J = 6.1 Hz, 1H), 3.94 (s, 3H), 3.90 (s, 3H), 3.80 – 3.71 (m, 2H), 3.45-3.33 (m, 2H), 3.22 – 3.11 (m, 2H), 2.79 – 2.68 (m, 2H), 1.71 – 1.62 (m, 2H), 1.40 (s, 9H). **¹³C NMR** (151 MHz, CDCl₃) δ 162.6, 156.7, 154.5, 150.8, 130.9, 129.3, 108.2, 102.1, 79.5, 73.5, 61.6, 56.5, 56.5, 44.3, 37.3, 34.1, 29.7, 28.5 **HRMS**: m/z : [M+Na]⁺ Calcd for [C₂₁H₃₂N₂O₈S₂Na]⁺ Theo mass: 527.1492; Found: 527.1490



UTA155: methyl 6-methoxybenzo[b]thiophene-2-carboxylate (1.109)

General Procedure C: Domino Aldol-S_NAR

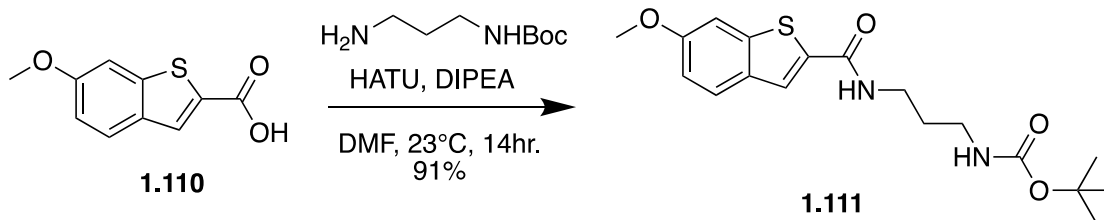
¹H NMR (599 MHz, MeOD) δ 7.99 (s, 1H), 7.80 (d, *J* = 8.8 Hz, 1H), 7.44 (d, *J* = 1.8 Hz, 1H), 7.04 (dd, *J* = 8.8, 2.2 Hz, 1H), 3.90 (s, 3H), 3.88 (s, 3H). ¹³C NMR (151 MHz, MeOD) δ 161.3, 145.7, 134.1, 131.7, 127.5, 117.1, 105.3, 56.1, 52.8. **HRMS:** *m/z*: [M+H]⁺ Calcd for [C₁₁H₁₁O₃S]⁺ Theo mass: 223.0423; Found: 223.0424



UTA165: 6-methoxybenzo[b]thiophene-2-carboxylic acid (1.110)

General Procedure D: Saponification

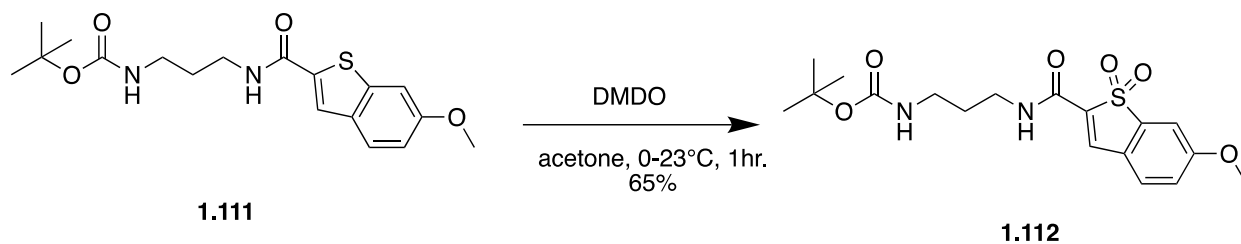
¹H NMR (599 MHz, DMSO) δ 8.00 (s, 1H), 7.87 (d, *J* = 8.8 Hz, 1H), 7.59 (d, *J* = 2.1 Hz, 1H), 7.06 (dd, *J* = 8.8, 2.3 Hz, 1H), 3.84 (s, 3H). **¹³C NMR** (151 MHz, DMSO) δ 163.7, 159.1, 143.5, 132.6, 131.9, 130.2, 126.6, 115.8, 104.9, 55.6. **HRMS**: *m/z*: [M-H]⁻ Calcd for [C₁₀H₇O₃S]⁻ Theo mass: 207.0121; Found: 207.0125



UTA229: tert-butyl (3-(6-methoxybenzo[b]thiophene-2-carboxamido)propyl)carbamate (1.111)

General Procedure E: HATU Amide Coupling

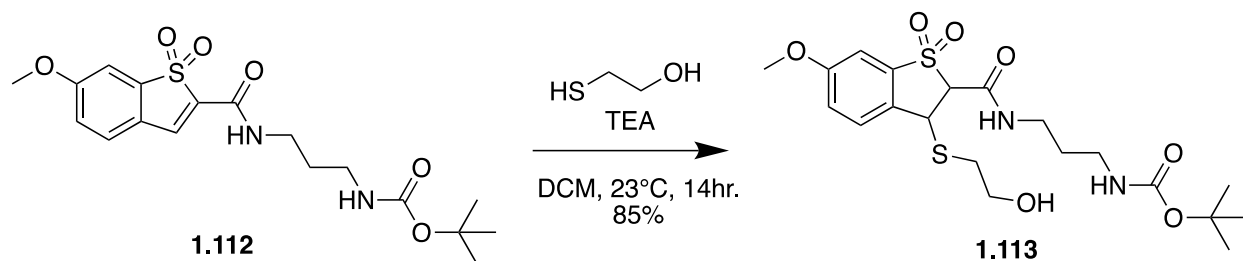
¹H NMR (599 MHz, CDCl₃) δ 7.74 (s, 1H), 7.69 (d, *J* = 8.8 Hz, 1H), 7.38 (s, 1H), 7.28 (d, *J* = 1.3 Hz, 1H), 6.99 (dd, *J* = 8.8, 2.1 Hz, 1H), 4.98 (s, 1H), 3.87 (s, 3H), 3.50 (dd, *J* = 12.2, 6.2 Hz, 2H), 3.26 (d, *J* = 5.5 Hz, 2H), 1.76 – 1.65 (m, 2H), 1.46 (s, 9H). **¹³C NMR** (151 MHz, CDCl₃) δ 162.8, 158.9, 157.3, 143.0, 133.4, 125.9, 124.7, 115.6, 104.6, 55.7, 38.8, 37.1, 36.2, 30.4, 28.6 **HRMS**: *m/z*: [M+Na]⁺ Calcd for [C₁₈H₂₄N₂O₄SNa]⁺ Theo mass: 387.1349; Found: 387.1350



UTA245: tert-butyl (3-(6-methoxy-1,1-dioxidocinnamamido)propyl)carbamate
(1.112)

General Procedure B: DMSO oxidation

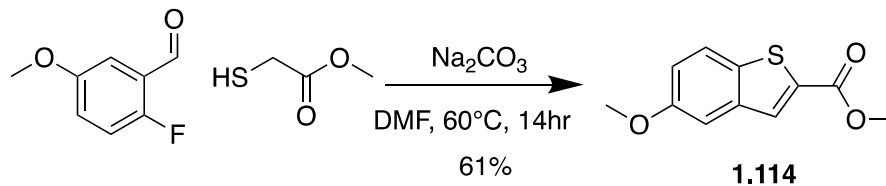
¹H NMR (599 MHz, CDCl₃) δ 7.78 (s, 1H), 7.41 (d, *J* = 8.4 Hz, 1H), 7.26 (s, 1H), 7.08 (dd, *J* = 8.4, 2.2 Hz, 1H), 6.76 (s, 1H), 4.97 (s, 1H), 3.91 (s, 3H), 3.49 (q, *J* = 6.4 Hz, 2H), 3.20 (d, *J* = 5.6 Hz, 2H), 1.79-1.71 (m, 2H), 1.44 (s, 9H). **¹³C NMR** (151 MHz, MeOD) δ 165.09 (s), 160.4, 158.6, 141.0, 136.5, 135.9, 129.8, 122.0, 109.0, 108.9, 80.1, 56.9, 38.7, 38.1, 30.7, 28.8, 28.7. **HRMS:** *m/z*: [M+MeOH+Na]⁺ Calcd for [C₁₉H₂₈N₂O₇SNa]⁺ Theo mass: 451.1509; Found: 451.1511



UTA256: tert-butyl (3-(3-((2-hydroxyethyl)thio)-6-methoxy-1,1-dioxido-2,3-dihydrobenzo[b]thiophene-2-carboxamido)propyl)carbamate (1.113)

General Procedure E: Thia-Micheal Addition

¹H NMR (599 MHz, CDCl₃) δ 7.63 (d, *J* = 8.7 Hz, 1H), 7.27 (s, 1H), 7.18 (dd, *J* = 8.6, 2.4 Hz, 1H), 7.11 (d, *J* = 2.2 Hz, 1H), 5.09 (d, *J* = 6.8 Hz, 1H), 4.96 (s, 1H), 4.57 (d, *J* = 6.8 Hz, 1H), 3.85 (s, 3H), 3.82 – 3.74 (m, 2H), 3.50 – 3.34 (m, 2H), 3.26 – 3.14 (m, 2H), 2.85-2.70 (m, 2H), 1.76 – 1.67 (m, 2H), 1.42 (s, 9H). **¹³C NMR** (151 MHz, CDCl₃) δ 162.2, 160.9, 156.8, 138.9, 129.2, 128.5, 122.8, 103.9, 79.7, 73.7, 61.8, 56.1, 44.0, 37.3, 34.2, 29.9, 28.5. **HRMS**: *m/z*: [M+Na]⁺ Calcd for [C₂₀H₃₀N₂O₇S₂Na]⁺ Theo mass: 497.1387; Found: 497.1386

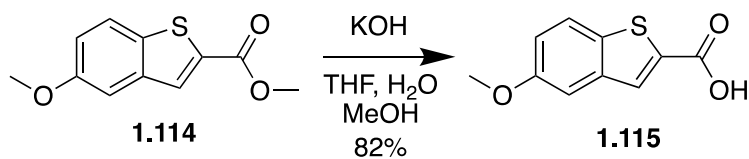


UTA156: methyl 5-methoxybenzo[b]thiophene-2-carboxylate (1.114)

General Procedure C: Domino Aldol-S_NAR

¹H NMR (599 MHz, CDCl₃) δ 7.98 (s, 1H), 7.72 (d, *J* = 8.9 Hz, 1H), 7.28 (d, *J* = 2.4 Hz, 1H), 7.11 (dd, *J* = 8.9, 2.5 Hz, 1H), 3.94 (s, 3H), 3.88 (s, 3H). **¹³C NMR** (151 MHz, CDCl₃) δ 163.4, 158.0, 139.8, 135.1, 134.4, 130.4, 123.6, 118.3, 106.6, 55.7, 52.6.

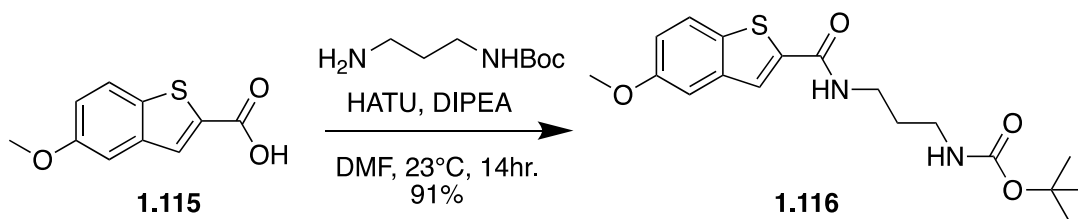
HRMS: *m/z*: [M+H]⁺ Calcd for [C₁₁H₁₁O₃S]⁺ Theo mass: 223.0423; Found: 223.0425



UTA169: 5-methoxybenzo[b]thiophene-2-carboxylic acid (1.115)

General Procedure D: Saponification

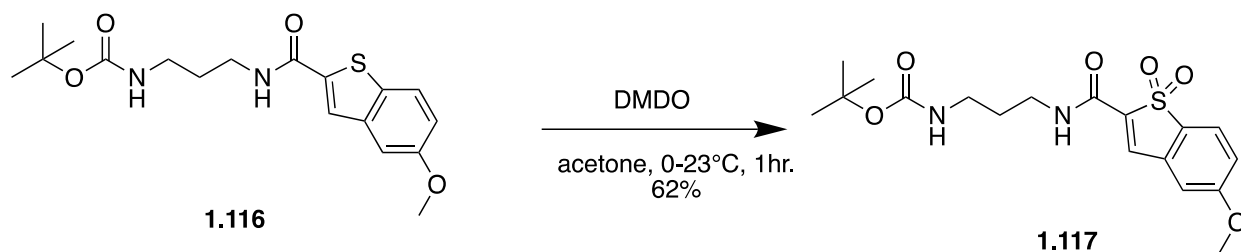
¹H NMR (599 MHz, MeOD) δ 7.98 (s, 1H), 7.76 (d, J = 8.9 Hz, 1H), 7.41 (d, J = 2.0 Hz, 1H), 7.11 (dd, J = 8.9, 2.3 Hz, 1H), 3.86 (s, 3H). **¹³C NMR** (151 MHz, MeOD) δ 165.9, 159.4, 141.4, 136.6, 136.2, 131.4, 124.4, 119.2, 107.5, 56.0. **HRMS**: m/z : [M-H]⁻ Calcd for [C₁₀H₇O₃S]⁻ Theo mass: 207.0122; Found: 207.0122



UTA232: tert-butyl (3-(5-methoxybenzo[b]thiophene-2-carboxamido)propyl)carbamate (1.116)

General Procedure E: HATU Amide Coupling

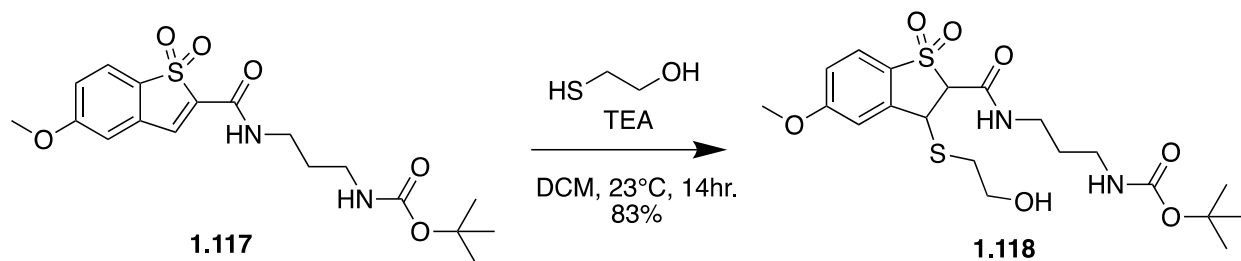
¹H NMR (599 MHz, CDCl₃) δ 7.75 (s, 1H), 7.70 (d, *J* = 8.8 Hz, 1H), 7.39 (s, 1H), 7.25 (d, *J* = 2.2 Hz, 1H), 7.06 (dd, *J* = 8.9, 2.4 Hz, 1H), 4.93 (s, 1H), 3.86 (s, 3H), 3.51 (dd, *J* = 12.3, 6.2 Hz, 2H), 3.27 (dd, *J* = 12.0, 6.1 Hz, 2H), 1.76-1.70 (m, 2H), 1.47 (s, 9H). ¹³C NMR (151 MHz, CDCl₃) δ 162.7, 157.9, 157.3, 140.4, 133.7, 124.8, 123.5, 117.1, 106.5, 79.8, 55.7, 37.1, 36.2, 30.4, 28.1. **HRMS:** *m/z*: [M+H]⁺ Calcd for [C₁₈H₂₄N₂O₄SNa]⁺ Theo mass: 387.1349; Found: 387.1347



UTA244: tert-butyl (3-(5-methoxy-1,1-dioxidocinnamamido)propyl)carbamate(1.117)

General Procedure B: DMSO oxidation

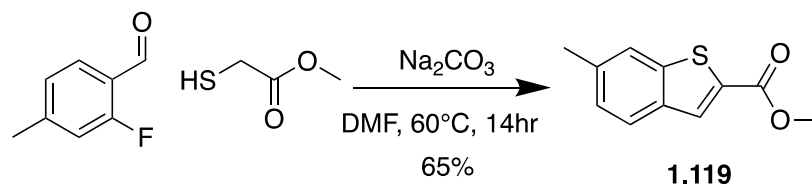
¹H NMR (599 MHz, CDCl₃) δ 7.72 (s, 1H), 7.62 (d, *J* = 8.4 Hz, 1H), 7.01 (dd, *J* = 8.4, 1.8 Hz, 1H), 6.96 (d, *J* = 1.9 Hz, 1H), 6.91 (s, 1H), 5.04 (s, 1H), 3.87 (s, 3H), 3.46 (q, *J* = 6.4 Hz, 2H), 3.17 (d, *J* = 4.9 Hz, 2H), 1.76 – 1.70 (m, 2H), 1.41 (s, 9H). **¹³C NMR** (151 MHz, CDCl₃) δ 164.4, 157.6, 156.5, 138.4, 135.9, 131.7, 128.7, 123.7, 116.4, 113.3, 56.2, 37.1, 37.1, 30.1, 28.6. **HRMS:** *m/z*: [M+MeOH+Na]⁺ Calcd for [C₁₉H₂₈N₂O₇SNa]⁺ Theo mass: 451.1509; Found: 451.1513



UTA255: tert-butyl (3-(3-((2-hydroxyethyl)thio)-5-methoxy-1,1-dioxido-2,3-dihydrobenzo[b]thiophene-2-carboxamido)propyl)carbamate (1.118)

General Procedure E: Thia-Micheal Addition

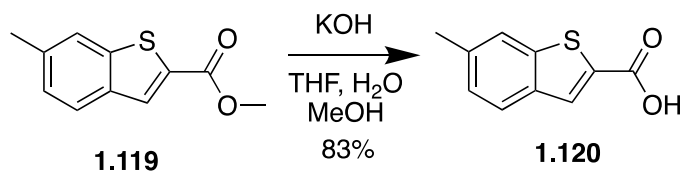
$^1\text{H NMR}$ (599 MHz, CDCl_3) δ 7.58 (d, $J = 8.7$ Hz, 1H), 7.39 (s, 1H), 7.19 (d, $J = 1.5$ Hz, 1H), 6.98 (dd, $J = 8.7, 2.0$ Hz, 1H), 5.11 (d, $J = 7.0$ Hz, 1H), 5.02 (s, 1H), 4.57 (d, $J = 7.0$ Hz, 1H), 3.87 (s, 3H), 3.81 – 3.73 (m, 2H), 3.44 – 3.35 (m, 2H), 3.25 – 3.13 (m, 2H), 2.82 – 2.71 (m, 2H), 1.71 – 1.66 (m, 2H), 1.41 (s, 9H). **$^{13}\text{C NMR}$** (151 MHz, CDCl_3) δ 164.7, 162.3, 156.8, 140.4, 129.9, 123.0, 117.1, 111.0, 79.7, 73.5, 61.8, 56.1, 44.2, 37.3, 34.2, 29.8, 28.5. **HRMS:** m/z : $[\text{M}+\text{Na}]^+$ Calcd for $[\text{C}_{20}\text{H}_{30}\text{N}_2\text{O}_7\text{S}_2\text{Na}]^+$ Theo mass: 497.1387; Found: 497.1384



UTA159: methyl 6-methylbenzo[b]thiophene-2-carboxylate (1.119)

General Procedure C: Domino Aldol-S_NAR

¹H NMR (599 MHz, MeOD) δ 8.03 (s, 1H), 7.81 (d, *J* = 8.2 Hz, 1H), 7.72 (s, 1H), 7.27 (d, *J* = 8.2 Hz, 1H), 3.92 (s, 3H), 2.48 (s, 3H). ¹³C NMR (151 MHz, MeOD) δ 164.8, 143.9, 139.0, 138.0, 133.1, 131.7, 128.0, 126.3, 123.2, 52.9, 21.8. **HRMS:** *m/z*: [M+H]⁺ Calcd for [C₁₁H₁₁O₂S]⁺ Theo mass: 207.0474; Found: 207.0471



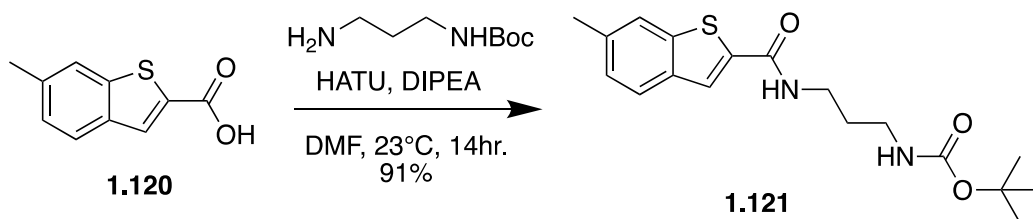
UTA172: 6-methylbenzo[b]thiophene-2-carboxylic acid (1.120)

General Procedure D: Saponification

¹H NMR (599 MHz, MeOD) δ 7.98 (s, 1H), 7.79 (d, $J = 8.2$ Hz, 1H), 7.70 (s, 1H), 7.25 (d, $J = 8.2$ Hz, 1H), 2.47 (s, 3H).

¹³C NMR

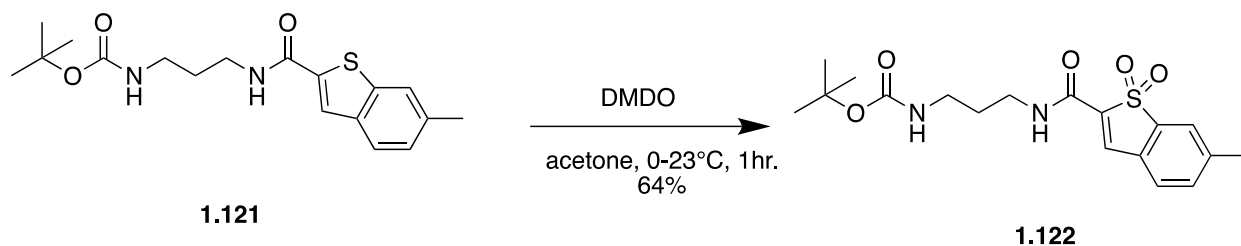
HRMS: m/z : [M-H]⁻ Calcd for [C₁₀H₇O₂S]⁻ Theo mass: 191.0167; Found: 191.0165



UTA230: tert-butyl (3-(6-methylbenzo[b]thiophene-2-carboxamido)propyl)carbamate (1.121)

General Procedure E: HATU Amide Coupling

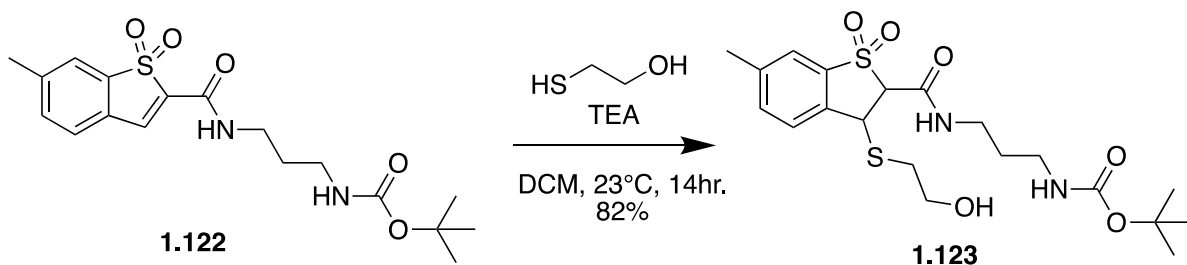
¹H NMR (599 MHz, CDCl₃) δ 7.78 (s, 1H), 7.70 (d, *J* = 8.2 Hz, 1H), 7.63 (s, 1H), 7.40 (s, 1H), 7.19 (dd, *J* = 8.1, 0.8 Hz, 1H), 3.50 (dd, *J* = 12.3, 6.2 Hz, 2H), 3.26 (d, *J* = 5.6 Hz, 2H), 2.47 (s, 3H), 1.75 – 1.68 (m, 2H), 1.46 (s, 9H). **¹³C NMR** (151 MHz, CDCl₃) δ 162.9, 157.2, 141.5, 138.0, 137.2, 136.5, 126.8, 124.8, 124.8, 122.5, 37.1, 36.2, 30.3, 28.5, 21.9. **HRMS:** *m/z*: [M+Na]⁺ Calcd for [C₁₈H₂₄N₂O₃SNa]⁺ Theo mass: 341.1400; Found: 341.1401



UTA243: tert-butyl (3-(6-methyl-1,1-dioxidocinnamamido)propyl)carbamate (1.122)

General Procedure B: DMSO oxidation

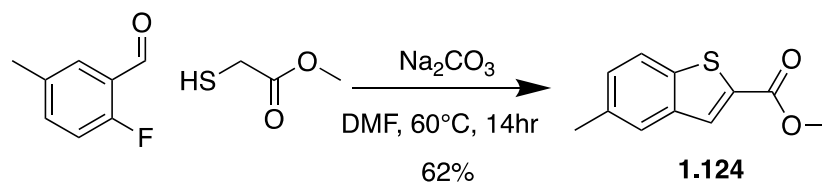
¹H NMR (599 MHz, CDCl₃) δ 7.77 (s, 1H), 7.53 (s, 1H), 7.40 (d, *J* = 7.6 Hz, 1H), 7.37 (d, *J* = 7.7 Hz, 1H), 6.80 (s, 1H), 4.99 (s, 1H), 3.48 (dd, *J* = 12.8, 6.4 Hz, 2H), 3.19 (d, *J* = 5.6 Hz, 2H), 2.46 (s, 3H), 1.79 – 1.71 (m, 2H), 1.43 (s, 9H). **¹³C NMR** (151 MHz, CDCl₃) δ 157.7, 156.4, 143.9, 137.4, 136.4, 134.8, 126.9, 126.6, 122.6, 79.4, 37.4, 37.0, 30.1, 28.5, 21.9. **HRMS**: *m/z*: [M+Na]⁺ Calcd for [C₁₈H₂₄N₂O₅SNa]⁺ Theo mass: 403.1298; Found: 403.1301



UTA254: tert-butyl (3-(3-((2-hydroxyethyl)thio)-6-methyl-1,1-dioxido-2,3-dihydrobenzo[b]thiophene-2-carboxamido)propyl)carbamate (1.123)

General Procedure E: Thia-Micheal Addition

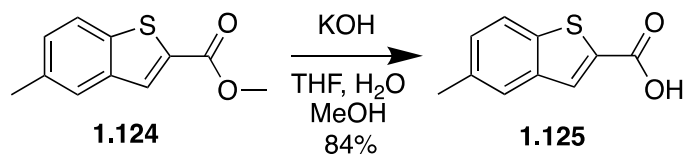
¹H NMR (599 MHz, CDCl₃) δ 7.66 (d, *J* = 8.0 Hz, 1H), 7.49 (s, 1H), 7.47 (d, *J* = 8.1 Hz, 1H), 7.11 (s, 1H), 5.12 (d, *J* = 7.3 Hz, 1H), 4.89 (s, 1H), 4.51 (d, *J* = 7.3 Hz, 1H), 3.81 (qdd, *J* = 11.5, 6.4, 4.7 Hz, 2H), 3.50 – 3.38 (m, 2H), 3.23 (qd, *J* = 14.2, 7.5 Hz, 2H), 2.83 (ddd, *J* = 14.2, 5.8, 4.6 Hz, 1H), 2.76 (ddd, *J* = 14.3, 7.1, 4.8 Hz, 1H), 1.75-1.66 (m, 2H), 1.43 (s, 9H). **¹³C NMR** (151 MHz, CDCl₃) δ 162.3, 156.6, 140.4, 137.6, 135.4, 134.7, 127.1, 121.1, 79.3, 73.1, 61.5, 44.0, 37.3, 37.2, 34.0, 29.5, 28.4, 21.1. **HRMS:** *m/z*: [M+Na]⁺ Calcd for [C₂₀H₃₀N₂O₆S₂Na]⁺ Theo mass: 481.1437; Found: 481.1438



UTA160: methyl 5-methylbenzo[b]thiophene-2-carboxylate (1.124)

General Procedure C: Domino Aldol-S_NAR

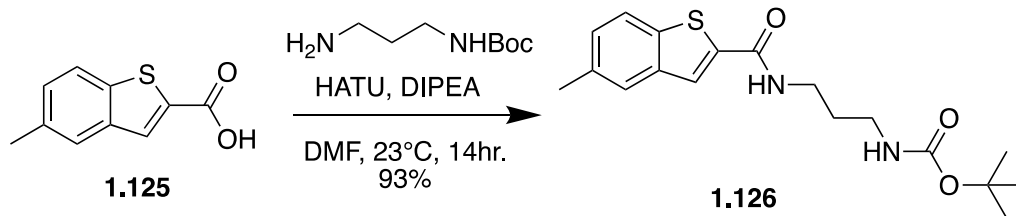
¹H NMR (599 MHz, CDCl₃) δ 7.99 (s, 1H), 7.74 (d, *J* = 8.3 Hz, 1H), 7.66 (s, 1H), 7.29 (dd, *J* = 8.3, 1.1 Hz, 1H), 3.94 (s, 3H), 2.47 (s, 3H). ¹³C NMR (151 MHz, CDCl₃) δ 163.3, 139.5, 139.0, 134.8, 133.3, 130.4, 128.9, 125.3, 122.4, 52.4, 21.4. HRMS: *m/z*: [M+H]⁺ Calcd for [C₁₁H₁₁O₂S]⁺ Theo mass: 207.0474; Found: 207.0474



UTA234: 5-methylbenzo[b]thiophene-2-carboxylic acid (1.125)

General Procedure D: Saponification

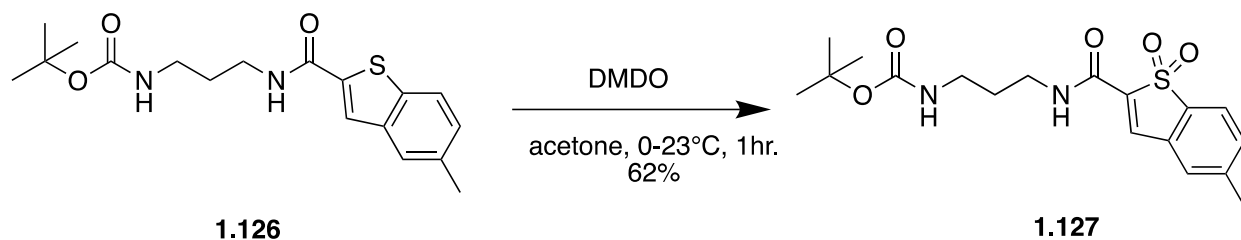
¹H NMR (599 MHz, MeOD) δ 7.96 (s, 1H), 7.78 (d, $J = 8.3$ Hz, 1H), 7.71 (s, 1H), 7.31 (d, $J = 8.3$ Hz, 1H), 2.46 (s, 3H). **¹³C NMR** (151 MHz, MeOD) δ 166.0, 140.9, 140.7, 136.1, 135.7, 131.4, 130.0, 126.2, 123.3, 21.3. **HRMS**: m/z : [M-H]⁻ Calcd for [C₁₀H₇O₂S]⁻ Theo mass: 191.0172; Found: 191.0173



UTA218: tert-butyl (3-(5-methylbenzo[b]thiophene-2-carboxamido)propyl)carbamate (1.126)

General Procedure E: HATU Amide Coupling

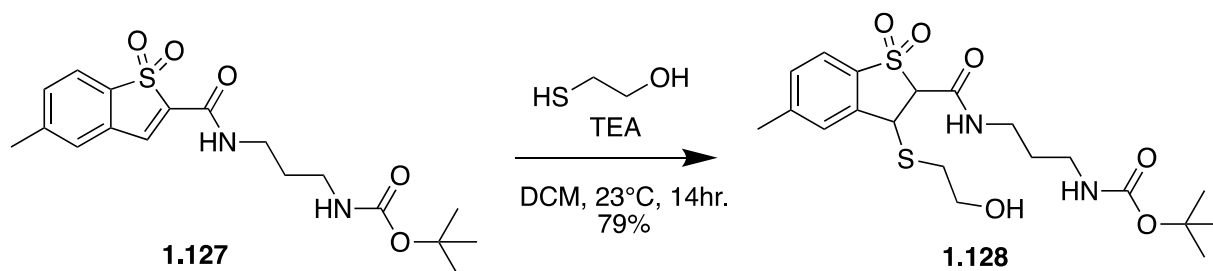
¹H NMR (599 MHz, CDCl₃) δ 7.76 (s, 1H), 7.70 (d, *J* = 8.3 Hz, 1H), 7.57 (s, 1H), 7.56 (s, 1H), 7.21 (dd, *J* = 8.3, 0.9 Hz, 1H), 5.09 (s, 1H), 3.50 (dd, *J* = 12.2, 6.2 Hz, 2H), 3.25 (d, *J* = 5.7 Hz, 2H), 2.43 (s, 3H), 1.75 – 1.67 (m, 2H), 1.45 (s, 9H). ¹³C NMR (151 MHz, CDCl₃) δ 162.9, 157.2, 139.7, 139.2, 138.3, 134.6, 128.1, 124.9, 124.7, 122.4, 79.7, 37.1, 36.3, 30.2, 28.5, 21.4. **HRMS:** *m/z*: [M+Na]⁺ Calcd for [C₁₈H₂₄N₂O₃SNa]⁺ Theo mass: 341.1400; Found: 341.1403



UTA242: tert-butyl (3-(5-methyl-1,1-dioxidocinnamamido)propyl)carbamate (1.127)

General Procedure B: DMSO oxidation

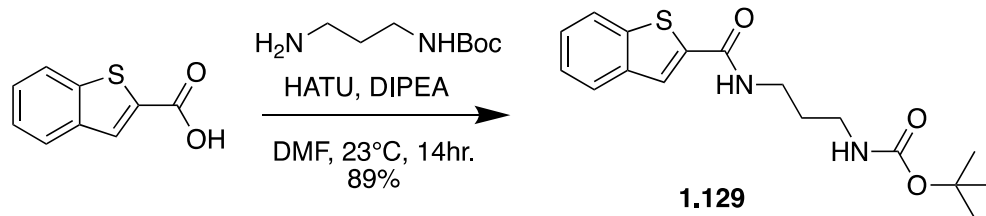
¹H NMR (599 MHz, CDCl₃) δ 7.76 (s, 1H), 7.62 (d, *J* = 7.8 Hz, 1H), 7.40 (d, *J* = 7.7 Hz, 1H), 7.29 (s, 1H), 6.82 (s, 1H), 4.97 (s, 1H), 3.49 (q, *J* = 6.4 Hz, 2H), 3.20 (d, *J* = 5.6 Hz, 2H), 2.45 (s, 3H), 1.83 – 1.72 (m, 2H), 1.44 (s, 9H). **¹³C NMR** (151 MHz, CDCl₃) δ 157.7, 156.5, 145.6, 137.4, 136.4, 134.4, 132.8, 129.6, 127.8, 121.9, 37.4, 37.0, 30.1, 28.5, 21.9. **HRMS:** *m/z*: [M+MeOH+Na]⁺ Calcd for [C₁₉H₂₈N₂O₆SNa]⁺ Theo mass: 435.1560; Found: 435.1559



UTA246: tert-butyl (3-(3-((2-hydroxyethyl)thio)-5-methyl-1,1-dioxido-2,3-dihydrobenzo[b]thiophene-2-carboxamido)propyl)carbamate (1.128)

General Procedure E: Thia-Micheal Addition

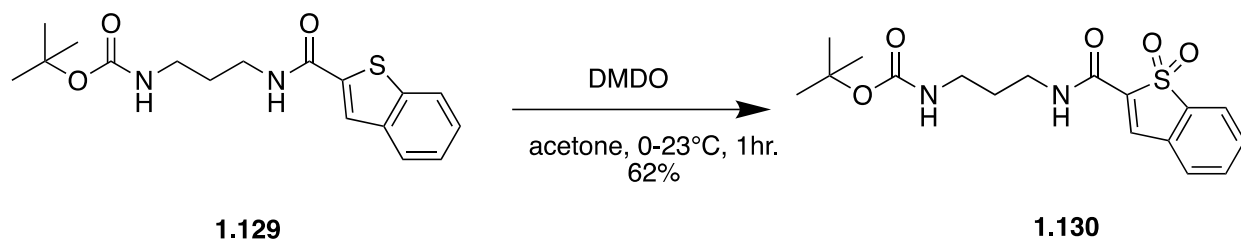
¹H NMR (599 MHz, CDCl₃) δ 7.60 (s, 1H), 7.51 (d, *J* = 7.2 Hz, 2H), 7.24 (d, *J* = 8.1 Hz, 1H), 5.18 (s, 1H), 5.08 (d, *J* = 6.6 Hz, 1H), 4.54 (d, *J* = 6.5 Hz, 1H), 3.74-3.71 (m, 2H), 3.35-3.30 (m, 2H), 3.16 – 3.08 (m, 3H), 2.76 – 2.67 (m, 2H), 2.40 (s, 2H), 1.67 – 1.58 (m, 2H), 1.37 (s, 9H). **¹³C NMR** (151 MHz, CDCl₃) δ 162.4, 156.6, 145.6, 137.8, 135.0, 130.7, 127.6, 121.1, 79.4, 73.2, 61.6, 44.2, 37.3, 34.2, 29.6, 28.4, 21.9. **HRMS:** *m/z*: [M+Na]⁺ Calcd for [C₂₀H₃₀N₂O₆S₂Na]⁺ Theo mass: 481.1437; Found: 481.1440



UTA219: tert-butyl (3-(benzo[b]thiophene-2-carboxamido)propyl)carbamate (1.129)

General Procedure E: HATU Amide Coupling

¹H NMR (599 MHz, MeOD) δ 7.92 (s, 1H), 7.89 (dd, $J = 14.1, 8.0$ Hz, 2H), 7.42 (p, $J = 7.1$ Hz, 2H), 6.67 (s, 1H), 3.43 (t, $J = 6.8$ Hz, 2H), 3.15 (t, $J = 6.3$ Hz, 2H), 1.83 – 1.71 (m, 2H), 1.44 (s, 9H). **¹³C NMR** (151 MHz, MeOD) δ 164.6, 158.5, 142.1, 140.6, 139.9, 127.3, 126.3, 126.1, 125.9, 123.5, 80.0, 38.8, 38.4, 30.7, 28.8. **HRMS:** m/z : $[\text{M}+\text{Na}]^+$
 Calcd for $[\text{C}_{17}\text{H}_{22}\text{N}_2\text{O}_3\text{SNa}]^+$ Theo mass: 357.1243; Found: 357.1242

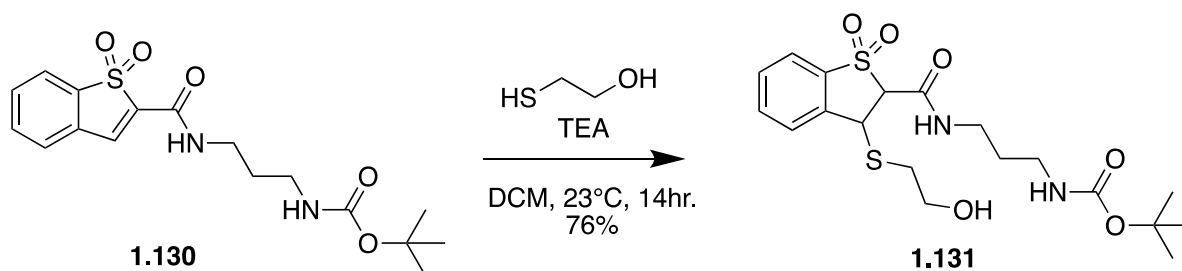


UTA228: tert-butyl (3-(1,1-dioxidocinnamamido)propyl)carbamate (1.130)

General Procedure B: DMSO oxidation

¹H NMR (599 MHz, CDCl₃) δ 7.82 (s, 1H), 7.76 – 7.73 (m, 1H), 7.65 – 7.61 (m, 2H), 7.53 – 7.49 (m, 1H), 6.84 (s, 1H), 4.94 (s, 1H), 3.51 (q, *J* = 6.4 Hz, 2H), 3.21 (d, *J* = 4.9 Hz, 2H), 1.77 (p, *J* = 6.5 Hz, 2H), 1.45 (s, 9H). **¹³C NMR** (151 MHz, CDCl₃) δ 157.5, 156.5, 137.2, 136.2, 134.3, 132.4, 129.3, 127.1, 122.1, 79.5, 37.4, 37.0, 30.1, 28.5.

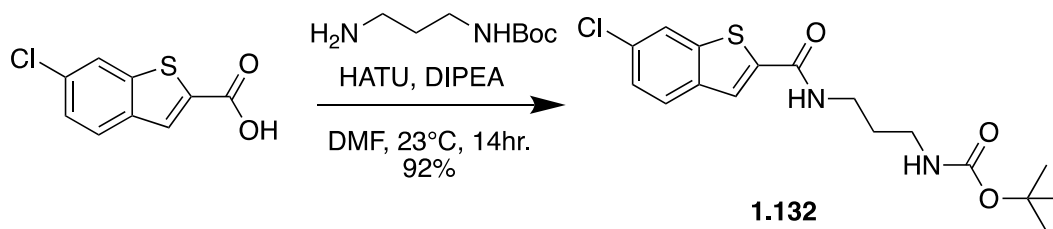
HRMS: *m/z*: [M+Na]⁺ Calcd for [C₁₇H₂₂N₂O₅SNa]⁺ Theo mass: 389.1142; Found: 389.1143



UTA132: tert-butyl (3-(3-((2-hydroxyethyl)thio)-1,1-dioxido-2,3-dihydrobenzo[b]thiophene-2-carboxamido)propyl)carbamate (1.131)

General Procedure E: Thia-Micheal Addition

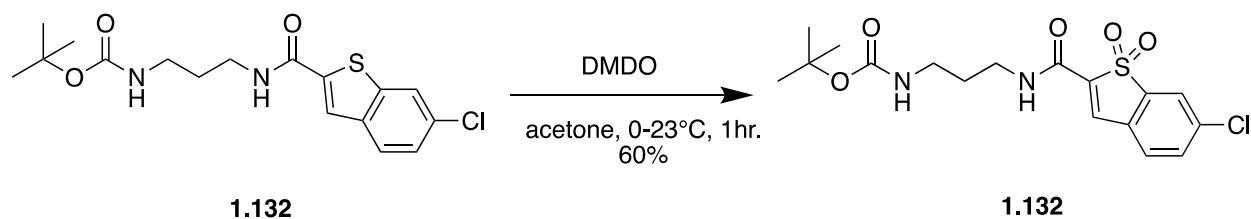
¹H NMR (599 MHz, CDCl₃) δ 7.79 (d, *J* = 7.8 Hz, 1H), 7.71 – 7.65 (m, 2H), 7.51 (t, *J* = 7.5 Hz, 1H), 7.23 (s, 1H), 5.17 (d, *J* = 7.3 Hz, 1H), 4.92 (s, 1H), 4.55 (d, *J* = 7.3 Hz, 1H), 3.86 – 3.74 (m, 2H), 3.44 (qd, *J* = 14.3, 7.6 Hz, 2H), 3.28 – 3.14 (m, 2H), 2.86 – 2.80 (m, 1H), 2.79 – 2.72 (m, 1H), 1.76 – 1.67 (m, 2H), 1.43 (s, 9H). **¹³C NMR** (151 MHz, CDCl₃) δ 162.2, 156.9, 137.9, 137.7, 134.5, 129.9, 127.5, 121.5, 79.8, 73.1, 61.8, 44.4, 37.3, 37.3, 34.3, 29.9, 28.5. **HRMS:** *m/z*: [M+Na]⁺ Calcd for [C₁₉H₂₈N₂O₆S₂Na]⁺ Theo mass: 467.1281; Found: 467.1285



UTA216: tert-butyl (3-(6-chlorobenzo[b]thiophene-2-carboxamido)propyl)carbamate (1.132)

General Procedure E: HATU Amide Coupling

¹H NMR (599 MHz, CDCl₃) δ 7.83 (d, *J* = 1.5 Hz, 1H), 7.79 (s, 1H), 7.74 (d, *J* = 8.5 Hz, 1H), 7.60 (s, 1H), 7.34 (dd, *J* = 8.5, 1.9 Hz, 1H), 4.92 (s, 1H), 3.51 (dd, *J* = 12.2, 6.2 Hz, 2H), 3.27 (dd, *J* = 11.7, 6.0 Hz, 2H), 1.76 – 1.68 (m, 2H), 1.47 (s, 9H). **¹³C NMR** (151 MHz, CDCl₃) δ 162.4, 157.5, 142.1, 137.8, 132.5, 126.0, 125.9, 124.3, 122.4, 37.1, 36.3, 30.2, 28.5. **HRMS:** *m/z*: [M+Na]⁺ Calcd for [C₁₇H₂₁ClN₂O₃SNa]⁺ Theo mass: 391.0854 ; Found: 391.0856



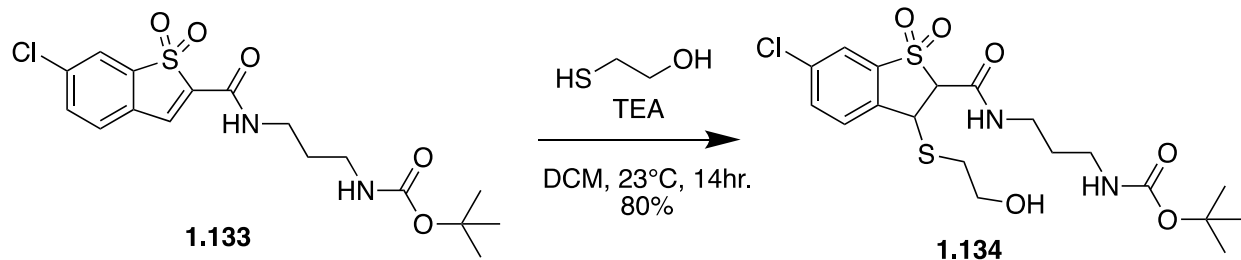
UTA227: tert-butyl (3-(6-chloro-1,1-dioxidocinnamamido)propyl)carbamate (1.133)

General Procedure B: DMSO oxidation

¹H NMR (599 MHz, CDCl₃) δ 7.78 (s, 1H), 7.71 (s, 1H), 7.59 (dd, *J* = 8.0, 1.8 Hz, 1H), 7.45 (d, *J* = 8.0 Hz, 1H), 6.91 (s, 1H), 4.93 (s, 1H), 3.49 (q, *J* = 6.4 Hz, 2H), 3.21 (d, *J* = 5.8 Hz, 2H), 1.79 – 1.71 (m, 2H), 1.44 (s, 9H). **¹³C NMR** (151 MHz, CDCl₃) δ 157.2, 156.6, 139.0, 138.6, 137.6, 135.1, 134.3, 127.9, 127.6, 122.7, 37.4, 37.0, 30.1, 28.5.

HRMS: *m/z*: [M+MeOH+Na]⁺ Calcd for [C₁₈H₂₅ClN₂O₆SNa]⁺ Theo mass: 455.1014;

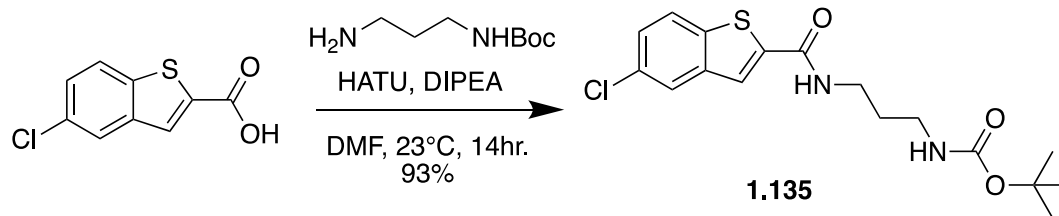
Found: 455.1010



UTA250: tert-butyl (3-(6-chloro-3-((3-hydroxypropyl)thio)-1,1-dioxido-2,3-dihydrobenzo[b]thiophene-2-carboxamido)propyl)carbamate (1.134)

General Procedure E: Thia-Micheal Addition

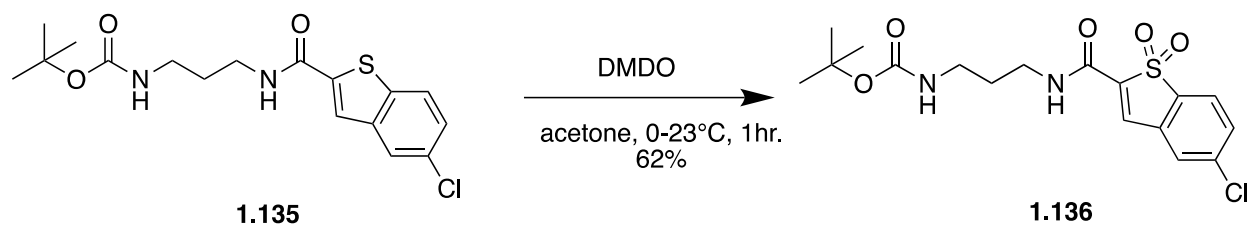
¹H NMR (599 MHz, CDCl₃) δ 7.70 (d, *J* = 8.4 Hz, 1H), 7.61 (s, 1H), 7.58 (d, *J* = 1.9 Hz, 1H), 7.57 (d, *J* = 1.9 Hz, 1H), 5.11 (d, *J* = 6.9 Hz, 1H), 5.05 (s, 1H), 4.62 (d, *J* = 6.8 Hz, 1H), 3.82 – 3.68 (m, 2H), 3.38 (qd, *J* = 13.2, 7.0 Hz, 2H), 3.18 (qd, *J* = 14.1, 7.2 Hz, 2H), 2.85 – 2.68 (m, 2H), 1.68 (p, *J* = 6.2 Hz, 2H), 1.41 (s, 9H). **¹³C NMR** (151 MHz, CDCl₃) δ 161.9, 156.9, 139.2, 136.2, 135.8, 134.7, 129.0, 121.4, 79.7, 73.4, 61.6, 44.1, 37.3, 34.4, 29.8, 28.5. **HRMS:** *m/z*: [M+Na]⁺ Calcd for [C₁₉H₂₇ClN₂O₆S₂Na]⁺ Theo mass: 501.0891 ; Found: 501.0887



UTA221: tert-butyl (3-(5-chlorobenzo[b]thiophene-2-carboxamido)propyl)carbamate (1.135)

General Procedure E: HATU Amide Coupling

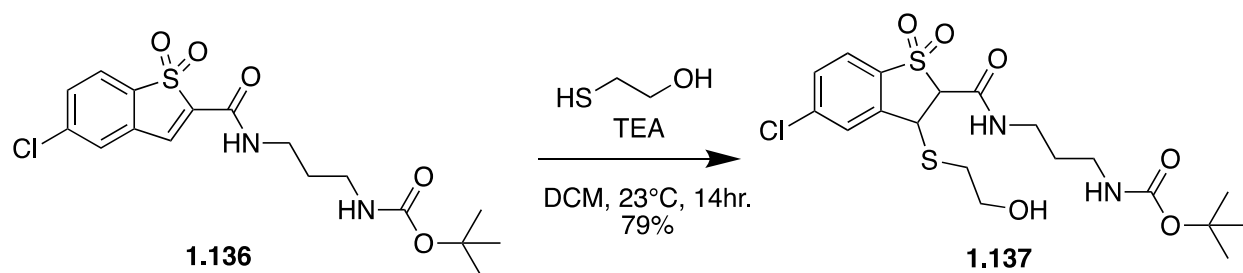
¹H NMR (599 MHz, CDCl₃) δ 7.80-7.73 (m, 3H), 7.70 (s, 1H), 7.35 (dd, *J* = 8.6, 1.8 Hz, 1H), 4.97 (s, 1H), 3.51 (dd, *J* = 12.1, 6.1 Hz, 2H), 3.27 (dd, *J* = 11.6, 5.9 Hz, 2H), 1.78 – 1.65 (m, 2H), 1.46 (s, 3H). **¹³C NMR** (151 MHz, CDCl₃) δ 162.3, 157.3, 141.4, 140.4, 139.0, 131.0, 126.6, 124.4, 123.8, 123.8, 79.7, 53.5, 37.1, 36.3, 30.1, 28.5. **HRMS:** *m/z*: [M+Na]⁺ Calcd for [C₁₇H₂₁ClN₂O₃SNa]⁺ Theo mass: 391.0854 ; Found: 391.0854



UTA226: tert-butyl (3-(5-chloro-1,1-dioxidocinnamamido)propyl)carbamate (1.136)

General Procedure B: DMSO oxidation

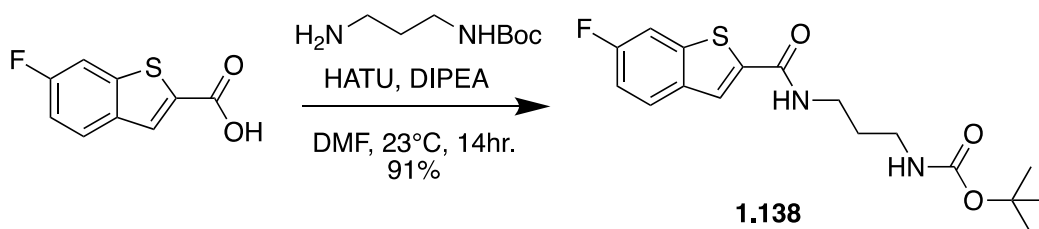
¹H NMR (599 MHz, MeOD) δ 7.88 (s, 1H), 7.78 (d, *J* = 8.5 Hz, 1H), 7.72 (s, 1H), 7.71 (s, 1H), 6.65 (s, 1H), 3.39 (t, *J* = 6.8 Hz, 2H), 3.15-3.08 (m, 2H), 1.78 – 1.70 (m, 2H), 1.44 (s, 9H). **¹³C NMR** (151 MHz, MeOD) δ 159.8, 158.6, 141.2, 139.5, 137.2, 134.2, 133.9, 132.3, 128.5, 123.8, 80.1, 38.7, 38.2, 30.6, 28.8. **HRMS**: *m/z*: [M+Na]⁺ Calcd for [C₁₇H₂₁ClN₂O₅SNa]⁺ Theo mass: 423.0752 ; Found: 423.0749



UTA249: tert-butyl (3-(5-chloro-3-((2-hydroxyethyl)thio)-1,1-dioxido-2,3-dihydrobenzo[b]thiophene-2-carboxamido)propyl)carbamate (1.137)

General Procedure E: Thia-Micheal Addition

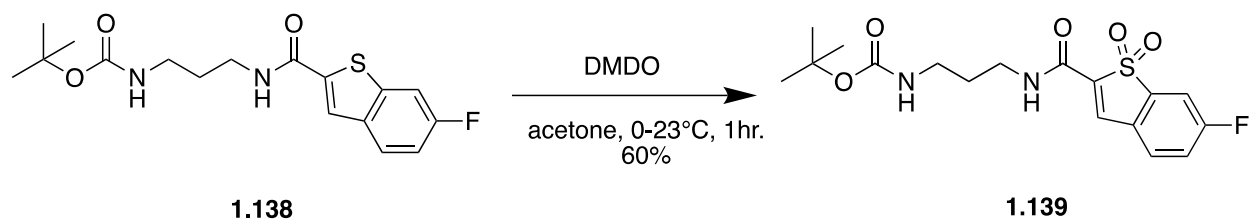
¹H NMR (599 MHz, CDCl₃) δ 7.74 (s, 1H), 7.59 (d, *J* = 8.3 Hz, 1H), 7.54 (s, 1H), 7.43 (dd, *J* = 8.3, 0.8 Hz, 1H), 5.11 (d, *J* = 7.0 Hz, 1H), 5.07 (s, 1H), 4.60 (d, *J* = 6.9 Hz, 1H), 3.82 – 3.71 (m, 2H), 3.44-3.32 (m, 2H), 3.23 – 3.07 (m, 2H), 2.82-2.77 (m, 1H), 2.77 – 2.71 (m, 1H), 1.68 (p, *J* = 6.2 Hz, 2H), 1.40 (s, 9H). **¹³C NMR** (151 MHz, CDCl₃) δ 162.0, 156.8, 140.9, 140.0, 136.2, 130.3, 127.7, 122.7, 79.6, 73.1, 61.7, 44.1, 37.4, 37.3, 34.4, 29.7, 28.5. **HRMS:** *m/z*: [M+Na]⁺ Calcd for [C₁₉H₂₇ClN₂O₆S₂Na]⁺ Theo mass: 501.0891 ; Found: 501.0894



UTA231: tert-butyl (3-(6-fluorobenzo[b]thiophene-2-carboxamido)propyl)carbamate (1.138)

General Procedure E: HATU Amide Coupling

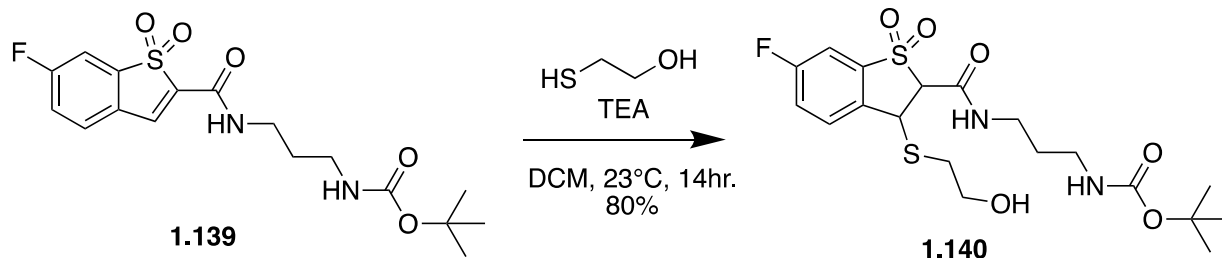
¹H NMR (599 MHz, CDCl₃) δ 7.79 (s, 1H), 7.74 (dd, *J* = 8.5, 5.2 Hz, 1H), 7.67 (s, 1H), 7.50 (dd, *J* = 8.7, 2.0 Hz, 1H), 7.11 (td, *J* = 8.8, 2.3 Hz, 1H), 5.05 (s, 1H), 3.49 (dd, *J* = 12.2, 6.1 Hz, 2H), 3.25 (d, *J* = 5.7 Hz, 2H), 1.76 – 1.66 (m, 2H), 1.45 (s, 9H). **¹³C NMR** (151 MHz, CDCl₃) δ 162.4 (d, *J* = 4.5 Hz), 160.7, 157.3, 142.2 (d, *J* = 10.9 Hz), 139.3 (d, *J* = 4.5 Hz), 135.9, 126.4 (d, *J* = 9.7 Hz), 124.2, 114.2 (d, *J* = 24.8 Hz), 108.7 (d, *J* = 25.5 Hz), 79.8, 37.1, 36.2, 30.2, 28.5. **HRMS**: *m/z*: [M+Na]⁺ Calcd for [C₁₇H₂₁FN₂O₃SNa]⁺ Theo mass: 375.1149 ; Found: 375.1149



UTA241: tert-butyl (3-(6-fluoro-1,1-dioxidocinnamamido)propyl)carbamate (1.139)

General Procedure B: DMSO oxidation

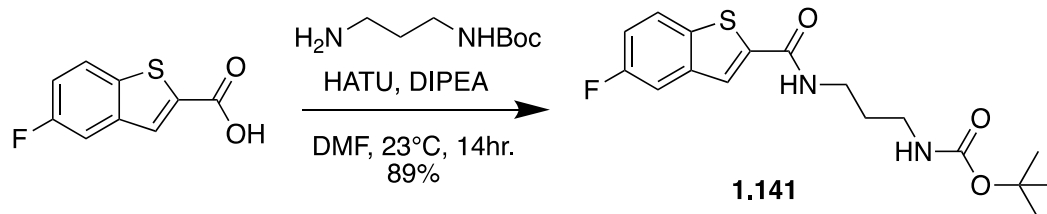
¹H NMR (599 MHz, CDCl₃) δ 7.79 (s, 1H), 7.51 (dd, *J* = 8.3, 4.5 Hz, 1H), 7.47 (dd, *J* = 6.3, 1.9 Hz, 1H), 7.32 (td, *J* = 8.3, 2.1 Hz, 1H), 6.87 (s, 1H), 3.50 (q, *J* = 6.3 Hz, 2H), 3.21 (d, *J* = 5.6 Hz, 2H), 1.76 (p, *J* = 6.4 Hz, 2H), 1.45 (s, 9H). **¹³C NMR** (151 MHz, CDCl₃) δ 165.9, 164.1, 157.2, 156.6, 139.3 (d, *J* = 10.1 Hz), 137.9 (d, *J* = 5.6 Hz), 135.2, 128.8 (d, *J* = 9.1 Hz), 125.2 (d, *J* = 3.8 Hz), 121.2 (d, *J* = 23.4 Hz), 110.8 (d, *J* = 26.9 Hz), 79.6, 37.4, 37.0, 30.1, 28.5. **HRMS:** *m/z*: [M+MeOH+Na]⁺ Calcd for [C₁₈H₂₅FN₂O₆SNa]⁺ Theo mass: 439.1310; Found: 439.1312



UTA253: tert-butyl (3-(6-fluoro-3-((2-hydroxyethyl)thio)-1,1-dioxido-2,3-dihydrobenzo[b]thiophene-2-carboxamido)propyl)carbamate (1.140)

General Procedure E: Thia-Micheal Addition

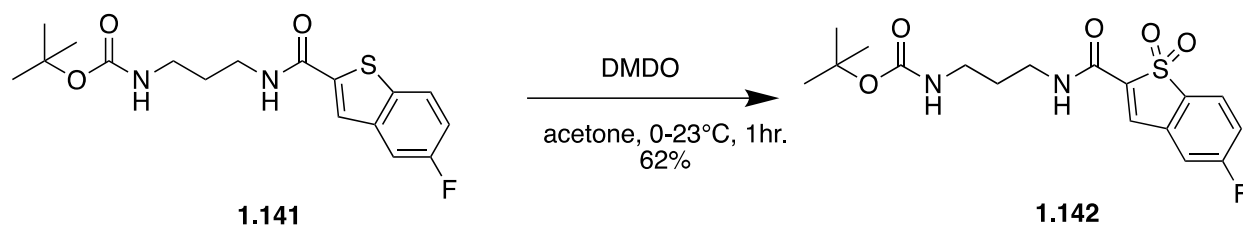
$^1\text{H NMR}$ (599 MHz, CDCl_3) δ 7.75 (dd, $J = 9.2, 4.3$ Hz, 1H), 7.46 (s, 1H), 7.38 – 7.30 (m, 2H), 5.12 (d, $J = 6.8$ Hz, 1H), 5.02 (s, 1H), 4.64 (d, $J = 6.8$ Hz, 1H), 3.84 – 3.73 (m, 2H), 3.47 – 3.32 (m, 2H), 3.19 (tt, $J = 14.2, 7.3$ Hz, 2H), 2.84 – 2.71 (m, 2H), 1.72 – 1.65 (m, 2H), 1.41 (s, 9H). **$^{13}\text{C NMR}$** (151 MHz, CDCl_3) δ 163.7 (s), 162.0 (d, $J = 8.0$ Hz), 156.9 (s), 139.4 (d, $J = 8.2$ Hz), 133.4 (d, $J = 3.0$ Hz), 129.6 (d, $J = 8.8$ Hz), 122.2 (d, $J = 23.4$ Hz), 108.4 (d, $J = 25.5$ Hz), 79.8, 73.7, 61.8, 44.1, 37.3, 34.4, 29.8, 28.5. **HRMS:** m/z : $[\text{M}+\text{Na}]^+$ Calcd for $[\text{C}_{19}\text{H}_{27}\text{FN}_2\text{O}_6\text{S}_2\text{Na}]^+$ Theo mass: 485.1187 ; Found: 485.1184



UTA217: tert-butyl (3-(5-fluorobenzo[b]thiophene-2-carboxamido)propyl)carbamate (1.141)

General Procedure E: HATU Amide Coupling

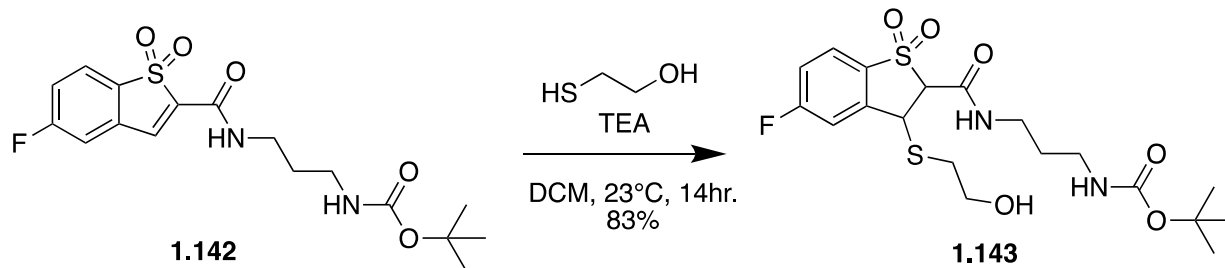
¹H NMR (599 MHz, MeOD) δ 7.89 (dd, $J = 9.0, 4.9$ Hz, 1H), 7.87 (s, 1H), 7.57 (dd, $J = 9.3, 2.1$ Hz, 1H), 7.23 (td, $J = 8.9, 2.2$ Hz, 1H), 3.42 (t, $J = 6.9$ Hz, 2H), 3.15 (t, $J = 6.5$ Hz, 2H), 1.82 – 1.74 (m, 2H), 1.43 (s, 9H). **¹³C NMR** (151 MHz, CDCl₃) δ 162.3 (d, $J = 12.7$ Hz), 161.8, 160.2, 157.3 (d, $J = 3.7$ Hz), 141.9, 140.3 (d, $J = 9.8$ Hz), 136.5, 124.3 (d, $J = 5.5$ Hz), 124.1 (d, $J = 9.6$ Hz), 115.3 (d, $J = 25.8$ Hz), 110.2 (d, $J = 23.0$ Hz), 79.9, 37.1, 36.2, 30.2, 28.5. **HRMS:** m/z : [M+Na]⁺ Calcd for [C₁₇H₂₁FN₂O₃SNa]⁺ Theo mass: 375.1149 ; Found: 375.1146



UTA225: tert-butyl (3-(5-fluoro-1,1-dioxidocinnamamido)propyl)carbamate (1.142)

General Procedure B: DMSO oxidation

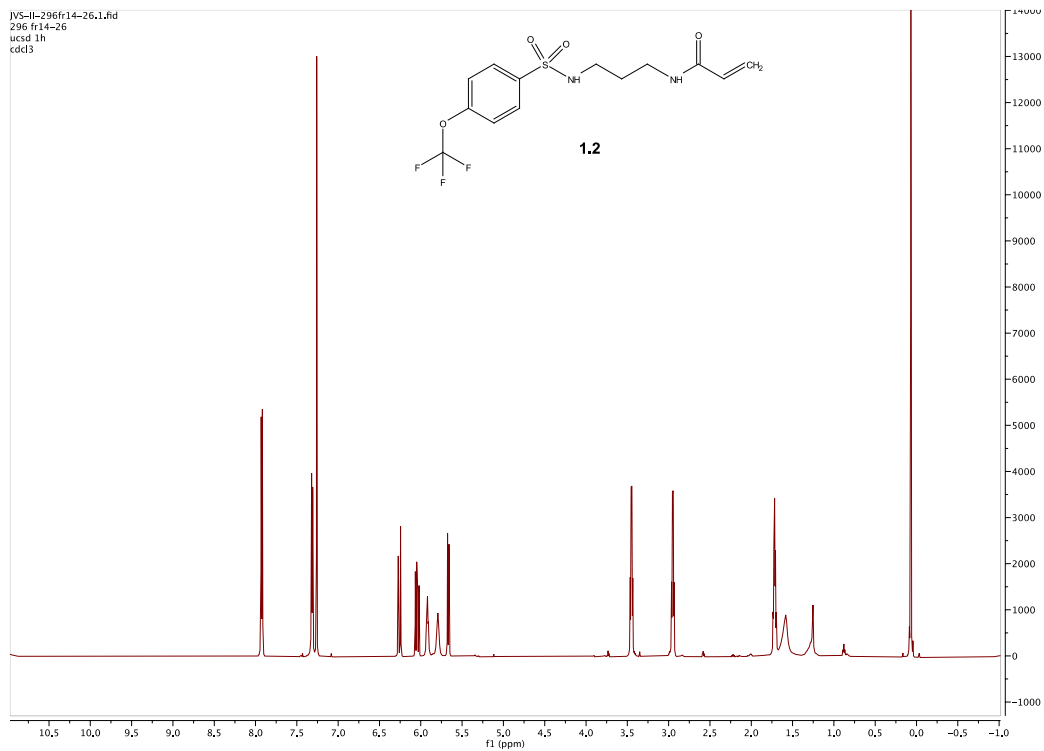
¹H NMR (599 MHz, MeOD) δ 7.88 (s, 1H), 7.84 (dd, *J* = 8.3, 4.7 Hz, 1H), 7.49 – 7.42 (m, 2H), 3.39 (t, *J* = 6.9 Hz, 2H), 3.12 (t, *J* = 6.6 Hz, 2H), 1.75 (p, *J* = 6.6 Hz, 2H), 1.44 (s, 9H). **¹³C NMR** (151 MHz, CDCl₃) δ 166.9, 165.2, 157.1, 156.6, 139.1, 134.5 (s), 132.9 (d, *J* = 3.7 Hz), 132.3 (d, *J* = 10.2 Hz), 124.2 (d, *J* = 10.1 Hz), 119.0 (d, *J* = 24.1 Hz), 114.8 (d, *J* = 25.1 Hz), 79.6, 37.4, 37.0, 30.1, 28.5. **HRMS**: *m/z*: [M+Na]⁺ Calcd for [C₁₇H₂₁FN₂O₅SNa]⁺ Theo mass: 407.1047 ; Found: 407.1048



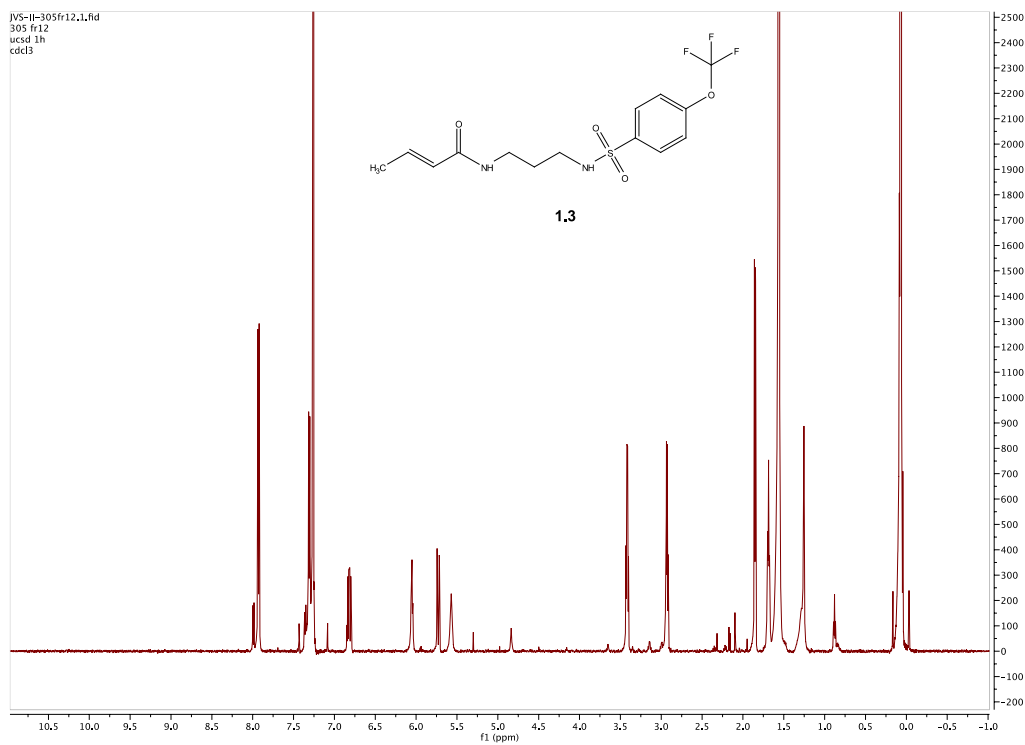
UTA248: tert-butyl (3-(5-fluoro-3-((2-hydroxyethyl)thio)-1,1-dioxido-2,3-dihydrobenzo[b]thiophene-2-carboxamido)propyl)carbamate (1.143)

General Procedure E: Thia-Micheal Addition

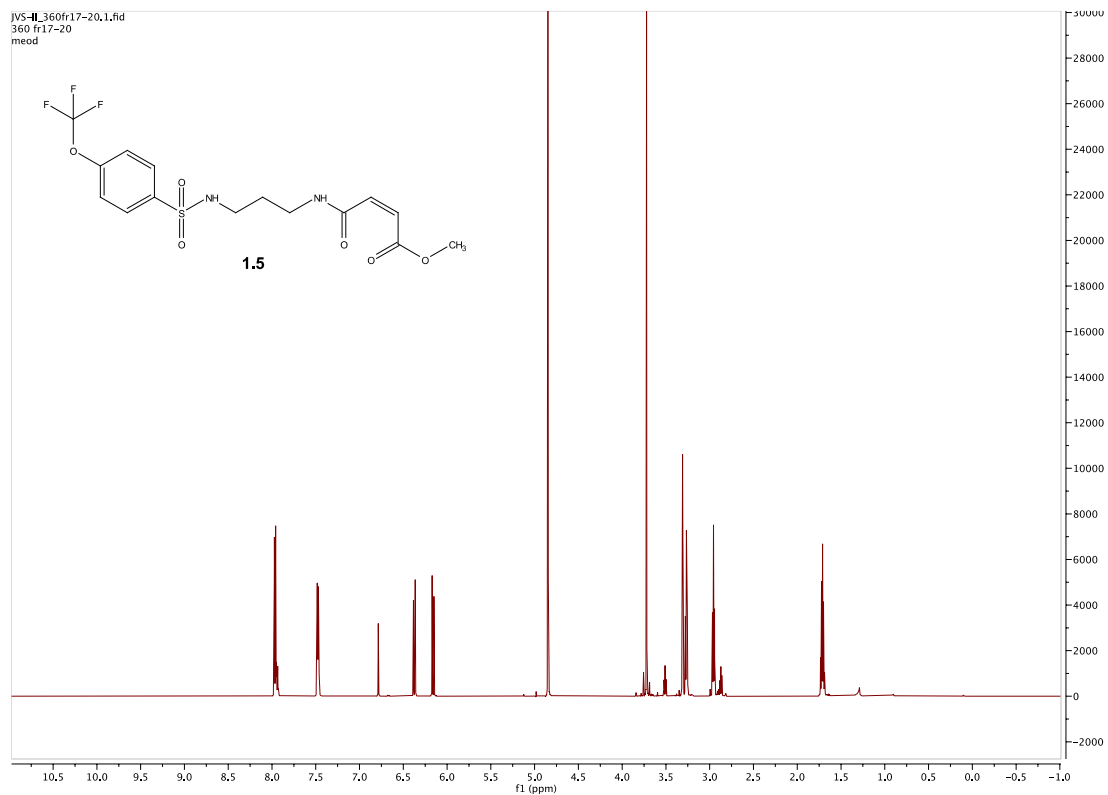
¹H NMR (599 MHz, CDCl₃) δ 7.65 (dd, *J* = 8.4, 4.6 Hz, 1H), 7.56 (s, 1H), 7.42 (d, *J* = 7.7 Hz, 1H), 7.15 (t, *J* = 8.2 Hz, 1H), 5.12 (s, 1H), 5.11 (d, *J* = 7.0 Hz, 1H), 4.61 (d, *J* = 6.7 Hz, 1H), 3.76 (dt, *J* = 13.0, 6.5 Hz, 2H), 3.36 (d, *J* = 3.7 Hz, 2H), 3.21 – 3.06 (m, 2H), 2.81 – 2.65 (m, 2H), 1.70 – 1.61 (m, 2H), 1.39 (s, 9H). **¹³C NMR** (151 MHz, CDCl₃) δ 167.1, 165.4, 162.0, 156.7, 141.4 (d, *J* = 9.4 Hz), 133.6, 123.8 (d, *J* = 9.8 Hz), 117.8 (d, *J* = 24.1 Hz), 114.5 (d, *J* = 24.3 Hz), 79.5, 73.2, 61.6, 44.0, 37.3 (d, *J* = 10.8 Hz), 34.2, 29.5, 28.4. **HRMS:** *m/z*: [M+Na]⁺ Calcd for [C₁₉H₂₇FN₂O₇S₂Na]⁺ Theo mass: 485.1187 ; Found: 485.1190



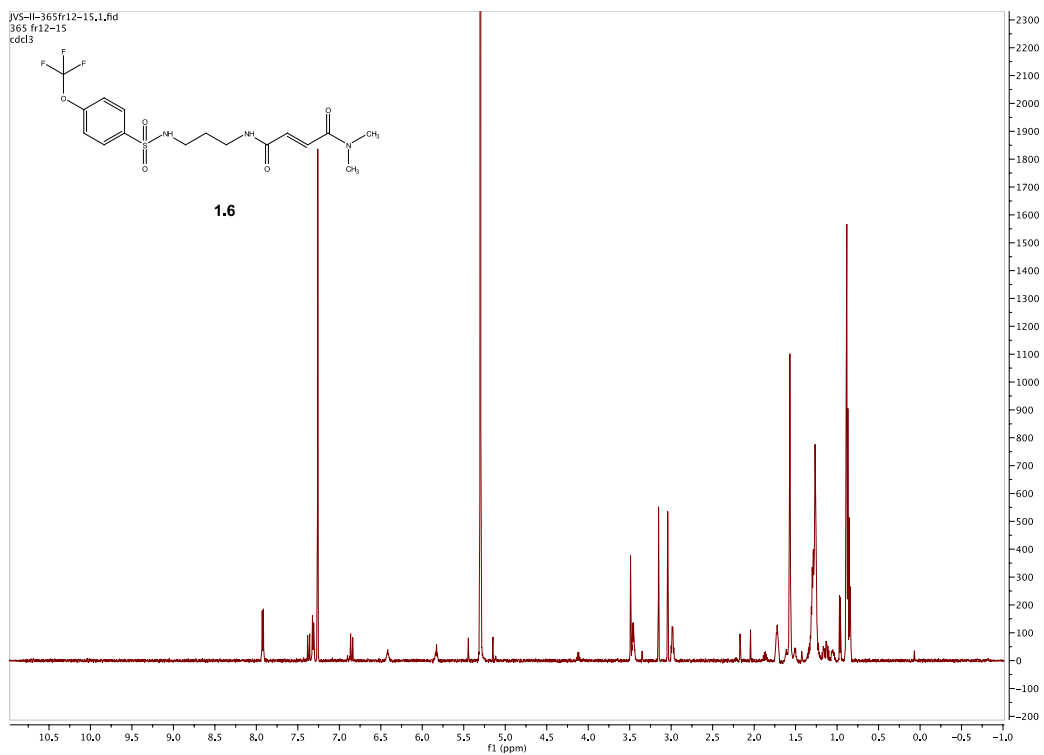
Spectra 1.1 ¹H NMR Spectrum of compound 1.2



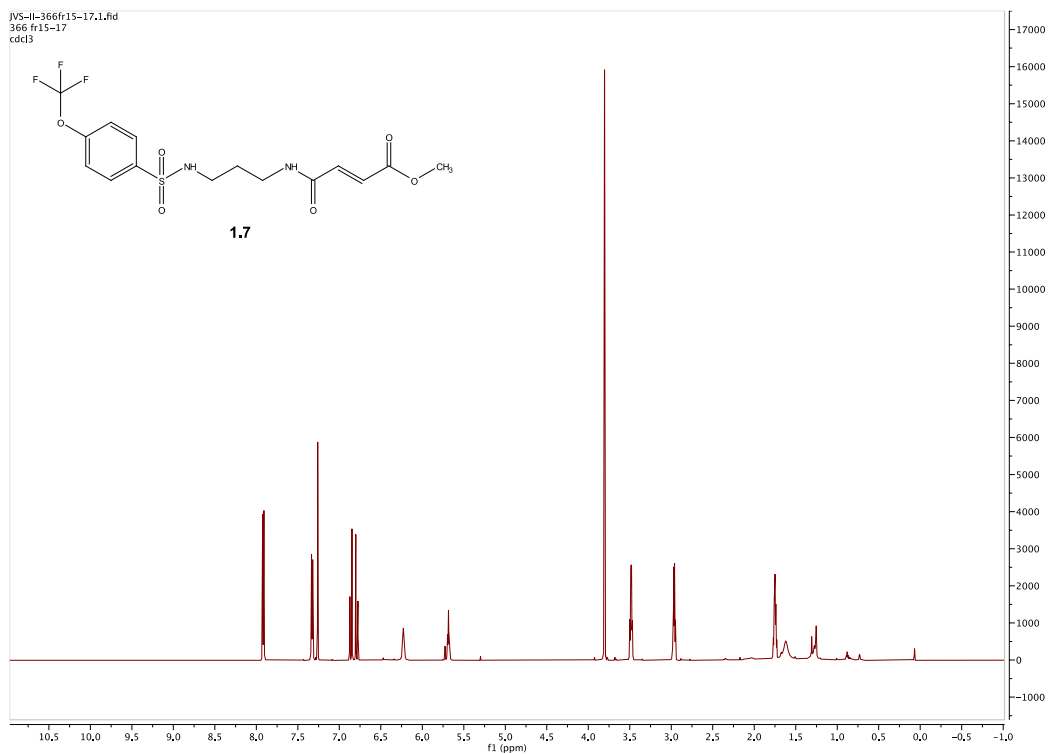
Spectra 1.2 ¹H NMR Spectrum of compound 1.3



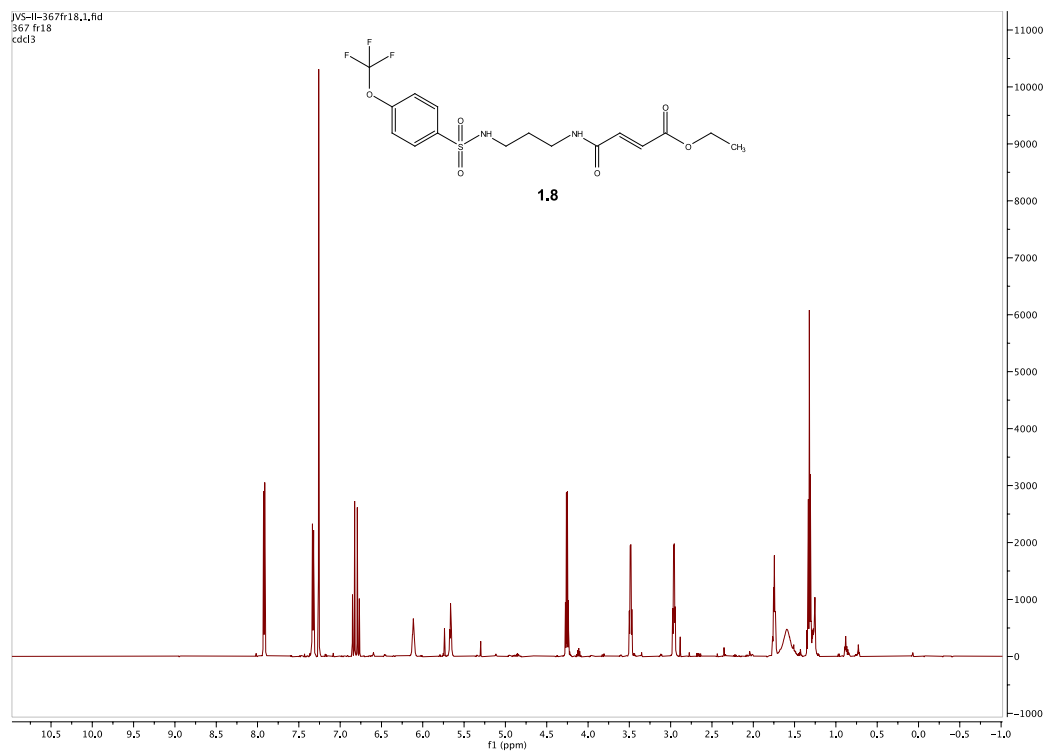
Spectra 1.3 ^1H NMR Spectrum of compound **1.5**



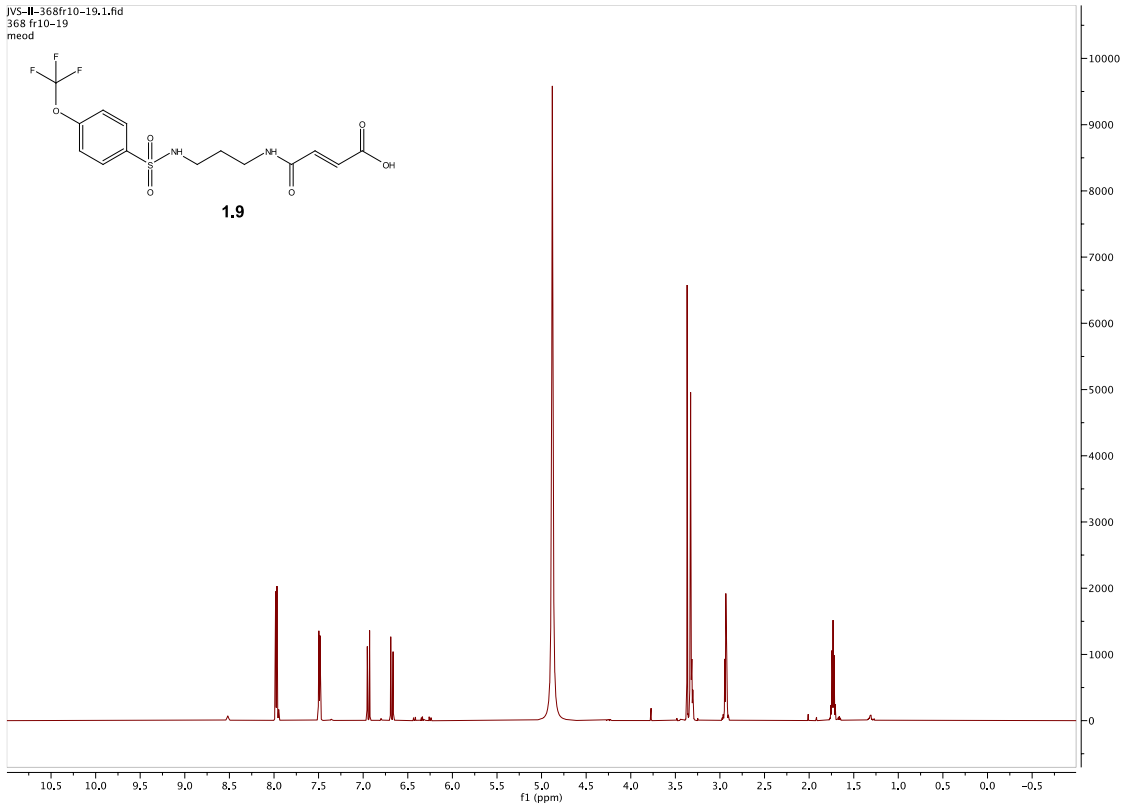
Spectra 1.4 ^1H NMR Spectrum of compound **1.6**



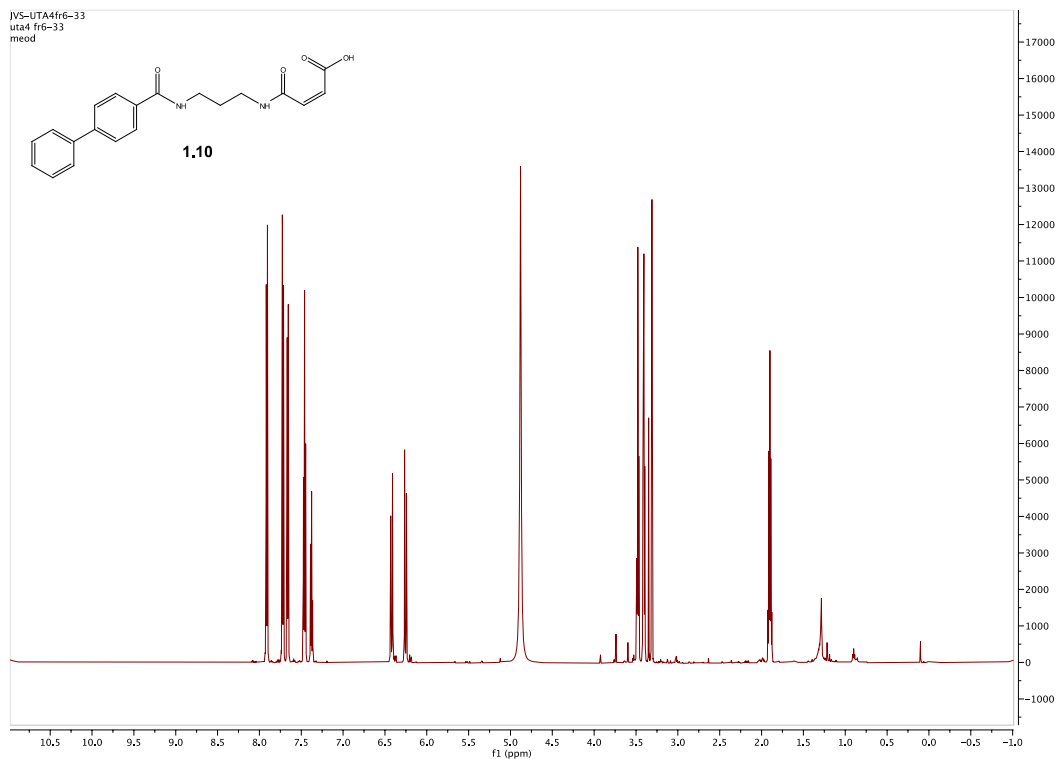
Spectra 1.5 ^1H NMR Spectrum of compound **1.7**



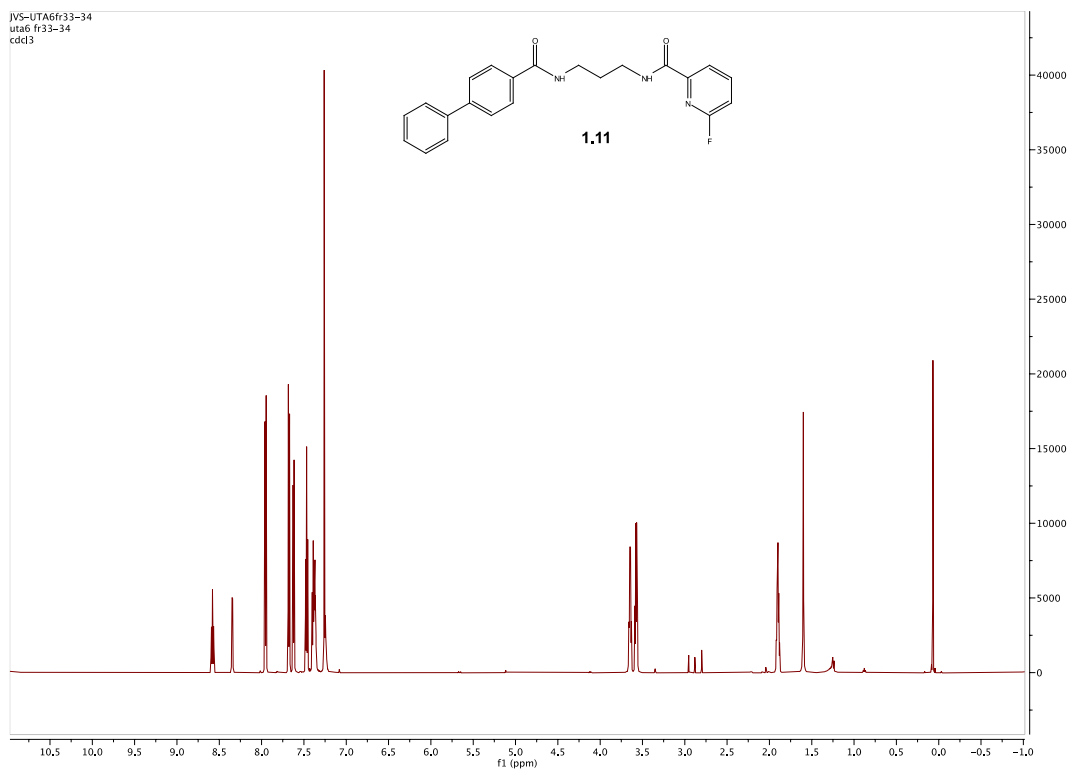
Spectra 1.6 ^1H NMR Spectrum of compound **1.8**



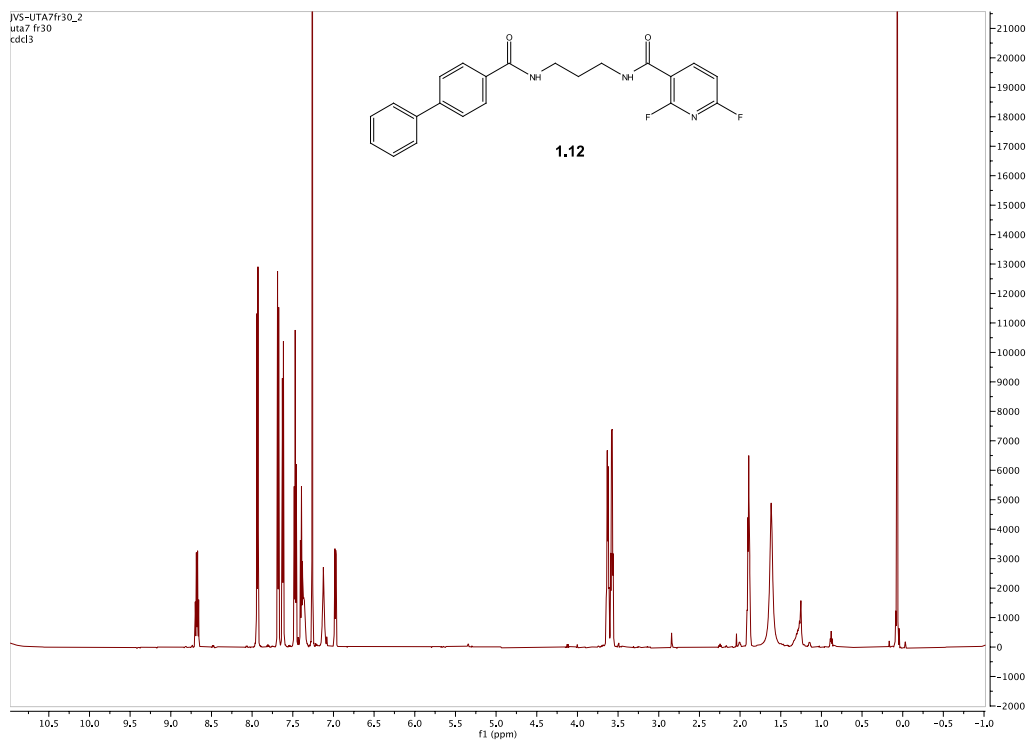
Spectra 1.7 ^1H NMR Spectrum of compound **1.9**



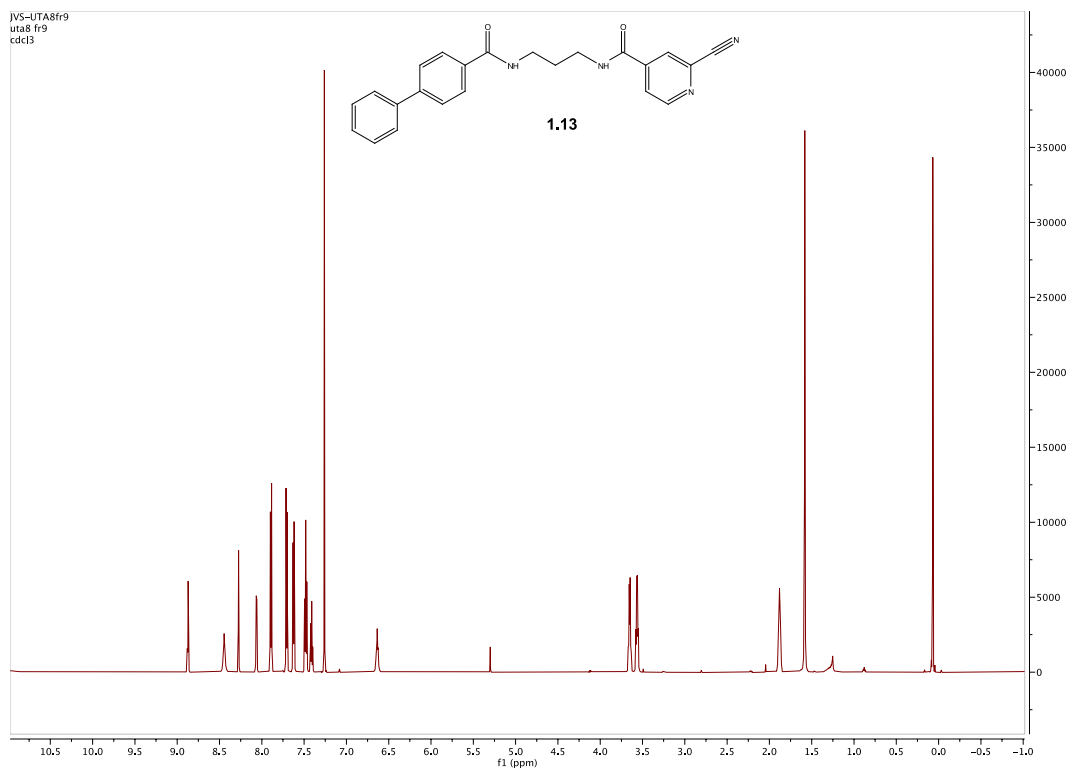
Spectra 1.8 ^1H NMR Spectrum of compound **1.10**



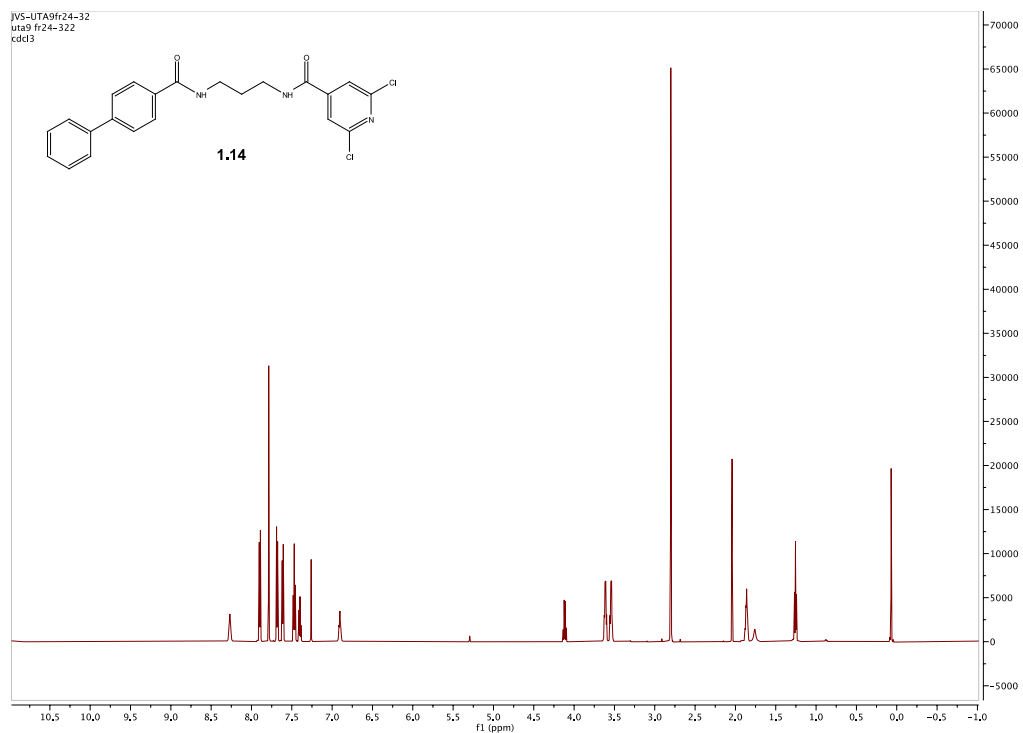
Spectra 1.9 ^1H NMR Spectrum of compound **1.11**



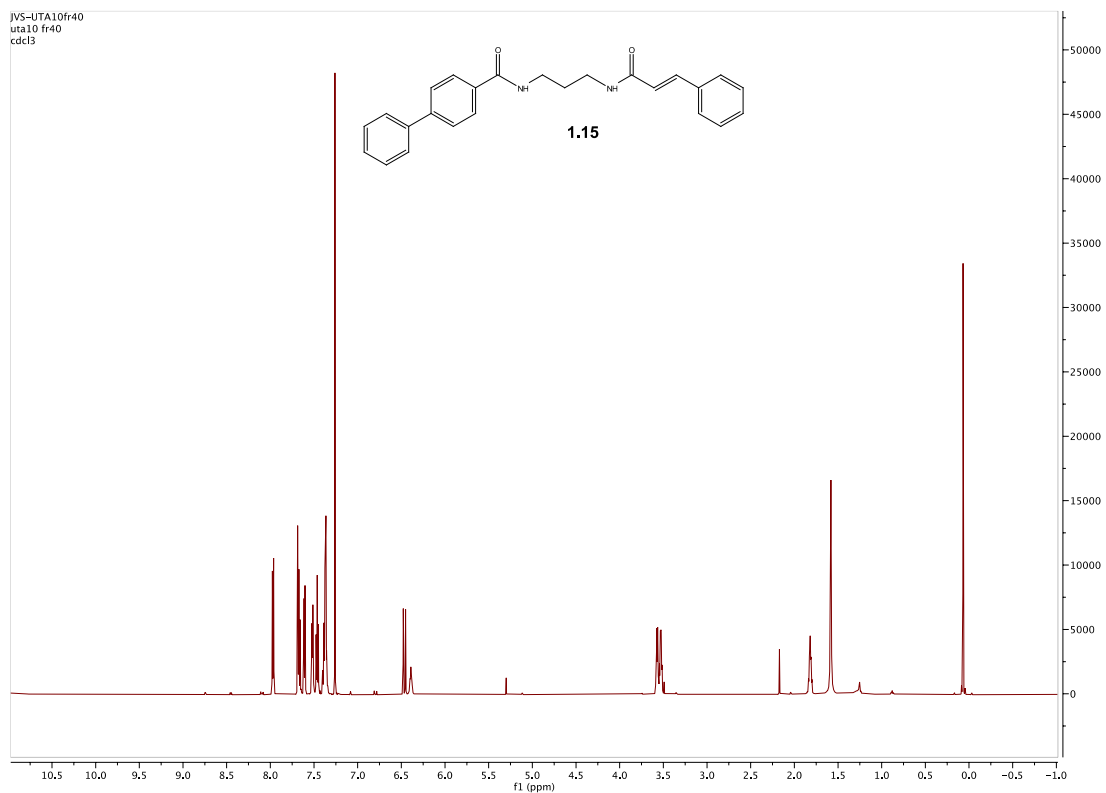
Spectra 1.10 ^1H NMR Spectrum of compound **1.12**



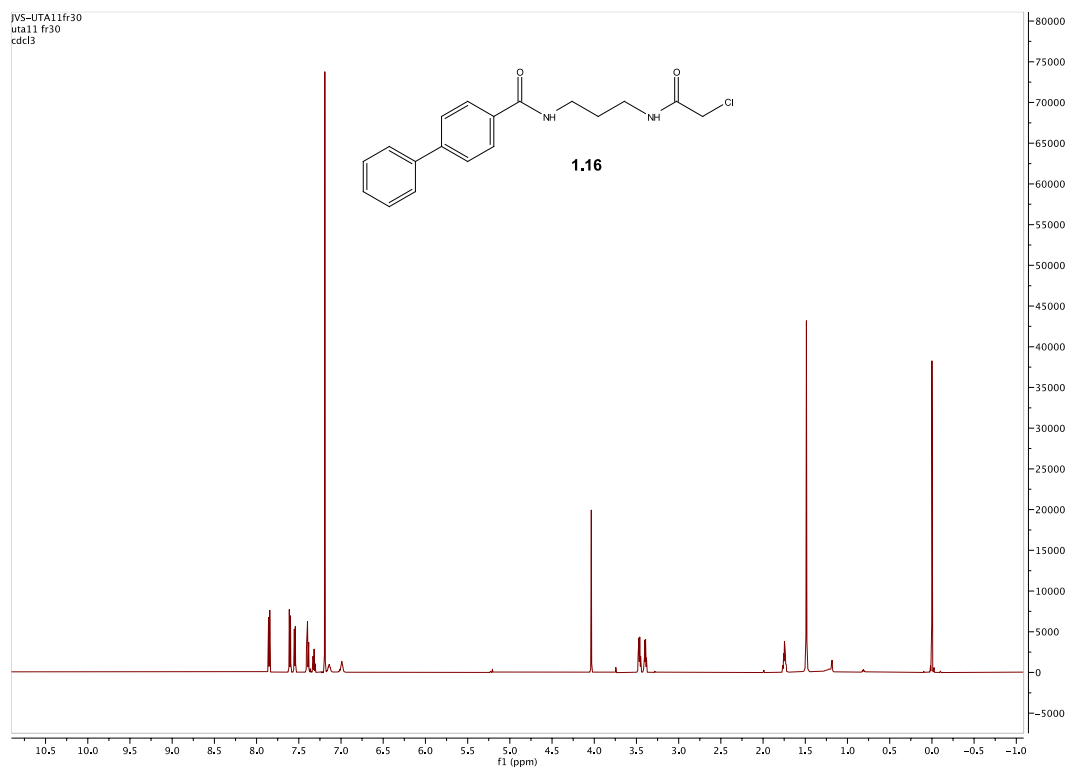
Spectra 1.11 ¹H NMR Spectrum of compound 1.13



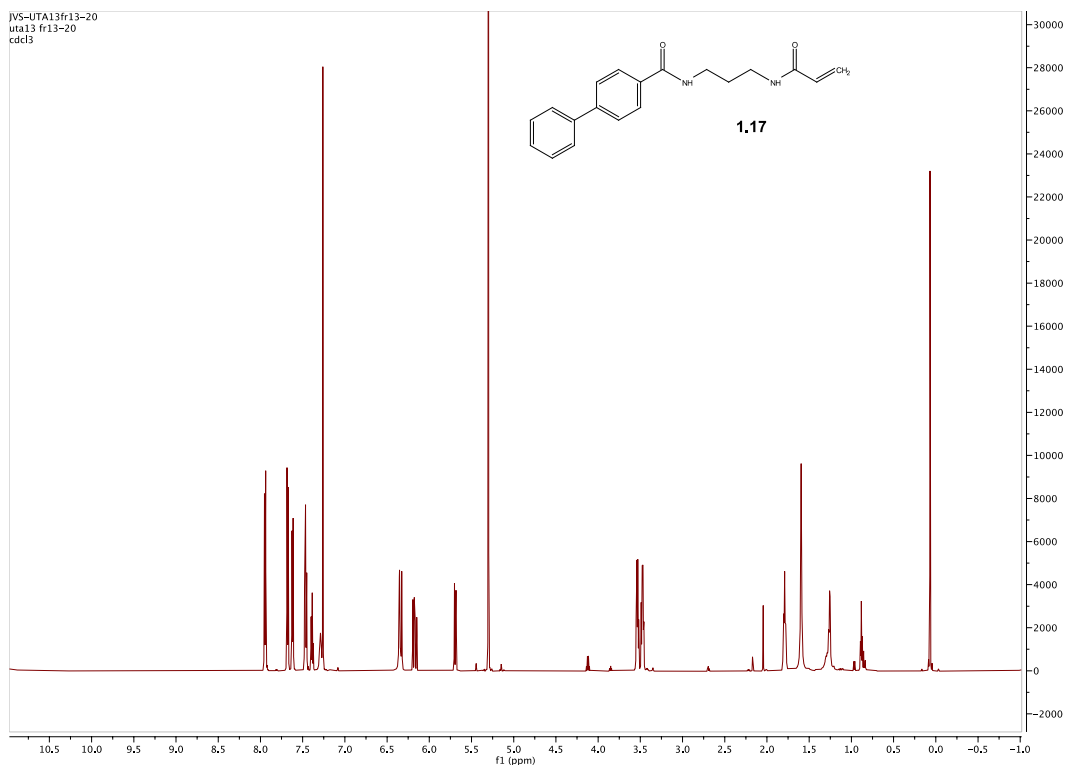
Spectra 1.12 ¹H NMR Spectrum of compound 1.14



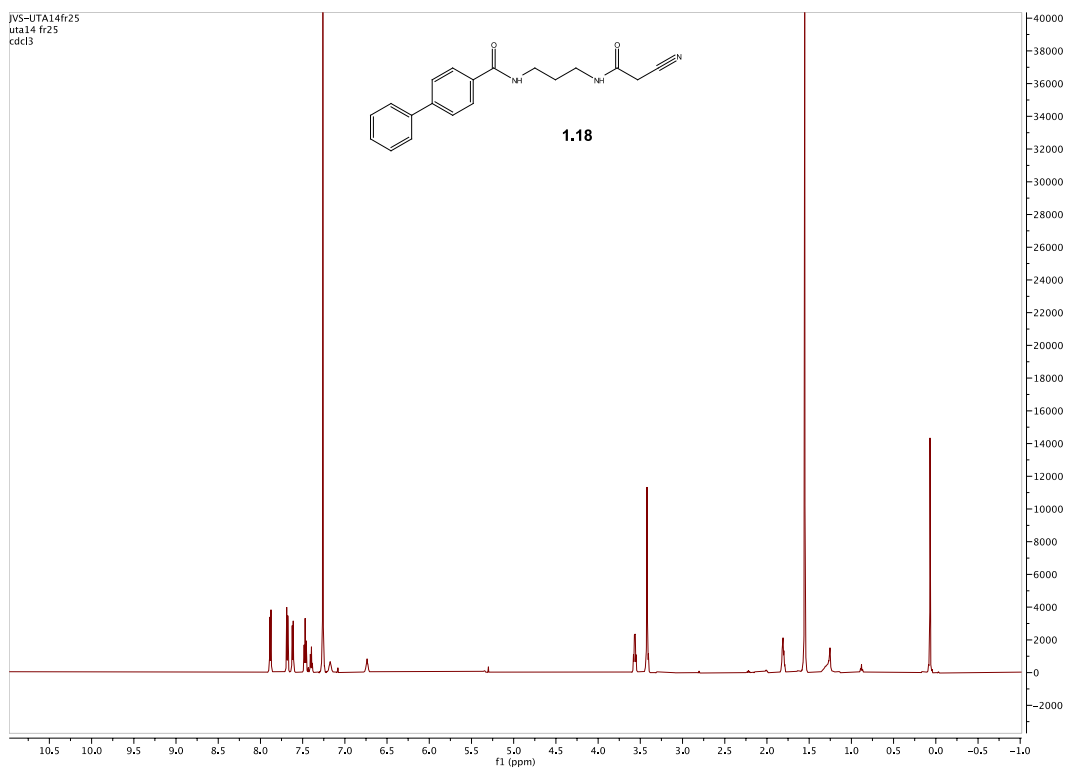
Spectra 1.13 ¹H NMR Spectrum of compound 1.15



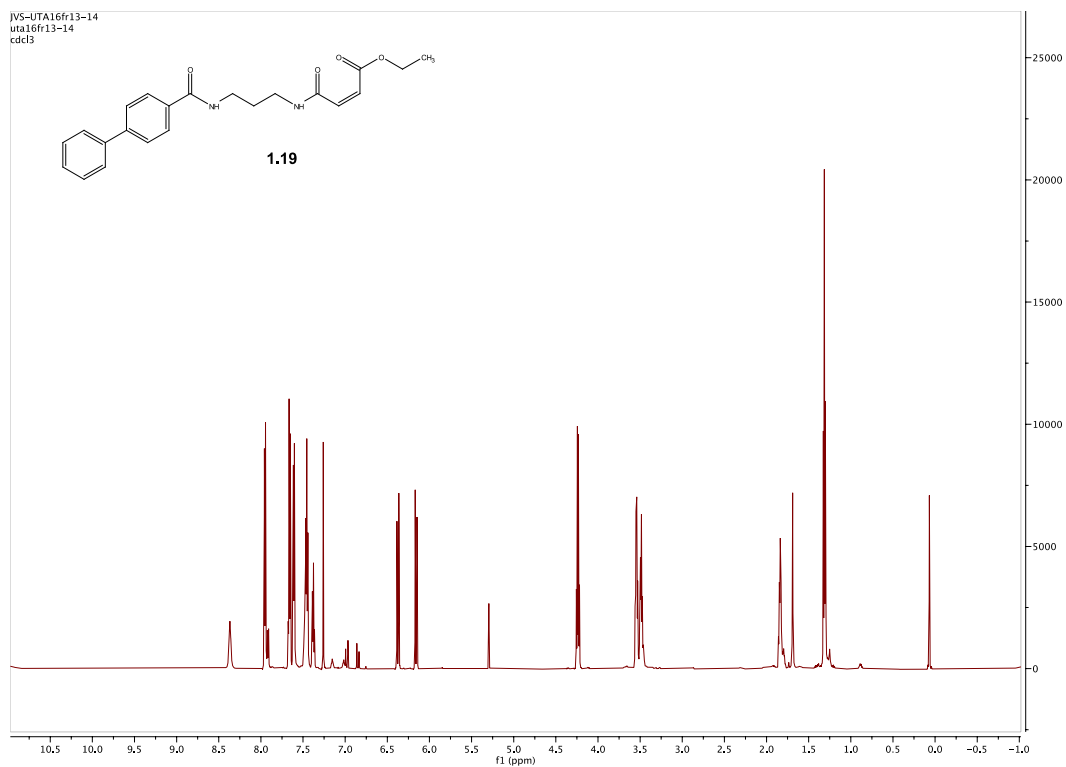
Spectra 1.14 ¹H NMR Spectrum of compound 1.16



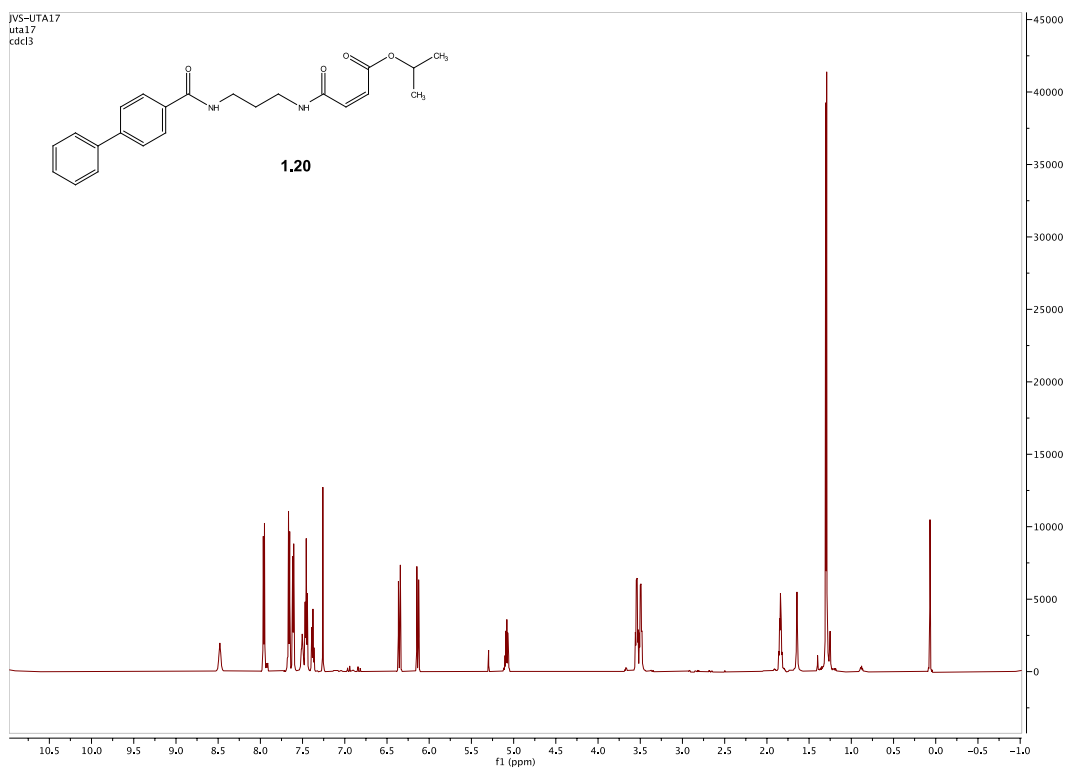
Spectra 1.15 ^1H NMR Spectrum of compound **1.17**



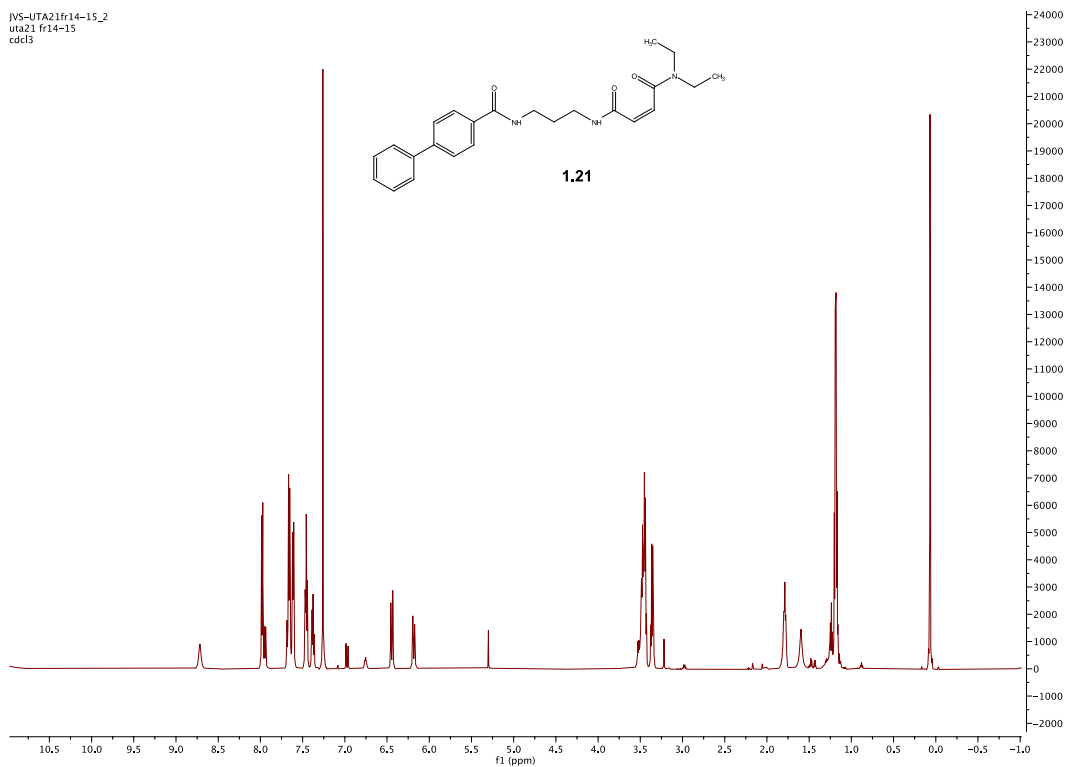
Spectra 1.16 ^1H NMR Spectrum of compound **1.16**



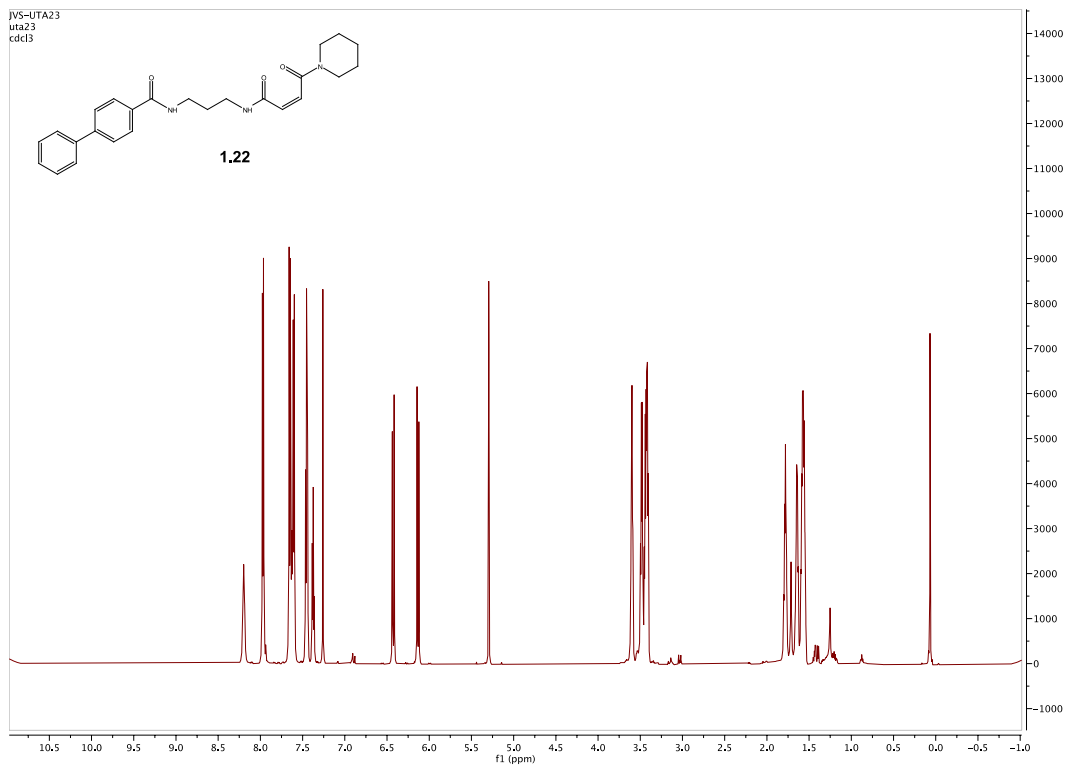
Spectra 1.17 ^1H NMR Spectrum of compound **1.19**



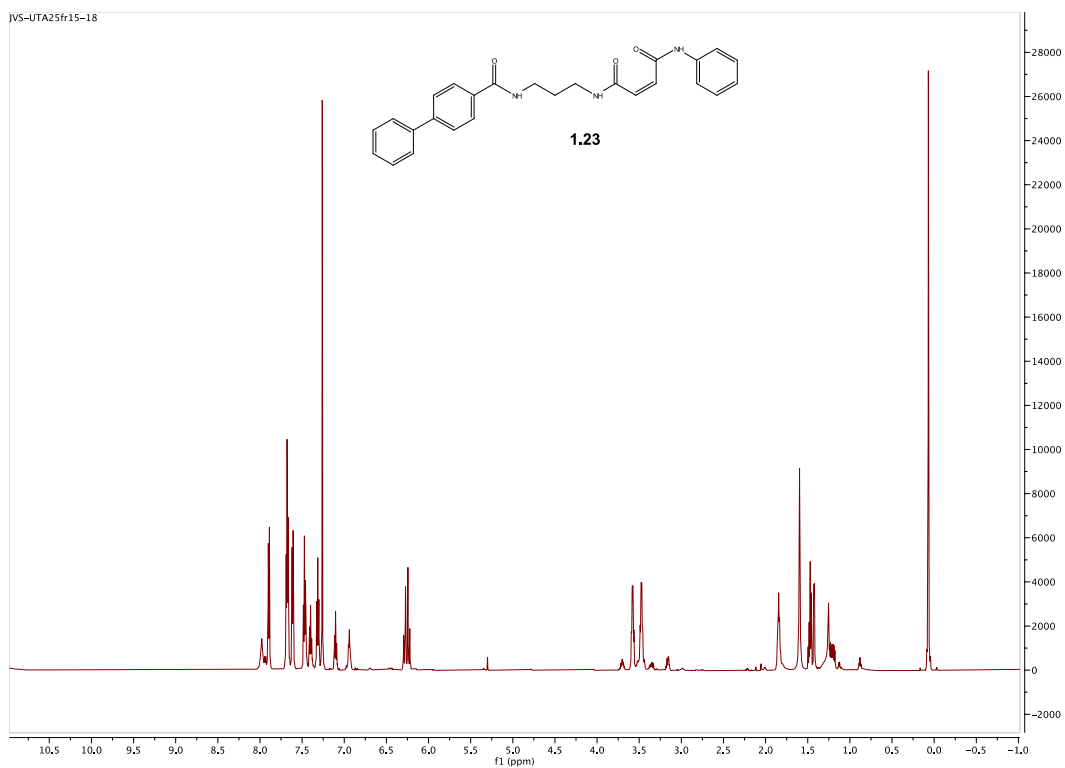
Spectra 1.18 ^1H NMR Spectrum of compound **1.20**



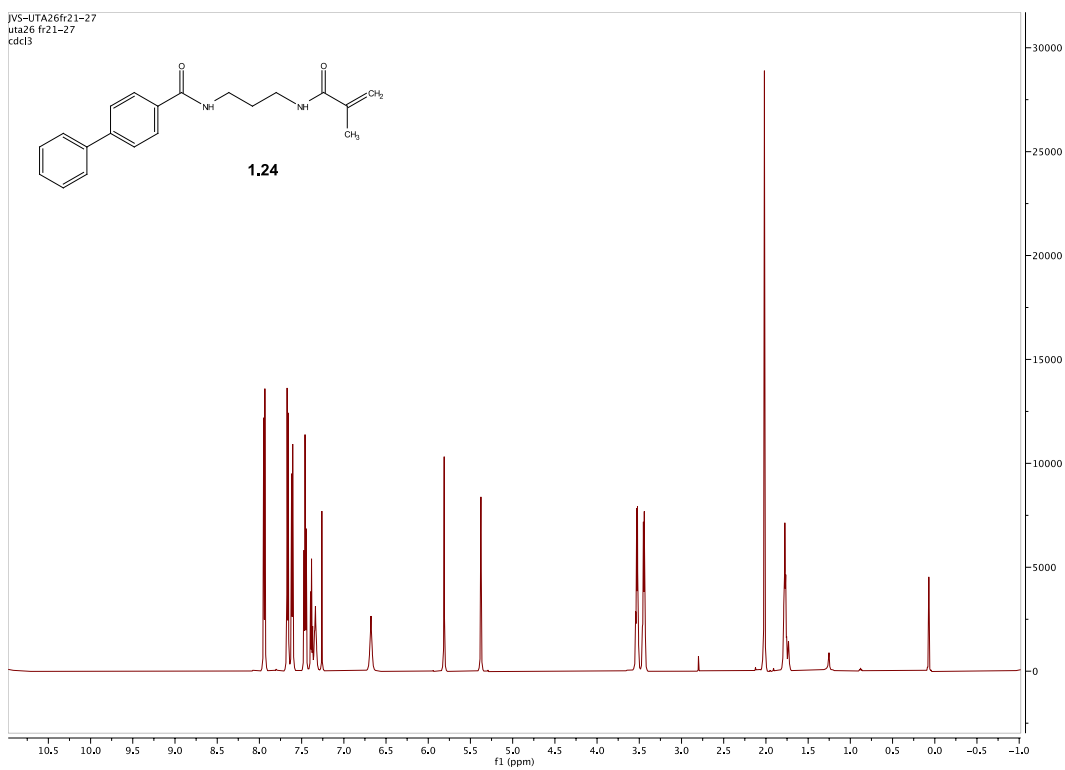
Spectra 1.19 ^1H NMR Spectrum of compound **1.21**



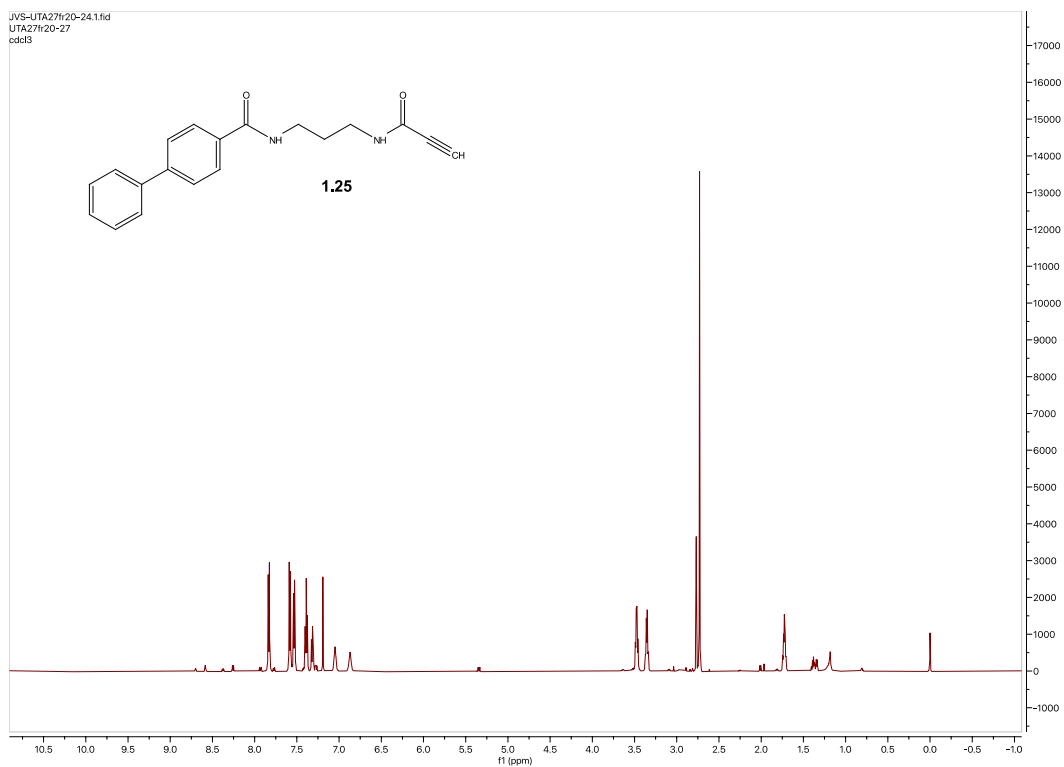
Spectra 1.20 ^1H NMR Spectrum of compound **1.22**



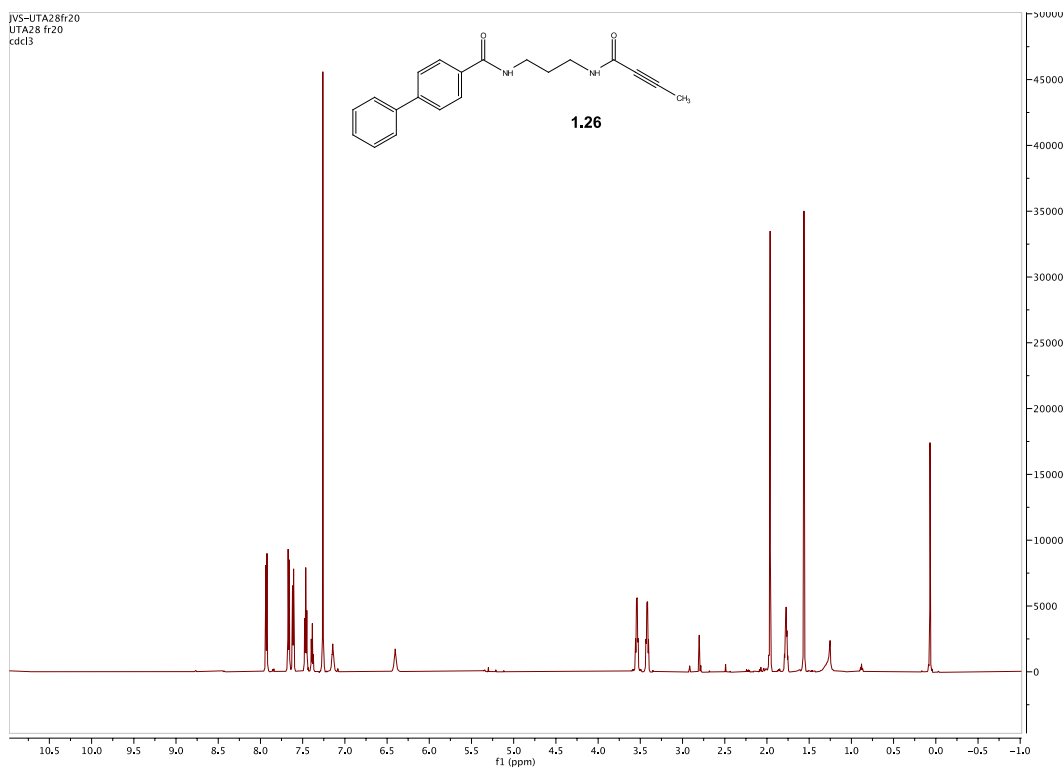
Spectra 1.21 ¹H NMR Spectrum of compound 1.23



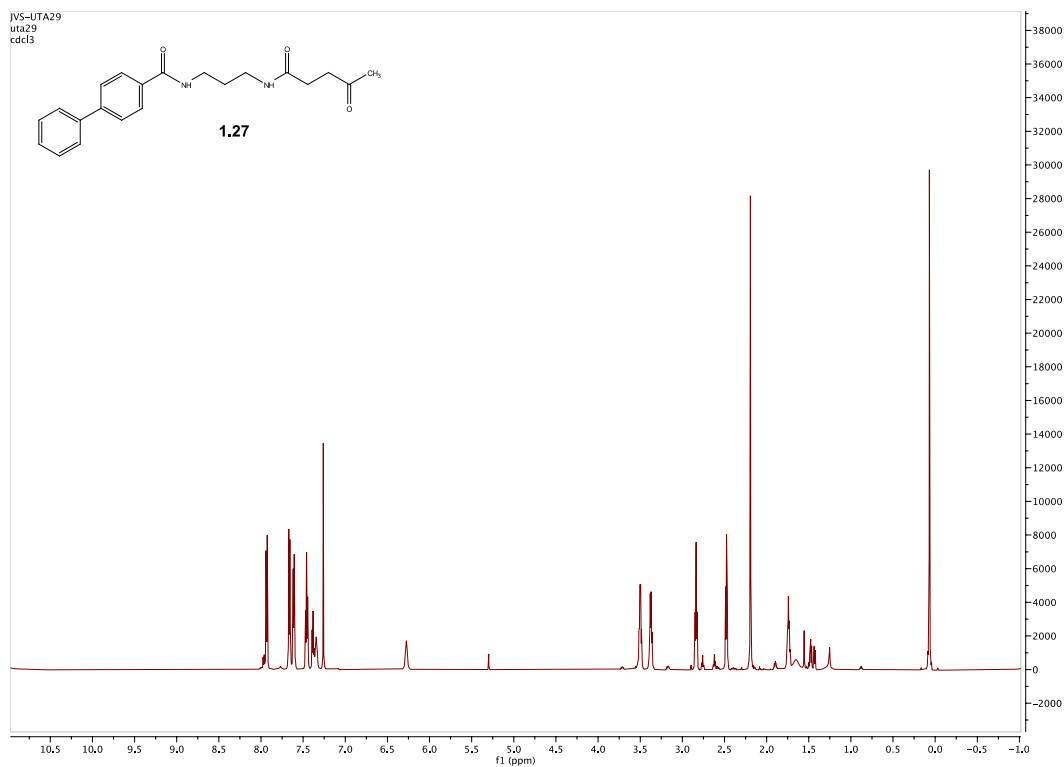
Spectra 1.22 ¹H NMR Spectrum of compound 1.24



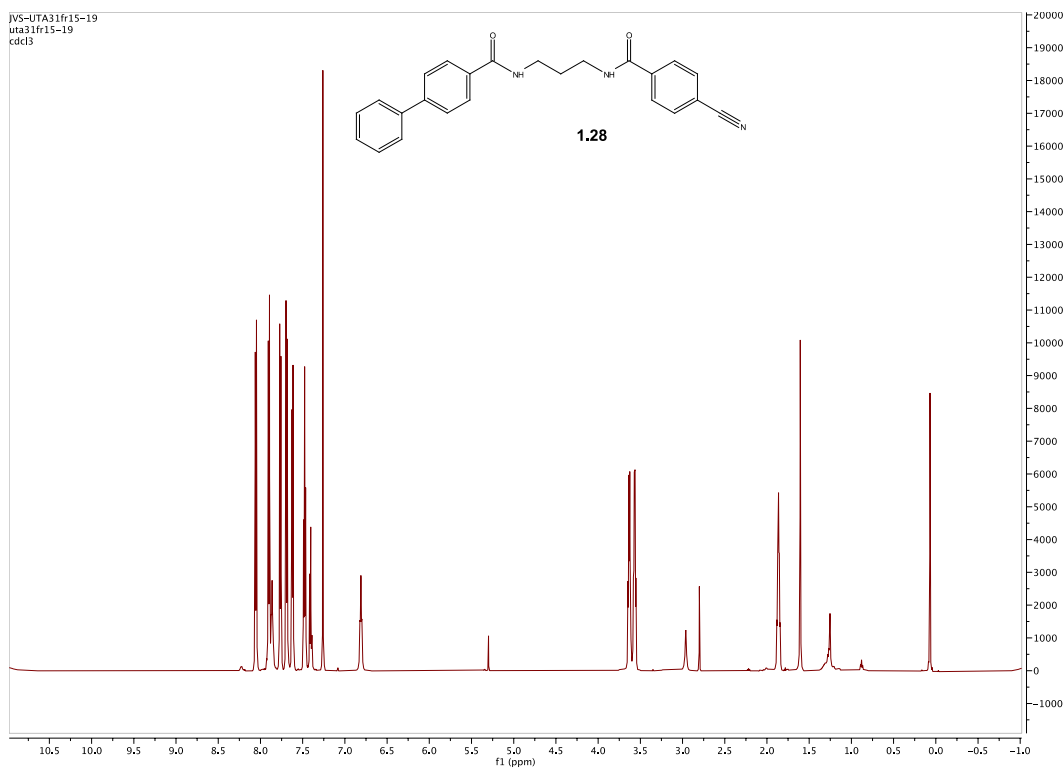
Spectra 1.23 ^1H NMR Spectrum of compound **1.25**



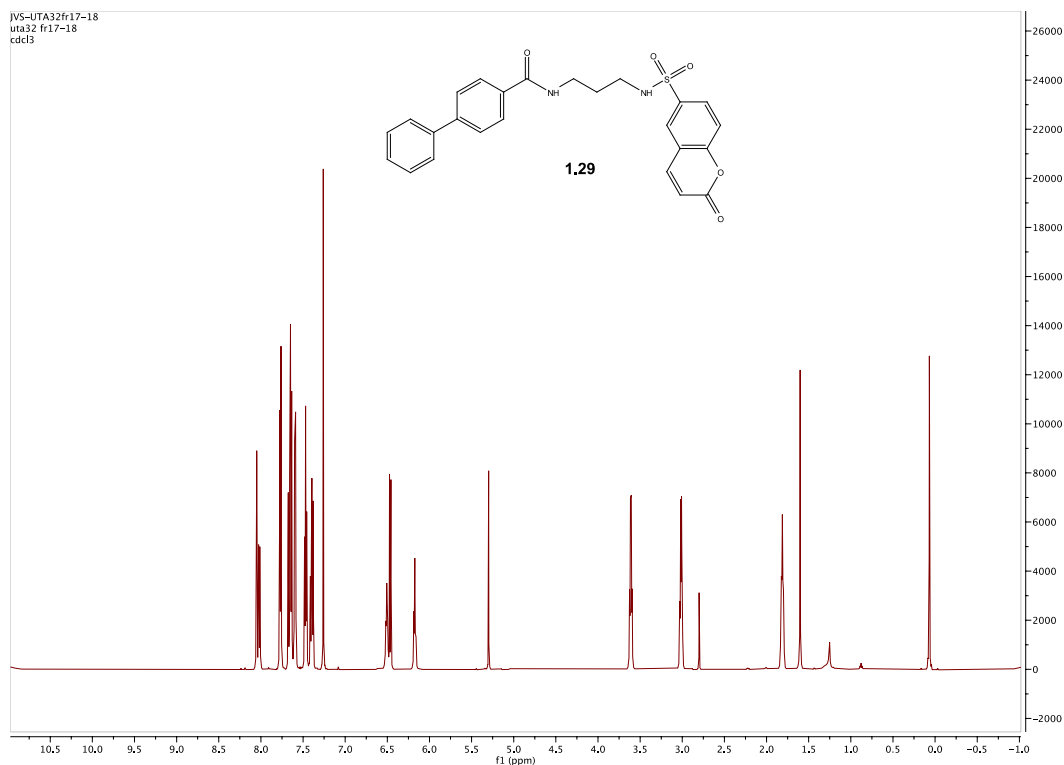
Spectra 1.24 ^1H NMR Spectrum of compound **1.26**



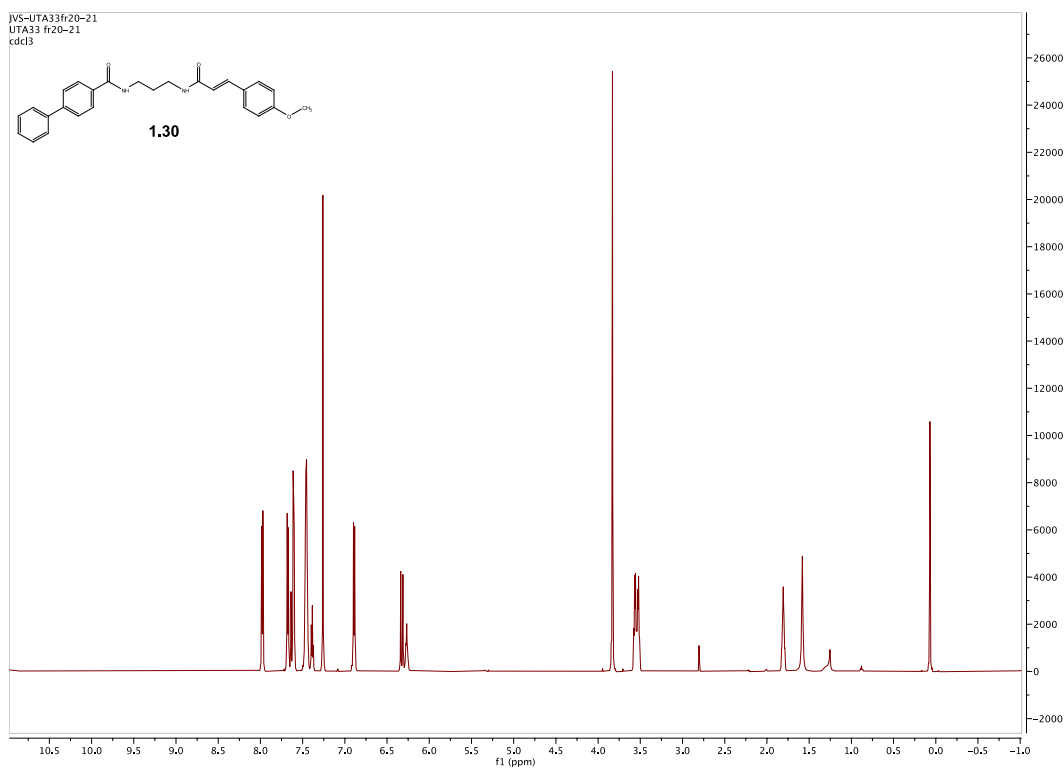
Spectra 1.25 ^1H NMR Spectrum of compound **1.27**



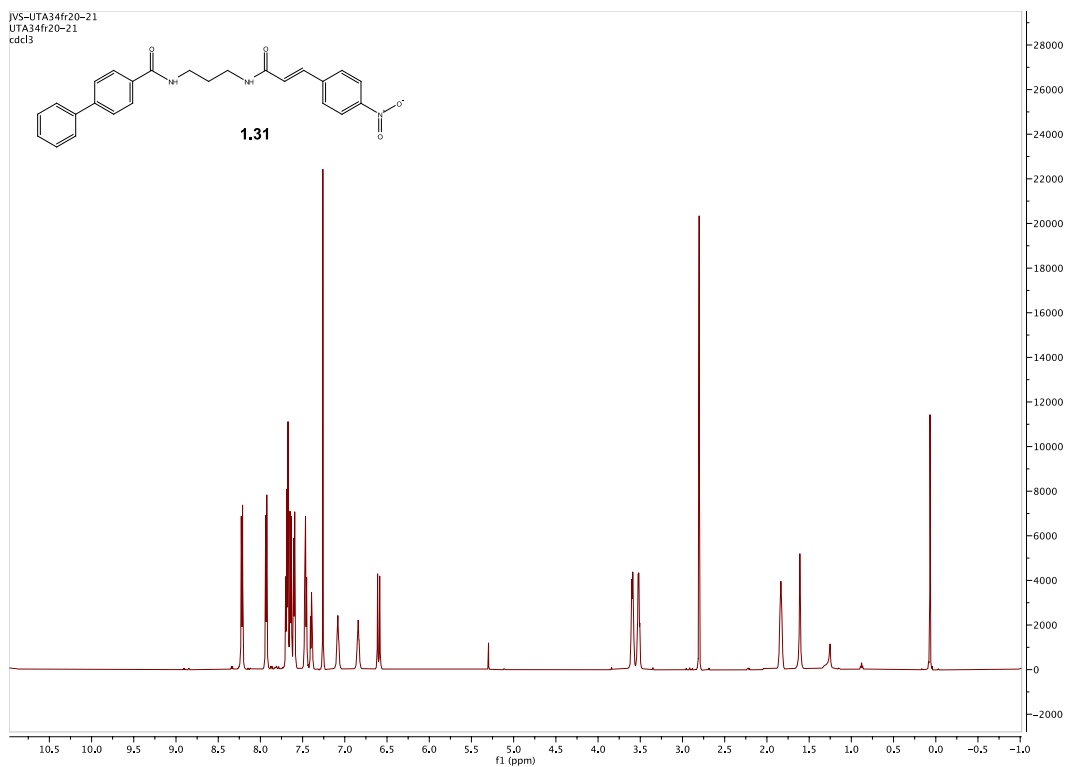
Spectra 1.26 ^1H NMR Spectrum of compound **1.28**



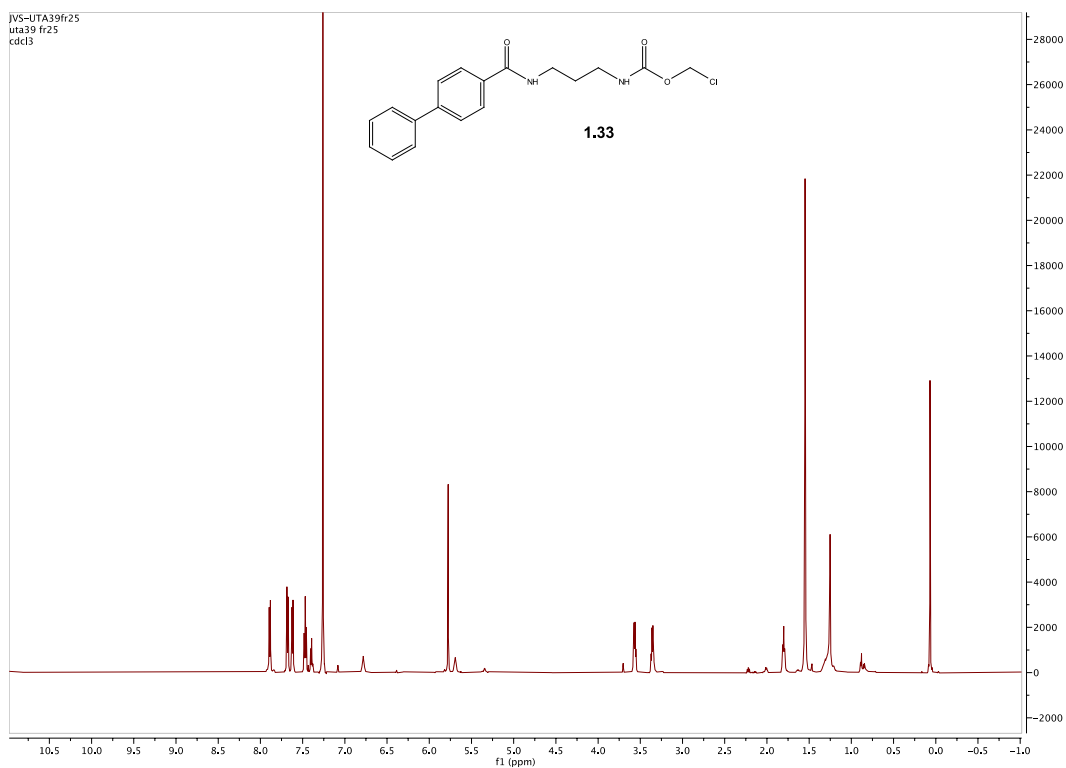
Spectra 1.27 ¹H NMR Spectrum of compound 1.29



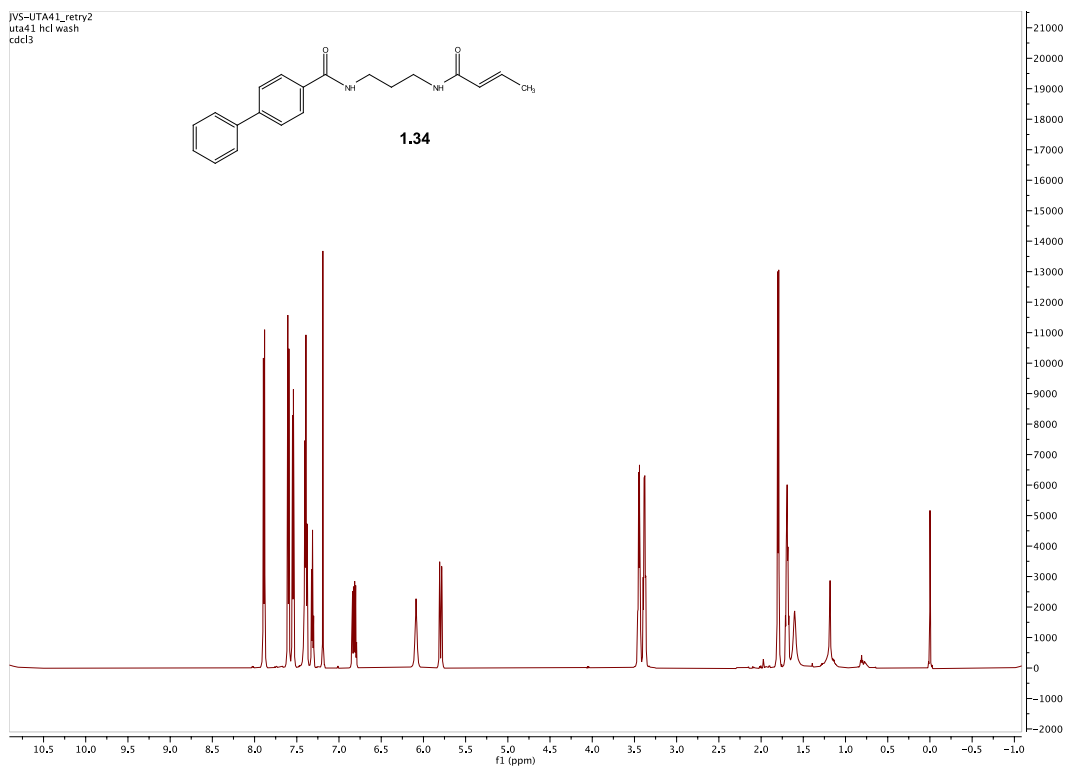
Spectra 1.28 ¹H NMR Spectrum of compound 1.30



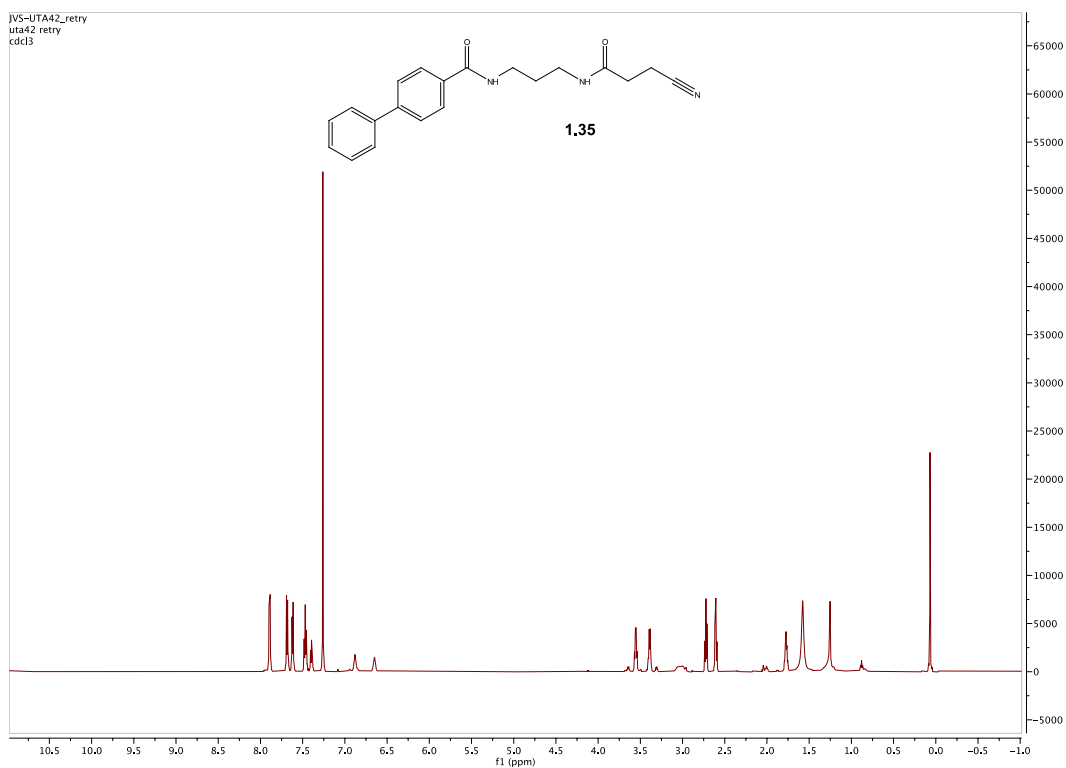
Spectra 1.29 ^1H NMR Spectrum of compound **1.31**



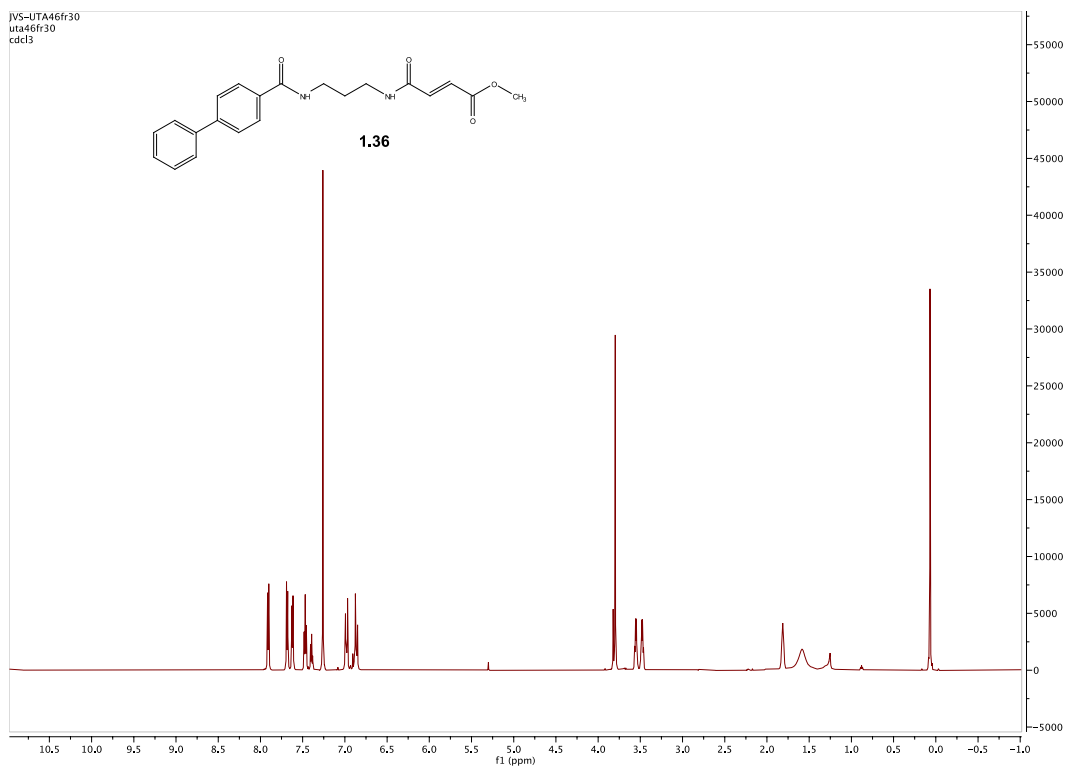
Spectra 1.30 ^1H NMR Spectrum of compound **1.33**



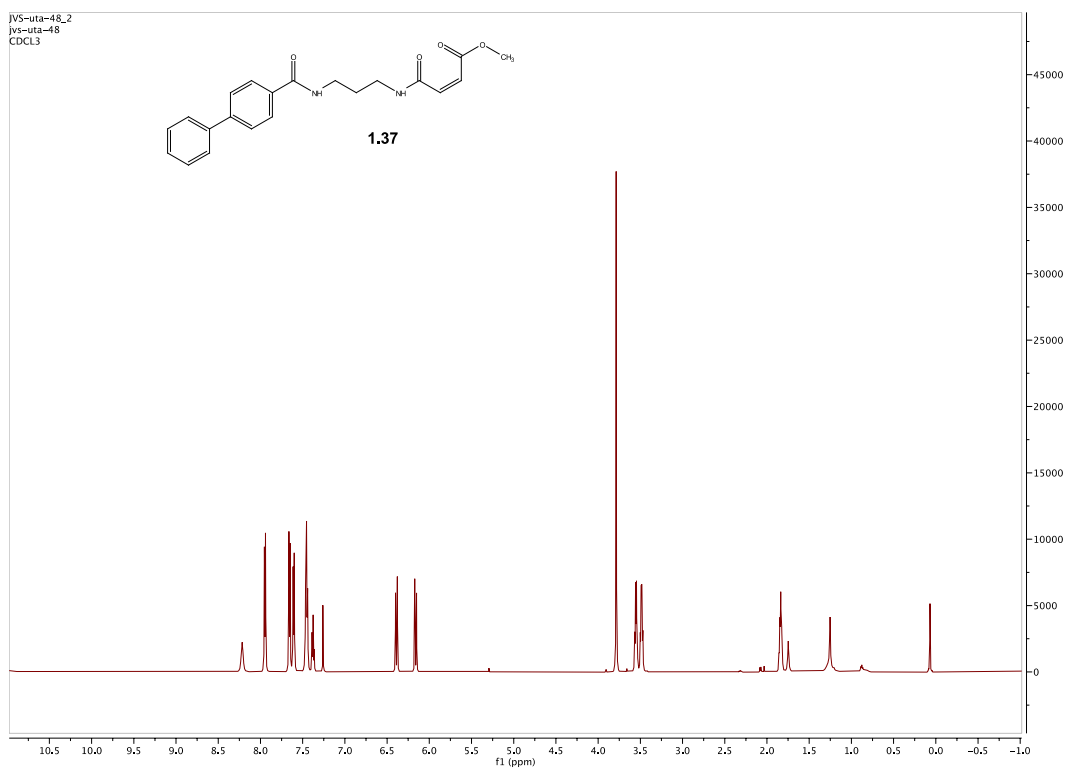
Spectra 1.31 ^1H NMR Spectrum of compound **1.34**



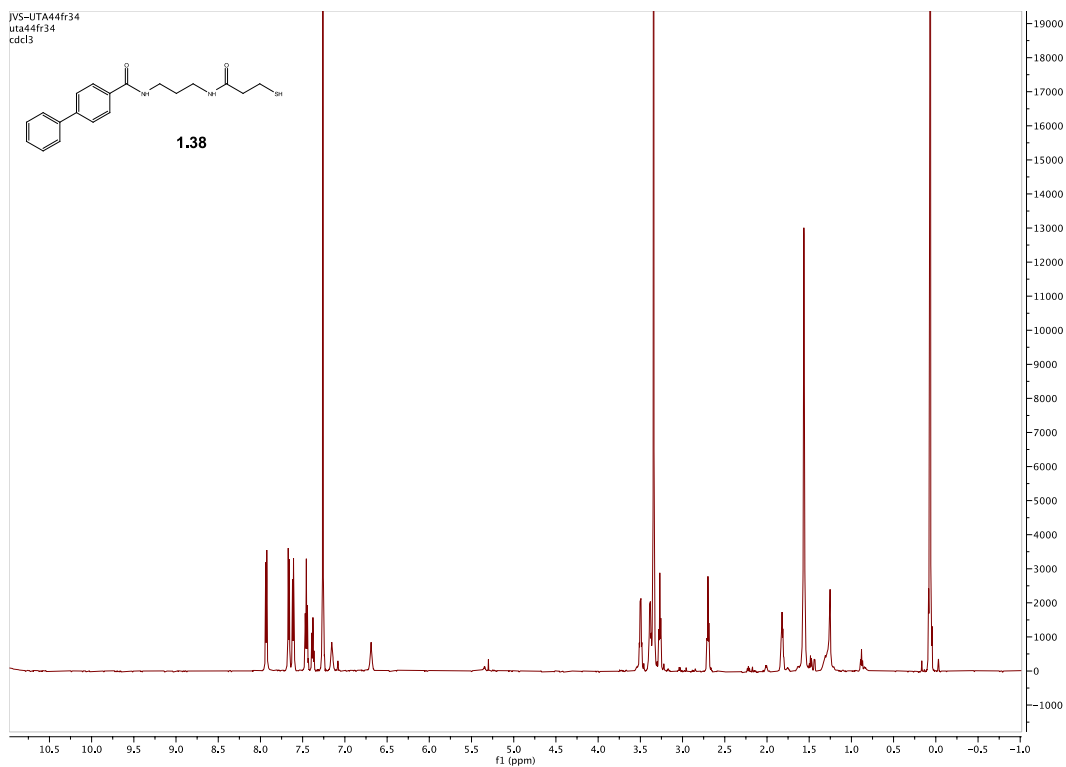
Spectra 1.32 ^1H NMR Spectrum of compound **1.35**



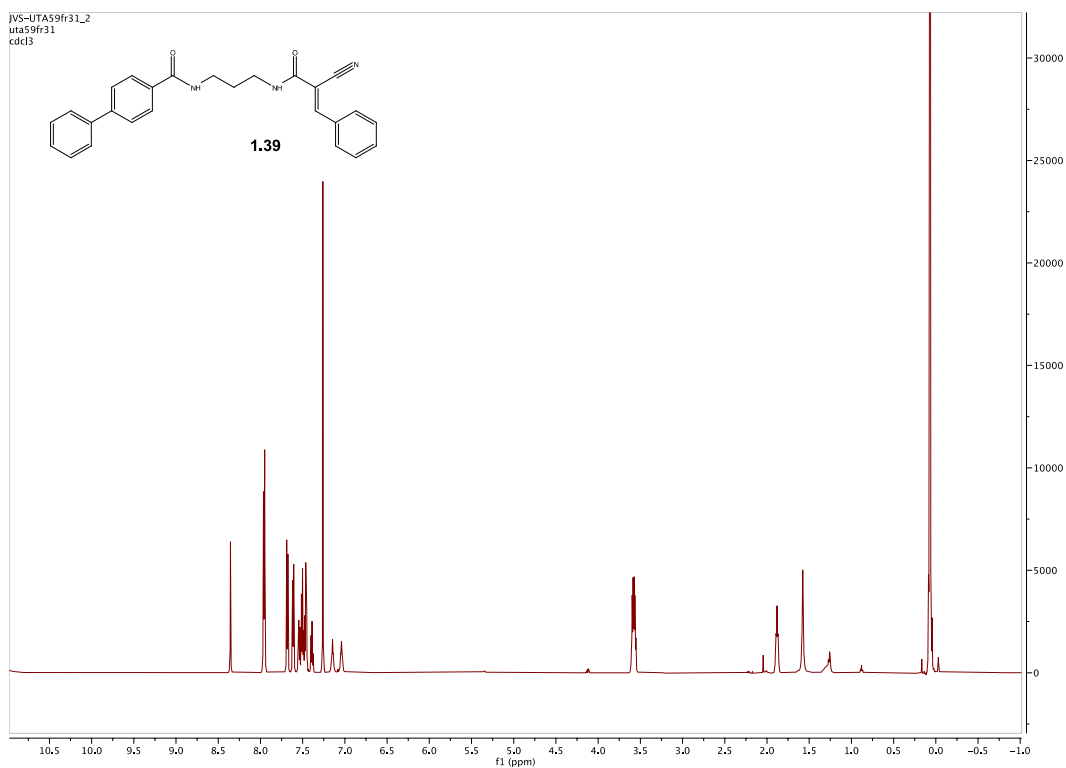
Spectra 1.33 ^1H NMR Spectrum of compound **1.36**



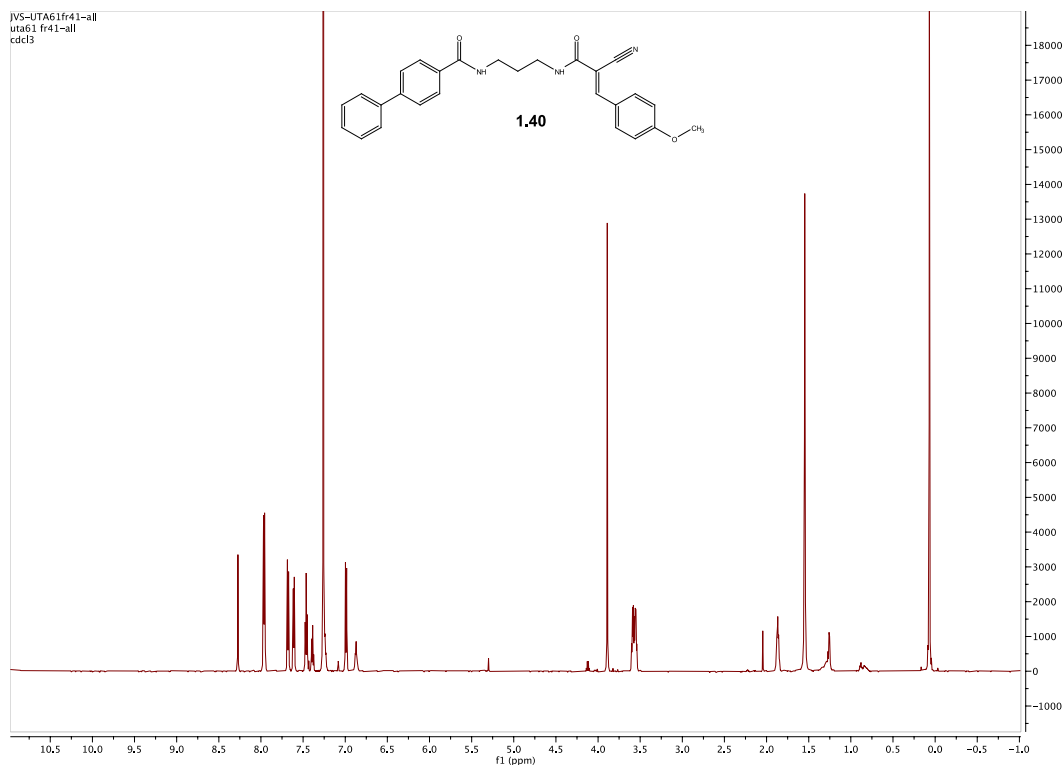
Spectra 1.34 ^1H NMR Spectrum of compound **1.37**



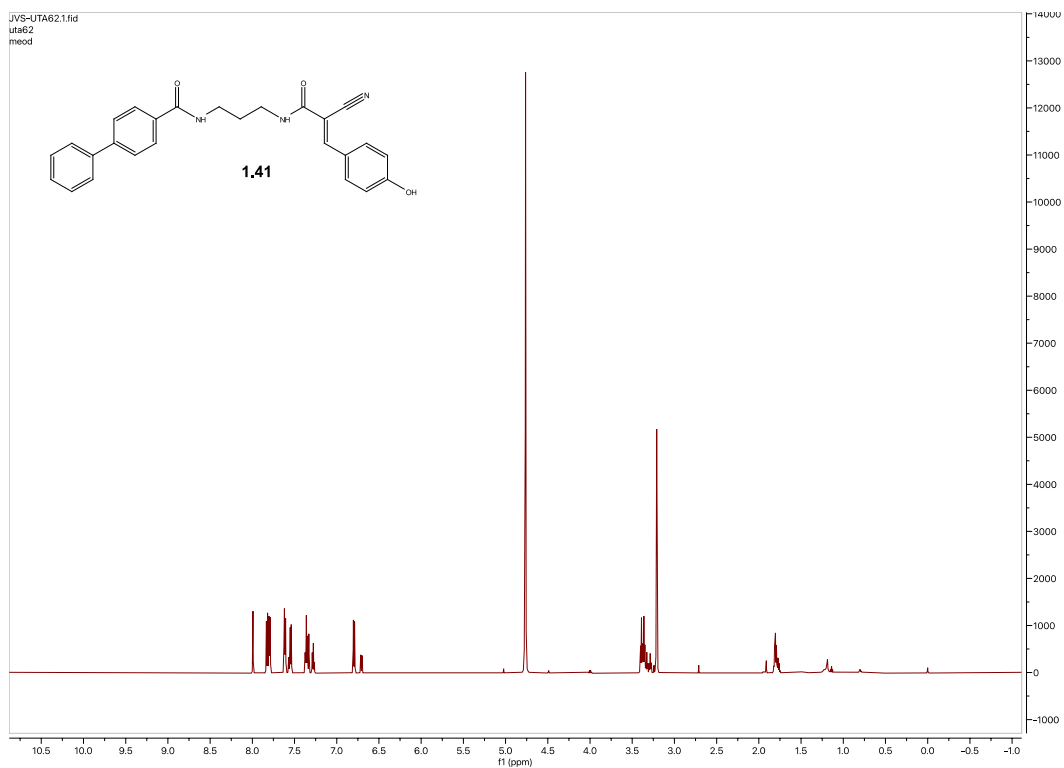
Spectra 1.35 ^1H NMR Spectrum of compound **1.38**



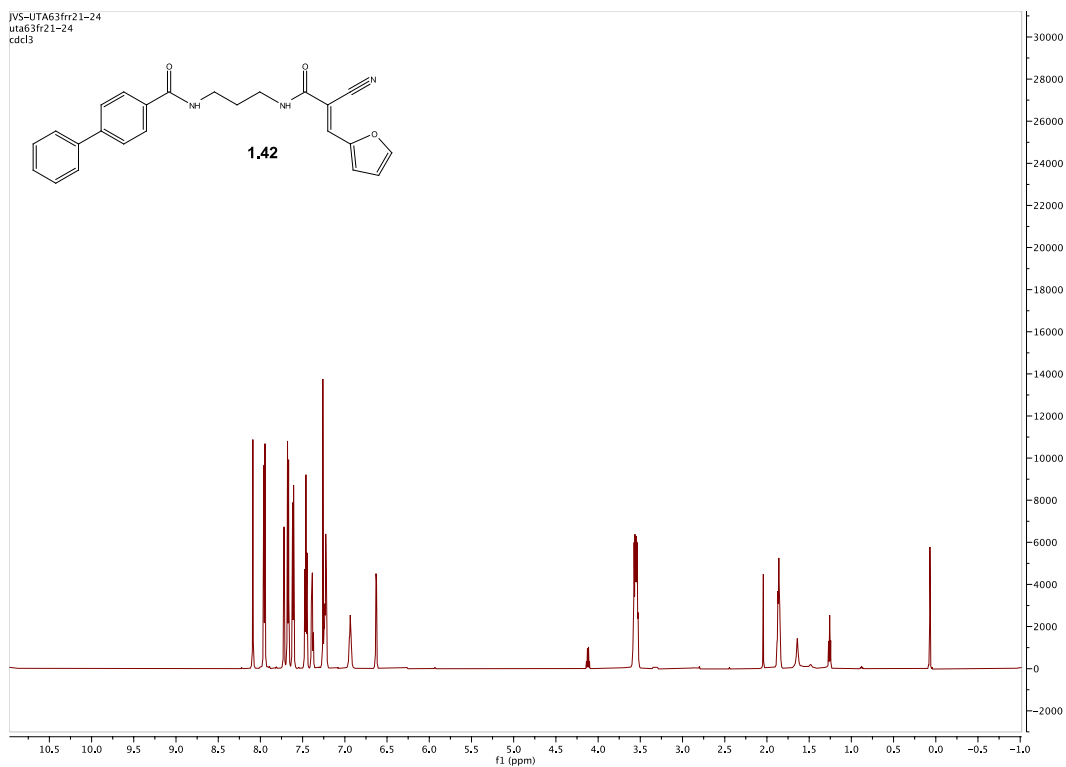
Spectra 1.36 ^1H NMR Spectrum of compound **1.39**



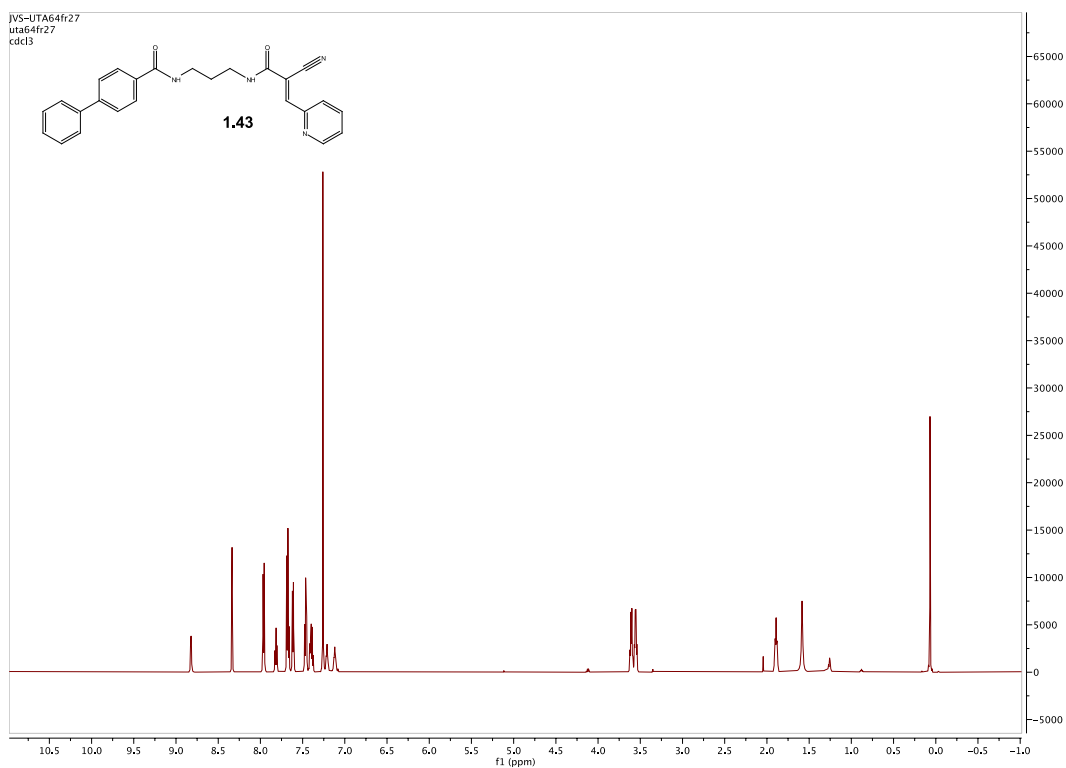
Spectra 1.37 ^1H NMR Spectrum of compound **1.40**



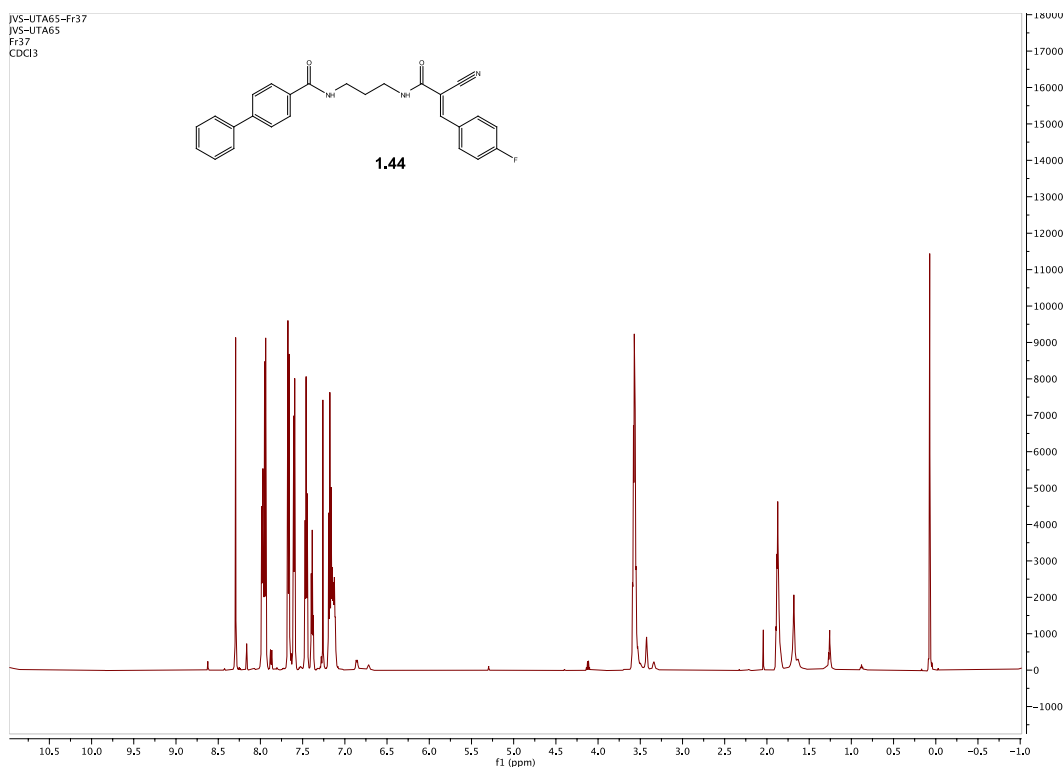
Spectra 1.38 ^1H NMR Spectrum of compound **1.41**



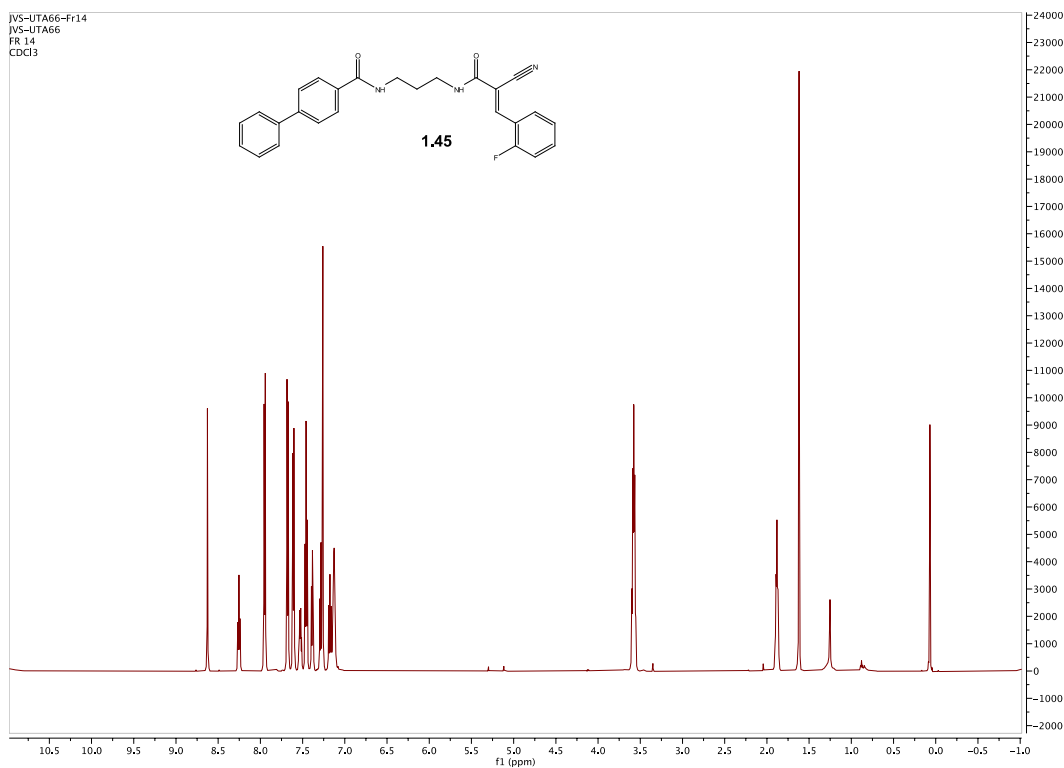
Spectra 1.39 ^1H NMR Spectrum of compound **1.42**



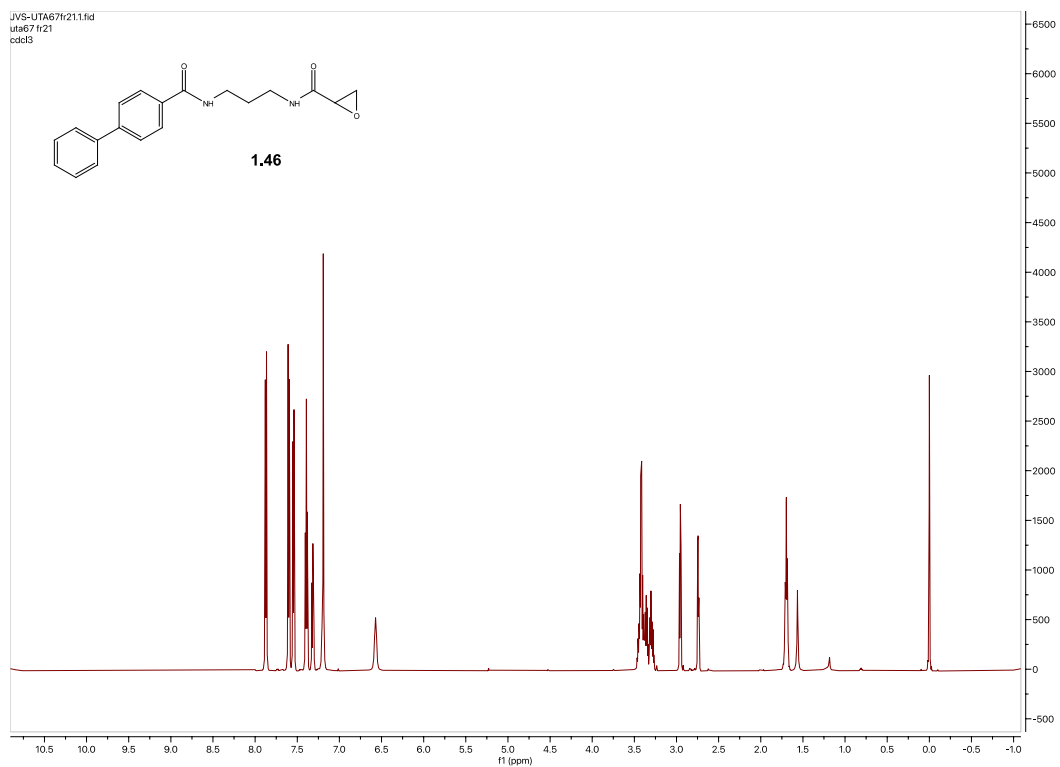
Spectra 1.40 ^1H NMR Spectrum of compound **1.43**



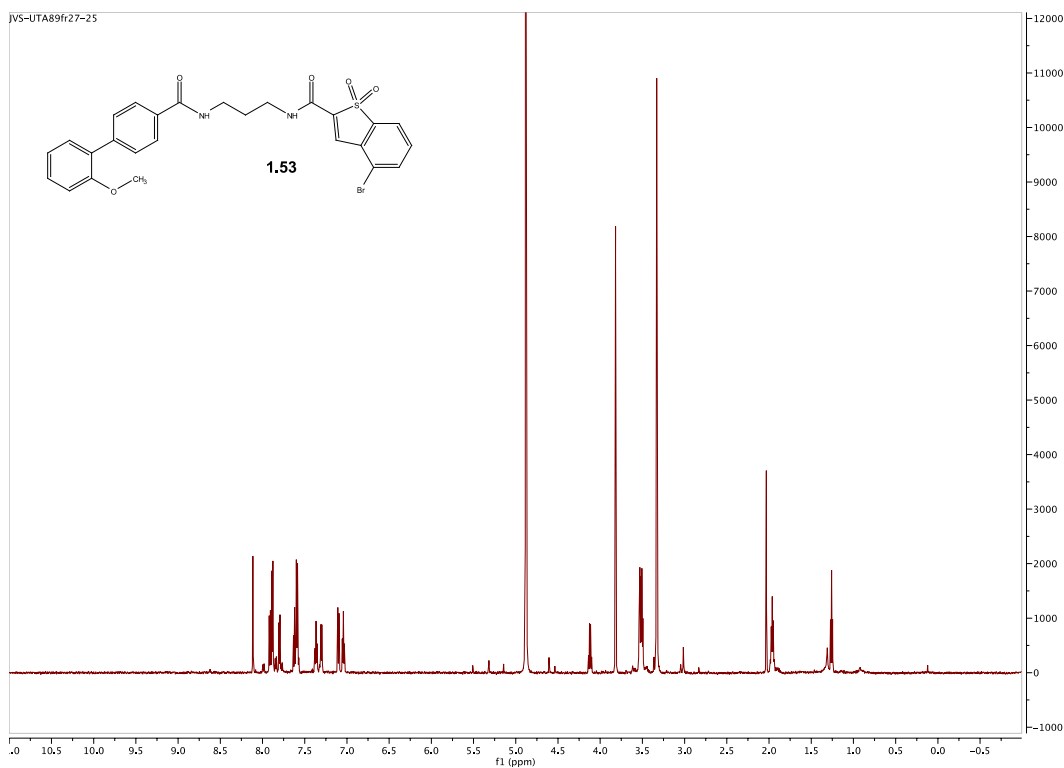
Spectra 1.41 ^1H NMR Spectrum of compound **1.44**



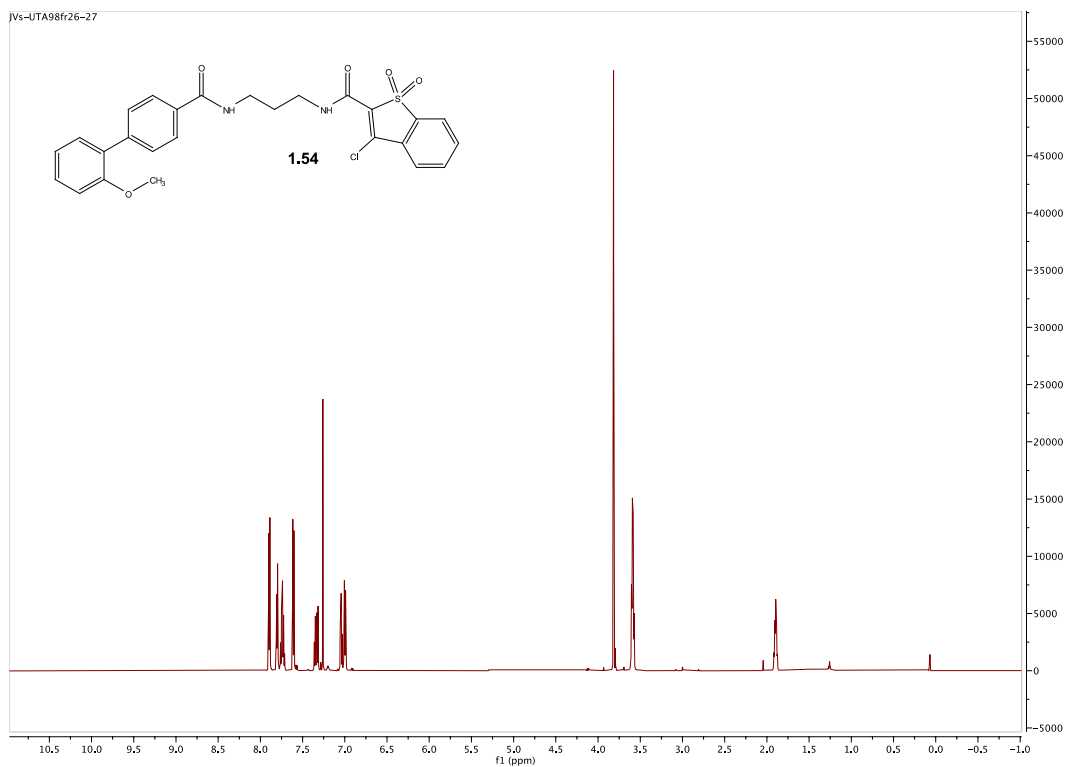
Spectra 1.42 ^1H NMR Spectrum of compound **1.45**



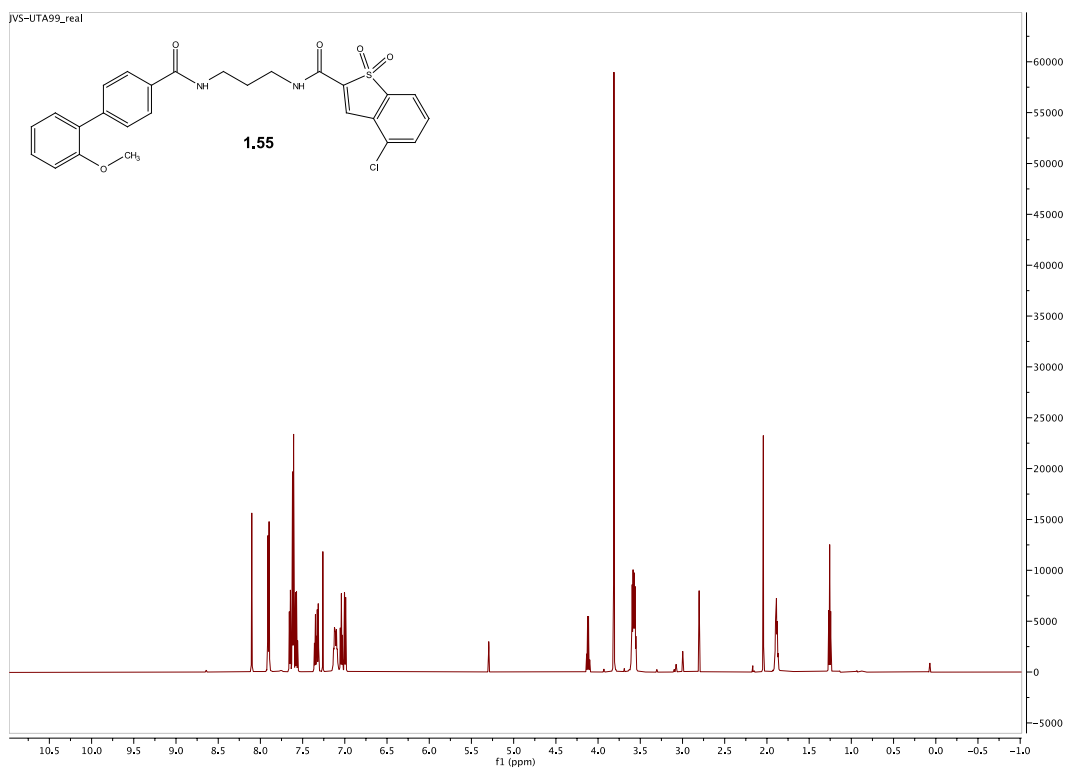
Spectra 1.43 ^1H NMR Spectrum of compound **1.46**



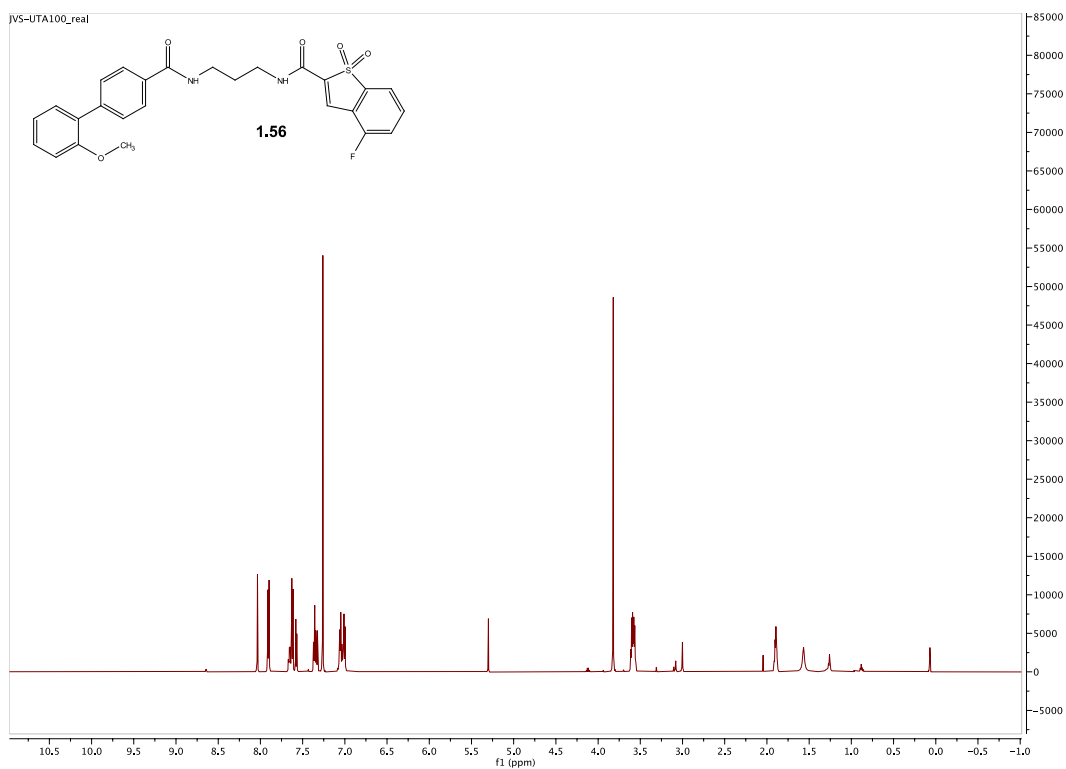
Spectra 1.44 ^1H NMR Spectrum of compound **1.53**



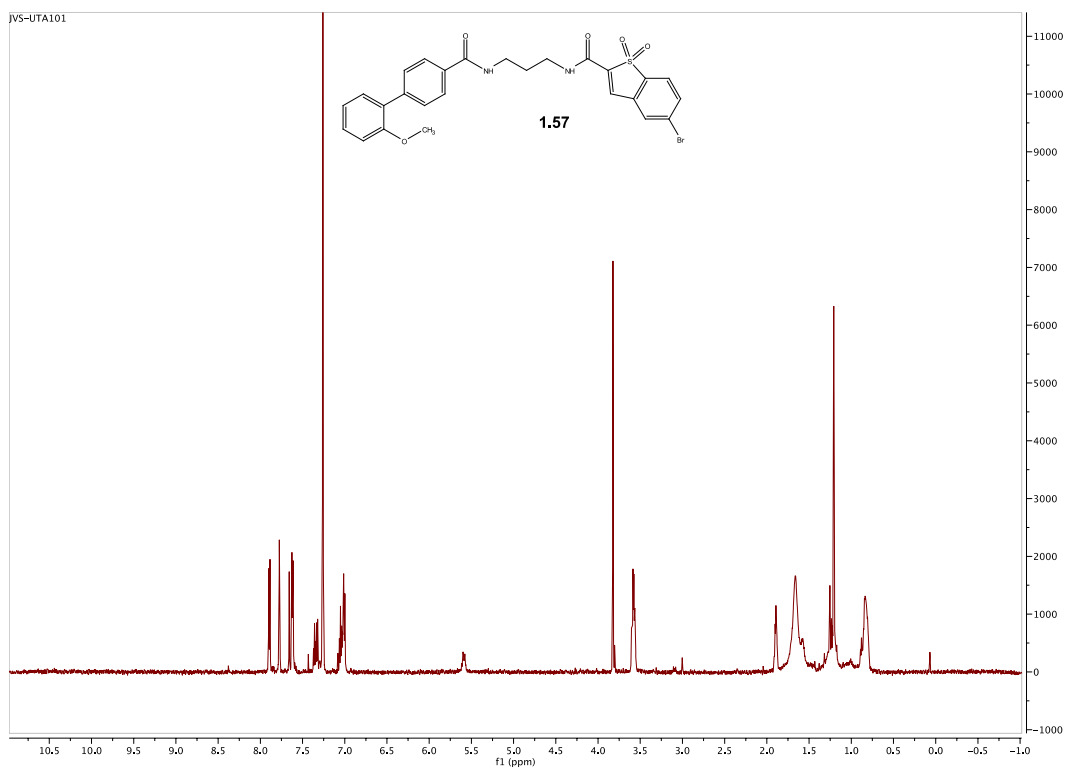
Spectra 1.45 ^1H NMR Spectrum of compound **1.54**



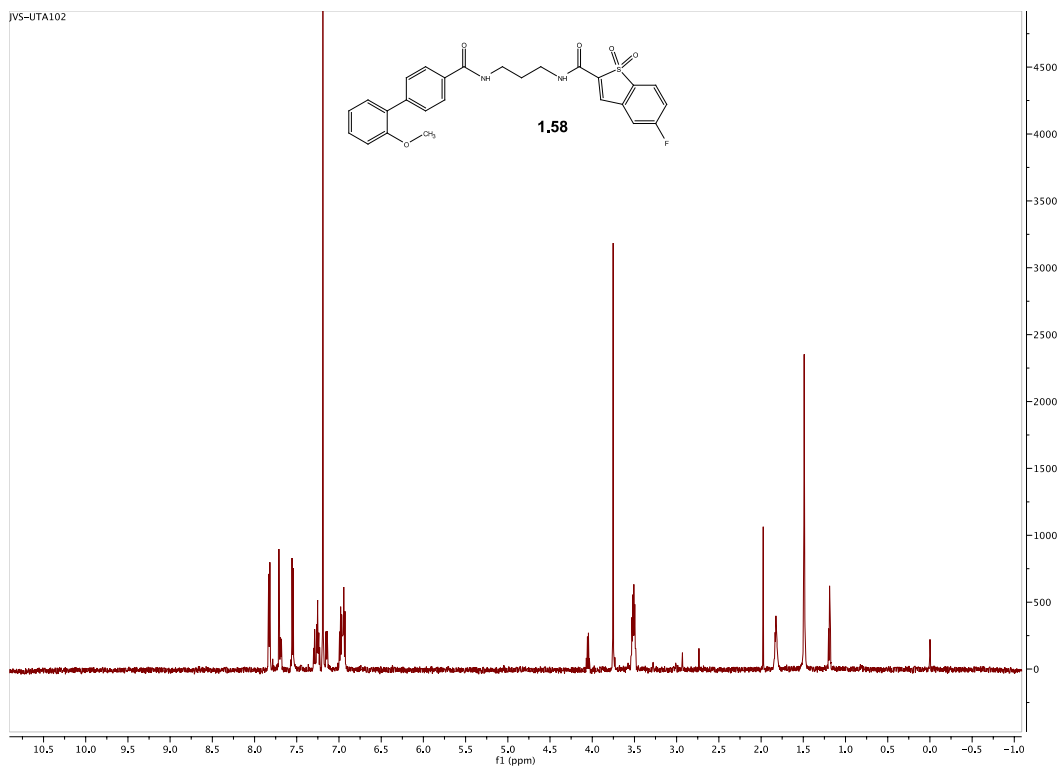
Spectra 1.46 ^1H NMR Spectrum of compound **1.55**



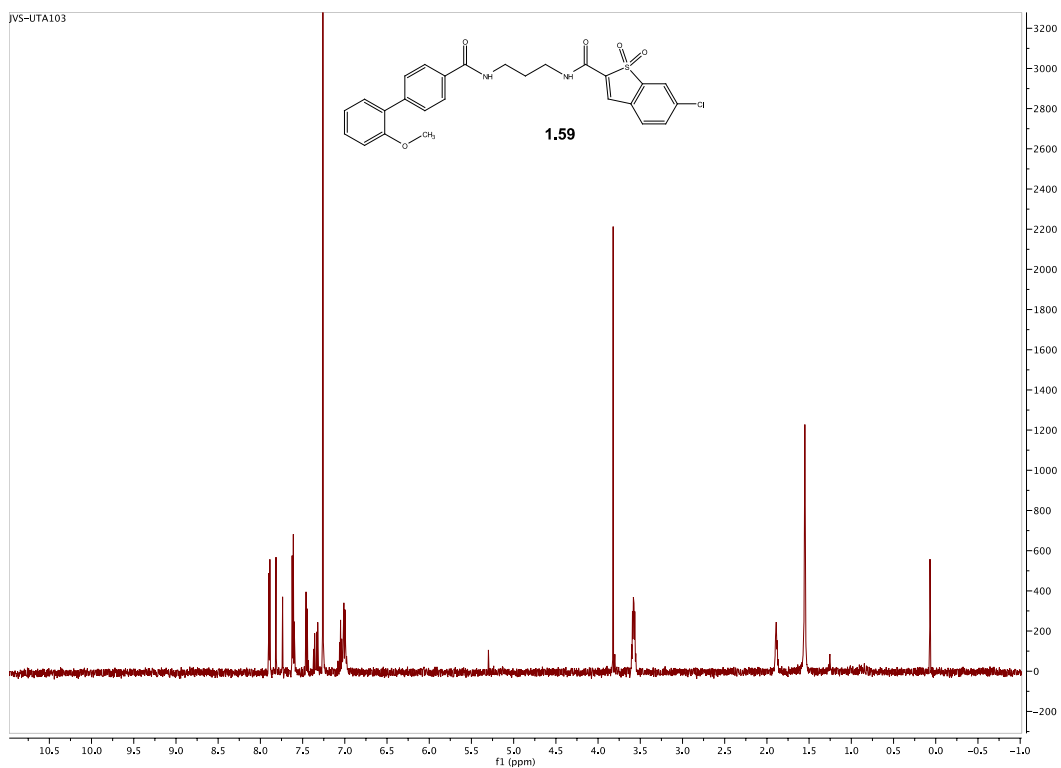
Spectra 1.47 ^1H NMR Spectrum of compound **1.56**



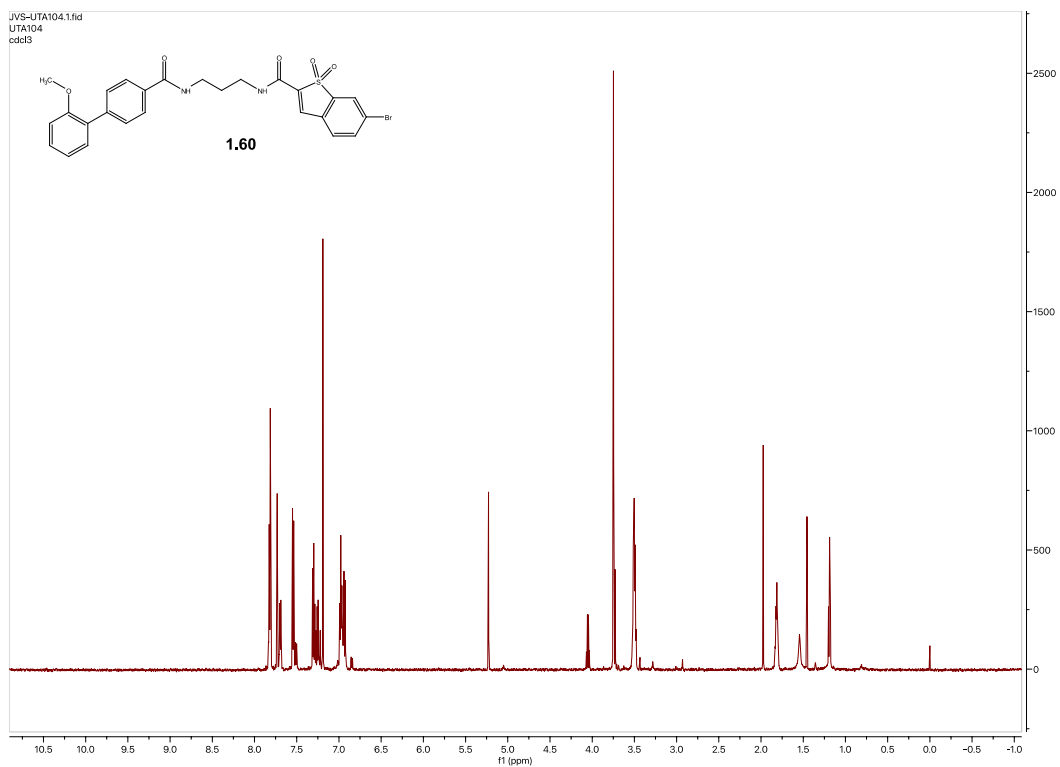
Spectra 1.48 ^1H NMR Spectrum of compound **1.57**



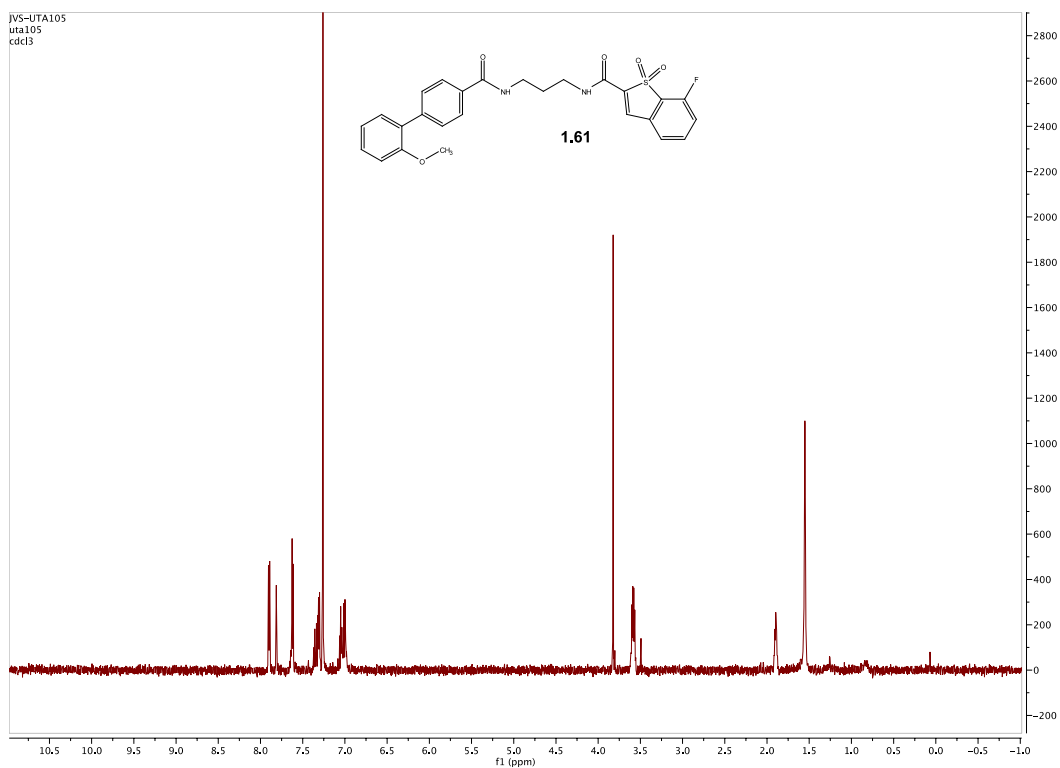
Spectra 1.49 ^1H NMR Spectrum of compound **1.58**



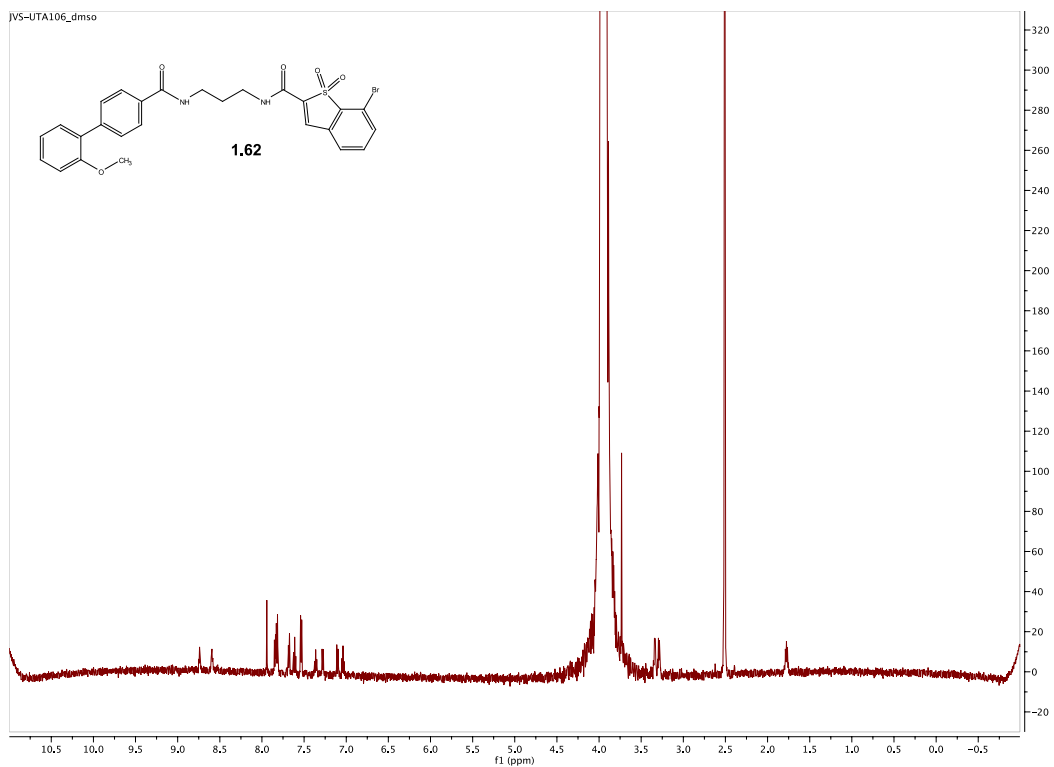
Spectra 1.50 ^1H NMR Spectrum of compound **1.59**



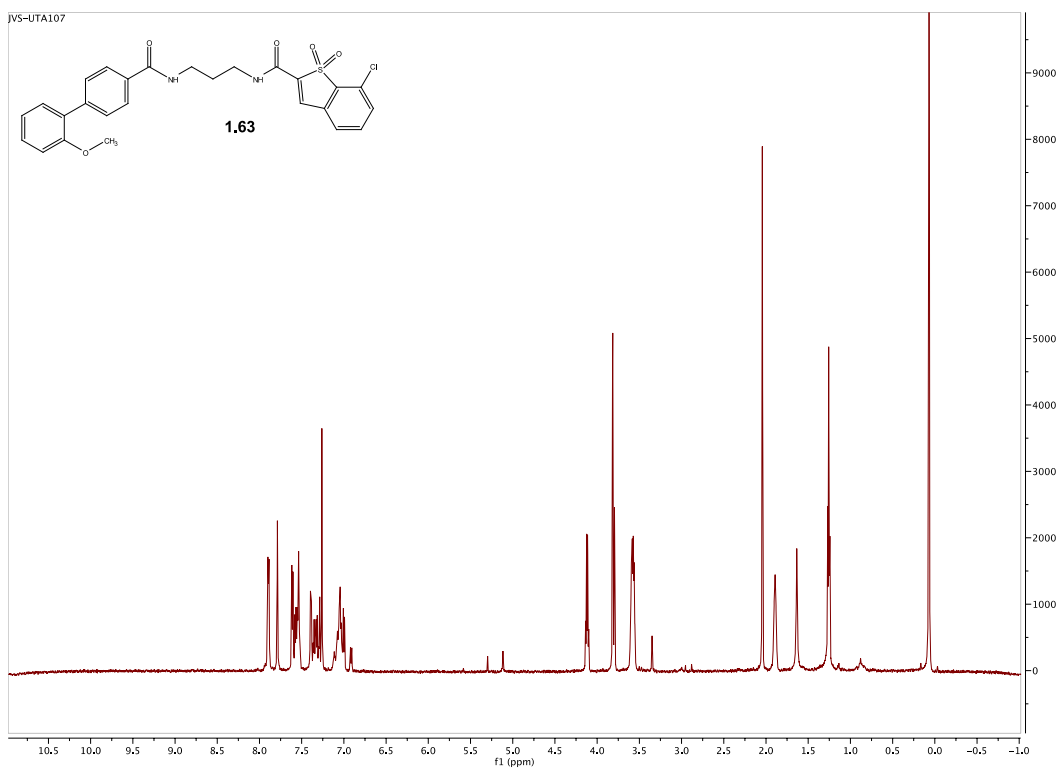
Spectra 1.51 ^1H NMR Spectrum of compound **1.60**



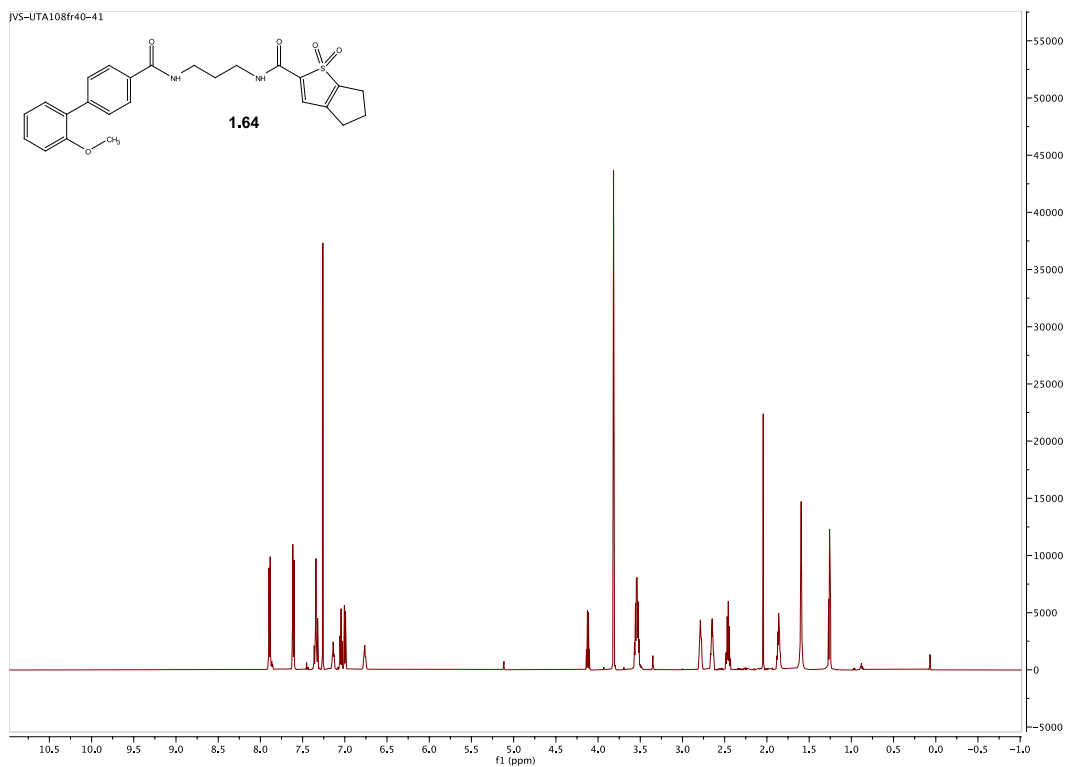
Spectra 1.52 ^1H NMR Spectrum of compound **1.61**



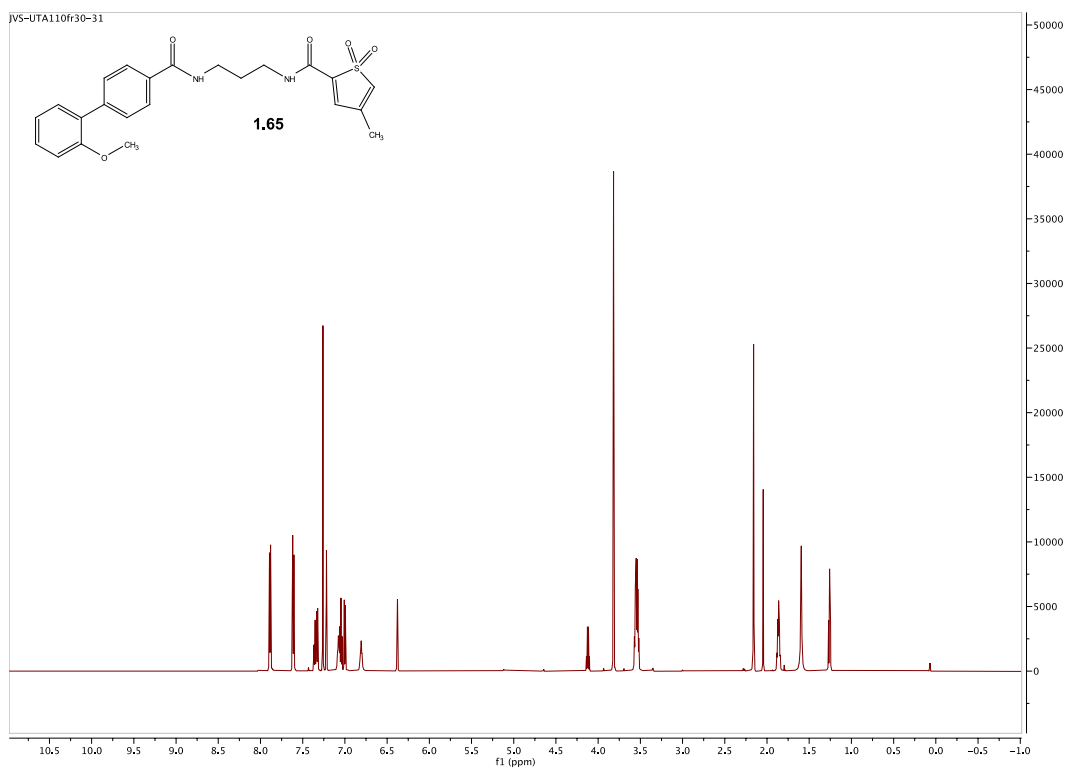
Spectra 1.53 ^1H NMR Spectrum of compound **1.62**



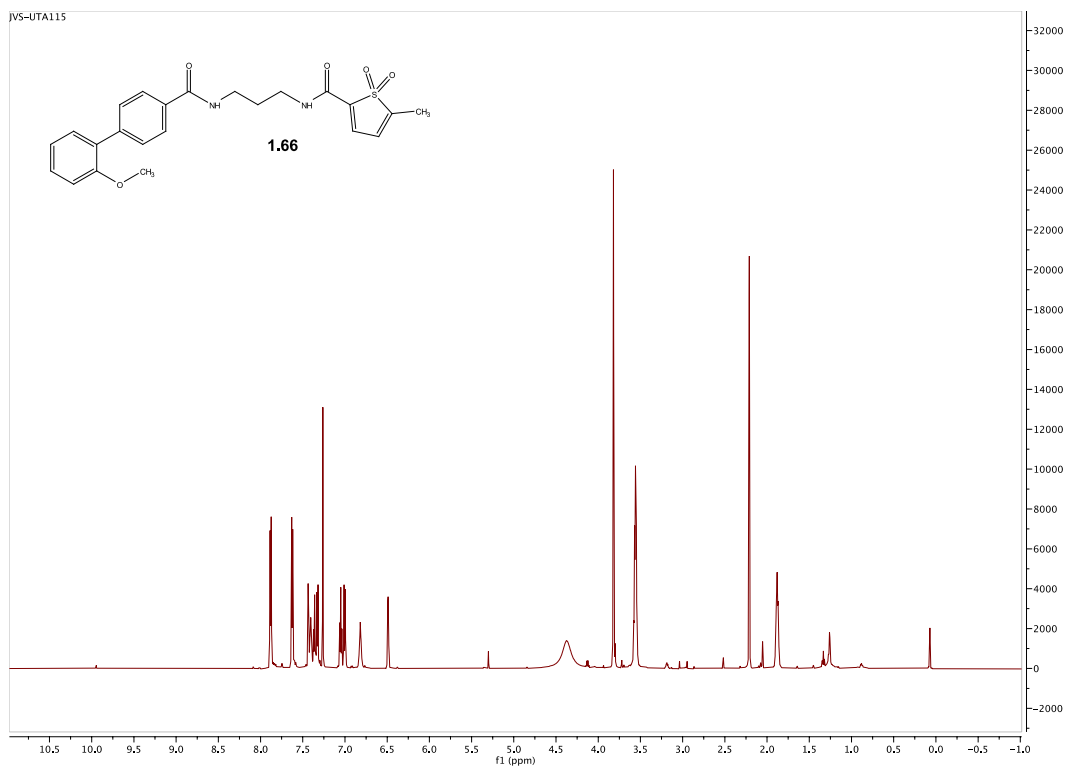
Spectra 1.54 ^1H NMR Spectrum of compound **1.63**



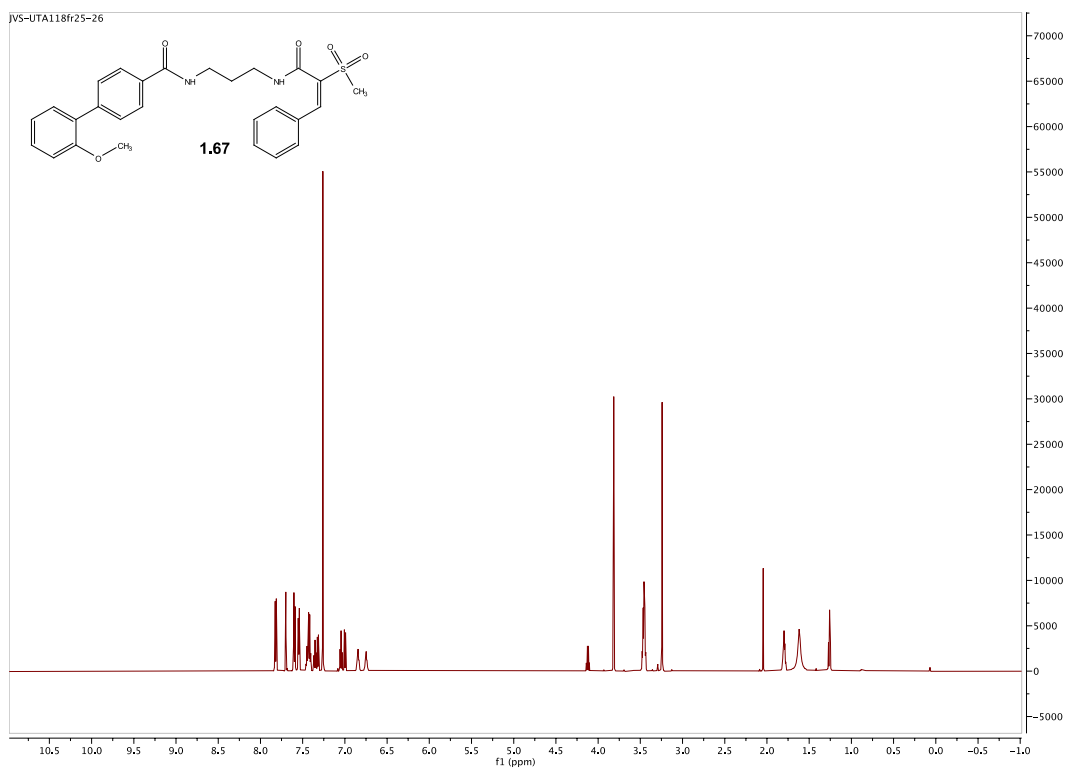
Spectra 1.55 ^1H NMR Spectrum of compound **1.64**



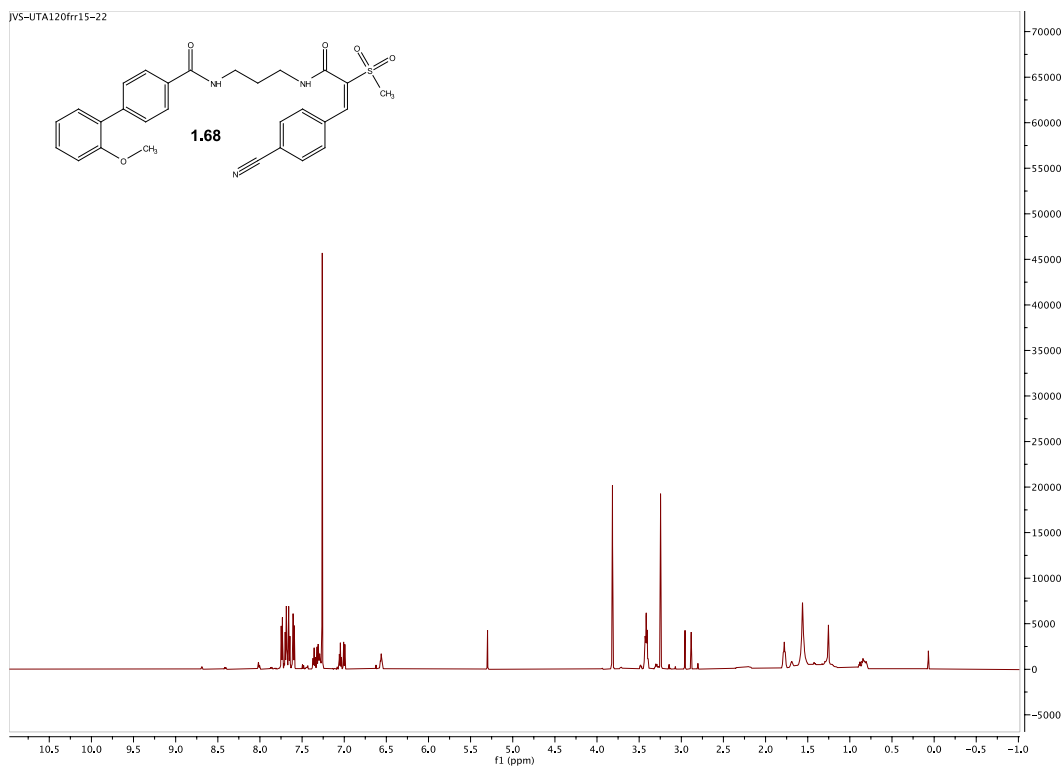
Spectra 1.56 ^1H NMR Spectrum of compound **1.65**



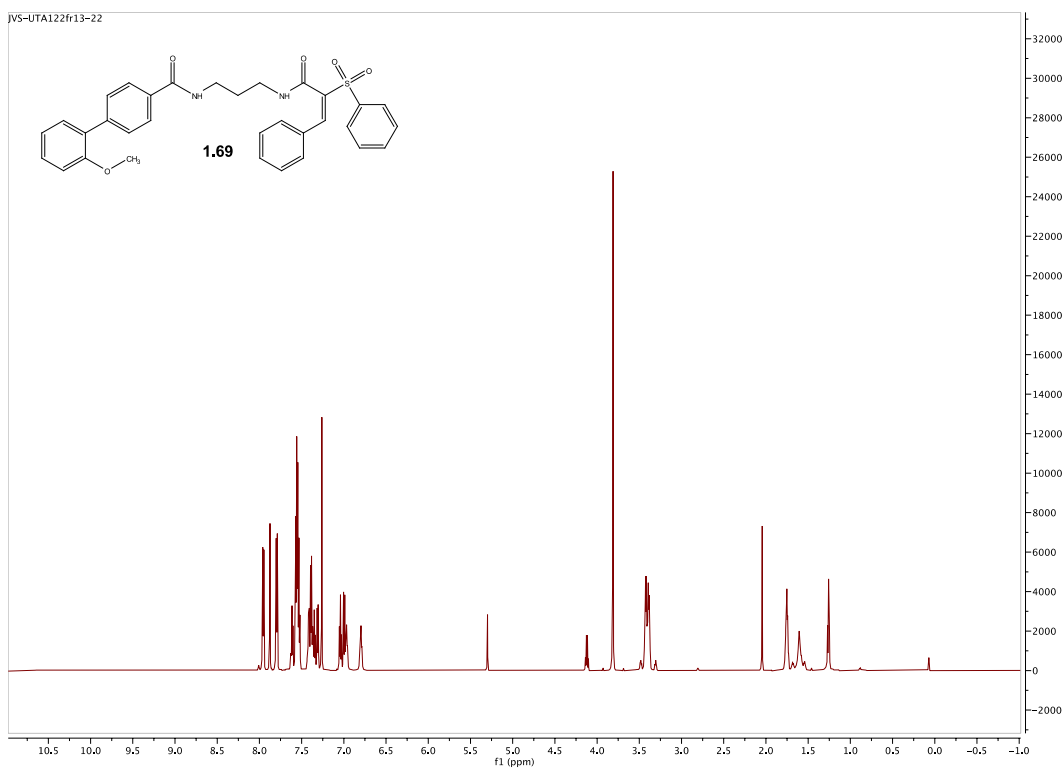
Spectra 1.57 ^1H NMR Spectrum of compound **1.66**



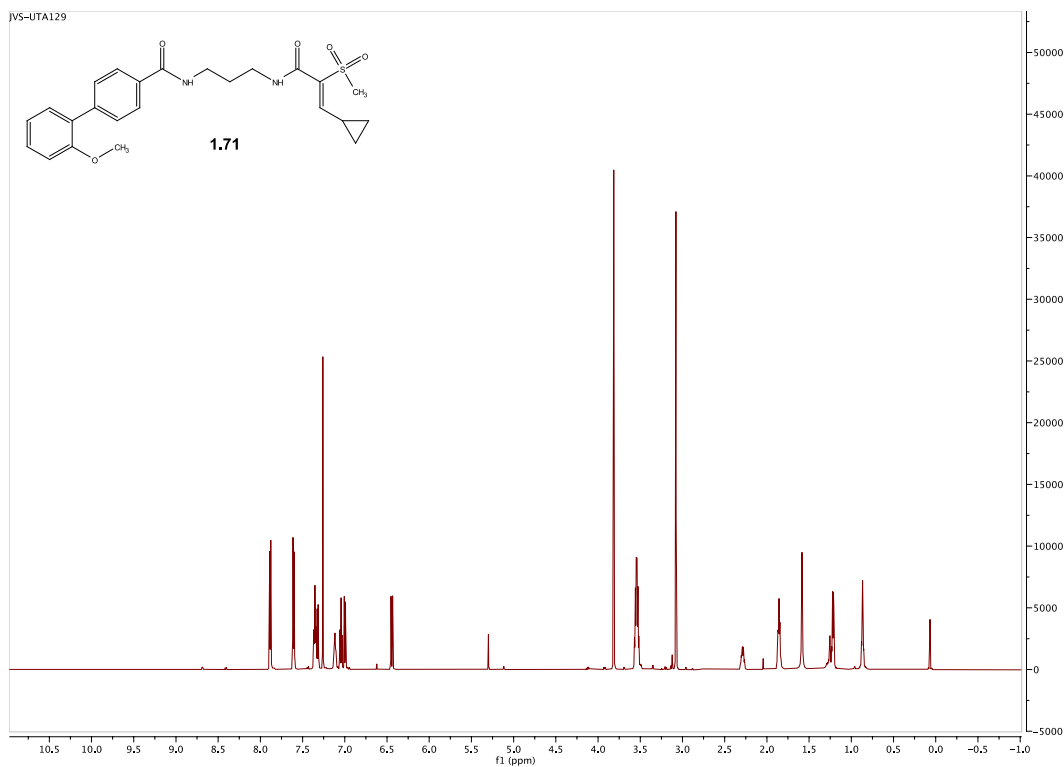
Spectra 1.58 ^1H NMR Spectrum of compound **1.67**



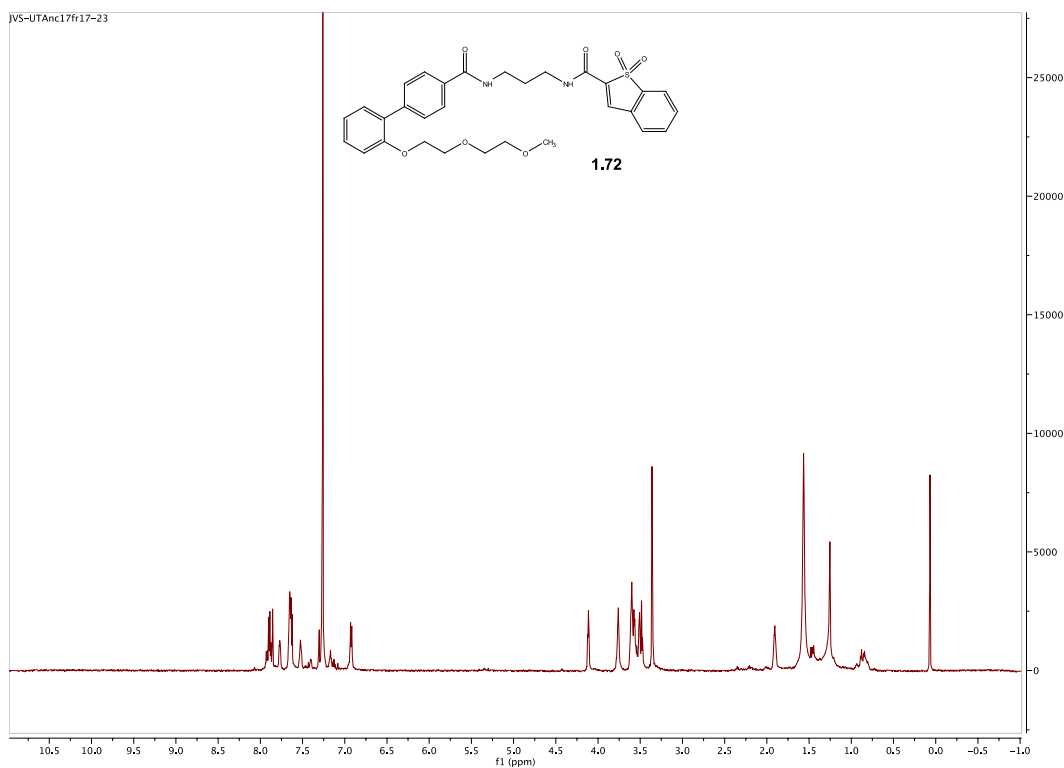
Spectra 1.59 ^1H NMR Spectrum of compound **1.68**



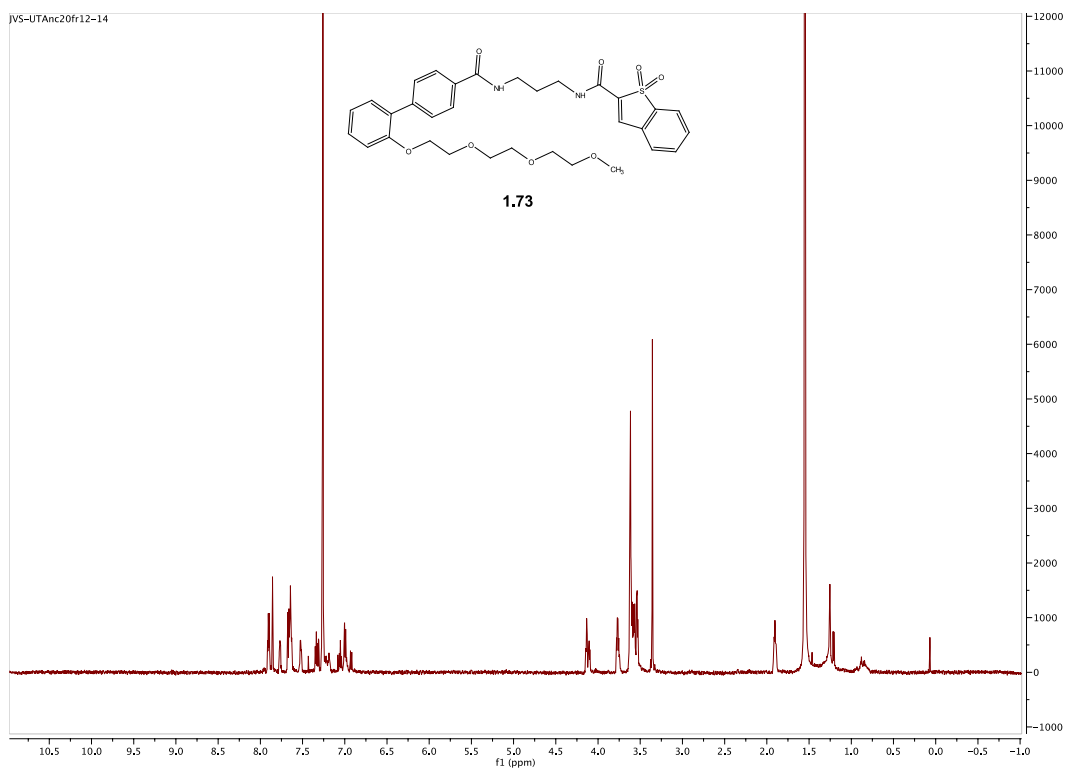
Spectra 1.60 ^1H NMR Spectrum of compound **1.69**



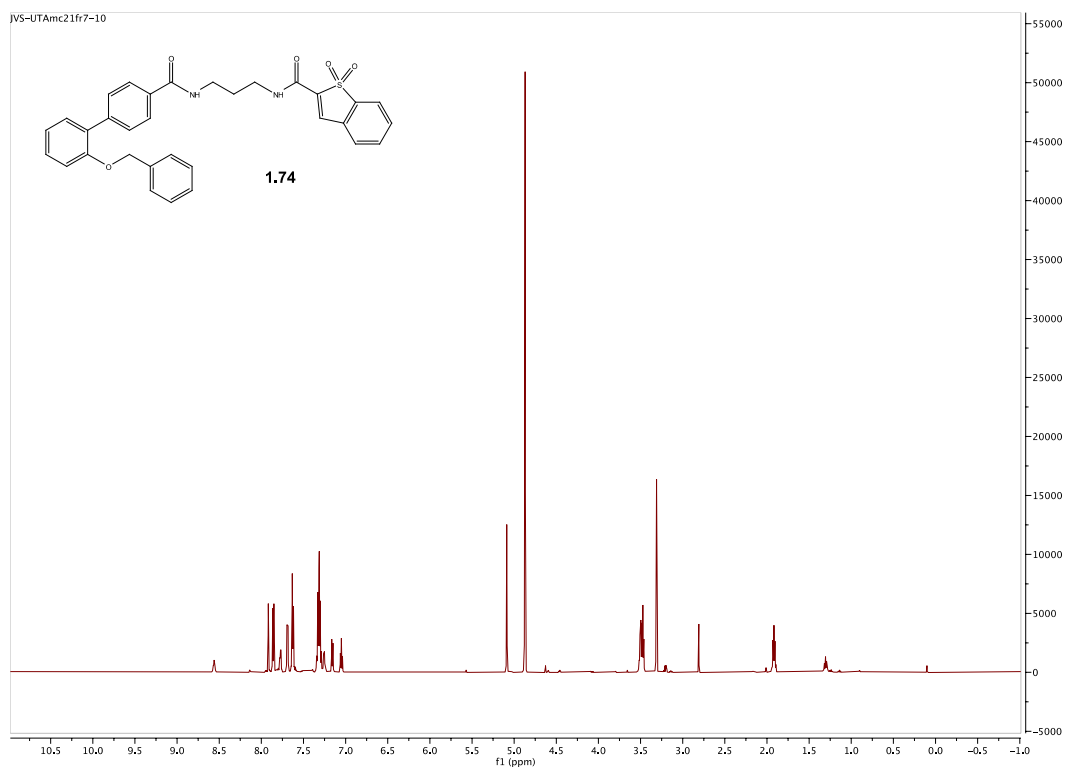
Spectra 1.61 ^1H NMR Spectrum of compound **1.71**



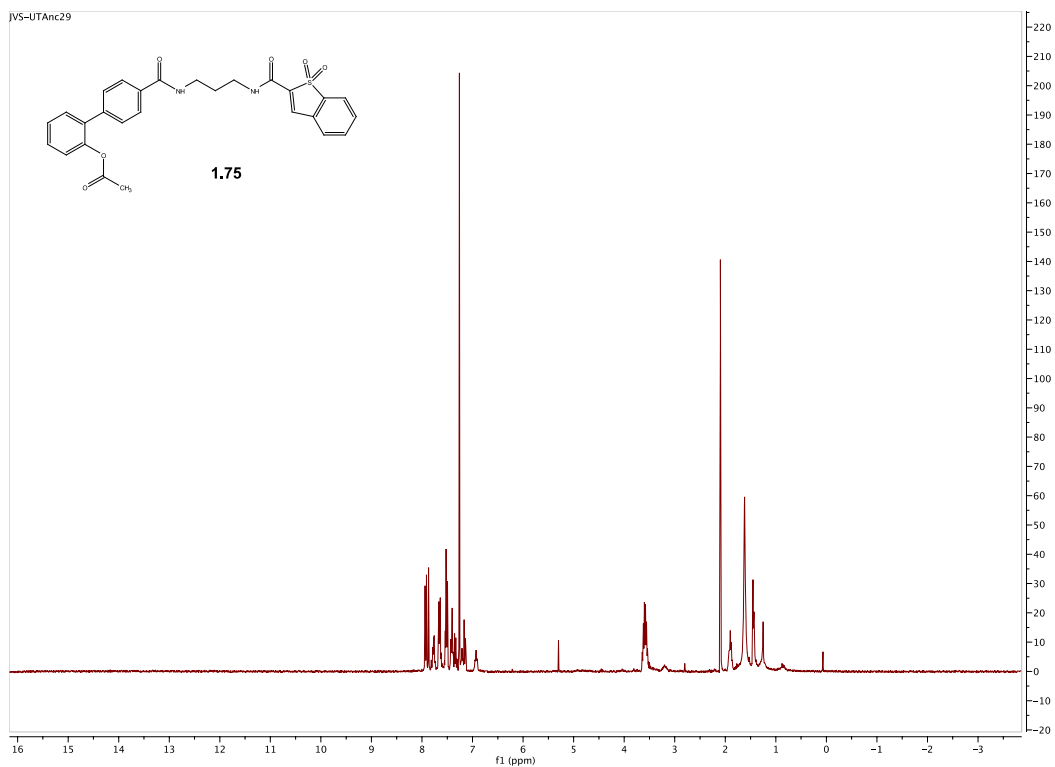
Spectra 1.62 ^1H NMR Spectrum of compound **1.72**



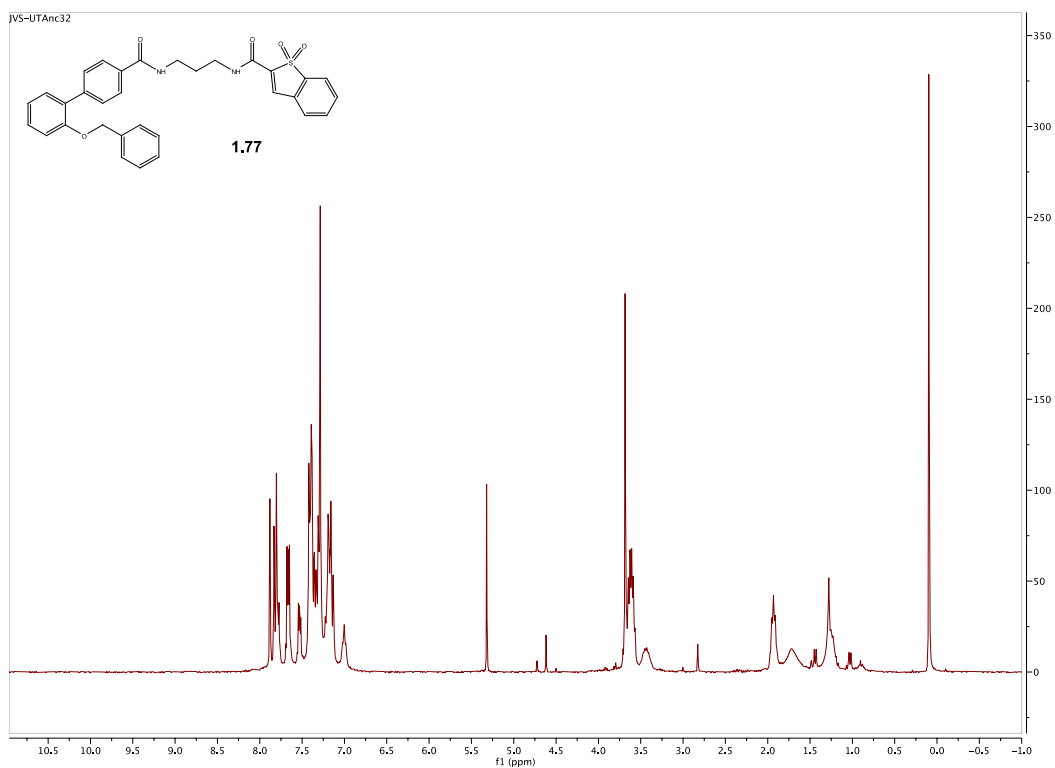
Spectra 1.63 ^1H NMR Spectrum of compound **1.73**



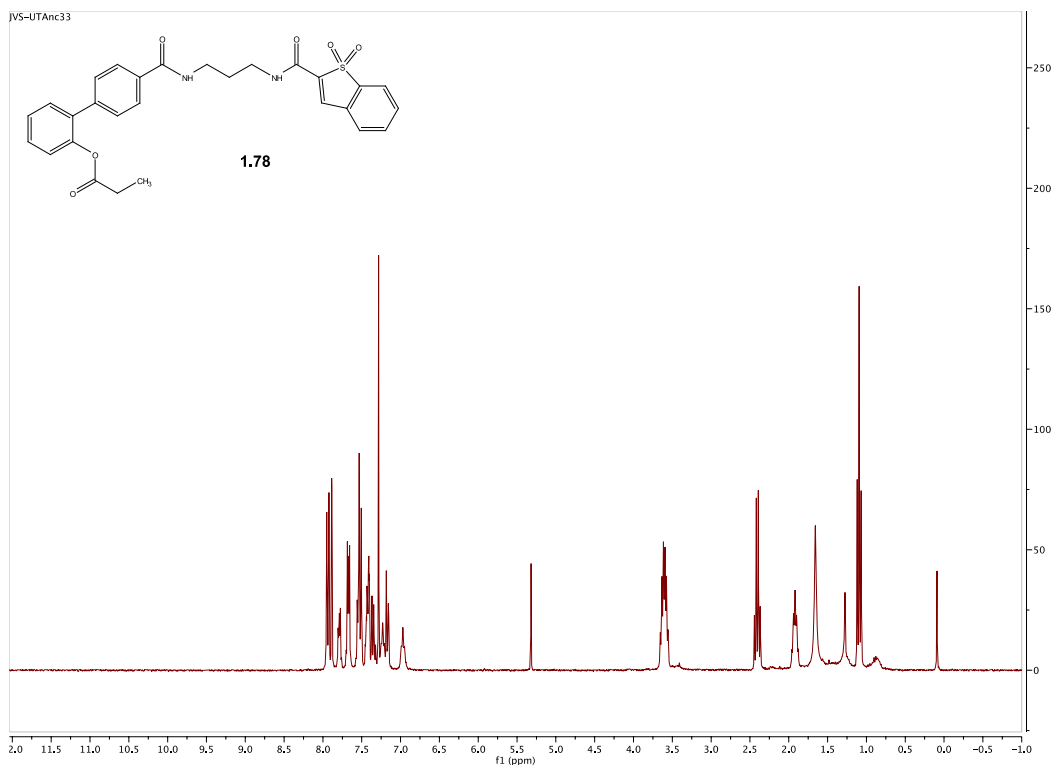
Spectra 1.64 ^1H NMR Spectrum of compound **1.74**



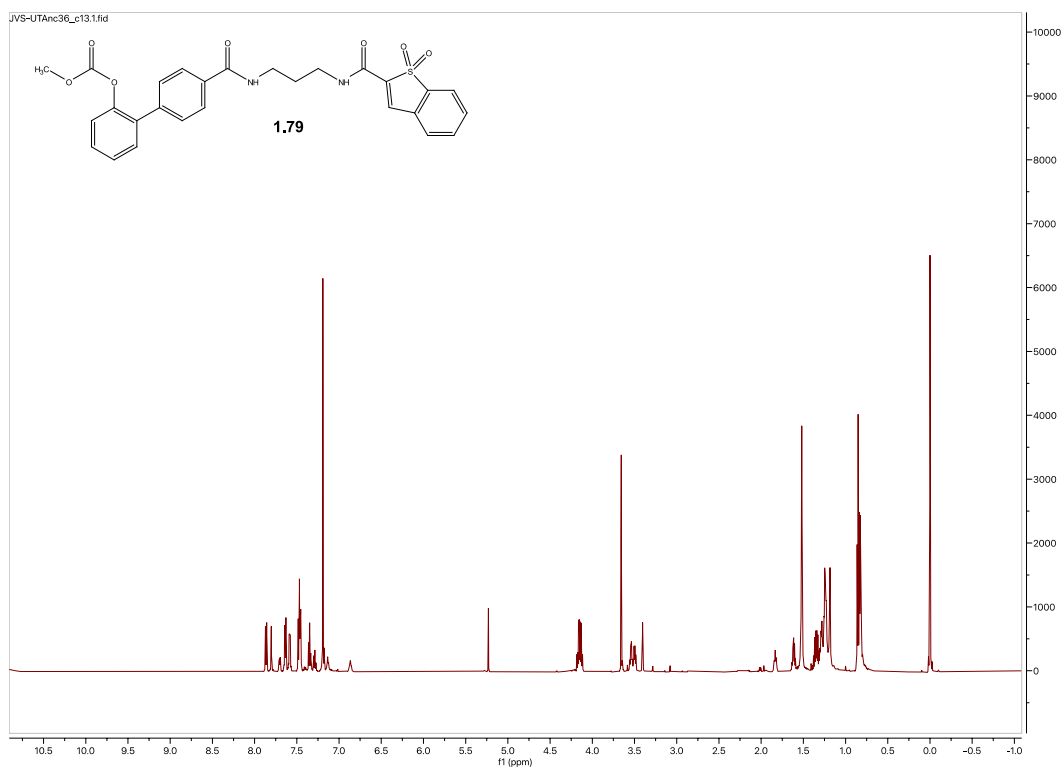
Spectra 1.65 ^1H NMR Spectrum of compound **1.75**



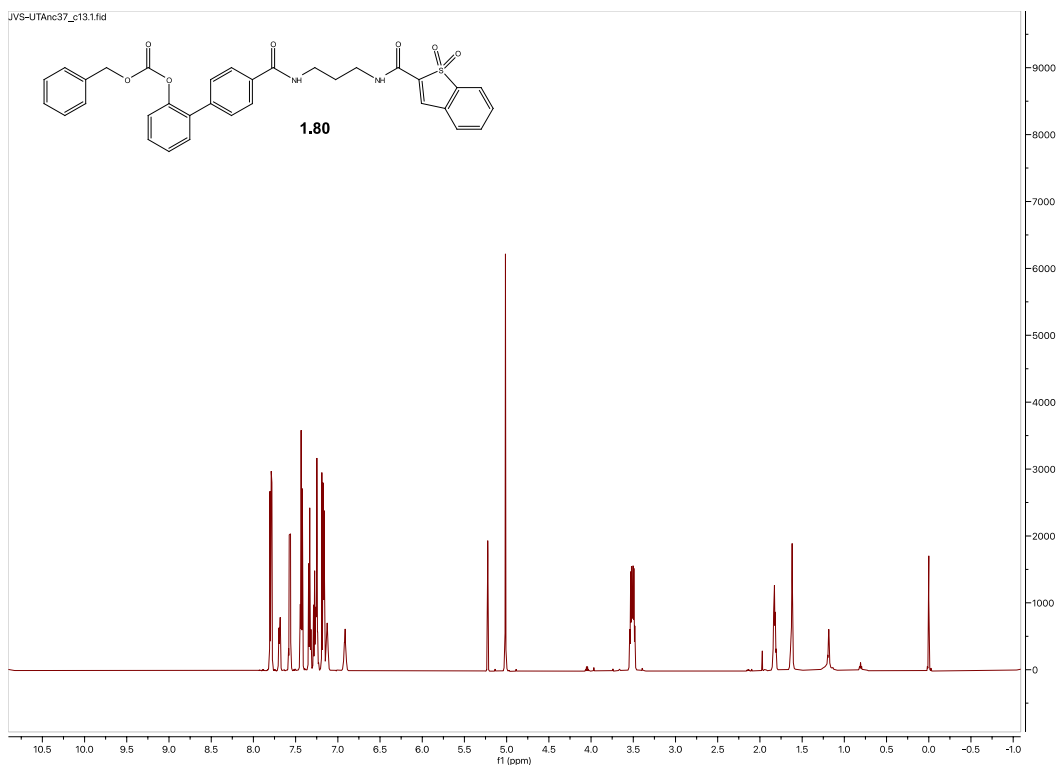
Spectra 1.66 ^1H NMR Spectrum of compound **1.77**



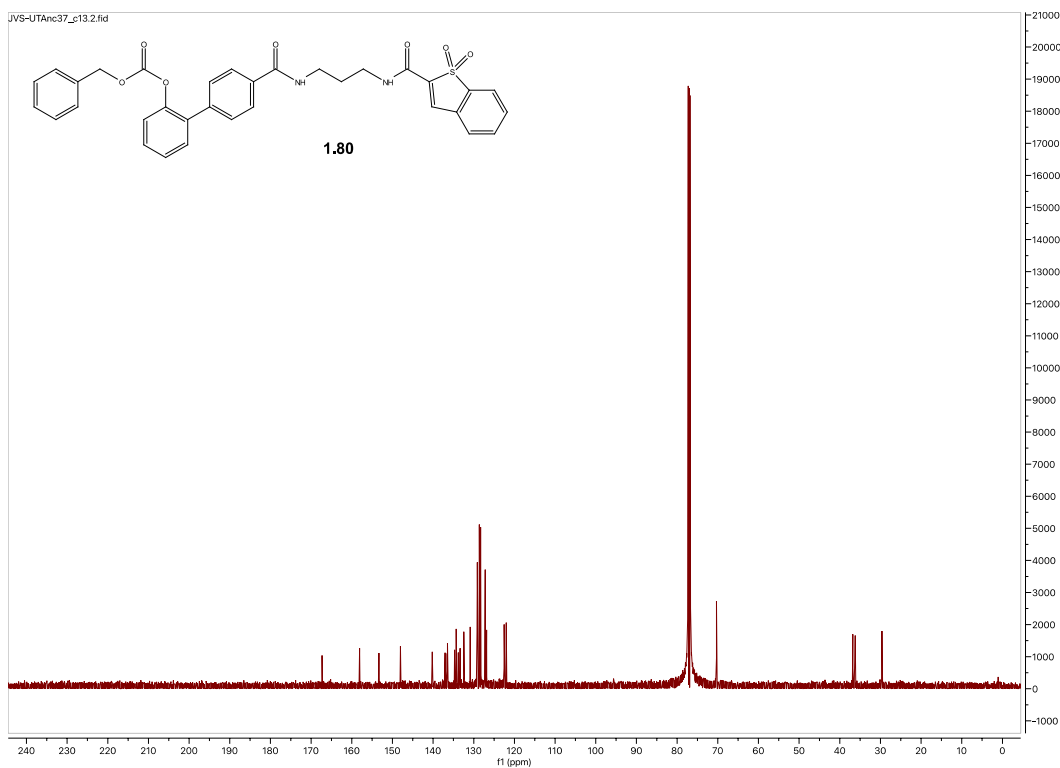
Spectra 1.67 ^1H NMR Spectrum of compound **1.78**



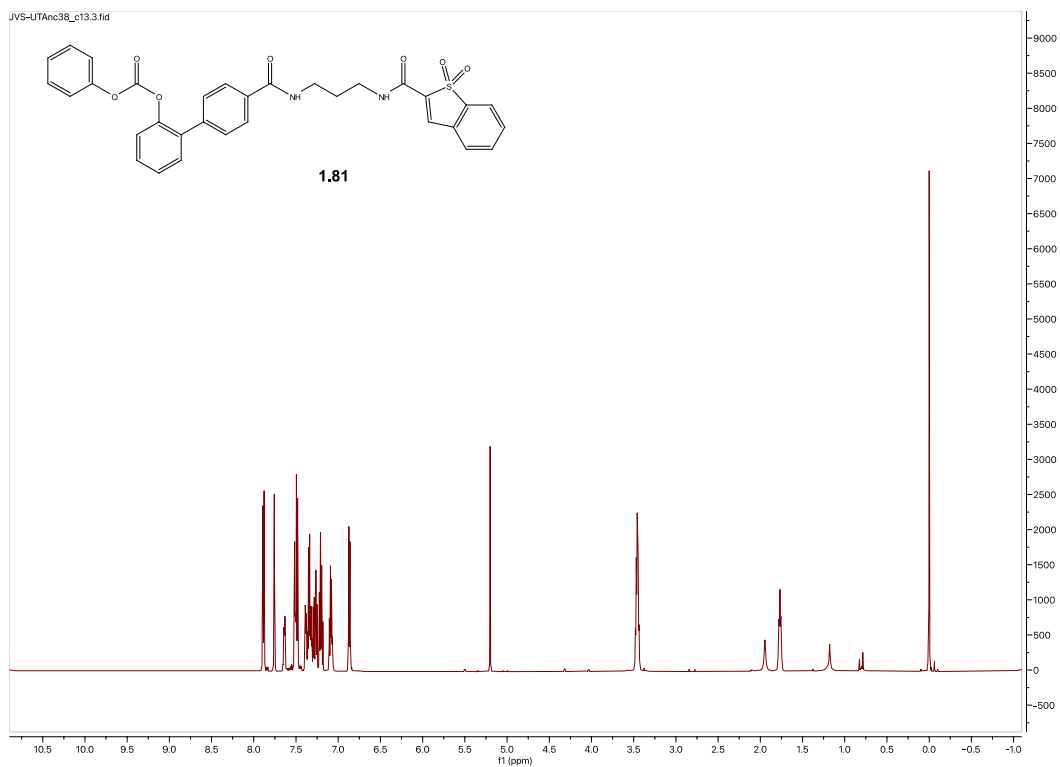
Spectra 1.68 ^1H NMR Spectrum of compound **1.79**



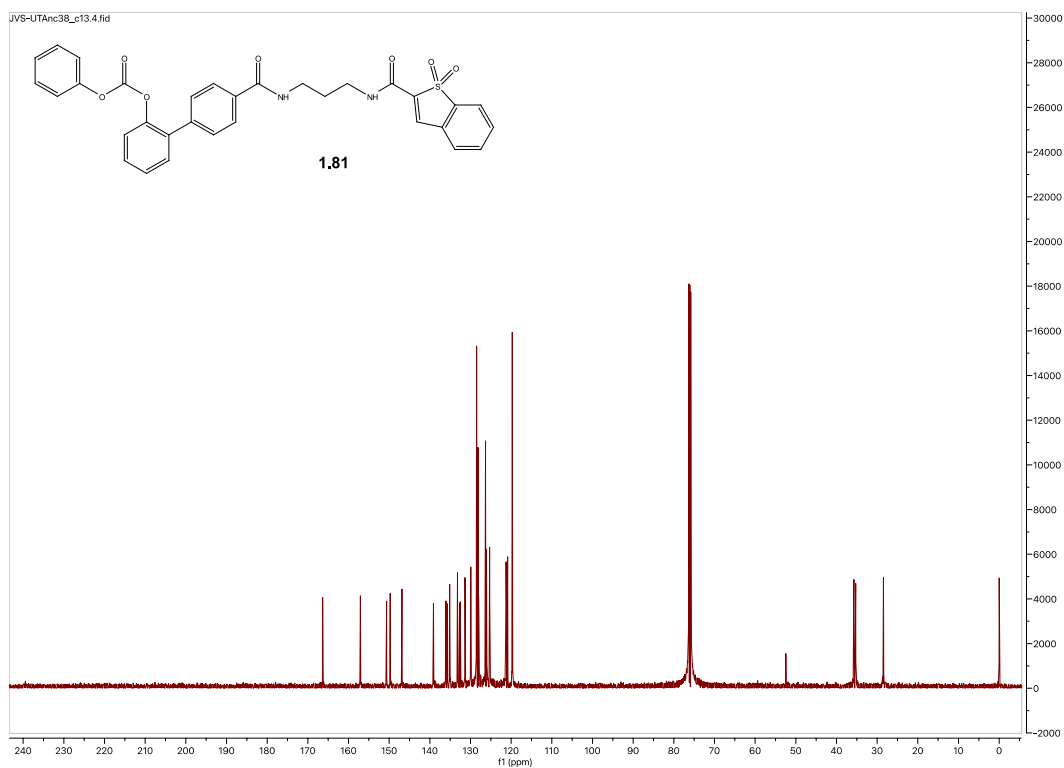
Spectra 1.69 ^1H NMR Spectrum of compound **1.80**



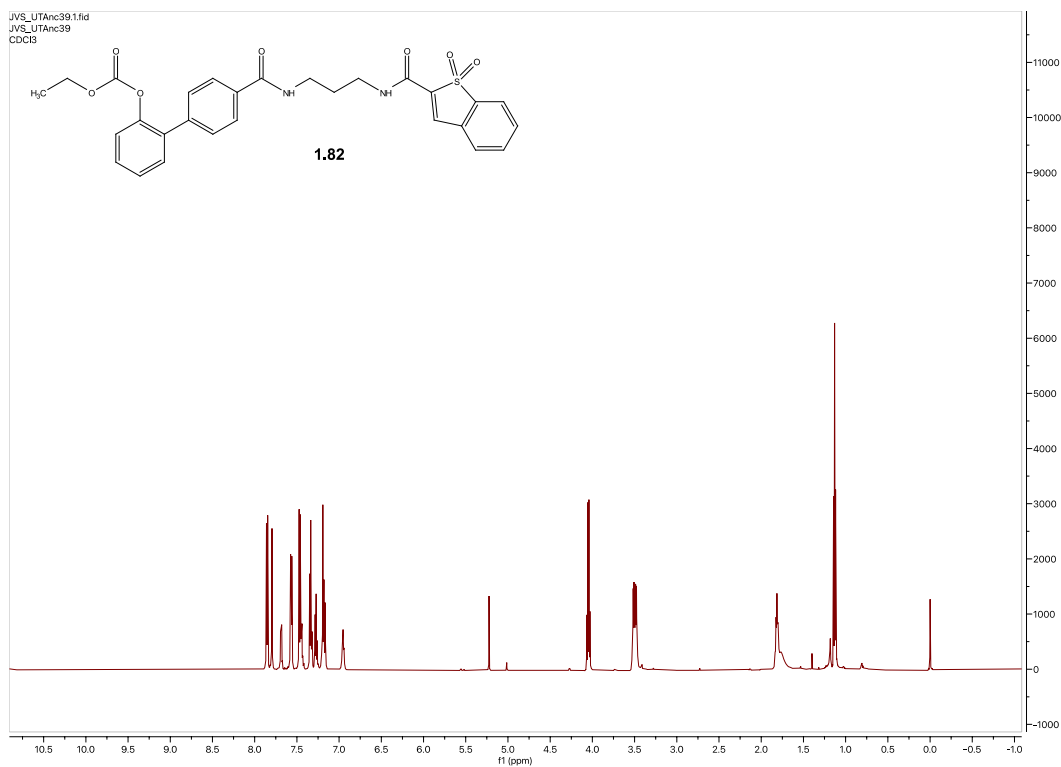
Spectra 1.70 ^{13}C NMR Spectrum of compound **1.80**



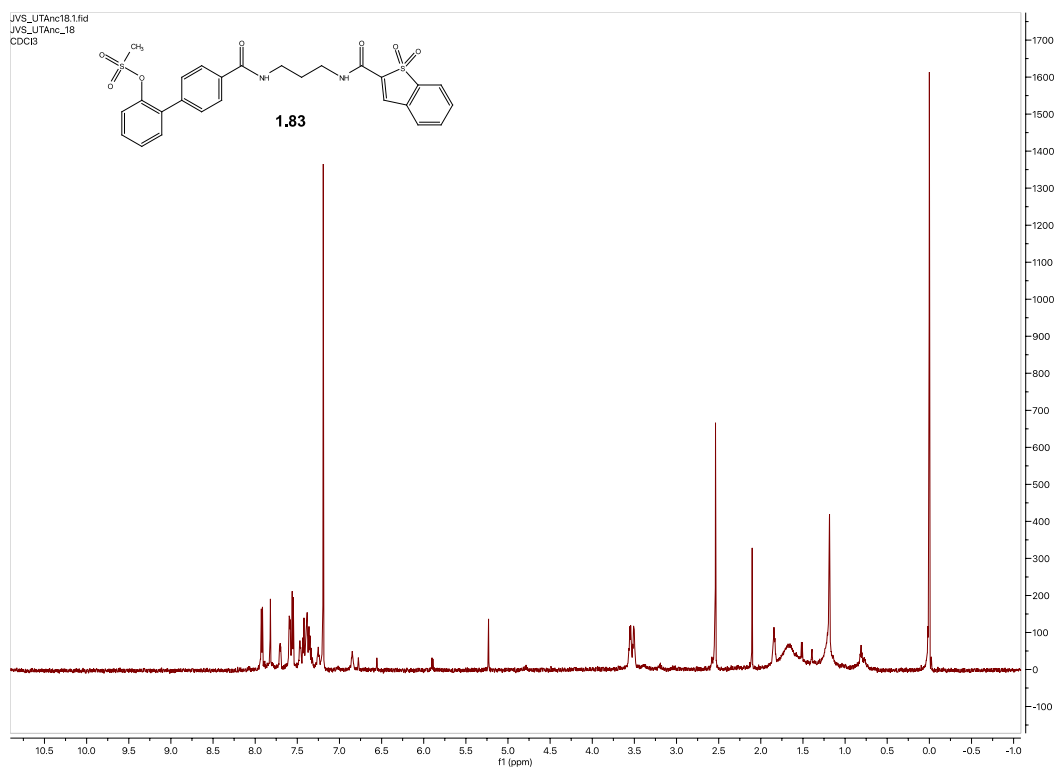
Spectra 1.71 ^1H NMR Spectrum of compound 1.81



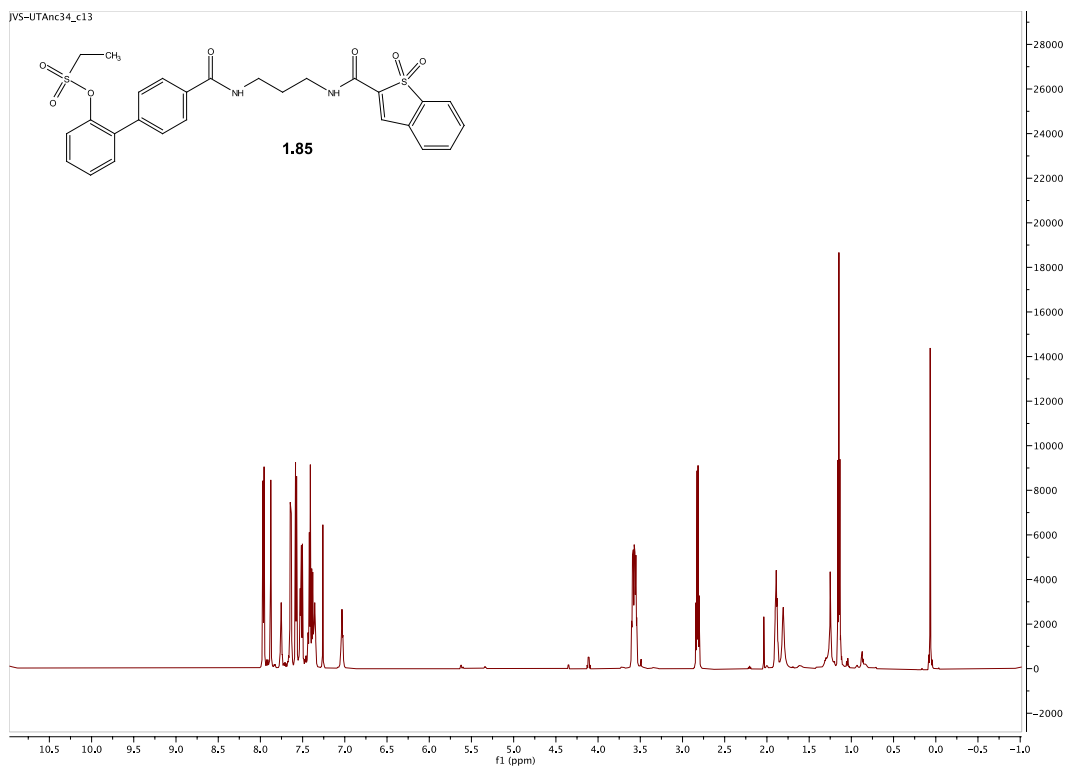
Spectra 1.72 ^{13}C NMR Spectrum of compound 1.81



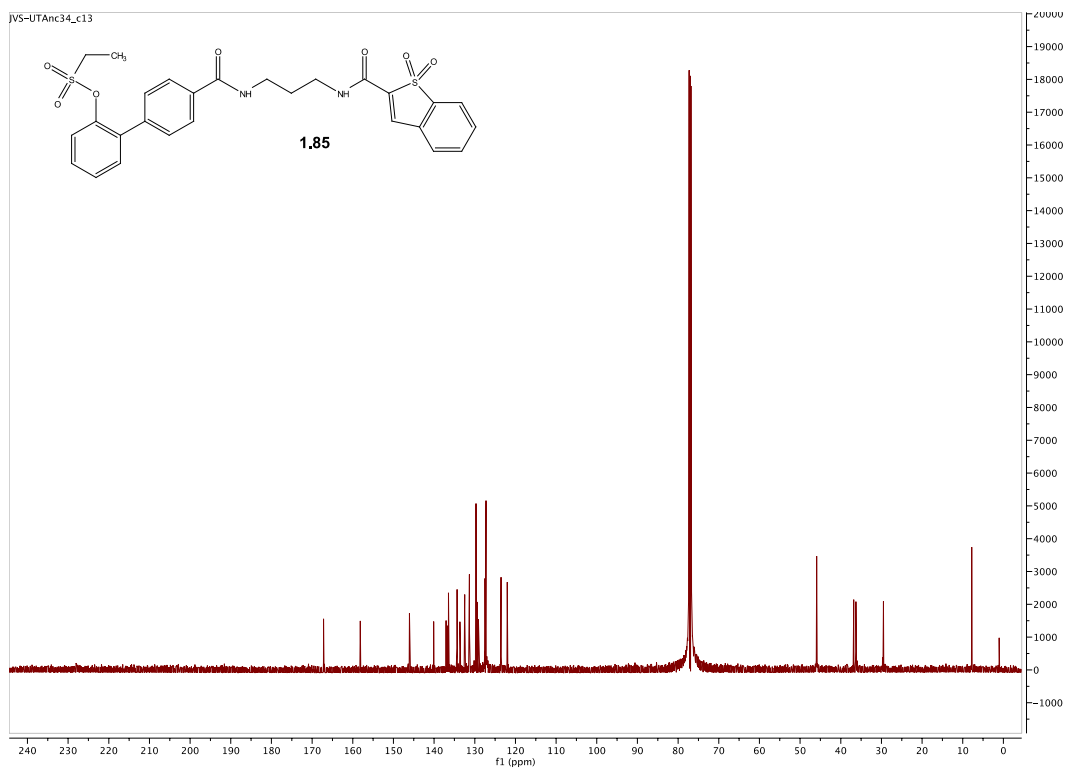
Spectra 1.73 ¹H NMR Spectrum of compound 1.82



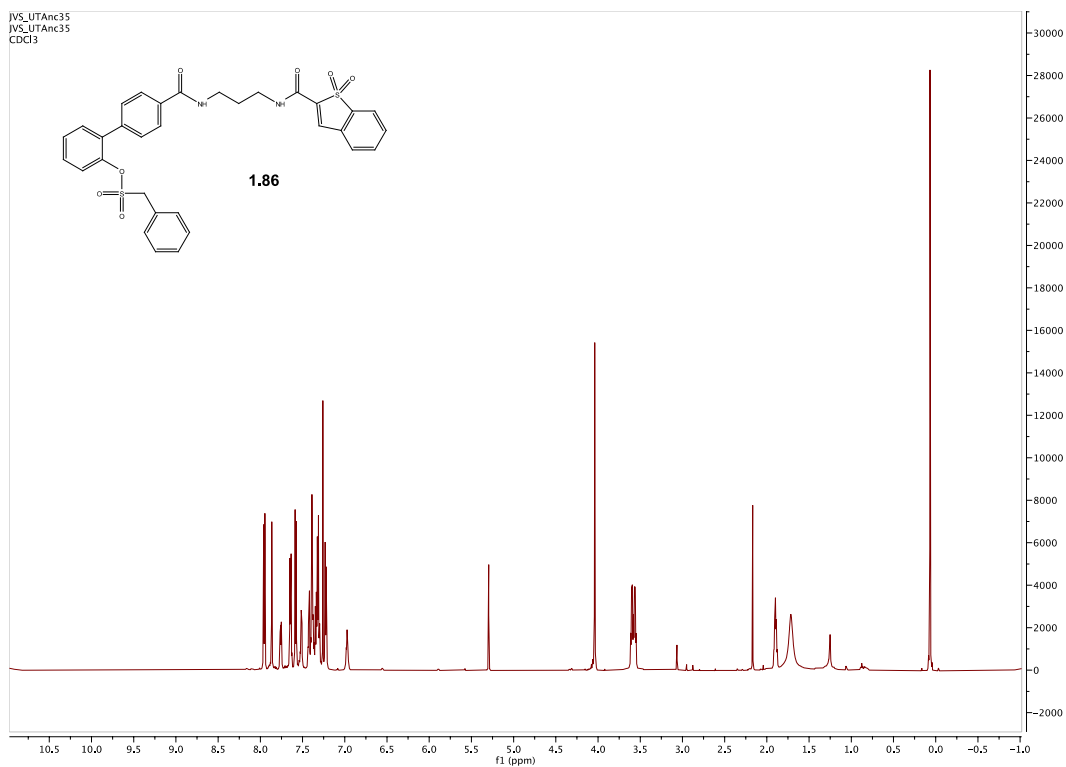
Spectra 1.74 ¹H NMR Spectrum of compound 1.83



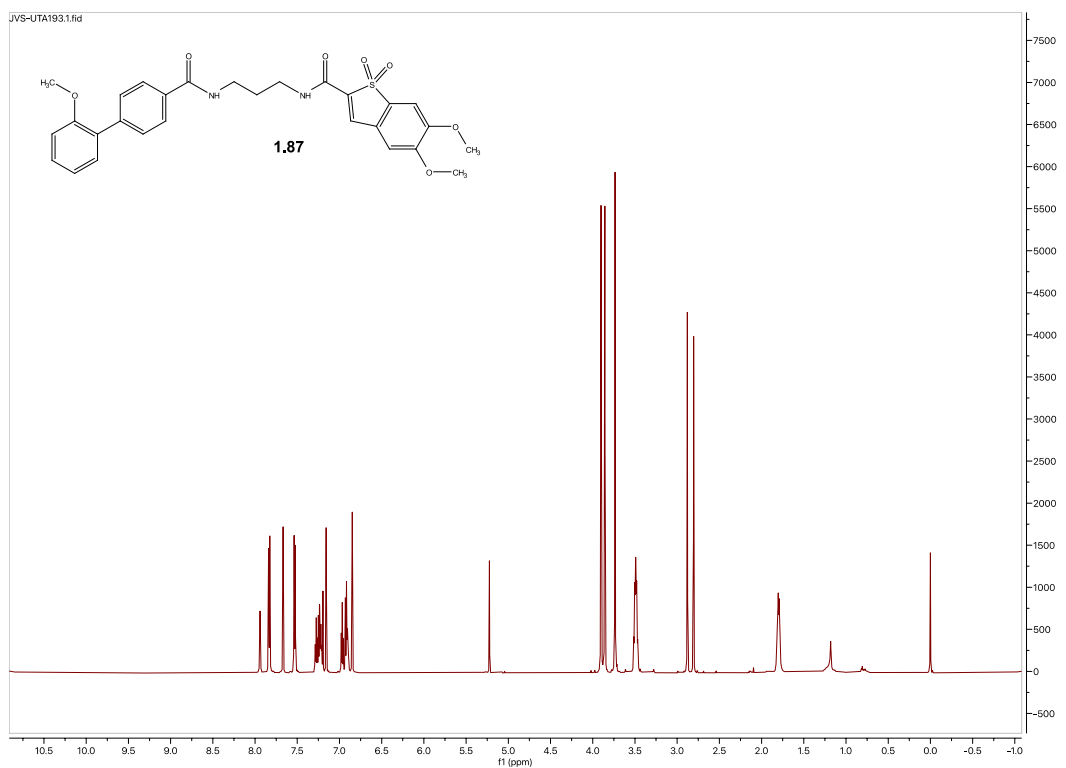
Spectra 1.75 ^1H NMR Spectrum of compound **1.84**



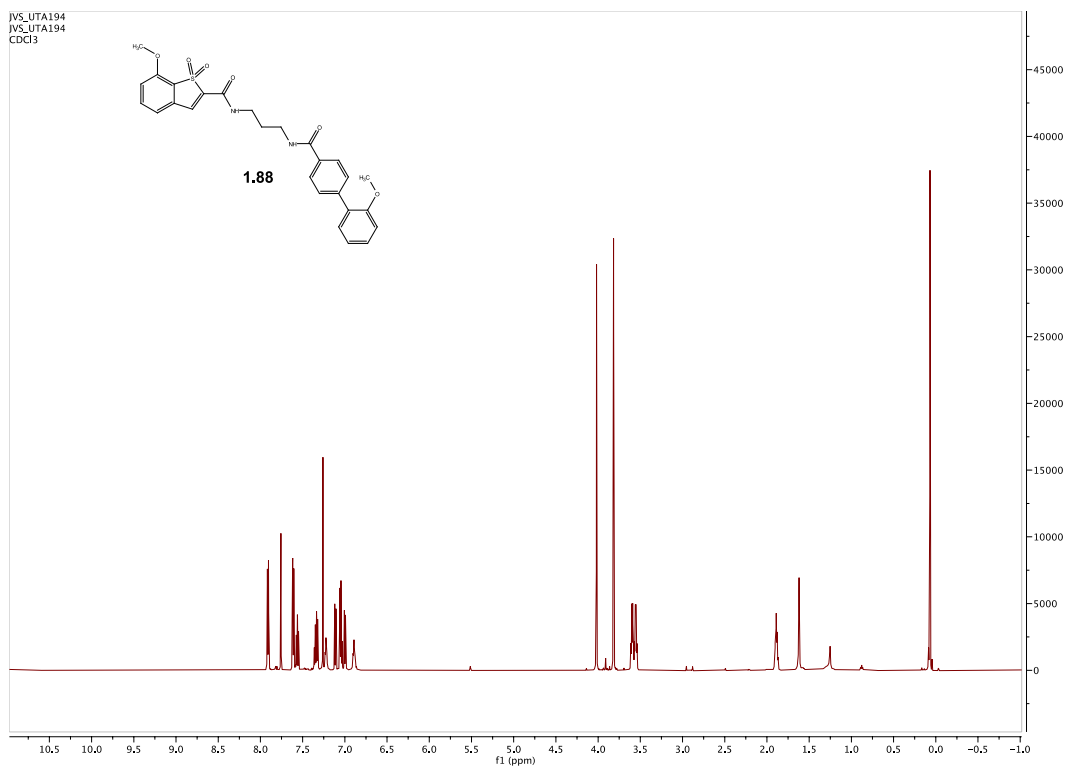
Spectra 1.76 ^{13}C NMR Spectrum of compound **1.85**



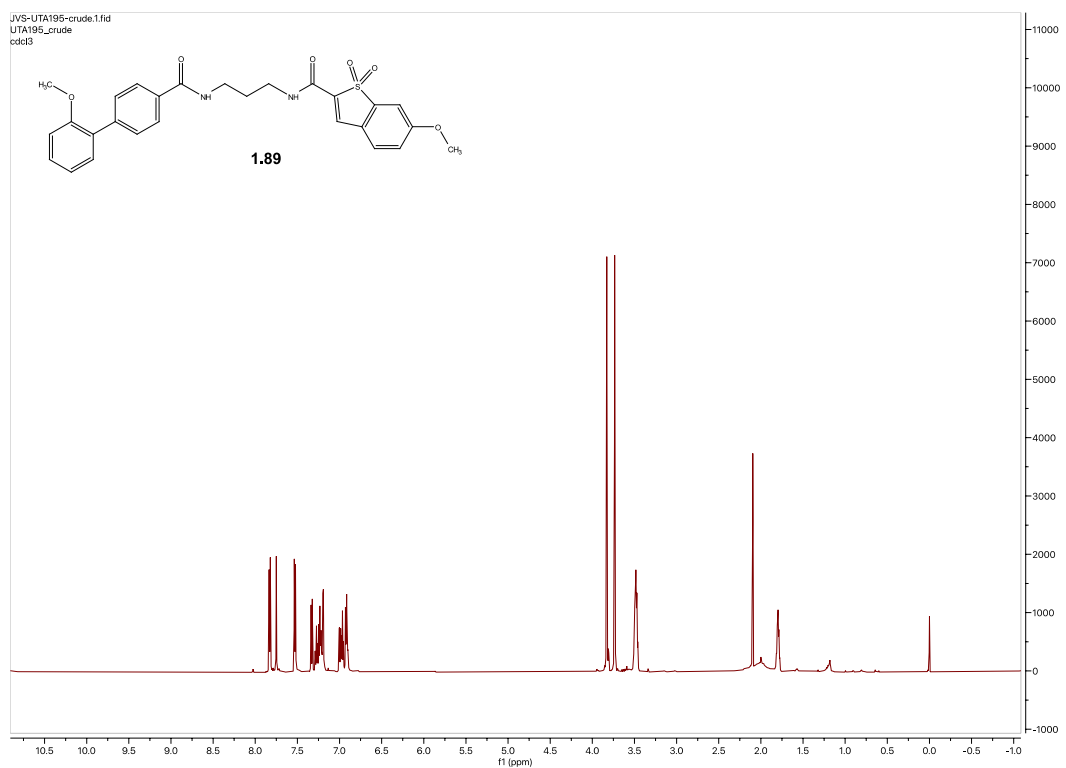
Spectra 1.77 ¹H NMR Spectrum of compound 1.86



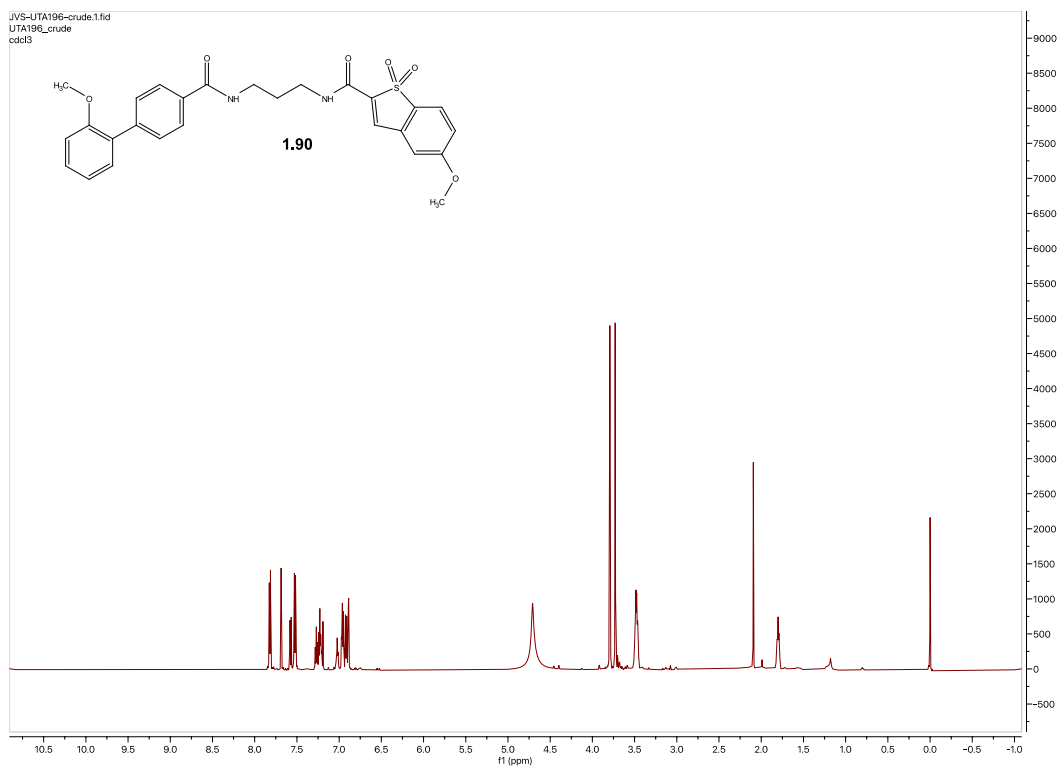
Spectra 1.78 ¹H NMR Spectrum of compound 1.87



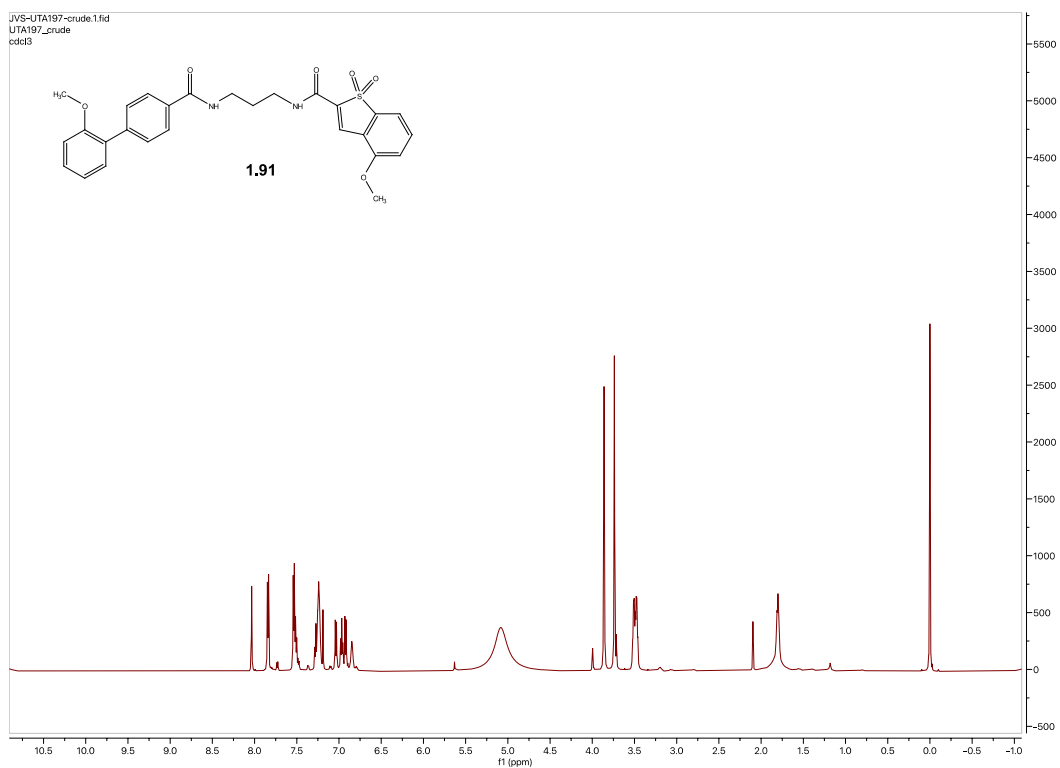
Spectra 1.79 ¹H NMR Spectrum of compound **1.88**



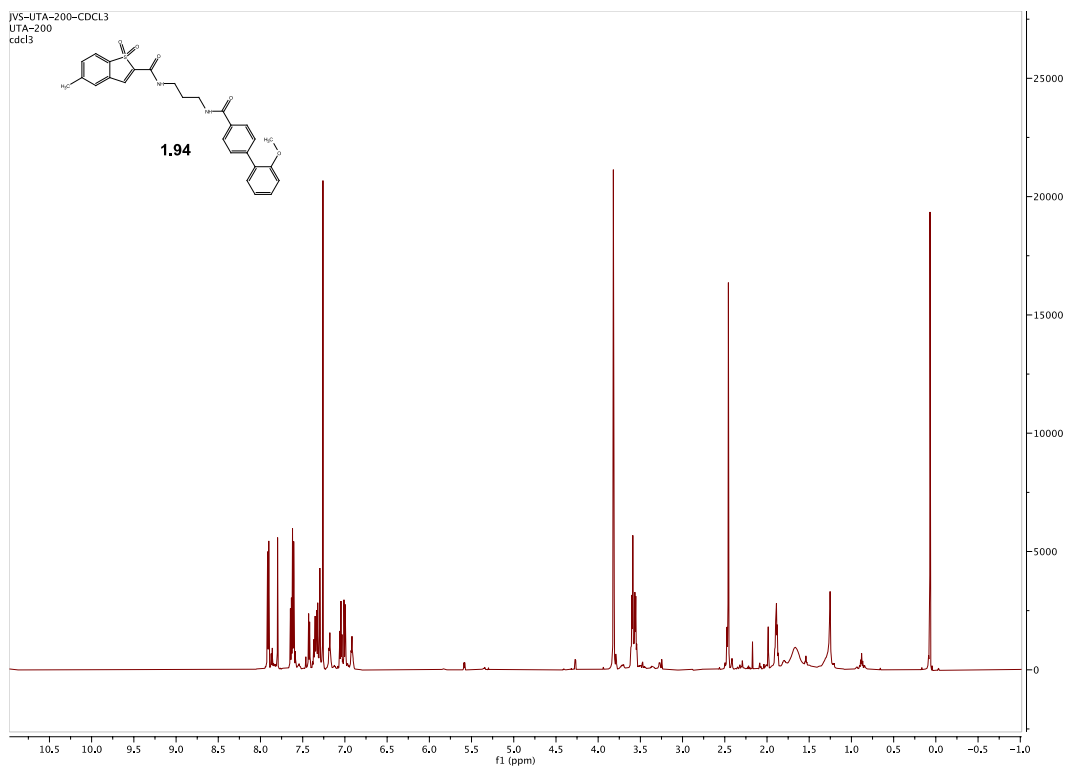
Spectra 1.80 ¹H NMR Spectrum of compound **1.89**



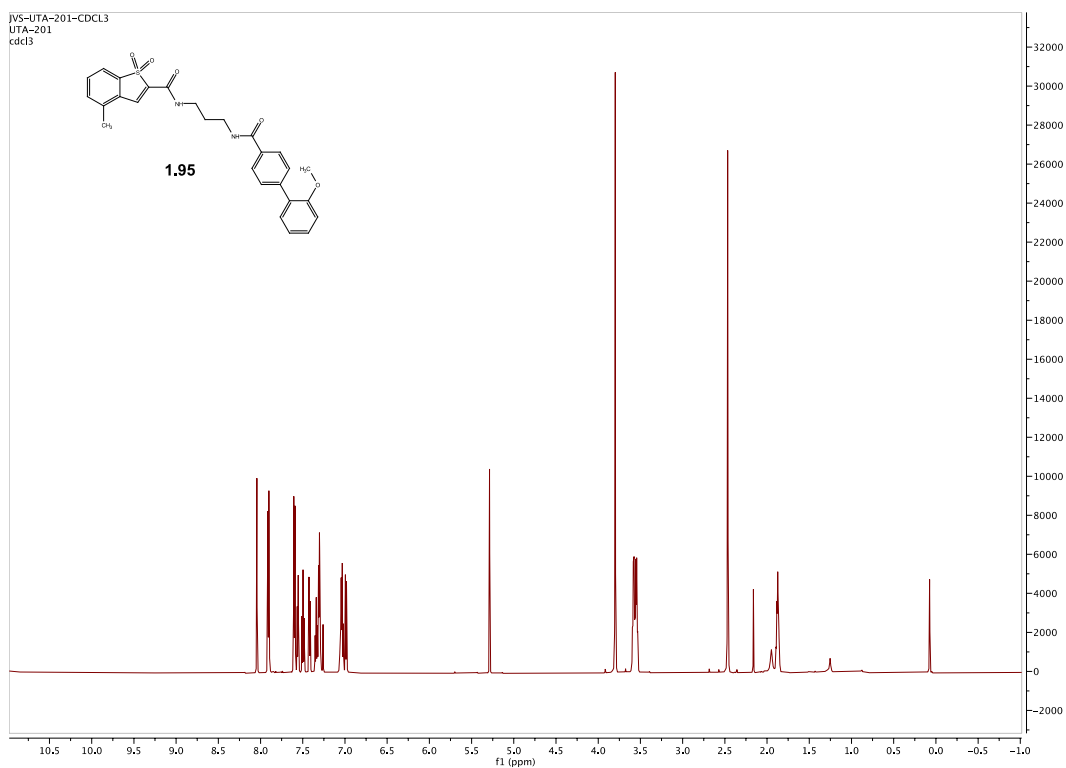
Spectra 1.81 ^1H NMR Spectrum of compound **1.90**



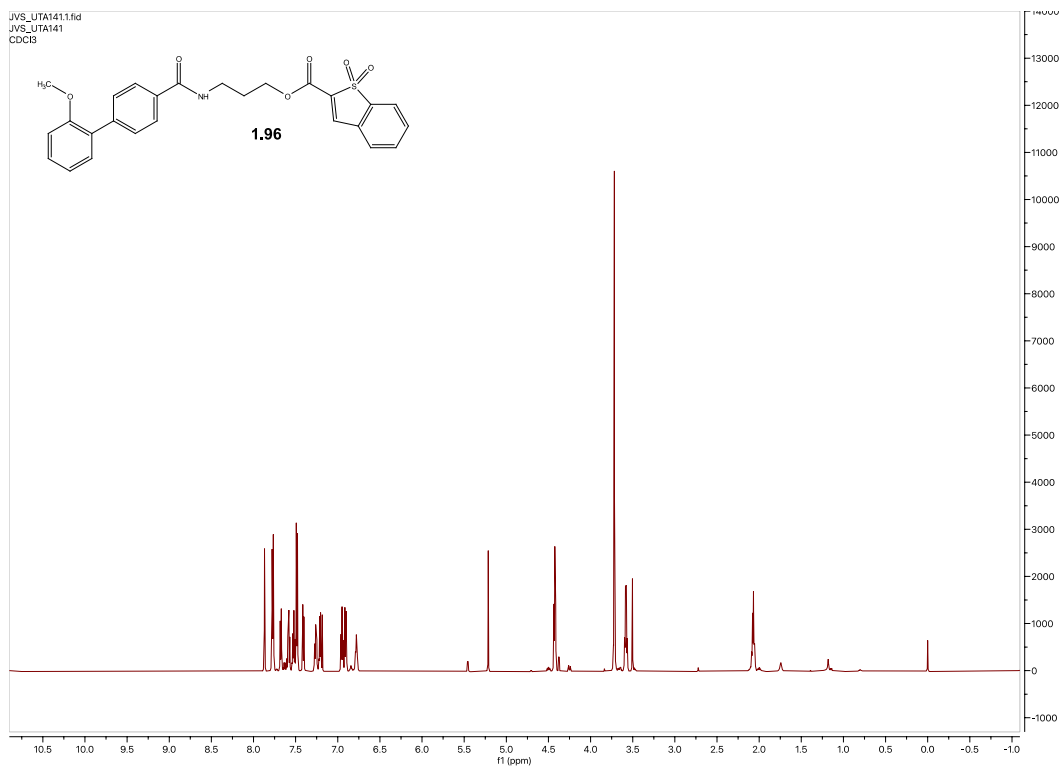
Spectra 1.82 ^1H NMR Spectrum of compound **1.91**



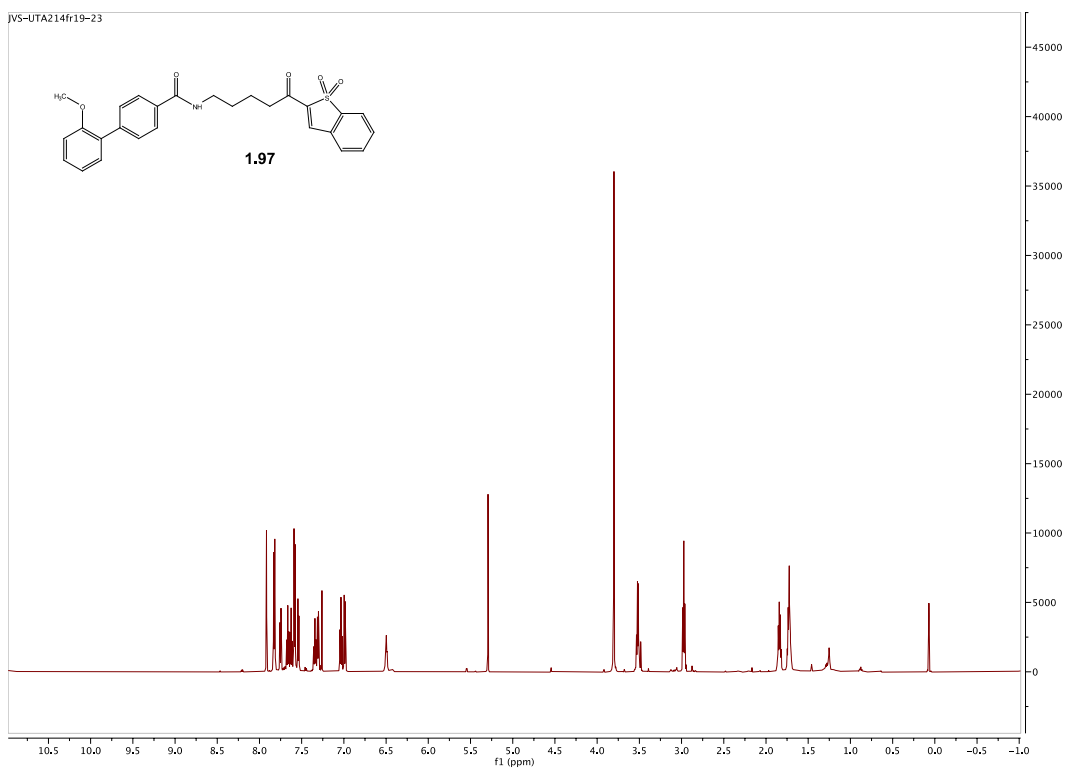
Spectra 1.83 ^1H NMR Spectrum of compound **1.94**



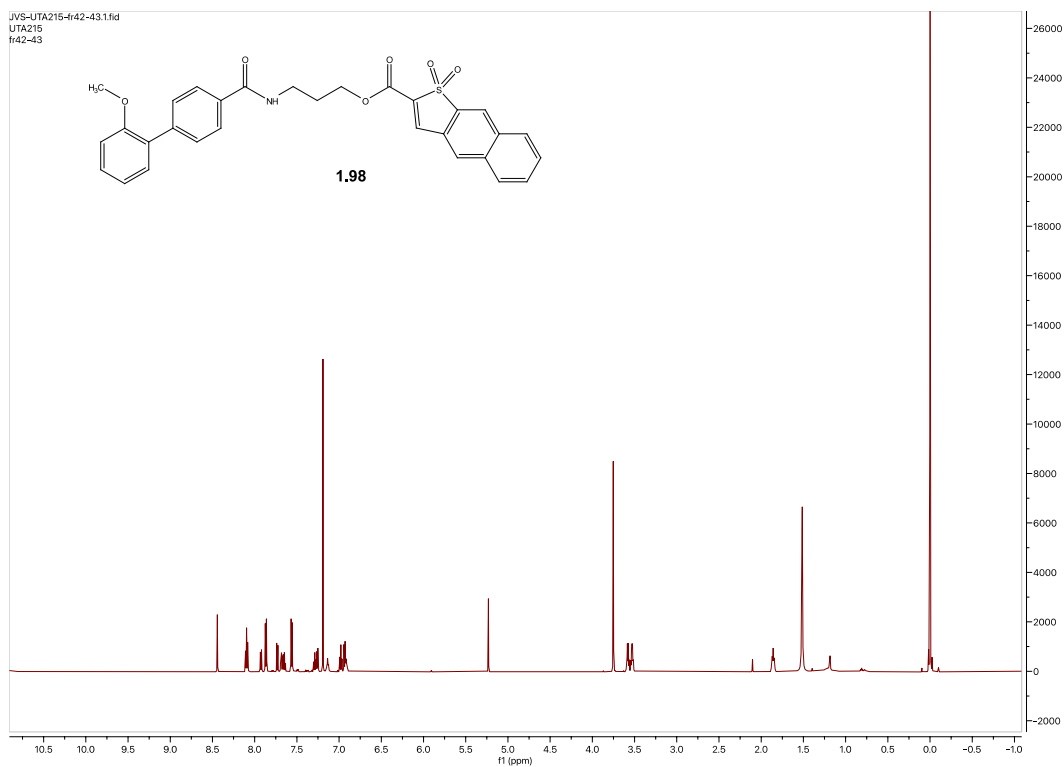
Spectra 1.84 ^1H NMR Spectrum of compound **1.95**



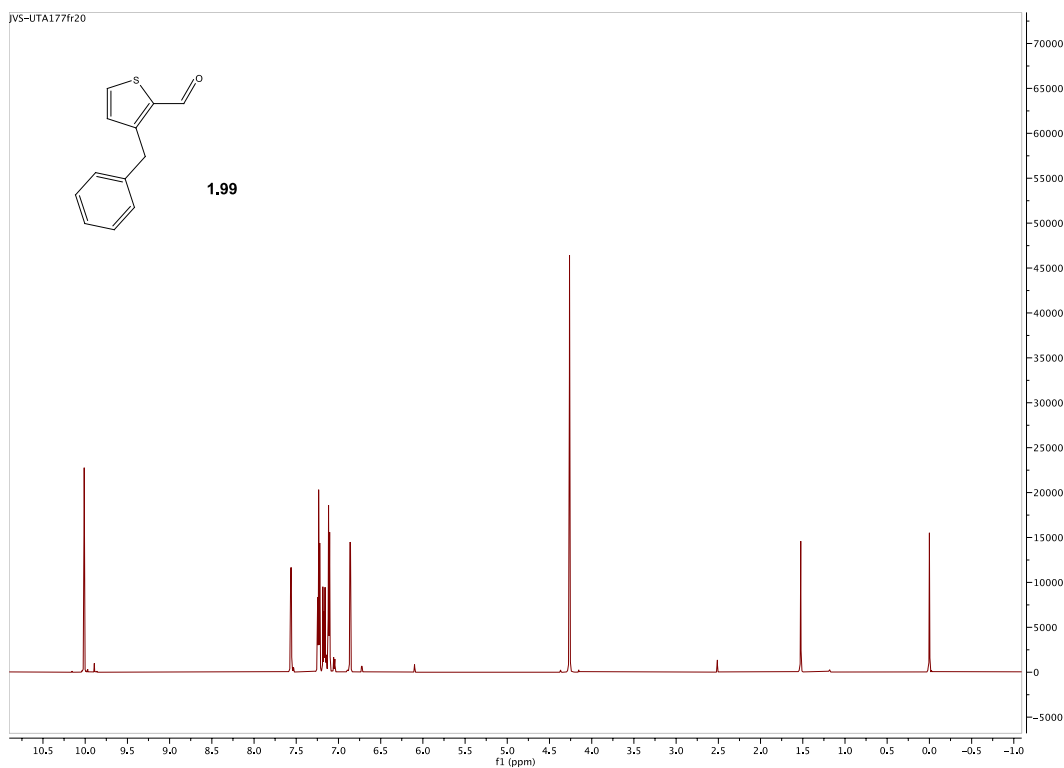
Spectra 1.85 ^1H NMR Spectrum of compound **1.96**



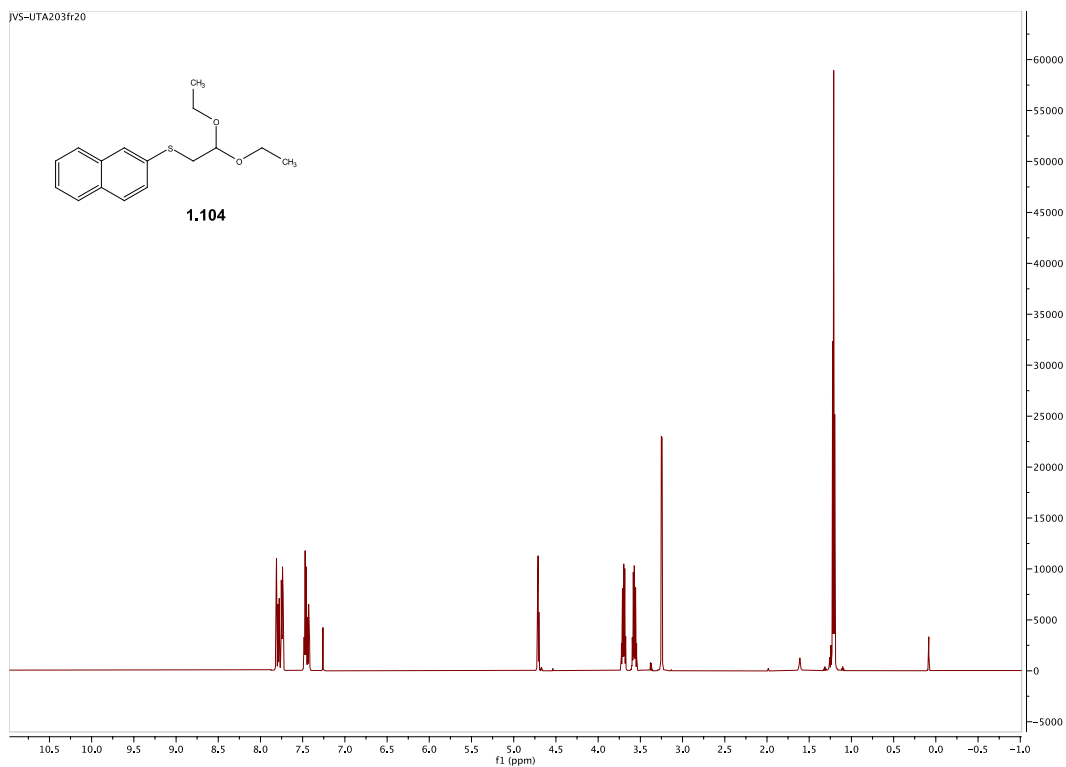
Spectra 1.86 ^1H NMR Spectrum of compound **1.97**



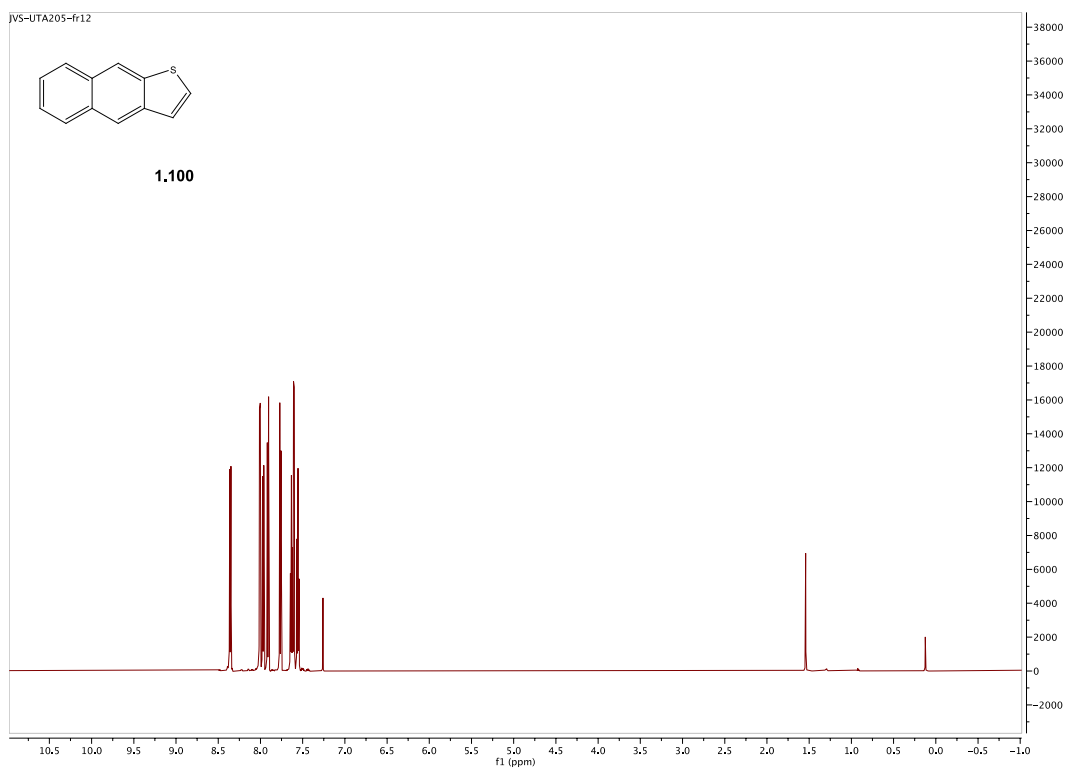
Spectra 1.87 ^1H NMR Spectrum of compound 1.98



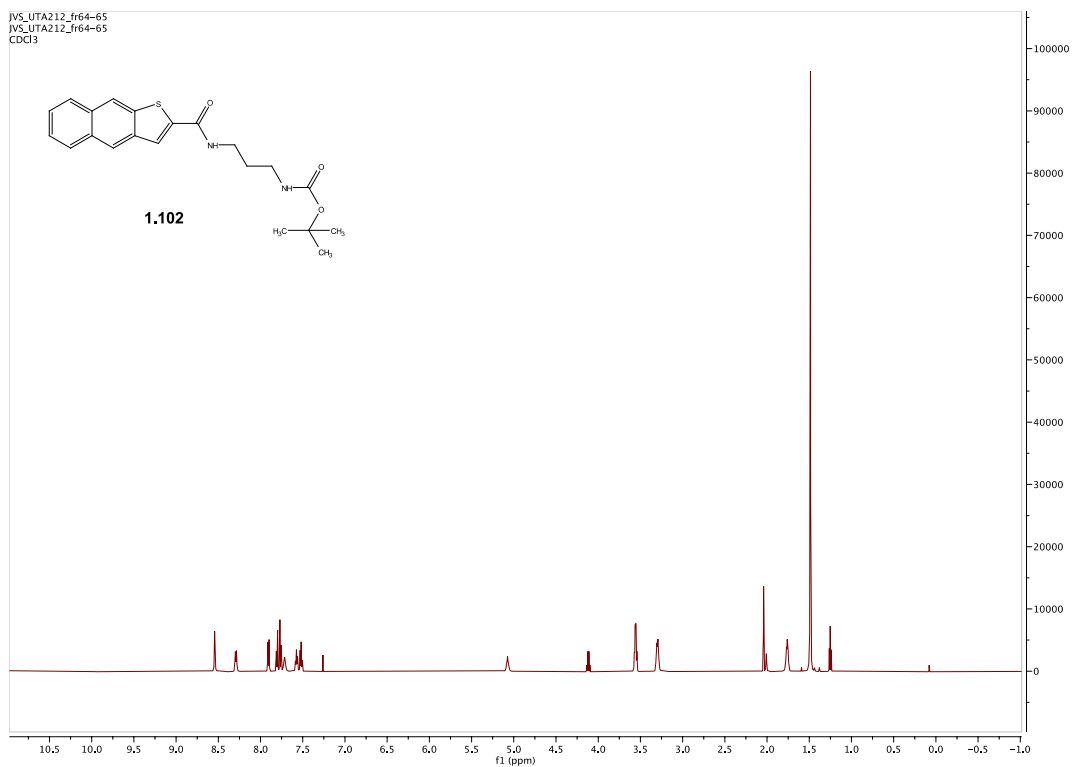
Spectra 1.88 ^1H NMR Spectrum of compound 1.99



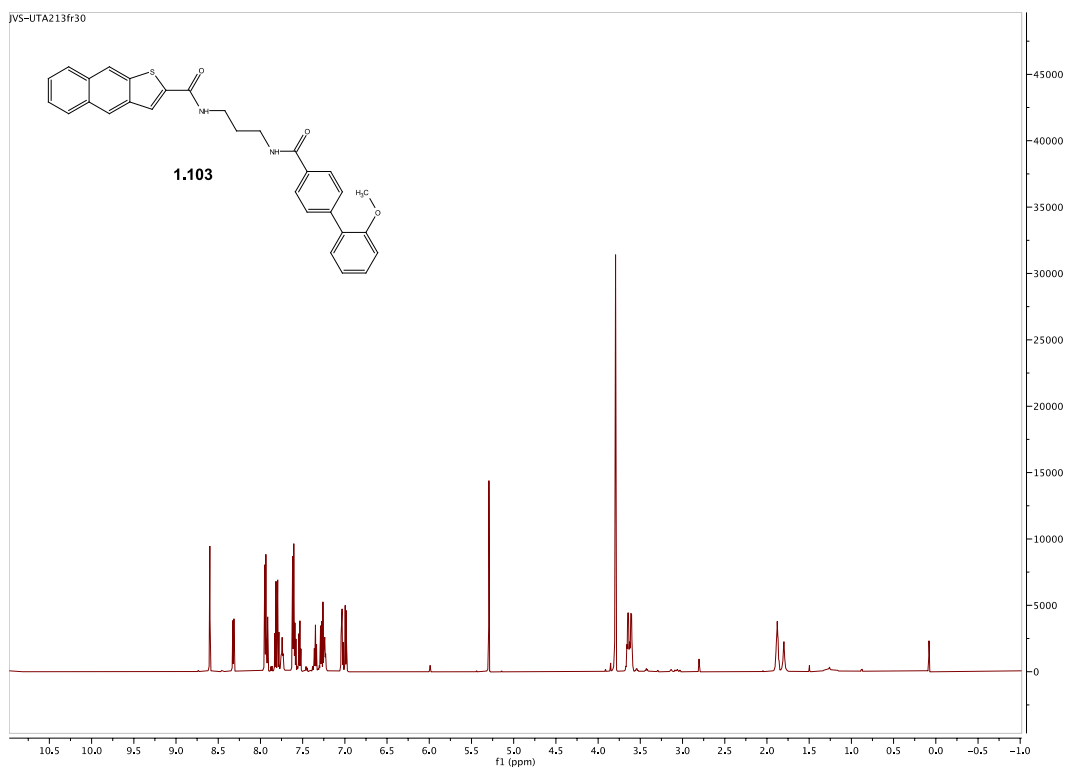
Spectra 1.89 ^1H NMR Spectrum of compound **1.104**



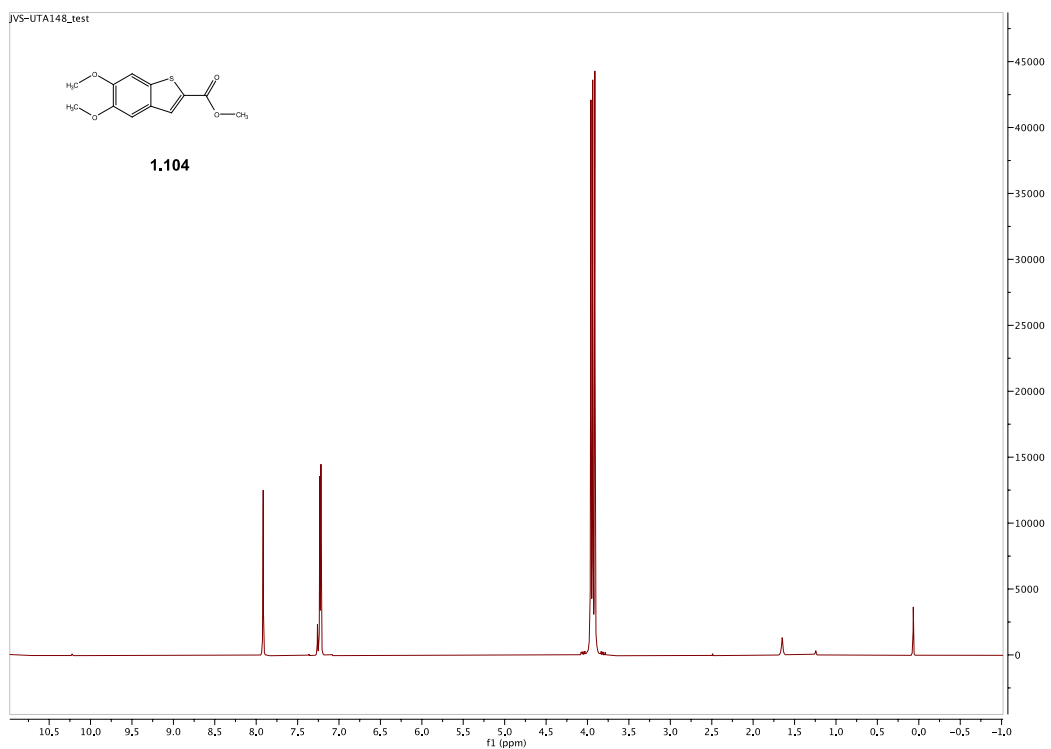
Spectra 1.90 ^1H NMR Spectrum of compound **1.100**



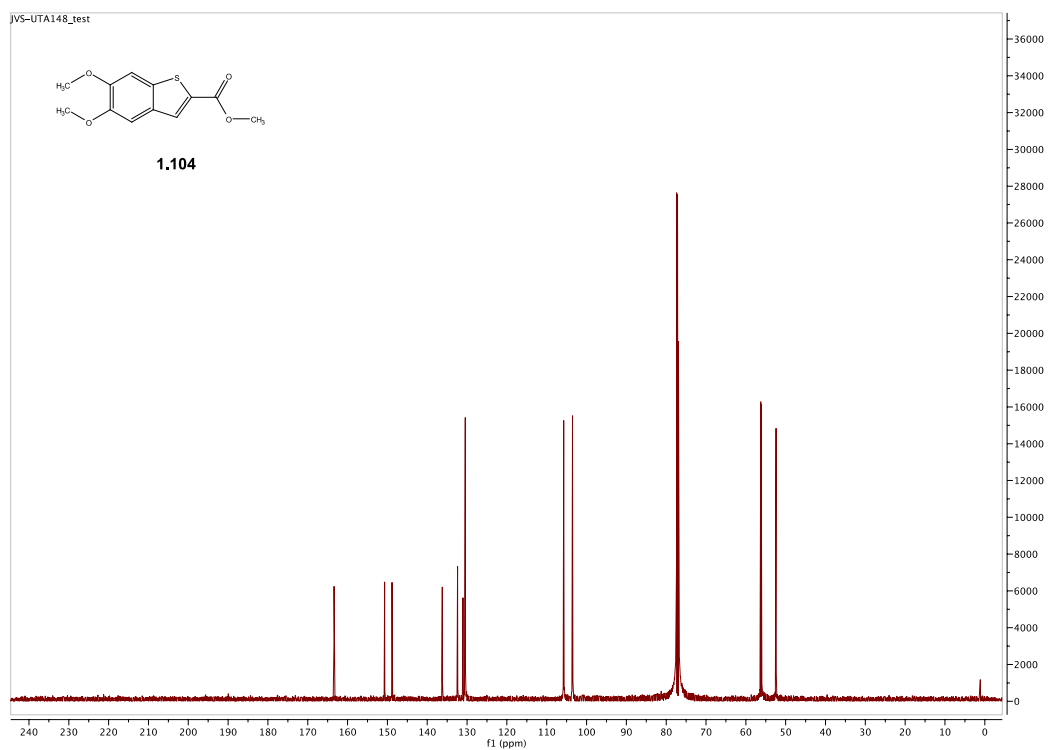
Spectra 1.91 ¹H NMR Spectrum of compound **1.102**



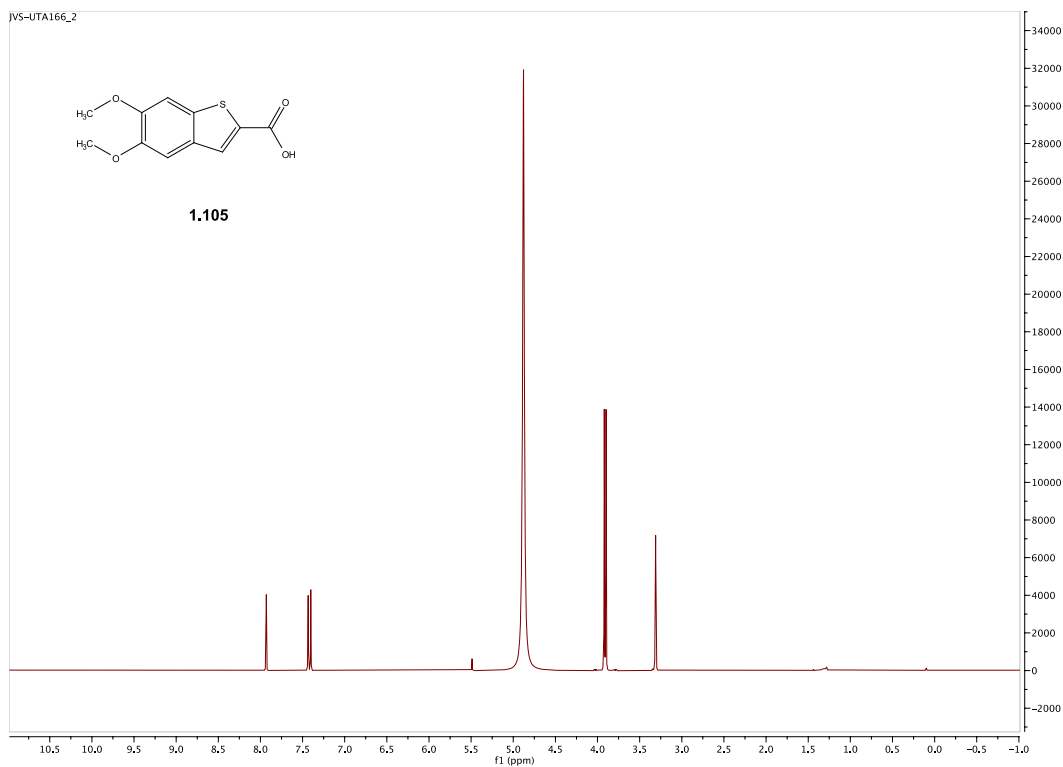
Spectra 1.92 ¹H NMR Spectrum of compound **1.103**



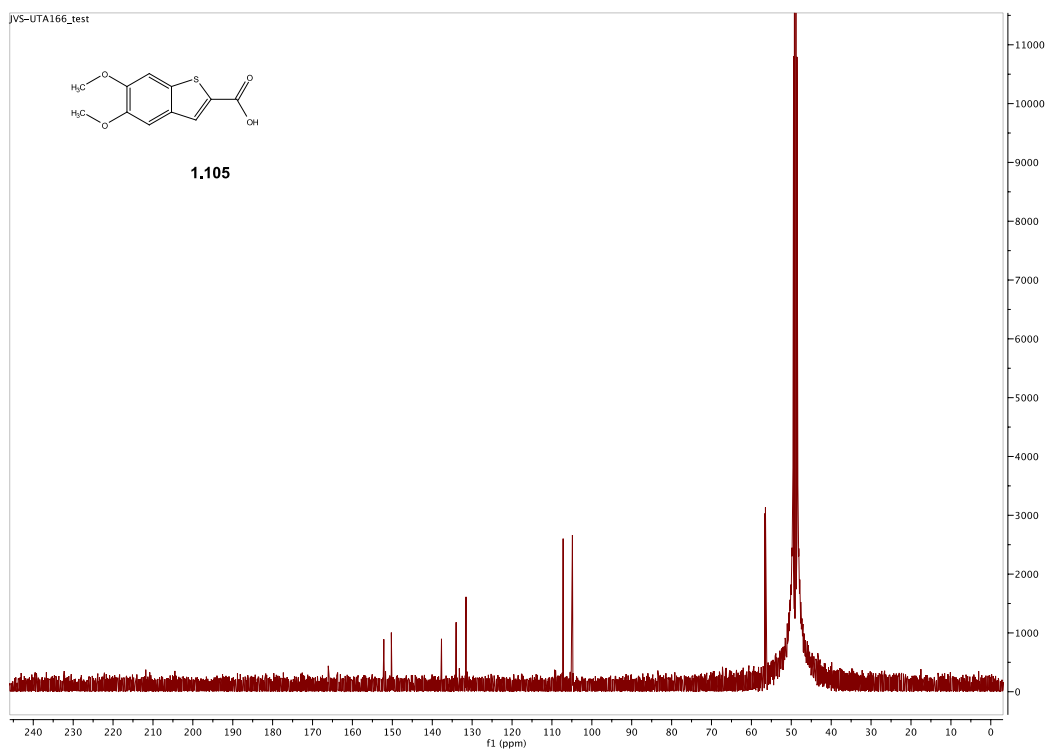
Spectra 1.93 ^1H NMR Spectrum of compound **1.104**



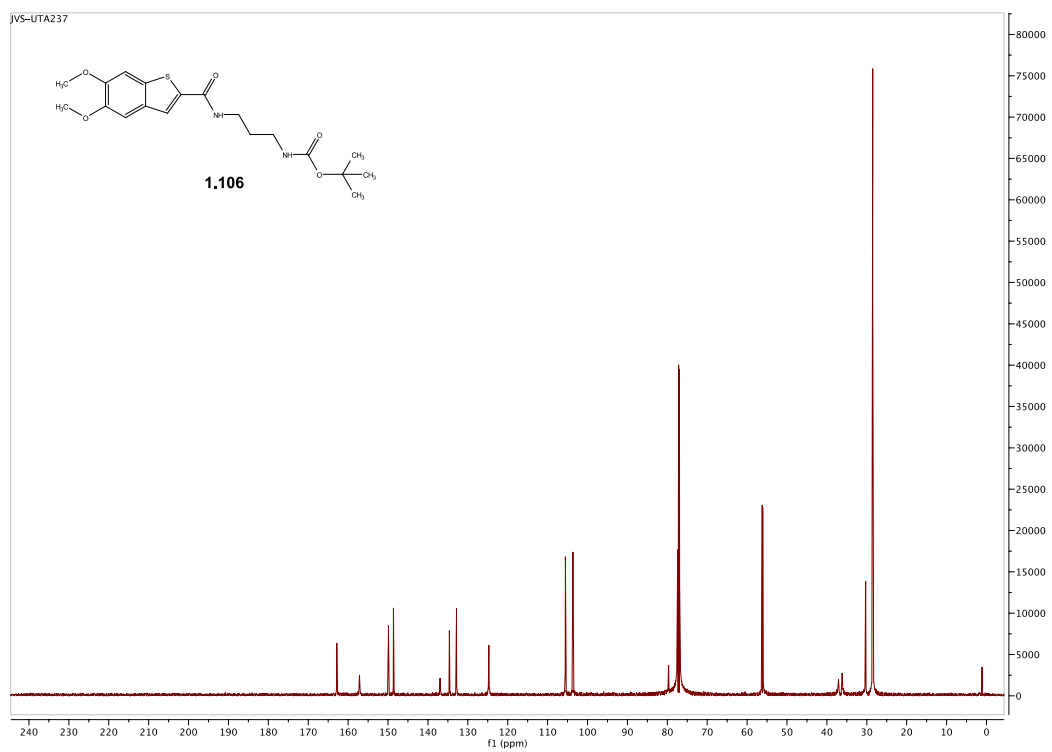
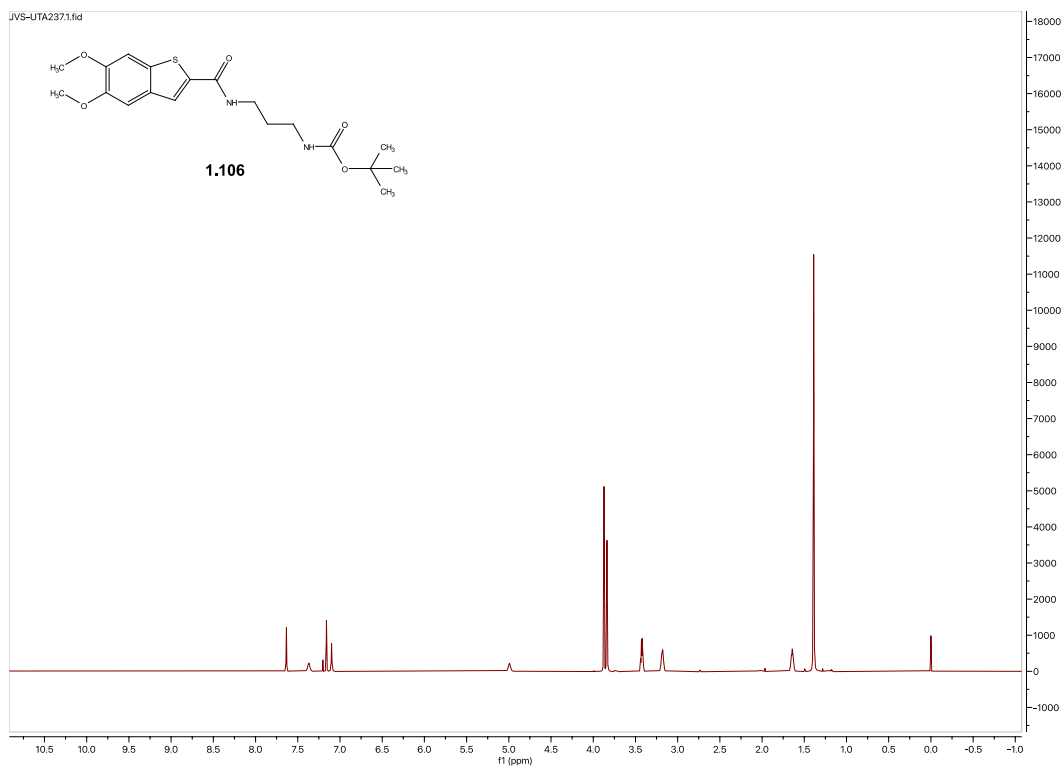
Spectra 1.94 ^{13}C NMR Spectrum of compound **1.104**

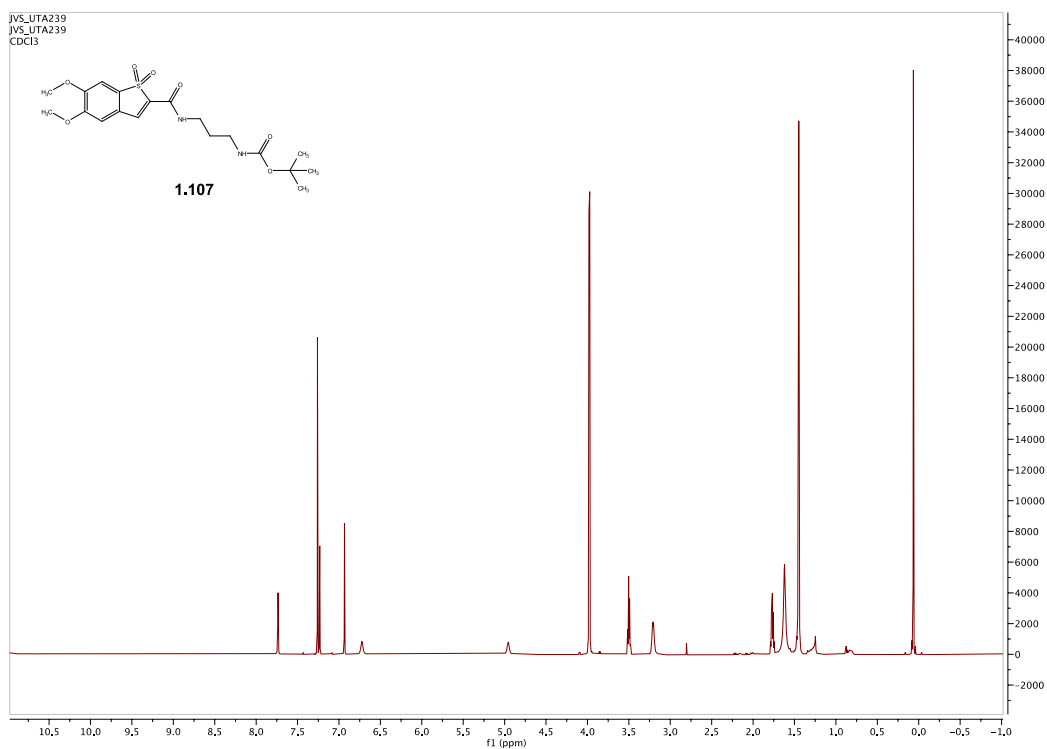


Spectra 1.95 ^1H NMR Spectrum of compound **1.105**

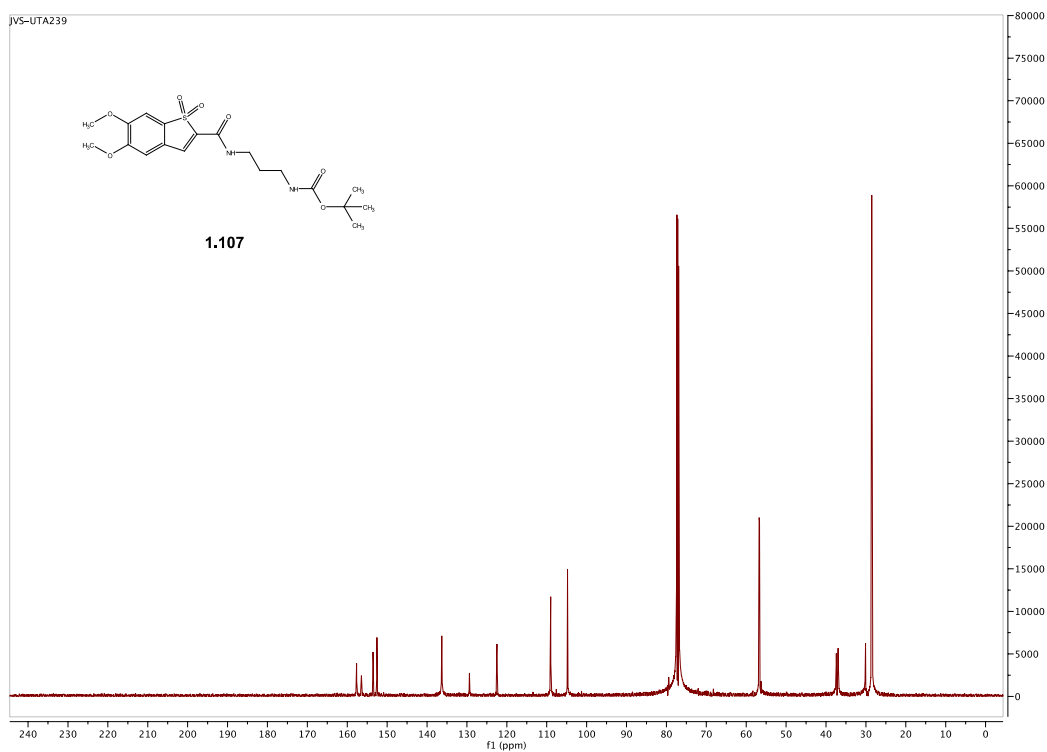


Spectra 1.95 ^{13}C NMR Spectrum of compound **1.105**

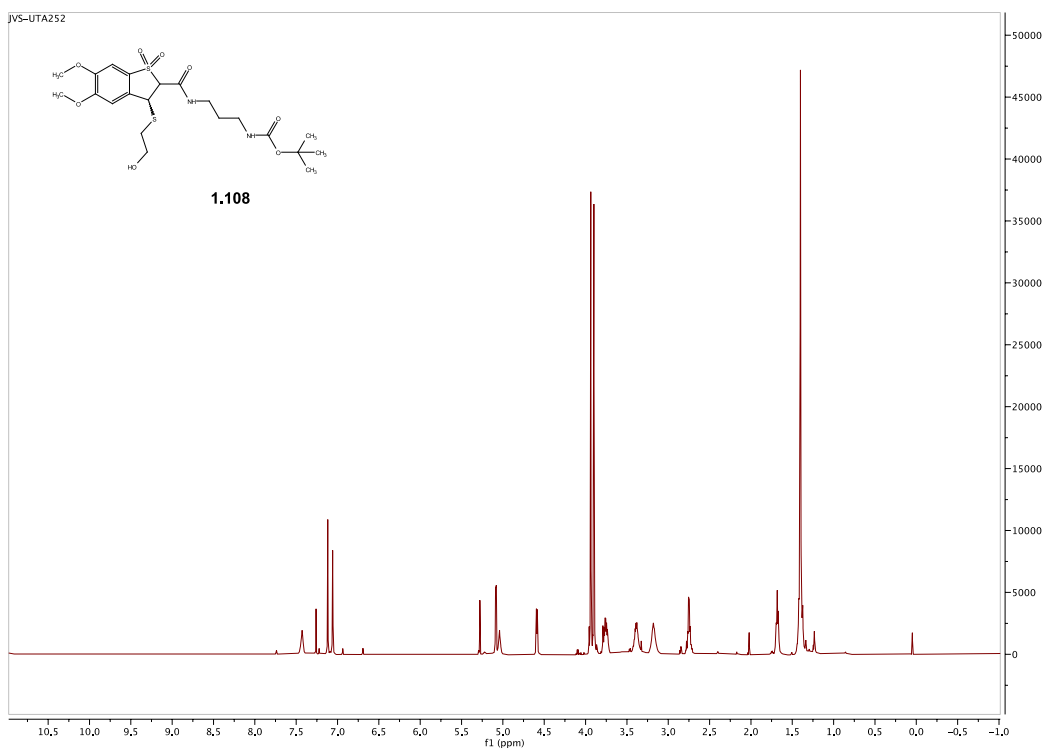




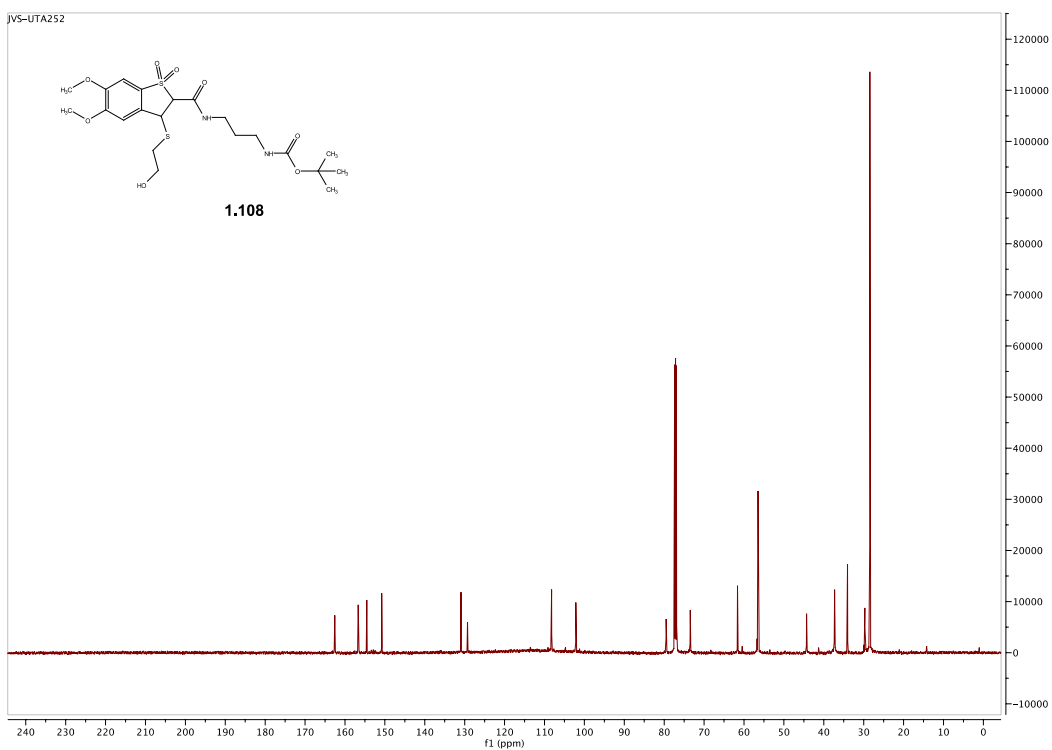
Spectra 1.98 ¹H NMR Spectrum of compound **1.107**



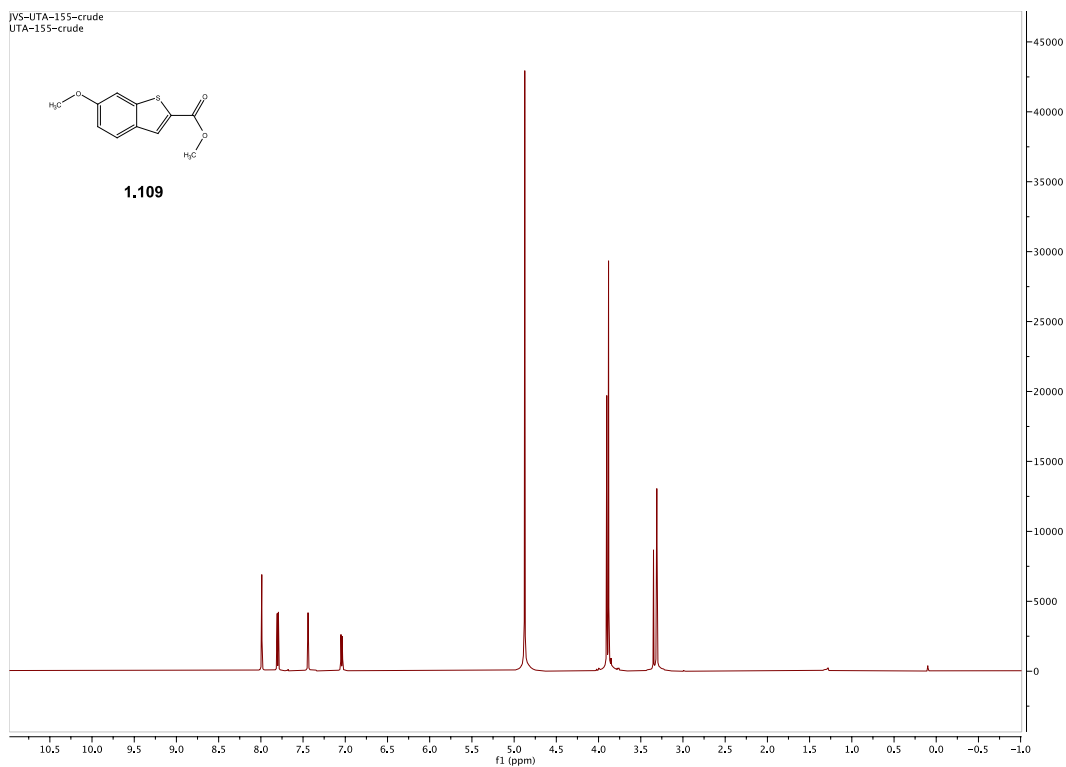
Spectra 1.99 ¹³C NMR Spectrum of compound **1.107**



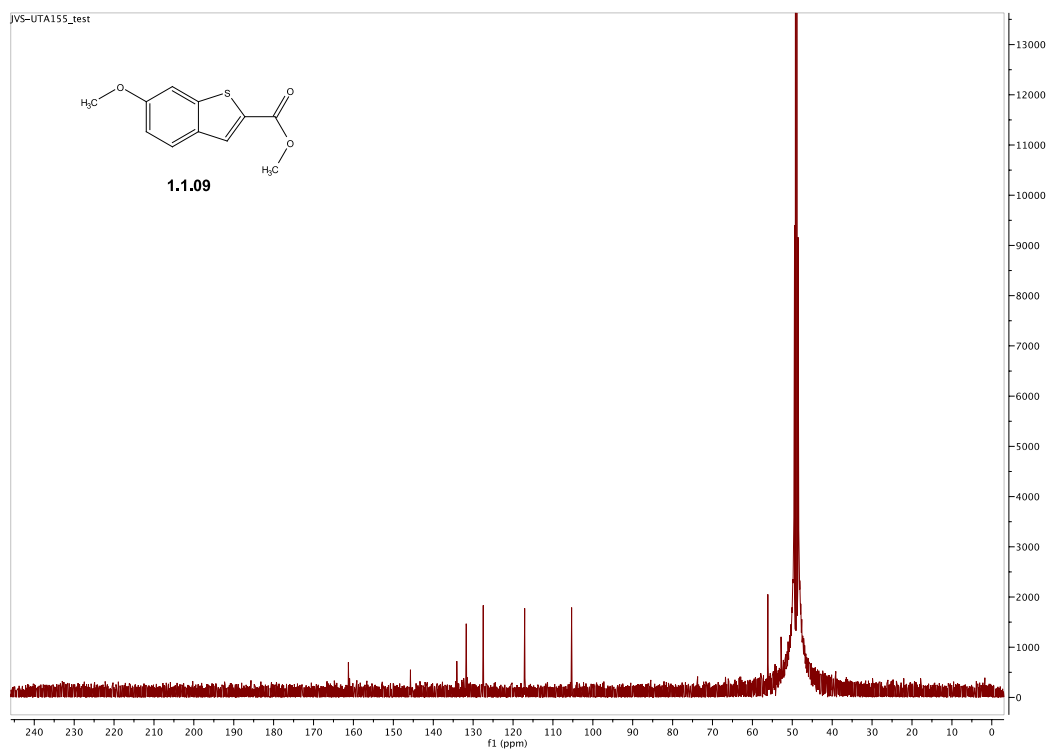
Spectra 1.100 ^1H NMR Spectrum of compound **1.108**



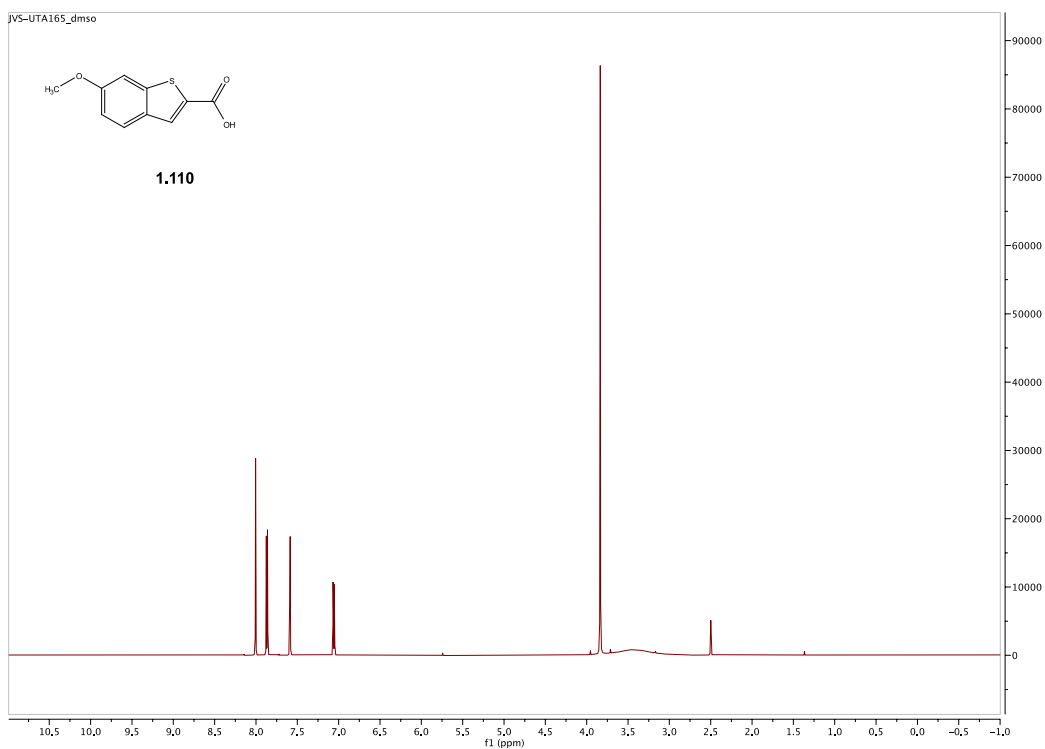
Spectra 1.101 ^{13}C NMR Spectrum of compound **1.108**



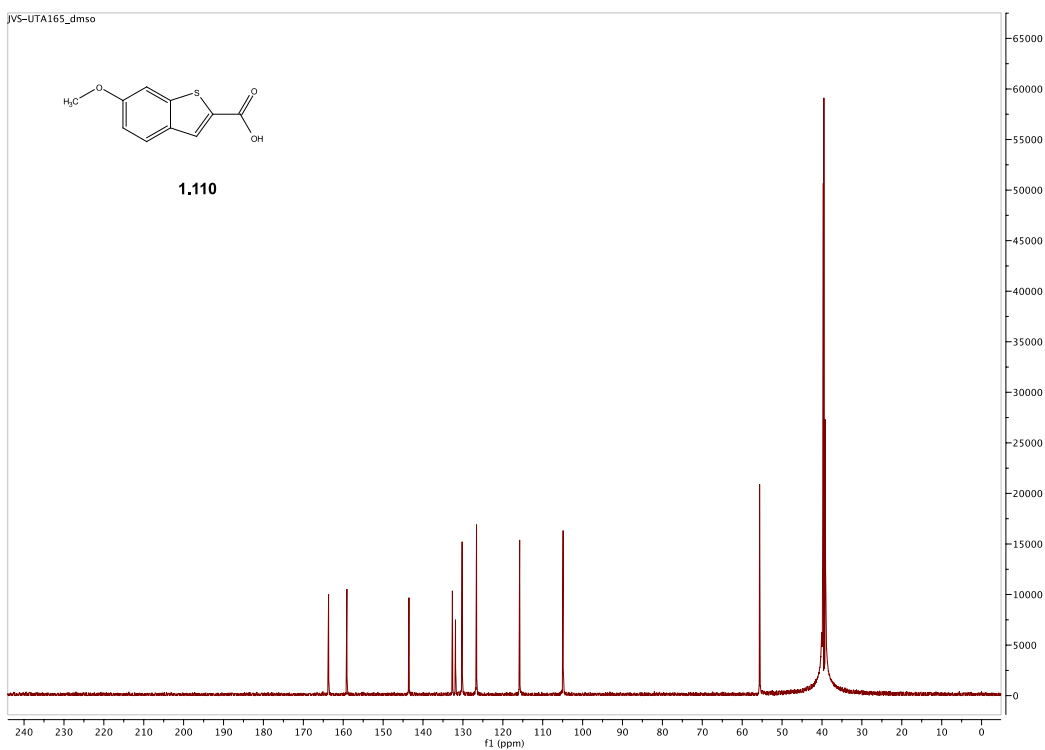
Spectra 1.102 ^1H NMR Spectrum of compound **1.109**



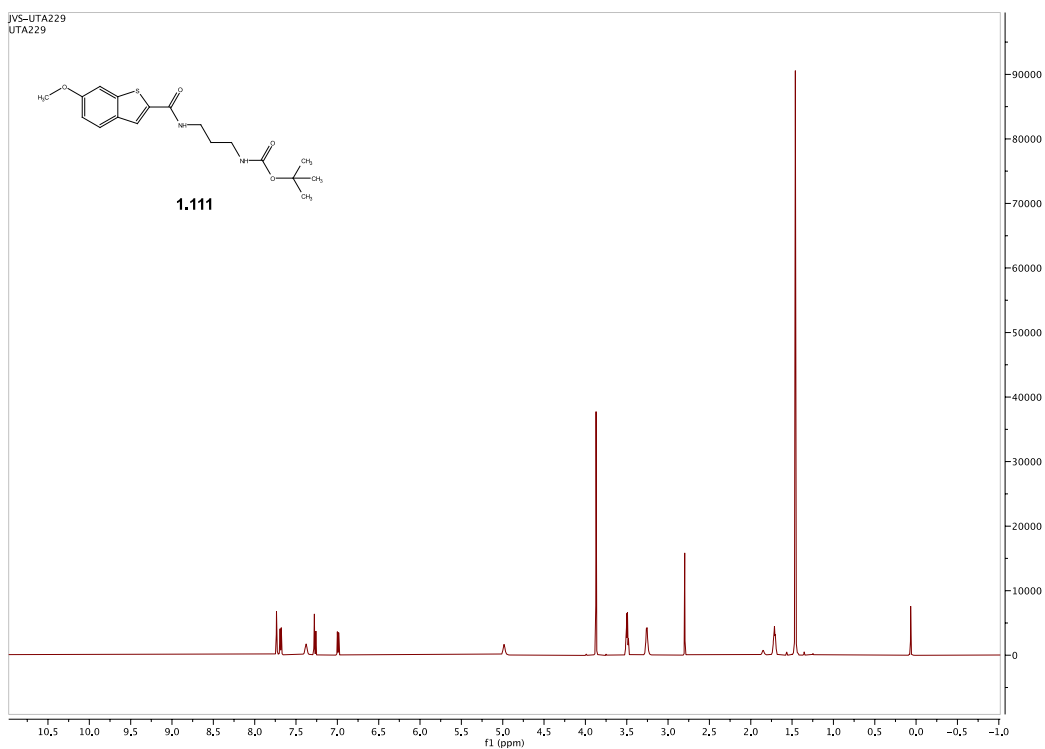
Spectra 1.103 ^{13}C NMR Spectrum of compound **1.109**



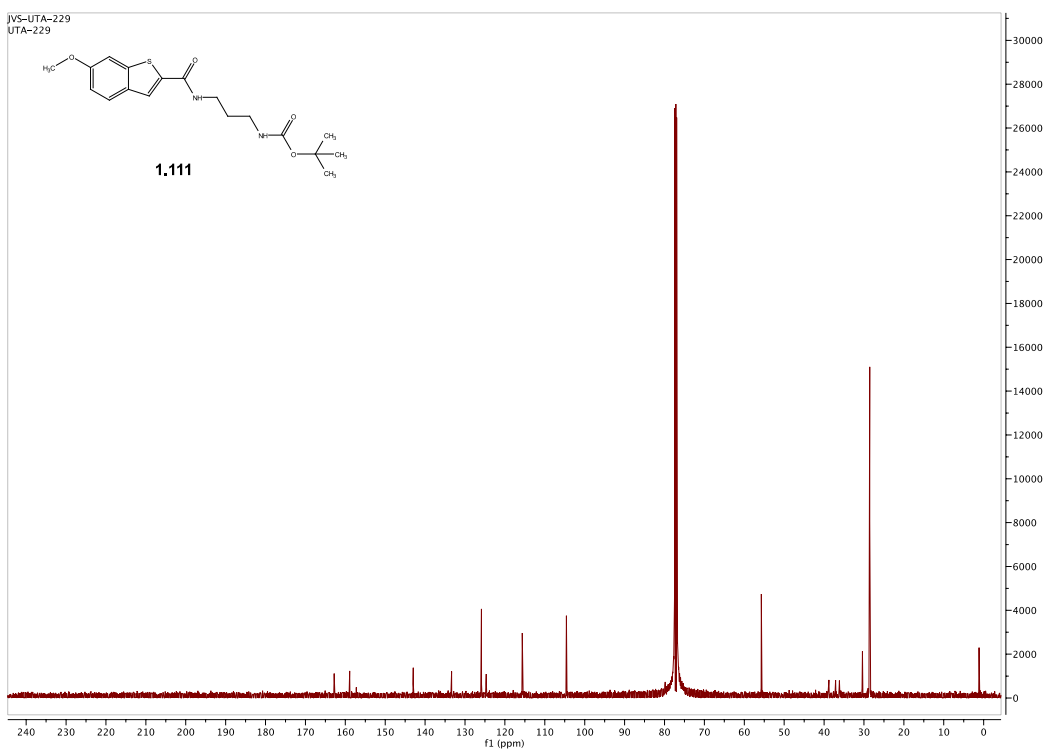
Spectra 1.104 ^1H NMR Spectrum of compound **1.110**



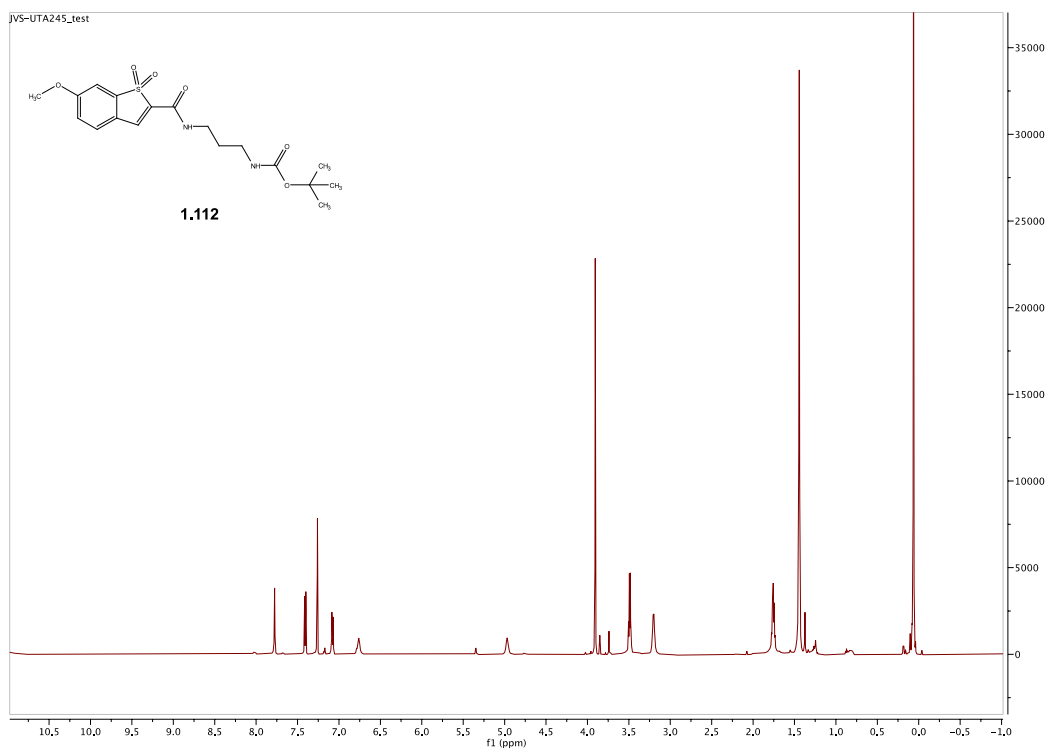
Spectra 1.105 ^{13}C NMR Spectrum of compound **1.110**



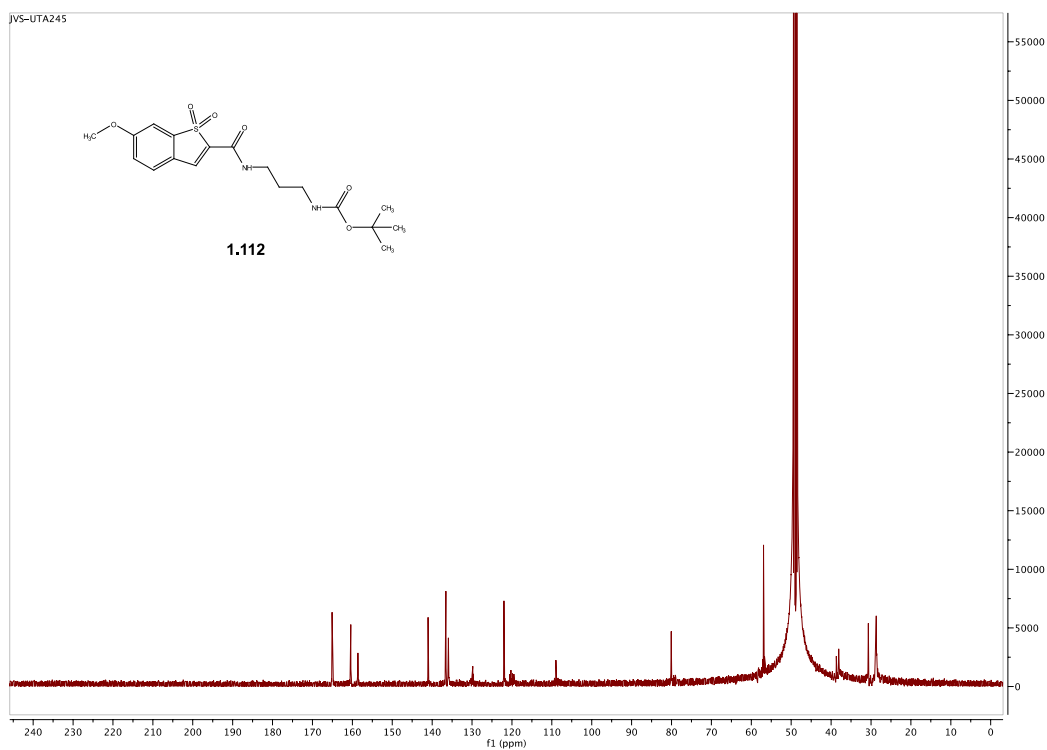
Spectra 1.106 ^1H NMR Spectrum of compound **1.111**



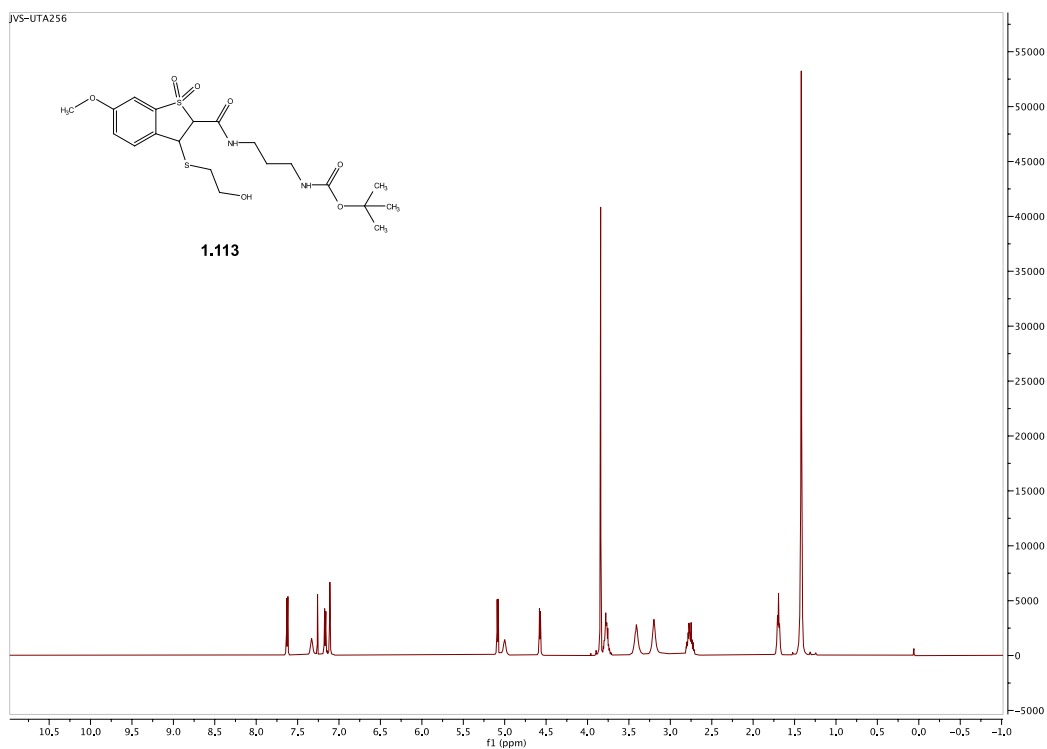
Spectra 1.107 ^{13}C NMR Spectrum of compound **1.111**



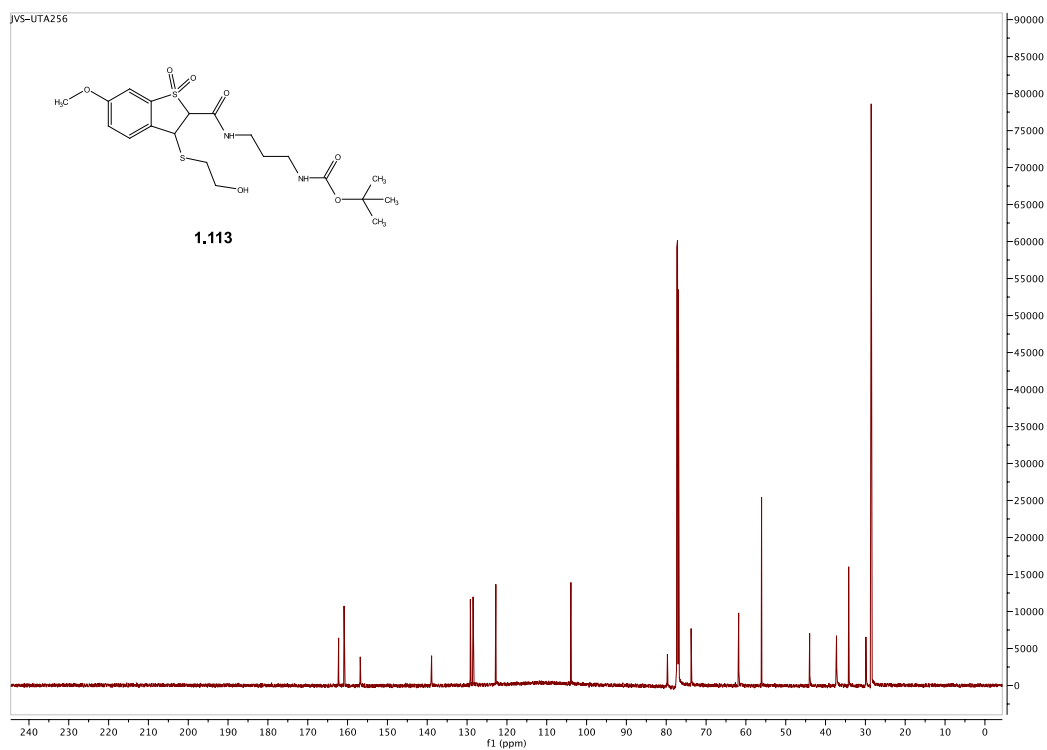
Spectra 1.108 ^1H NMR Spectrum of compound **1.112**



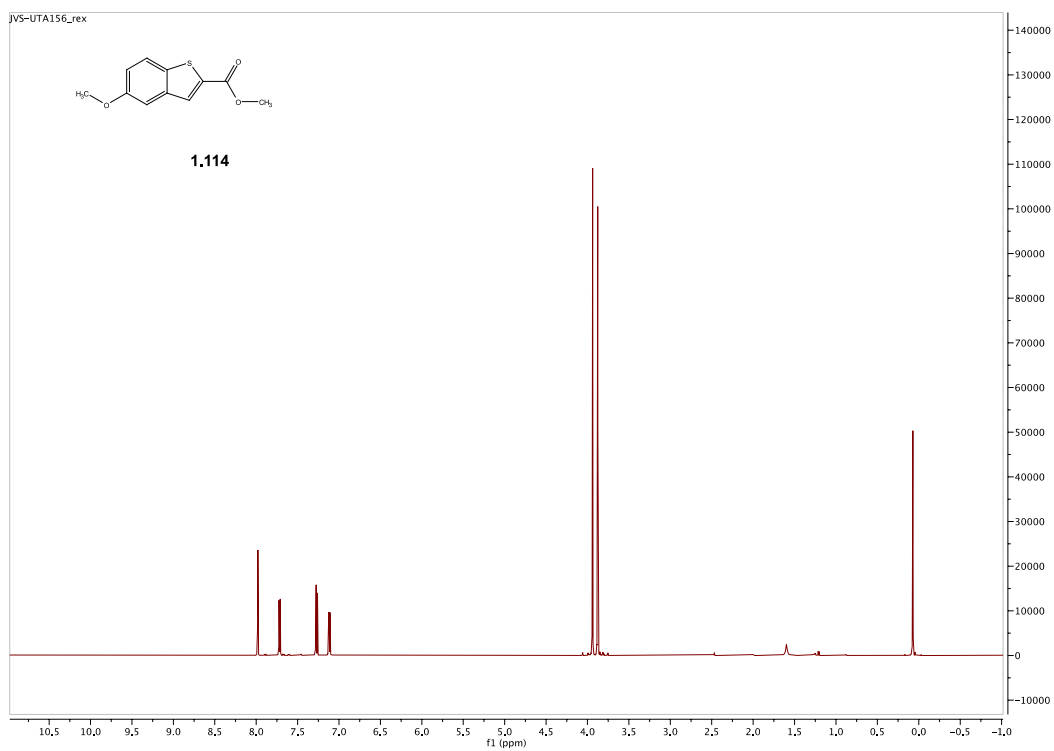
Spectra 1.109 ^{13}C NMR Spectrum of compound **1.112**



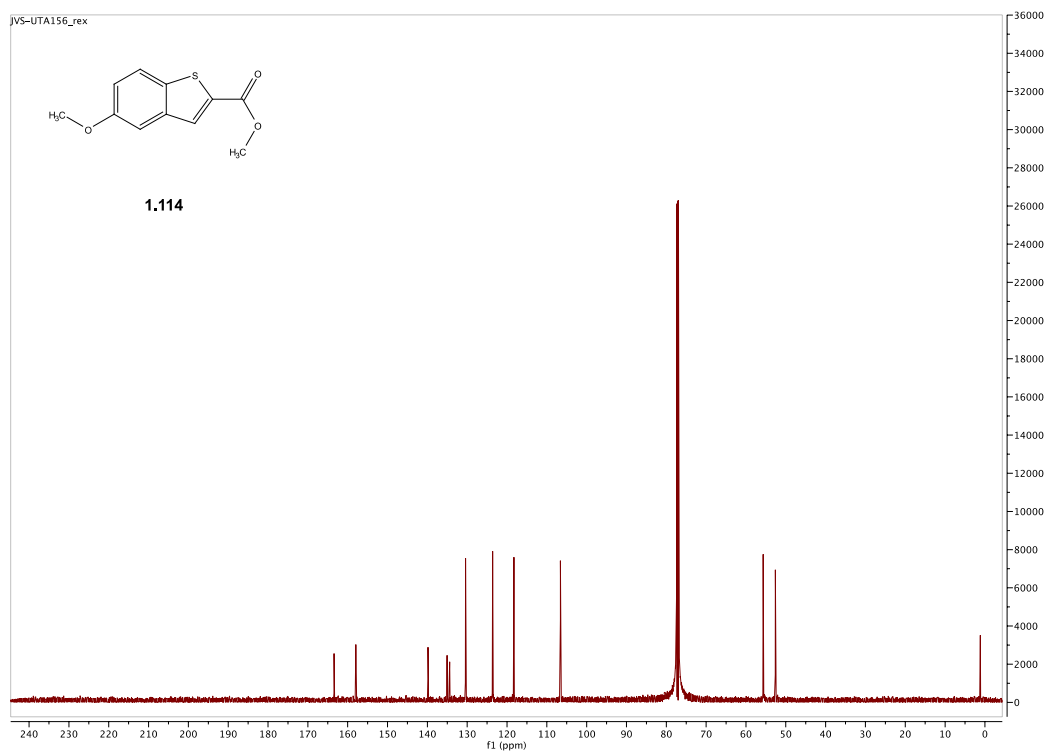
Spectra 1.110 ^1H NMR Spectrum of compound **1.113**



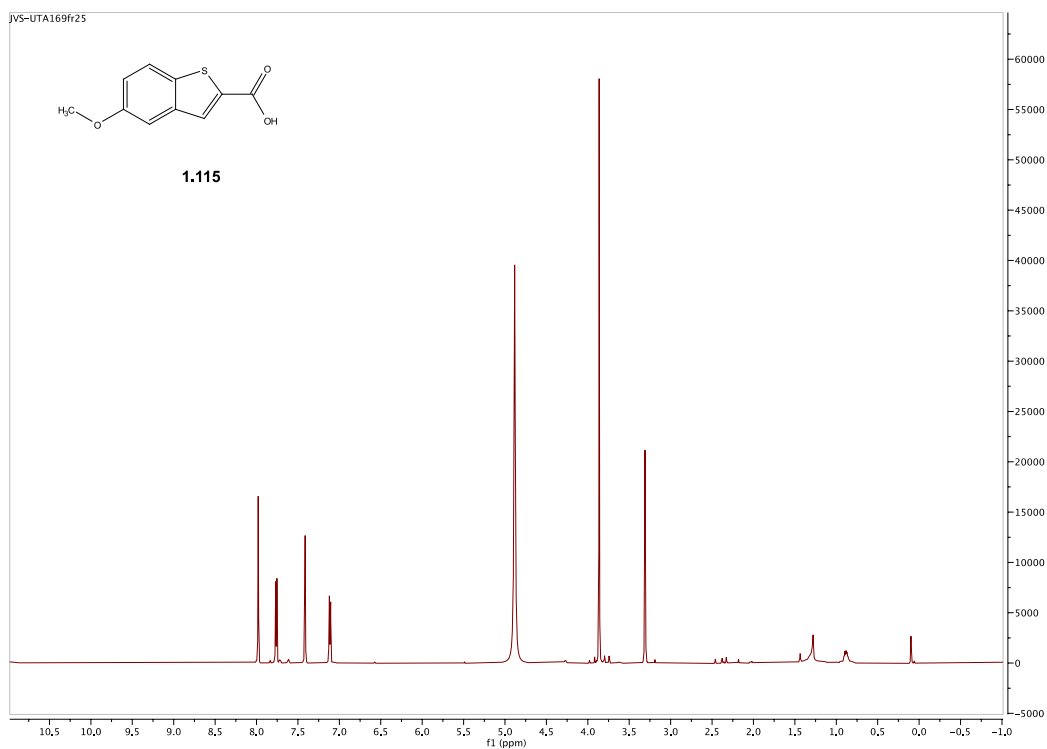
Spectra 1.111 ^{13}C NMR Spectrum of compound **1.113**



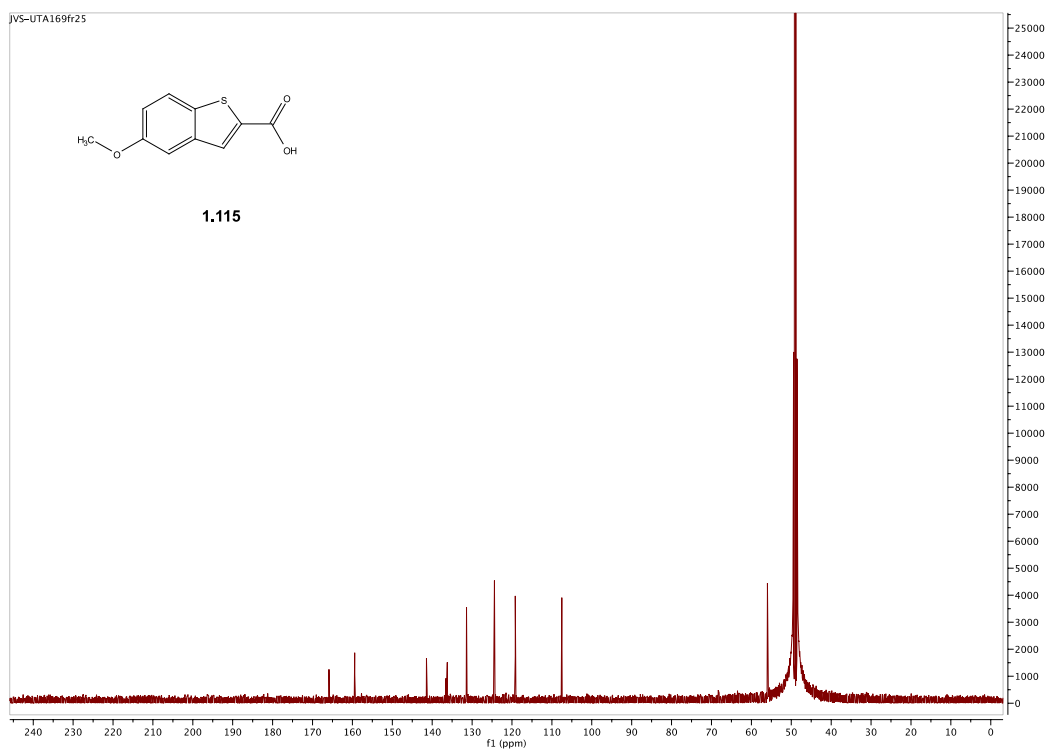
Spectra 1.112 ^1H NMR Spectrum of compound **1.114**



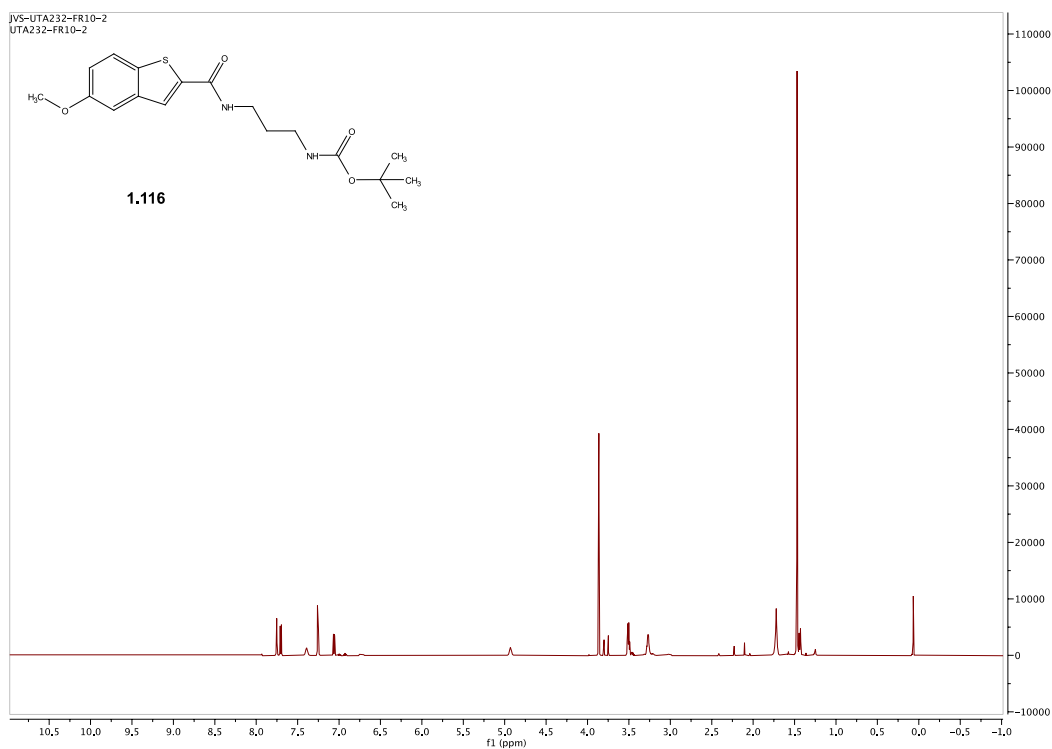
Spectra 1.113 ^{13}C NMR Spectrum of compound **1.114**



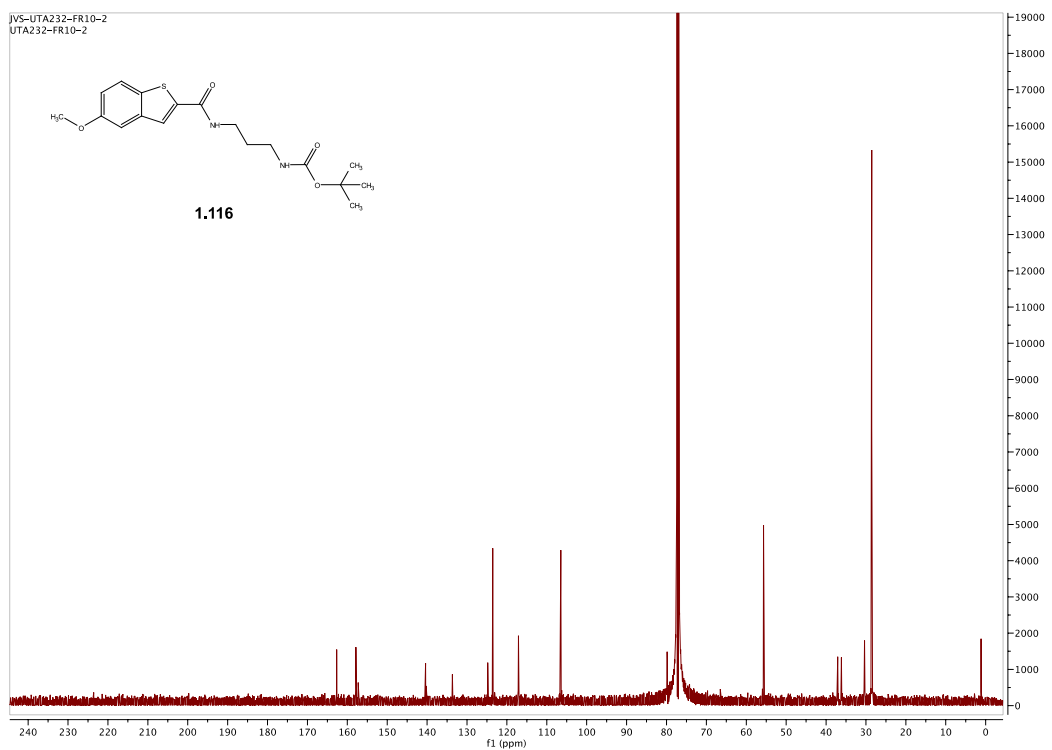
Spectra 1.114 ^1H NMR Spectrum of compound **1.115**



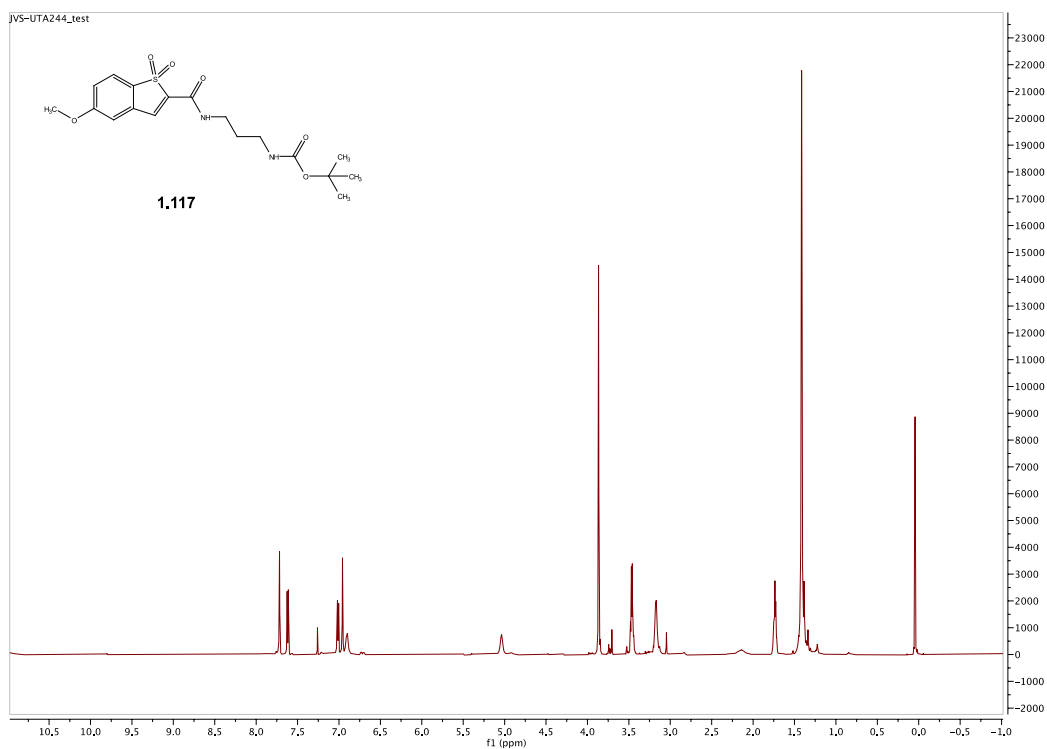
Spectra 1.115 ^{13}C NMR Spectrum of compound **1.115**



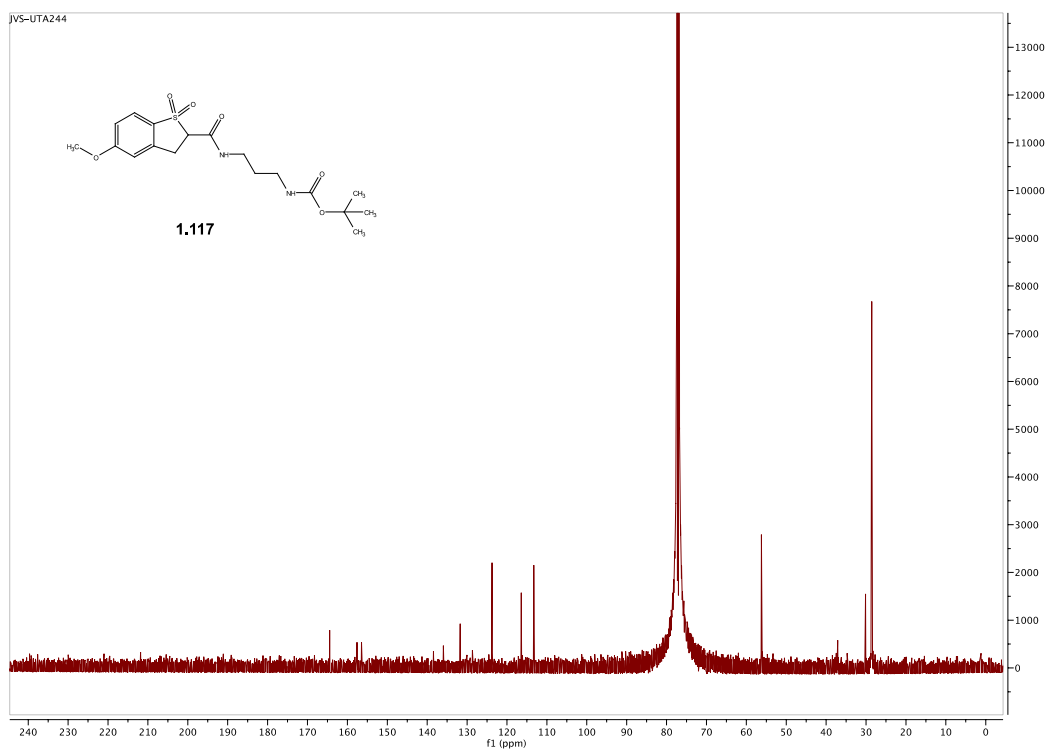
Spectra 1.116 ^1H NMR Spectrum of compound **1.116**



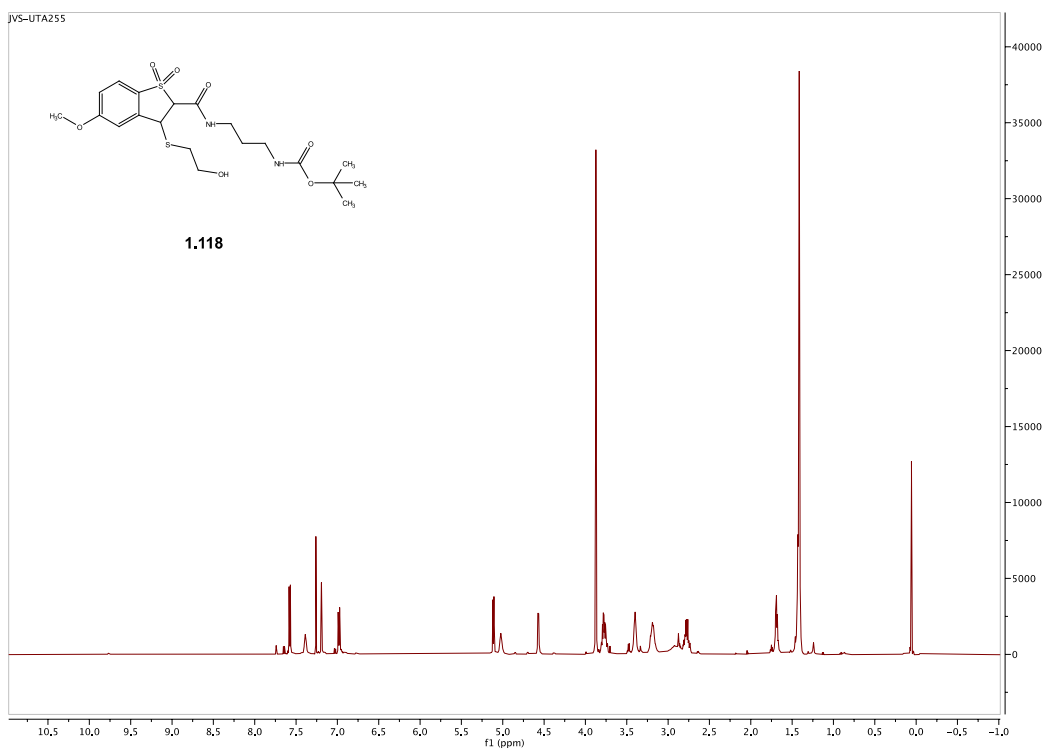
Spectra 1.117 ^{13}C NMR Spectrum of compound **1.116**



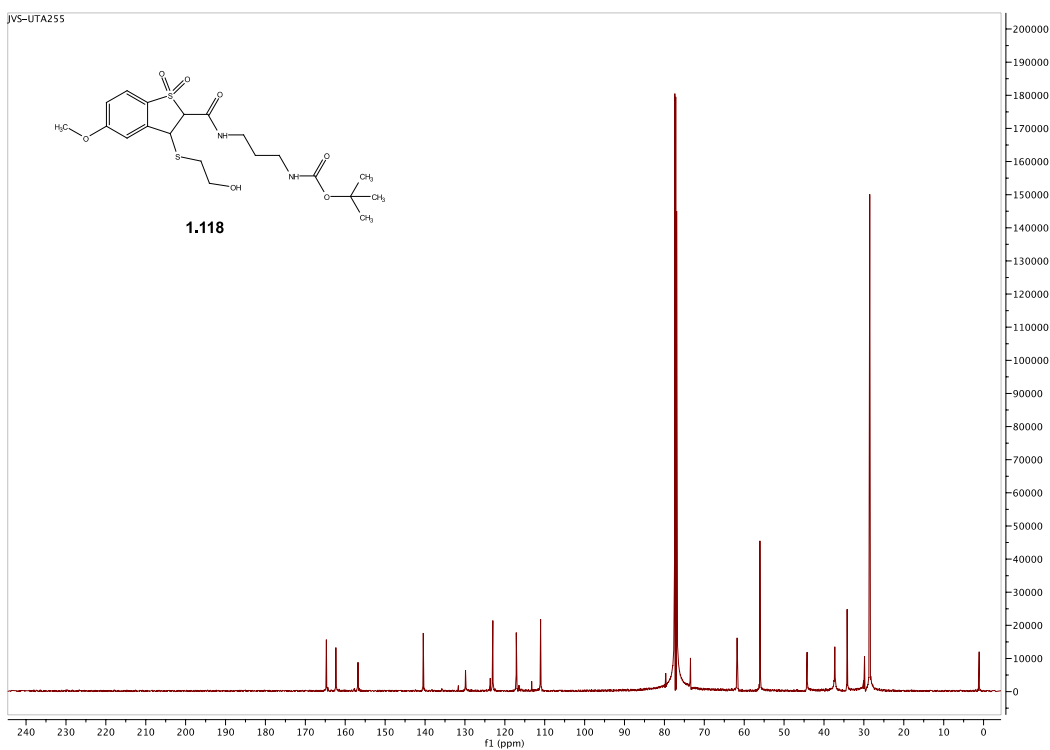
Spectra 1.118 ¹H NMR Spectrum of compound 1.117



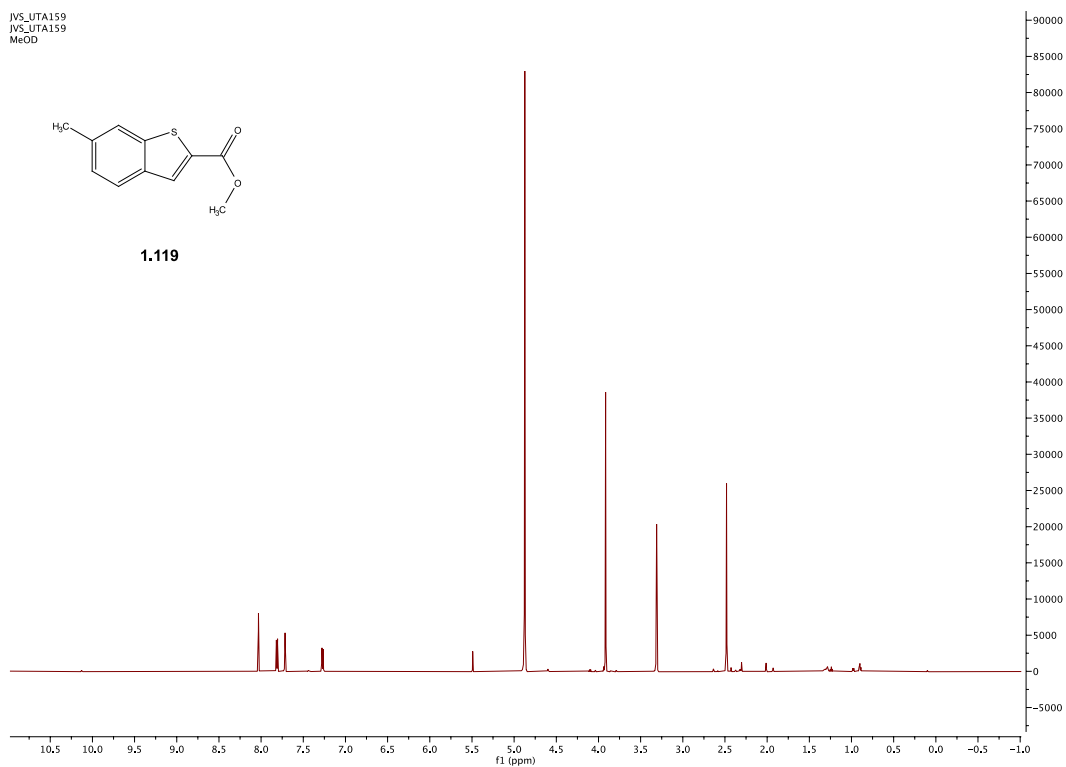
Spectra 1.119 ¹³C NMR Spectrum of compound 1.117



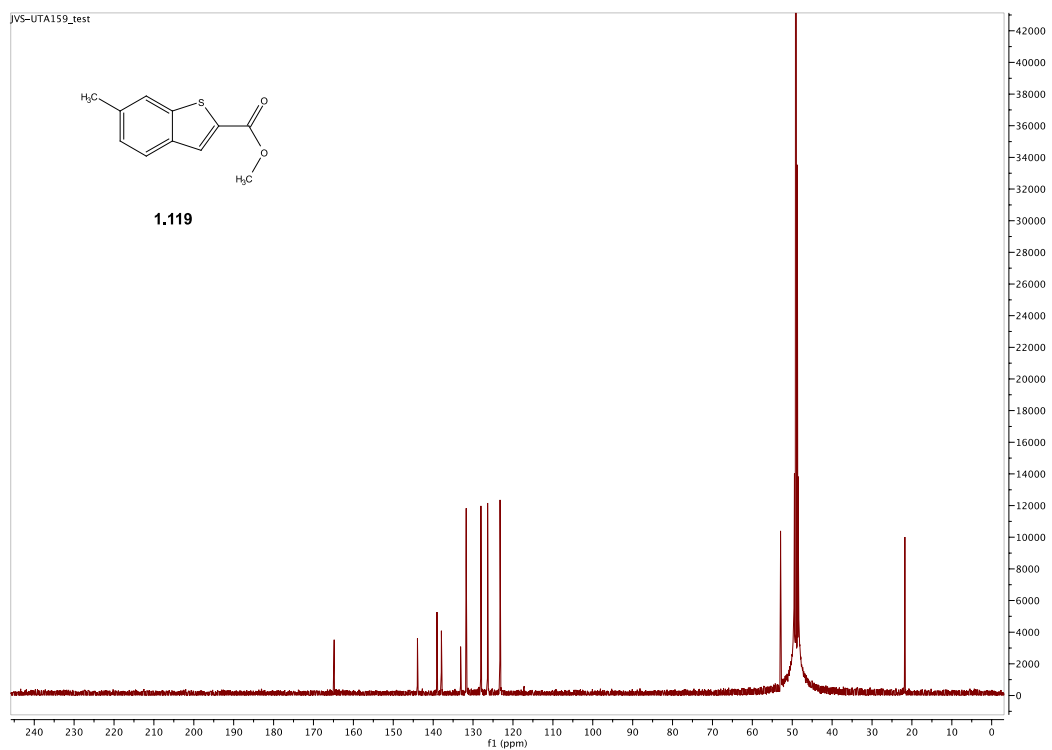
Spectra 1.120 ^1H NMR Spectrum of compound **1.118**



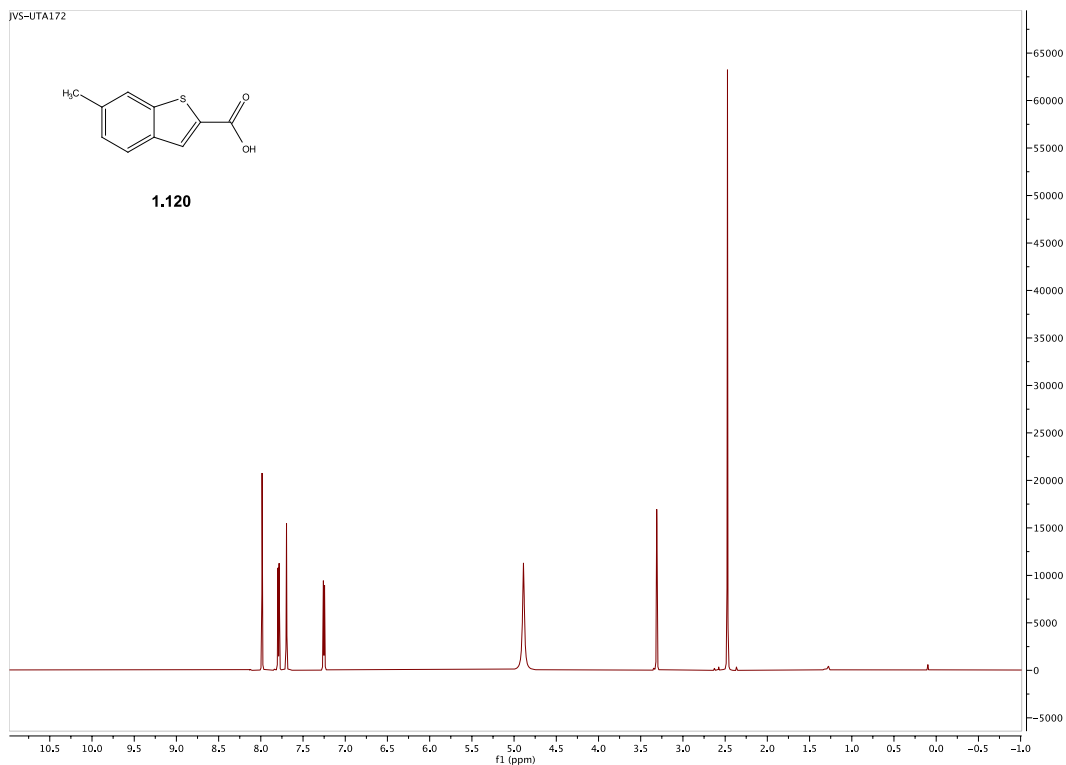
Spectra 1.121 ^{13}C NMR Spectrum of compound **1.118**



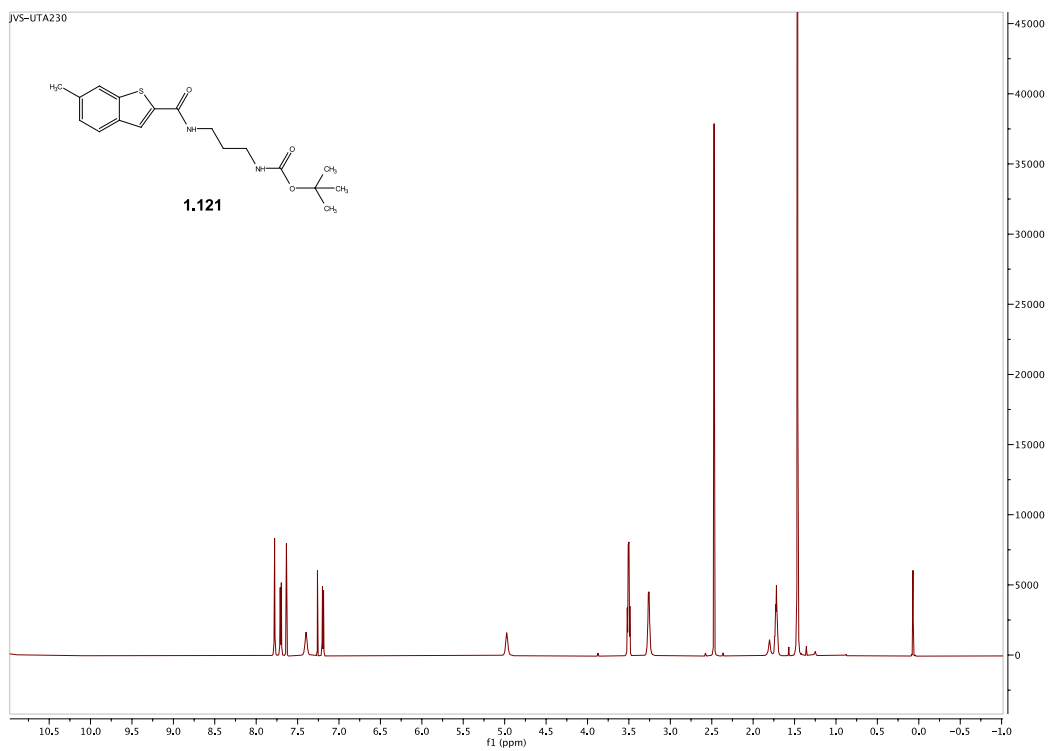
Spectra 1.122 ^1H NMR Spectrum of compound **1.119**



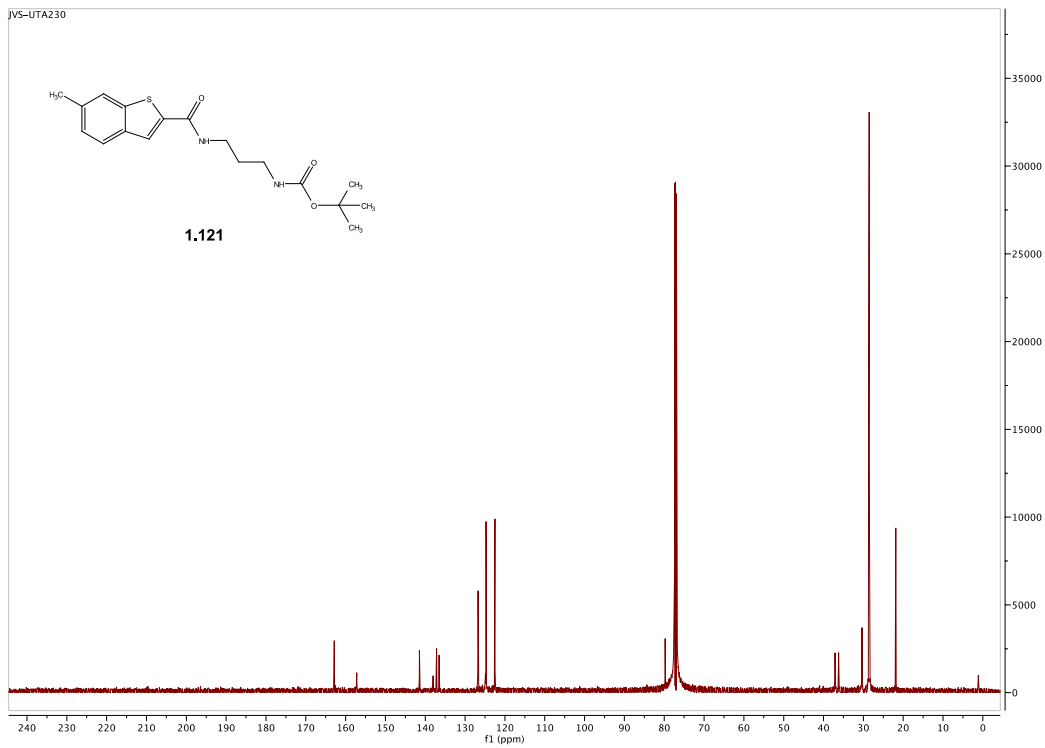
Spectra 1.123 ^{13}C NMR Spectrum of compound **1.119**



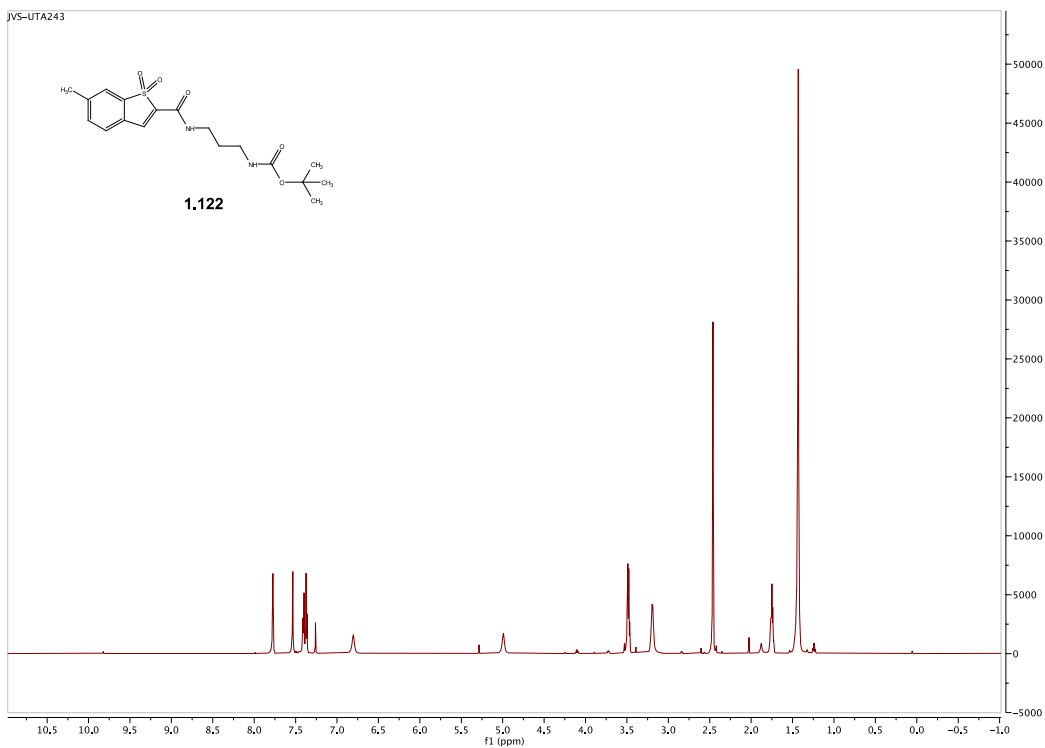
Spectra 1.124 ^1H NMR Spectrum of compound **1.120**



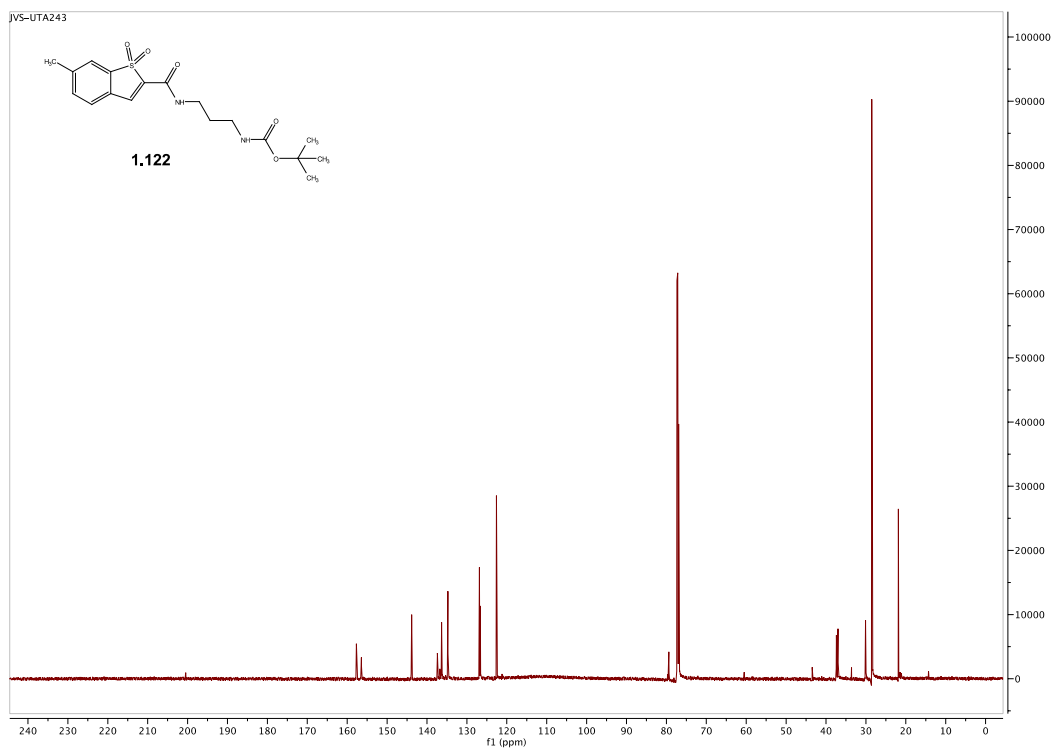
Spectra 1.125 ^1H NMR Spectrum of compound **1.121**



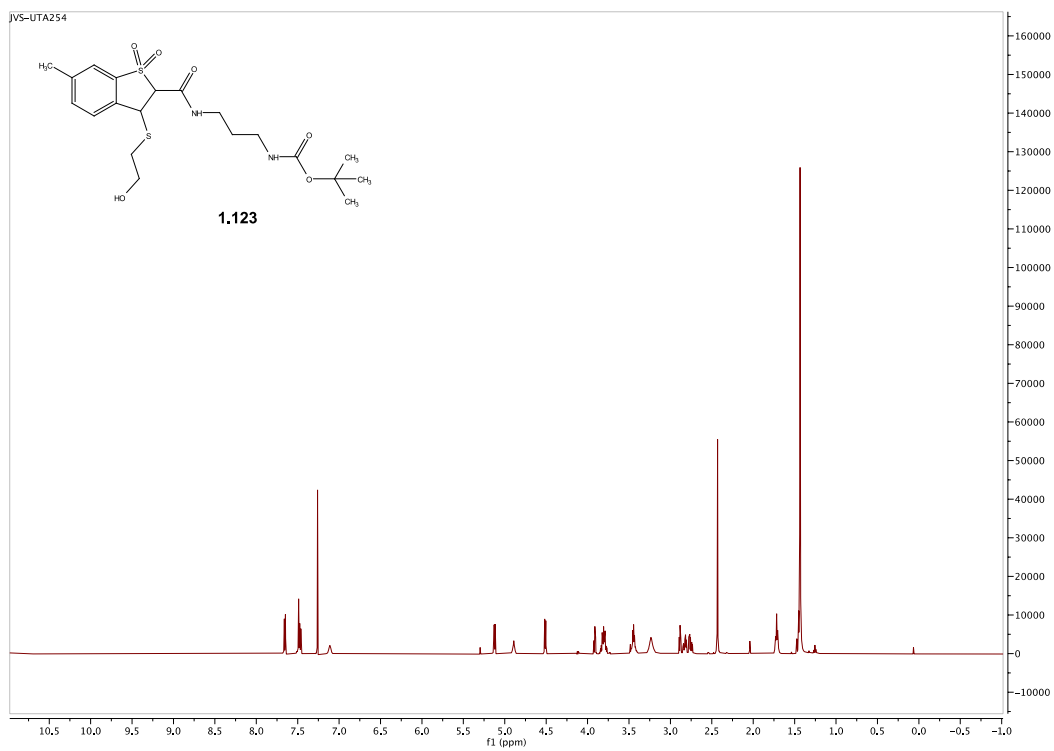
Spectra 1.126 ^{13}C NMR Spectrum of compound **1.121**



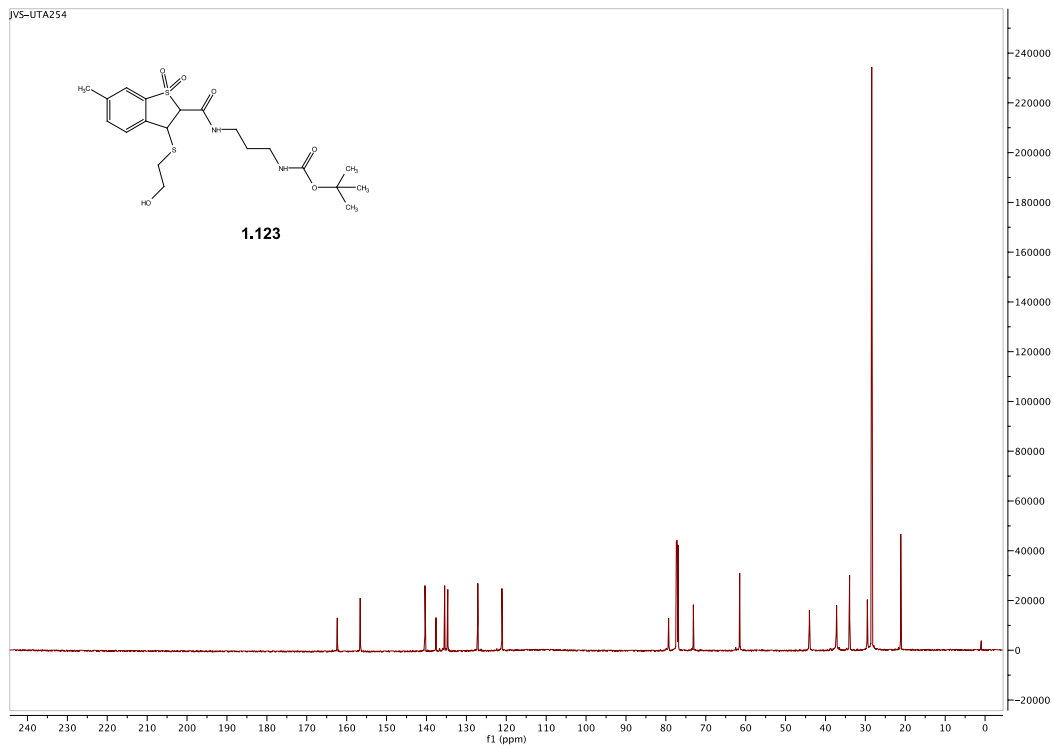
Spectra 1.127 ^1H NMR Spectrum of compound **1.122**



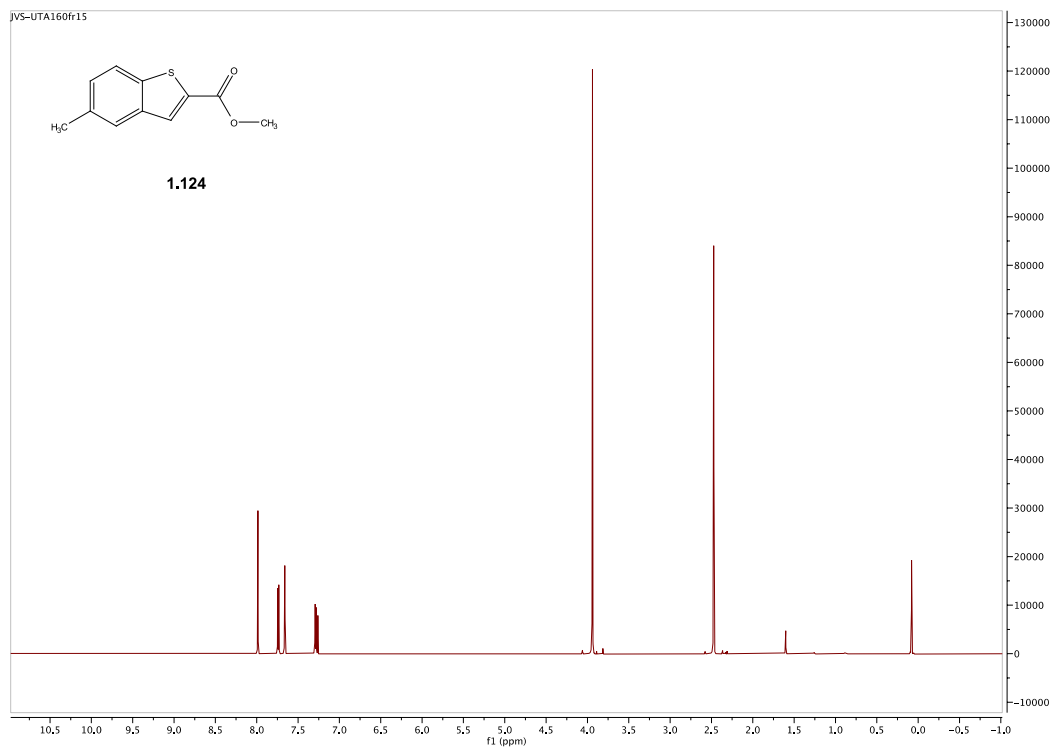
Spectra 1.128 ^{13}C NMR Spectrum of compound **1.122**



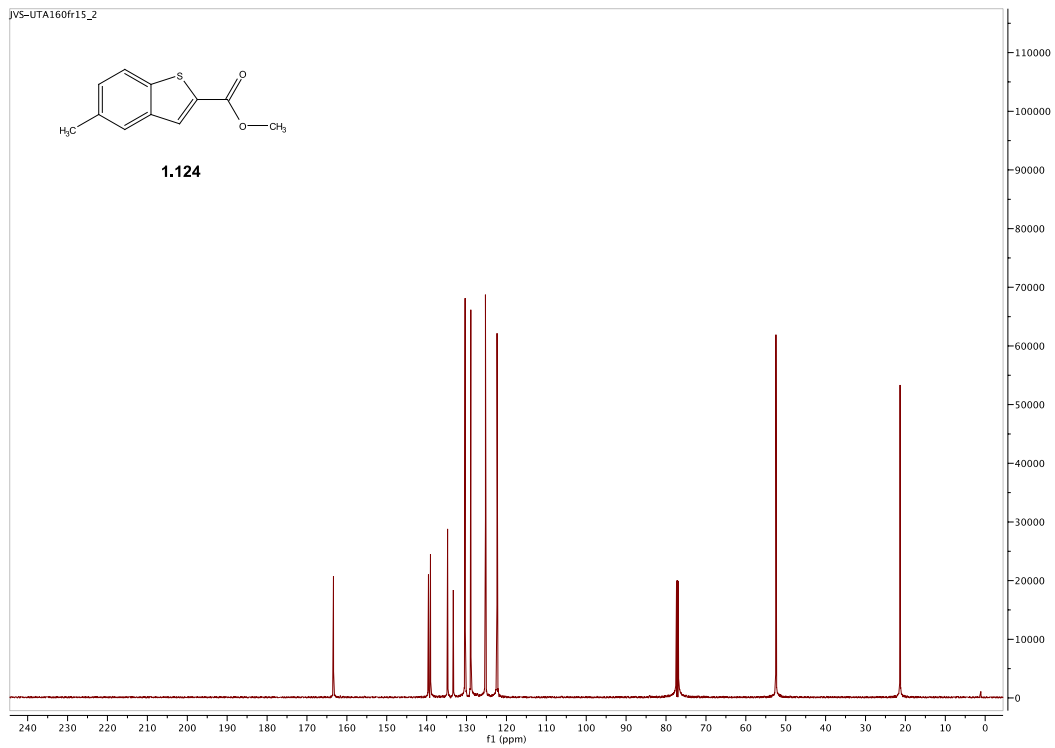
Spectra 1.129 ^1H NMR Spectrum of compound **1.123**



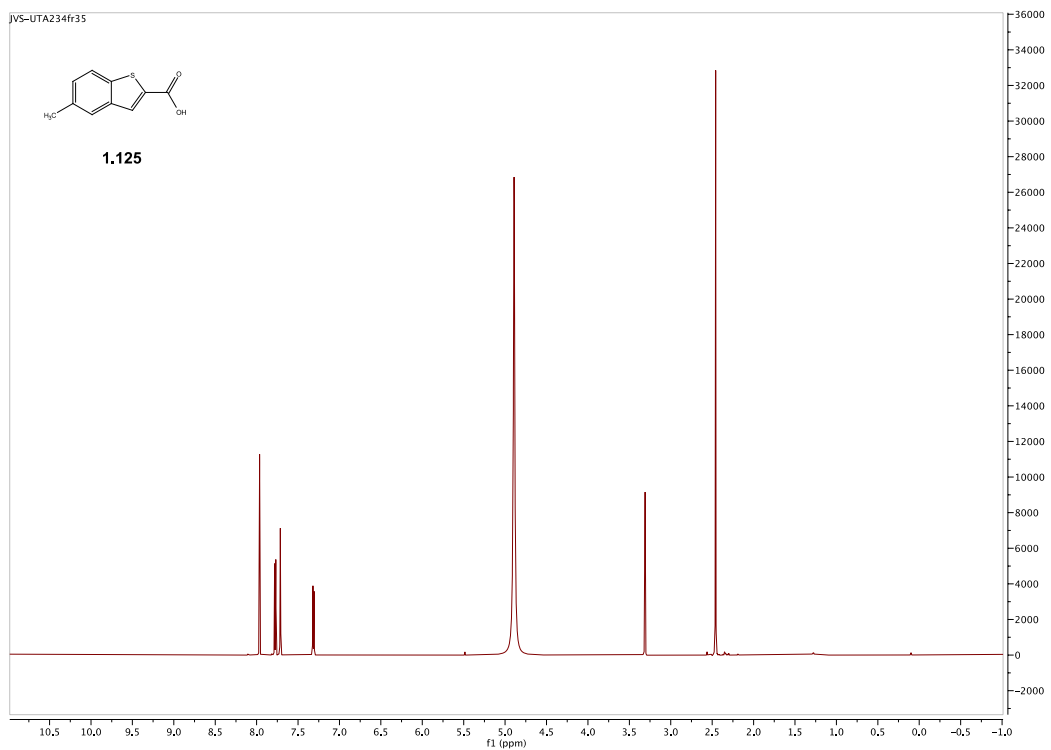
Spectra 1.130 ¹³C NMR Spectrum of compound 1.123



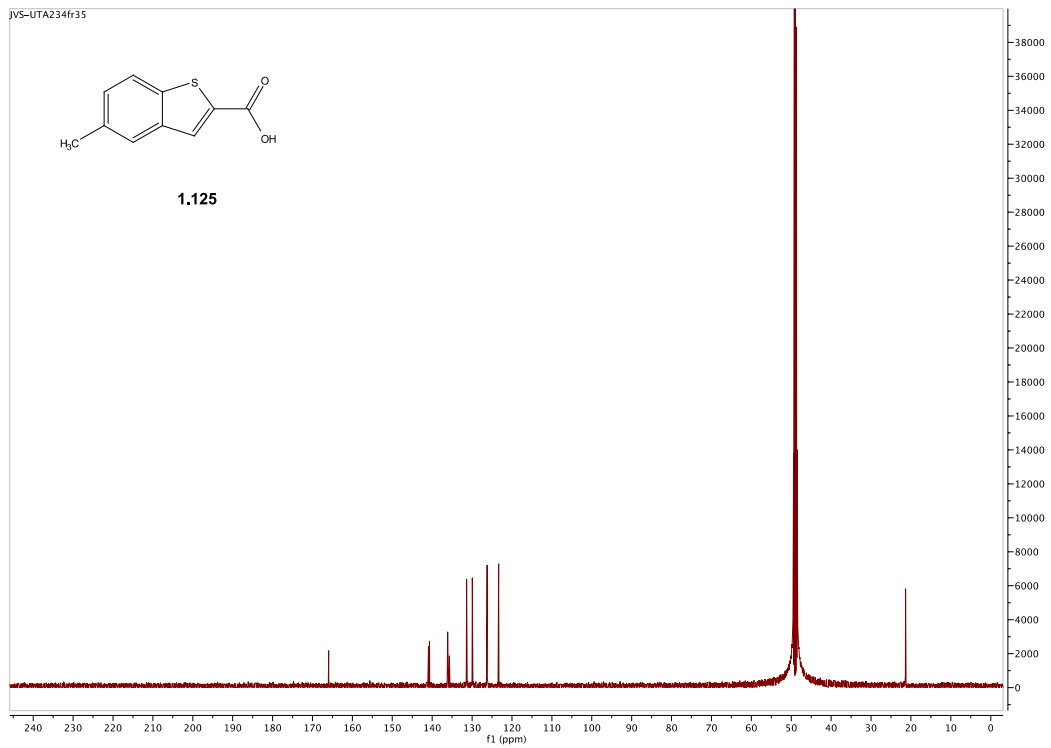
Spectra 1.131 ¹H NMR Spectrum of compound 1.124



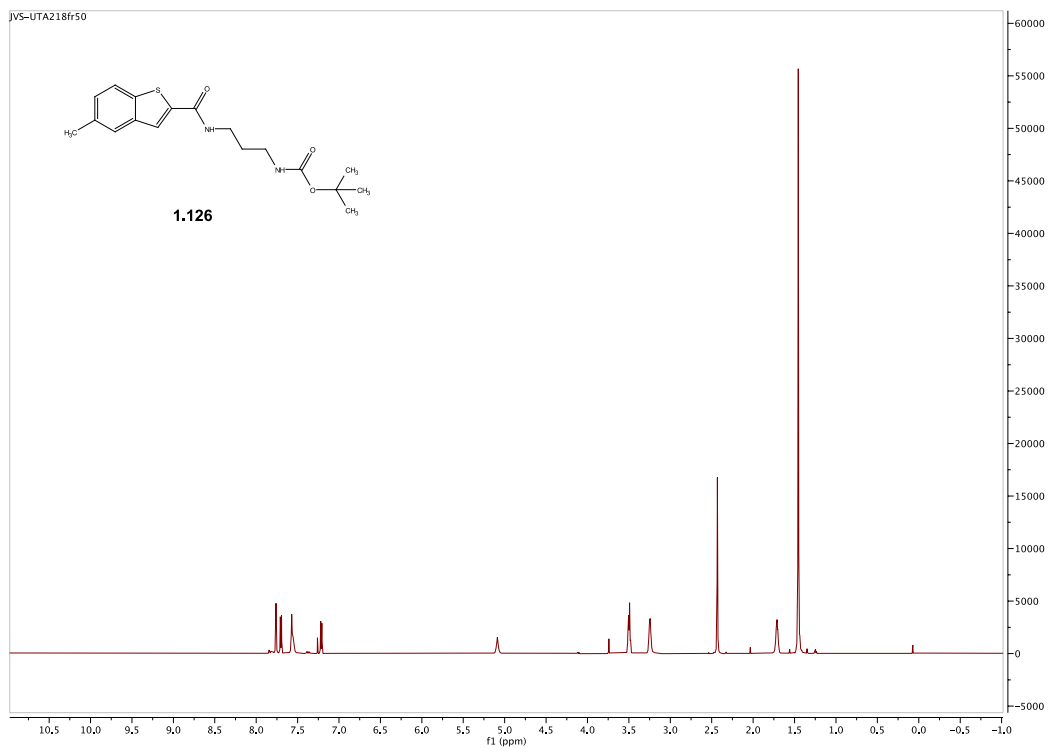
Spectra 1.132 ^{13}C NMR Spectrum of compound **1.124**



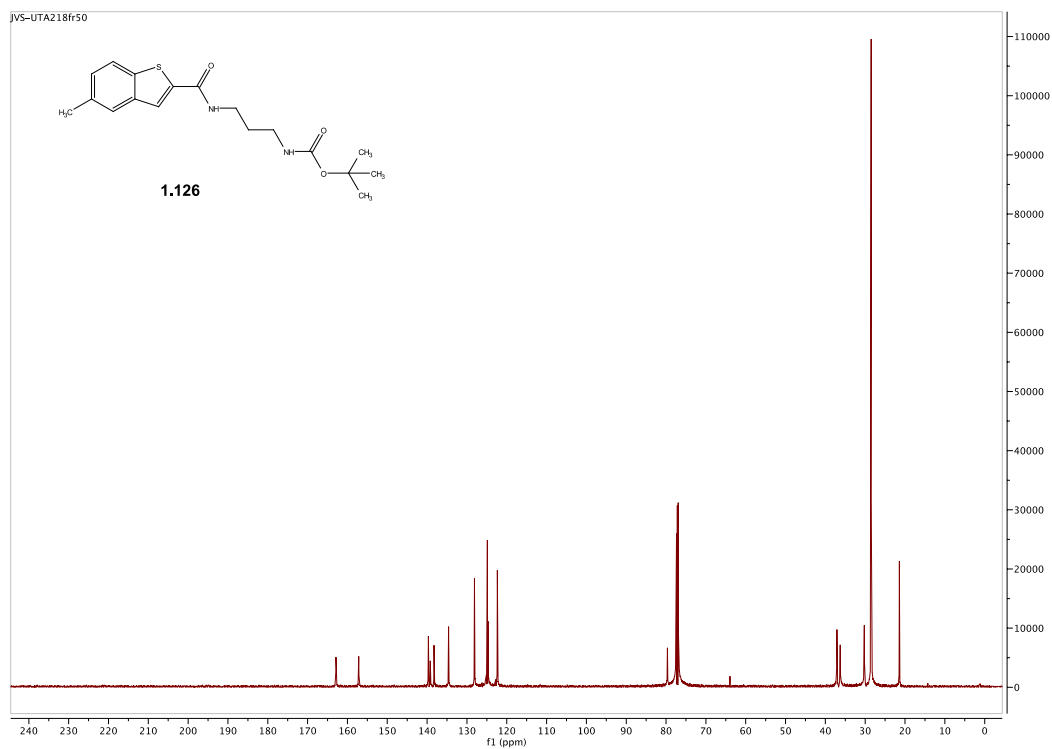
Spectra 1.133 ^1H NMR Spectrum of compound **1.125**



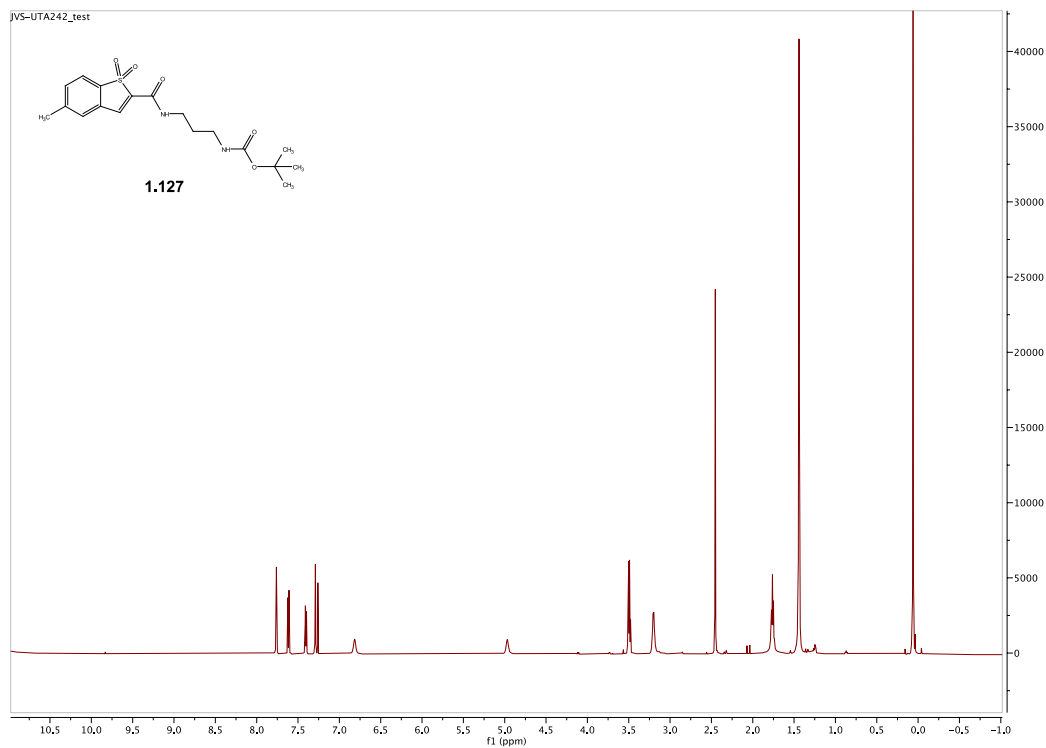
Spectra 1.134 ^{13}C NMR Spectrum of compound **1.125**



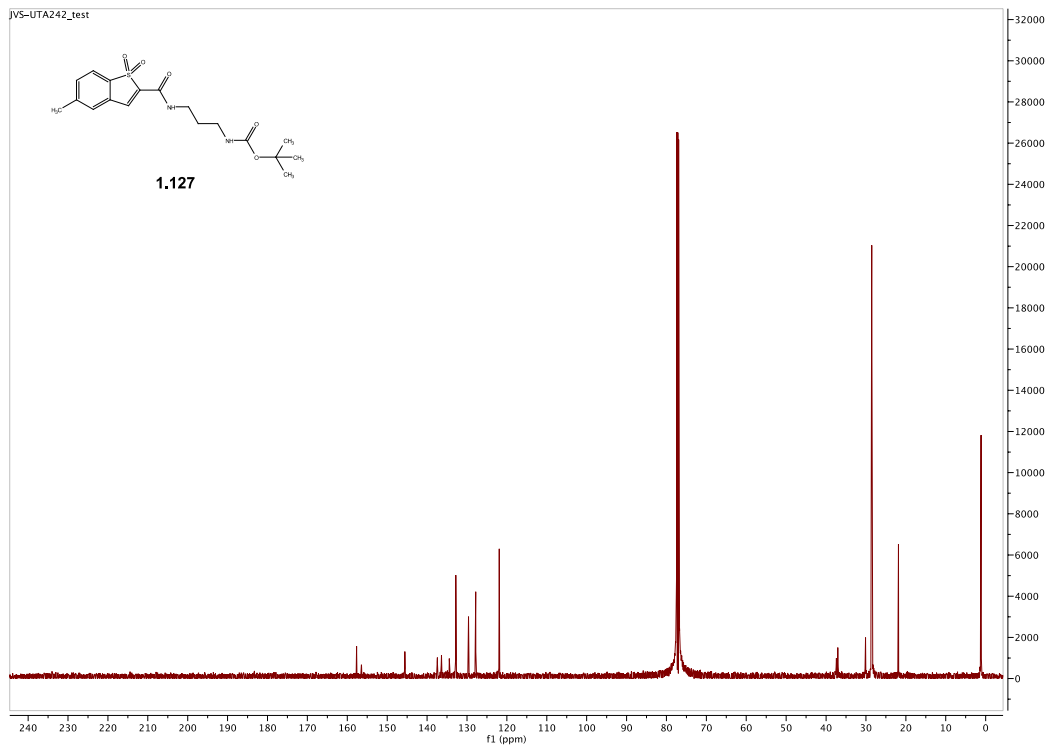
Spectra 1.135 ^1H NMR Spectrum of compound **1.126**



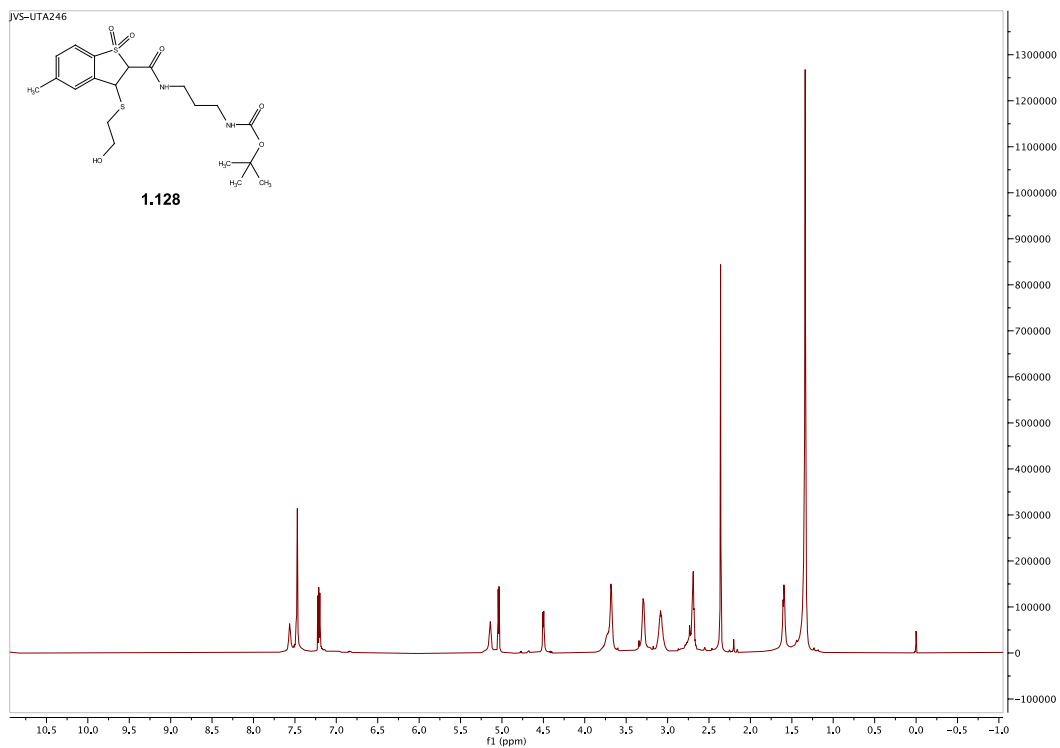
Spectra 1.136 ^{13}C NMR Spectrum of compound **1.126**



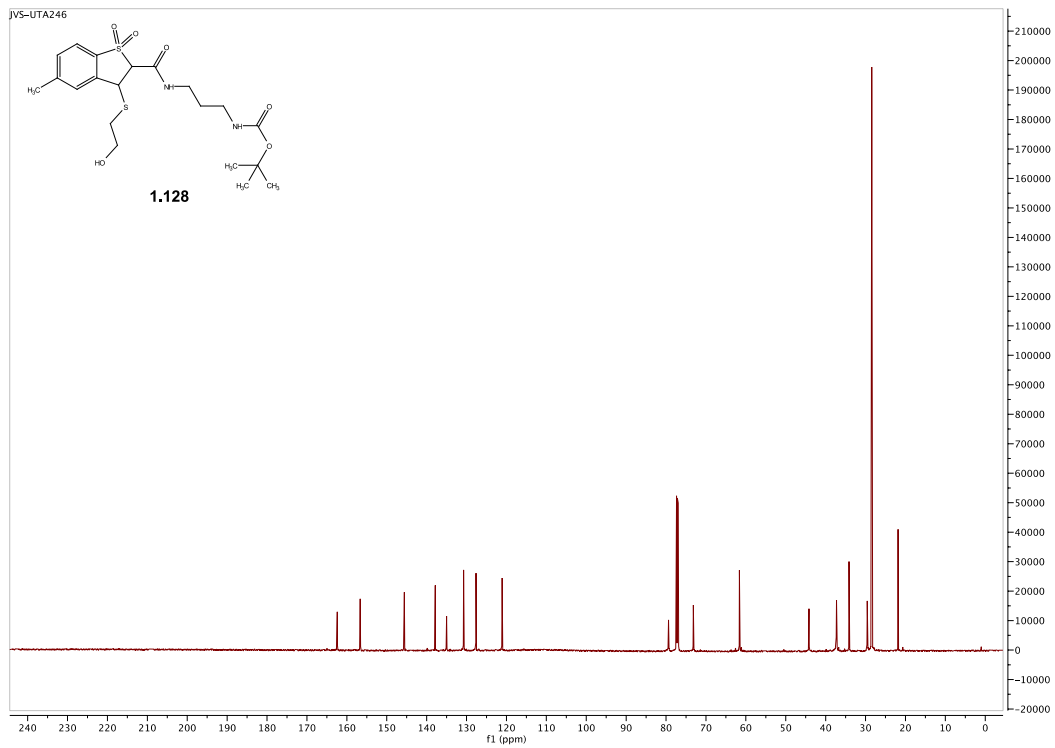
Spectra 1.137 ^1H NMR Spectrum of compound **1.127**



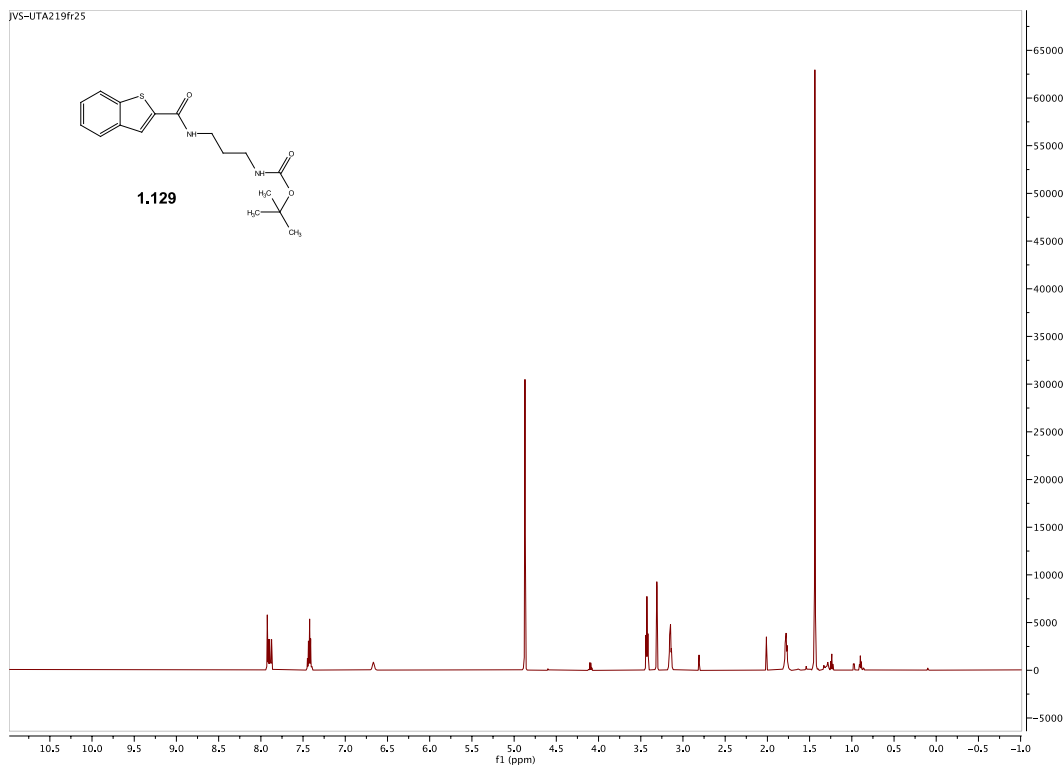
Spectra 1.138 ^{13}C NMR Spectrum of compound **1.127**



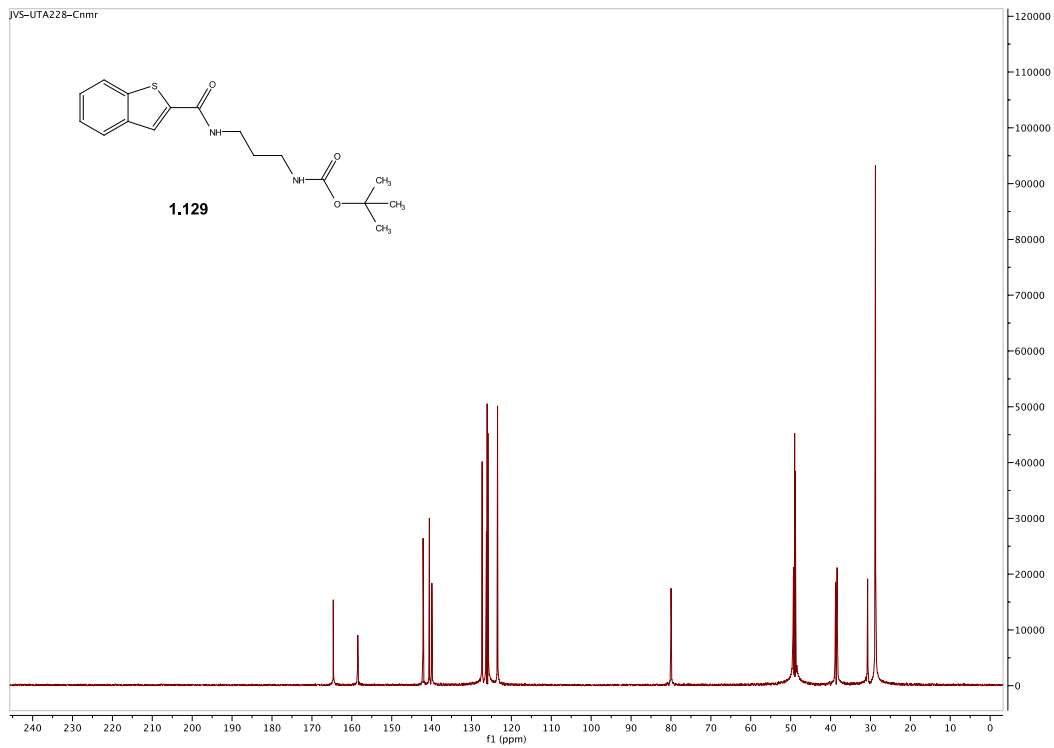
Spectra 1.139 ^1H NMR Spectrum of compound **1.128**



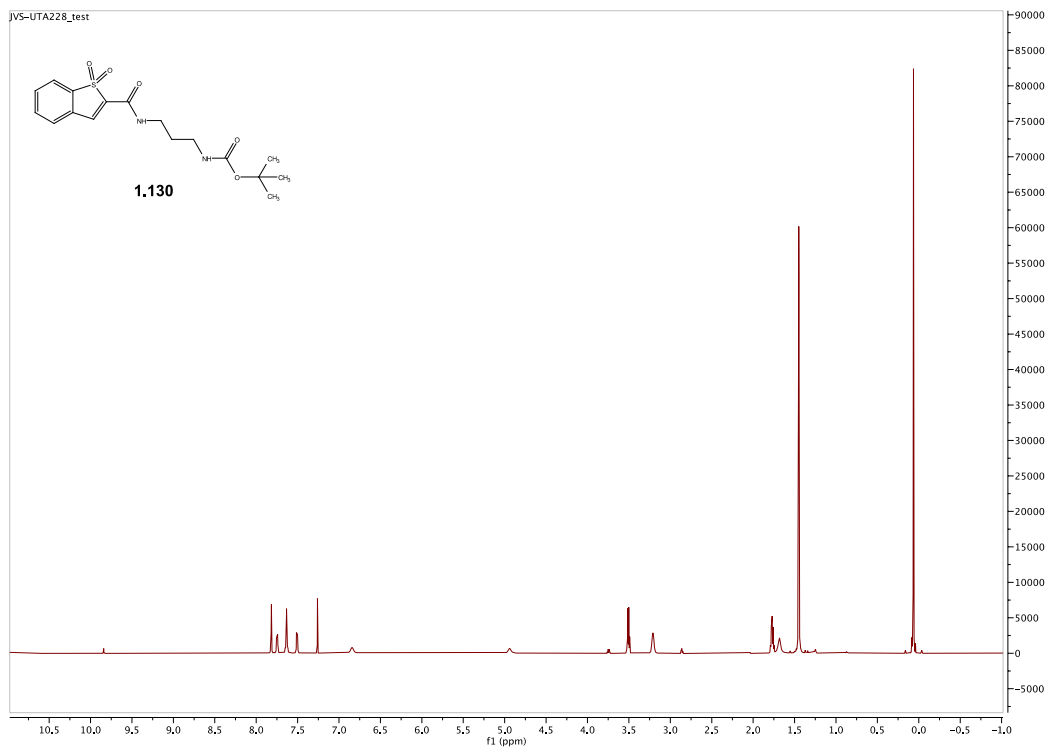
Spectra 1.140 ^{13}C NMR Spectrum of compound **1.128**



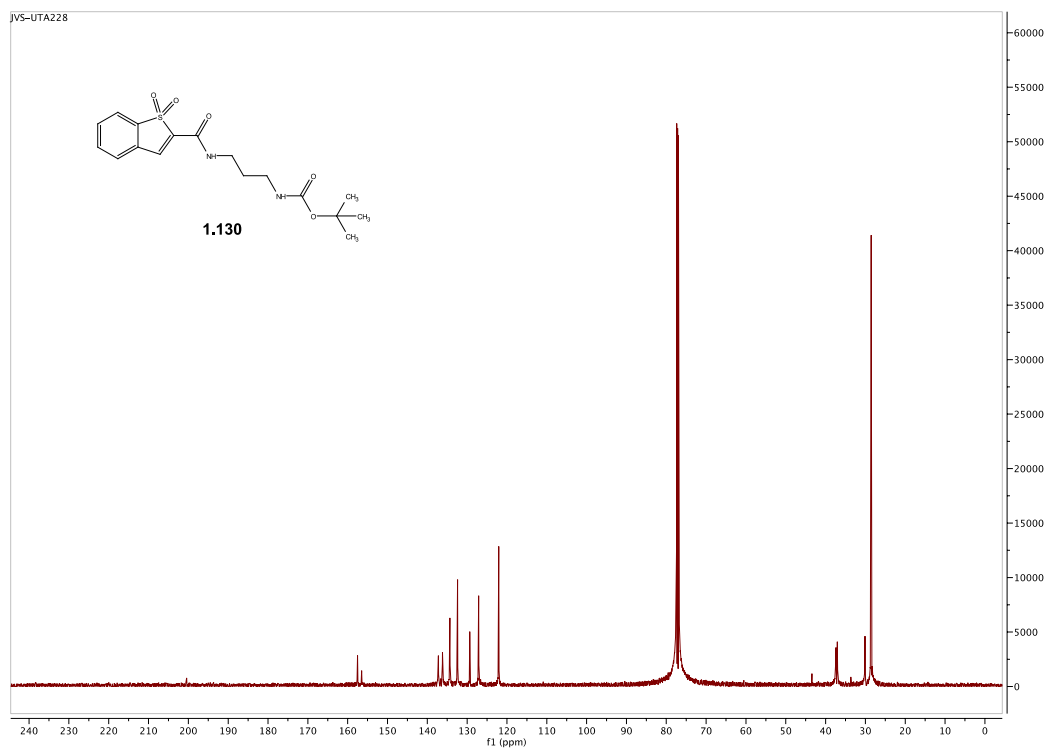
Spectra 1.141 ^1H NMR Spectrum of compound **1.129**



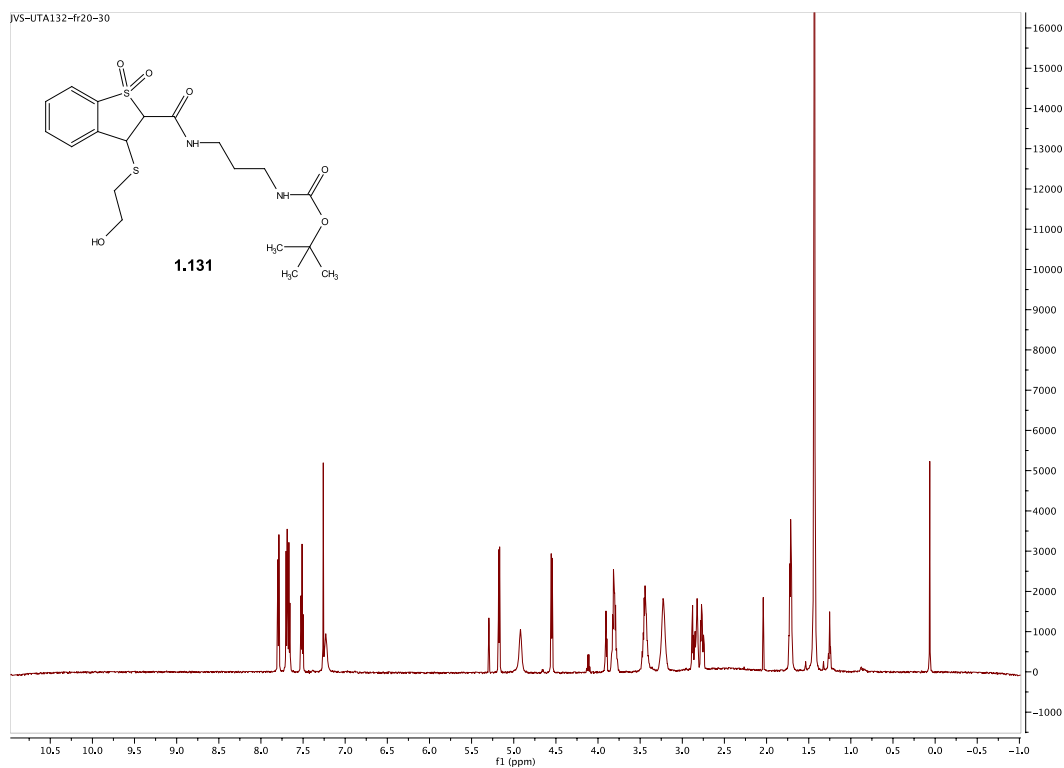
Spectra 1.142 ^{13}C NMR Spectrum of compound **1.129**



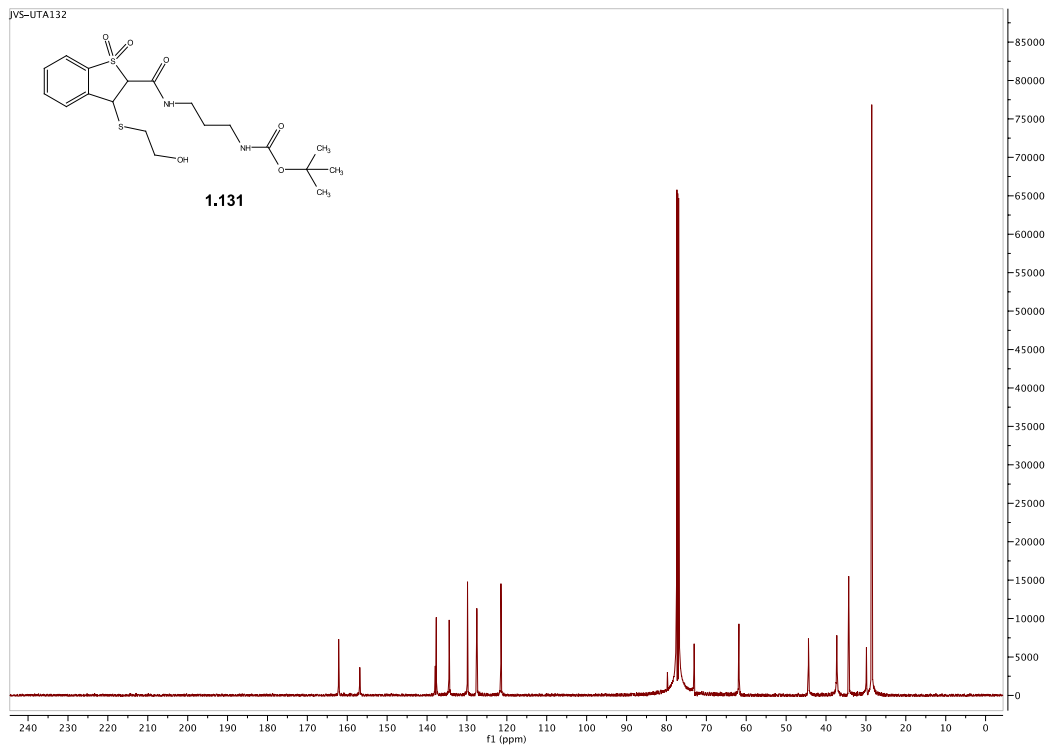
Spectra 1.143 ^1H NMR Spectrum of compound **1.130**



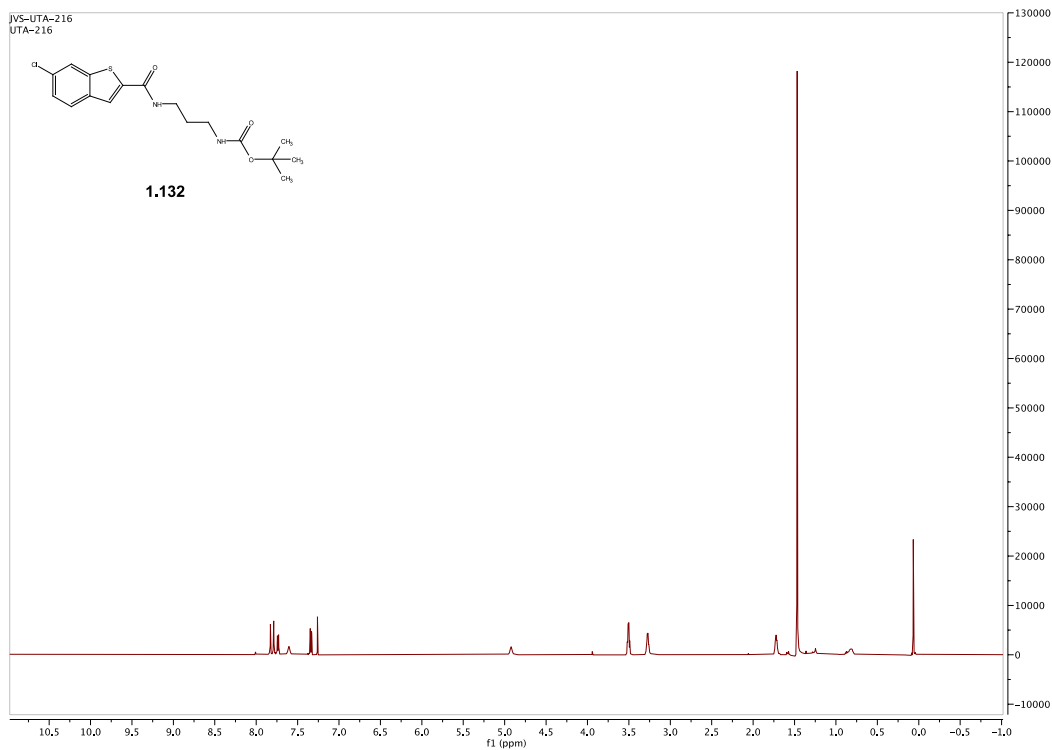
Spectra 1.144 ^{13}C NMR Spectrum of compound **1.130**



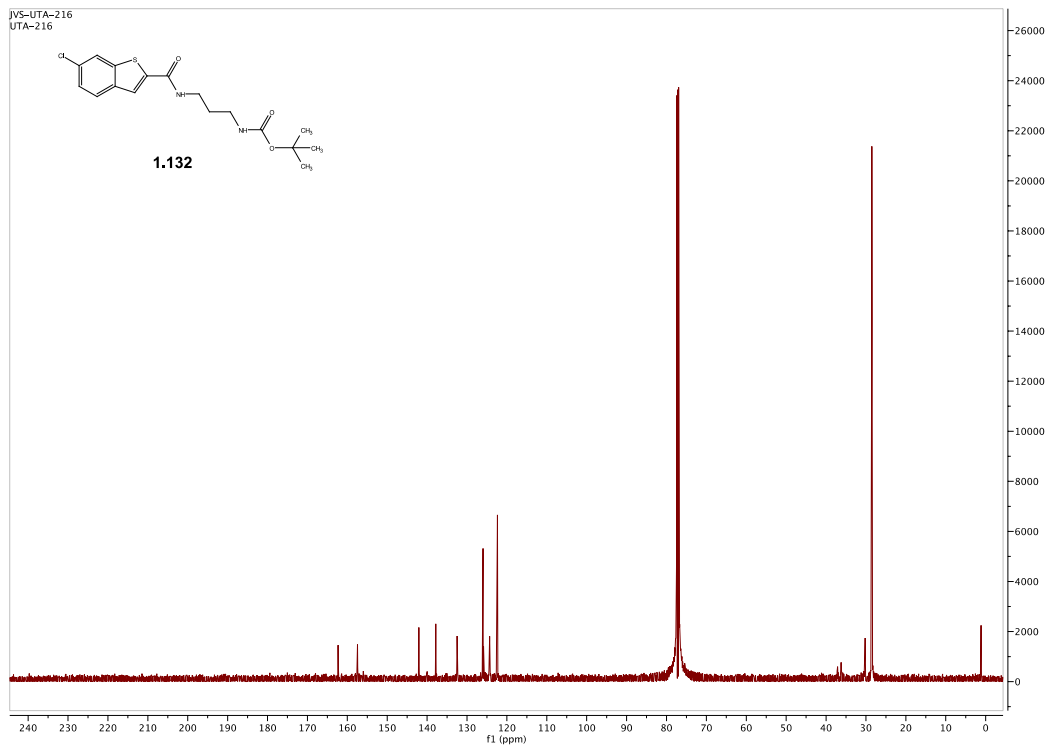
Spectra 1.145 ^1H NMR Spectrum of compound **1.131**



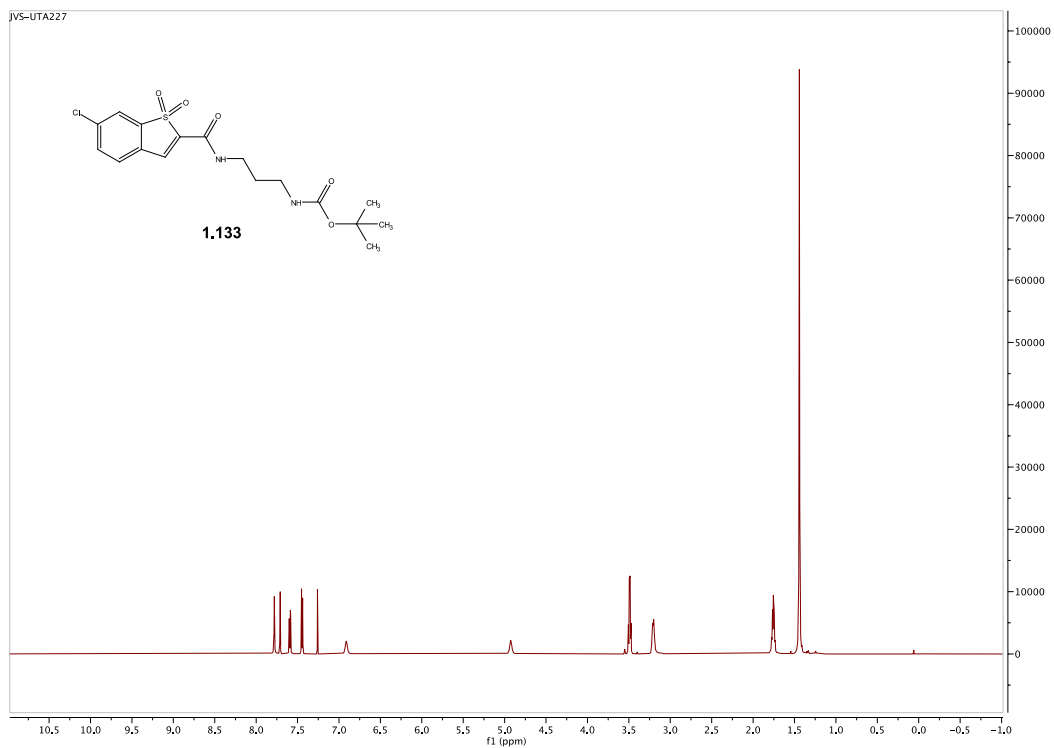
Spectra 1.146 ^{13}C NMR Spectrum of compound **1.131**



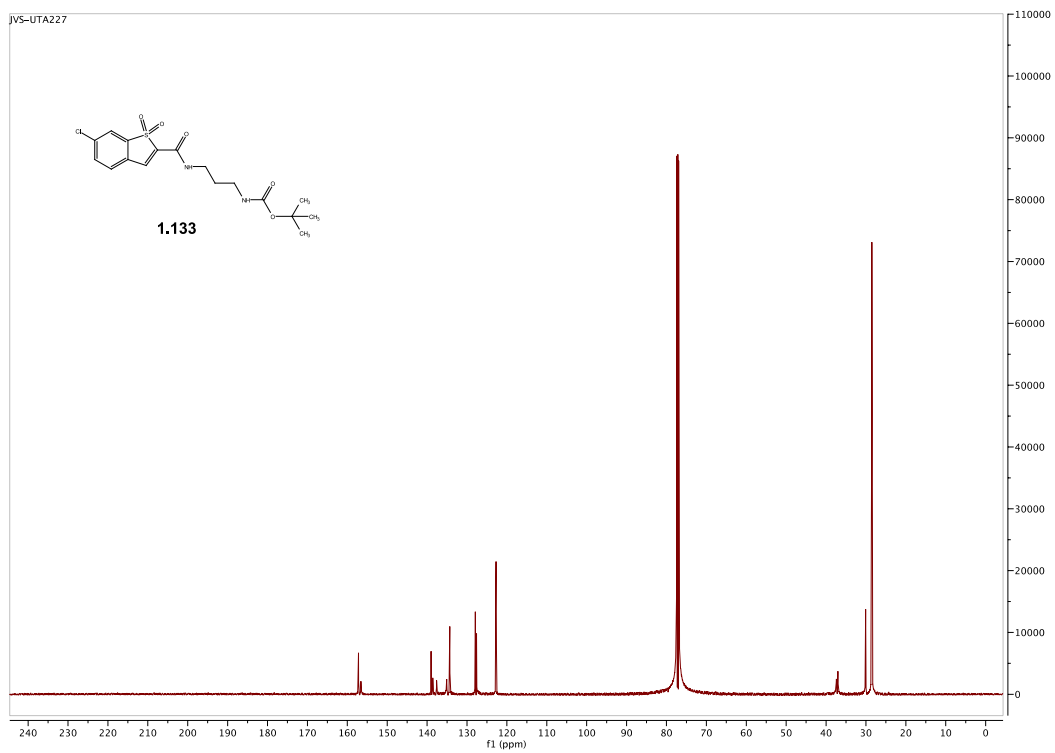
Spectra 1.147 ^1H NMR Spectrum of compound **1.132**



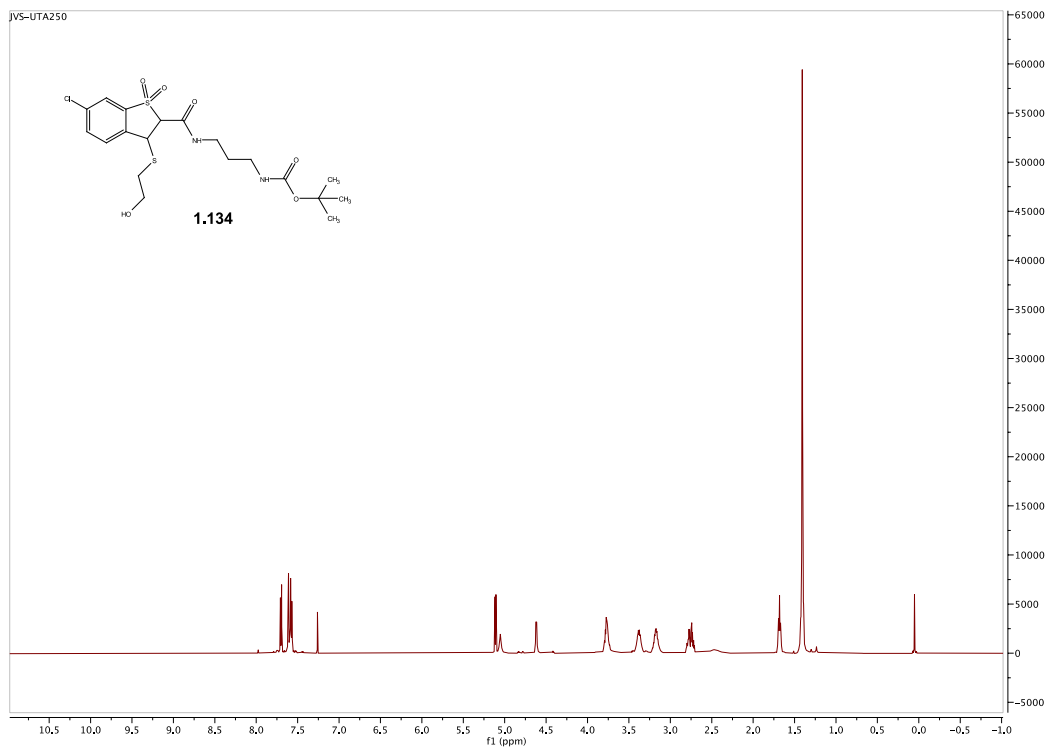
Spectra 1.148 ^{13}C NMR Spectrum of compound **1.132**



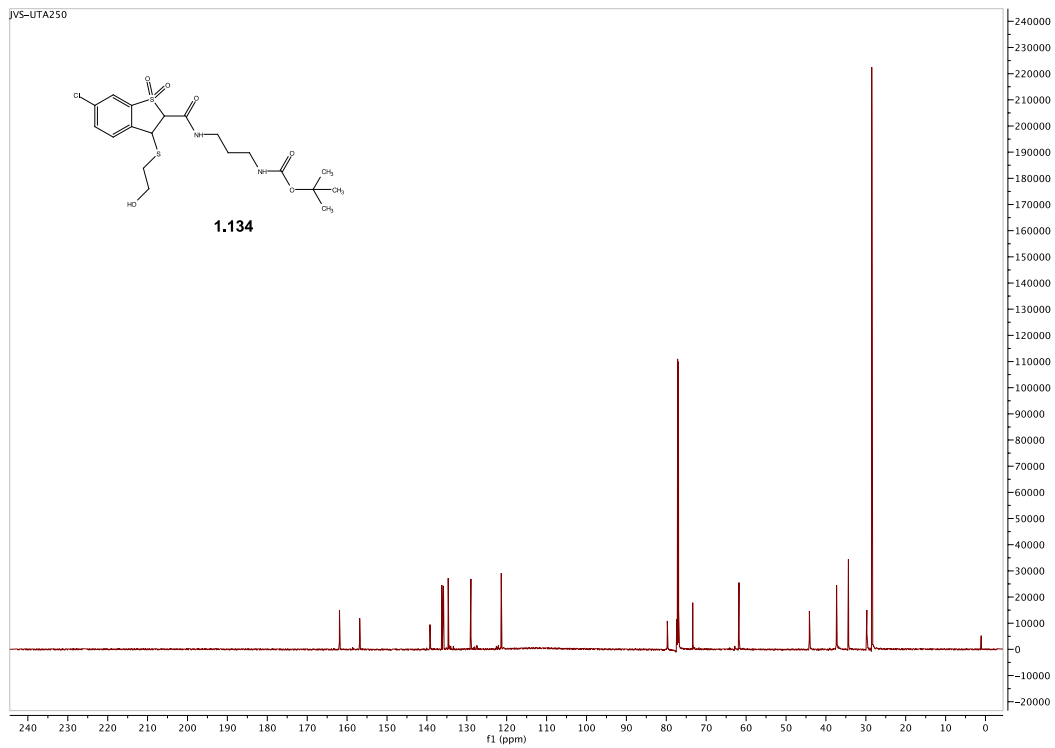
Spectra 1.149 ^1H NMR Spectrum of compound **1.133**



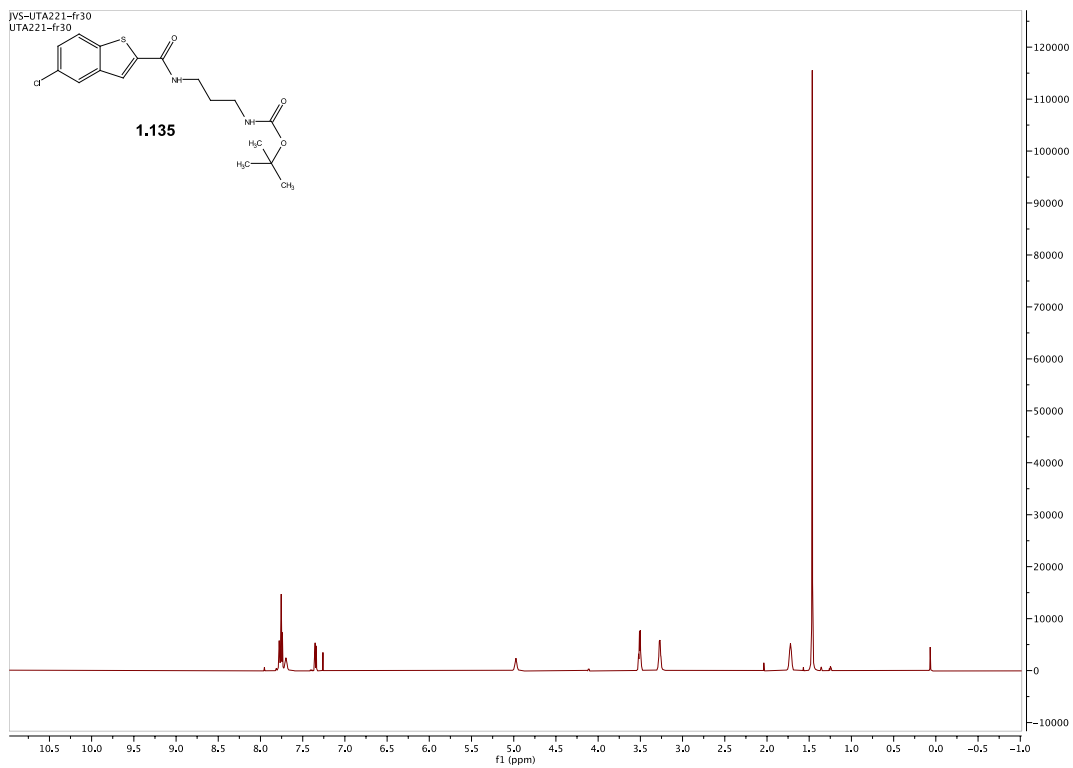
Spectra 1.150 ^{13}C NMR Spectrum of compound **1.133**



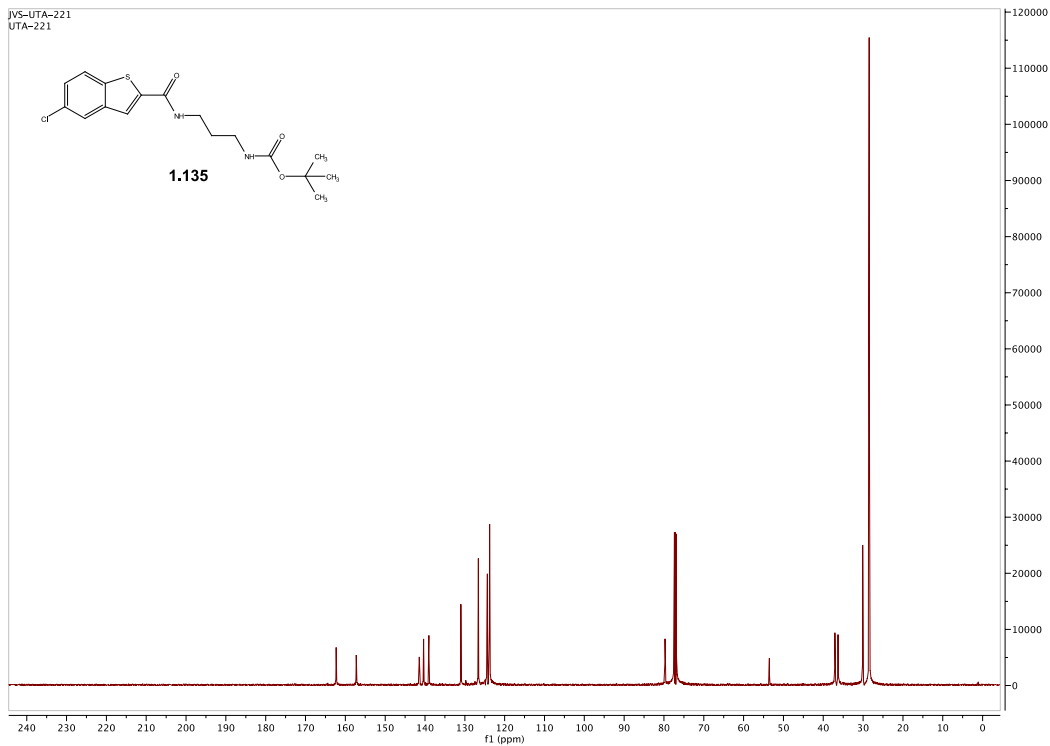
Spectra 1.151 ^1H NMR Spectrum of compound **1.134**



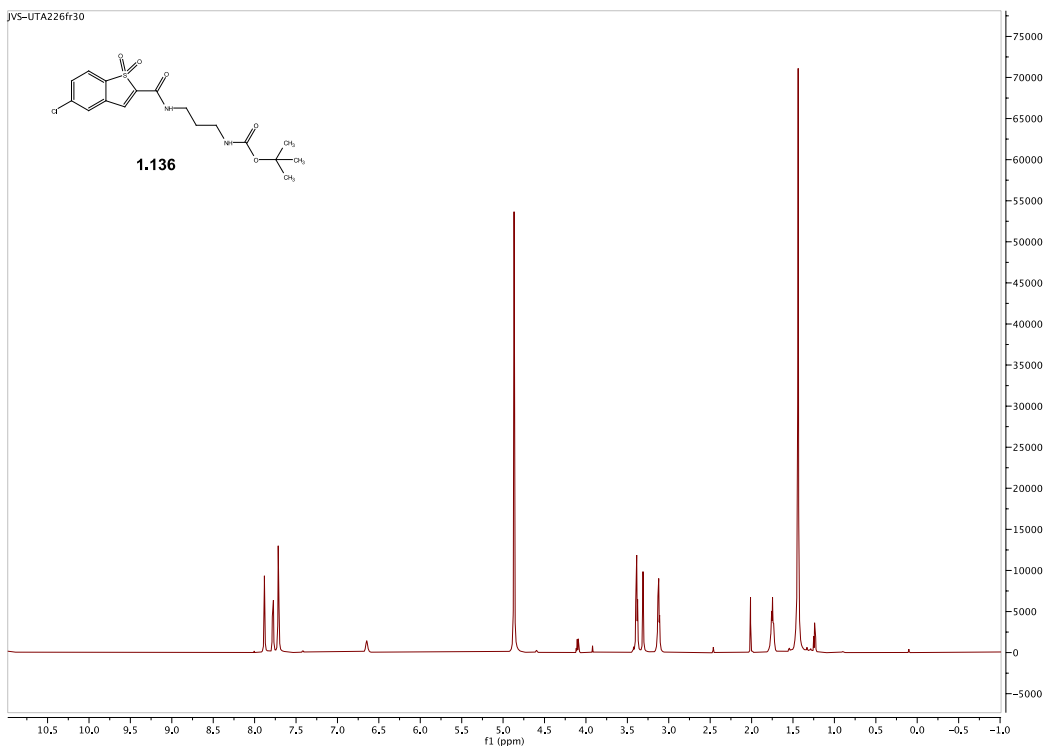
Spectra 1.152 ^{13}C NMR Spectrum of compound **1.134**



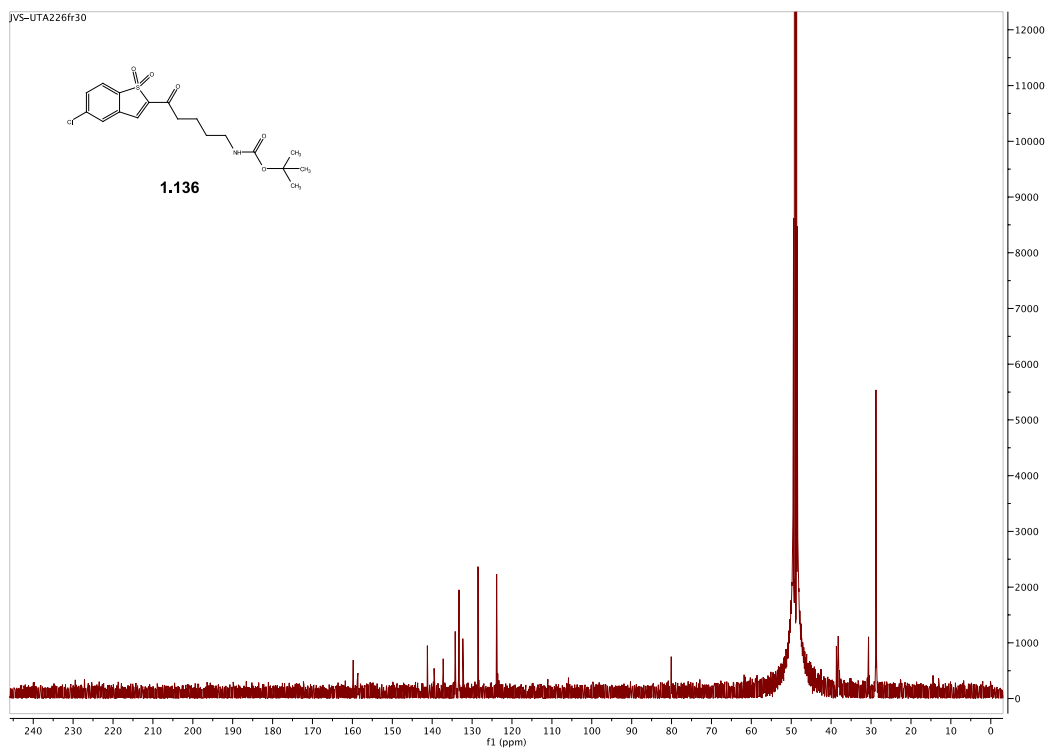
Spectra 1.153 ^1H NMR Spectrum of compound **1.135**



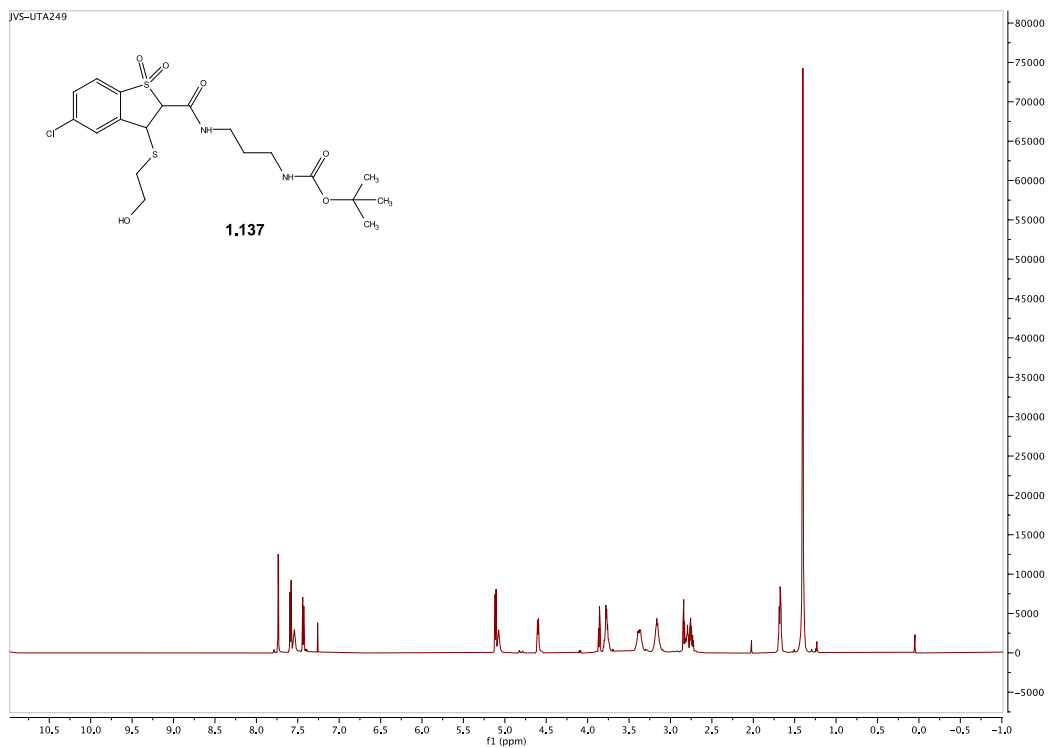
Spectra 1.154 ^{13}C NMR Spectrum of compound **1.135**



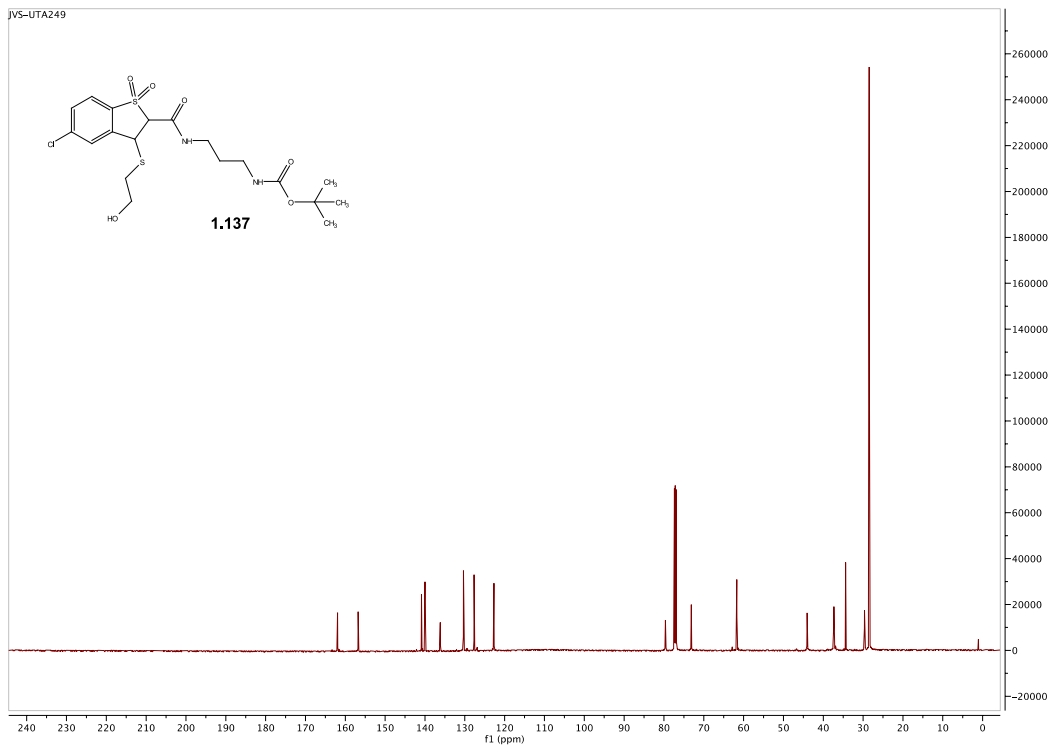
Spectra 1.155 ^1H NMR Spectrum of compound **1.136**



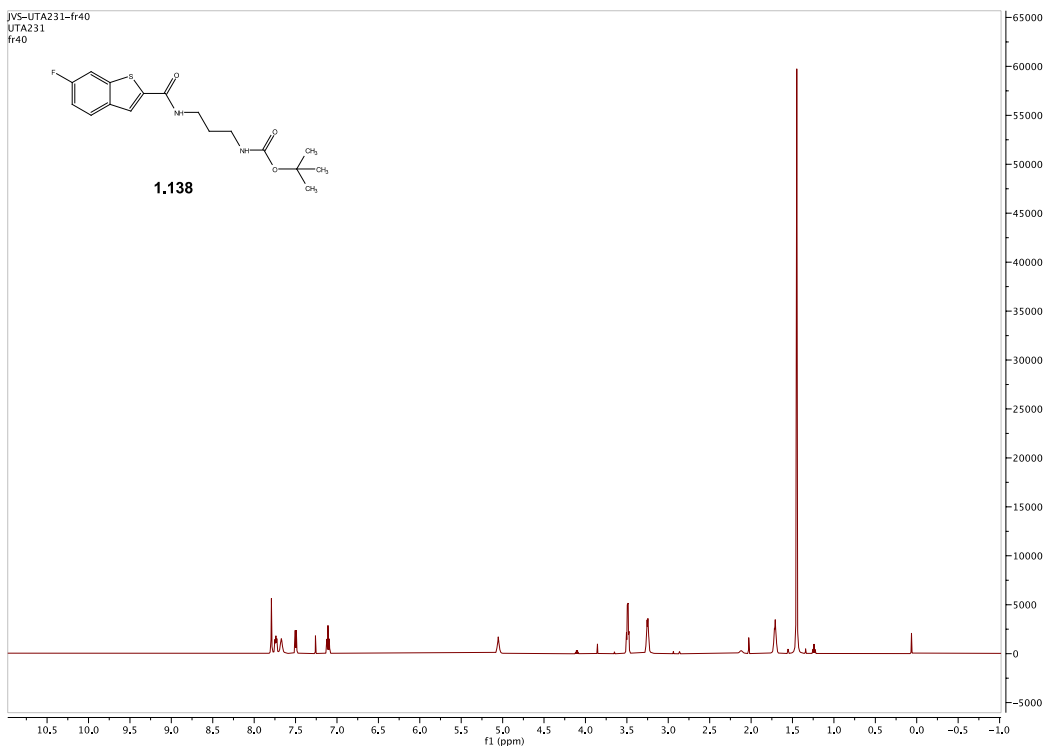
Spectra 1.156 ^{13}C NMR Spectrum of compound **1.136**



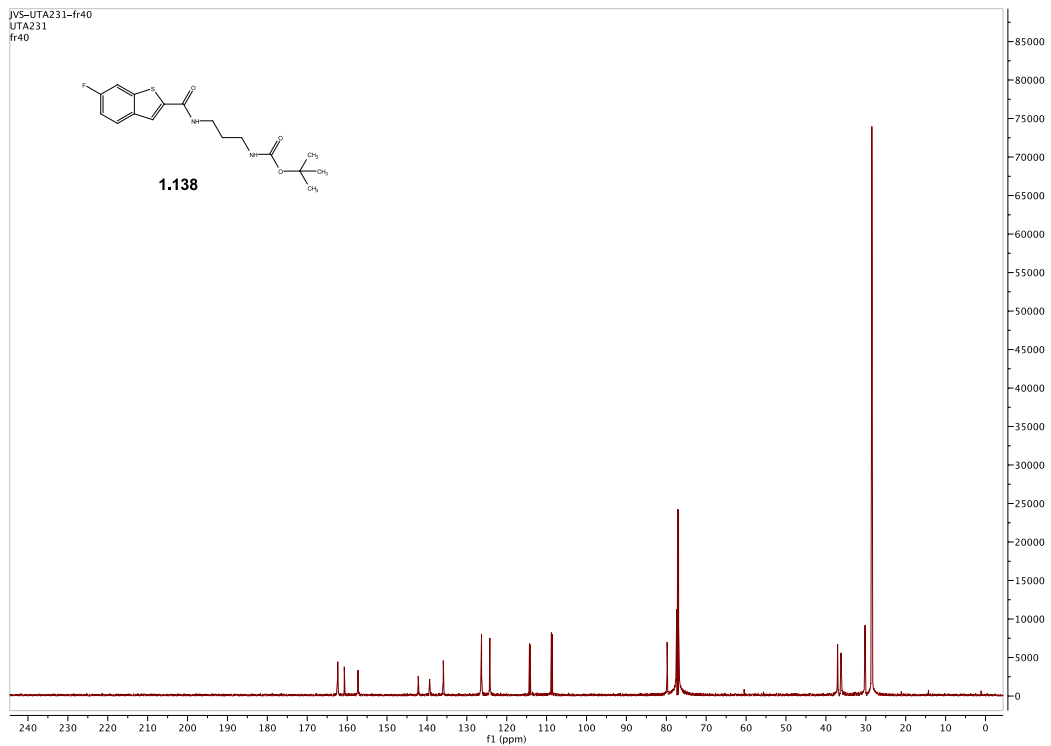
Spectra 1.157 ^1H NMR Spectrum of compound **1.137**



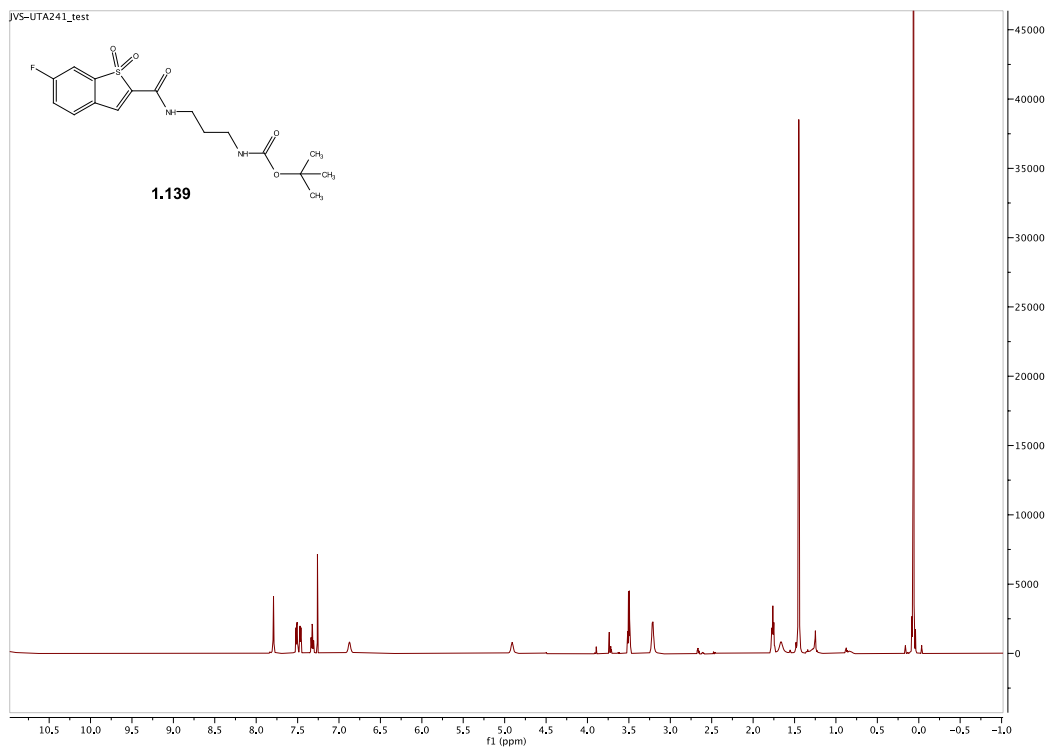
Spectra 1.158 ^{13}C NMR Spectrum of compound **1.137**



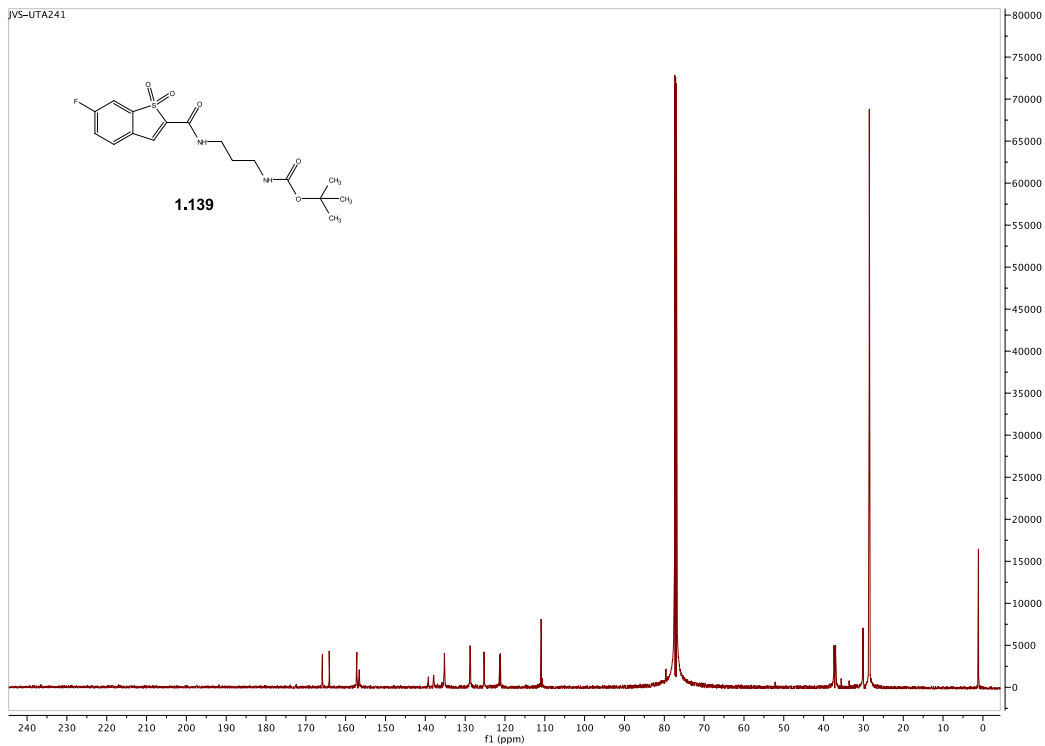
Spectra 1.159 ^1H NMR Spectrum of compound **1.138**



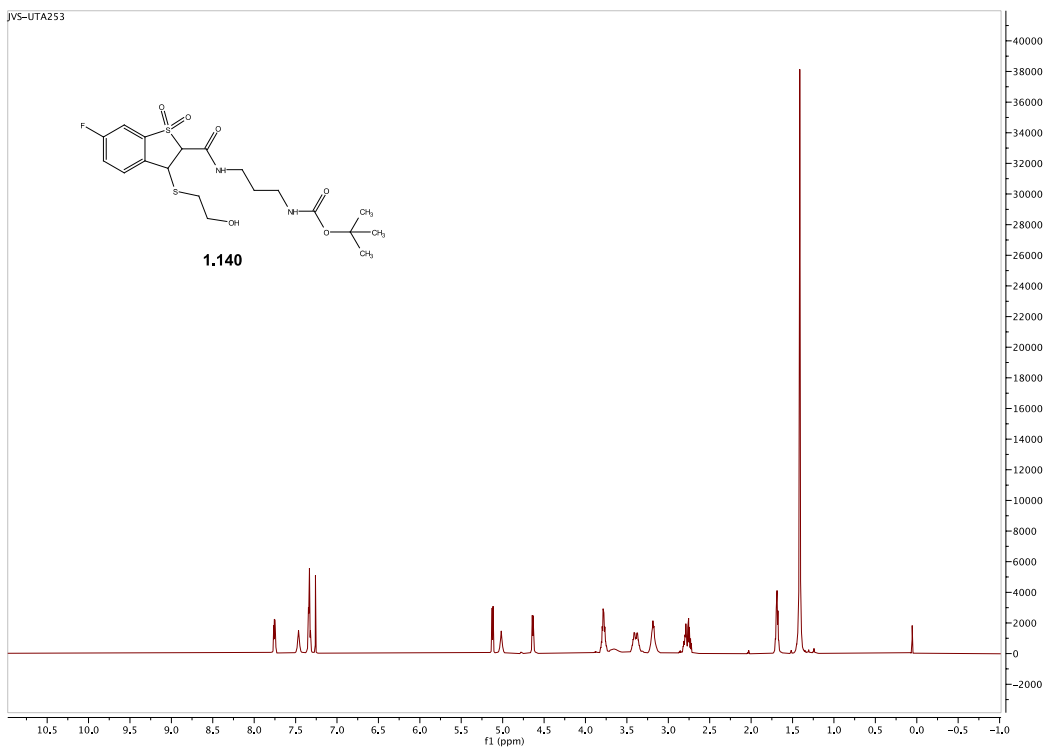
Spectra 1.160 ^{13}C NMR Spectrum of compound **1.138**



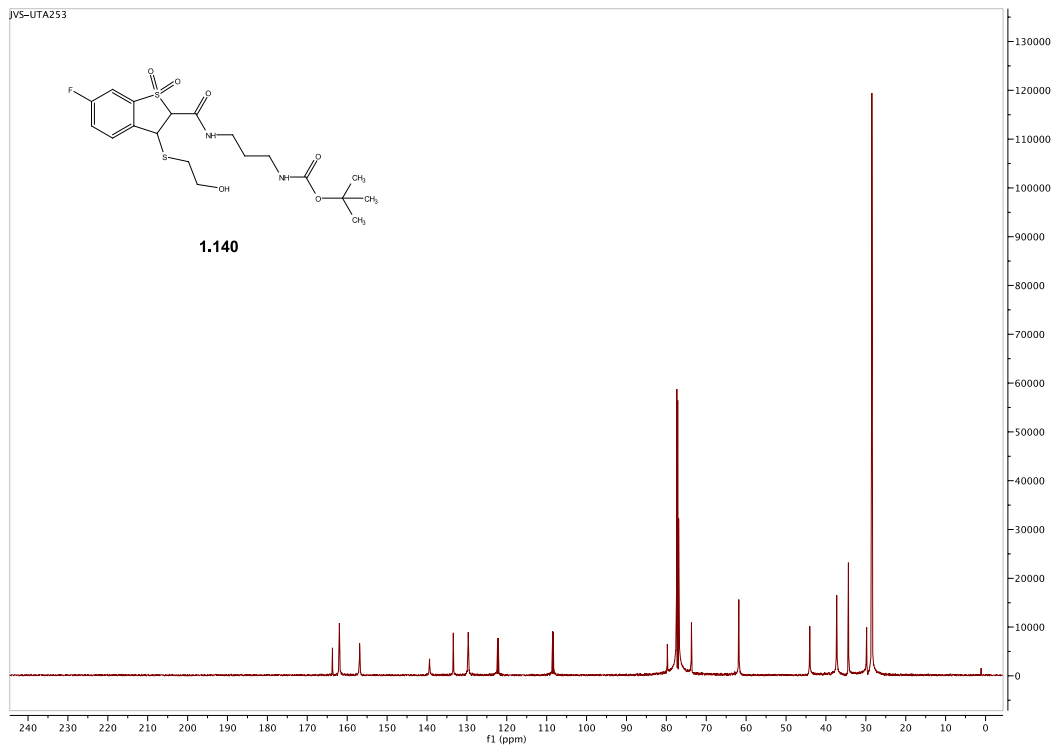
Spectra 1.161 ^1H NMR Spectrum of compound **1.139**



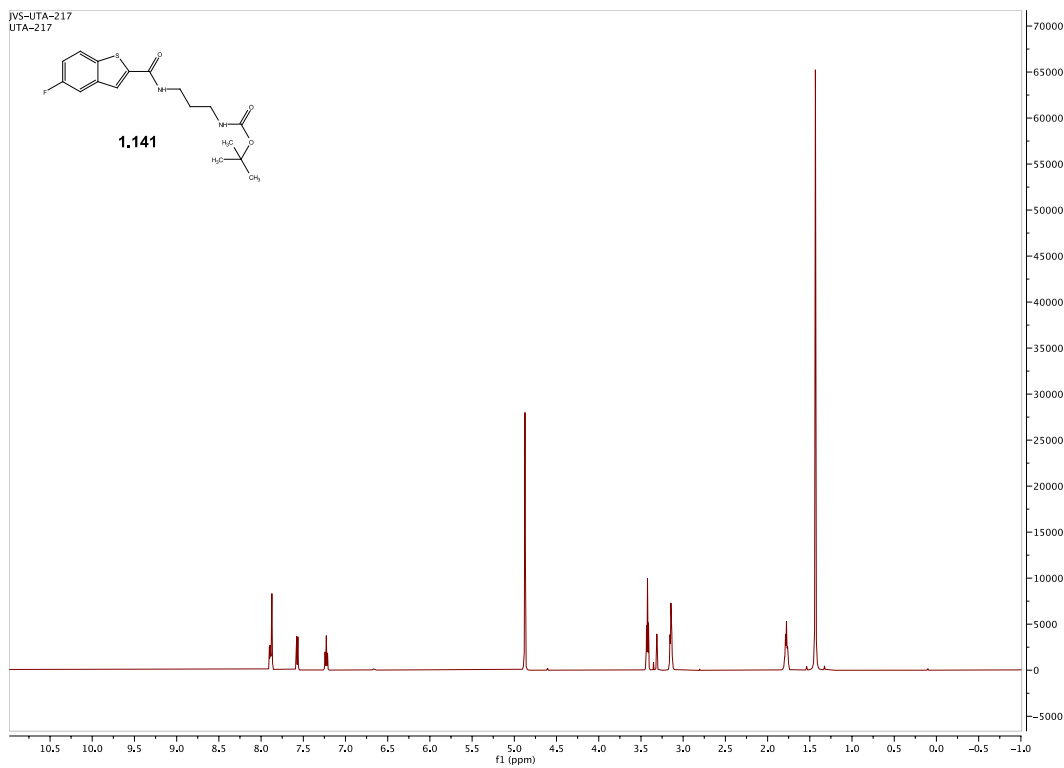
Spectra 1.162 ^{13}C NMR Spectrum of compound **1.139**



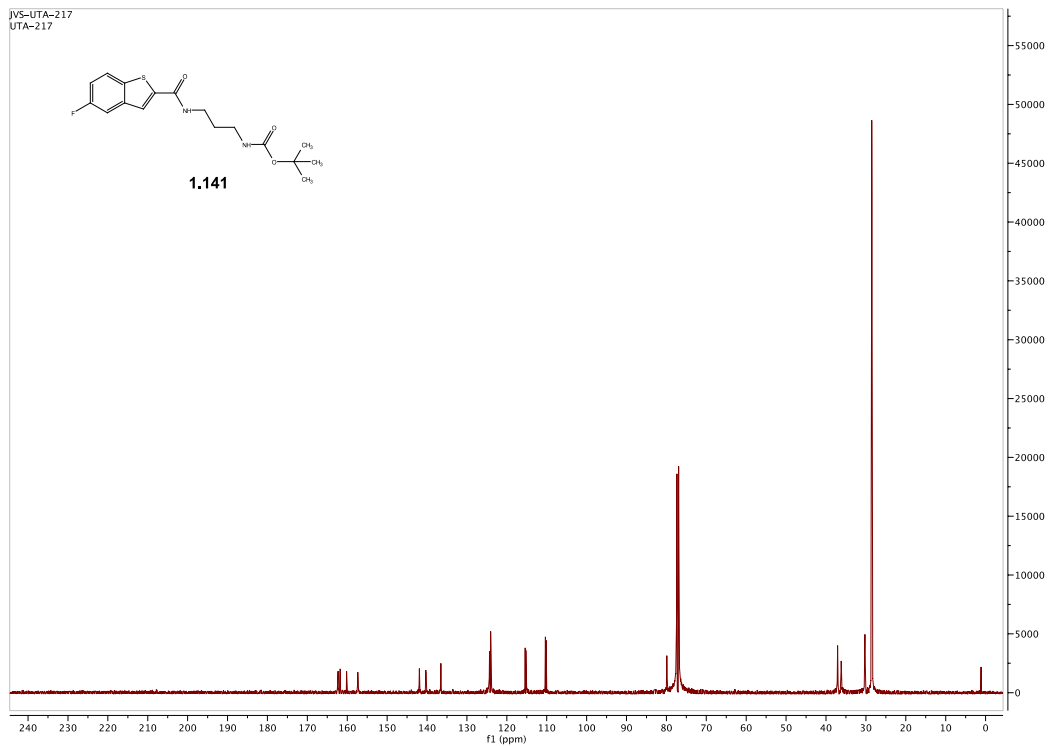
Spectra 1.163 ^1H NMR Spectrum of compound **1.140**



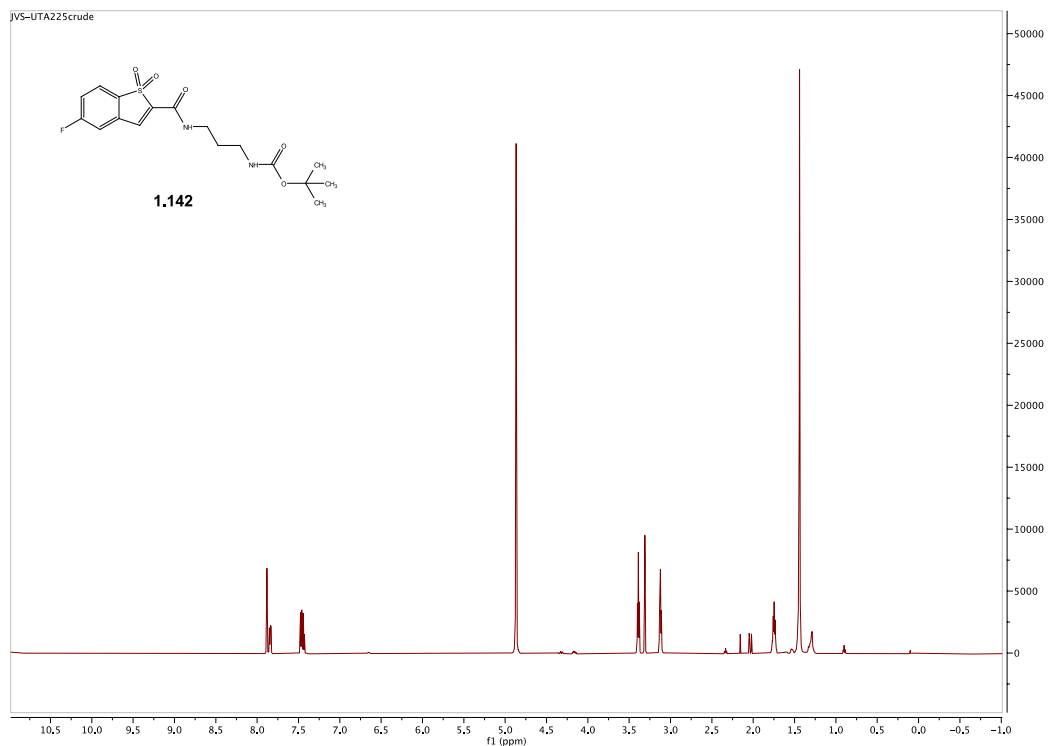
Spectra 1.164 ^{13}C NMR Spectrum of compound **1.140**



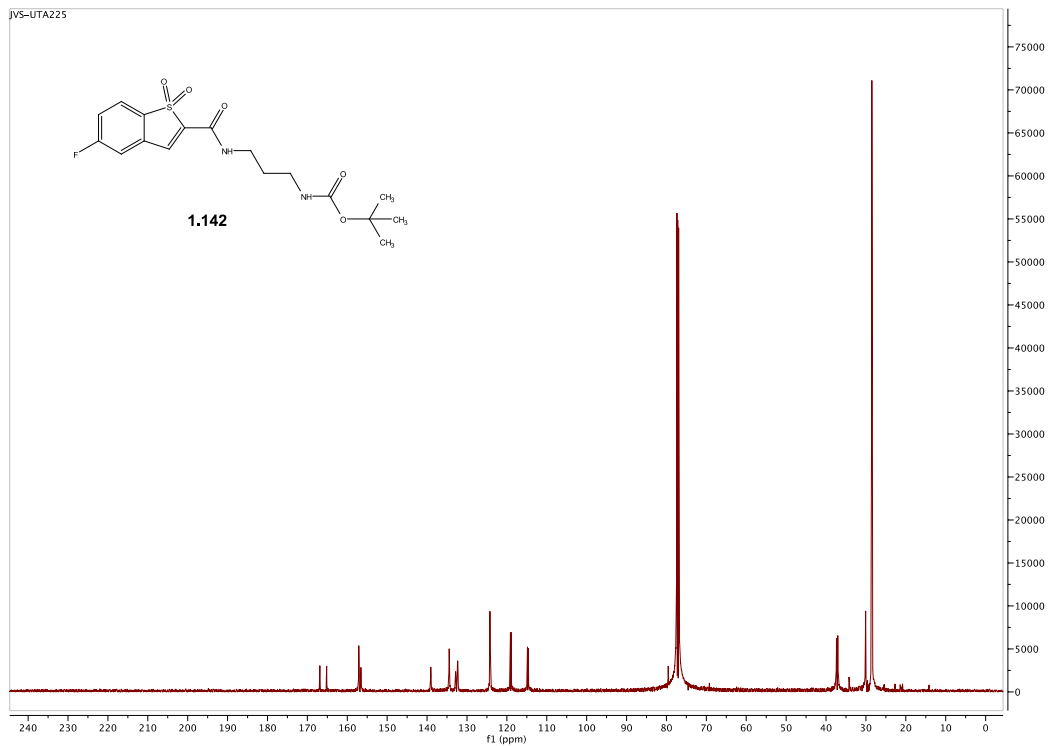
Spectra 1.165 ^1H NMR Spectrum of compound **1.141**



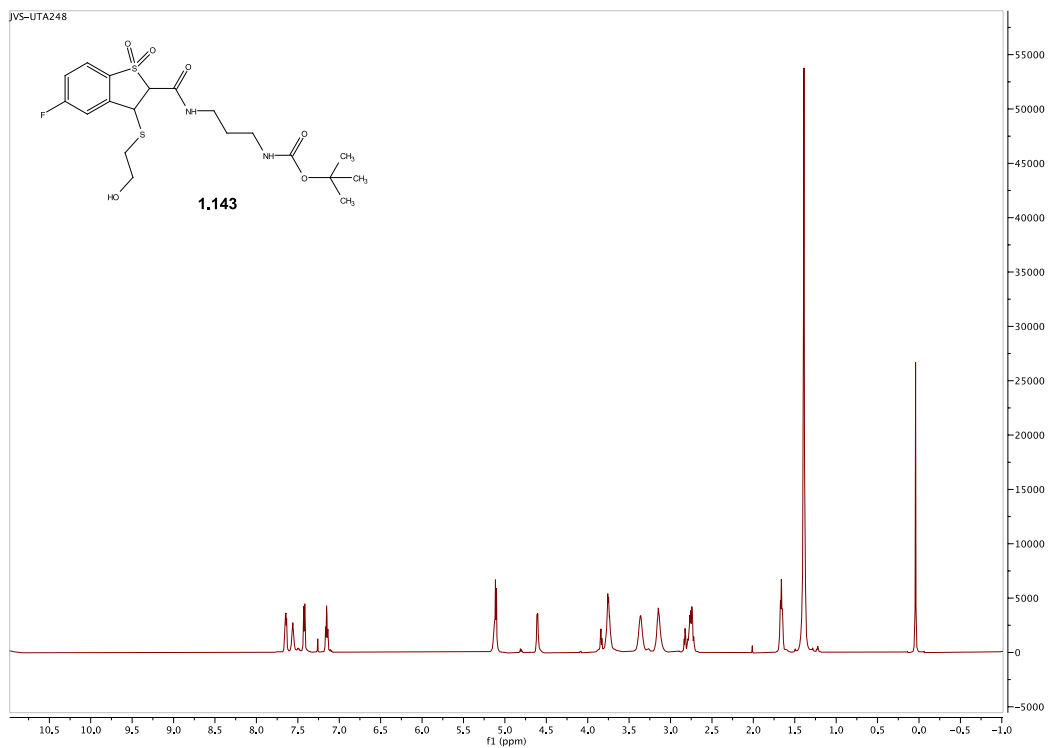
Spectra 1.166 ^{13}C NMR Spectrum of compound **1.141**



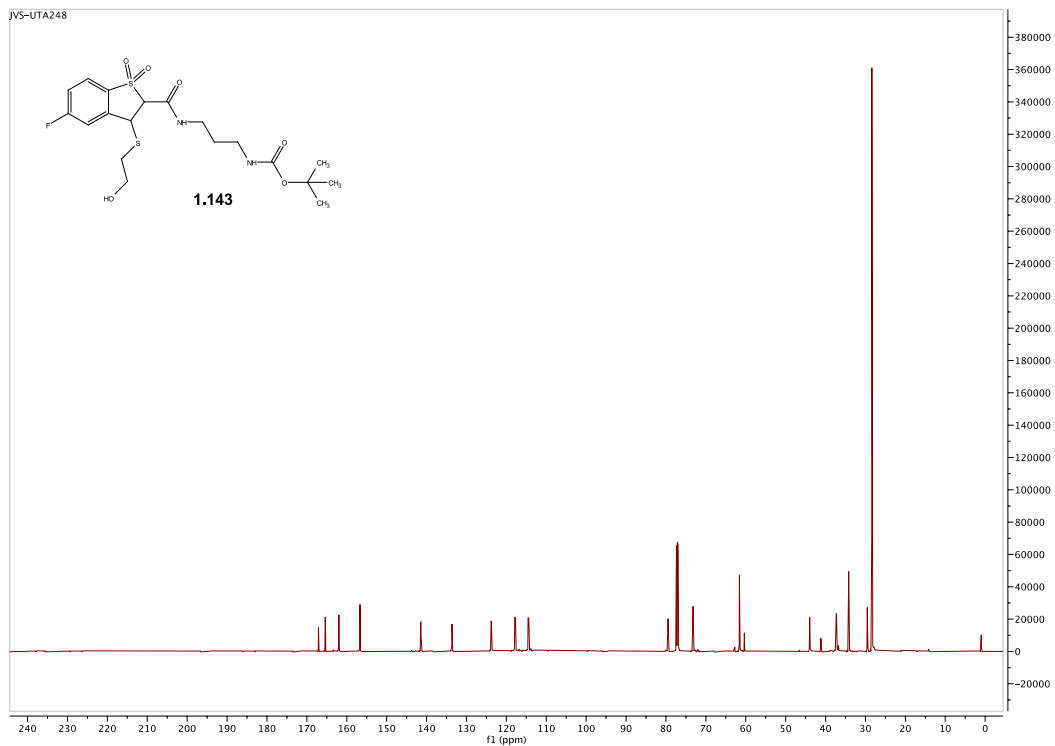
Spectra 1.167 ^1H NMR Spectrum of compound **1.142**



Spectra 1.168 ^{13}C NMR Spectrum of compound **1.142**



Spectra 1.169 ^1H NMR Spectrum of compound **1.143**



Spectra 1.170 ^{13}C NMR Spectrum of compound **1.143**

References

- 1) Stupp, R.; Mason, W.P.; Van den Bent, M.J.; Weller, M.; Fisher, B.; Taphoorn, M.J.. Radiotherapy plus concomitant and adjuvant temozolomide for glioblastoma. *N Engl J Med.* **2005**, 352, 987–996.
- 2) Wen, P.Y.; Kesari, S. Malignant gliomas in adults. *N Engl J Med.* **2008**, 359, 492–507.
- 3) Ohgaki, H. Epidemiology of brain tumors. *Methods Mol Biol.* **2009**, 472, 323–342.
- 4) Martinez, R.; Schackert, G.; Yaya-Tur, R.; Rojas-Marcos, I.; Herman, J.G.; Esteller, M. Frequent hypermethylation of the DNA repair gene MGMT in long-term survivors of glioblastoma multiforme. *J Neurooncol.* **2007**, 83, 91–93.
- 5) Stanford Health Care Home Page. <https://stanfordhealthcare.org/medical-treatments/c/cancer-surgery/complications.html>
- 6) Caner Home Page. <https://www.cancer.gov/about-cancer/treatment/types/radiation-therapy/side-effects>
- 7) Woo. Radiotherapy-Induced Glioblastoma: Distinct Differences in Overall Survival, Tumor Location, pMGMT Methylation and Primary Tumor Epidemiology in Hong Kong Chinese Patients. *British journal of neurosurgery.* **2024**, 38 (2). <https://doi.org/10.1080/02688697.2021.1881445>.
- 8) Medline Plus Home Page. <https://medlineplus.gov/druginfo/meds/a601250.html>
- 9) Krex, D.; Klink, B.; Hartmann, C.; Von Deimling, A.; Pietsch, T.; Simon, M. Long-term survival with glioblastoma multiforme. *Brain.* **2007**, 130 (10), 2596–2606.
- 10) Zhou, W.; Wahl, D.R. Metabolic abnormalities in glioblastoma and metabolic strategies to overcome treatment resistance. *Cancers.* **2019**, 11(9), 1231.
- 11) Pearson J.R.D.; Regad, T. Targeting cellular pathways in glioblastoma multiforme. *Signal Transduct Target Ther.* **2017**, 2, 17040. DOI: 10.1038/sigtrans.2017.40
- 12) Ballas, N.; Mandel, G. The Many Faces of REST Oversee Epigenetic Programming of Neuronal Genes. *Curr. Opin. Neurobiol.* **2005**, 15, 500–506.
- 13) Schoenherr, C.; Anderson, D. The Neuron-Restrictive SilencerFactor (NRSF): A Coordinate Repressor of Multiple Neuron-Specific Genes. *Science.* **1995**, 267, 1360–1363.
- 14) Gregory, N.; Xiaohua, S.; Roger, P.; Zvi, C.; Frederick, L.; Raymond, S.; Sadhan, M. Many human medulloblastoma tumors overexpress repressor element-1 silencing transcription (REST)/neuron-restrictive silencer factor, which can be functionally countered by REST-VP16. *Mol Cancer Ther.* **2005**, 4(3), 343–349. <https://doi.org/10.1158/1535-7163.MCT-04-0228>
- 15) Conti, L.; Crisafulli, L.; Caldera, V.; Tortoreto, M.; Brilli, E.; Conforti, P.; Zunino, F.; Magrassi, L.; Schiffer, D.; Cattaneo, E. REST Controls Self-Renewal and Tumorigenic Competence of Human Glioblastoma. *Cells.* **2012**, 7, 38486.

- 16) Lawinger, P.; Venugopal, R.; Guo, Z. S.; Immaneni, A.; Sengupta, D.; Lu, W.; Rastelli, L.; Marin Dias Carneiro, A.; Levin, V.; Fuller, G. N.; Echelard, Y.; Majumder, S. The Neuronal Repressor REST/NRSF Is an Essential Regulator in Medulloblastoma *Cells. Nat. Med.* **2000**, *6*, 826–831.
- 17) Spencer, E. M.; Chandler, K. E.; Haddley, K.; Howard, M. R.; Hughes, D.; Belyaev, N. D.; Coulson, J. M.; Stewart, J. P.; Buckley, N. J.; Kipar, A.; Walker, M. C.; Quinn, J. P. Regulation and Role of REST and REST4 Variants in Modulation of Gene Expression in in Vivo and in Vitro in Epilepsy Models. *Neurobiol Dis.* **2006**, *24*, 41–52.
- 18) Natali, G.; Michetti, C.; Alicja, K. R.; Floss, T.; Cesca, F.; Benfenati, F. Conditional knockout of REST/NRSF in excitatory neurons reduces seizure susceptibility to chemical kindling. *Frontiers in Cellular Neuroscience.* **2023**, *17*.
- 19) Shawn, M.; Gary, B.; Celine, D.; Seeta, R.; Shruti, I.; Cristina, R.; Christophe, B.; Tallie, B. The transcription factor NRSF contributes to epileptogenesis by selective repression of a subset of target genes. *eLife*, **2014**, *3*.
- 20) Song, Z.; Zhao, D.; Zhao, H.; Yang, L. NRSF: An Angel or a Devil in Neurogenesis and Neurological Diseases. *J. Mol. Neurosci.* **2015**, *56*, 131–144.
- 21) Nassar, A.; Satarker, S.; Gurram, P. C. Repressor Element-1 Binding Transcription Factor (REST) as a Possible Epigenetic Regulator of Neurodegeneration and MicroRNA-Based Therapeutic Strategies. *Mol Neurobiol.* **2023**, *60*, 5557–5577. <https://doi.org/10.1007/s12035-023-03437-1>
- 22) Pajarillo, E.; Rizer, A.; Son, D. S.; Aschner, M.; Lee, E. The transcription factor REST up-regulates tyrosine hydroxylase and antiapoptotic genes and protects dopaminergic neurons against manganese toxicity. *J Biol Chem.* **2020**, *295*(10), 3040-3054. DOI: 10.1074/jbc.RA119.011446
- 23) Cheng, Y.; Yin, Y.; Zhang, A. Transcription factor network analysis identifies REST/NRSF as an intrinsic regulator of CNS regeneration in mice. *Nat Commun.* **2022**, *13*, 4418. <https://doi.org/10.1038/s41467-022-31960-7>
- 24) Buckley, N. J.; Johnson, R.; Zuccato, C.; Bithell, A.; Cattaneo, E. The Role of REST in Transcriptional and Epigenetic Dysregulation in Huntington's Disease. *Neurobiol Dis.* **2010**, *39*, 28–39.
- 25) Zuccato, C.; Belyaev, N.; Conforti, P.; Ooi, L.; Tartari, M.; Papadimou, E.; MacDonald, M.; Fossale, E.; Zeitlin, S.; Buckley, N.; Cattaneo, E. Widespread Disruption of Repressor Element-1 Silencing Transcription Factor/Neuron-Restrictive Silencer Factor Occupancy at Its Target Genes in Huntington's. *Disease. J. Neurosci.* **2007**, *27*, 6972–6983.
- 26) Orozco-Díaz, R.; Sánchez-Álvarez, A.; Hernández-Hernández, J. M.; Tapia-Ramírez, J. The interaction between RE1-silencing transcription factor (REST) and heat shock protein 90 as new therapeutic target against Huntington's disease. *Plos One.* **2019**, *14*(7), 220-393. DOI: 10.1371/journal.pone.0220393
- 27) Ravache, M.; Weber, C.; Mérienne, K.; Trottier, Y. Transcriptional Activation of REST by Sp1 in Huntington's Disease Models. *Plos One.* **2010** *5*(12), 14311.

- 28) Jee-Yeon, H.; Suzanne, Z. REST, a master transcriptional regulator in neurodegenerative disease. *Current Opinion in Neurobiology*. **2018**, 48, 193-200.
- 29) Chiara, Z.; Nikolai, B.; Paola, C.; Lezanne, O.; Marzia, T.; Evangelia, P.; Marcy, M.; Elisa, F.; Scott, Z.; Noel, B.; Elena, C. Widespread Disruption of Repressor Element-1 Silencing Transcription Factor/Neuron-Restrictive Silencer Factor Occupancy at Its Target Genes in Huntington's Disease. *Journal of Neuroscience*. **2007**, 27 (26) 6972-6983.
- 30) Kamal, M. M.; Sathyan, P.; Singh, S. K.; Zinn, P. O.; Marisetty, A. L.; Liang, S.; Gumin, J.; El-Mesallamy, H. O.; Suki, D.; Colman, H.; Fuller, G. N.; Lang, F. F.; Majumder, S. REST Regulates Oncogenic Properties of Glioblastoma Stem Cells. *Stem Cells*. **2012**, 30, 405-414.
- 31) Singh, S. K.; Kagalwala, M. N.; Parker-Thornburg, J.; Adams, H.; Majumder, S. REST Maintains Self-Renewal and Pluripotency of Embryonic Stem Cells. *Nature*. **2008**, 453, 223-227
- 32) Fuller, G. N.; Su, X.; Price, R. E.; Cohen, Z. R.; Lang, F. F.; Sawaya, R.; Majumder, S. Many Human Medulloblastoma Tumors Overexpress Repressor Element-1 Silencing Transcription (REST)/Neuron-Restrictive Silencer Factor, Which Can Be Functionally Countered by REST-VP16. *Mol. Cancer Ther*. **2005**, 4, 343-349.
- 33) Chong, J. A.; Tapia-Ramirez, J.; Kim, S.; Toledo-Aral, J. J.; Zheng, Y.; Boutros, M. C.; Altshuler, Y. M.; Frohman, M. A.; Kraner, S. D.; Mandel, G. REST: A Mammalian Silencer Protein That Restricts Sodium Channel Gene Expression to Neurons. *Cell*. **1995**, 80, 949-957.
- 34) Chen, A.; Koehler, A. N. Transcription Factor Inhibition: Lessons Learned and Emerging Targets. *Trends Mol Med*. **2020**, 26(5), 508-518. DOI: 10.1016/j.molmed.2020.01.004.
- 35) Basu, S.; Martínez-Cristóbal, P.; Frigolé-Vivas, M. Rational optimization of a transcription factor activation domain inhibitor. *Nat Struct Mol Biol*. **2023**, 30, 1958-1969. <https://doi.org/10.1038/s41594-023-01159-5>
- 36) Huang, Z.; Bao, S. Ubiquitination and deubiquitination of REST and its roles in cancers, *FEBS Letters*. **2012**, 586, DOI: 10.1016/j.febslet.2012.04.052
- 37) Guardavaccaro, D.; Frescas, D.; Dorrello, N.V.; Peschiaroli, A.; Multani, A.S.; Cardozo, T. Control of chromosome stability by the beta-TrCP-REST-Mad2 axis. *Nature*. **2008**; 452(7185), 365-9.
- 38) Nesti, E.; Corson, G.M.; McCleskey, M.; Oyer, J.A.; Mandel, G. C-terminal domain small phosphatase 1 and MAP kinase reciprocally control REST stability and neuronal differentiation. *Proc Natl Acad Sci USA*. **2014**, 111(37), 3929-3936.
- 39) Yeo, M.; Lin, P. S.; Dahmus, M. E.; Gill, G. N. A Novel RNAPolymerase II C-Terminal Domain Phosphatase That Preferentially Dephosphorylates Serine. *J. Biol. Chem*. **2003**, 278, 26078-26085.
- 40) Burkholder, N. T.; Mayfield, J. E.; Yu, X.; Irani, S.; Arce, D. K.; Jiang, F.; Matthews, W. L.; Xue, Y.; Zhang, Y. J. Phosphatase Activity of Small C-Terminal Domain

Phosphatase 1 (SCP1) Controls the Stability of the Key Neuronal Regulator RE1-Silencing Transcription Factor (REST). *J. Biol. Chem.* **2018**, 293, 16851–16861.

- 41) Swingle, M.; Ni, L.; Honkanen, R.E. Small-molecule inhibitors of ser/thr protein phosphatases: specificity, use and common forms of abuse. *Methods Mol Biol.* **2007**, 365, 23-38. DOI: 10.1385/1-59745-267-X:23.
- 42) Mochen, G.; Zekun, L.; Mingxiao, G.; Junrui, G.; Qidong, Y.; Lei, W. Targeting phosphatases: From molecule design to clinical trials. *European Journal of Medicinal Chemistry.* **2024**, 264.
- 43) Vintonyak, V.V.; Waldmann, H.; Rauh, D. Using small molecules to target protein phosphatases. *Bioorg Med Chem.* **2011**, 19(7), 2145-55. DOI: 10.1016/j.bmc.2011.02.047.
- 44) Mullard, A. Phosphatases start shedding their stigma of undruggability. *Nat Rev Drug Discov.* **2018**, 847–849. <https://doi.org/10.1038/nrd.2018.201>
- 45) Victor, C.; Yuhong, F.; Dingyin, T.; Harichandra, D.; Tagad, S.; Yuhong, W.; Surendra, K.; Kelly, L.; Zhen-Dan, S.; Olga, V.; Christophe, A.; Rebecca, E.; Min, S.; Samarjit, P.; Ettore, A.; Nathan, C.; Matthew, H.; Daniel, H. Appella. *ACS Pharmacology & Translational Science* **2022** 5 (10), 993-1006.
- 46) Erika, R.; Jonathan, M.; Neil, M.; Xavier, M.; Ka Kei, H.; Nadine, L.; Annette, S.; Marianna, M.; Karen, P.; Christophe, E.; Eric, L.; Ramón, V.; Rüdiger, W. *ACS Chemical Biology.* **2006** 1 (12), 780-790
- 47) Pestell, K.; Ducruet, A.; Wipf, P. Small molecule inhibitors of dual specificity protein phosphatases. *Oncogene* **19**, 6607–6612 (2000).
- 48) Kimberly, M.; Rita, A.; David, C.; Sudeh, I.; Danica, W.; Abbey, P.; Jaya, S.; David, K.; Daniela, S.; Maxwell, C.; Janna, K.; Agnes, S.; Shen, Y.; Divya, H.; Daniel, M.; Nilesh, Z.; Yixuan, G.; David, B.; Stephen, P.; Cynthia, S.; William, O.; Alice, L.; Alexander, K.; John, S.; Rosalie, S.; Analisa, D.; Yiannis, I.; Michael, O.; Goutham, N.; Matthew, G. Small-Molecule Activators of Protein Phosphatase 2A for the Treatment of Castration-Resistant Prostate Cancer. *Cancer Res.* **2018**, 78 (8), 2065–2080
- 49) Tanja, G.; Marleen, H.; Lena, K.; Silke, M.; Thomas, U.; Mayer, Christof, R.; Hauck, L. A selective small-molecule inhibitor of the integrin phosphatase, PPM1F, blocks cancer cell invasion. *Cell Chemical Biology*, **2022**, 29 (6), 930-946.
- 50) Quinzii, C.M.; Luna-Sanchez, M.; Ziosi, M.; Hidalgo-Gutierrez, A.; Kleiner, G.; Lopez, L.C. The Role of Sulfide Oxidation Impairment in the Pathogenesis of Primary CoQ Deficiency. *Front Physiol.* **2017**, 25 (80), 525.
- 51) Fichtner, T.; Fischer, A.R.; Dornack, C. Nitrate consumption by the oxidation of sulfides during an enhanced natural attenuation project at a contaminated site in Berlin, Germany. *Environ Sci Eur.* **2021**, 33 (103). <https://doi.org/10.1186/s12302-021-00546-3>

- 52) Tang, C.; Li, J.; Shen, Y. A sulfide-sensor and a sulfane sulfur-sensor collectively regulate sulfur-oxidation for feather degradation by *Bacillus licheniformis*. *Commun Biol.* **2023**, *6*, 167. <https://doi.org/10.1038/s42003-023-04538-2>
- 53) Brenda, M.; Wanjie, Y.; Srihari, K.; Jiajun, D.; Seema, I.; Haoyi, W.; Wendy, M.; Zhong-Yin, Z.; Dionico, S.; Yan, Z. *Journal of Medicinal Chemistry.* **2022**, *65* (1), 507-519
- 54) Huang, F.; Han, X.; Xiao, X.; Zhou, J. Covalent Warheads Targeting Cysteine Residue: The Promising Approach in Drug Development. *Molecules.* **2022**, *27*(22), 7728.
- 55) Boike, L.; Henning, N.J.; Nomura, D.K. Advances in covalent drug discovery. *Nat Rev Drug Discov.* **2022**, *21*, 881–898. <https://doi.org/10.1038/s41573-022-00542-z>
- 56) Serafimova, I.M.; Pufall, M.A.; Krishnan, S.; Duda, K.; Cohen, M.S.; Maglathlin, R.L.; McFarland, J.M.; Miller, R.M.; Frödin, M.; Taunton, J. Reversible targeting of noncatalytic cysteines with chemically tuned electrophiles. *Nat Chem Biol.* **2012**, *8*(5), 471-476. DOI: 10.1038/nchembio.925.
- 57) Rambabu, N.; Reddi, R.; Adi, R.; Boddu, R.; Ronen, G.; Kim, G.; Neta, G.; Daniel, Z.; Alexander, P.; Haim, B.; Ziv, S.; Nir, L. Tunable Methacrylamides for Covalent Ligand . *Chemistry Journal of the American Chemical Society.* **2021** *143* (13), 4979-4992.
- 58) James, M.; Claire, M.; Daniel, F.; Ian, G. Characterising covalent warhead reactivity. *Bioorganic & Medicinal Chemistry*, **2019**, *27* (10) , 2066-2074.
- 59) Kim, H.; Hauner, D.; Laureanti, J.A. Mechanistic investigation of SARS-CoV-2 main protease to accelerate design of covalent inhibitors. *Sci Rep.* **2022**, *12*, 21037. <https://doi.org/10.1038/s41598-022-23570-6>.
- 60) John, S. A Perspective on the Kinetics of Covalent and Irreversible Inhibition. *SLAS Discovery.* 2017, *22* (1) , 3-20.
- 61) Chaikuad, A.; Koch, P.; Laufer, A.; Knapp, S. *Angew. Chem. Int. Ed.* **2018**, *57*, 4372.
- 62) Peter, M.; Robert, D.; Avner, S. Encounter and React: Computer-Guided Design of Covalent Inhibitors, *Cell Chemical Biology.* **2019**, *26*(1) ,6-8.
- 63) Zheng, L.; Li, Y.; Wu, D. Development of covalent inhibitors: principle, design and application in cancer. *MedComm – Oncology.* **2023**, *2*, 56. doi:10.1002/mog2.56
- 64) Lonsdale, R.; Ward, R. *Chem. Soc. Rev.* **2018**, *47*, 3816-3830.
- 65) Simon, C.C.; Lucas, J.; Henry, B.; Sarah, H.; Hannah, S.; Benjamin, C.; Whitehurst, X. Covalent hits and where to find them. *SLAS Discovery*, **2024**, *29*(3) , 100142.
- 66) Péter, Á.; László, P.; Tímea, I.; Péter, S.; Andrea, S.; Martina, H.; Ana, M.; Urša, F.; Krisztina, N.; Hélène, B.; David, R.; Kata, H.; György, F.; Janko, K.; Janez, I.; Stanislav, G.; György, K. A road map for prioritizing warheads for cysteine targeting covalent inhibitors. *European Journal of Medicinal Chemistry*, **2018**, *160*, 94-107.
- 67) Serafimova, I. Reversible Targeting of Noncatalytic Cysteines with Chemically Tuned Electrophiles. *Nature chemical biology.* **2012**, *8*(5), 471–476.

- 68) Jack, T. Targeting kinases with reversible covalent fragments. *Cancer Res.* **2014**; 74.
- 69) Lee, J.; Park, S.B. Extended Applications of Small-Molecule Covalent Inhibitors toward Novel Therapeutic Targets. *Pharmaceuticals.* **2022**, 15, 1478. <https://doi.org/10.3390/ph15121478>
- 70) Ray, S.; Murkin, A.S. New Electrophiles and Strategies for Mechanism-Based and Targeted Covalent Inhibitor Design. *Biochemistry.* **2019**, 58(52), 5234-5244. DOI: 0.1021/acs.biochem.9b00293.
- 71) Jin-Young, M.; Kyung-Soo, C.; Do-Hee, K. The versatile utility of cysteine as a target for cancer treatment. *Frontiers in Oncology.* **2023**, 12.
- 72) Fangjiao, H.; Xiaoli, H.; Xiaohui, X.; Jinming, Z. Covalent Warheads Targeting Cysteine Residue: The Promising Approach in Drug Development. *Molecules.* **2022**, 27(22), 7728.
- 73) Thomas, S.; Max, R.; Kay, A.; Alexandre, S.; Tanja, S.; Bernd, E.; Simon, G. Vinyl sulfone building blocks in covalently reversible reactions with thiols. *New J. Chem.* **2015**, 39, 5841-5853.
- 74) James, P.; David, R.; Jeffrey, K.; Dieter, B. *Journal of Medicinal Chemistry.* **1995**, 38 (17), 3193-3196.
- 75) Iain, K.; Ji, L.; Christopher, F.; Rachael, M.; Mathias, R.; Mohammed, S.; Kailash, P.; Conor, C.; Jennifer, L.; Elizabeth, H.; James, M.; Charles, C.; Philip, R.; Linda, B. Vinyl Sulfones as Antiparasitic Agents and a Structural Basis for Drug Design. *Journal of Biological Chemistry*, **2009**, 284(38), 25697-25703.
- 76) Jung, S.; Fuchs, N.; Johe, P.; Wagner, A.; Diehl, E.; Yuliani, T.; Zimmer, C.; Barthels, F.; Zimmermann, R.A.; Klein, P.; Waigel, W.; Meyr, J.; Opatz, T.; Tenzer, S.; Distler, U.; Räder, H.J.; Kersten, C.; Engels, B.; Hellmich, U.A.; Klein, J.; Schirmeister, T. Fluorovinylsulfones and -Sulfonates as Potent Covalent Reversible Inhibitors of the Trypanosomal Cysteine Protease Rhodesain: Structure-Activity Relationship, Inhibition Mechanism, Metabolism, and In Vivo Studies. *J Med Chem.* **2021**, 64(16), 12322-12358. DOI: 10.1021/acs.jmedchem.1c01002.
- 77) Huang, F.; Han, X.; Xiao, X.; Zhou, J. Covalent Warheads Targeting Cysteine Residue: The Promising Approach in Drug Development. *Molecules.* **2022**, 27(22), 7728. DOI: 10.3390/molecules27227728.
- 78) Iain, K.; Ji, L.; Christopher, F.; Rachael, M.; Mathias, R.; Mohammed, S.; Kailash, P.; Conor, C.; Jennifer, L.; Elizabeth, H.; James, M.; Charles, C.; Philip, R.; Linda, B. Vinyl Sulfones as Antiparasitic Agents and a Structural Basis for Drug Design. *Journal of Biological Chemistry*, **2009**, 284(38), 25697-25703.
- 79) Boike, L.; Henning, N.J.; Nomura, D.K. Advances in covalent drug discovery. *Nat Rev Drug Discov.* **2022**, 21, 881–898. <https://doi.org/10.1038/s41573-022-00542-z>.
- 80) Claudio, Z.; Ekaterina, V.; Xiaotian, Q.; Jonathan, I.; Radu, S.; Minseob, K.; Kristine, S.; Stormi, R.; Brittany, B.; Jason, C.; Arnab, C.; Peng, L.; Peter, S.; Benjamin, C.; Michael, B. *Journal of the American Chemical Society.* **2020**, 142 (19), 8972-8979.

- 81) Huaisheng, Z.; Jasmine, C.; Rogers, N.; Olamide, C.; Oluwatomi, A.; Victor, O. Vinyl sulfone-based inhibitors of trypanosomal cysteine protease rhodesain with improved antitrypanosomal activities. *Bioorganic & Medicinal Chemistry Letters*. **2020**, 30(14), 127217.
- 82) Xiao, Y. C.; Chen, F. E. The vinyl sulfone motif as a structural unit for novel drug design and discovery. *Expert Opinion on Drug Discovery*. **2024**, 19(2), 239–251. <https://doi.org/10.1080/17460441.2023.2284201>.
- 83) Zhang, T.; Hatcher, J.M.; Teng, M.; Gray, N.S.; Kostic, M. Recent Advances in Selective and Irreversible Covalent Ligand Development and Validation. *Cell Chem Biol*. **2019**, 26(11), 1486-1500. DOI: 10.1016/j.chembiol.2019.09.012.
- 84) Kerr, I.D.; Lee, J.H.; Farady, C.J.; Marion, R.; Rickert, M.; Sajid, M.; Pandey, K.C.; Caffrey, C.R.; Legac, J.; Hansell, E.; McKerrow, J.H.; Craik, C.S.; Rosenthal, P.J.; Brinen, L.S. Vinyl sulfones as antiparasitic agents and a structural basis for drug design. *J Biol Chem*. **2009**, 284(38), 25697-703. DOI: 10.1074/jbc.M109.014340.
- 85) Klein, P.; Barthels, F.; Johe, P.; Wagner, A.; Tenzer, S.; Distler, U.; Le, T.A.; Schmid, P.; Engel, V.; Engels, B.; et al. Naphthoquinones as Covalent Reversible Inhibitors of Cysteine Proteases—Studies on Inhibition Mechanism and Kinetics. *Molecules*. **2020**, 25, 2064. <https://doi.org/10.3390/molecules25092064>.
- 86) Gil, E.; Jiménez-Moreno, E.; Oliveira, B.L.; Navo, C.D.; Jiménez-Osés, G.; Robina, I.; Moreno-Vargas, A.J.; Bernardes, G.J.L. Azabicyclic vinyl sulfones for residue-specific dual protein labelling. *Chem Sci*. **2019**, 10(16), 4515-4522. DOI: 10.1039/c9sc00125e.
- 87) Boike, L.; Henning, N.J.; Nomura, D.K. Advances in covalent drug discovery. *Nat Rev Drug Discov*. **2022**, 21(12), 881-898. DOI: 10.1038/s41573-022-00542-z.
- 88) Zambaldo, C.; Vinogradova, E.V.; Qi, X. 2-Sulfonylpyridines as Tunable, Cysteine-Reactive Electrophiles. *Journal of the American Chemical Society*. **2020**, 142(19), 8972-8979. DOI: 10.1021/jacs.0c02721.
- 89) Alves, E.T.M.; Pernichelle, F.G.; Nascimento, L.A.; Ferreira, G.M.; Ferreira, E.I. Covalent Inhibitors for Neglected Diseases: An Exploration of Novel Therapeutic Options. *Pharmaceuticals*. **2023**, 16, 1028. <https://doi.org/10.3390/ph16071028>.
- 90) Mons, E.; Kim, R. Q.; Doodewaerd, B. R.; Veelen, P. A.; Mulder, M. P. C.; Ovaa, H. Exploring the versatility of the covalent thiol-alkyne reaction with substituted propargyl warheads: a deciding role for the cysteine protease. *Journal Of the American Chemical Society*. **2021**, 143(17), 6423-6433. DOI:10.1021/jacs.0c10513.
- 91) Bogyo, M.; McMaster, J.S.; Gaczynska, M.; Tortorella, D.; Goldberg, A.L.; Ploegh, H. Covalent modification of the active site threonine of proteasomal beta subunits and the Escherichia coli homolog HslV by a new class of inhibitors. *Proc Natl Acad Sci U S A*. **1997**, 94(13), 6629-34. DOI: 10.1073/pnas.94.13.6629.
- 92) Shenai, B.R.; Lee, B.J.; Alvarez-Hernandez, A.; Chong, P.Y.; Emal, C.D.; Neitz, R.J.; Roush, W.R.; Rosenthal, P.J. Structure-Activity Relationships for Inhibition of Cysteine Protease Activity and Development of Plasmodium falciparum by Peptidyl Vinyl Sulfones. *Antimicrob Agents Chemother*. **2013**, 47.

- 93) Shyam, K.; Rand, M.; Boxue, T.; Dyche, M.; Matthew, J.; Jack, T. Design of Reversible, Cysteine-Targeted Michael Acceptors Guided by Kinetic and Computational Analysis. *Journal of the American Chemical Society*. **2014**, *136* (36), 12624-12630.
- 94) Panina, S.B.; Schweer, J.V.; Zhang, Q. Targeting of REST with rationally-designed small molecule compounds exhibits synergetic therapeutic potential in human glioblastoma cells. *BMC Biol.* **2024**, *22* (83). <https://doi.org/10.1186/s12915-024-01879-0>.
- 95) Gehringer, M.; Laufer, S. Emerging and Re-Emerging Warheads for Targeted Covalent Inhibitors: Applications in Medicinal Chemistry and Chemical Biology. *Journal of Medicinal Chemistry*. **2019**, *62* (12), 5673-5724. DOI: 10.1021/acs.jmedchem.8b01153.
- 96) Michele, P.; Mark, D. *Journal of Medicinal Chemistry*. **2009**, *52* (5), 1231-1246 DOI: 10.1021/jm8008597.
- 97) Douglas, J.; Eranthie, W.; Benjamin, C. Strategies for discovering and derisking covalent, irreversible enzyme inhibitors. *Future Medicinal Chemistry*. **2010** *2*(6), 949-964.
- 98) Kalgutkar, A. S.; Dalvie, D. K. Drug discovery for a new generation of covalent drugs. *Expert Opinion on Drug Discovery*. **2012**, *7*(7), 561–581.
- 99) Johansson, M.H. Reversible Michael additions: covalent inhibitors and prodrugs *Mini-Rev. Med. Chem.* **2012**, *12*, 1330-1344.
- 100) Wilson, A.J. Keep calm, and carry on covalently. *J. Med. Chem.* **2013**, *56*, 7463-7476.
- 101) Johansson, M.H. Reversible Michael additions: covalent inhibitors and prodrugs *Mini-Rev. Med. Chem.* **2012**, *12*, 1330-1344.
- 102) Mark, Flanagan.; Joseph, Abramite.; Dennis, Anderson.; Ann, Aulabaugh.; Upendra, Dahal.; Adam, Gilbert.; Chao, L.; Justin, M.; Stacey, O.; Tim, R.; Brandon, S.; Daniel, U.; Gregory, W.; Yan, W.; Matthew, B.; Jinshan, C.; Matthew, H.; Mark, N.; Scott, O.; Laurence, P.; Veerabahu, S.; Michael, S.; Jeremy, S.; Justin, S.; Ye, C. Chemical and Computational Methods for the Characterization of Covalent Reactive Groups for the Prospective Design of Irreversible Inhibitors. *Journal of Medicinal Chemistry*. **2014**, *57* (23), 10072-10079.
- 103) Rambabu, R.; Efrat, R.; Adi, R.; Boddu, R.; Ronen, G.; Kim, G.; Neta, G.; Daniel, Z.; Alexander, P.; Haim, B.; Ziv, S.; Nir, L. Tunable Methacrylamides for Covalent Ligand. *Chemistry Journal of the American Chemical Society*. **2021**, *143* (13), 4979-4992.
- 104) Jackson, P. A.; Widen, J. C.; Harki, D. A.; Brummond, K. M. Covalent Modifiers: A Chemical Perspective on the Reactivity of α,β -Unsaturated Carbonyls with Thiols via Hetero-Michael Addition Reactions. *J. Med. Chem.* **2017**, *60* (3), 839– 885.
- 105) Strelow, J. M. A Perspective on the Kinetics of Covalent and Irreversible Inhibition. *J. Biomol. Screen.* **2016**.

- 106) Martin, J. S.; MacKenzie, C. J.; Fletcher, D.; Gilbert, I. H. Characterising Covalent Warhead Reactivity. *Bioorg. Med. Chem.* **2019**, *27* (10), 2066– 2074. DOI: 10.1016/j.bmc.2019.04.002.
- 107) Birkholz, A.; Kopecky, D. J.; Volak, L. P.; Bartberger, M. D.; Chen, Y.; Tegley, C.; Arvedson, T. L.; McCarter, J. D.; Fotsch, C. H.; Cee, V. J. Systematic Study of the Glutathione (GSH) Reactivity of N-Phenylacrylamides: Effects of Acrylamide Substitution. *J. Med. Chem.* **2020**, *63*, 11602. DOI: 10.1021/acs.jmedchem.0c00749.
- 108) Cee, V. J.; Volak, L. P.; Chen, Y.; Bartberger, M. D.; Tegley, C.; Arvedson, T.; McCarter, J.; Tasker, A. S.; Fotsch, C. Systematic Study of the Glutathione (GSH) Reactivity of N-Arylacrylamides: 1. Effects of Aryl Substitution *J. Med. Chem.* **2015**, *58*, 9171– 9178 DOI: 10.1021/acs.jmedchem.5b01018.
- 109) Böhme, A.; Thaens, D.; Schramm, F.; Paschke, A.; Schüürmann, G. Thiol Reactivity and Its Impact on the Ciliate Toxicity of α,β -Unsaturated Aldehydes, Ketones, and Esters. *Chem. Res. Toxicol.* **2010**, *23*, 1905– 1912.
- 110) Schwöbel, J. A. H.; Wondrousch, D.; Koleva, Y. K.; Madden, J. C.; Cronin, M. T. D.; Schüürmann, G. Prediction of Michael-Type Acceptor Reactivity Toward Glutathione *Chem. Res. Toxicol.* **2010**, *23*, 1576– 1585 DOI: 10.1021/tx100172x.
- 111) Amslinger, S. The Tunable Functionality of α,β -Unsaturated Carbonyl Compounds Enables Their Differential Application in Biological Systems. *Chem Med Chem.* **2010**, *5*, 351– 356. DOI: 10.1002/cmdc.200900499.
- 112) Blewett, M. M.; Xie, J.; Zaro, B. W.; Backus, K. M.; Altman, A.; Teijaro, J. R.; Cravatt, B. F. Chemical Proteomic Map of Dimethyl Fumarate–Sensitive Cysteines in Primary Human T Cells. *Sci. Signaling.* **2016**, *9* (445). DOI: 10.1126/scisignal.aaf7694.
- 113) Ekkebus, R.; van Kasteren, S. I.; Kulathu, Y.; Scholten, A.; Berlin, I.; Geurink, P. P.; de Jong, A.; Goerdal, S.; Neefjes, J.; Heck, A. J. R.; Komander, D.; Ova, H. On Terminal Alkynes That Can React with Active-Site Cysteine Nucleophiles in Proteases. *J. Am. Chem. Soc.* **2013**, *135* (8), 2867– 2870.
- 114) Sommer, S.; Weikart, N. D.; Linne, U.; Mootz, H. D. Covalent Inhibition of SUMO and Ubiquitin-Specific Cysteine Proteases by an in Situ Thiol–Alkyne Addition. *Bioorg. Med. Chem.* **2013**, *21* (9), 2511– 2517. DOI: 10.1016/j.bmc.2013.02.039.
- 115) Terrier, F. Rate and Equilibrium Studies in Jackson-Meisenheimer Complexes. *Chem. Rev.* **1982**, *82* (2), 77– 152. DOI: 10.1021/cr00048a001.
- 116) Terrier, F. *Modern Nucleophilic Aromatic Substitution*, 1st ed.; Wiley-VCH: Weinheim, **2013**.
- 117) Sanger, F. The Free Amino Groups of Insulin. *Biochem. J.* **1945**, *39* (5), 507– 515.
- 118) Singh, J.; Petter, R.; Baillie, T. The resurgence of covalent drugs. *Nat Rev Drug Discov.* **2011**, *10*, 307–317. <https://doi.org/10.1038/nrd3410>.
- 119) Miller, R. M.; Taunton, J. Targeting Protein Kinases with Selective and Semipromiscuous Covalent Inhibitors. *Methods in Enzymology.* **2014**, *548*, 93– 116. DOI: 10.1016/B978-0-12-397918-6.00004-5.

- 120) Serafimova, I. M.; Pufall, M. A.; Krishnan, S.; Duda, K.; Cohen, M. S.; Maglathlin, R. L.; McFarland, J. M.; Miller, R. M.; Frödin, M.; Taunton, J. Reversible Targeting of Noncatalytic Cysteines with Chemically Tuned Electrophiles. *Nat. Chem. Biol.* **2012**, *8* (5), 471– 476. DOI: 10.1038/nchembio.925.
- 121) Bradshaw, J. M.; McFarland, J. M.; Paavilainen, V. O.; Bisconte, A.; Tam, D.; Phan, V. T.; Romanov, S.; Finkle, D.; Shu, J.; Patel, V.; Ton, T.; Li, X.; Loughhead, D. G.; Nunn, P. A.; Karr, D. E.; Gerritsen, M. E.; Funk, J. O.; Owens, T. D.; Verner, E.; Brameld, K. A.; Hill, R. J.; Goldstein, D. M.; Taunton, J. Prolonged and Tunable Residence Time Using Reversible Covalent Kinase Inhibitors. *Nat. Chem. Biol.* **2015**, *11* (7), 525– 531. DOI: 10.1038/nchembio.1817.
- 122) Krishnan, S.; Miller, R. M.; Tian, B.; Mullins, R. D.; Jacobson, M. P.; Taunton, J. Design of Reversible, Cysteine-Targeted Michael Acceptors Guided by Kinetic and Computational Analysis. *J. Am. Chem. Soc.* **2014**, *136* (36), 12624– 12630. DOI: 10.1021/ja505194w.
- 123) Krenske, E. H.; Petter, R. C.; Houk, K. N. Kinetics and Thermodynamics of Reversible Thiol Additions to Mono- and Diactivated Michael Acceptors: Implications for the Design of Drugs That Bind Covalently to Cysteines. *J. Org. Chem.* **2016**, *81* (23), 11726– 11733. DOI: 10.1021/acs.joc.6b02188.
- 124) Mecozzi, S.; West, A.P.; Dougherty, D.A. Cation-pi interactions in aromatics of biological and medicinal interest: electrostatic potential surfaces as a useful qualitative guide. *Proc Natl Acad Sci U S A.* **1996**, *93*(20), 10566-71. DOI: 10.1073/pnas.93.20.10566.
- 125) Chennakesava, R.; Javed, S.; Ramakrishna, G. Bhat *The Journal of Organic Chemistry.* **2020**, *85* (11), 6924-6934. DOI: 10.1021/acs.joc.0c00154.
- 126) Yu, X.; Lu, X. Efficient Synthesis of 9-Tosylaminofluorene Derivatives by Boron Trifluoride Etherate-Catalyzed Aza-Friedel–Crafts Reaction of *in situ* Generated *N*-Tosylbenzaldimines. *Adv. Synth. Catal.*, **2011**, *353*, 569-574.
- 127) Danni, R.; Tao, Y.; Huixu, F.; Qi, A.; Shaofeng, Z.; Jinghua, Y.; Xuelian, R.; Xingxing, D.; He, H.; Wei, T.; Shilin, X. Discovery and Structural Optimization of Covalent ZAP-70 Kinase Inhibitors against Psoriasis. *Journal of Medicinal Chemistry*, **2023**, *66* (17) , 12018-12032.
- 128) Uetrecht, J. Immune-mediated adverse drug reactions *Chem. Res. Toxicol.* **2009**, *22*, 24– 34.
- 129) Zhang, X.; Liu, F.; Chen, X.; Zhu, X.; Uetrecht, J. Involvement of the immune system in idiosyncratic drug reactions. *Drug Metab. Pharmacokinet.* **2011**, *26*, 47– 59.
- 130) Lanning, B. R.; Whitby, L. R.; Dix, M. M.; Douhan, J.; Gilbert, A. M.; Hett, E. C.; Johnson, T. O.; Joslyn, C.; Kath, J. C.; Niessen, S.; Roberts, L. R.; Schnute, M. E.; Wang, C.; Hulce, J. J.; Wei, B.; Whiteley, L. O.; Hayward, M. M.; Cravatt, B. F. A road map to evaluate the proteome-wide selectivity of covalent kinase inhibitors *Nat. Chem. Biol.* **2014**, *10*, 760– 767.

- 131) Krishnan, S.; Miller, R. M.; Tian, B.; Mullins, R. D.; Jacobson, M. P.; Taunton, J. Design of Reversible, Cysteine-Targeted Michael Acceptors Guided by Kinetic and Computational Analysis. *J. Am. Chem. Soc.* **2014**, *136*, 12624–12630.
- 132) Paul, G.; Shir, M.; Mike, B.; Julia, H.; Silke, K.; Amit, S.; Christian, D.; Ronen, G.; Jan, W.; Matthias, M.; Galit, C.; Ilana, B.; Khriesto, S.; Liat, A.; Efrat, R.; Haim, B.; Daniel, R.; Nir, L. Optimization of Covalent MKK7 Inhibitors via Crude Nanomole-Scale Libraries. *Journal of Medicinal Chemistry.* **2022**, *65* (15), 10341-10356.

Covalent Guanosine GNAS Inhibitors

Introduction

Natural Nucleosides

Nucleosides constitute a group of small intracellular compounds crucially involved in various biochemical processes. Primarily, they serve as the biochemical precursors to nucleotides, the fundamental building blocks of nucleic acids (DNA and RNA), which are responsible for transmitting genetic information¹. While both nucleosides and nucleotides are composed of a heterocyclic nitrogenous base (pyrimidine or purine) that are linked to a 5-carbon sugar through a β -N-glycosidic bond, the key difference is the presence of one to three phosphate groups attached at the 5' position of the pentose sugar. Nucleotides play essential roles in metabolic regulation, such as facilitating ATP-dependent phosphorylation of crucial metabolic enzymes, modulating enzyme activity through allosteric regulation by ATP, AMP, and CTP, and governing the rate of oxidative phosphorylation through ADP control¹.

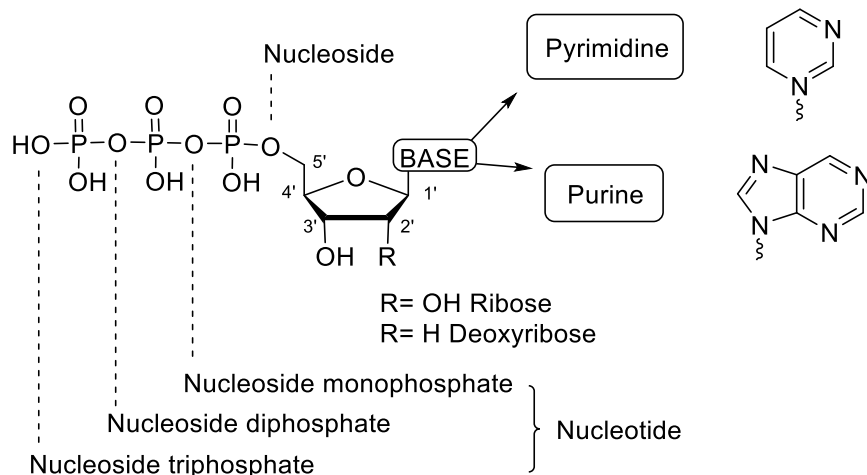


Figure 2.1 General structure of nucleosides and nucleotides

Purine and pyrimidines make up the two categories of nitrogenous bases found in DNA and RNA. The three pyrimidines are uracil (Ura), thymine (Thy), and cytosine (Cyt) and the two purines are guanine (Gua), and adenine (Ade). Presence of a hydroxyl substituent at the 2' position of the pentose sugar dictates whether it is D-ribose or 2-deoxy-D-ribose. D-ribose nucleosides and 2-deoxy-D-ribose nucleosides are labeled ribonucleosides and deoxyribonucleosides respectively. Ribonucleotides are the monomer units that make up RNA. These monomers consist of adenosine (Ado), guanosine (Guo), cytidine (Cyd), and uridine (Urd). Deoxyribonucleotides are the monomer units that make up DNA. These monomer units consist of deoxyadenosine (dAdo), deoxycytidine (dCyt), deoxyguanosine (dGuo), and thymidine (Thd).

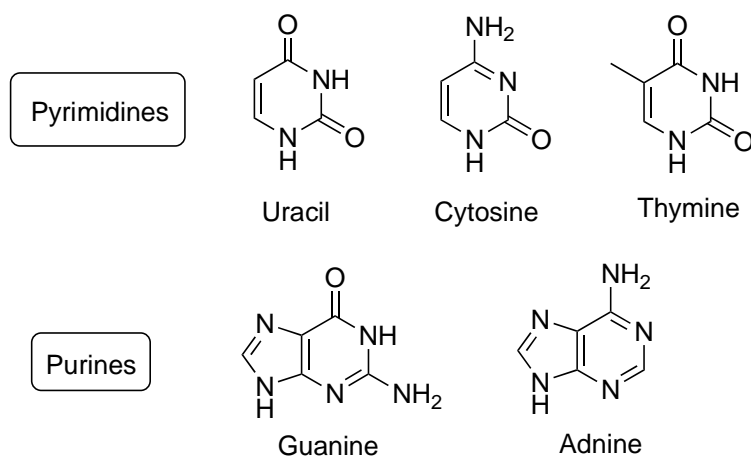


Figure 2.2 DNA and RNA nitrogenous bases

Mechanism of Action of Nucleoside Analogues

Therapeutic nucleoside analogues currently in use leverage the same metabolic pathways as naturally occurring nucleosides or nucleotides. NAs gain access to the cytoplasm by utilizing integral membrane proteins such as nucleoside transporters¹¹⁻¹². The first phosphorylation step is the rate-limiting step for pharmacological activation, and the nucleoside monophosphate can be dephosphorylated by 5'-nucleosidases (5'-NT)¹³⁻¹⁴. Additionally catabolic enzymes, such as deaminases, can decrease the amount of active metabolites². The incorporation of the second and third phosphates proceed smoothly to furnish the active nucleoside analogue 5'-triphosphate. Once endogenous kinase enzymes generate the di- and tri- phosphate form of the NAs, they accumulate and are available to be incorporated into the cancerous or virally infected cells, however they are susceptible to inhibition by enzymes involved in nucleotide metabolism such as Ribonucleotide reductase M1 (RR)². Active phosphorylated NAs that do not contain the 3' hydroxyl group prevent the formation of 3'-5' phosphodiester bond formation and lead to termination of chain elongation¹⁸. DNA damage sensors identify these occurrences and initiate survival mechanisms like cell cycle arrest and DNA repair. Nevertheless, if the extent of DNA damage surpasses the capacity of these processes, the sensors may also initiate signals for the apoptotic pathway¹⁵⁻¹⁷.

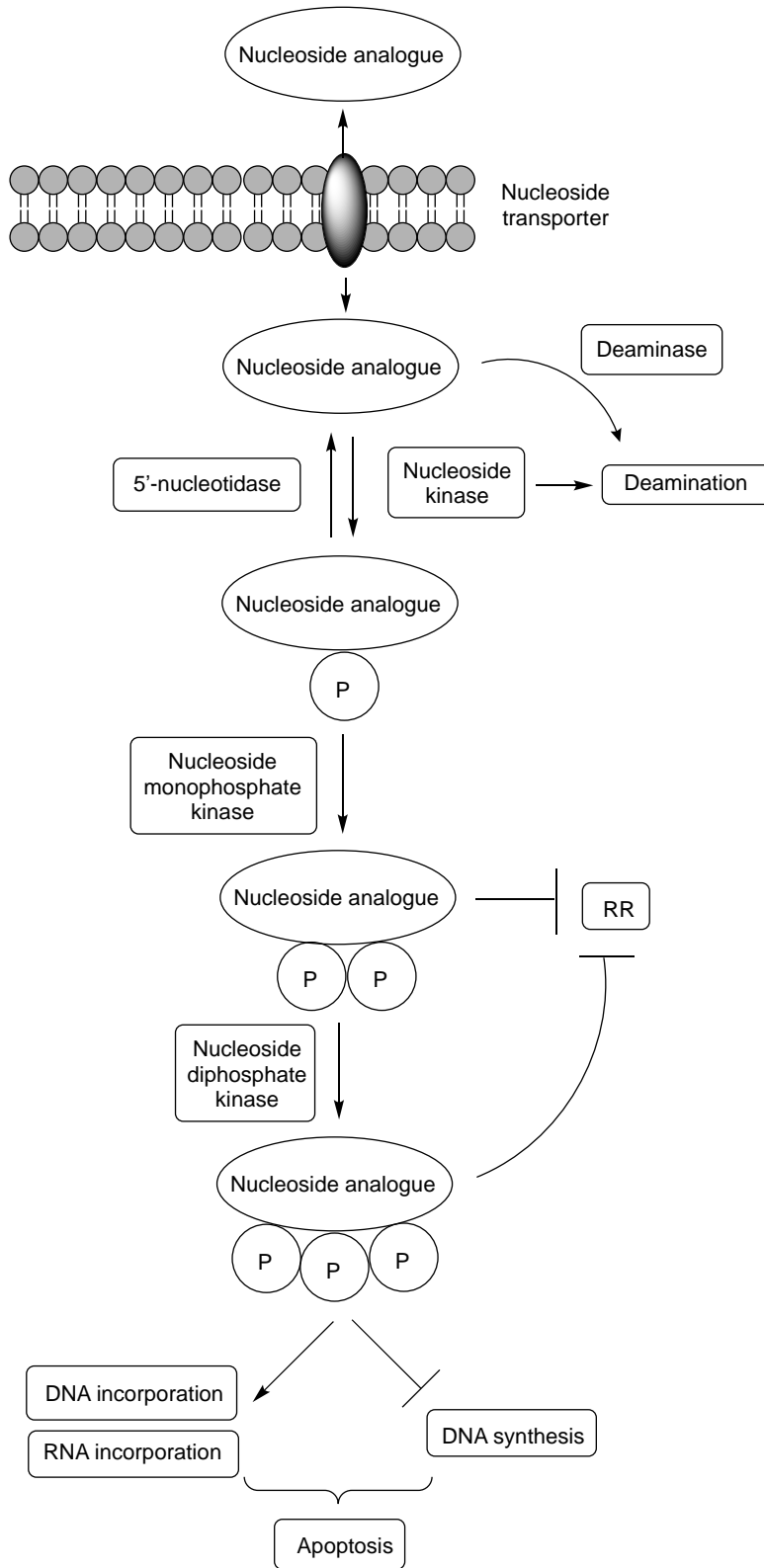


Figure 2.3 Nucleoside analogues mechanism of action

Anticancer Nucleoside Analogues

Due to the versatile mechanisms of action and proven track record as cancer therapeutics, the number of FDA approved purine and pyrimidine nucleobase and nucleosides is growing.

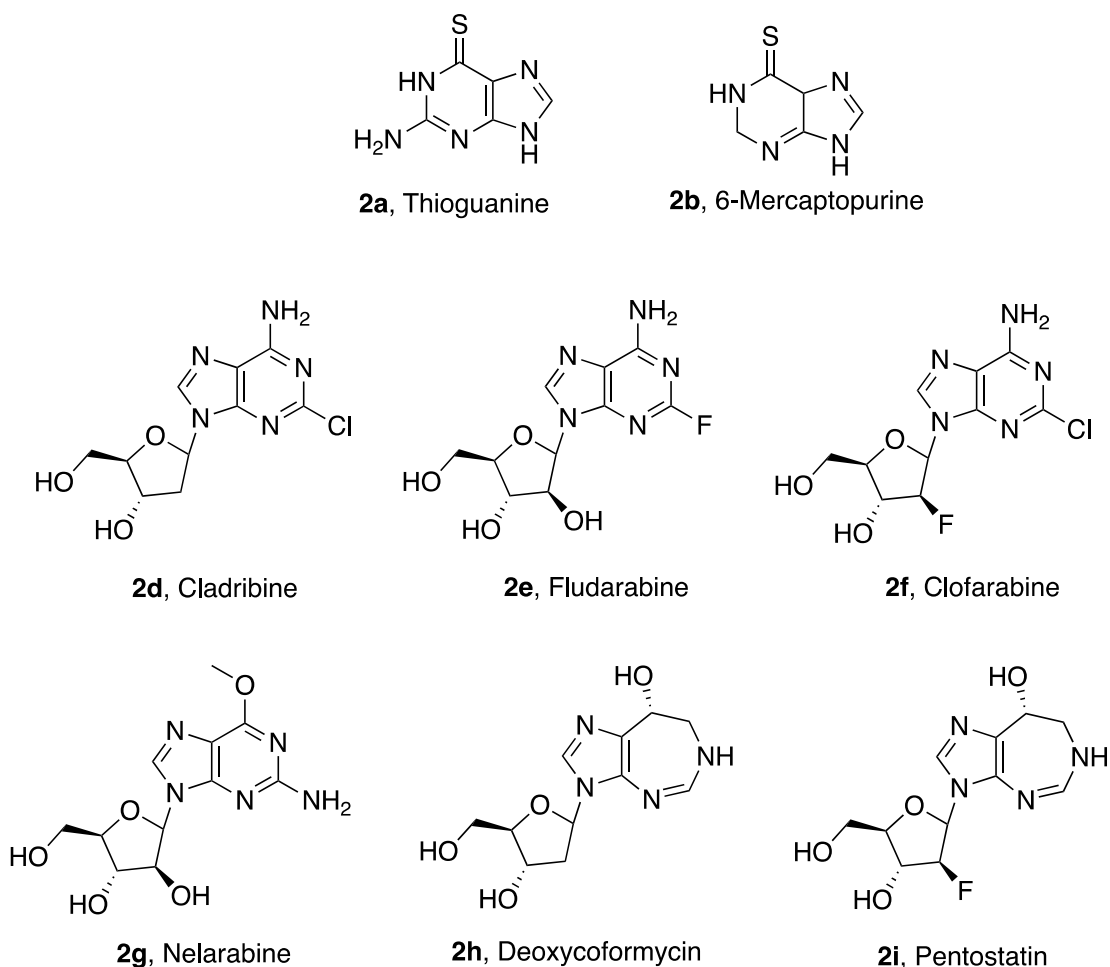


Figure 2.4 Anticancer purine nucleobases and nucleosides

Although more accurately described as nucleobases, thioguanine (6-TG, **2a**) can be viewed as a guanine derivative just as 6-mercaptopurine (6-MP, **2b**) is a derivative of hypoxanthine. These nucleobases become activated when hypoxanthine-guanine phosphoribosyl-transferase phosphorylates them generating the monophosphate that

will subsequently be converted into the triphosphates and be misincorporated into DNA¹⁹. Thiopurines play an integral role in the management of childhood acute lymphoblastic leukaemia¹⁹.

Cladribine (2Cda, **2d**), Fludarabine (FA, **2e**), and Clofarabine (CAFdA, **2f**), are adenosine derivatives. 2Cda shows cytotoxicity in both resting and dividing cells by incorporating its active triphosphate metabolite form into DNA²⁰⁻²¹. Both 2Cda and FA show resistance to deamination by adenosine deaminase (ADA)²². FA initiates the termination of chain elongation mediated by DNA polymerases α ²³. While CAFdA utilizes the same mechanisms of action as 2Cda and FA it was designed for improved efficacy. CAFdA showed improved plasma stability, higher cell retention, higher affinity for nucleoside transporters, and highest lipophilicity among purine analogs this next generation deoxyadenosine derivative and activity against DNA polymerase²⁴.

Nelarabine (**2g**) is a guanosine analogue functionalized with a 6-methoxy thereby increasing water solubility by 10x and generating a prodrug of arabinosylguanine (Ara-G). Adenosine deaminase is responsible for the conversion of nelarabine to the parent nucleoside Ara-G. Nelarabine was shown to be toxic towards T-lymphocytes and T-lymphoblastoid cells²⁵.

Deoxycoformycin (dCF, **2h**) is an effective treatment against hairy cell leukemia. As the exact mechanism of action has not been elucidated, it is speculated that dCF is an inhibitor of ADA resulting in increased levels of deoxyadenosine (dAdo) and adenosine (Ado) in the plasma. Down stream effects are seen through the accumulation of DNA strand breaks in lymphocytes, leading to the activation of p53, the release of cytochrome c from mitochondria, and ultimately triggering apoptosis²⁶.

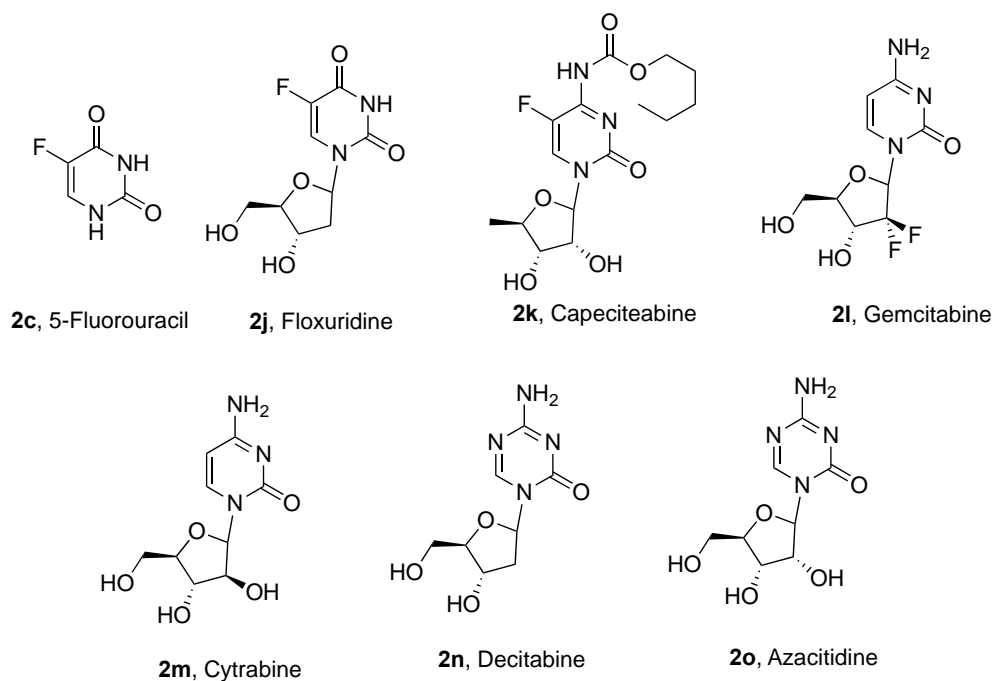


Figure 2.5 Anticancer pyrimidine nucleobases and nucleosides

The uracil nucleobase analogue 5-fluorouracil (5-FU, **2c**) is used for a wide range of cancers including colorectal, breast, and ovarian. In order to become activated 5-FU must be converted into one of the nucleoside forms like floxuridine (FUdR, **2j**). After a phosphorylation event the nucleotide forms can form covalent linkages with thymidylate synthase (TS) forming a quaternary complex and thus inhibiting the enzyme. The nucleotide triphosphate is produced through a series of enzymatic steps leading to inhibition of DNA synthesis and downstream function²⁷. Capecitabine (**2k**) is a 5-FU prodrug containing a liable carbamate group. This orally available fluoropyrimidine carbamate was designed to generate 5-FU in the liver by sequential metabolism by a carboxylesterase, deaminase, and lastly thymidine phosphorylase²⁷.

Although cytarabine (**2m**) does not show activity against solid tumors, is a common treatment used for haematological malignant diseases. Cytarabine cytotoxicity arises from direct inhibition of DNA polymerases and the incorporation of arabinosyl cytidine triphosphate (CTP) into DNA. This incorporation leads to chain termination and arrest of DNA synthesis¹⁹. Due to low affinity for deoxycytidine kinase and rapid elimination of the active triphosphate alternative deoxycytidine derivatives were explored.

Gemcitabine (**2l**) is a deoxycytidine derivative and one of the most active agents in cancer treatment and unlike cytarabine does have effect on solid tumors. It has shown activity among non-small cell lung cancer, pancreatic, bladder, and breast cancer. After crossing into the cell via nucleoside transporters and enzymatic transformation into the di (dFdCDP) and tri (dFdCTP) nucleotide forms, both of which are responsible for cytotoxic actions, it can be incorporated into the DNA and cause strand termination. Synergy between gemcitabine and several other antineoplastic agents has been observed in experimental models, indicating specific pharmacodynamic interactions²⁸.

Although decitabine (DAC, **2n**) and azacytidine (5-AC, **2o**) are structurally similar to the deoxycytidine analogues they induce altered physiological effects. The discovery that these compounds inhibit DNA methylation in human cell lines, offered a mechanistic explanation for their activity in modulating differentiation²⁹. After azanucleosides have been metabolized to 5-aza-2'-deoxycytidine-triphosphate, they can become substrates for the DNA replication machinery and will be incorporated into DNA. DNA methyltransferase recognizes the azacytosine-guanine dinucleotides as

natural substrates and the azanucleotide remains covalently bound leading to enzyme degradation³⁰.

Nucleoside and Nucleotide Analogues as Therapeutics

Apart from being monomers composing RNA and DNA, nucleoside and nucleotide compounds are fundamental to other biological processes such as cellular metabolism², cell signaling³, neurotransmission⁴, and regulation of cardiovascular activity⁵. Due to the widespread physiological utility of nucleoside and nucleotides, their chemical analogs, nucleoside analogs (NAs) are promising therapeutics.

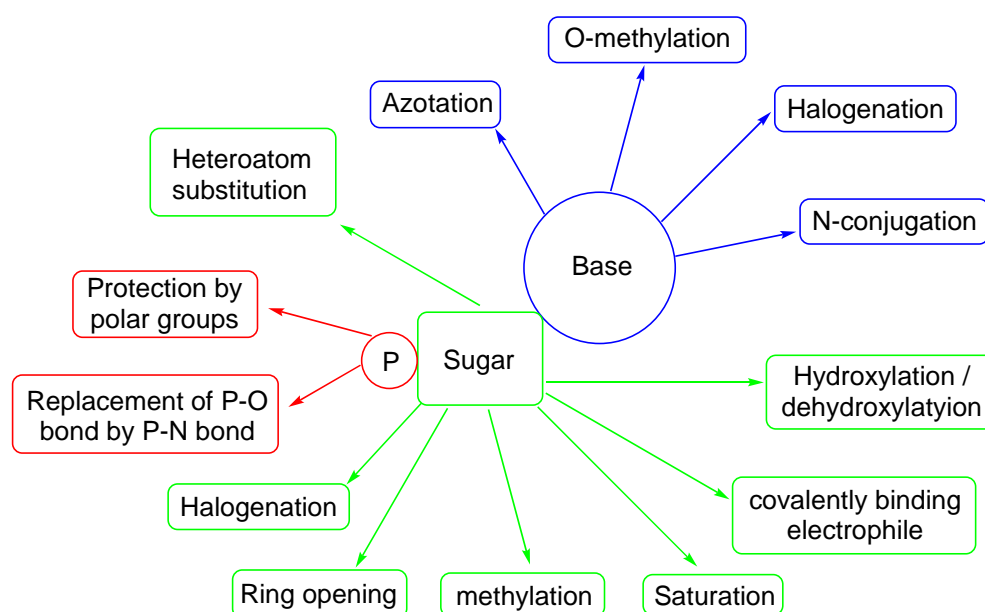


Figure 2.6 Modifications to the nucleobase, carbohydrate, and phosphate group

Nucleobases in which functional groups have been strategically moved or substituted, named pseudo-bases, can enhance stability by resisting the cleavage of the glycosidic bond and incorporate more or stronger intermolecular interactions. Even though slight alteration to the heterobase moiety is tolerated a close correlation to the endogenous counterpart is necessary to undergo cellular metabolism and be incorporated into nucleic acids. Drastic alteration to the heterobase has been shown to be associated with ineffectiveness against Tick-borne encephalitis virus (TBEV) and

cytotoxic effects⁶. A structure activity relationship study altering the substitutions at the 2', 3', and 4' positions of the sugar has shown low tolerance for substitution when tested against TBEV and cytotoxicity⁶. Chemical alteration to the sugar moiety has proved to alter both selectivity and effectiveness in both anticancer and antiviral agents⁷. While initial efforts to optimize NAs were focused on alteration to the nitrogenous base and sugar, much focus has shifted towards optimization of the phosphate group. Although various nucleoside and nucleotide analogs are currently used in clinical practice, there remains a necessity for the development of novel agents with enhanced properties to address challenges such as drug resistance⁸, limited oral bioavailability⁹, and long-term toxicity¹⁰. A review composed by Seley-Radtke and Yates describes the diverse structural variations to both heterobase and carbohydrate, examples of each, and their biological implications³¹.

Prodrug Strategy

Prodrugs are a biologically inactive component that convert into the active parent drug within the body. Used to treat dopamine deficiency in those who have Parkinson's disease, levodopa is the prodrug to the active component dopamine. Dopamine itself is not lipophilic enough to cross the blood-brain barrier (BBB) and so addition of a carboxy group increases its amino acid characteristics enough to enable transportation across the BBB using transporters of neutral amino acids (LAT1). Once across the BBB, levodopa is decarboxylated by the endogenous aromatic L-amino acid decarboxylase revealing the active drug dopamine³³.

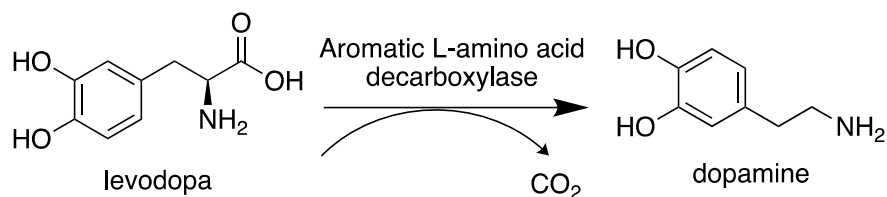


Figure 2.7 Endogenous decarboxylation of levodopa to dopamine

The ideal prodrug would address parameters including solubility, barrier permeability, good enzymatic and chemical stability, low toxicity, and efficient transformation to active metabolite in the desired cell³². Modification of drug's physio-chemical properties is a powerful, well-developed strategy in overcoming some of these problems³⁴⁻³⁵.

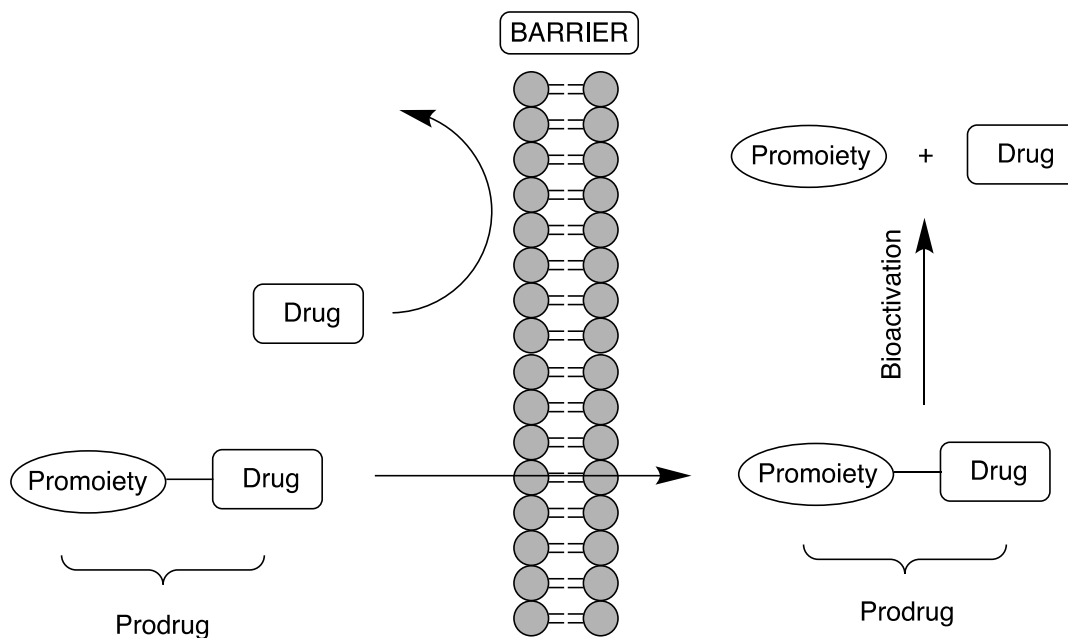


Figure 2.8 General depiction of the prodrug strategy

The prodrug strategy has been successfully applied to nucleoside analogs as the active triphosphates are too polar which hinders their translocation across cell membrane. In the process of nucleoside analog phosphate activation, the initial phosphorylation step is frequently recognized as the bottleneck. This recognition has prompted medicinal chemists to develop stable masked monophosphate nucleosides, enabling the delivery of nucleoside monophosphates into the cell³⁶. Addition of the first phosphate group circumvents the rate limiting step however at physiological pH, the monophosphate's anionic characteristic hinders cell membrane permeability. To overcome this issue numerous prodrug strategies have been developed increasing bioavailability by masking the negative charge. The masked monophosphate can now translocate to the intracellular environment, shed the masking components through bioactivation, and convert to the active triphosphate through endogenous enzymes.

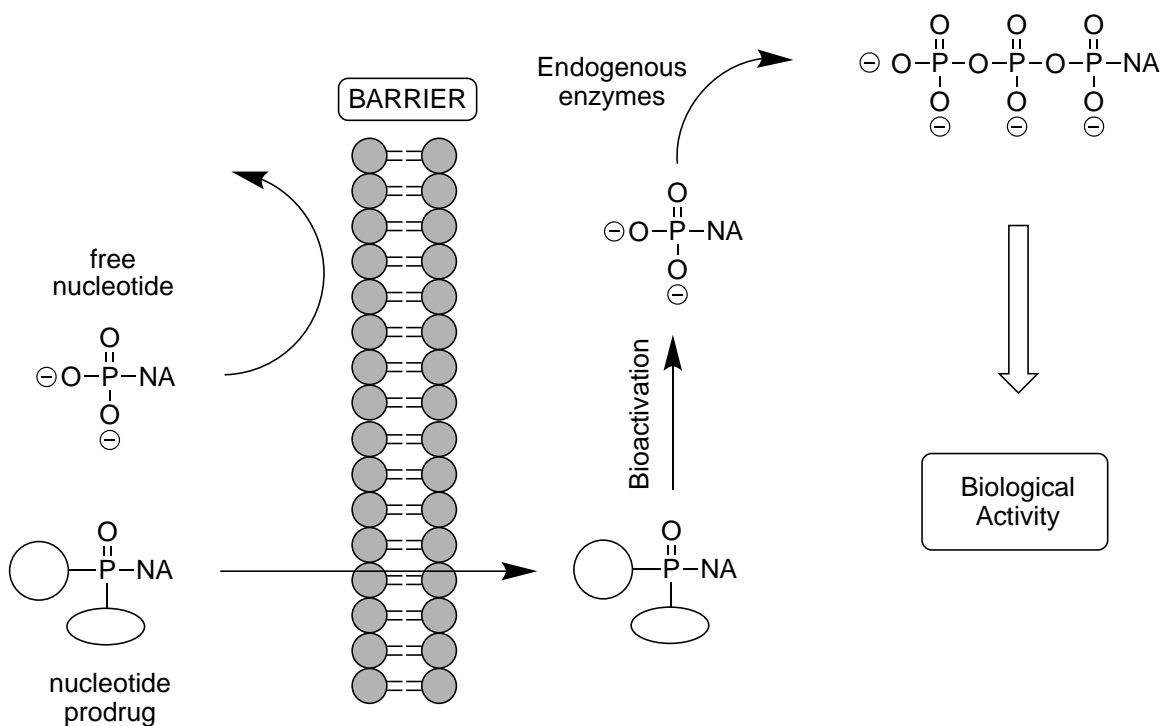


Figure 2.9 The pronucleotide “ProTide” strategy

In 1983 Farquhar published his investigations into the use of acyloxymethyl groups as biologically reversible phosphate protecting groups used to increase cell membrane permeability of nucleotides³⁷. This was the first published work using bis(carboxyloxymethyl) as a masking group. Since then both masking groups have shown to increase oral bioavailability⁴⁶⁻⁴⁷.

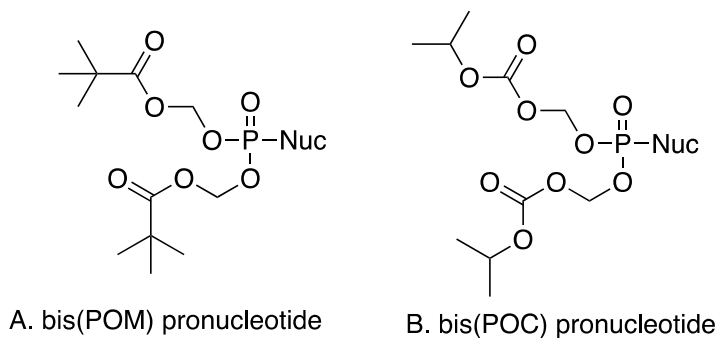


Figure 2.10 Generic structure of bis(POM) (A) and bis(POC) (B) pronucleotides

Utilization of the bis(POM) and bis (POC) groups have been applied many other nucleosides including tenofovir³⁸, acyclic nucleoside phosphonates adefovir³⁹, AZT⁴⁰, thymidine⁴¹, and 2',3'-dideoxyuridine (ddU)⁴². Adefovir dipivoxil (**2p**) is an orally available prodrug to adefovir which was discontinued in 1999 due to renal toxicity, yet gained FDA approval in 2002 for treatment of chronic HBV infections at decreased dosages⁴³. Tenofovir disoproxil fumarate (**2q**) is the prodrug to tenofovir used to treat HIV. It is also orally available and gained FDA approval⁴⁴. Also used as an HBV treatment, LB80380 (**2r**), has made it through phase II clinical trials⁴⁵.

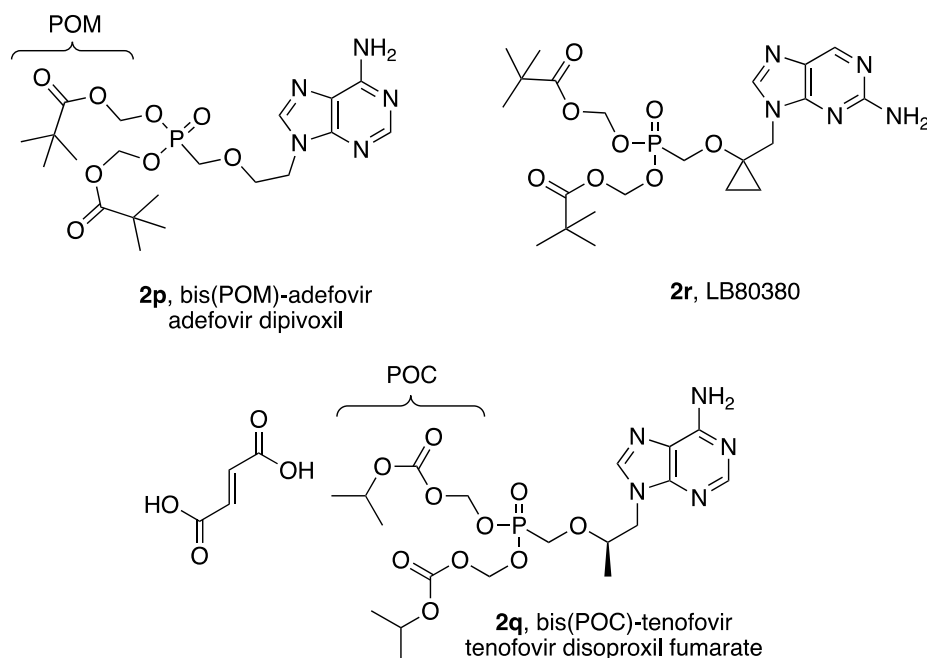
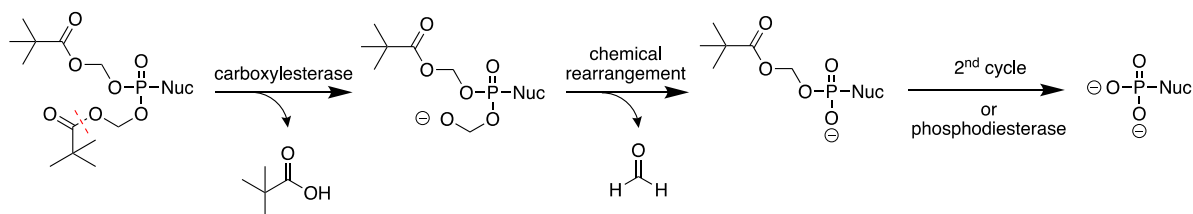


Figure 2.11 FDA approved POM and POC nucleotide prodrugs

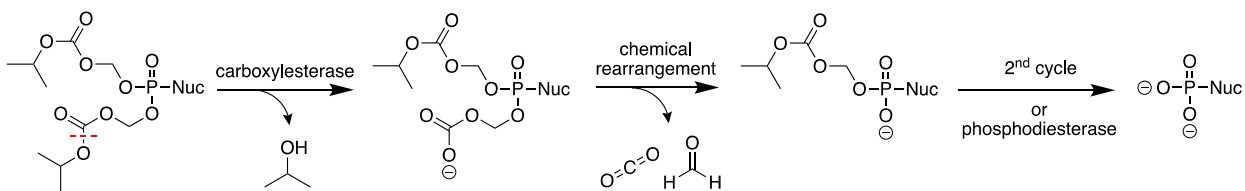
The first step in the bioactivation of bio(POM) prodrug cleavage of pivalic acid by a carboxylase leaving an unstable hydroxymethyl alcoholate intermediate. This unstable intermediate undergoes a chemical rearrangement liberating one molecule of formaldehyde resulting in the mono-ester form. After repetition of this cycle one more time, or by direct cleavage by a phosphodiesterase, the free monophosphate

nucleoside is formed. In the bioactivation of a bis(POM) protected analogue two molecules of pivalic acid and formaldehyde are released in the cell. These potentially toxic metabolites spurred the use of bis(POC) as a protecting group instead. Following a similar bioactivation pathway, a carboxylesterase catalyzes the release of one molecule of isopropanol. The unstable carbamate rearranges leading to the release of formaldehyde and carbon dioxide. Following a second cycle or by cleavage by a phosphodiesterase, the monophosphate nucleoside is free from masking groups. Although both bis(POM) and bis(POC) were successful in masking the phosphate group, their degradation generated potentially toxic metabolite in the cell. The need for a better solution is desirable.

A. Bioactivation pathway of bis(POM) pronucleotide



B. Bioactivation pathway of bis(POC) pronucleotide



Scheme 2.1 The endogenous activation mechanism of bis(POM) (A) and bis(POC) (B) pronucleotides

The synthetic approaches to carbonyloxymethyl phosphate nucleoside prodrugs can be seen in **Figure 2.12**. **A** shows the coupling of a nucleoside monophosphate with a halogenated carbonyloxymethyl derivative such as POM-Cl. The direct substitution of nucleoside alcohol and bis(POM)-Cl under basic conditions is shown by **B**. A Mitsunobu between the nucleoside and bis(POM)-OH is depicted by **C**. Iodination of the 5' position

of the nucleoside followed by substitution using the bis(POM) alkoxide salt can lead to the desired substitution product (**D**).

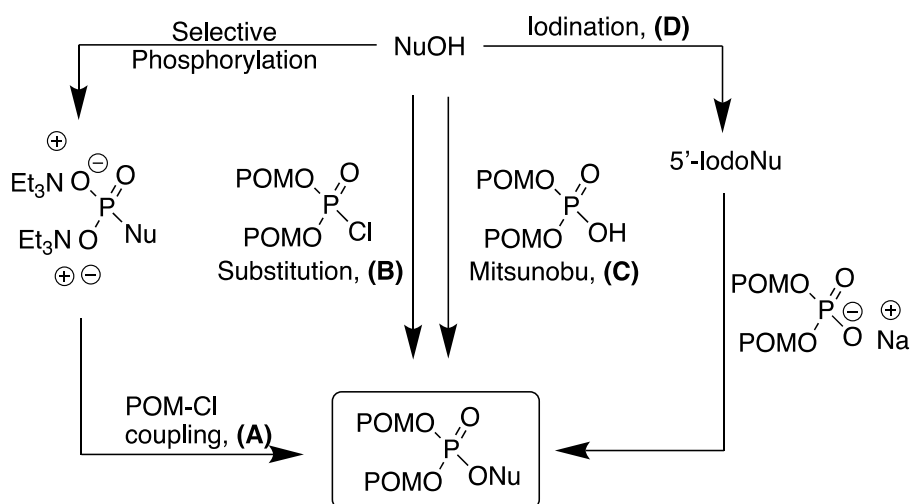
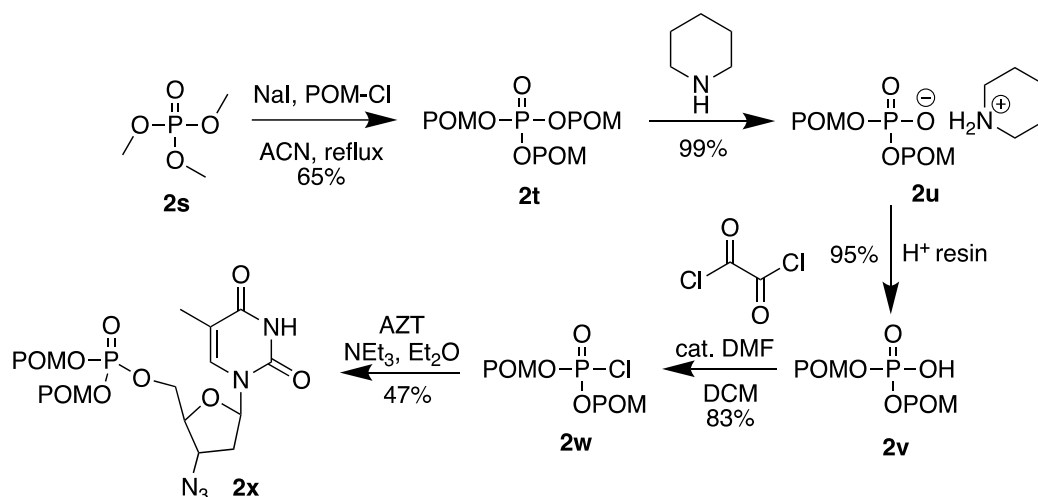


Figure 2.12 Common routes to access carbonyloxymethyl phosphate nucleoside prodrugs

In order to address the poor yields and reactivity seen from both routes **C** and **D**, Hwang and Cole develop a route utilizing the bis(POM)-phosphochloridate⁴⁸. **Scheme 2.2** shows the synthesis of the more reactive bis(POM)-chloridate (**2w**) starting from a common intermediate trimethylphosphate (**2s**). Refluxing **2s** with sodium iodide and chloromethyl pivalate in ACN yields the trisubstituted tri(POM) (**2t**) in 65% yields. Stirring **2t** in piperidine gives rise to the piperidine salt (**2u**) that leads to the bis(POM)-OH intermediate (**2v**). This intermediate can be used as seen in **C**, taking advantage of the Mitsunobu reaction or be further processed into the increasingly reactive bis(POM)-Cl (**2w**). Coupling **2w** and AZT in a basic environment led to the desired AZT bis(POM)-monophosphate prodrug **2x** in a 47% yield.



Scheme 2.2 Hwang and Cole's route to bis(POM)-phosphochloridate

A more recent phosphorous masking strategy that does not introduce a potentially toxic metabolite to the intracellular environment is seen through the aryloxyphosphoamidates, also known as ProTides. The first description of this strategy came from the pioneering work of Chris McGuigan and coworkers seen through its application on AZT⁴⁹⁻⁵⁰. The general structure of a ProTide can be seen in **Figure 2.13**. The phosphorous atom contains an amino acid alkyl ester and an aryloxy group which mask the negative charges of the monophosphate nucleoside. Presently the ProTides are generally synthesized as diastereomeric mixtures, however there is a great surge in research efforts to enable the generation of single enantiomers of the ProTide nucleotide analogues.

INX189 (**2aa**), a deoxyguanosine phosphoamidate analogue, was the leading antiviral compounds developed by McGuigan's group. Sofosbuvir (**2z**) was originally developed by the company Pharmasset, however it was acquired by Gilead and gained FDA approval in 2013 as a treatment of HCV infections⁵⁴. Gilead Sciences also developed compound **2y** known as Remdesivir. Although being an inhibitor of RNA-

dependent RNA polymerase and being used as a treatment for COVID-19⁵¹ it did not meet efficacy endpoints in clinical trials for the treatment of Ebola virus⁵². Even though the FDA utilized an emergency authorization approval in 2020 the world health organization (WHO) recommended against the use of Remdesivir regardless of disease severity⁵³.

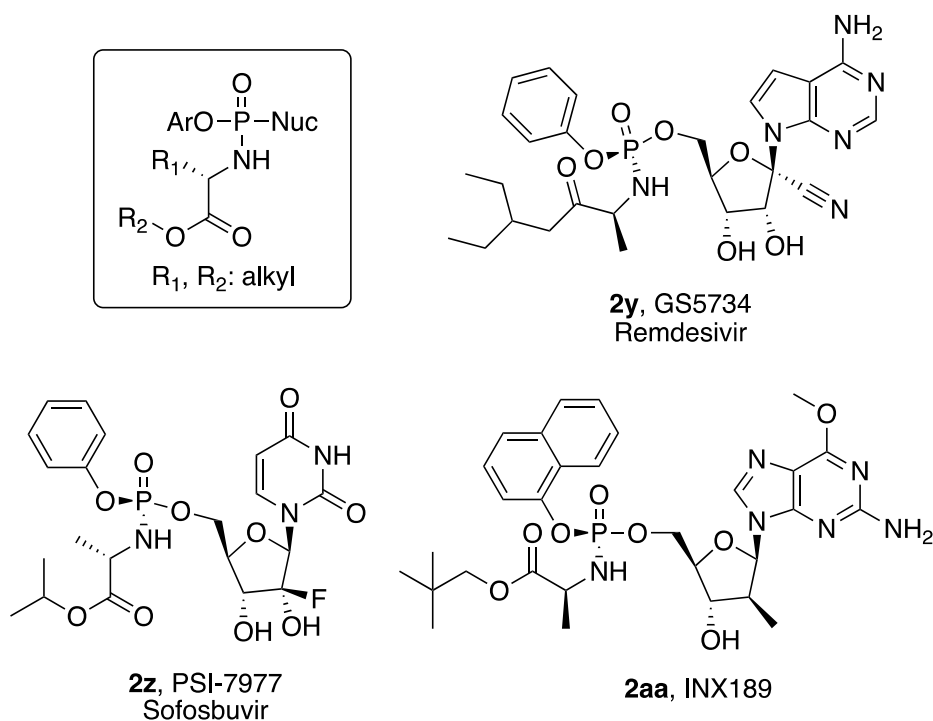
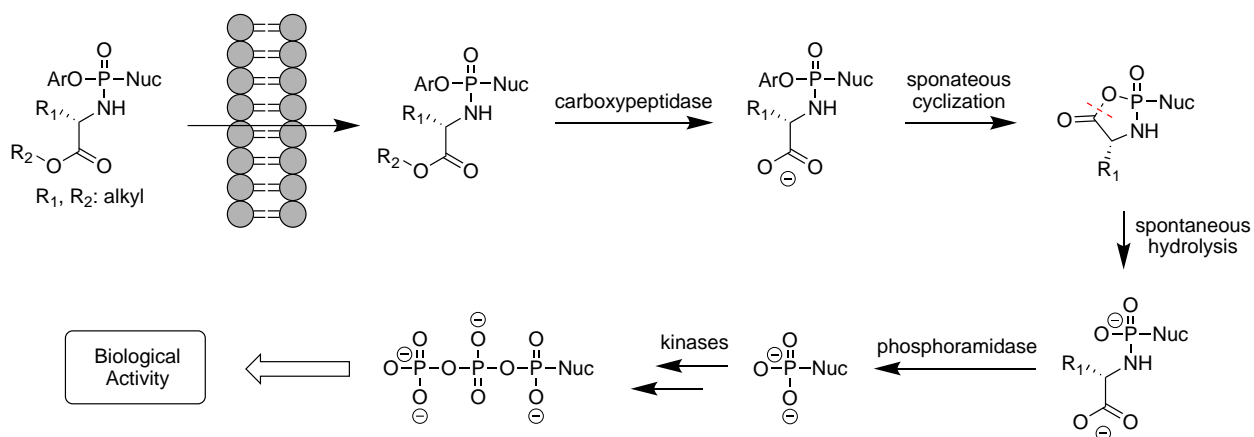


Figure 2.13 Generic phosphoramidate structure and FDA-approved nucleoside protides

Scheme 2.3 shows the proposed biochemical activation. Although the fully elucidated mechanism is not known, much research has led to this current understanding⁵⁵⁻⁵⁶. Unlike the carbonyloxymethyl phosphate nucleoside prodrugs, the Protide nucleotide prodrugs can pass the cell membrane through diffusion⁵⁶. After crossing the cell membrane endogenous carboxylic-ester hydrolases or carboxypeptidase enzymes catalyze the ester cleavage leading to a carboxylate intermediate⁵⁷. Spontaneous cyclization proceeding through an addition-elimination

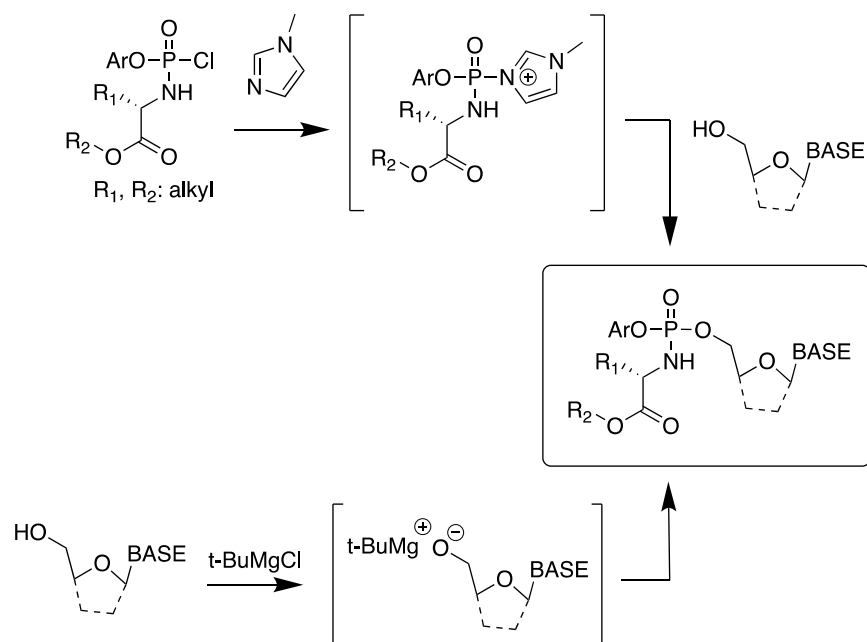
reaction generates the transient cyclized intermediate. The combination of mass spectrometry and ion spectroscopy showed the first experimental evidence of this elusive intermediate⁵⁸. Hydrolysis of the cyclic anhydride leads to a phosphoramidate diester. Cleavage of the P-N bond by phosphoramidase enzymes leads to the parent monophosphate nucleoside. Subsequent phosphorylations generate the triphosphorylated nucleotide which can generate the biological effect.



Scheme 2.3 The endogenous activation mechanism of aryloxyphosphoramidates pronucleotides

Even though recent efforts have given methods to leading to enantiopure phosphoramidate nucleosides, these methods rely on intricate chiral auxiliaries⁵¹, costly catalysts⁵⁹, or microwave reactors⁶². Most preparations of phosphochloridates generate 1:1 mixtures of R_p and S_p diastereomers. Subsequent reaction of diastereomeric phosphochloridates with enantiopure nucleosides generates the formation of two diastereomer products which are notoriously difficult to separate by chromatography and crystallization methods. **Scheme 2.4** shows the two main reaction conditions used to attach phosphochloridates to nucleosides. First seen in the synthesis of AZT aryloxyphosphosmidate prodrug, McGuigan laid the path for the synthesis of many other ProTide analogues⁶⁰⁻⁶¹. In the NMI-mediated coupling, *n*-methylimidazole forms

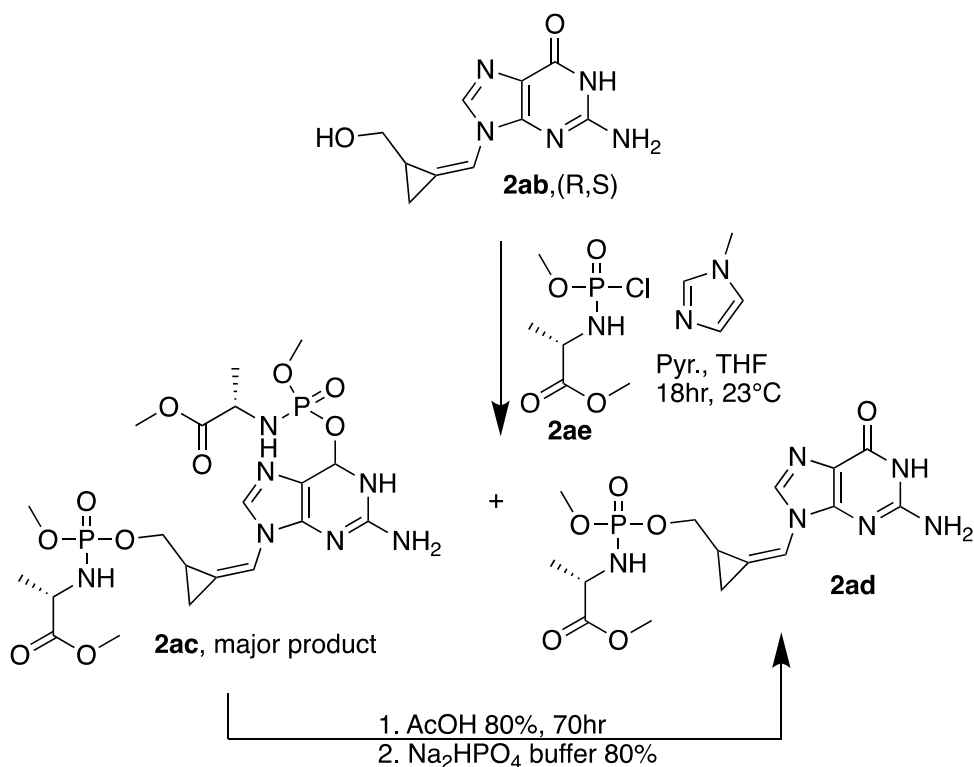
an activated imidazolium intermediate than can be attacked by the 5' hydroxyl of the nucleoside⁶³. The second method incorporates tert-butyl magnesium chloride as a strong base to deprotonates the 5' hydroxyl forming an alkoxide that participates in a substitution reaction with the phosphochloridate. In both methods the reaction is substrate dependent leading to unpredictable outcomes.



Scheme 2.4 Main pathways to conjugate phosphochloridates and nucleosides

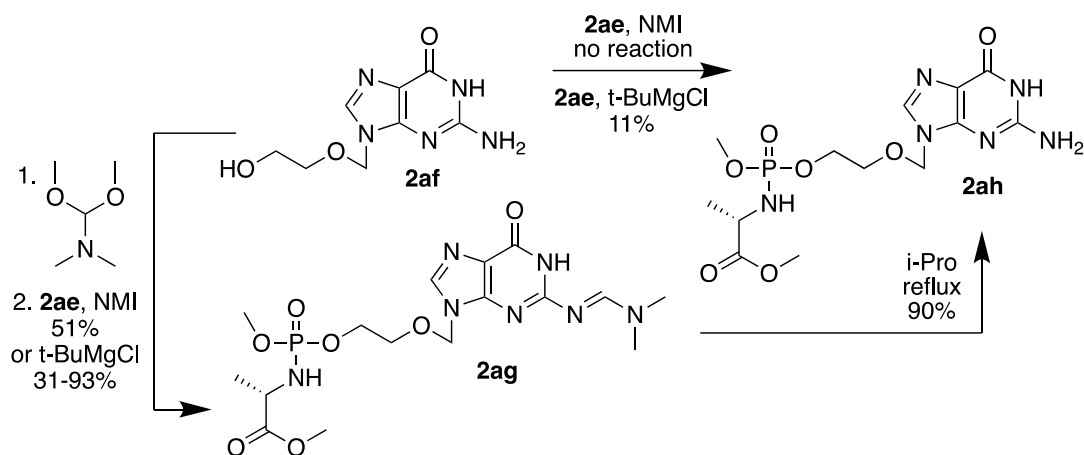
Factors that impact reaction efficiency include the presence of other free hydroxyl on the carbohydrate backbone and the nature of the heterobase. The presence of multiple free hydroxyl groups can lead to the mono and di-substituted phosphorylation products. While a mixture of 5'-mono and 3',5'-disubstituted products can be separated by chromatography, the regioisomers 3' and 5'-mono phosphorylated products are generally inseparable⁶⁴⁻⁶⁶. The reactivity of the heterobase also impacts the efficiency which the ProTide can be incorporated onto the nucleoside. While uridine and adenine are well behaved in both methods, it is nucleobases with competitive nucleophiles

where challenges arise. **Scheme 2.5** shows the case where a guanosine analog **2ab** has competitive reactivity at the amide's carbonyl oxygen. Difunctionalization at both the 5' hydroxyl and O⁶ position has been proven to be the major product in many nucleosides⁶⁷ as shown in **2ac**. A subsequent hydrolysis step under acid conditions led to the desired monophosphorylated ProTide **2ad**. Not only does competitive O⁶ phosphorylation impact guanosine like heterobases efficiency but their low solubility lead NMI-mediated reaction to fail⁶⁸. Methylation at the O⁶ position prior to coupling with phosphochloridates increases solubility and protects from phosphorylation at this position. **2aa** is an example of a deoxyguanosine ProTide analogue with an O⁶ methylation.



Scheme 2.5 Competitive O⁶-phosphorylation and hydrolysis

Increasing solubility and mitigating N⁴ reactivity, use of a protecting group may be necessary. McGuigan⁶⁹ opted to utilize the N²-dimethylformamide protection group after failing to phosphorylate acyclovir (**2af**) via the NMI-mediated coupling pathway and only yielding 11% by the grignard route. N²-dimethylformamide protection of acyclovir yielded the monophosphorylated intermediate in as much as 93% yield. Subsequent deprotection by reflux in isopropanol generated a 90% yield however much of the product is lost to multiple purification steps. Nevertheless, protection of competing reactive sites produced the desired acyclovir aryloxyphosphoamidate prodrug (**2ah**) in higher yields than direct phosphorylation.



Scheme 2.6 Masking the competitive 2-NH₂ with the dimethylformamide group

G-Protein Coupled Receptors (GPCRs)

G-protein coupled receptors are one of the largest and most diverse families of membrane proteins found in eukaryotic cells. Interaction with extracellular chemical messengers induce a complex chain of events linked to signal transduction.

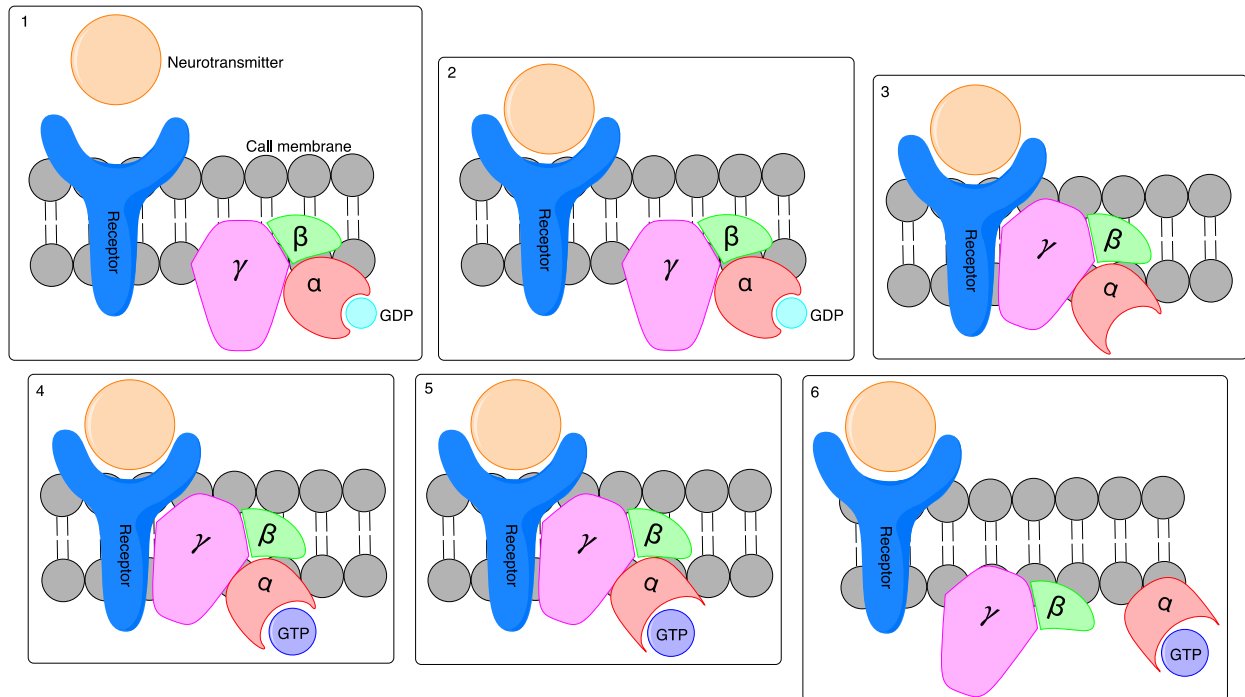


Figure 2.14 Extracellular activation and signal transduction through a G-protein coupled receptor

Figure 2.14 shows the activation of G-protein coupled receptors and its interactions with G-proteins. Box 1 shows an activator compound, such as a neurotransmitter, that is on the outside of the cell binding to the transmembrane GPCR. A conformation change in the receptor generates a binding site for the G-proteins. Once the G-proteins have interacted with the newly formed binding site, conformational change to the guanyl binding site causes the $G\alpha$ subunit ($G\alpha_s$) to release Guanosine diphosphate (GDP). Box 4 shows that the guanyl binding site does not stay empty yet is now the correct shape to bind guanosine triphosphate (GTP). The binding on GTP

induces a conformation shift in the $G\alpha$ which weakens its attraction with the β ($G\beta$ s) and γ ($G\gamma$ s) subunits. Box 6 shows the dissociation of all G-proteins from the receptor, however $G\beta$ s and $G\gamma$ s remain dimerized as a complex, $G\beta\gamma$ s, and $G\alpha$ s dissociates entirely still bound to GTP.

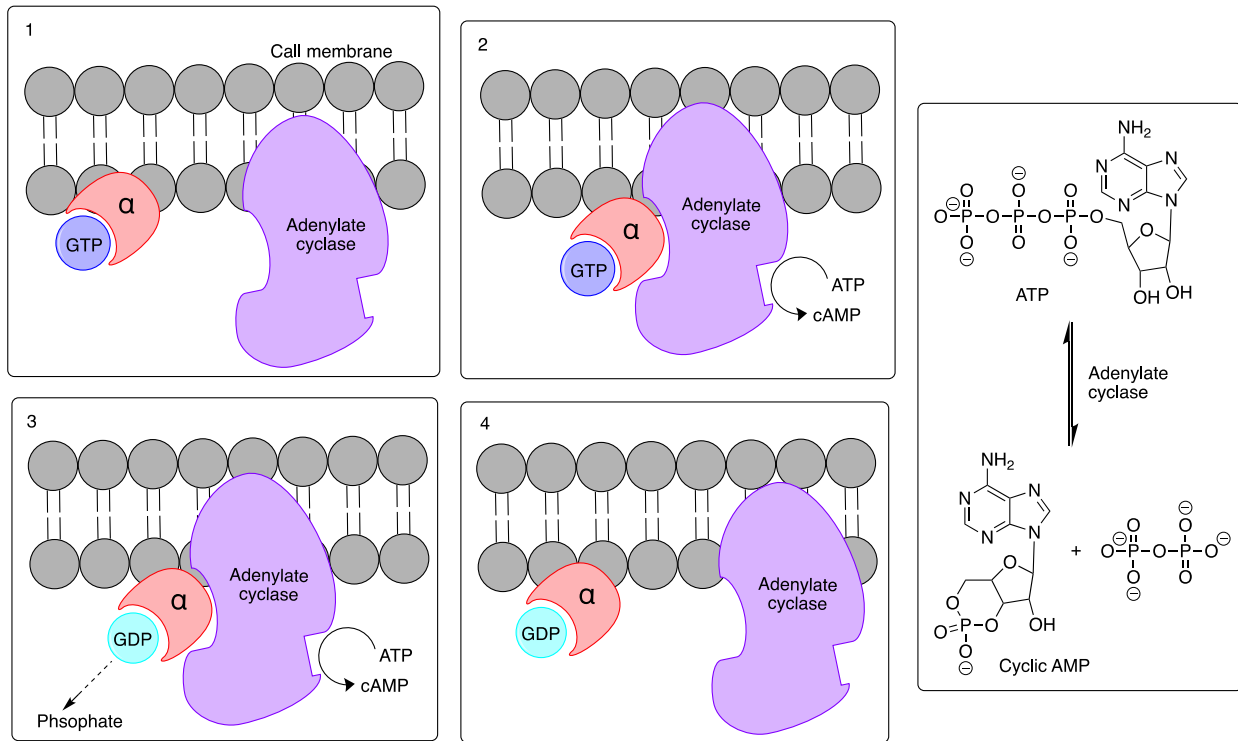


Figure 2.15 Interaction of $G\alpha$ s and adenylate cyclase leading to intracellular signal transduction as well as conversion of ATP to cAMP

Figure 2.15 shows the interaction of the $G\alpha$ s with adenylate cyclase and the synthesis of cyclic AMP (cAMP). $G\alpha$ s still bound to GTP can interact with adenylate cyclase another membrane bound protein. The binding of $G\alpha$ s and GTP activates a proximal catalytic site on adenylate cyclase which subsequently converts adenosine triphosphate (ATP) to cAMP. cAMP is a secondary messenger, a molecule that moves into the cytoplasm and continues the signal transduction. As long as $G\alpha$ s is bound to adenylate cyclase the conversion of ATP to cAMP will occur generating an amplification

effect. The $G\alpha_s$ can hydrolyze GTP back to GDP which finally deactivates adenylate cyclase.

Gas^{R201C} as a Target to Modulate Tumorigenesis

The GNAS gene, responsible for encoding the Gas subunit of heterotrimeric G proteins, exhibits the second highest mutation frequency in mucinous appendiceal adenocarcinoma (AA), occurring in approximately 50% of tumors, and in Pseudomyxoma Peritonei (PMP), affecting around 75% of tumors. In non-mucinous AA, it ranks third, observed in roughly 25% of tumors. These statistics show its potential as a promising target for therapeutic intervention in addressing this rare medical condition⁷⁰. As GNAS has been identified to play a key role in oncogenic processes in various cancers including gastric adenocarcinoma⁷¹, pancreatic⁷², colon⁷³, appendiceal⁷⁴, as well as others⁷⁵. Despite being traditionally considered as druggable targets, there are currently no commercially available inhibitors specifically targeting Gas. Additionally GNAS^{R201} stands out because it is the most cancer-causing mutation of all heterotrimeric G-proteins⁷⁶. For these reasons chemical modulation of G α s is a promising strategy.

The point mutation GNAS^{R201C} has been shown by Dr. Shen at the MD Anderson Cancer Center to significantly increase tumor growth in Ls174T cells. With use of his self-developed software Pocket Finder⁷⁷⁻⁷⁸, Dr. Ruben Abagayan utilized x-ray crystallographic structures of GDP bound to GNAS^{R201C} to identify a druggable site⁷⁹. It was discovered that cysteine 201 is close enough to the GDP binding site in order to utilize target covalent inhibitors to inhibit the mutated Gas. **Figure 2.16** shows GDP (on left) bound to GNAS^{R201C} and for comparison a covalent guanosine analog containing an electrophilic epoxide ingrained in the carbohydrate structure. The epoxide has demonstrated close enough proximity to form a covalent linkage with cysteine 201. The

Abagayan lab used Molsoft ICM software to model both GDP and the guanosine-epoxide ligands within the GNAS^{R201C} binding site⁷⁷⁻⁷⁸.

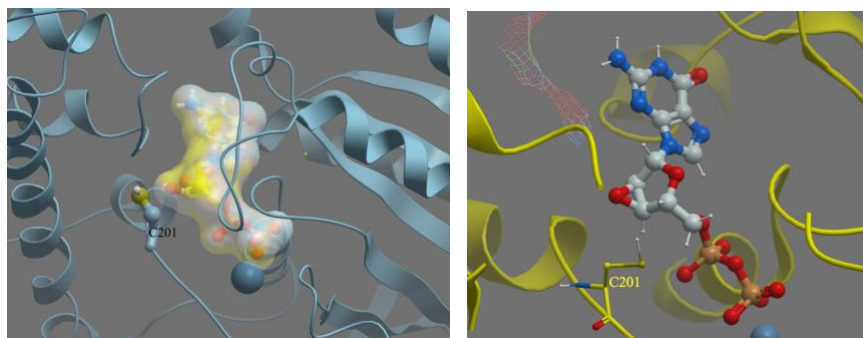
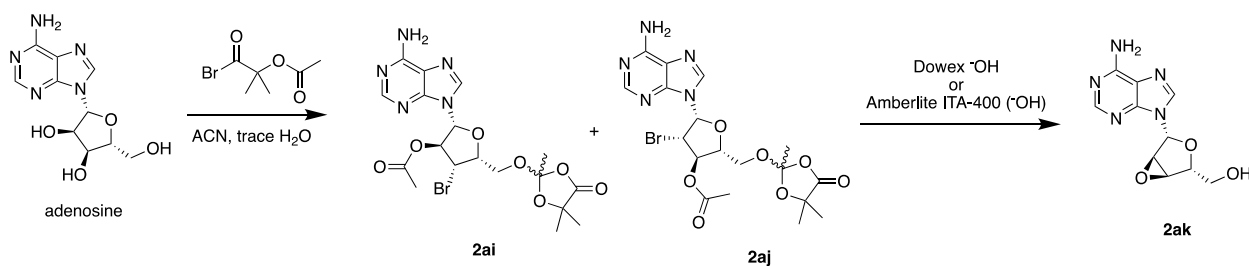


Figure 2.16 GDP and guanosine-epoxide bound to the GNAS^{R201C} active site

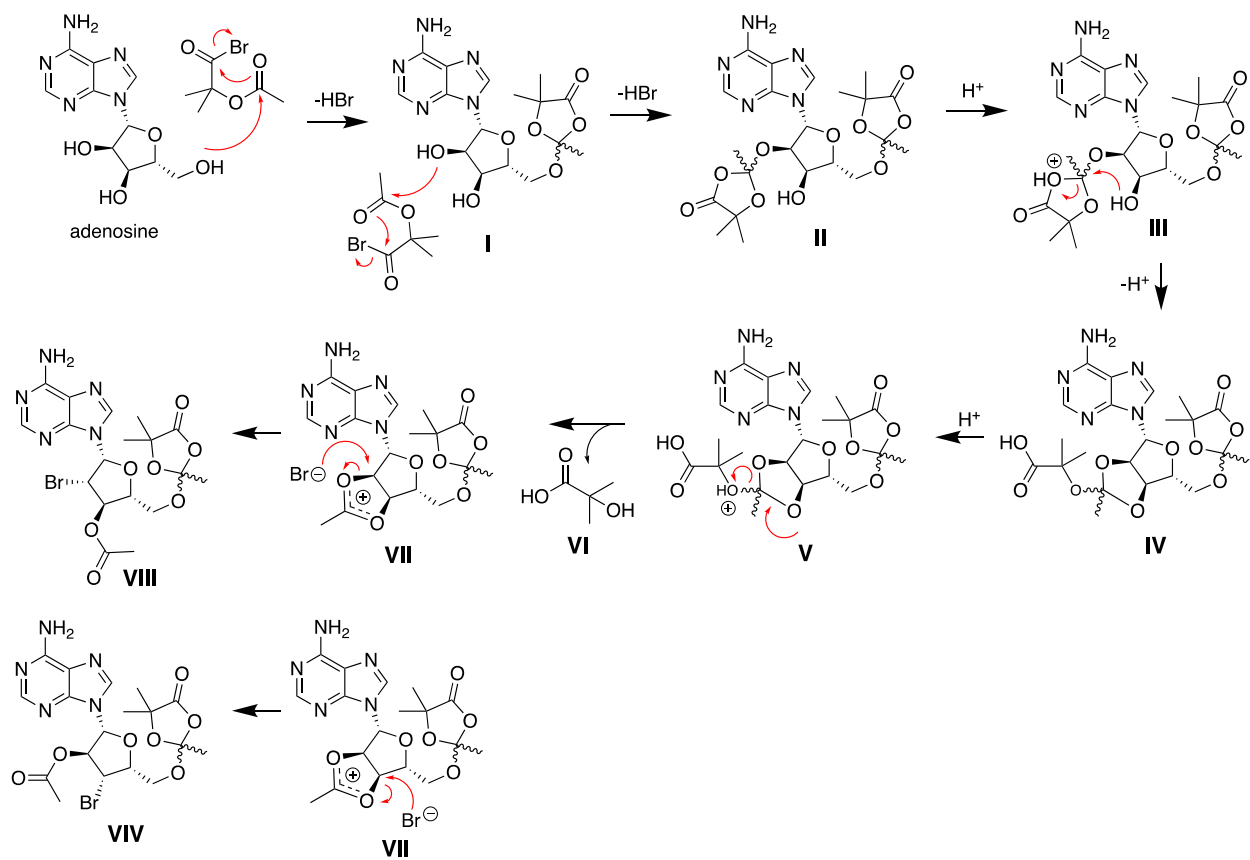
An early example of generating an electrophilic epoxide on the carbohydrate of a nucleoside comes from Morris Robins⁸⁰ seen in **Scheme 2.7**. Adenosine, as the starting material, was subjected to 4 molar equivalents of α -acetoxyisobutryl bromide in ACN with trace amounts of water (10:1). These reaction conditions yielded both regioisomers **2ai** and **2aj**. This crude reaction product was treated with hydroxide bound resin, leading to the formation of the epoxide. Others have successfully applied the same synthetic scheme to other nucleosides⁸¹⁻⁸⁴.



Scheme 2.7 Traditional route to generate epoxide on carbohydrate of nucleoside

Moffatt was the first to use α -acetoxyisobutryl halides on diols imbedded in nucleosides which is an abnormal Mattocks reaction⁸⁵⁻⁸⁷. It was found that α -

acetoxyisobutryl chloride in hot ACN led to cleavage of the glycosidic bond, while utilization of the more reactive α -acetoxyisobutryl bromide in room temperature solvent generated the desired product. *cis*-Cycloalkane-1,2-diols are converted into *trans*-2-bromocycloalkyl acetates with inversion of one stereocenter. **Scheme 2.8** shows the proposed mechanism through which this abnormal Mattocks reaction proceeds. Adenosine's primary alcohol acts as a nucleophile adding into the ester of α -acetoxyisobutryl bromide. Electrons flow to the acid bromide eliminating a bromide ion. The same reaction takes place at one of the sugar alcohols generating an intermediate (**II**) containing two dioxalone moieties. An acid catalyzed rearrangement leads to the elimination of 2-hydroxy-2-methylpropanoic acid (**VI**) resulting in the formation of acetoxonium ion intermediate (**VII**). Depending on which carbon is attacked by a bromide ion both *trans*-2-bromocycloalkyl acetates isomers **VIII** and **VIV** are formed.



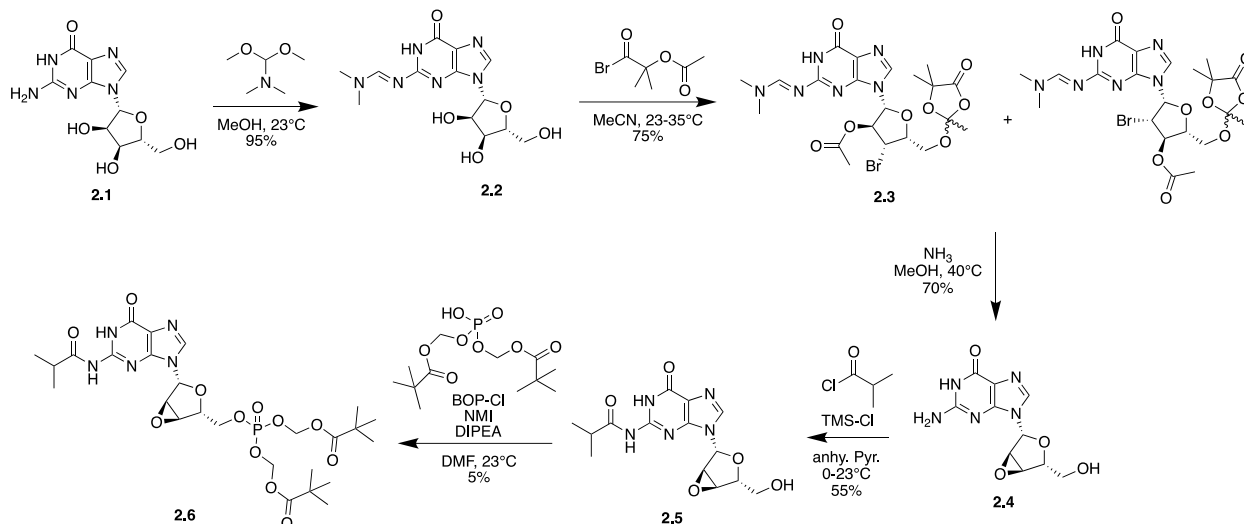
Scheme 2.8 Proposed mechanism through which the abnormal Mattocks reaction proceeds

Results

Synthesis of Guanosine-Epoxyde and its Prodrug

Although adenosine could be reacted directly with α -acetoxyisobutryl bromide, guanosine was unreactive in the 0-23°C temperature range which was also encountered by Gong-Xin He from the Gilead group⁸³. Guanosines low solubility in organic solvents may be blame. Additionally, a complex mixture of products at elevated temperatures was also encountered like what Lei Zhang encountered⁸⁸. The 2-NH₂ group on the purine is an additional reactivity center leading to unintended products. To address the reactivity and solubility issues unique to guanosine, it was reacted with N,N-dimethylformamide dimethyl acetal in methanol yielding the more soluble intermediate (**2.2**) bearing a methylene dimethylamine protecting group. This heterogeneous reaction allowed for the easy purification by filtration and generated a high yield of 95%. Now that **2.2** contains a 2-NH₂ protection group it is suitable of the abnormal Mattocks reaction. **2.2** was stirred at room temp in neat α -acetoxyisobutryl bromide overnight at room temperature. The next day the reaction was heated to 35°C with ACN until the solution went clear (15-30min) at which time the reaction was worked up with NaHCO₃ and purified on a silica column to yield **2.3** and its regioisomer in a 75% yield. Following the many literature examples⁸⁵⁻⁸⁷, **2.3** was stirred in resin bound hydroxide which yielded the desired product **2.4**, however it led to unsatisfactory yields. Although the same reaction conditions described by Zhang⁸⁸ and Porcari⁸⁹ are reported to give different products, utilization of this method produced the intended product **2.4**. Stirring **2.3** with 7M methanolic ammonia in a pressurized round bottom overnight

removed all protecting groups and led to the formation of the epoxide in 70% yield after purification of C18 silica column.



Scheme 2.9 Reaction path to guanosine-epoxide and its prodrug

Following McGuigan's strategy to increase solubility and mitigate competitive reactivity at the N⁴ amine the isobutryl group was installed. Yupeng Fan describes a convenient method to install acyl protecting groups to the amine of guanosine⁹⁰. This method firstly utilizes TMS-Cl for the transient protection of the oxygen atoms, followed by the introduction of an acid chloride which reacts at the desired amino group. Both classic method (NMI- coupling and t-BuMgCl) to introduce carbonyloxymethyl masked phosphate through bis(POM)-Cl failed. A thorough optimization effort altering conditions including solvent, base, temperature, equivalents was fruitless. Interestingly activation of bis(POM)-OH with BOP-Cl and NMI in the presence of DIPEA did generate the desired carbonyloxymethyl phosphate guanosine prodrug **2.6**. Although the yield was extremely poor, scale up of material was enough to provide sufficient material to attempt cleavage of the isobutryl protection group.

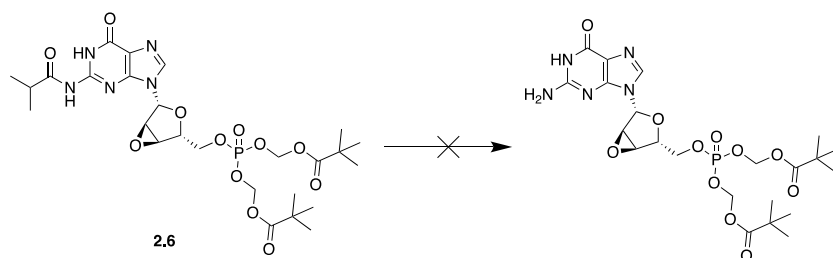
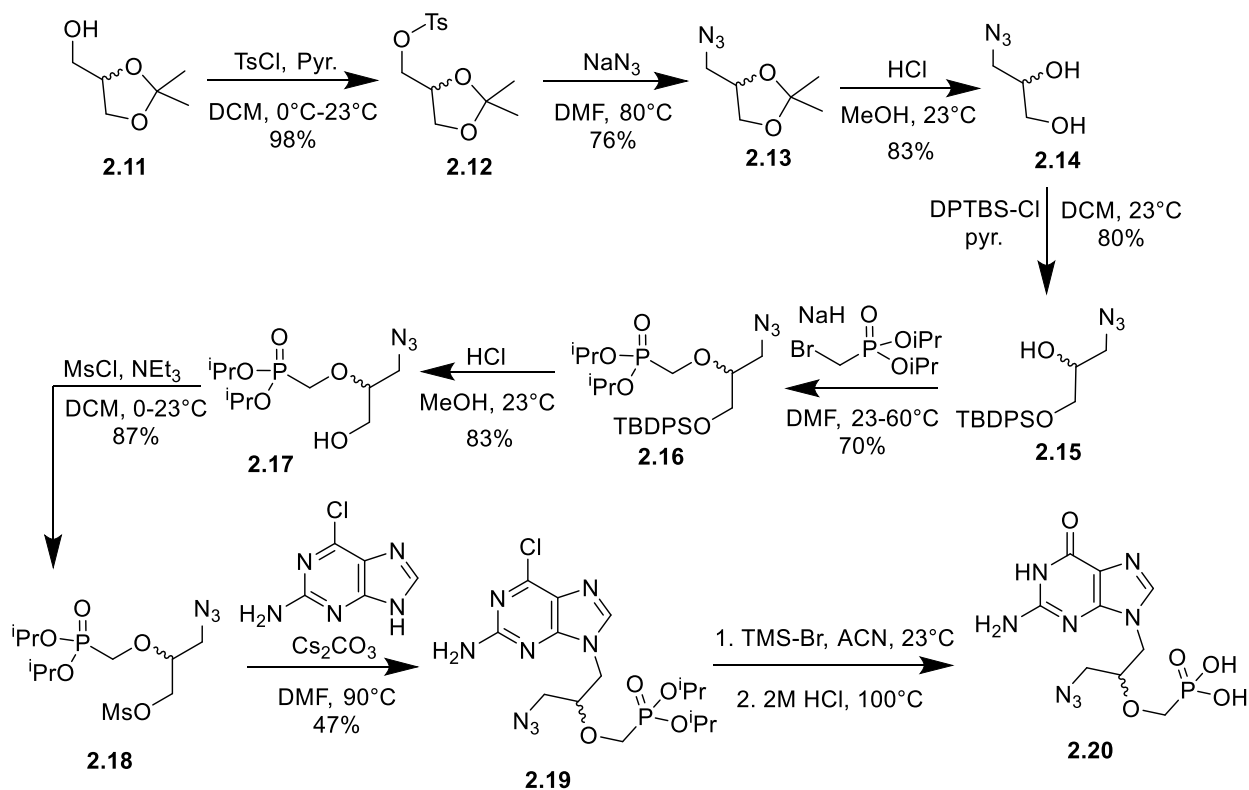


Figure 2.17 Deprotection of isobutryl amide (**2.6**) failed

Deprotection of the isobutryl protected amine was attempted using a variety of conditions. Attempting an optimization strategy by altering base (NH_3 or EtNH_2), solvent (THF or MeOH), and temperature (0 - 23°C) failed to remove the isobutryl group before 5'-OH-P bond was cleaved. Use the conditions 1.3% methylamine, 2.6% ethanol, and 96% DCM by weight of starting material generated cleavage of 50% of the isobutryl group on guanosine's amine in 18 hours⁹⁰. Same reaction conditions for the acetyl and phenoxyacetyl protected guanosines took 4.5 hours and 4.7 min respectively to cleave 50%. Cleavage of the 5'-OH-P bond was observed by TLC instantaneously, so an alternative strategy was necessary. Orthogonal reactivity could provide a solution. Moving away from deprotection conditions using a nucleophile seems logical. The carboxybenzyl (Cbz) protection group on guanosine can be removed under hydrogenation conditions in 1 hour⁹¹.

Covalent Acyclic Guanosine Inhibitors

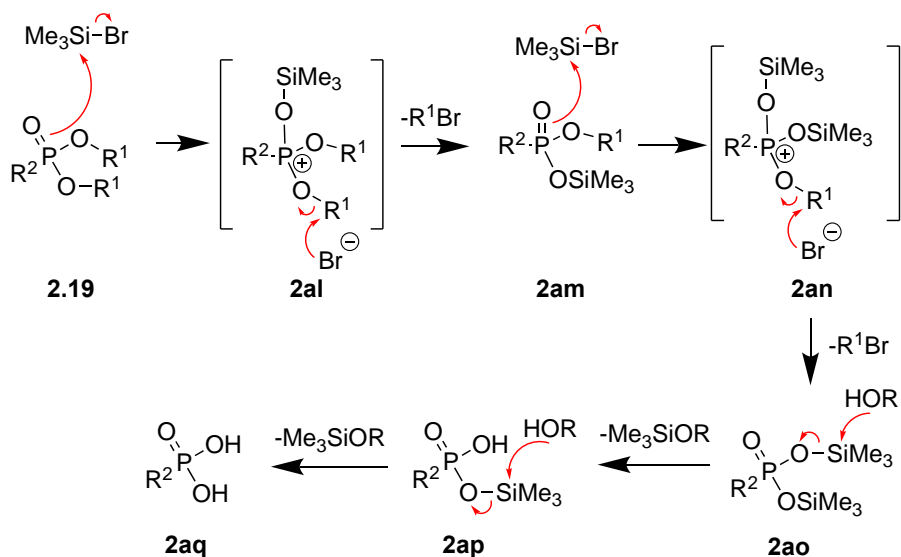
The nucleotide prodrug strategy has been proven to be effective. Merging the target covalent inhibitor strategy with nucleotide prodrugs has exciting potential. Addition of a chemical attachment point for the incorporation of electrophiles on the nucleoside would allow a perfectly tuned covalent warhead to be incorporated into the nucleotide. Ganciclovir prodrugs have already shown potent cytotoxicity and contain an attachment point for electrophilic warhead⁹².



Scheme 2.10 Route towards acyclic guanosine prodrugs

The synthetic pathway chosen to yield an acyclic guanosine analogue starts with commercially available solketal (**2.11**) as seen in **Scheme 2.10**. Tosylation of the primary alcohol generates a good leaving group which is displaced by sodium azide. The azide in **2.13** is the amine synthon that will be used for attachment of electrophilic

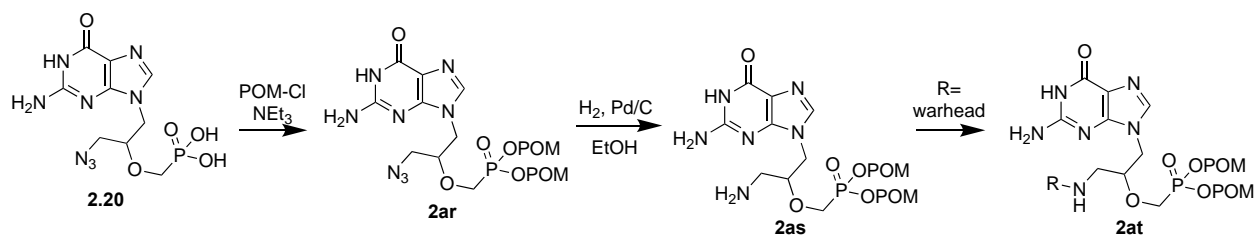
warheads. Cleavage of the acetonide with aqueous hydrochloric acid in methanol released the diol **2.14**. Use of the bulky protection group DPTBS-Cl allows the selective protection of the primary alcohol in 80% yield. Attachment of the masked phosphate diisopropyl (bromomethyl)phosphonate using Finkelstein conditions failed. Instead, generation of the secondary alkoxide with sodium hydride by heating in DMF and then addition of diisopropyl (bromomethyl)phosphonate generated the desired product **2.16** in modest yields. Deprotection of the silyl ether to the free alcohol through acidic conditions generated product **2.17** in 83% yield. Initial efforts to attach the chloro-purine via the tosylated acyclic sugar failed potentially due to steric hinderance. Shifting towards a smaller leaving group, **2.17**'s primary alcohol was mesylated with methanesulfonyl chloride to give **2.18**. The mesylate's acyclic sugar fragment was attached to 2-amino-6-chloropurine using Cs₂CO₃ in 90°C DMF.



Scheme 2.11 Mechanism through which the McKenna reaction proceeds

Employment of the McKenna reaction generates the phosphorous acid from the organophosphorus ester **2.19**. **Scheme 2.11** shows the reaction method through which

the McKenna reaction proceeds. Initially the organophosphorus ester **2.19** undergoes two cycles transesterification generating the trimethylsilyl ester **2ao**. Next, the trimethylsilyl esters are cleaved through a solvolysis reaction forming the phosphorous acid **2aq**. Hydrolysis under acidic conditions leads to the conversion of chloro-purine to guanosine analog **2.20**. The next step was transformation of the free phosphoric acid into the bis(POM) phosphorous ester **2ar**. Hydrogenation of the azide, reducing it to a free amine, allows for the attachment of electrophilic warheads.



Scheme 2.12 Continuation of the route towards acyclic guanosine prodrugs

Although the esterification of phosphoric acids such as **2au-2aw** and others is well documented⁹³⁻¹⁰², the yields are very low and often leads to inseparable mixtures. The conversion of **2.20** to **2ar** was unsuccessful even after optimization efforts including systematically changing bases, temperature, and solvents.

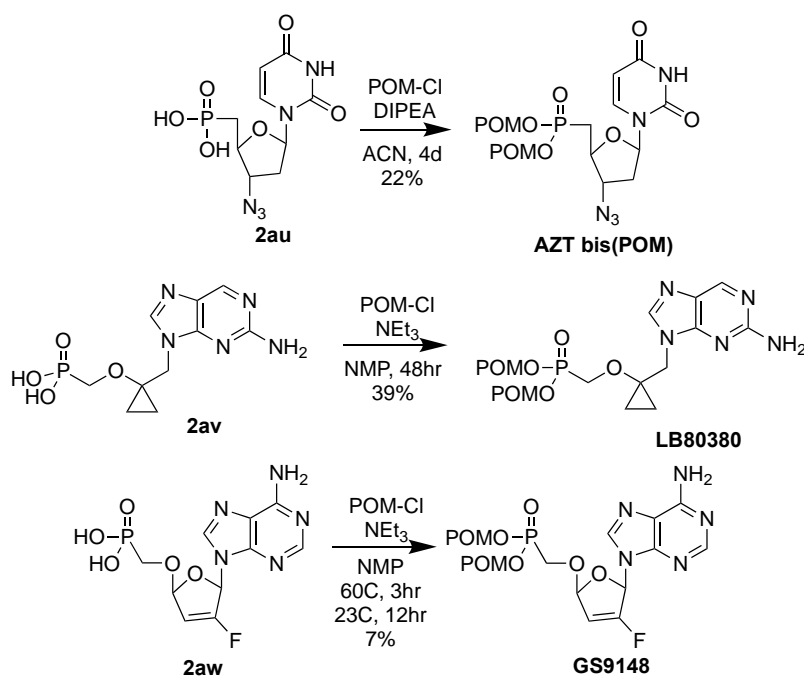
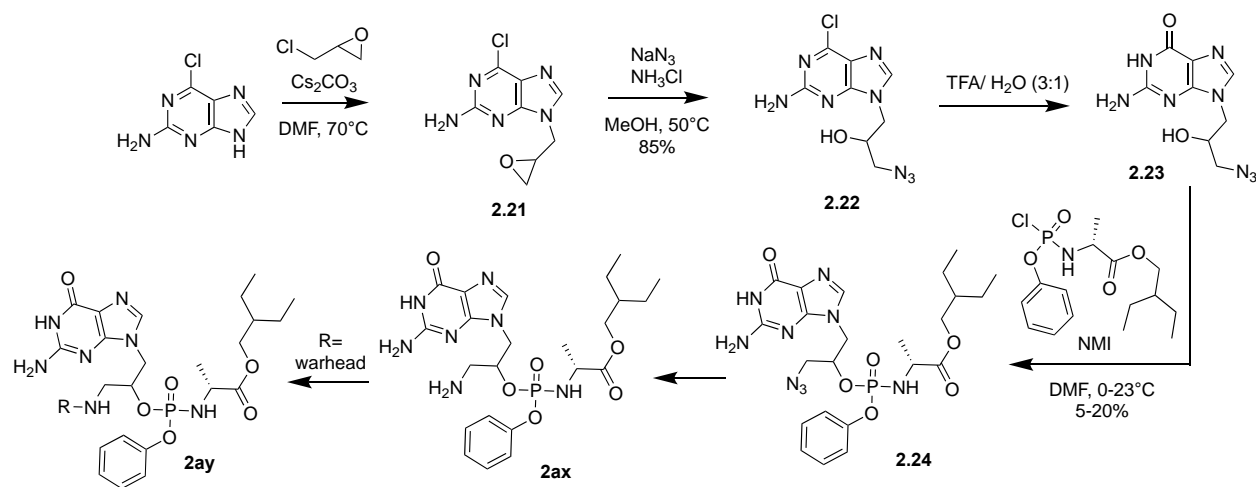


Figure 2.18 Esterification of phosphoric acid intermediates with POM-Cl

As efforts towards esterifying phosphoric acid intermediates were fruitless, the strategy was shifted toward use of the phosphoamidates. **Scheme 2.13** shows the commercially available 2-amino-6-chloropurine reacting with racemic epichlorohydrin to generate the epoxide intermediate **2.21**. Opening the epoxide ring with sodium azide gave the amine synthon which will be used for attachment of the electrophilic warhead. Hydrolysis in 3:1 TFA/H₂O of the chloro-purine leads to the increasingly polar intermediate **2.23**. Generation of the acyclic guanosine phosphoamidate (**2.24**) was achieved using NMI-coupling and a phosphochloridate, however yields were less than optimal and not consistent. Use of diastereomeric phosphochloridate generates a diastereomer pair of isomers in **2.24**, which complicates NMR interpretation. Reducing conditions converting azide (**2.24**) to amine (**2ax**) failed. Both catalytic hydrogenation and attempts of the Staudinger reaction failed to generate the desired amine. Additionally, hydrogenation and Staudinger with Boc₂O in the reaction failed to yield the

desired amine protected carbamate which could have aided in the purification. The next step, functionalization of the amine with a warhead, would have given rise to the final product.



Scheme 2.13 Alternate route towards acyclic guanosine prodrugs

In attempts to produce acyclic guanosine phosphoamidates in a more concise manner, **Scheme 2.14** was devised. NMI and t-BuMgCl coupling were potentially failing due to sterics so use of ganciclovir gives more space between the phosphochloridate and nucleoside compared to the last scheme. The arrangement of atoms between the purine's nitrogen and primary alcohol is the same.

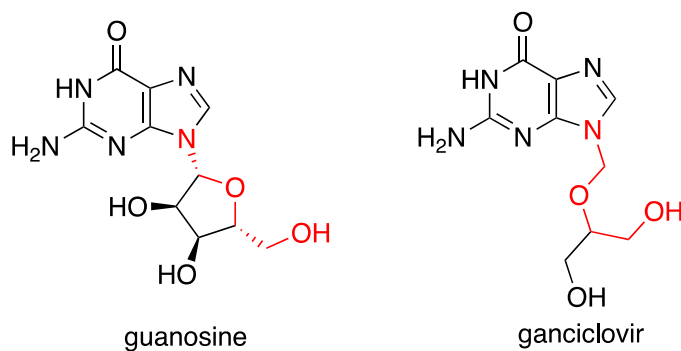
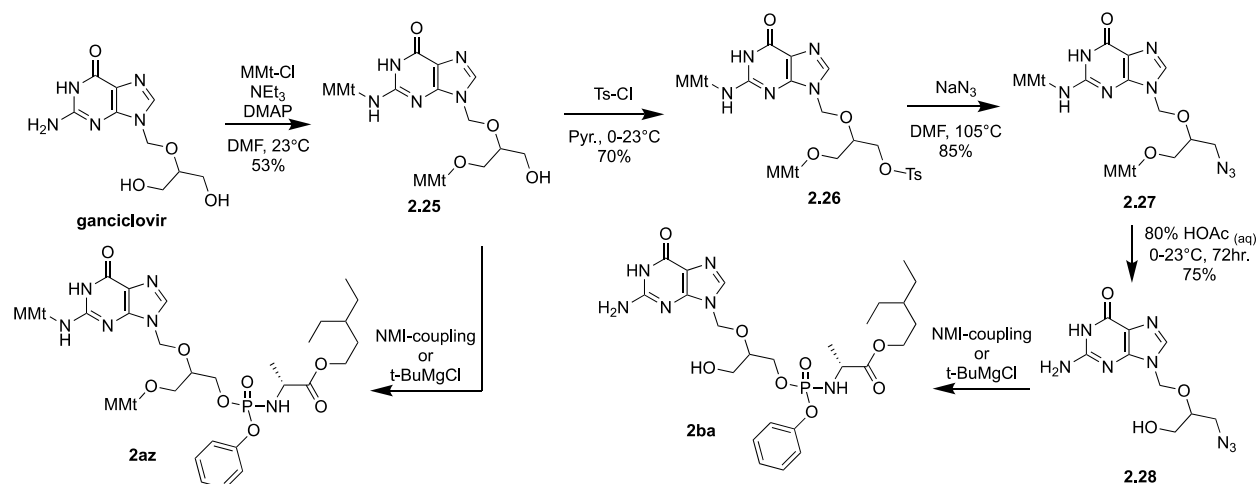


Figure 2.19 Comparing the structural similarity of guanosine and ganciclovir

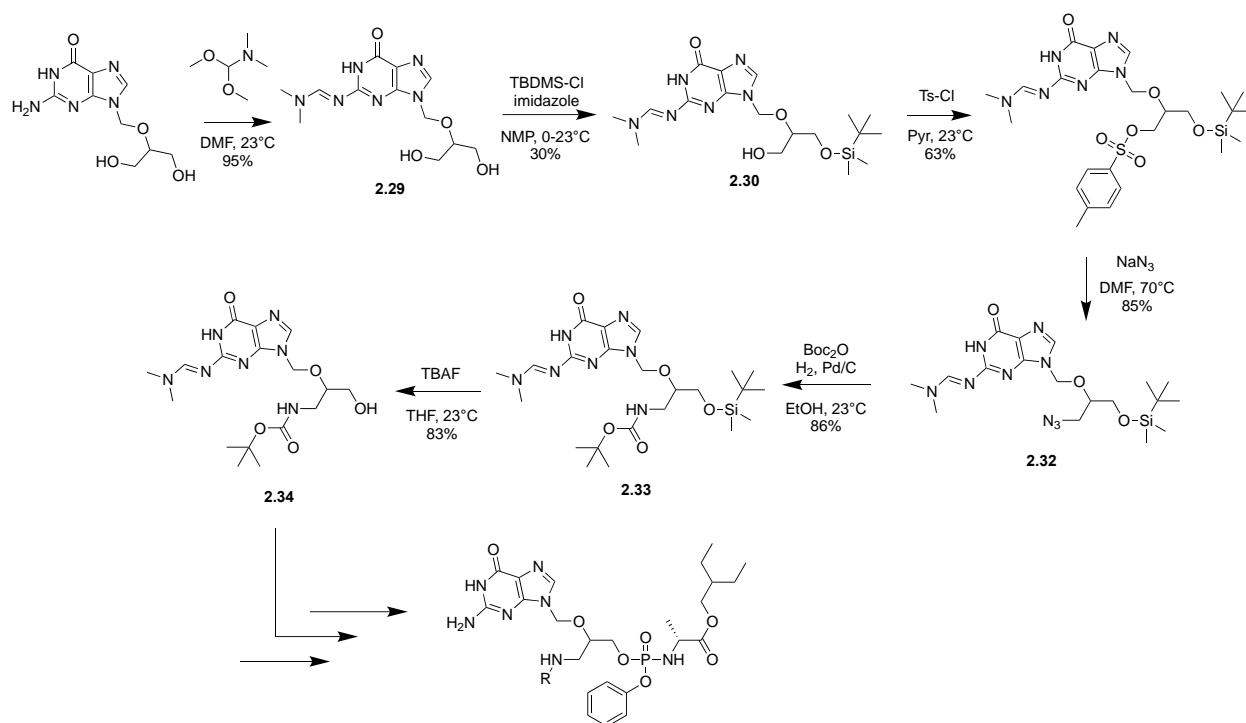
Starting at the commercially available acyclic guanosine analog, ganciclovir is protected using the bulky monomethoxy trityl group (MMt) on the 2-NH₂ and one of the primary hydroxyls. Strategically a bulky protecting group was chosen to leave one hydroxy open for subsequent reaction. Attempts to attach the phosphochloridate at this stage were futile. Tosylation of the free alcohol generates a good leaving group (**2.26**).

Displacement of the tosylate allows substitution for an azide, the amine synthon used for attachment of the warhead. Use of MMt has been widely employed in the synthesis of nucleotides¹⁰³⁻¹⁰⁹, yet despite the many examples and reaction conditions, removal of the MMt protecting group was inconsistent. After a systematic optimization experiment, the best reaction conditions entailed stirring **2.27** in 80% HOAc initially at 0°C and allowing it to warm to room temperature. This was stirred for 3 days generating a 75% yield. Again, the attachment of phosphochloridate to the nucleoside failed. NMI, t-BuMgCl, and Bop-Cl coupling failed to generate the desired acyclic guanosine phosphoamidate **2ba**.



Scheme 2.14 Route towards acyclic guanosine analogs starting with ganciclovir

Although compound **2.25** masked competitive reactive site, the (MMt) groups are very bulky. Coupling of **2.28** does not contain the bulky protecting groups however does contain competitive reactive site potentially leading to the failed coupling with the phosphochloridate. To address the bulky protecting groups and competitive reactive sites the **Scheme 2.15** was devised. Ganciclovir's 2-NH₂ was protected using a dimethylformamidine group to yield **2.29** in a 95% yield. Cold temperatures, slow addition, and strict controlling equivalents of TBDMS-Cl allows the monosilyl ether **2.30** in 30% yield. TBDMS-Cl was chosen as it is a smaller oxygen selective protecting group compared to MMt. Tosylation of the primary hydroxyl and subsequent substitution with sodium azide generates intermediate **2.32**. Catalytic hydrogenation reduced the azide to amine however purification was difficult, so addition of Boc₂O to the reaction allowed for an easier purification. Selective deprotection of the silyl ether with TBAF generates a free hydroxyl which is now available to couple with a phosphochloridate. Even with the competitive reactive site protected, and a less bulky protection group near the free hydroxy, coupling with the phosphochloridate were not successful.



Scheme 2.15 Route towards acyclic guanosine prodrug using less bulky protecting groups.

The common point at which most of these reaction schemes fail is the coupling of nucleoside and masked phosphate. To determine the optimal conditions for this coupling reaction a model study was undertaken. Using benzyl alcohol or p-methoxy benzyl alcohol as the nucleoside surrogate a systemic alteration of coupling reagent, base, and catalyst was used to find the best reaction conditions. The outcomes were determined based on crude NMR. The chemical shift of the benzylic protons as well as conversion of bis(POM)-OH were used to dictate the quality of reaction conditions. The initial stage of this study used benzyl alcohol and focus was put towards finding a coupling reagent which was compatible for the phosphate coupling. The classic conditions (**1**) using the phosphochloridate and triethylamine consumed all starting material however led to a complex mixture of products. Due to the high reactivity and need for fresh preparation, attention was shifted towards coupling with the phosphoric

acid intermediate. Conditions **2-3** used the phosphonium salt PyBOP as the coupling agent and varied catalysts. No shift of the benzylic protons or consumption of the bis(POM)-OH was observed. Shifting to the carbodiimide EDC (**4-5**), and altering the catalyst showed trace amounts of product however it was heavily dominated by starting material. Mitsunobu conditions (**6**) led to an undesirable complex reaction mixture. Activation of bis(POM)-OH with BOP-Cl, DIPEA as a base, and NMI as a catalyst did consume all bis(POM)-OH starting material, generate a product with shifted benzylic protons, and had a clean spectrum. These encouraging results became the framework for further optimization. Because changes in chemical shifts were easier to identify the nucleoside surrogate was changed to p-methoxy benzyl alcohol. While conditions **8** used DMAP in excess intending it to function as both a base and catalyst, these conditions showed only trace amounts of the conjugated product. Conditions **9** excluded DIPEA and used NMI in excess as a base and catalyst. While these conditions were better than **8**, there was still incomplete conversion of starting materials. **10** showed the most promise as all starting bis(POM)-OH was consumed and the desired conjugated product was the major product. As NMI participates as catalyst and generates the imidazolium intermediate, incorporation of an electron withdrawing group would destabilize the cation intermediate making it more reactive. **11** utilized the top performing conditions but included 2-nitro-1,2,4-triazole as a catalyst. While these conditions did lead to the desired product conditions, **10** provided a higher conversion and a cleaner spectrum.

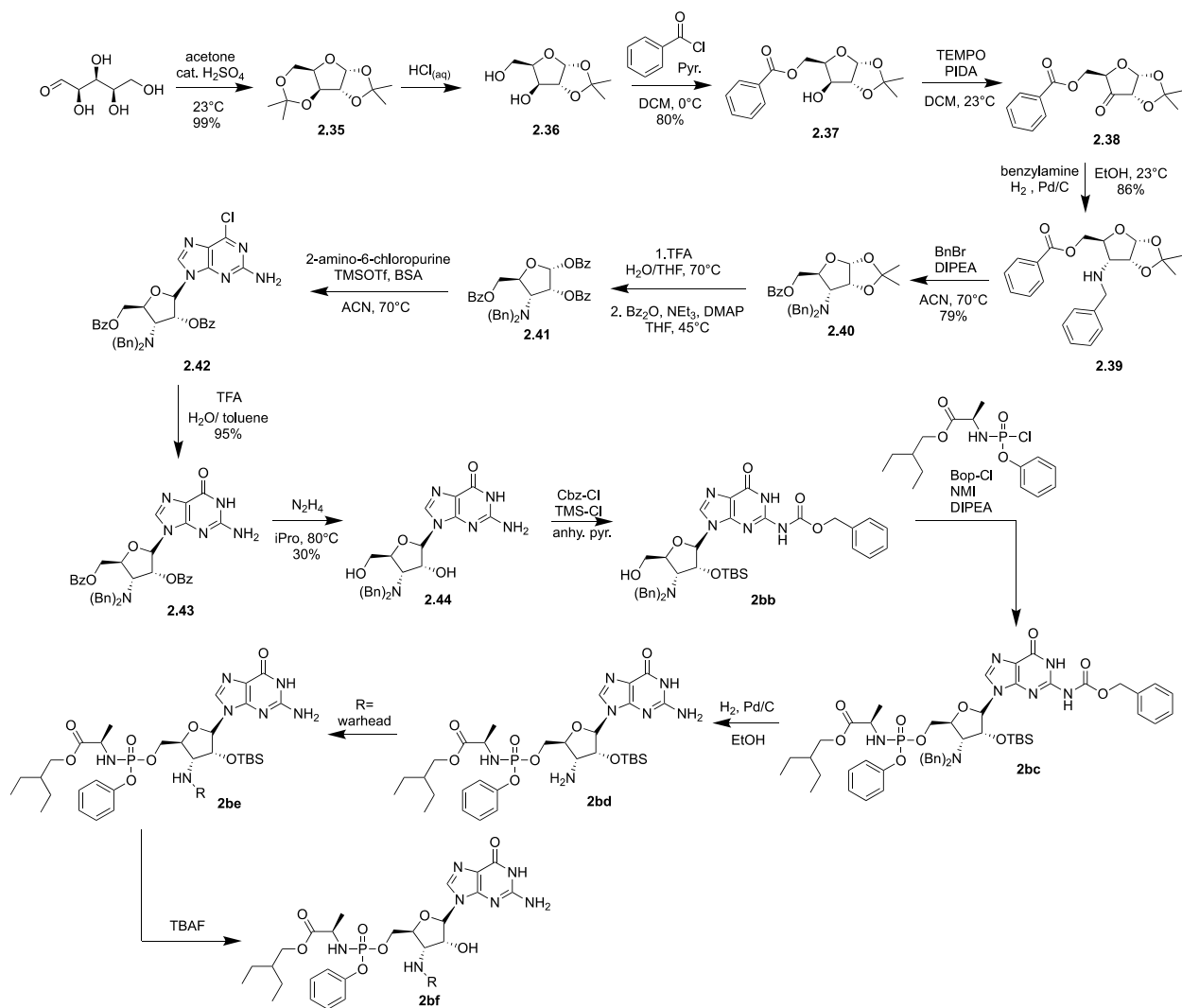
Table 2.1 Optimization conditions for the conjugation of nucleoside and masked phosphate

	nucleoside surrogate	masked phosphate	coupling reagent	base	catalyst
1	benzyl alcohol	bis(POM)-Cl		NEt ₃	
2	benzyl alcohol	bis(POM)-OH	PyBOP	DIPEA	DMAP
3	benzyl alcohol	bis(POM)-OH	PyBOP	DIPEA	NMI
4	benzyl alcohol	bis(POM)-OH	EDC	DIPEA	DMAP
5	benzyl alcohol	bis(POM)-OH	EDC	DIPEA	NMI
6	benzyl alcohol	bis(POM)-OH	DIAD		PPh ₃
7	benzyl alcohol	bis(POM)-OH	Bop-Cl	DIPEA	NMI
8	p-methoxy benzyl alcohol	bis(POM)-OH	Bop-Cl	DMAP	
9	p-methoxy benzyl alcohol	bis(POM)-OH	Bop-Cl		NMI
10	p-methoxy benzyl alcohol	bis(POM)-OH	Bop-Cl	DIPEA	NMI
11	p-methoxy benzyl alcohol	bis(POM)-OH	Bop-Cl	DIPEA	3-nitro-1,2,4-triazole

Updated Covalent Guanosine Phosphoamidates

Similar to the acyclic guanosine analogs the goal is to generate a library of covalent guanosine phosphoamidate. Incorporation of an amine to the carbohydrate moiety would allow a reactive group for the attachment of electrophilic warheads. Starting with the commercially available D-xylose a diacetonide (**2.35**) is formed using acetone in acidic conditions. Selective cleave of the 1,3 acetonide under aqueous acidic conditions yields xylofuranose (**2.36**). Dropwise addition of benzoyl chloride at 0°C in pyridine ensured the reaction took place at the intended primary alcohol, resulting in the desired monoester. Oxidation of the secondary alcohol using TEMPO/PIDA conditions generates the desired ketone. Although, it was found that TEMPO/bleach oxidation generated the desired product with an easier purification. Reductive hydrogenation outperformed classical reductive amination conditions using NaBH₄, although both generated the benzylamine intermediate **2.39**. Subsequent reductive amination failed however the substitution conditions using benzyl bromide and Hunig's base succeeded in producing the desired tertiary amine **2.40**. Deprotection of the acetonide revealed the 1,2 diols that were subsequently benzoylated. To form the glycosidic bond Vorbruggen conditions were employed. When **2.41** is activated with BSA and TMSOTf it forms a cyclic carbocation intermediate on the α -face directing substitution to occur on the β -face of the carbohydrate. 6-chloro-2-aminopurine is silylated at the 2 and 7 amino positions allowing the 9-NH to form the glycosidic bond on the β -face of the carbohydrate, generating the desired protected chloro-nucleoside **2.42**. Hydrolysis of the chloro-purine with TFA in a H₂O/toluene mixture gives rise to **2.43** in 85% yield. Cleaving the benzoyl group by hydrazine in 2-propanol generated a complex mixture of

products. Use of KOH in a H₂O/THF solvent gave rise to a better yield and a less complex mixture to purify. The next step was to protect the 2-NH₂ in order to reduce competitive reactive site when going into the phosphate coupling. Use of a Cbz group will reduce the number of synthetic steps as hydrogenation conditions will be used to deprotect the benzyl protected amine. NMI coupling with BOP-Cl, DIPEA, and the phosphochloridate would result in the masked nucleotide **2bc**. Hydrogenation conditions would reveal both the 2-NH₂ and the 3'-NH₂ free amines. Incorporation of an electrophilic warhead to the more reactive 3'-NH₂ followed by silyl ether deprotection with TBAF would give rise to the final covalent guanosine nucleotide **2bf**.



Scheme 2.16 Synthetic approach towards covalent guanosine prodrugs

Conclusion

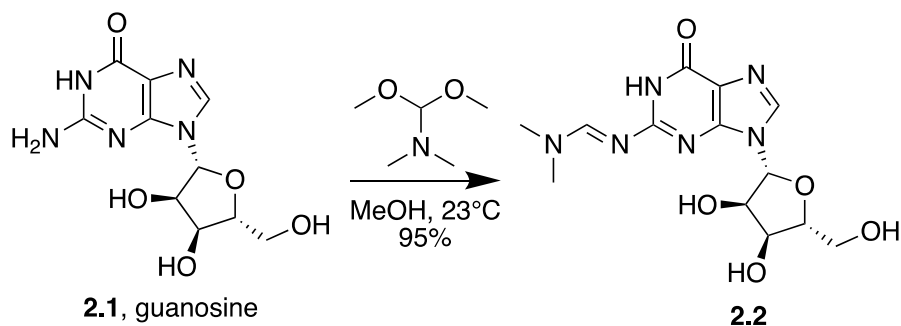
Described herein are synthetic routes affording both cyclic and acyclic covalent guanosine inhibitors targeting the most cancer-causing mutation of all heterotrimeric G-proteins, GNAS^{R201}. Throughout the life cycle of this project the common bottleneck arose in the transformation of nucleoside to nucleotide prodrug. Although optimized reaction parameters were developed and described, yields were not sufficient enough to generate the desired library of covalent guanosine phosphoamidates or carbonyloxymethyl phosphate guanosine prodrugs.

Experimental Section

General Information

All reactions were performed in flame- or oven-dried glassware sealed with rubber septa and under a nitrogen atmosphere unless otherwise indicated. Air- and/or moisture-sensitive liquids or solutions were transferred by cannula or syringe. Organic solutions were concentrated by rotary evaporator at 30 millibars with the water bath heated to not more than 40°C unless specified otherwise. Tetrahydrofuran (THF), dichloromethane (DCM), toluene (PheMe), diethyl ether (Et₂O) was purified with a Pure-Solve MD-5 Solvent Purification System (Innovative Technology). Acetonitrile (ACN, 99.9%, anhydrous) was purchased from FisherScientific. N,N,-Dimethylformamide (DMF, 99.8%, anhydrous) was purchased from Acros. Ethanol (EtOH, 200 proof, absolute) and methanol (MeOH, 99.8%, anhydrous) were purchased from Sigma-Aldrich. Analytical thin-layer chromatography (TLC) was carried out using commercial silica plates (silica gel 60, F254, Sigma-Aldrich) and was visualized by UV lamp, ceric ammonium molybdate (CAM), aqueous potassium permanganate (KMnO₄), or in an iodine (I₂) chamber. Nuclear Magnetic Resonance (NMR) spectra were collected at 298 K on a Bruker Avance III spectrometer (¹H NMR at 600 MHz; ¹³C NMR 151 MHz) fitted with a 1.7 mm or 5 mm triple resonance cryoprobe with z-axis gradients. All spectra were taken in Methanol-d₄ with shifts reported in parts per million (ppm) referenced to the proton or carbon of the solvent (3.31 or 49.00, respectively). All spectra were taken in chloroform-d with shifts reported in parts per million (ppm) referenced to the proton or carbon of the solvent (7.26 or 77.0, respectively). All spectra were taken in dimethyl sulfoxide-d₆ with shifts reported in parts per million (ppm) referenced to the proton or

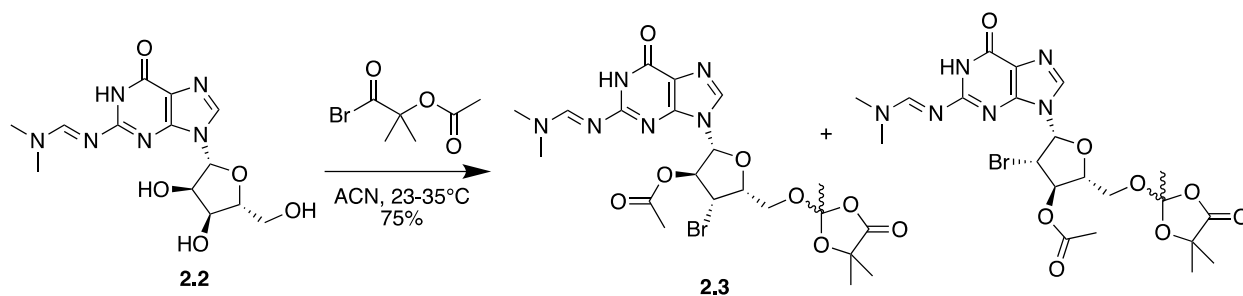
carbon of the solvent (2.50 or 39.5, respectively). All spectra were taken in benzene-d₆ with shifts reported in parts per million (ppm) referenced to the proton or carbon of the solvent (7.16 or 128.1, respectively). Coupling constants are reported in Hertz (Hz). Data for ¹H-NMR are reported as follows: chemical shift (ppm, reference to protium; s = single, d = doublet, t = triplet, q = quartet, dd = doublet of doublets, m = multiplet, coupling constant (Hz), and integration).



(E)-N'-((2R,3S,4R,5S)-3,4-dihydroxy-5-(hydroxymethyl)tetrahydrofuran-2-yl)-6-oxo-6,9-dihydro-1H-purin-2-yl)-N,N-dimethylformimidamide (2.2)

Guanosine **2.1** (10.0 g, 35 mmol, 1 eq.) was dissolved in 100 mL of anhydrous methanol, and (17.4 mL, 0.13 mol, 3.7 eq.) of dimethylformamide dimethyl acetal was added under argon. The suspension was stirred for 96 h at 23 °C. The resulting white precipitate was removed by filtration, washed with cold methanol (20 mL), and dried under reduced pressure to afford the product **2.2** (11.3 g, 33.5mmol, 95%) as a white solid.

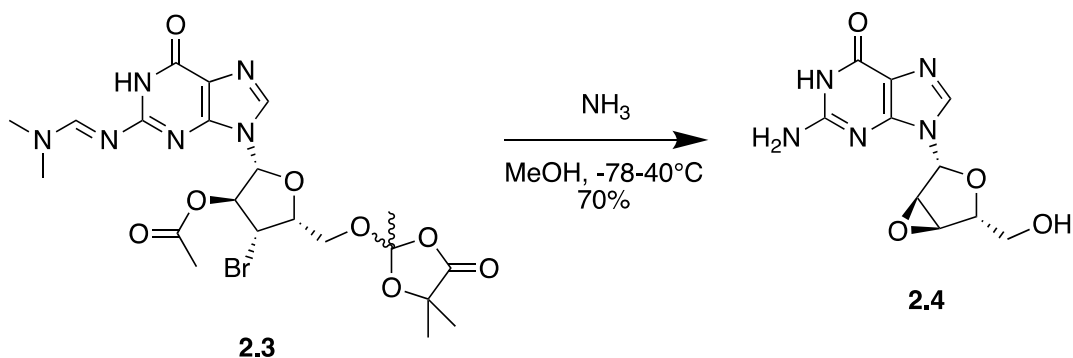
¹H NMR (599 MHz, DMSO) δ 8.53 (s, 1H), 8.04 (s, 1H), 5.79 (d, *J* = 6.1 Hz, 1H), 5.41 (d, *J* = 6.2 Hz, 1H), 5.17 (d, *J* = 4.6 Hz, 1H), 5.02 (t, *J* = 5.6 Hz, 1H), 4.48 (dd, *J* = 11.3, 5.9 Hz, 1H), 4.11 (dd, *J* = 8.1, 4.6 Hz, 1H), 3.90 (q, *J* = 3.8 Hz, 1H), 3.63 (dt, *J* = 11.8, 4.6 Hz, 1H), 3.54 (ddd, *J* = 11.8, 5.8, 4.1 Hz, 1H), 3.15 (s, 3H), 3.03 (s, 3H).



((2S,3R,4R,5R)-4-acetoxy-3-bromo-5-(2-(((E)-(dimethylamino)methylene)amino)-6-oxo-1,6-dihydro-9H-purin-9-yl)tetrahydrofuran-2-yl)methyl 2-acetoxy-2-methylpropanoate (2.3)

In an oven dried 20mL scintillation vial with 1-bromo-2-methyl-1-oxopropan-2-yl acetate (1.04mL, 7.09 mmol, 12 eq.) was added **2.2** (200mg, 591 μ mol, 1eq.) and put under Argon. The reaction was stirred at room temp. for 14hr at which time 3mL of MeCN was added and heated to 35°C for 30 minutes. The crude reaction mixture was evaporated to dryness and dissolved in DCM (10mL). The organic solution was carefully washed with water (10mL), NaHCO₃ solution (3x10mL), and brine (10mL). The organic solution was dried (MgSO₄) and concentrated under reduced pressure. The crude residue was purified by silica gel chromatography (DCM:MeOH (0-5%)) to afford 2 isomers of **2.3** (250 mg , 0.44 mmol, 75%).

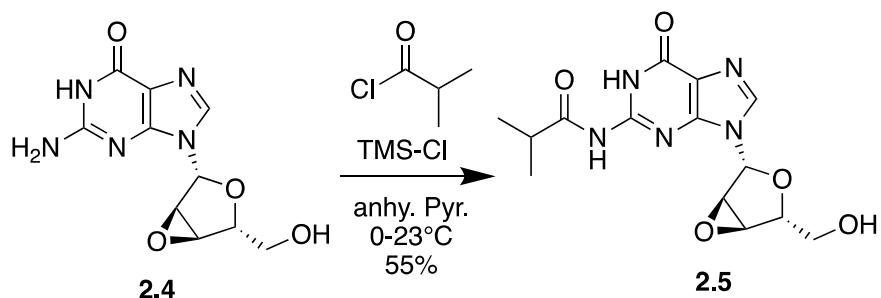
R_f = 0.36 (DCM:MeOH 9:1) **¹H NMR** (599 MHz, CDCl₃) δ 8.63 (s, 1H), 7.95 (s, 1H), 6.06 (s, 1H), 5.96 (d, *J* = 2.0 Hz, 1H), 4.55 – 4.43 (m, 3H), 4.38 (d, *J* = 3.4 Hz, 1H), 3.19 (s, 3H), 3.08 (s, 3H), 2.18 (s, 3H), 2.05 (s, 3H), 1.56 (d, *J* = 4.9 Hz, 6H).



2-amino-9-((1S,2R,4S,5S)-4-(hydroxymethyl)-3,6-dioxabicyclo[3.1.0]hexan-2-yl)-1,9-dihydro-6H-purin-6-one (2.4)

To a pressure flask was added solid **2.3** (50mg, 88 μmol , 1 eq.) and dissolved in 10 mL of methanol. After cooling the flask to -78°C and initiating rapid stirring, liquid ammonia (0.19 mL, 8.8 mmol, 100 eq.) was added slowly. The flask was sealed, allowed to come to room temperature and then heated to 40°C for 14 hours. The crude reaction mixture was evaporated to dryness and purified utilizing C18 silica gel chromatography ($\text{H}_2\text{O}:\text{MeCN}:\text{TFA}$ (100:3:0.01-100:10:0.01)) to afford **2.4** as a white solid (16 mg, 61 μmol , 70%)

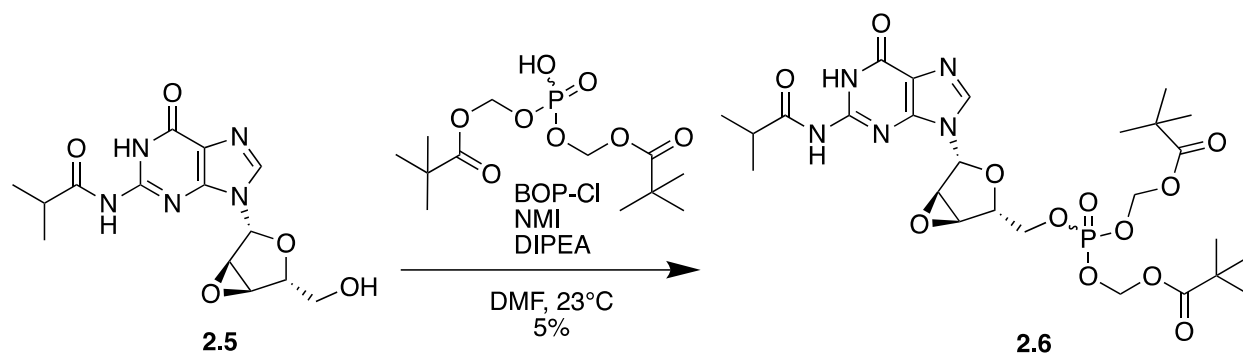
$R_f = 0.28$ (DCM:MeOH 8:2) $^1\text{H NMR}$ (599 MHz, DMSO) δ 7.89 (s, 1H), 6.54 (s, 2H), 5.95 (s, 1H), 5.06 (t, $J = 5.0$ Hz, 1H), 4.35 (d, $J = 2.6$ Hz, 1H), 4.15 (d, $J = 2.5$ Hz, 1H), 3.55 – 3.46 (m, 2H), 3.16 (d, $J = 4.7$ Hz, 1H).



N-(9-((1S,2R,4S,5S)-4-(hydroxymethyl)-3,6-dioxabicyclo[3.1.0]hexan-2-yl)-6-oxo-6,9-dihydro-1H-purin-2-yl)isobutyramide (2.5)

2.4 (1.0 g, 4 mmol, 1 eq.) was dried by co-evaporation in dry pyridine (3x10 mL). The residue was redissolved in dry pyridine (25mL), put under argon, and neat chlorotrimethylsilane (4.0 mL, 0.03 mol, 7.5 eq.) was added. After the reaction was stirred at room temperature for 2 hours and then cooled to 0°C, neat isobutryl chloride (0.5 mL, 4 mmol, 1.15 eq.) was added dropwise over 20 minutes. The reaction mixture was allowed to come to room temperature and stir for 3 hours. Cooling the reaction back down to 0°C, the reaction was quenched with 5 mL of water and stirred for 15 min. Subsequently concentrated aqueous NH₄OH (10 mL) was added and allowed to stir for another 15 min. The reaction was diluted with H₂O (50 mL) and DCM (30 mL). The aqueous layer was collected and evaporated in vacuo. The residue was purified silica gel chromatography (DCM:MeOH (2-10%)) to yield the product **2.5** (0.7 g, 4 mmol, 55%) as a white solid.

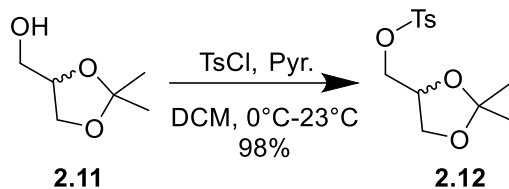
R_f = 0.1 (DCM:MeOH 9:1) **¹H NMR** (599 MHz, DMSO) δ 8.21 (s, 1H), 6.05 (s, 1H), 5.05 (t, *J* = 5.0 Hz, 1H), 4.46 (d, *J* = 2.6 Hz, 1H), 4.19 (t, *J* = 3.9 Hz, 2H), 3.55 – 3.48 (m, 2H), 2.82 – 2.71 (m, 1H), 1.13 (s, *J* = 6.8 Hz, 3H), 1.12 (s, 3H).



To a stirring solution of DIPEA (231 mg, 312 μL , 3 Eq, 1.79 mmol) in dry dmf (5 mL) was added 1-methyl-1H-imidazole (147 mg, 143 μL , 3 Eq, 1.79 mmol), BOP-Cl (182 mg, 1.2 Eq, 716 μmol), ((hydroxyphosphoryl)bis(oxy))bis(methylene) bis(2,2-dimethylpropanoate) (234 mg, 1.2 Eq, 716 μmol), and allowed to stir for 5 min before adding **2.5** (200 mg, 1 Eq, 596 μmol). The reaction was put under argon atmosphere and allowed to stir for 14 hours. Upon completion the reaction was diluted with EtOAc (20 mL), washed with water (4x 20 mL), brine (20 mL), dried with Na_2SO_4 , filtered, and concentrated under reduced pressure. The residue was purified by silica gel chromatography (DCM:MeOH (0-3%)) to yield the product **2.6** (19 mg, 30 μmol , 5.0 %).

$R_f = 0.45$ (DCM:MeOH 9.5:0.5) **$^1\text{H NMR}$** (599 MHz, CDCl_3) δ 7.66 (s, 1H), 5.96 (s, 1H), 5.77 (dd, $J = 13.3, 5.2$ Hz, 1H), 5.70 (dd, $J = 14.0, 5.2$ Hz, 1H), 5.59 (d, $J = 12.9$ Hz, 2H), 5.27 (dd, $J = 20.8, 9.9$ Hz, 1H), 4.44 (dd, $J = 11.2, 5.2$ Hz, 1H), 4.38 (d, $J = 2.6$ Hz, 1H), 4.01 (d, $J = 2.6$ Hz, 1H), 3.97 (ddd, $J = 9.5, 6.9, 5.3$ Hz, 1H), 2.81 – 2.74 (m, 1H), 1.27 (s, 9H), 1.22 (s, 3H), 1.21 (s, 3H), 1.16 (s, 9H).

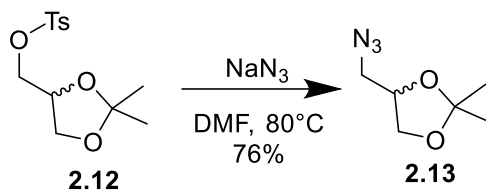
LRMS: m/z: $[\text{M}+\text{Na}]^+$ Calcd for $[\text{C}_{19}\text{H}_{26}\text{O}_5\text{SNa}]^+$ Theo mass: 666.22; Found: 666.31



(2,2-dimethyl-1,3-dioxolan-4-yl)methyl 4-methylbenzenesulfonate (2.12)

Solketal **2.11** (19 mL, 0.15 mol, 1 eq.) was added to a RBF and dissolved in DCM (10 mL) at 0°C. To this was added pyridine (61 mL, 0.76 mol, 5 eq.) and then tosyl-Cl (35 g, 0.18 mol, 1.2 eq.). The reaction was stirred at 0 °C for 15 min and then allowed to come to 23 °C for 14 hour. After this time 2M aqueous HCl was added to the reaction and allowed to stir. The organic phase was collected, washed with brine, filtered, dried over Na₂SO₄, and concentrated in vacuo. The crude oil was purified by silica gel chromatography (Hexanes:EtOAc (0-20%)) to afford the tosylated product **2.12** (42.5 g, 0.15 mol, 98%) as a yellow oil.

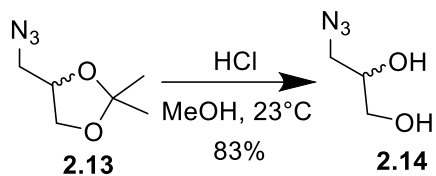
¹H NMR (599 MHz, CDCl₃) δ 7.79 (d, *J* = 8.3 Hz, 1H), 7.35 (d, *J* = 8.1 Hz, 1H), 4.30 – 4.23 (m, 1H), 4.07 – 3.99 (m, 1H), 3.97 (dd, *J* = 10.1, 6.1 Hz, 1H), 3.76 (dd, *J* = 8.8, 5.1 Hz, 1H), 2.45 (s, 3H), 1.33 (s, 3H), 1.31 (s, 3H).



4-(azidomethyl)-2,2-dimethyl-1,3-dioxolane (**2.13**)

To a stirring solution of **2.12** (46.34 g, 161.8 mmol, 1 eq.) in DMF (300mL) was added sodium azide (21.04 g, 323.7 mmol, 2 eq.) and the reaction was heated to 70°C for 14 hr. The reaction was then diluted with EtOAc (400 mL), washed with 2M LiCl (4 x 200 mL), brine (200 mL), dried with Na₂SO₄, and concentrated in vacuo to yield **2.13** (19.0 g, 161.8 mmol, 76%) as a brown oil. No purification was necessary.

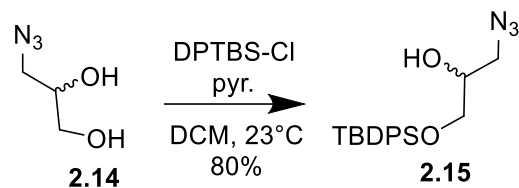
¹H NMR (599 MHz, CDCl₃) δ 4.20-4.27 (m, 1H), 4.00 (dd, J=6.4, 8.4 Hz, 1H), 3.74 (dd, J=6.0, 8.4 Hz, 1H), 3.36 (dd, J=4.8, 12.8 Hz, 1H), 3.26 (dd, J=5.6, 12.8 Hz, 1H), 1.43 (s, 3H), 1.33 (s, 3H).



3-azidopropane-1,2-diol (**2.14**)

To A stirring solution of **2.13**(450 mg, 1 Eq, 2.86 mmol) dissolved in MeOH (10 mL) was added conc. HCl (313 mg, 4.29 mL, 2 molar, 3 Eq, 8.59 mmol) and stirred at 23 °C for 14 hour. Upon completion the solvent was evaporated and yielded the product **2.14** (0.24 g, 2.1 mmol, 73 %) without need for purification.

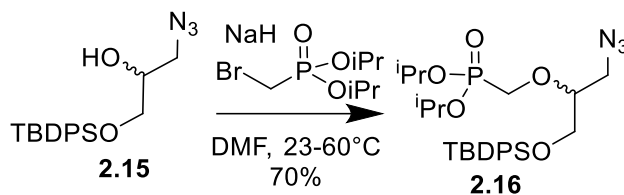
¹H NMR (599 MHz, CDCl₃) δ 3.90 (m, 1H), 3.81-3.58 (m, 2H), 3.44 (m, 2H)



1-azido-3-((tert-butyldiphenylsilyl)oxy)propan-2-ol (**2.15**)

To a stirring solution of **2.14** (1.72 g, 1 Eq, 14.7 mmol) and pyridine (1.43 mL, 17.6 mmol, 1.2 eq) in DCM (30 mL) at 23 °C was added tert-butyldichlorodiphenylsilane (4.58 mL, 17.6 mmol, 1.2 eq.). After 14 hour the reaction was washed with 2M HCl (15mL), brine (15mL), dried by MgSO₄, and concentrated in vacuo, The crude residue was purified by silica gel chromatography (Hexanes:EtOAc (10-20%)) and visualized by CAM stain to afford the product **2.15** (4.2 g, 12 mmol, 80 %).

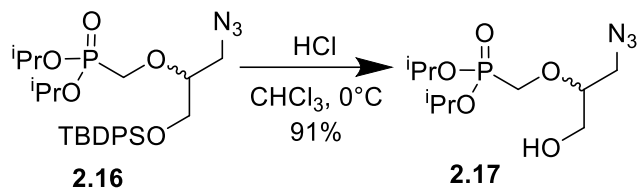
R_f = 0.4 (Hexanes:EtOAc (4:1)) **¹H NMR** (599 MHz, CDCl₃) δ 7.68 – 7.64 (m, 4H), 7.46 (t, *J* = 7.3 Hz, 2H), 7.43 – 7.36 (m, 4H), 3.88 (d, *J* = 4.4 Hz, 1H), 3.73 – 3.64 (m, 2H), 3.38 (d, *J* = 5.5 Hz, 2H), 2.46 (d, *J* = 3.7 Hz, 1H), 1.08 (s, 9H).



diisopropyl (((1-azido-3-((tert-butyldiphenylsilyl)oxy)propan-2-yl)oxy)methyl)phosphonate (2.16)

Sodium hydride (1.36 g, 60% Wt, 33.9 mmol, 2.5 eq.) was added to a solution of **2.15** (4.88 g, 13.6 mmol, , 1 eq.) in DMF (200 mL) and was stirred at 60 °C for 15 min. After diisopropyl (bromomethyl)phosphonate (5.28 g, 20.4 mmol, 1.5 eq.) was added the reaction was put under argon and stirred at 23 °C for 14 hour. The reaction was quenched with H₂O (20 mL), evaporated to dryness, redissolved in EtOAc (300mL), washed with H₂O (200 mL), brine (200 mL), dried by Na₂SO₄, and concentrated under vacuo. The residue was purified by silica gel chromatography (Hexanes:EtOAc (16-50%)) to afford the product **2.16** (4.7 g, 8.8 mmol, 65 %) as a colorless oil.

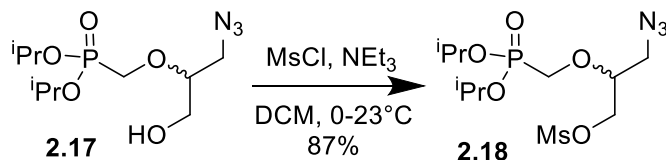
R_f = 0.52 (Hexanes:EtOAc (1:1)) **¹H NMR** (599 MHz, CDCl₃) δ 7.35 (d, *J* = 7.6 Hz, 4H), 7.24 (t, *J* = 7.6 Hz, 4H), 7.20-7.15 (m, 2H), 4.73 – 4.60 (m, 1H), 3.77 (dd, *J* = 13.6, 9.0 Hz, 1H), 3.69 (dd, *J* = 13.6, 8.8 Hz, 1H), 3.57 – 3.52 (m, 1H), 3.37 (qd, *J* = 12.9, 5.2 Hz, 2H), 3.18 (qd, *J* = 10.2, 5.3 Hz, 2H), 1.31 – 1.17 (m, 12H).



diisopropyl (((1-azido-3-hydroxypropan-2-yl)oxy)methyl)phosphonate (**2.17**)

To a stirring solution **2.16** (100 mg, 186 μmol , 1eq.) in CHCl_3 (5 mL) at 0 $^\circ\text{C}$ was added conc. HCl (5.01 μL , 205 μmol , 1.1 eq.) and allowed stir for 1 hour. Once all starting material had been consumed the solvent was evaporated and the crude product was purified by silica gel chromatography (Hexanes:EtOAc (25-50%)) which afforded the product **2.17** (50 mg, 0.17 mmol, 91 %).

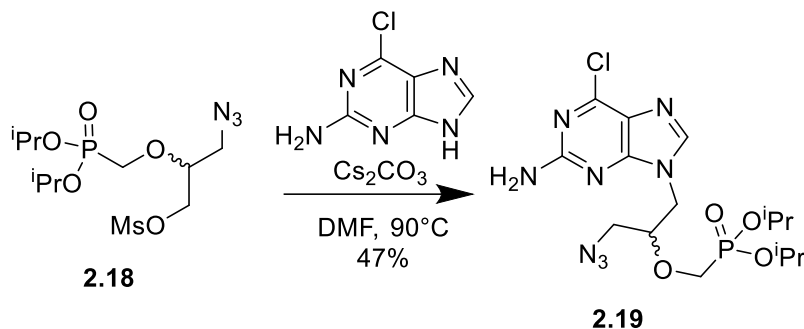
$^1\text{H NMR}$ (599 MHz, CDCl_3) δ 4.84 – 4.77 (m, 1H), 4.77 – 4.70 (m, 1H), 4.08 (dd, $J = 14.2, 6.9$ Hz, 1H), 3.97 (s, 1H), 3.79 (dd, $J = 14.2, 8.9$ Hz, 1H), 3.75 (d, $J = 12.3$ Hz, 1H), 3.67 – 3.62 (m, 1H), 3.59 (d, $J = 12.0$ Hz, 1H), 3.43 (dd, $J = 13.0, 7.5$ Hz, 1H), 3.25 (dd, $J = 13.0, 4.0$ Hz, 1H), 1.36 (dd, $J = 6.1, 3.5$ Hz, 6H), 1.34 (d, $J = 6.2$ Hz, 6H).



3-azido-2-((diisopropoxyphosphoryl)methoxy)propyl methanesulfonate (2.18)

To a solution of **2.17** (0.82 g, 1 Eq, 2.8 mmol) and triethylamine (0.77 mL, 2 Eq, 5.6 mmol) in DCM (7 mL) was added mesyl-Cl (0.38 g, 0.26 mL, 1.2 Eq, 3.3 mmol) at 0 °C under an argon atmosphere which was stirred for 1 hour and slowly warmed to 23 °C for 1hr. Water (7 mL) was added to the reaction and was extracted from with DCM (2x 7mL). The combined organics were washed with brine, dried by MgSO₄, filtered, and concentrated. The residue was purified by silica gel chromatography (DCM:Acetone (10-30%)) to afford the product **2.18** (0.90 g, 2.4 mmol, 87 %) as an oil.

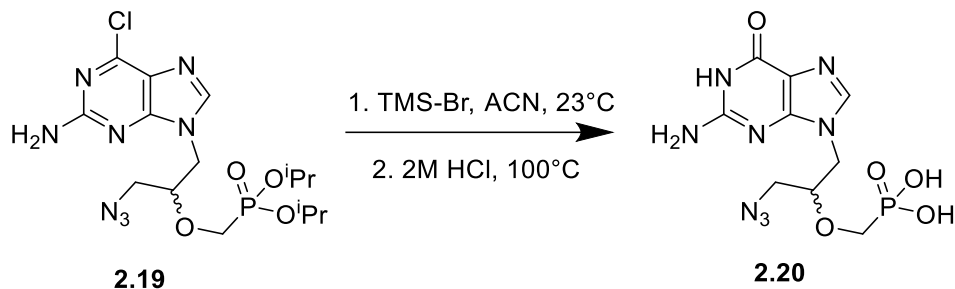
R_f = 0.26 (Hexanes:EtOAc (4:1)) visualized by KMnO₄ **¹H NMR** (599 MHz, CDCl₃) δ 4.80 – 4.69 (m, 2H), 4.34 (dd, *J* = 11.1, 4.5 Hz, 1H), 4.29 (dd, *J* = 11.1, 5.1 Hz, 1H), 3.91 – 3.84 (m, 3H), 3.52 (dd, *J* = 13.1, 4.7 Hz, 1H), 3.45 (dd, *J* = 13.1, 5.6 Hz, 1H), 3.07 (s, 3H), 1.34 (s, 6H), 1.33 (s, 6H).



diisopropyl (((1-(2-amino-6-chloro-9H-purin-9-yl)-3-azidopropan-2-yl)oxy)methyl)phosphonate (2.19)

2.18 (1.47 g, 1 Eq, 3.94 mmol), 6-chloro-9H-purin-2-amine (1.34 g, 2 Eq, 7.87 mmol), and cesium carbonate (2.82 g, 2.2 Eq, 8.66 mmol) were added to a RBF which containing dry DMF (15 mL), put under an argon atmosphere, and vigorously spun at 90 °C for 3 hour. Upon completion the reaction was brought to room temperature and filtered. The filtrate was diluted with EtOAc (40mL), washed with water (4x 30mL), brine (30mL), dried with Na₂SO₄, filtered, and concentrated under reduced pressure. The residue was purified by silica gel chromatography (DCM:MeOH (0-10%)) to afford the product **2.19** (0.83 g, 1.9 mmol, 47 %).

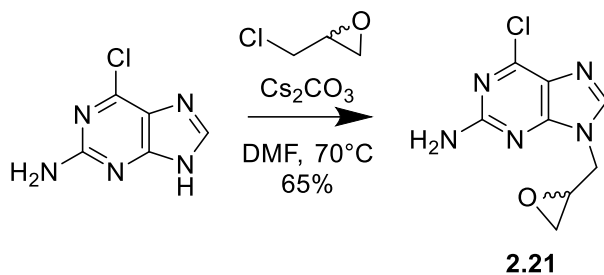
R_f = 0.43 (DCM:MeOH (9:1)) **¹H NMR** (599 MHz, CDCl₃) δ 7.92 (s, 1H), 5.23 (s, 2H), 4.76 – 4.64 (m, 2H), 4.31 (dd, *J* = 14.6, 4.0 Hz, 1H), 4.25 (dd, *J* = 14.6, 5.8 Hz, 1H), 3.94 – 3.90 (m, 1H), 3.85 (dd, *J* = 13.8, 8.4 Hz, 1H), 3.76 (dd, *J* = 13.8, 8.8 Hz, 1H), 3.48 (dd, *J* = 13.1, 5.0 Hz, 1H), 3.31 (dd, *J* = 13.1, 5.1 Hz, 1H), 1.32 (dd, *J* = 9.7, 6.3 Hz, 6H), 1.28 (dd, *J* = 18.0, 6.3 Hz, 6H).



(((1-(2-amino-6-oxo-1,6-dihydro-9H-purin-9-yl)-3-azidopropan-2-yl)oxy)methyl)phosphonic acid (2.20)

TMS-Br (874 mg, 740 μ L, 10 Eq, 5.71 mmol) was added drop wise to a solution of **2.19** (255 mg, 1 Eq, 571 μ mol) in dry ACN (250 μ L) which was under an argon atmosphere. This was stirred at 23 °C for 14 hour at which time the solvent was evaporated and subsequently dried under high vacuum. To this was added Acetone (2mL) and water (0.5mL) and was stirred at 23 °C for 6 hours. The precipitate was filtered, washed with Acetone (2mL) and water (0.5mL) and then stirred in HCl (20.8 mg, 285 μ L, 2 molar, 1 Eq, 571 μ mol) at 80 °C for 5 hours. Evaporation of the solvent left a residue that was crystalized from water to give the product **2.20** (49 mg, 0.14 mmol, 25 %).

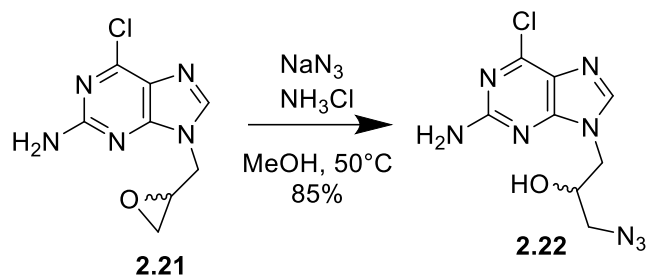
$^1\text{H NMR}$ (599 MHz, D_2O) δ 8.95 (s, 1H), 4.51 (d, $J = 15.0$ Hz, 1H), 4.41 (dd, $J = 14.7$, 7.3 Hz, 1H), 4.05 (d, $J = 2.7$ Hz, 1H), 3.91 (dd, $J = 12.9$, 9.0 Hz, 1H), 3.75 (dd, $J = 13.3$, 3.8 Hz, 1H), 3.65 (dd, $J = 12.4$, 10.8 Hz, 1H), 3.47 (dd, $J = 13.1$, 3.7 Hz, 1H). **LRMS:** m/z : $[\text{M}-\text{H}]^-$ Calcd for $[\text{C}_9\text{H}_{12}\text{N}_8\text{O}_5\text{P}]^-$ Theo mass: 343.07; Found: 343.15



6-chloro-9-(oxiran-2-ylmethyl)-9H-purin-2-amine (2.21)

To a stirring solution of 6-chloro-9H-purin-2-amine (10 g, 1 Eq, 59 mmol) and cesium carbonate (29 g, 1.5 Eq, 88 mmol) in dry DMF (100 mL) was added 2-(chloromethyl)oxirane (27 g, 23 mL, 5 Eq, 0.29 mol) slowly. After the reaction was heated to 70 °C for 1 hour it was allowed to come to room temperature, diluted with EtOAc (300mL), washed with water (4x 200mL), brine (200mL), dried with Na₂SO₄, filtered, and concentrated under reduced pressure. The crude residue was purified by silica gel chromatography (DCM:MeOH (0-5%)) to yield **2.21** (8.6 g, 38 mmol, 65 %).

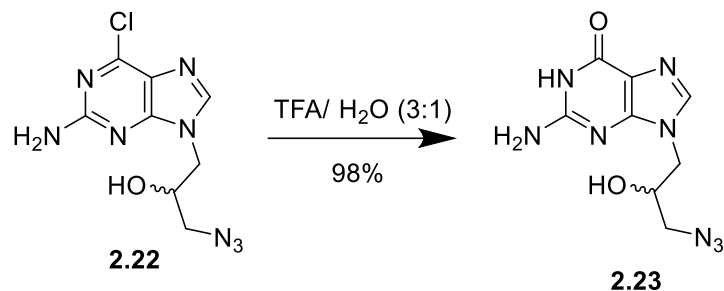
R_f = 0.2 (DCM:MeOH (9:1)) **¹H NMR** (599 MHz, MeOD) δ 8.05 (s, 1H), 4.51 (dd, *J* = 14.9, 3.3 Hz, 1H), 4.19 (dd, *J* = 15.0, 5.8 Hz, 1H), 3.38 (dt, *J* = 6.0, 3.5 Hz, 1H), 2.85 (t, *J* = 4.3 Hz, 1H), 2.57 (dd, *J* = 4.6, 2.5 Hz, 1H).



1-(2-amino-6-chloro-9H-purin-9-yl)-3-azidopropan-2-ol (**2.22**)

To a stirring solution of **2.21** (1.33 g, 1 Eq, 5.89 mmol) in MeOH (20 mL) was added ammonium chloride (946 mg, 3 Eq, 17.7 mmol) and sodium azide (1.15 g, 3 Eq, 17.7 mmol). The reaction was heated to 50 °C for 14 hour after which the reaction was evaporated to dryness and purified by silica gel chromatography (Hexanes: EtOAc (50-80%)) to yield **2.22** (1.3 g, 5.0 mmol, 85 %).

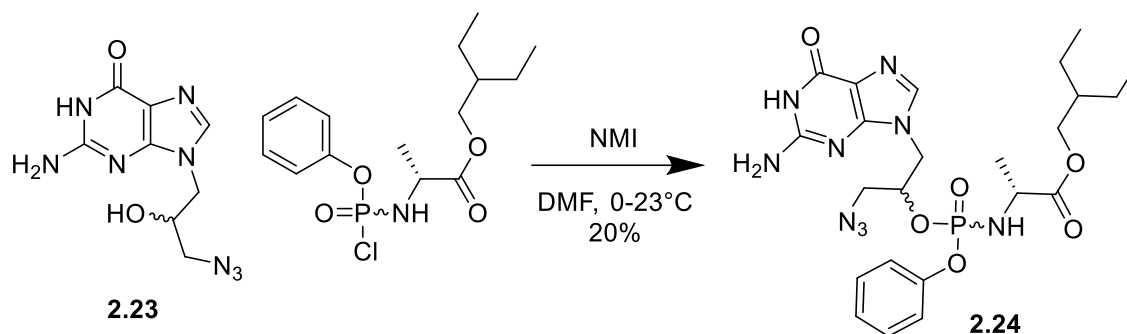
$R_f = 0.5$ (EtOAc) **¹H NMR** (599 MHz, DMSO) δ 8.05 (s, 1H), 6.88 (s, 2H), 5.66 (d, $J = 5.1$ Hz, 1H), 4.12 – 4.05 (m, 2H), 4.01 (dd, $J = 14.6, 9.3$ Hz, 1H), 3.36 (dd, $J = 13.0, 3.5$ Hz, 1H), 3.26 (dd, $J = 12.8, 6.0$ Hz, 1H).



2-amino-9-(3-azido-2-hydroxypropyl)-1,9-dihydro-6H-purin-6-one (2.23)

2.22 (200 mg, 1 Eq, 744 μmol) was dissolved in a mixture of TFA (1.5 mL) and H_2O (0.50 mL). This was stirred at 23 $^\circ\text{C}$ for 14 hour at which time toluene (4mL) was added and the solvents were evaporated off to dryness leaving and the orange solid **2.23** (0.18 g, 0.73 mmol, 98 %). Purification was not necessary.

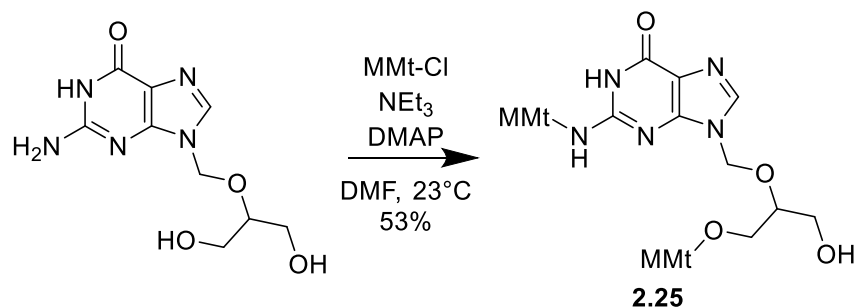
$^1\text{H NMR}$ (599 MHz, MeOD) δ 8.37 (s, 1H), 4.44 (dd, $J = 13.9, 2.8$ Hz, 1H), 4.31 (dd, $J = 13.8, 8.1$ Hz, 1H), 4.26-4.20 (m, 1H), 3.46 (dd, $J = 12.7, 3.9$ Hz, 1H), 3.37 (dd, $J = 12.6, 6.0$ Hz, 1H).



2-ethylbutyl (((1-(2-amino-6-oxo-1,6-dihydro-9H-purin-9-yl)-3-azidopropan-2-yl)oxy)(phenoxy)phosphoryl)-L-alaninate (2.24)

To a stirring solution of **2.23** (630 mg, 1 Eq, 2.52 mmol) and 1-methyl-1H-imidazole (413 mg, 401 μ L, 2 Eq, 5.04 mmol) at 0 °C in dry DMF (15 mL) under an argon atmosphere was added 2-ethylbutyl (chloro(phenoxy)phosphoryl)alaninate (963 mg, 1.1 Eq, 2.77 mmol) drop wise which was dissolved in dry DMF (3mL). The reaction was allowed to slowly come to 23 °C and was stirred for 14 hour. Upon completion the reaction was diluted with EtOAc (45mL), washed with water (4x 30 mL), brine (30mL), dried with Na₂SO₄, filtered, and concentrated under reduced pressure. The residue was purified by silica gel chromatography (DCM:MeOH (0-10%)) to yield **2.24** (0.28 g, 0.50 mmol, 20 %) as a pair of diastereomers.

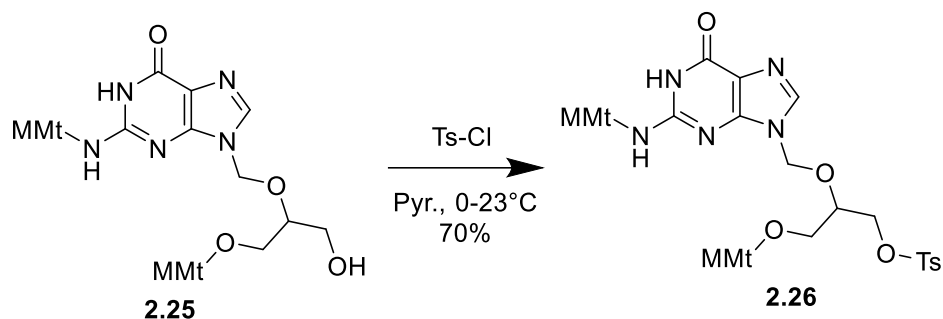
R_f = 0.3 (DCM:MeOH(9:1)) **¹H NMR** (599 MHz, MeOD) δ 8.04 (s, 1H), 7.39 – 6.99 (m, 5H), 4.30-4.20 (m 2H), 4.17 – 4.07 (m, 3H), 4.08-3.95 (m, 2H), 3.40 (d, *J* = 3.8 Hz, 1H), 1.53 (d, *J* = 7.3 Hz, 1H), 1.42 – 1.28 (m, 5H), 0.95-0.86 (m, 9H).



1,9-Dihydro-9-[[2-hydroxy-1-[[4-methoxyphenyl]diphenylmethoxy]methyl]ethoxy]methyl]-2-[[4-methoxyphenyl]diphenylmethyl]amino]-6H-purin-6-one (2.25)

A solution of ganciclovir (6000 mg, 1 Eq, 23.51 mmol), (chloro(4-methoxyphenyl)methylene)dibenzene (18.15 g, 2.5 Eq, 58.77 mmol), triethylamine (7.136 g, 9.83 mL, 3 Eq, 70.52 mmol), and DMAP (71.80 mg, 0.025 Eq, 587.7 μ mol) in DMF (40 mL) was stirred at 23 °C for 2 hour. The reaction was quenched with methanol (1mL), diluted with EtOAc (160mL), washed with water (4x 50mL), brine (50mL), dried by Na₂SO₄, filtered, and concentrated under reduced pressure. The residue was purified by silica gel chromatography (DCM:MeOH (2-6%)) to yield the colorless solid **2.25** (10 g, 12 mmol, 53 %).

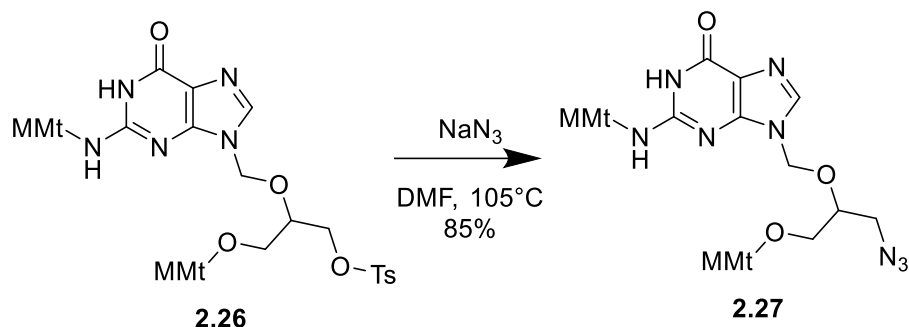
R_f = 0.6 (DCM:MeOH (9.5:0.5)) **¹H NMR** (599 MHz, MeOD) δ 7.78 (s, 1H), 7.30 – 7.24 (m, 11H), 7.21 (dd, *J* = 8.1, 5.1 Hz, 2H), 7.20 – 7.12 (m, 7H), 7.07 (t, *J* = 7.3 Hz, 2H), 6.85 (d, *J* = 8.8 Hz, 2H), 6.71 (d, *J* = 8.8 Hz, 2H), 5.06 – 5.01 (m, 2H), 3.80 (s, 3H), 3.63 (s, 3H), 3.57 – 3.51 (m, 1H), 3.24 (dd, *J* = 11.9, 2.8 Hz, 1H), 3.17 (dd, *J* = 11.9, 6.1 Hz, 1H), 2.82 (dd, *J* = 10.1, 6.1 Hz, 1H), 2.77 (dd, *J* = 10.1, 2.8 Hz, 1H).



N²-(p-anisyl)diphenylmethyl-9-[(1-(p-anisyl)diphenylmethoxy)-3-tosyloxy-2-propoxy]methyl]guanine (2.26)

2.25 (9.87 g, 1 Eq, 12.3 mmol) was dissolved in Pyridine (200 mL) under argon and cooled to 0 °C and tosyl-Cl (9.41 g, 4 Eq, 49.4 mmol) was added to it. After stirring at 0 °C for 30 min. the reaction was allowed to come to 23 °C for 48 hours. Ice water was added to quench the reaction and the majority of solvent was removed under reduced pressure. The residue was dissolved in toluene and removed on the rotary evaporator. The residue was purified by silica gel chromatography (DCM:MeOH (0-4%)) to yield **2.26** (8.2 g, 8.6 mmol, 70 %) as a white foam.

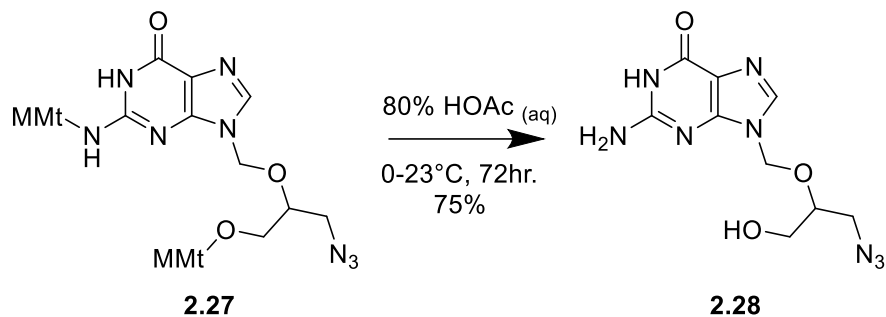
$R_f = 0.5$ (DCM:MeOH (9:1)) **¹H NMR** (599 MHz, MeOD) δ 7.69 (s, 1H), 7.65 (d, $J = 8.1$ Hz, 2H), 7.42 (d, $J = 8.0$ Hz, 2H), 7.30 – 7.18 (m, 14H), 7.16 (d, $J = 8.7$ Hz, 2H), 7.10 (dd, $J = 17.9, 8.2$ Hz, 6H), 7.01 (dd, $J = 14.0, 7.0$ Hz, 2H), 6.85 (d, $J = 8.7$ Hz, 2H), 6.69 (d, $J = 8.6$ Hz, 2H), 4.93 (s, 1H), 3.79 (s, 3H), 3.68 – 3.54 (m, 6H), 2.70 (d, $J = 4.0$ Hz, 2H), 2.46 (s, 3H).



N²-(p-anisylidiphenylmethyl)-9-((1-(p-anisylidiphenylmethoxy)-3-azido-2-propoxy)methyl)guanine (2.27)

A solution of **2.26** (4.52 g, 1 Eq, 4.74 mmol) and sodium azide (1.94 g, 6.3 Eq, 29.8 mmol) in DMF (20 mL) were heated to 105 °C for 72 hour. Upon completion the reaction was cooled and diluted with EtOAc (60mL), washed with water (4x 60mL), brine (60mL), dried by Na₂SO₄, filtered, and concentrated under reduced pressure. The product **2.27** (3.3 g, 4.0 mmol, 85 %) was obtained as a white foam by recrystallization with Hexanes and EtOAc.

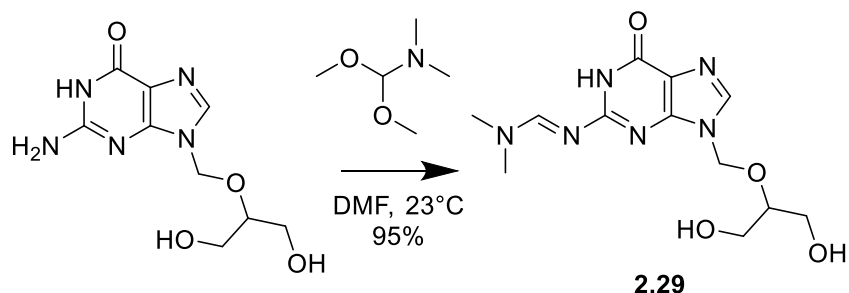
¹H NMR (599 MHz, MeOD) δ 7.76 (s, 1H), 7.30 (dt, $J = 19.6, 8.4$ Hz, 13H), 7.25 – 7.22 (m, 3H), 7.18 (dd, $J = 8.8, 4.6$ Hz, 4H), 7.13 (td, $J = 7.6, 2.6$ Hz, 4H), 7.07 (dd, $J = 7.7, 5.5$ Hz, 2H), 5.09 (d, $J = 11.5$ Hz, 1H), 4.99 (d, $J = 11.5$ Hz, 1H), 3.81 (s, 3H), 3.63 (s, 3H), 3.62 – 3.58 (m, 1H), 3.09 (dd, $J = 13.1, 7.9$ Hz, 1H), 2.86 (dd, $J = 13.0, 2.8$ Hz, 1H), 2.80 (dd, $J = 10.2, 3.0$ Hz, 1H).



2-amino-9-(((1-azido-3-hydroxypropan-2-yl)oxy)methyl)-1,9-dihydro-6H-purin-6-one (2.28)

To a stirring solution of acetic acid (80 mL) and water (20 mL) chilled to 0 °C was added **2.27** (1 g, 1 Eq, 1 mmol). This was held at 0 °C for 30min and then allowed to come to 23 °C for 72hr. Upon completion the solvent was removed under reduced pressure and the remaining residue was triturated with diethyl ether (40mL) to yield **2.28** (0.3 g, 0.9 mmol, 75 %).

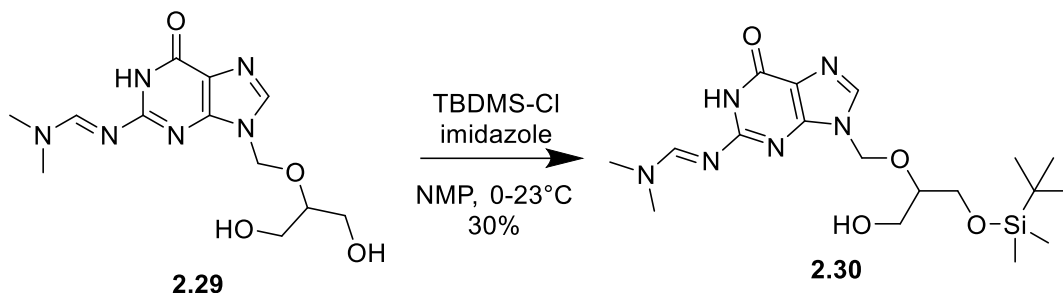
¹H NMR (599 MHz, MeOD) δ 7.87 (s, 1H), 5.59 (s, 2H), 3.92 – 3.87 (m, 1H), 3.57 (dd, $J = 11.8, 5.0$ Hz, 1H), 3.52 (dd, $J = 11.8, 5.6$ Hz, 1H), 3.35 (dd, $J = 13.1, 3.8$ Hz, 1H), 3.31 – 3.25 (m, 1H).



(E)-N'-(9-(((1,3-dihydroxypropan-2-yl)oxy)methyl)-6-oxo-6,9-dihydro-1H-purin-2-yl)-N,N-dimethylformimidamide (2.29)

To a stirring suspension of Ganciclovir (20 g, 1 Eq, 78 mmol) in DMF (250 mL) was added 1,1-dimethoxy-N,N-dimethylmethanamine (47 g, 52 mL, 5 Eq, 0.39 mol). The reaction was stirred at 23 °C for 14 hour at which time the bulk of solvent was evaporated. The remaining solution was filtered and triturated with ether (200 mL). The remaining solid was dried on high vacuum to yield **2.29** (23 g, 74 mmol, 95 %) as a white solid.

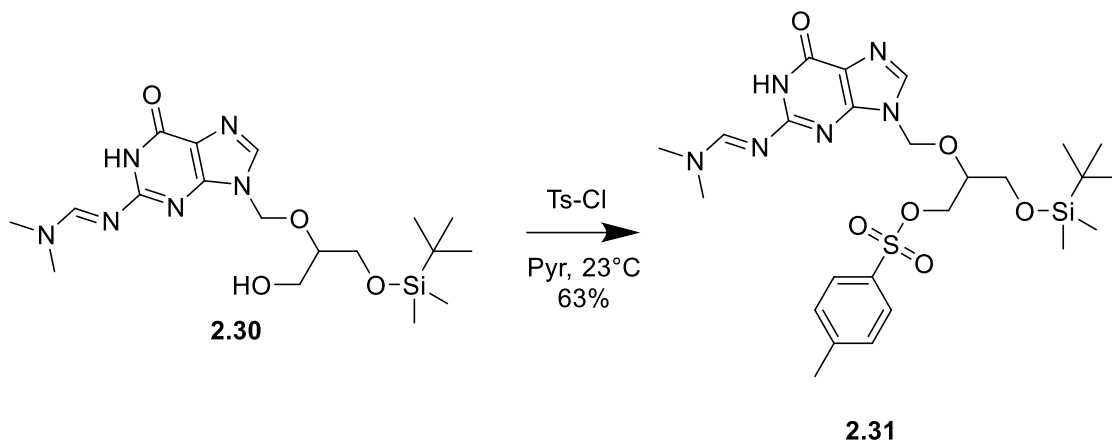
¹H NMR (599 MHz, MeOD) δ 8.61 (s, 1H), 7.86 (s, 1H), 5.57 (s, 2H), 3.69 – 3.64 (m, 1H), 3.50 (dd, $J = 11.7, 4.5$ Hz, 2H), 3.42 (dd, $J = 11.7, 6.1$ Hz, 2H), 3.12 (s, 3H), 3.03 (s, 3H).



(E)-N'-9-(((1-((tert-butyldimethylsilyl)oxy)-3-hydroxypropan-2-yl)oxy)methyl)-6-oxo-6,9-dihydro-1H-purin-2-yl)-N,N-dimethylformimidamide (2.30)

2.29 (100 mg, 1 Eq, 322 μmol) and imidazole (43.9 mg, 2 Eq, 645 μmol) were added to a scintillation vial containing NMP (15 mL) and was heated to create a homogeneous solution. The reaction was brought back down to 23 $^\circ\text{C}$ and tert-butyldimethylchlorosilane (31.6 mg, 0.65 Eq, 209 μmol) was added in very small portions. The reaction was allowed to continue until all starting material had been consumed by TLC. Upon completion the reaction was diluted with EtOAc (45mL), washed with water (4x40mL), brine (40mL), dried by Na_2SO_4 , filtered, and concentrated under reduced pressure. The residue was purified by silica gel chromatography (DCM:MeOH (0-10%)) to yield **2.30** (41 mg, 97 μmol , 30 %).

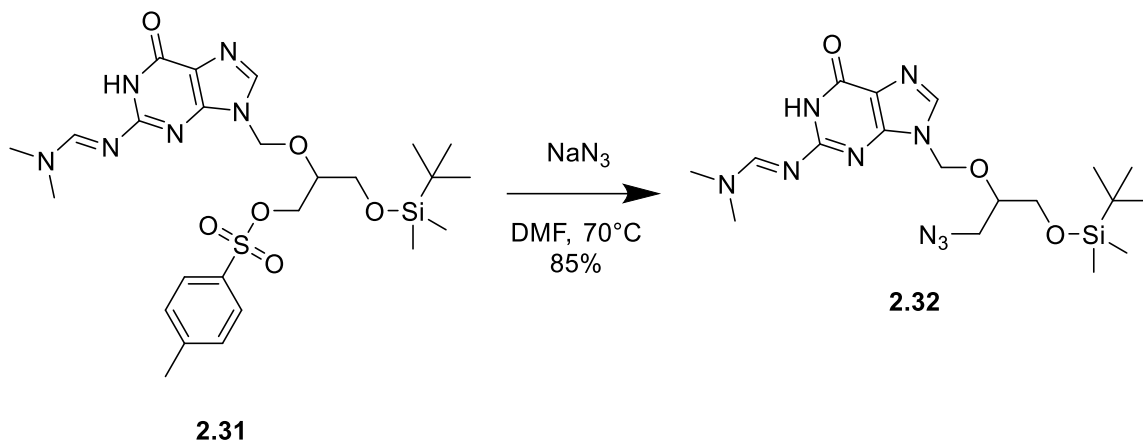
$R_f = 0.27$ (DCM:MeOH (9:1)) **$^1\text{H NMR}$** (599 MHz, MeOD) δ 8.71 (s, 1H), 7.95 (s, 1H), 5.66 (s, 2H), 3.80 (dt, $J = 10.3, 5.3$ Hz, 1H), 3.66 – 3.60 (m, 2H), 3.52 (ddd, $J = 10.6, 5.9, 3.2$ Hz, 2H), 3.21 (s, 3H), 3.13 (s, 3H), 0.84 (s, 9H), -0.00 (s, 3H), -0.02 (s, 3H).



(E)-3-((tert-butyl dimethylsilyl)oxy)-2-((2-(((dimethylamino)methylene)amino)-6-oxo-1,6-dihydro-9H-purin-9-yl)methoxy)propyl 4-methylbenzenesulfonate (2.31)

To a stirring solution of **2.30** (143 mg, 1 Eq, 337 μmol) in Pyridine (10 mL) at 23 $^\circ\text{C}$ was added tosyl-Cl (257 mg, 4 Eq, 1.35 mmol) and stirred for 14 hour. Upon completion the reaction was diluted with EtOAc (30mL), washed with a saturated solution of CuSO_4 (3x 60mL), brine (30mL), dried by Na_2SO_4 , filtered, and concentrated under reduced pressure. The residue was purified by silica gel chromatography (DCM:MeOH (0-2%)) to yield **2.31** (0.12 g, 0.21 mmol, 63 %).

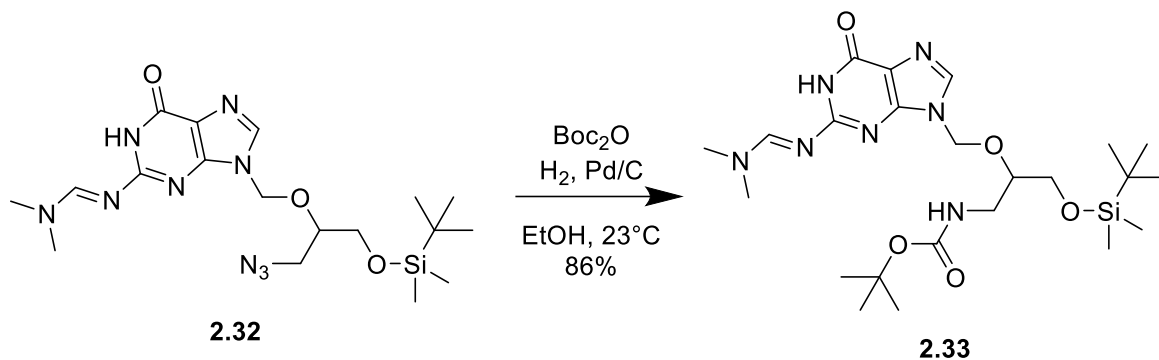
$R_f = 0.33$ (DCM:MeOH (9:1)) $^1\text{H NMR}$ (599 MHz, CDCl_3) δ 8.82 (s, 1H), 7.74 (d, $J = 8.2$ Hz, 2H), 7.67 (s, 1H), 7.34 (d, $J = 8.0$ Hz, 2H), 5.64 (d, $J = 11.1$ Hz, 1H), 5.49 (d, $J = 11.1$ Hz, 1H), 4.22 (d, $J = 9.0$ Hz, 1H), 4.02 – 3.93 (m, 2H), 3.49 – 3.41 (m, 2H), 3.33 (s, 23), 3.25 (s, 3H), 2.45 (s, 3H), 0.79 (s, 9H), -0.06 (s, 3H), -0.07 (s, 3H).



(E)-N'-9-(((1-azido-3-((tert-butyldimethylsilyl)oxy)propan-2-yl)oxy)methyl)-6-oxo-6,9-dihydro-1H-purin-2-yl)-N,N-dimethylformimidamide (2.32)

To a stirring solution of **2.31** (950 mg, 1 Eq, 1.64 mmol) in DMF (20 mL) was added sodium azide (320 mg, 3 Eq, 4.92 mmol). After reaction was heated to 70 °C for 14 hour it was cooled to 23 °C, diluted with EtOAc (70mL), washed with water (4x 50mL), brine (50mL), dried by Na₂SO₄, filtered, and concentrated under reduced pressure. The residue was purified by silica gel chromatography (DCM:MeOH (0-4%)) to yield **2.32** (0.63 g, 1.4 mmol, 85 %).

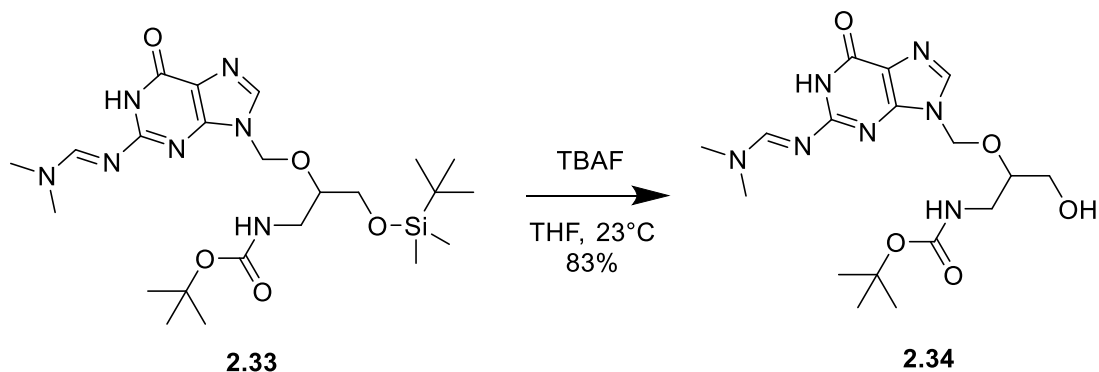
R_f = 0.42 (DCM:MeOH (9:1)) **¹H NMR** (599 MHz, MeOD) δ 8.72 (s, 1H), 7.96 (s, 1H), 5.67 (s, 2H), 3.95 (dt, *J* = 11.5, 5.6 Hz, 1H), 3.61 (dd, *J* = 10.7, 5.4 Hz, 1H), 3.56 (dd, *J* = 10.7, 5.6 Hz, 1H), 3.37 (dd, *J* = 13.0, 3.9 Hz, 1H), 3.21 (s, 3H), 3.14 (s, 3H), 0.86 (s, 9H), 0.02 (s, 3H), 0.01 (s, 3H).



***tert*-butyl (*E*)-(3-((*tert*-butyldimethylsilyl)oxy)-2-((2-
 (((dimethylamino)methylene)amino)-6-oxo-1,6-dihydro-9*H*-purin-9-
 yl)methoxy)propyl)carbamate (**2.33**)**

A mixture of **2.32** (212.2 mg, 1 Eq, 472.0 μmol) and boc2o (154.5 mg, 163 μL , 1.5 Eq, 708.0 μmol) in Ethanol (10 mL) was treated with palladium on carbon (25.11 mg, 10% Wt, 0.05 Eq, 23.60 μmol). The mixture was vigorously stirred under a hydrogen atmosphere for 14 hours. Upon completion the suspension was filtered through a pad of celite and washed with EtOH (5mL). The filtrate was concentrated in vacuo and purified by silica gel chromatography (DCM:MeOH (0-5%)) to afford **2.33** (0.21 g, 0.41 mmol, 86 %).

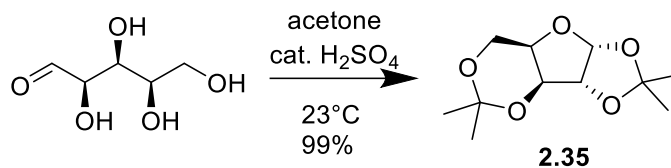
$R_f = 0.25$ (DCM:MeOH (9:1)) **$^1\text{H NMR}$** (599 MHz, MeOD) δ 8.74 (s, 1H), 7.93 (s, 1H), 5.62 (q, $J = 11.3$ Hz, 2H), 3.87 (s, 1H), 3.63 (dd, $J = 11.0, 4.4$ Hz, 1H), 3.53 (dd, $J = 10.9, 6.1$ Hz, 1H), 3.27 – 3.20 (m, 3H), 3.14 (s, 3H), 3.01 (dd, $J = 14.2, 7.2$ Hz, 1H), 1.39 (s, 9H), 0.86 (s, 9H), 0.02 (s, 3H), 0.01 (s, 3H).



***tert*-butyl (*E*)-(2-((2-(((dimethylamino)methylene)amino)-6-oxo-1,6-dihydro-9*H*-purin-9-yl)methoxy)-3-hydroxypropyl)carbamate (**2.34**)**

To a stirring solution **2.33** (112 mg, 1 Eq, 214 μmol) in THF (5 mL) was added TBAF (72.7 mg, 278 μL , 1 molar, 1.3 Eq, 278 μmol) dropwise at 23 °C and stirred for 3 hour. After the starting material had been consumed by TLC the reaction was diluted with EtOAc (20mL), washed with water (20mL), brine (20mL), dried by Na_2SO_4 , filtered, and concentrated under reduced pressure. The residue was purified by silica gel chromatography (DCM:MeOH (0-10%)) to yield **2.34** (73 mg, 0.18 mmol, 83 %).

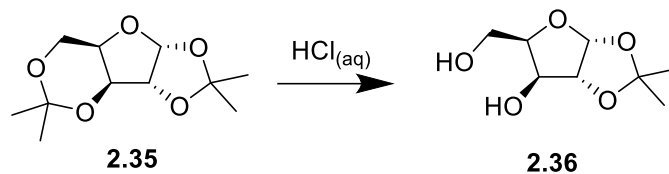
$R_f = 0.2$ (DCM:MeOH (9:1)) **$^1\text{H NMR}$** (599 MHz, MeOD) δ 8.73 (s, 1H), 7.94 (s, 1H), 5.62 (s, 2H), 3.80 (s, 1H), 3.58 (dd, $J = 11.9, 4.1$ Hz, 1H), 3.50 (dd, $J = 11.9, 5.9$ Hz, 1H), 3.26 – 3.20 (m, 4H), 3.13 (s, 3H), 3.03 (dd, $J = 14.2, 7.1$ Hz, 1H), 1.38 (s, 9H).



(3a*R*,3b*S*,7a*R*,8a*R*)-2,2,5,5-tetramethyltetrahydro-7*H*-[1,3]dioxolo[4',5':4,5]furo[3,2-*d*][1,3]dioxine (2.35)

To a stirring solution of D-xylose (32 g, 1 Eq, 0.21 mol) in acetone (780 mL) was added sulfuric acid (1.8 g, 28 mL, .66 molar, 0.088 Eq, 19 mmol) and allow to stir for 48hr at 23°C. Upon completion the reaction was filtered through celite and to the filtrate was added ammonia (5mL), and filtered again to remove ammonium sulfate. The filtrate was concentrated under reduced pressure and the residue was eluted through a silica plug with (Hexanes:EtOAc (3:2)) yielding **2.35** (49 g, 0.21 mol, 99 %) as yellow oil.

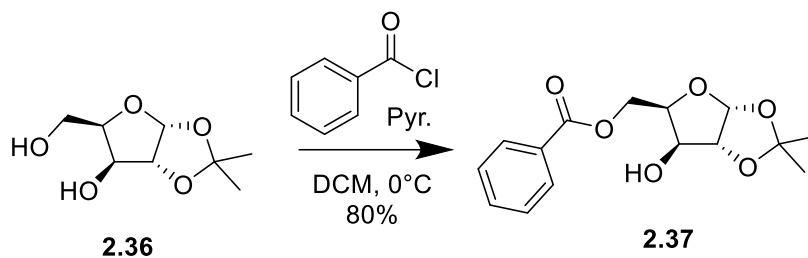
$R_f = 0.65$ (Hexanes:EtOAc (1:1)) $^1\text{H NMR}$ (599 MHz, CDCl_3) δ 6.00 (d, $J = 3.7$ Hz, 1H), 4.52 (d, $J = 3.6$ Hz, 1H), 4.29 (d, $J = 2.1$ Hz, 1H), 4.10 (d, $J = 11.2$ Hz, 1H), 4.06 (d, $J = 13.5$ Hz, 1H), 4.02 (d, $J = 1.3$ Hz, 1H), 1.49 (s, 3H), 1.44 (s, 3H), 1.38 (s, 3H), 1.32 (s, 3H). Spectrum matched: *J. Org. Chem.* **2022**, 87, 1925–1933



(3a*R*,5*R*,6*S*,6a*R*)-5-(hydroxymethyl)-2,2-dimethyltetrahydrofuro[2,3-*d*][1,3]dioxol-6-ol (2.36)

2.35 (49g , 1 Eq, 0.21 mol) was dissolved in 0.24M HCl (400mL) and stirred at 23°C for 1.5 hours, after which time the majority of solvent was removed with the rotovap. To the remaining solution was added ethanol (30mL) and toluene (30mL) in order to codistill the remaining water. The residue was loaded onto a silica plug and with eluted with (Hexanes:EtOAc (66-100%)) to yield **2.36** (39 g, 0.20 mol, 95 %) as a yellow oil.

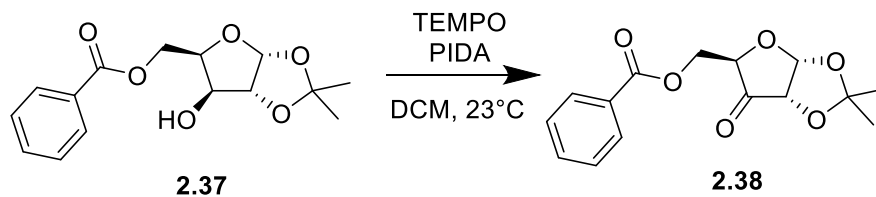
R_f = 0.13 (Hexanes:EtOAc (1:1)) **¹H NMR** (599 MHz, CDCl₃) δ 5.99 (d, *J* = 3.6 Hz, 1H), 4.53 (d, *J* = 3.6 Hz, 1H), 4.34 (d, *J* = 2.2 Hz, 1H), 4.18 (d, *J* = 3.6 Hz, 1H), 4.15 (d, *J* = 3.7 Hz, 1H), 4.06 (d, *J* = 10.7 Hz, 1H), 1.49 (s, 3H), 1.33 (s, 3H). Spectrum matched: *J*. *Org. Chem.* **2022**, 87, 1925–1933



((3a*R*,5*R*,6*S*,6a*R*)-6-hydroxy-2,2-dimethyltetrahydrofuro[2,3-*d*][1,3]dioxol-5-yl)methyl benzoate (2.37)

2.36 (5 g, 1 Eq, 0.03 mol) and pyridine (4 g, 4 mL, 2 Eq, 0.05 mol) were added to an argon flushed scintillation vial containing DCM (5 mL) at 0°C. To this was added benzoyl chloride (4 g, 3 mL, 1.08 Eq, 0.03 mol) dropwise over a 1 hour period and stirred for another hour. After the reaction was quenched with water (10mL), and the organic phase was washed with a 10% citric acid solution (20mL), saturated NaHCO₃ solution (20mL), brine (20mL), dried by Na₂SO₄, filtered, and concentrated in vacuo. The residue was purified by silica gel chromatography (Hexanes: EtOAc (10-50%)) to yield **2.37** (6 g, 0.02 mol, 80 %). This material can be telescoped to next reaction without purification.

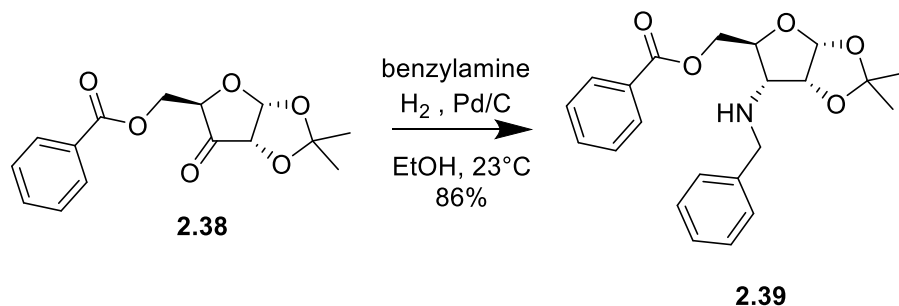
¹H NMR (599 MHz, CDCl₃) δ 8.06 (dd, *J* = 8.3, 1.1 Hz, 2H), 7.59 (t, *J* = 7.4 Hz, 1H), 7.46 (t, *J* = 7.8 Hz, 2H), 5.98 (d, *J* = 3.6 Hz, 1H), 4.79 (dd, *J* = 13.5, 9.4 Hz, 1H), 4.60 (d, *J* = 3.6 Hz, 1H), 4.42 (q, *J* = 5.0 Hz, 2H), 4.22 (d, *J* = 1.6 Hz, 1H), 1.52 (s, 3H), 1.33 (s, 3H). Spectrum matched: *J. Org. Chem.* **2022**, 87, 1925–1933



((3aR,5R,6aS)-2,2-dimethyl-6-oxotetrahydrofuro[2,3-d][1,3]dioxol-5-yl)methyl benzoate (2.38)

To a stirring solution of **2.37** (6 g, 0.02 mol, 80 %) in DCM (25mL) was added TEMPO (0.2 g, 0.05 Eq, 1 mmol) and phenyl-*I*-iodanediyl diacetate (0.01 kg, 1.5 Eq, 0.04 mol) portion wise at 23 °C and was allowed to react for 4 hours until the consumption of starting material was observed by TLC. To the reaction was added saturated sodium sulfite (25mL). The organic phase was washed with brine (25mL), dried by MgSO₄, filtered, and concentrated in vacuo. The residue was purified by silica gel chromatography (Hexanes: EtOAc (10-50%)) to yield **2.38** (6 g, 0.02 mol, 80 %). On large scale purification by recrystallizing with Hexanes is suitable.

¹H NMR (599 MHz, CDCl₃) δ 7.95 (d, *J* = 7.2 Hz, 2H), 7.57 (t, *J* = 7.4 Hz, 1H), 7.44 (t, *J* = 7.8 Hz, 2H), 6.14 (d, *J* = 4.4 Hz, 1H), 4.70 (dd, *J* = 16.7, 2.9 Hz, 1H), 4.46 (dd, *J* = 11.1, 2.7 Hz, 2H), 4.43 (d, *J* = 4.4 Hz, 1H), 1.51 (s, 3H), 1.43 (s, 3H). Spectrum matched: *J. Org. Chem.* **2022**, 87, 1925–1933

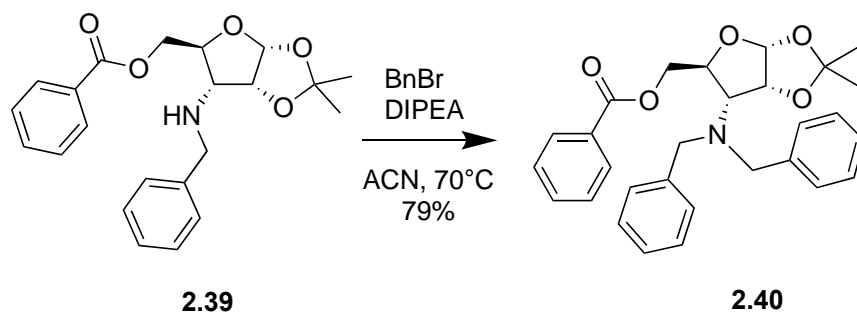


((3a*R*,5*S*,6*R*,6a*R*)-6-benzamido-2,2-dimethyltetrahydrofuro[2,3-*d*][1,3]dioxol-5-yl)methyl benzoate (2.39)

To an oven dried round bottom flask was added **2.38** (10.4 g, 1 Eq, 35.6 mmol) and dissolved in anhydrous EtOH (150 mL). To this was added benzylamine (5.72 g, 5.83 mL, 1.5 Eq, 53.4 mmol) and palladium on carbon (1.14 g, 10% Wt, 0.03 Eq, 1.07 mmol) with vigorous stirring. The reaction was put under a hydrogen atmosphere and stirred at 23 °C for 14 hour. Upon completion the reaction was filtered through a celite pad which was then washed with additional EtOH (30mL). The filtrate was concentrated in vacuo and purified by silica gel chromatography (Hexanes: EtOAc (10-30%)) to **2.39** (12 g, 31 mmol, 86 %). The crude product is clean enough to be telescoped to next reaction if needed.

¹H NMR (599 MHz, CDCl₃) δ 7.88 (d, *J* = 7.5 Hz, 2H), 7.47 (t, *J* = 7.4 Hz, 1H), 7.33 (t, *J* = 7.7 Hz, 2H), 7.28 (d, *J* = 7.5 Hz, 2H), 7.19 (dd, *J* = 8.6, 6.5 Hz, 2H), 7.11 (t, *J* = 7.3 Hz, 1H), 5.74 (d, *J* = 3.8 Hz, 1H), 4.65 (dd, *J* = 12.1, 1.9 Hz, 1H), 4.54 (t, *J* = 4.2 Hz, 1H), 4.29 (dd, *J* = 12.1, 5.3 Hz, 1H), 3.94 (dd, *J* = 5.3, 1.9 Hz, 1H), 3.91 (d, *J* = 13.4 Hz, 2H), 3.71 (d, *J* = 13.2 Hz, 1H), 2.94 (dd, *J* = 9.9, 4.6 Hz, 1H), 1.48 (s, 3H), 1.30 (s, 3H).

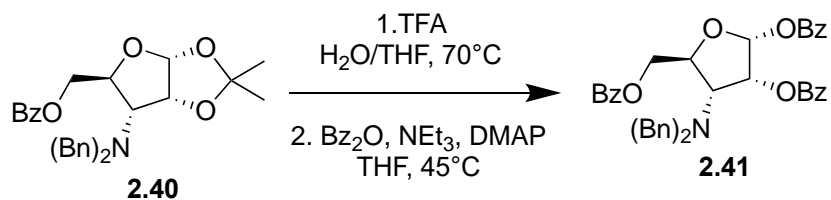
Spectrum matched: *J. Org. Chem.* **2022**, 87, 1925–1933



((3a*R*,5*S*,6*R*,6a*R*)-6-(dibenzylamino)-2,2-dimethyltetrahydrofuro[2,3-*d*][1,3]dioxol-5-yl)methyl benzoate (2.40)

To a stirring solution of **2.39** (13.6 g, 1 Eq, 35.5 mmol) in acn (150 mL) was added benzyl bromide (12.1 g, 8.44 mL, 2 Eq, 70.9 mmol) and DIPEA (13.8 g, 18.5 mL, 3 Eq, 106 mmol). This was stirred at 70 °C for 14 hour at which time the reaction was diluted with EtOAc (200mL), washed with 10% citric acid solution (200mL), brine (200mL), dried by Na₂SO₄, filtered, and concentrated under vacuum. The residue was purified and by silica gel chromatography (Hexanes: EtOAc (5-20%)) to yield **2.40** (13 g, 28 mmol, 79 %) as a yellow oil.

R_f = 0.46 (Hexanes:EtOAc (1:1)) **¹H NMR** (300 MHz, CDCl₃) δ 7.82 (dd, *J* = 5.1, 3.3 Hz, 2H), 7.53 (t, *J* = 7.4 Hz, 1H), 7.37 (dd, *J* = 7.3, 6.0 Hz, 5H), 7.28 – 7.20 (m, 5H), 7.14 (t, *J* = 7.2 Hz, 2H), 5.70 (d, *J* = 3.7 Hz, 1H), 4.80 (t, *J* = 4.0 Hz, 1H), 4.76 (dd, *J* = 13.0, 2.5 Hz, 1H), 4.60 (ddd, *J* = 10.5, 4.6, 1.9 Hz, 1H), 4.31 (dd, *J* = 12.3, 4.6 Hz, 1H), 4.10 (d, *J* = 14.1 Hz, 2H), 3.80 (d, *J* = 14.0 Hz, 2H), 3.14 (dd, *J* = 10.4, 4.0 Hz, 1H), 1.61 (s, 3H), 1.39 (s, 3H). Spectrum matched: *J. Org. Chem.* **2022**, 87, 1925–1933

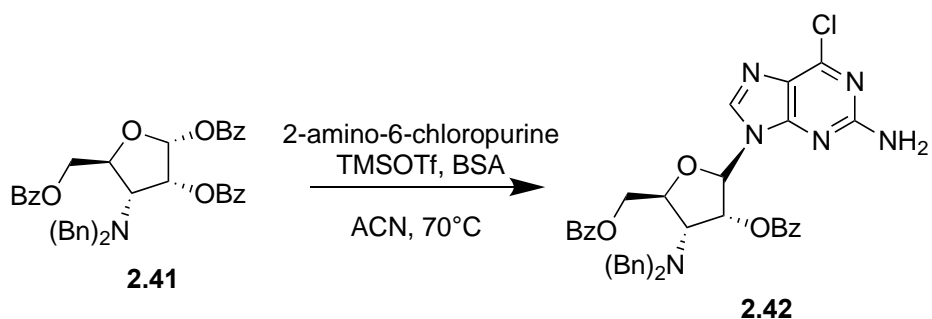


((2S,3S,4R,5S)-3-(N-benzoylbenzamido)-4,5-dihydroxytetrahydrofuran-2-yl)methyl benzoate (2.41)

To an argon flushed 100 mL flask, **2.40** (5.5 g, 1 Eq, 12 mmol), THF (16 mL), and water (8.0 mL) were charged to stir to a homogeneous solution. TFA (16 mL) was added to the reactor, and the solution was aged for 8 h at 70 °C on a heating mantle. The solution was then cooled to 10 °C and diluted with toluene (50 mL). The layer was separated, and the organic crude was washed with saturated NaHCO₃ (2x 20mL). The organic layer was washed with brine (20 mL), and the solution was used in the next step without further purification. To the solution was added DMAP (71 mg, 0.05 Eq, 0.58 mmol), triethylamine (3.5 g, 4.9 mL, 3 Eq, 35 mmol), and benzoic anhydride (6.6 g, 2.5 Eq, 29 mmol). The crude was aged at 45 °C on a heating mantle for 16 h. The reaction was washed with brine (40 mL), dried with Na₂SO₄, filtered, and concentrated on the rotovap. The residue was purified and by silica gel chromatography (Hexanes: EtOAc (10-20%)) to **2.41** (5.8 g, 9.1 mmol, 78 %) as a tan solid.

R_f = 0.4 (Hexanes:EtOAc (1:1)) **¹H NMR** (599 MHz, CDCl₃) δ 8.17 – 8.12 (m, 2H), 7.77 (d, *J* = 7.8 Hz, 2H), 7.68 (d, *J* = 7.2 Hz, 5H), 7.64 (dt, *J* = 14.8, 7.4 Hz, 1H), 7.57 (t, *J* = 7.5 Hz, 1H), 7.51 (dt, *J* = 15.7, 7.8 Hz, 7H), 7.41 (t, *J* = 7.4 Hz, 1H), 7.39 – 7.31 (m, 6H), 7.24 (t, *J* = 7.6 Hz, 4H), 7.14 (t, *J* = 7.3 Hz, 2H), 7.09 (t, *J* = 7.8 Hz, 2H), 6.43 (s, 1H),

5.87 (d, $J = 4.1$ Hz, 1H), 4.94 – 4.91 (m, 1H), 4.71 (dd, $J = 12.2, 2.3$ Hz, 1H), 4.44 (dd, $J = 12.2, 3.8$ Hz, 1H), 4.17 (d, $J = 13.6$ Hz, 2H), 4.00 (dd, $J = 9.8, 4.2$ Hz, 1H), 3.72 (d, $J = 13.6$ Hz, 2H). Spectrum matched: *J. Org. Chem.* **2022**, 87, 1925–1933



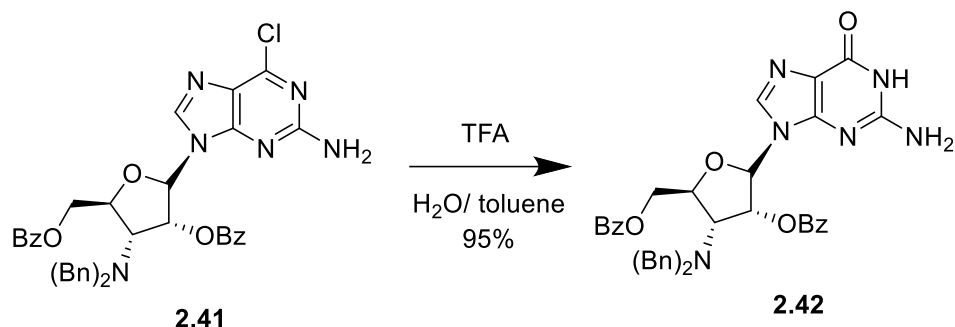
((2*S*,3*R*,4*R*,5*R*)-5-(2-amino-6-chloro-9*H*-purin-9-yl)-4-(benzoyloxy)-3-(dibenzylamino) tetrahydrofuran-2-yl)methyl benzoate (2.42)

To an argon backfilled flask with **2.41** (4.17 g, 1 Eq, 6.50 mmol) was added ACN (40 mL). To this solution was added 6-chloro-9*H*-purin-2-amine (2.20 g, 2 Eq, 13.0 mmol) and trimethylsilyl (E)-*N*-(trimethylsilyl)acetimidate (1.98 g, 2.38 mL, 1.5 Eq, 9.75 mmol) at 23°C to generate some precipitate. This was heated to 65°C for 20 minutes and then trimethylsilyl (E)-*N*-(trimethylsilyl)acetimidate (1.98 g, 2.38 mL, 1.5 Eq, 9.75 mmol) was added resulting in a homogeneous solution which was heated to 70°C for 7 hours. After the solution was cooled to 23°C it was quenched with a saturated NaHCO₃ solution (35mL). The reaction was extracted with toluene (40mL) and the organic phase was washed with a saturated NaHCO₃ solution (35mL), brine (35mL), dried with Na₂SO₄, filtered, and concentrated in vacuo. The residue was purified by silica gel chromatography (Hexanes: EtOAc (10-50%)) to **2.42** (3.1 g, 4.5 mmol, 70 %) as a tan solid. The product of this step can be telescoped to the next reaction without need for purification.

R_f = 0.5 (DCM:MeOH (9.5:0.5)) **¹H NMR** (300 MHz, CDCl₃) δ 8.13 (d, *J* = 7.1 Hz, 2H), 7.77 (dd, *J* = 8.3, 1.2 Hz, 2H), 7.66 (s, 1H), 7.52 (q, *J* = 7.5 Hz, 3H), 7.39 – 7.33 (m,

5H), 7.25 – 7.14 (m, 5H), 6.31 (dd, $J = 5.9, 1.6$ Hz, 1H), 5.94 (d, $J = 1.6$ Hz, 1H), 4.99 – 4.85 (m, 2H), 4.62 – 4.49 (m, 3H), 4.17 (d, $J = 14.1$ Hz, 2H), 3.93 (d, $J = 14.1$ Hz, 2H).

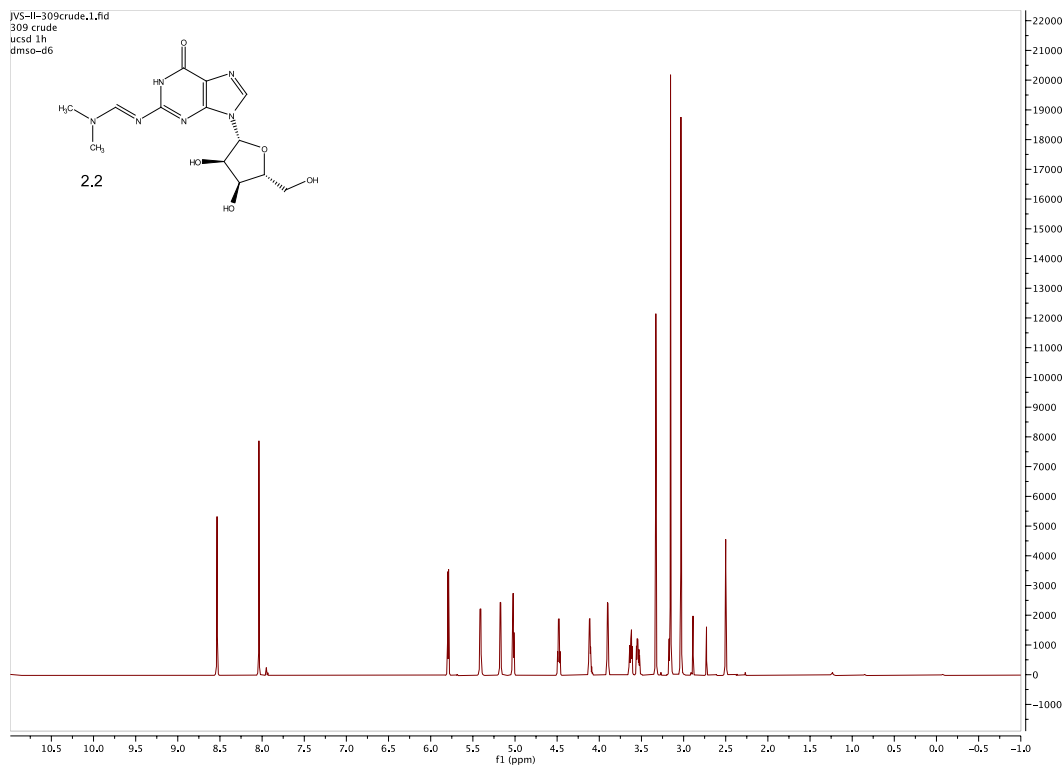
Spectrum matched: *J. Org. Chem.* **2022**, 87, 1925–1933



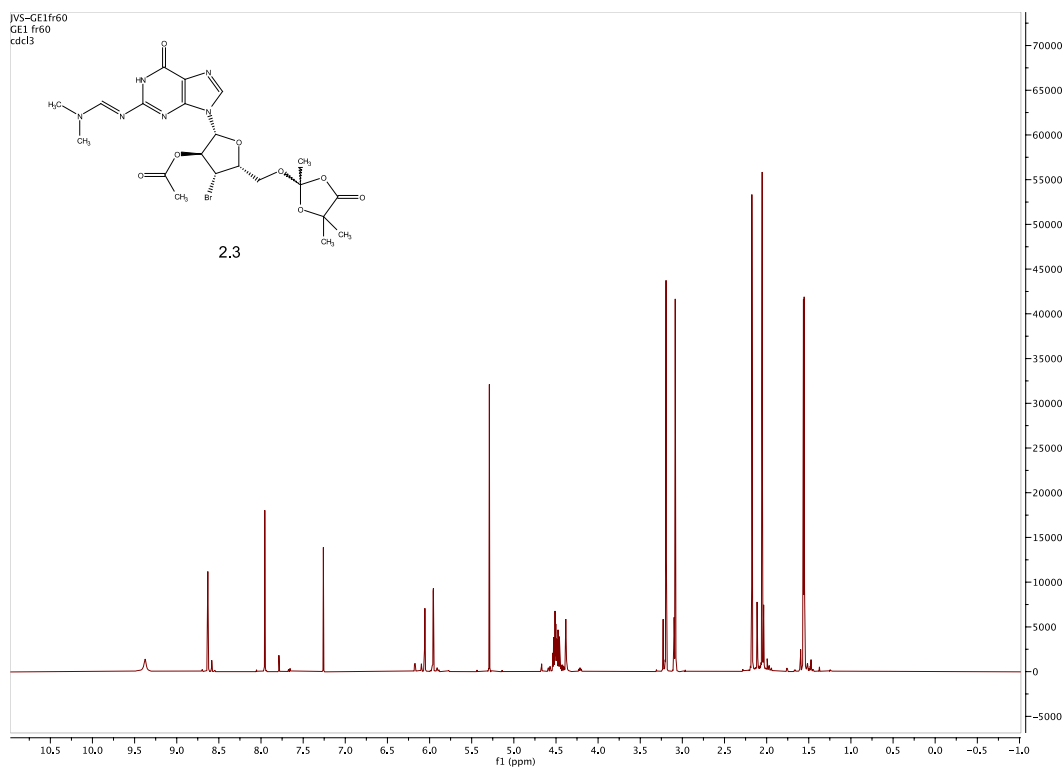
((2*S*,3*R*,4*R*,5*R*)-5-(2-amino-6-oxo-1,6-dihydro-9*H*-purin-9-yl)-4-(benzoyloxy)-3-(dibenzylamino) tetrahydrofuran-2-yl)methyl benzoate (2.42)

To a stirring solution of **2.41** (3.5 g, 1 Eq, 5.1 mmol) in toluene (15mL) and water (5mL) was added TFA (58 g, 39 mL, 100 Eq, 0.51 mol). This was stirred at 40C for 20 hours. After cooling back down to 23C the reaction was diluted with water (75mL) and toluene (30mL). The toluene layer was washed with saturated NaHCO₃ (3x 50mL), brine (50mL), dried by Na₂SO₄, filtered, and concentrated under reduced pressure. The residue was purified by silica gel chromatography (DCM: MeOH (0-4%)) to **2.42** (2.8 g, 4.2 mmol, 83 %) as a tan solid.

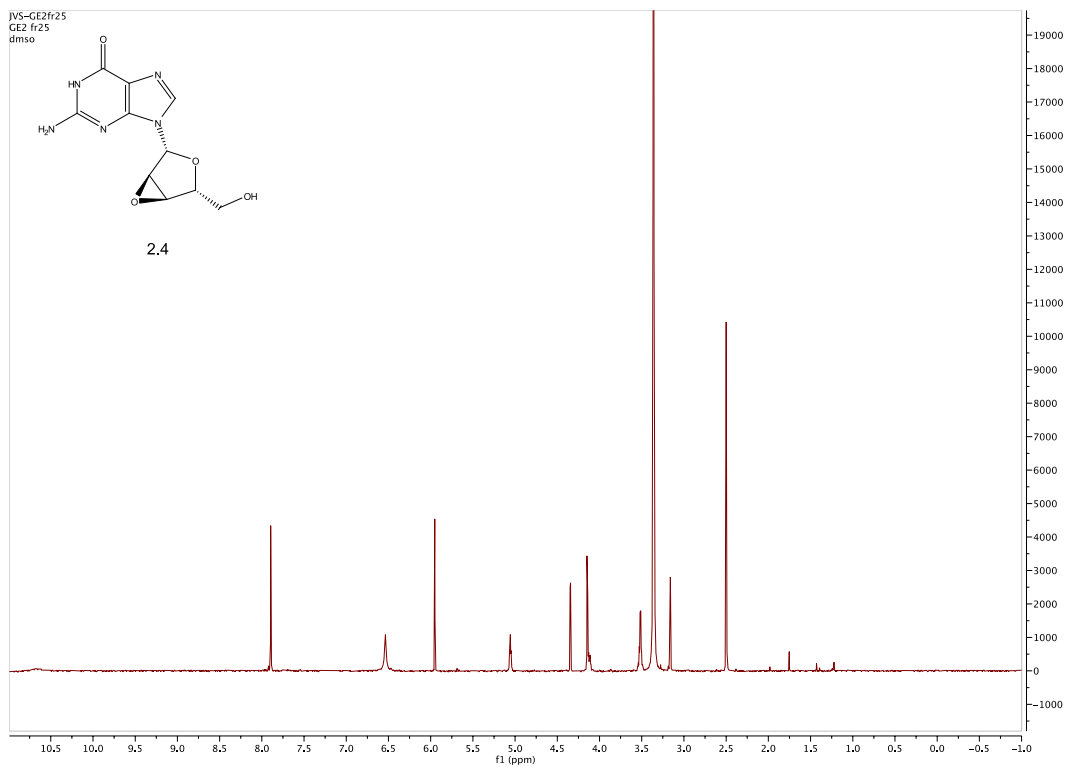
R_f = 0.14 (DCM:MeOH (9.5:0.5)) **¹H NMR** (599 MHz, DMSO) δ 10.73 (s, 1H), 8.11 (d, *J* = 7.3 Hz, 2H), 7.77 (d, *J* = 7.5 Hz, 2H), 7.74 (t, *J* = 7.3 Hz, 1H), 7.68 – 7.64 (m, 2H), 7.60 (t, *J* = 7.7 Hz, 2H), 7.48 (t, *J* = 7.7 Hz, 3H), 7.29 (d, *J* = 7.4 Hz, 5H), 7.20 (t, *J* = 7.4 Hz, 5H), 7.14 (t, *J* = 7.2 Hz, 3H), 6.14 (s, 4H), 5.02 – 4.96 (m, 1H), 4.72 (dd, *J* = 12.0, 2.5 Hz, 1H), 4.51 (dd, *J* = 12.0, 4.6 Hz, 1H), 4.15 (t, *J* = 7.4 Hz, 1H), 4.05 (d, *J* = 14.1 Hz, 2H), 3.86 (d, *J* = 14.2 Hz, 2H). Spectrum matched: *J. Org. Chem.* **2022**, 87, 1925–1933



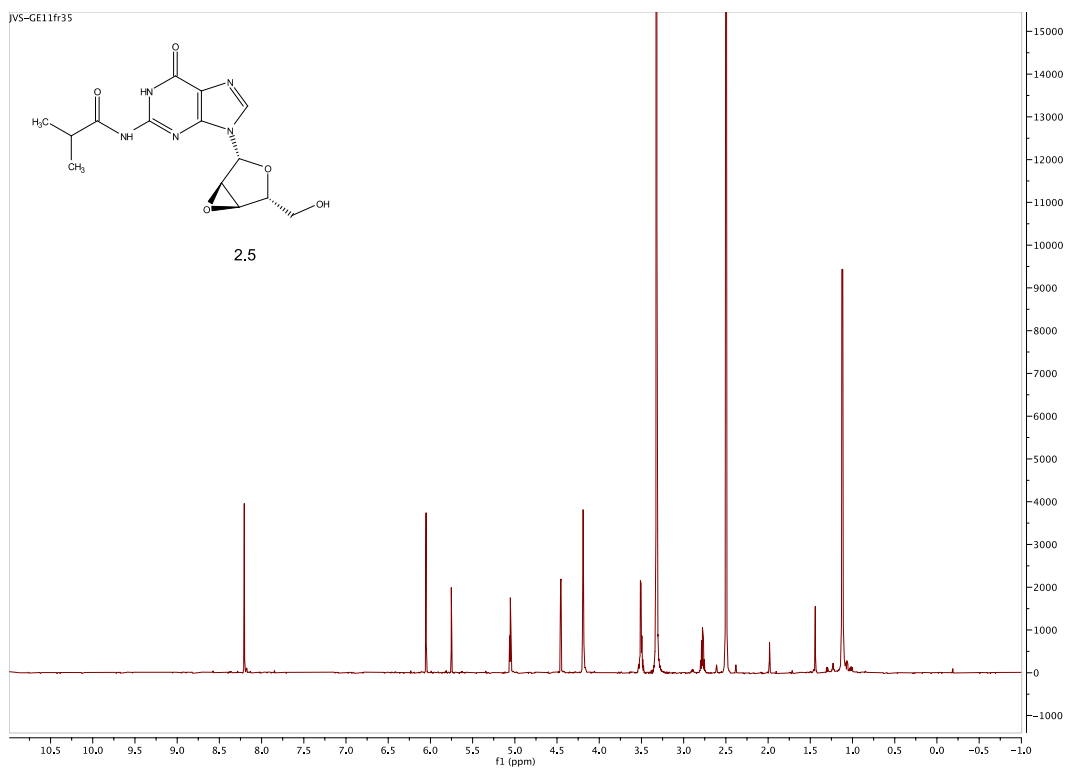
Spectra 2.1 ^1H NMR Spectrum of compound **2.2**



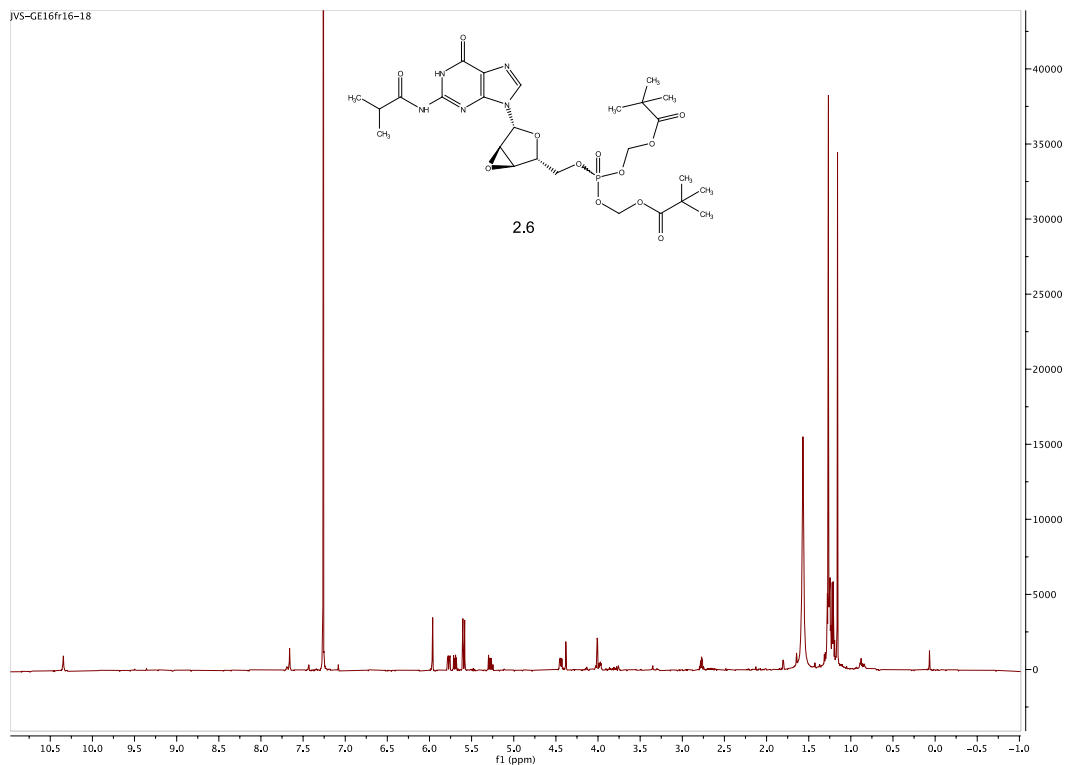
Spectra 2.2 ^1H NMR Spectrum of compound **2.3**



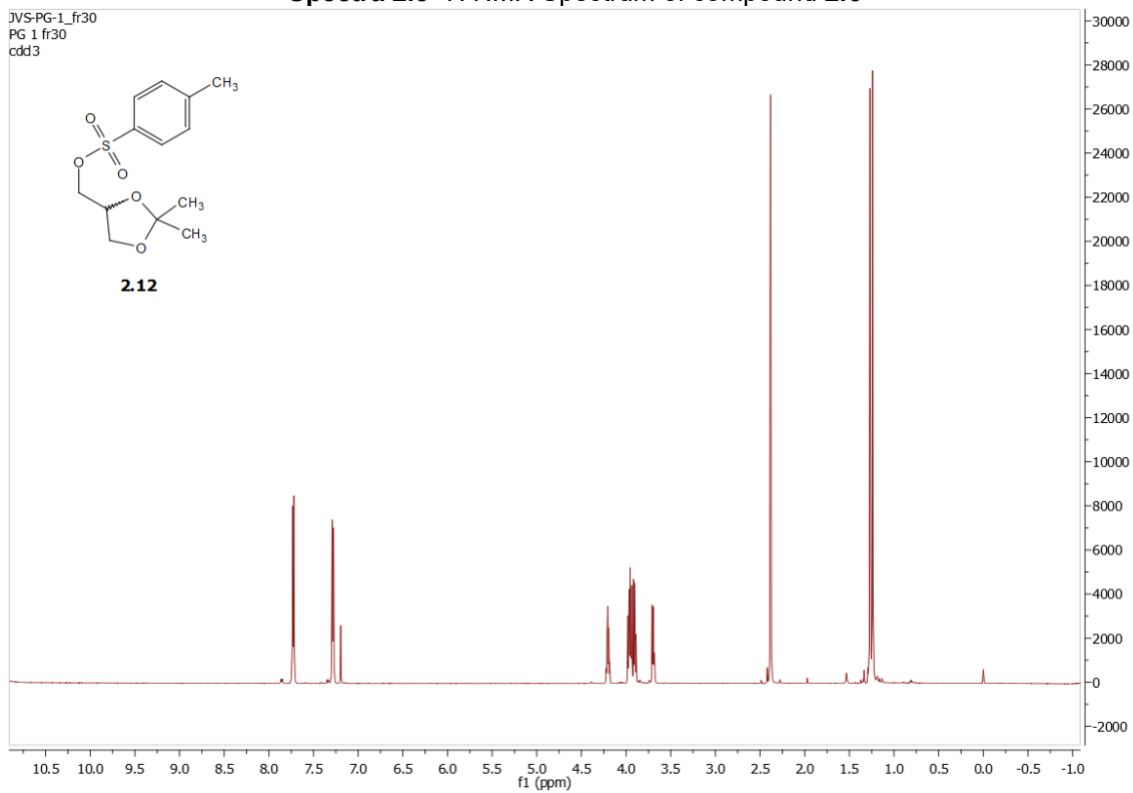
Spectra 2.3 ^1H NMR Spectrum of compound **2.4**



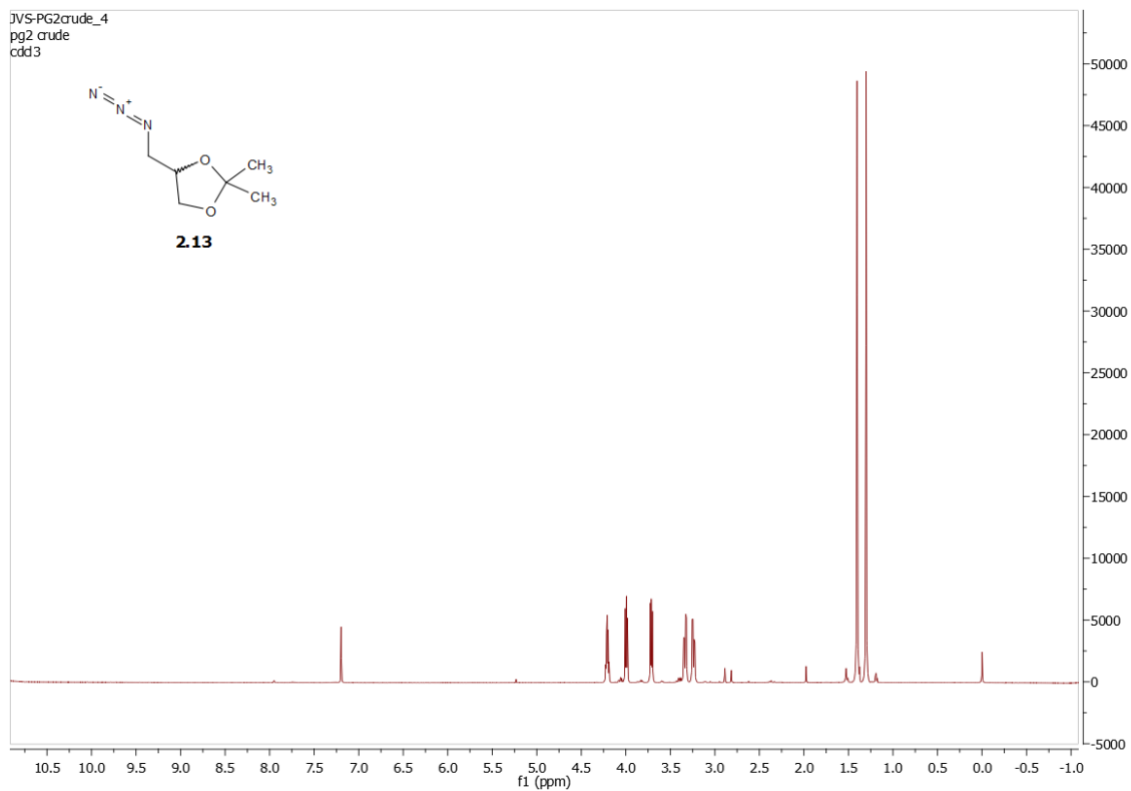
Spectra 2.4 ^1H NMR Spectrum of compound **2.5**



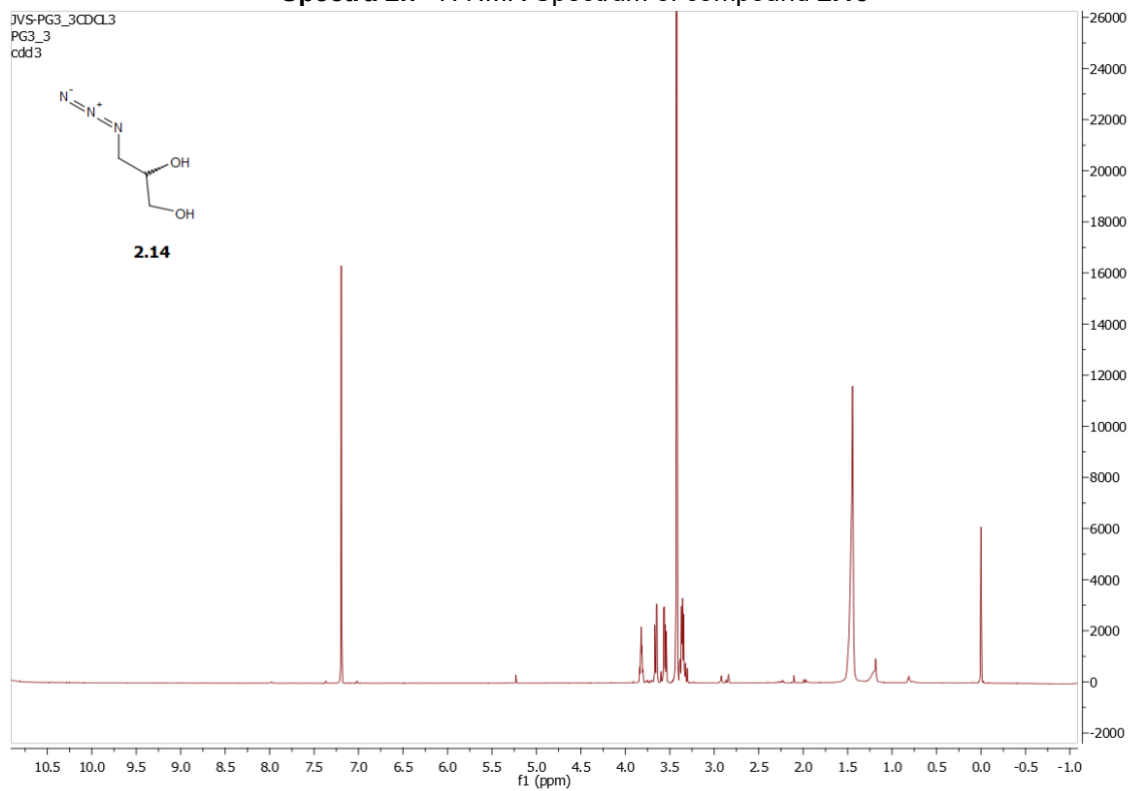
Spectra 2.5 ^1H NMR Spectrum of compound 2.6



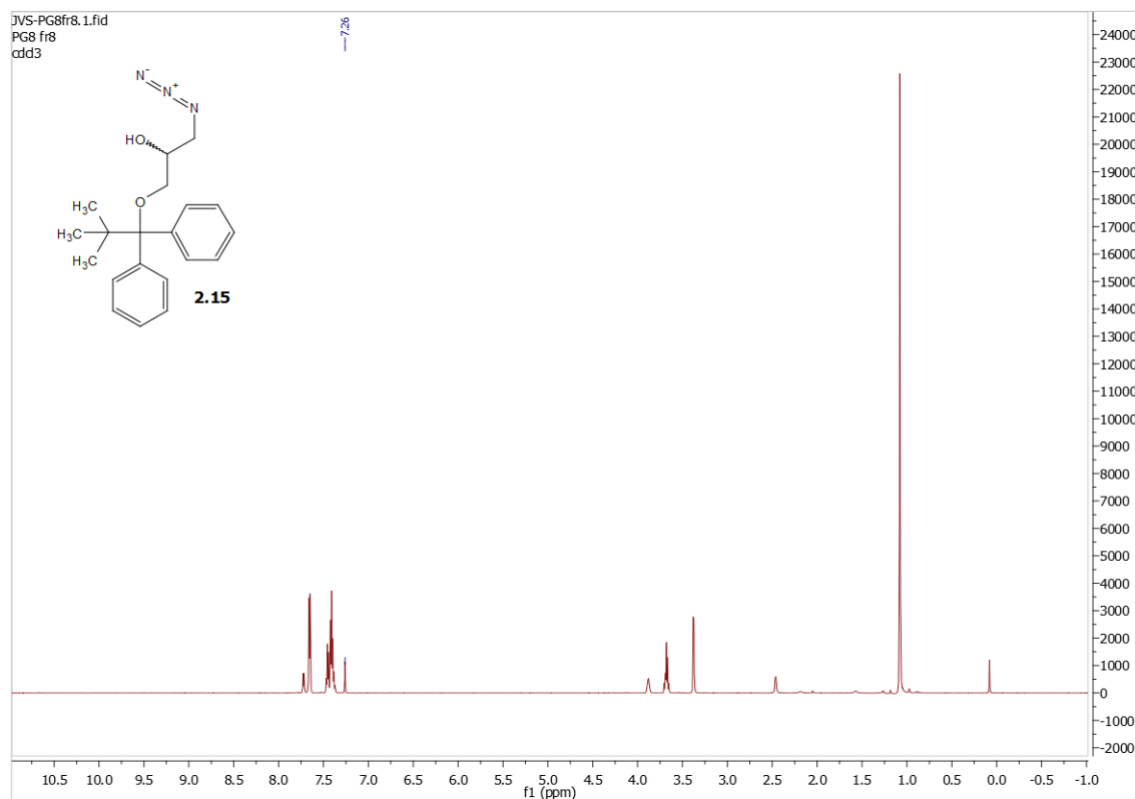
Spectra 2.6 ^1H NMR Spectrum of compound 2.12



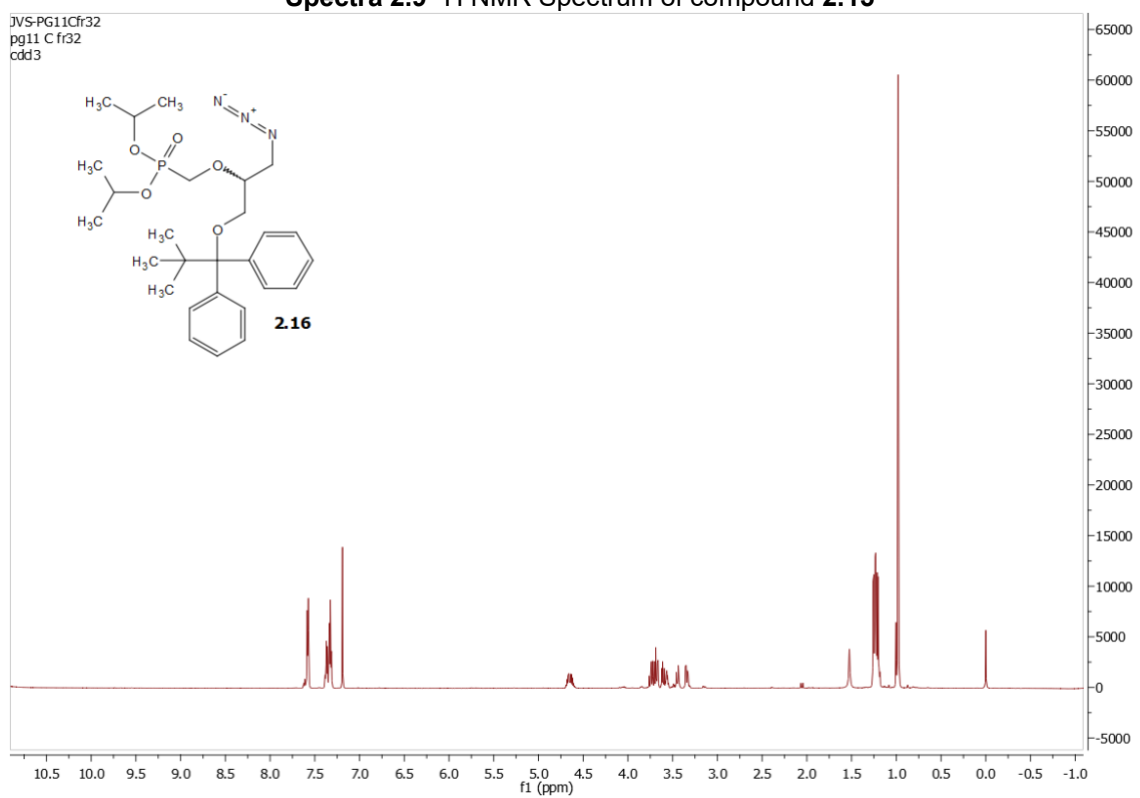
Spectra 2.7 ^1H NMR Spectrum of compound **2.13**



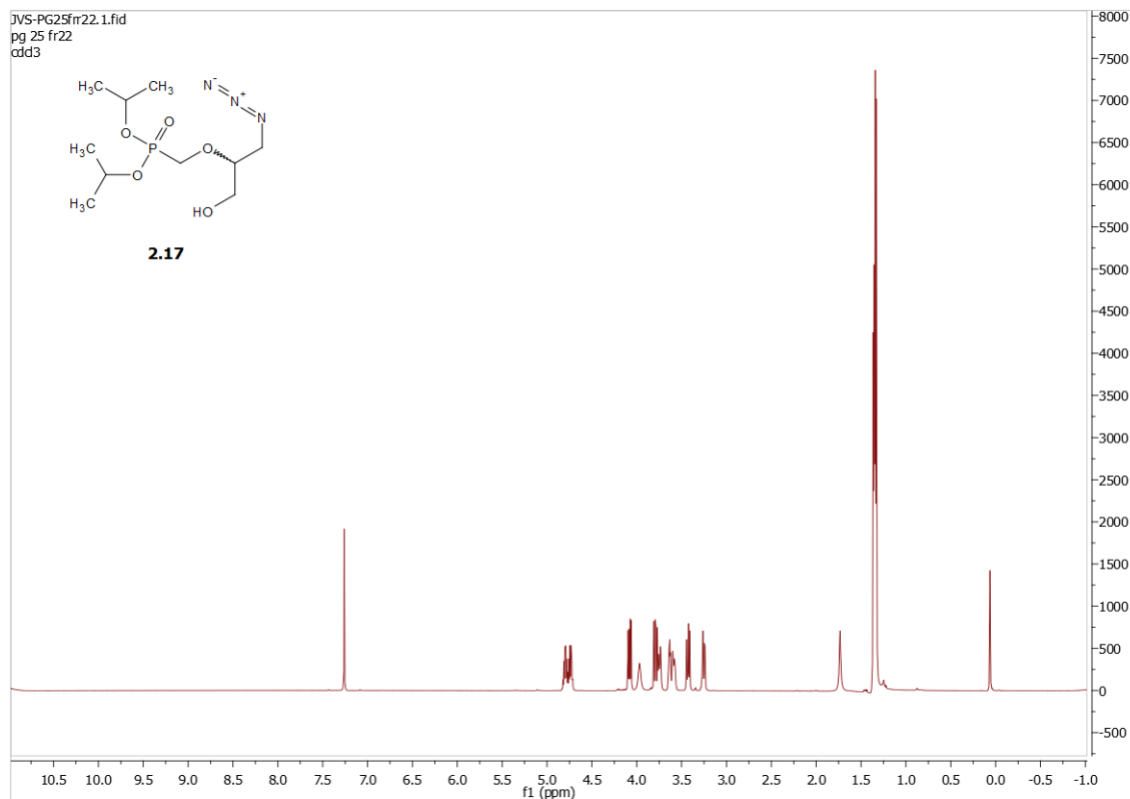
Spectra 2.8 ^1H NMR Spectrum of compound **2.14**



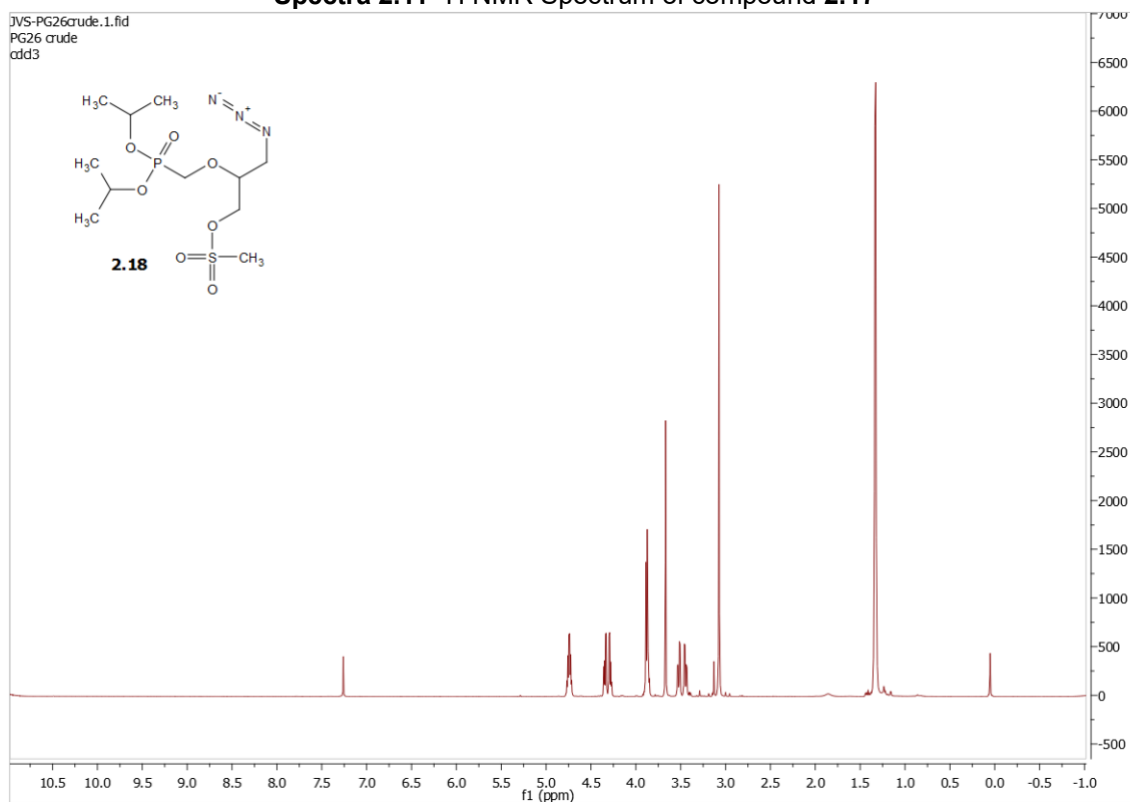
Spectra 2.9 ¹H NMR Spectrum of compound **2.15**



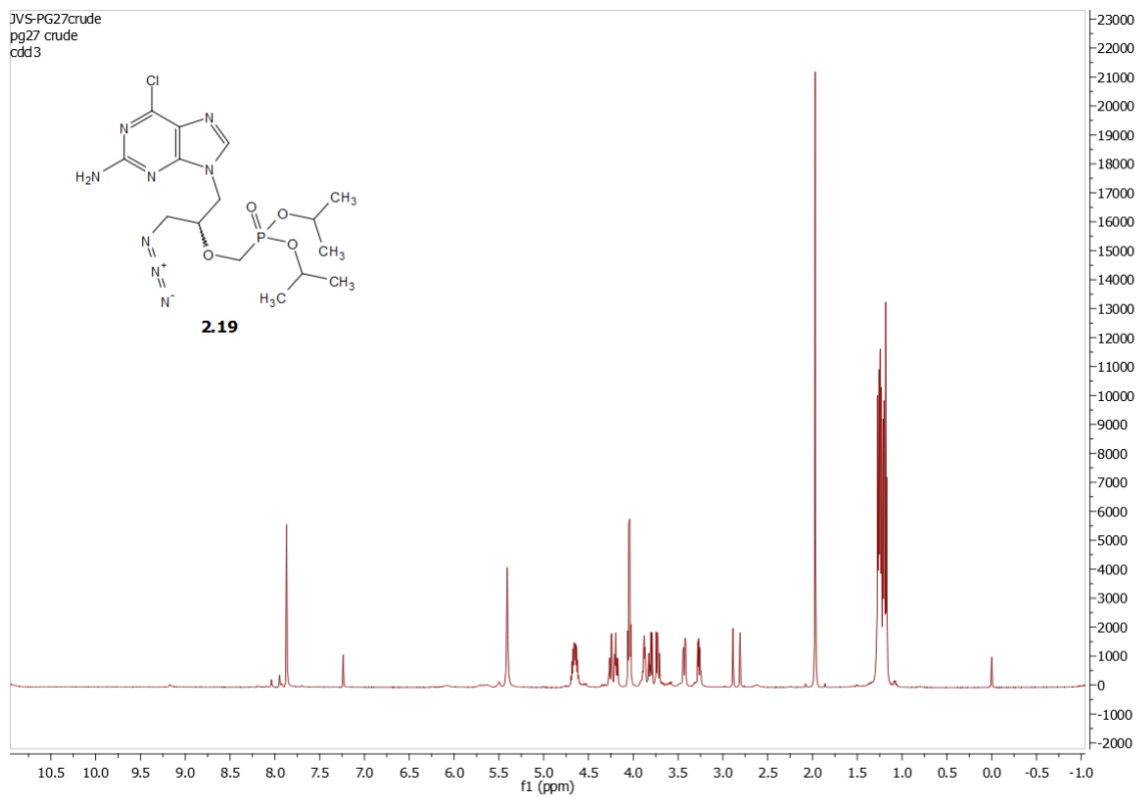
Spectra 2.10 ¹H NMR Spectrum of compound **2.16**



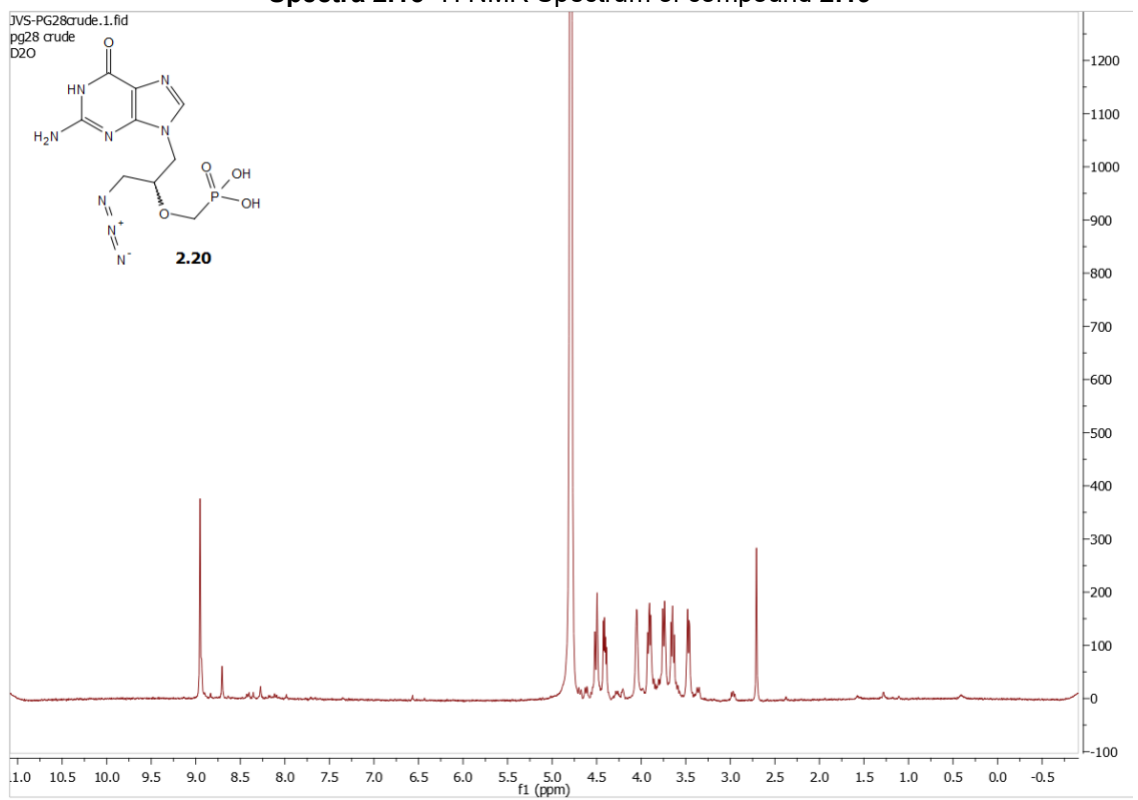
Spectra 2.11 ^1H NMR Spectrum of compound **2.17**



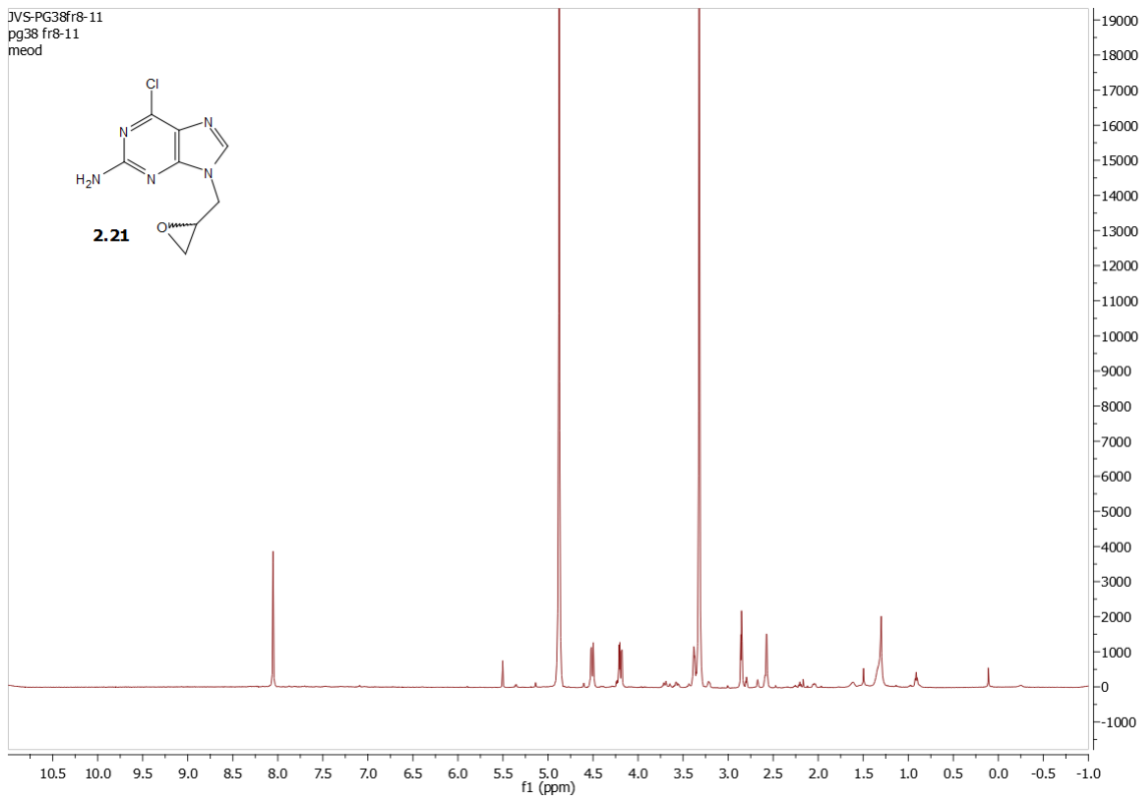
Spectra 2.12 ^1H NMR Spectrum of compound **2.18**



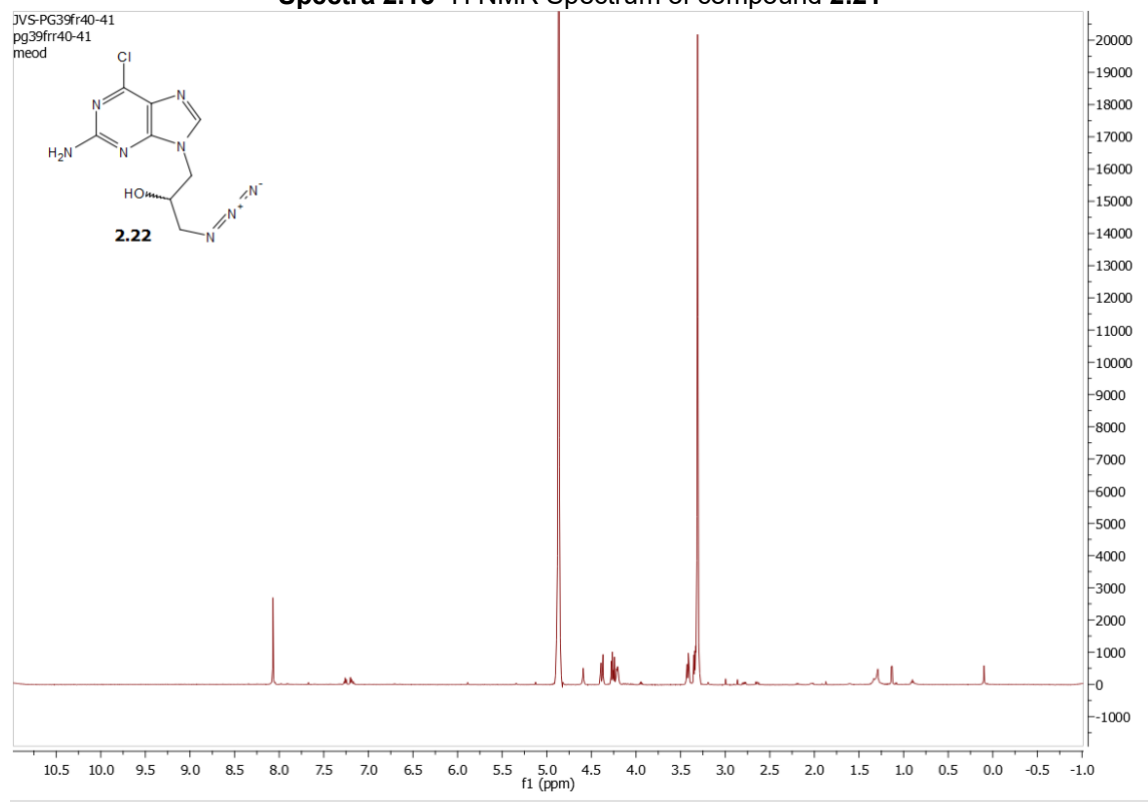
Spectra 2.13 ^1H NMR Spectrum of compound **2.19**



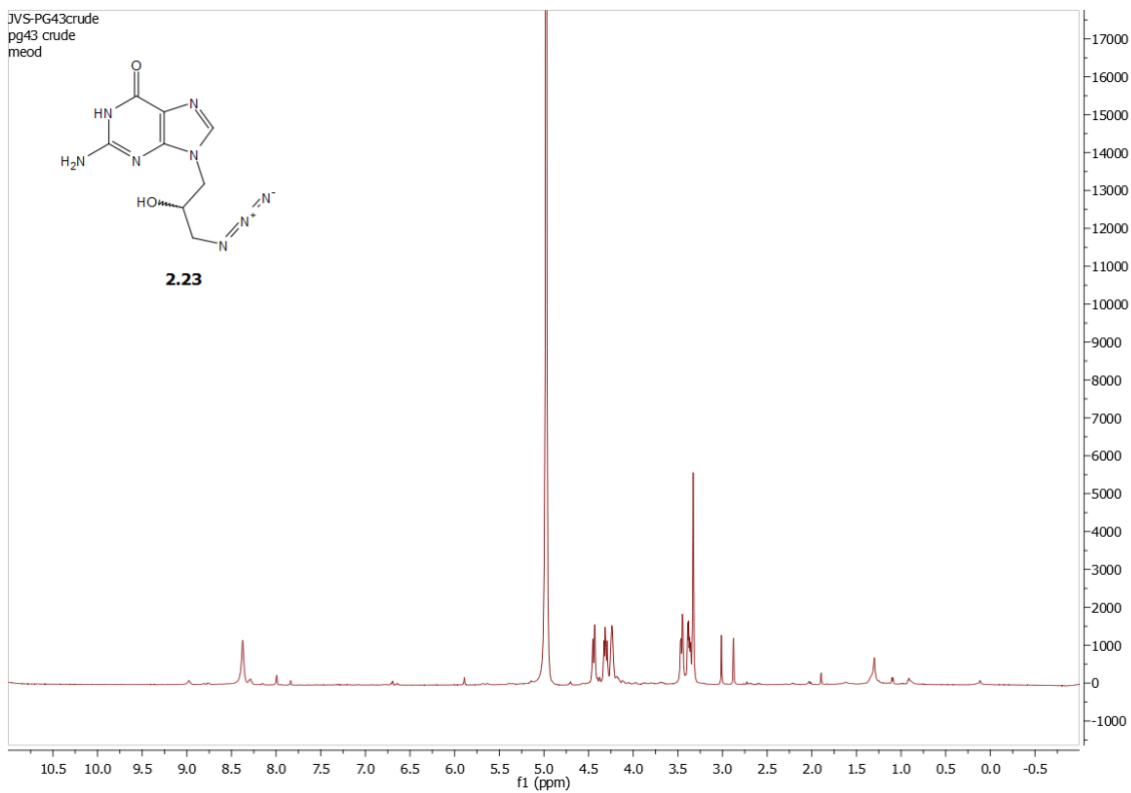
Spectra 2.14 ^1H NMR Spectrum of compound **2.20**



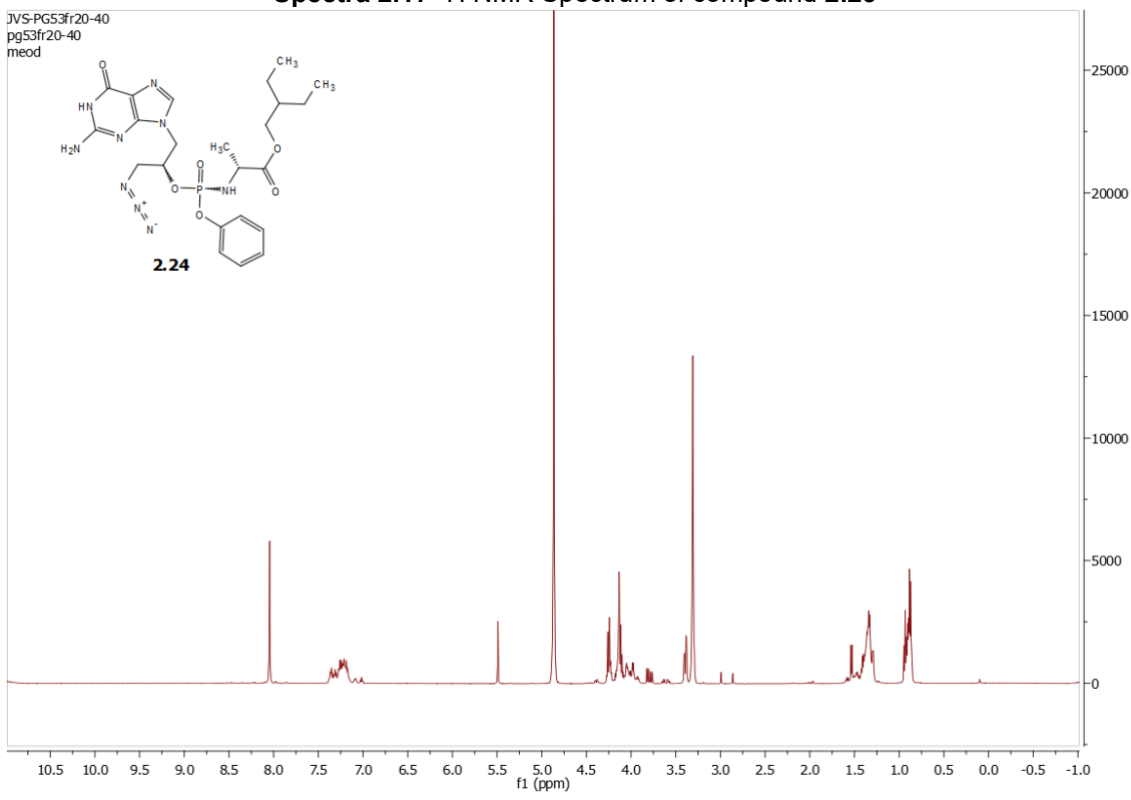
Spectra 2.15 ¹H NMR Spectrum of compound **2.21**



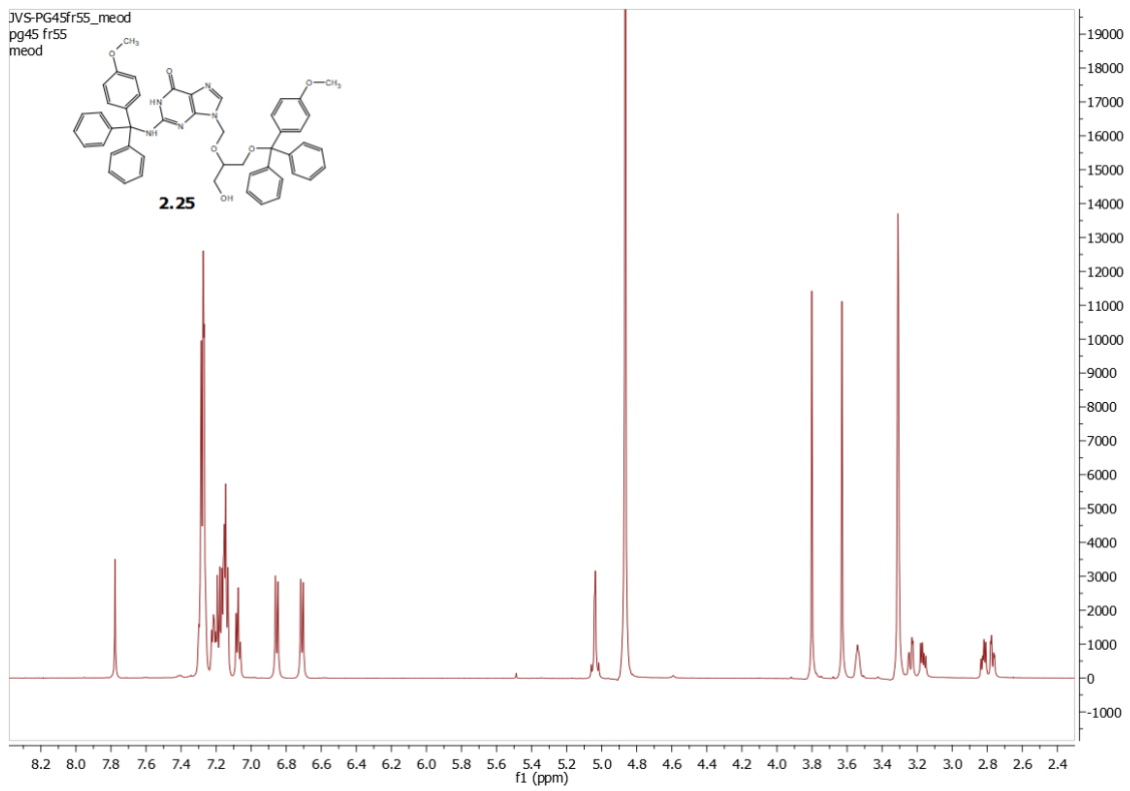
Spectra 2.16 ¹H NMR Spectrum of compound **2.22**



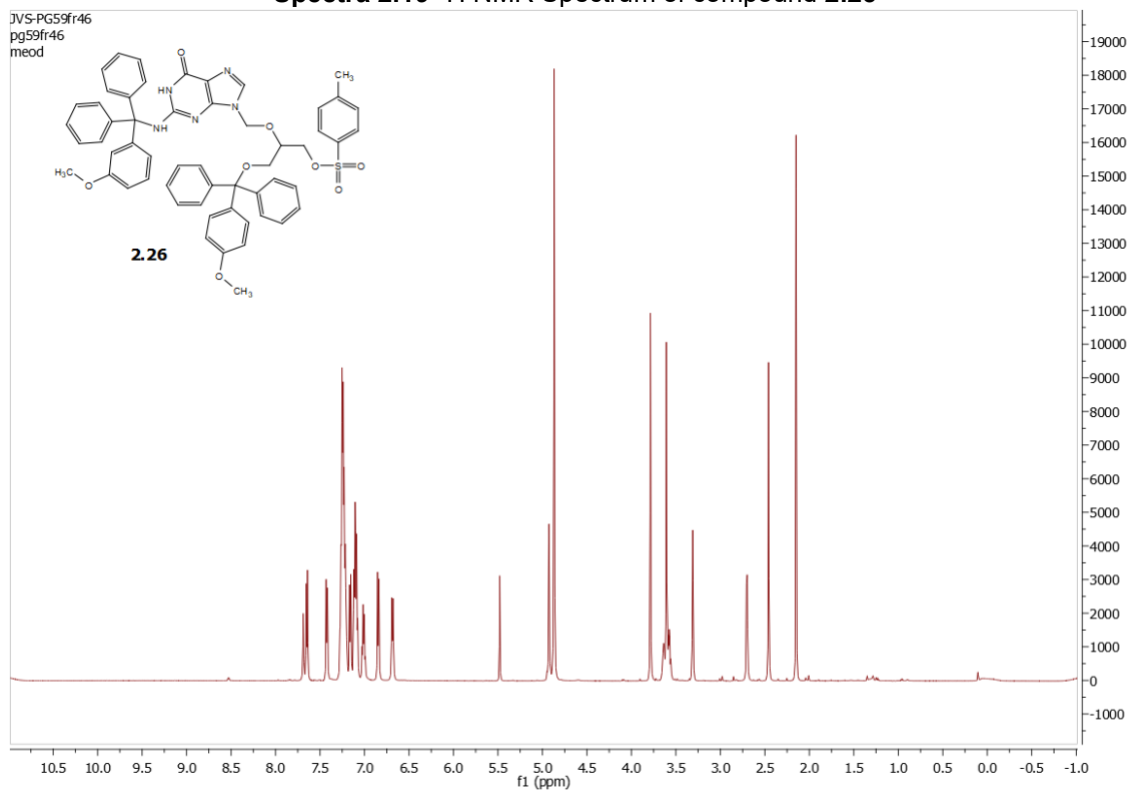
Spectra 2.17 ^1H NMR Spectrum of compound **2.23**



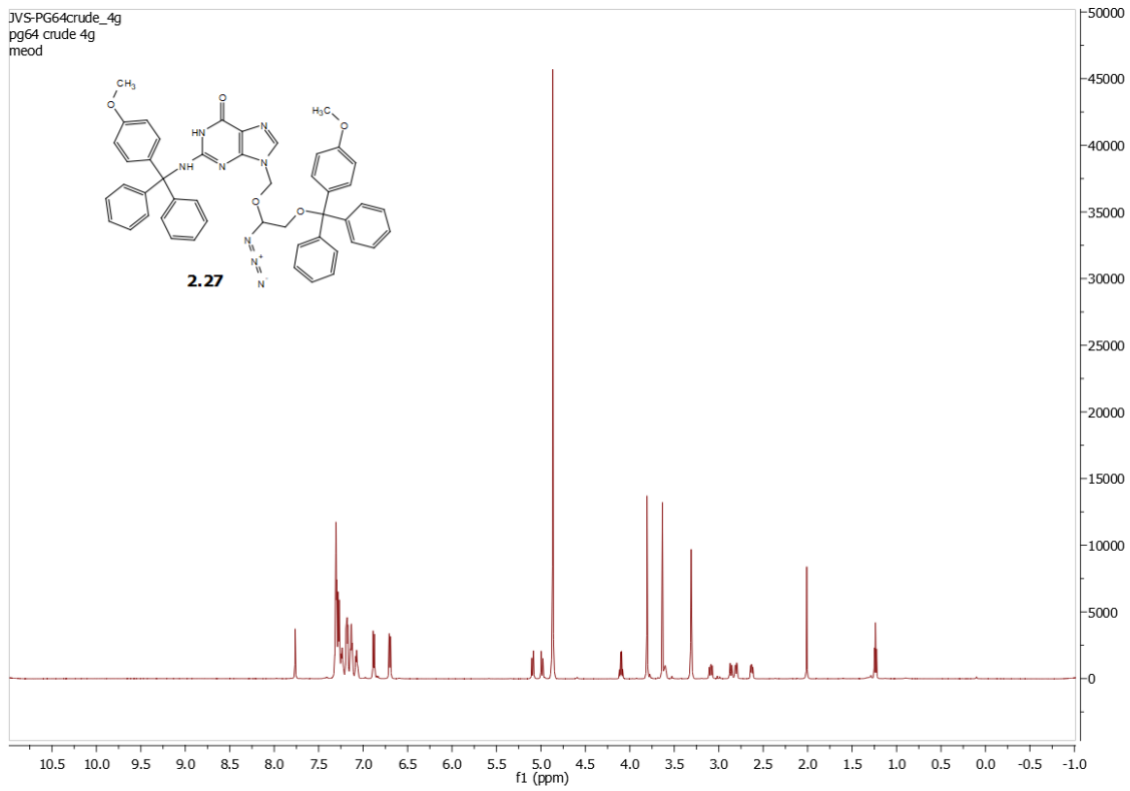
Spectra 2.18 ^1H NMR Spectrum of compound **2.24**



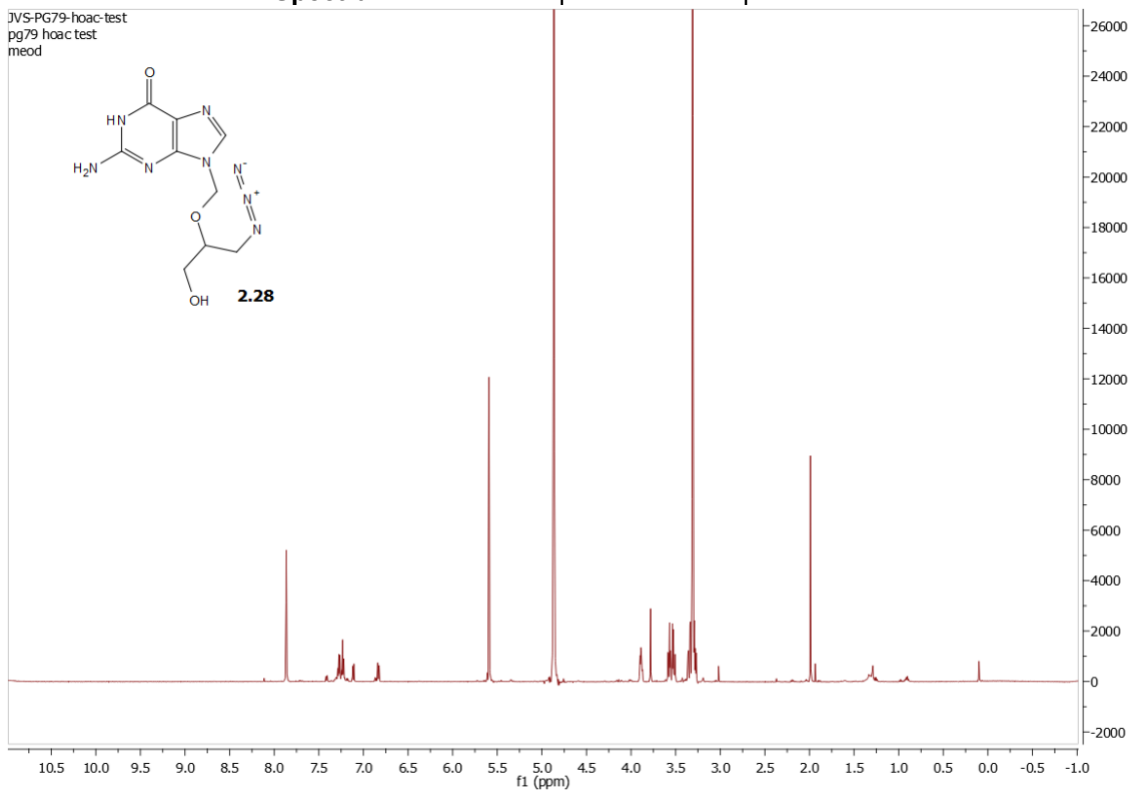
Spectra 2.19 ^1H NMR Spectrum of compound **2.25**



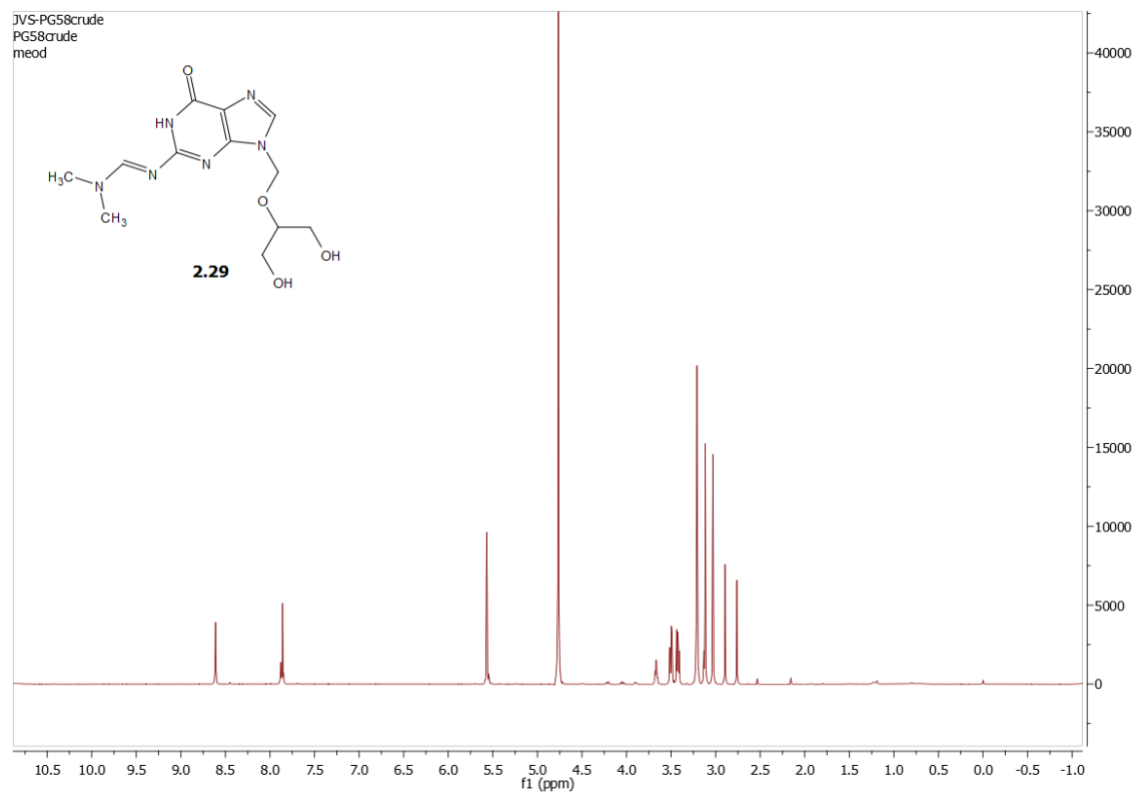
Spectra 2.20 ^1H NMR Spectrum of compound **2.26**



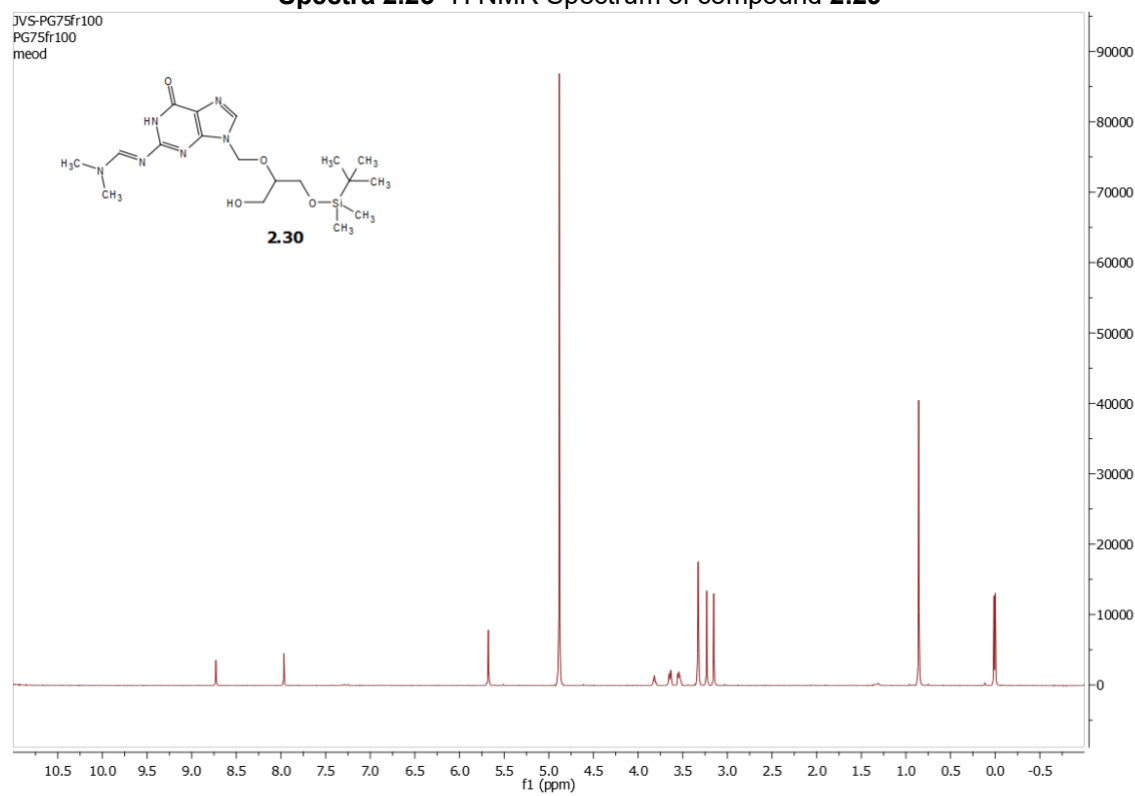
Spectra 2.21 ¹H NMR Spectrum of compound **2.27**



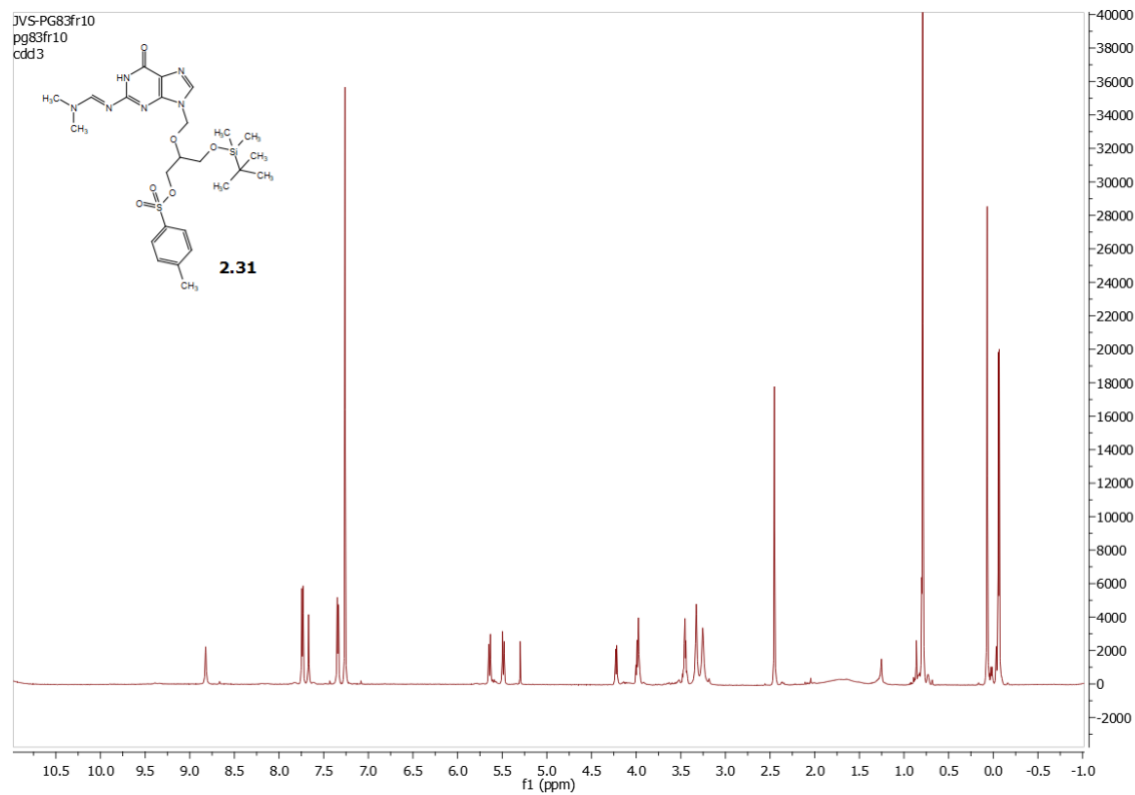
Spectra 2.22 ¹H NMR Spectrum of compound **2.28**



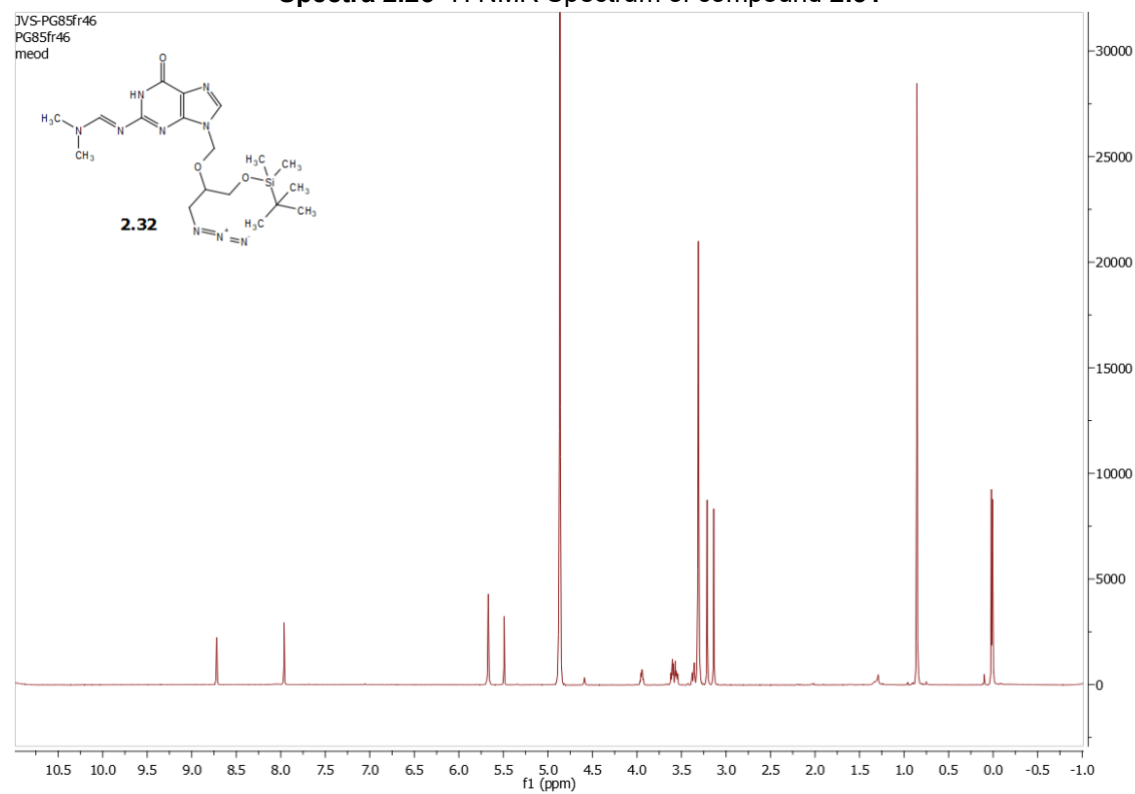
Spectra 2.23 ^1H NMR Spectrum of compound **2.29**



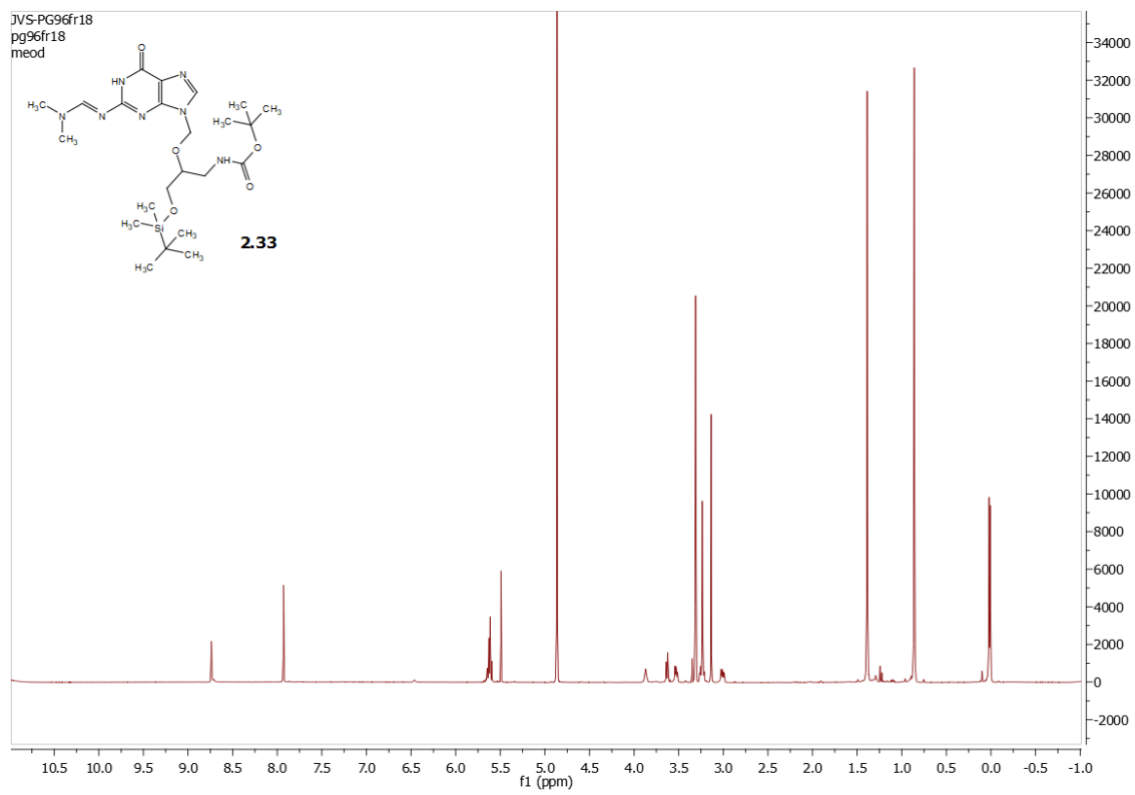
Spectra 2.24 ^1H NMR Spectrum of compound **2.30**



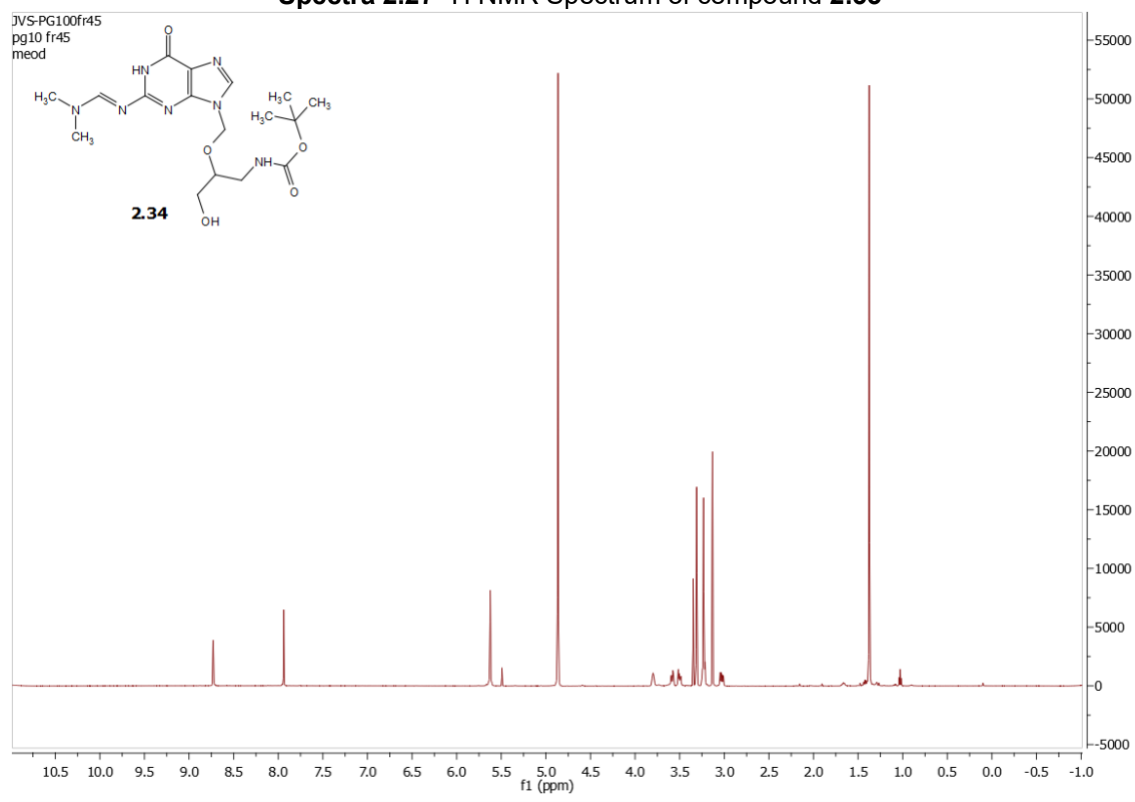
Spectra 2.25 ^1H NMR Spectrum of compound **2.31**



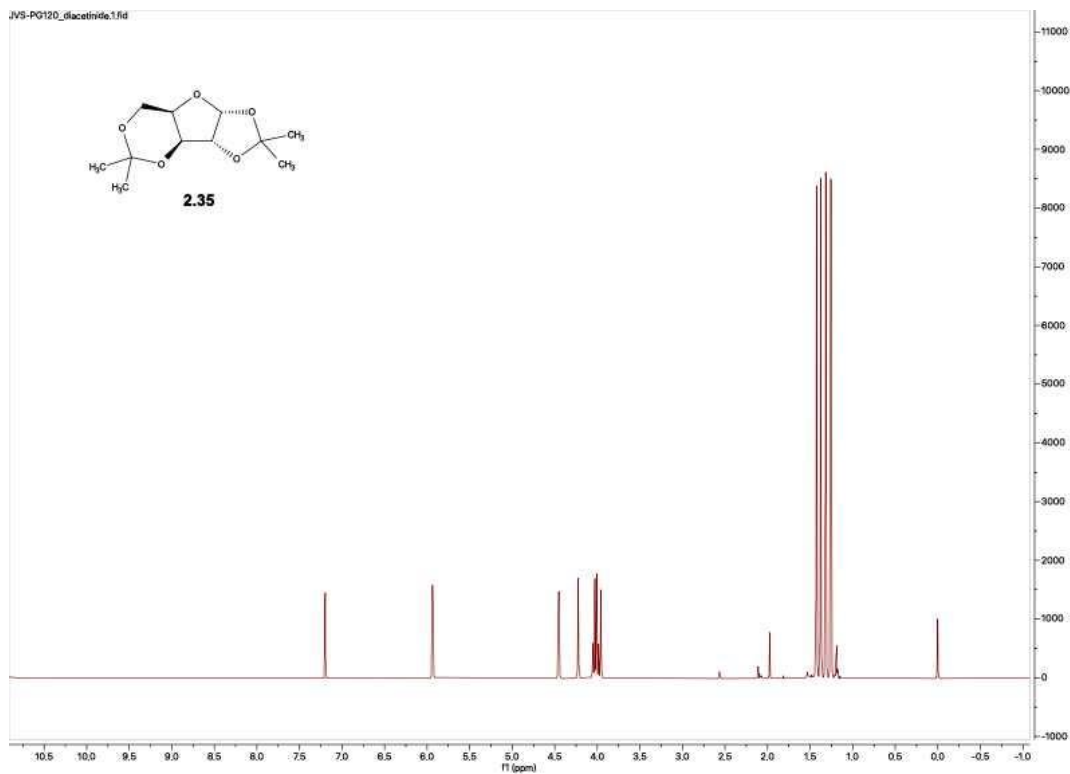
Spectra 2.26 ^1H NMR Spectrum of compound **2.32**



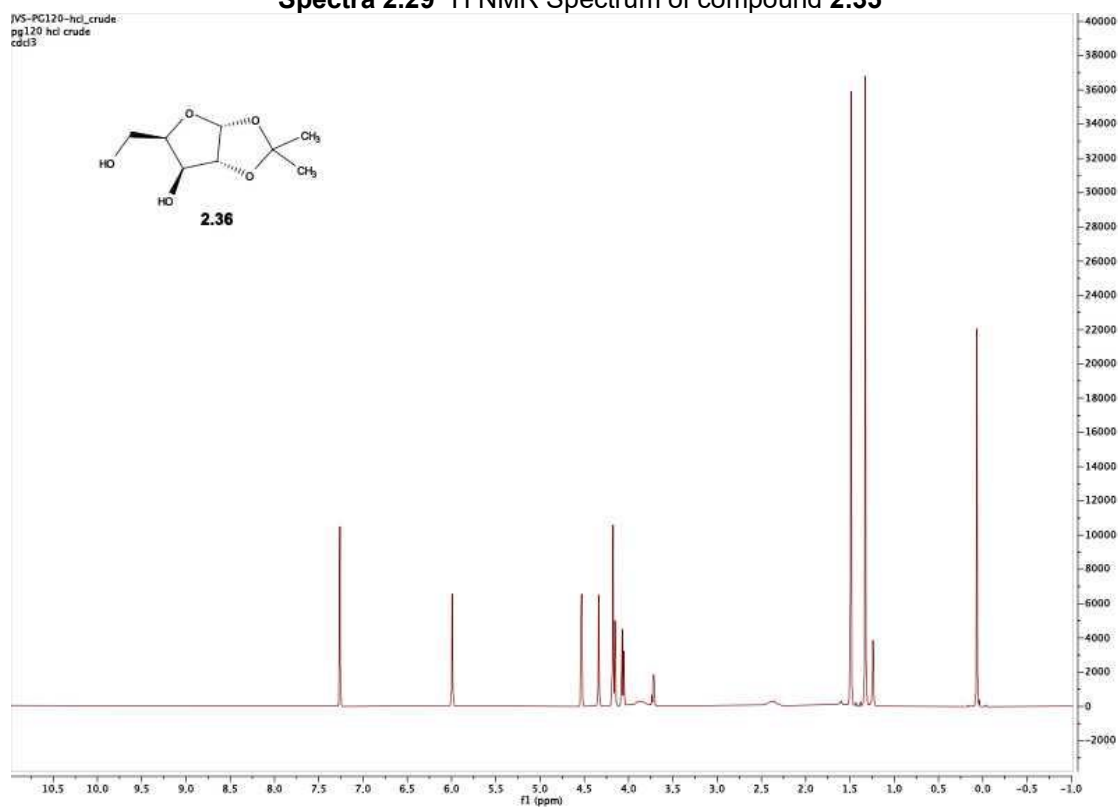
Spectra 2.27 ^1H NMR Spectrum of compound **2.33**



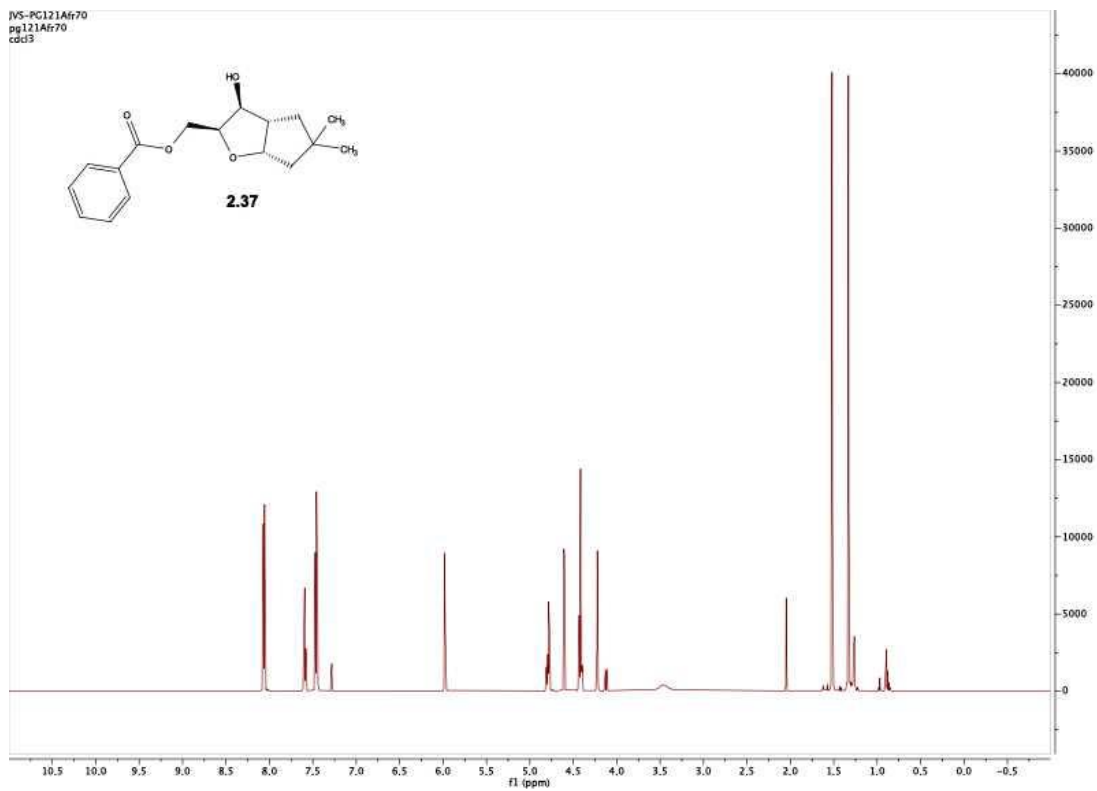
Spectra 2.28 ^1H NMR Spectrum of compound **2.34**



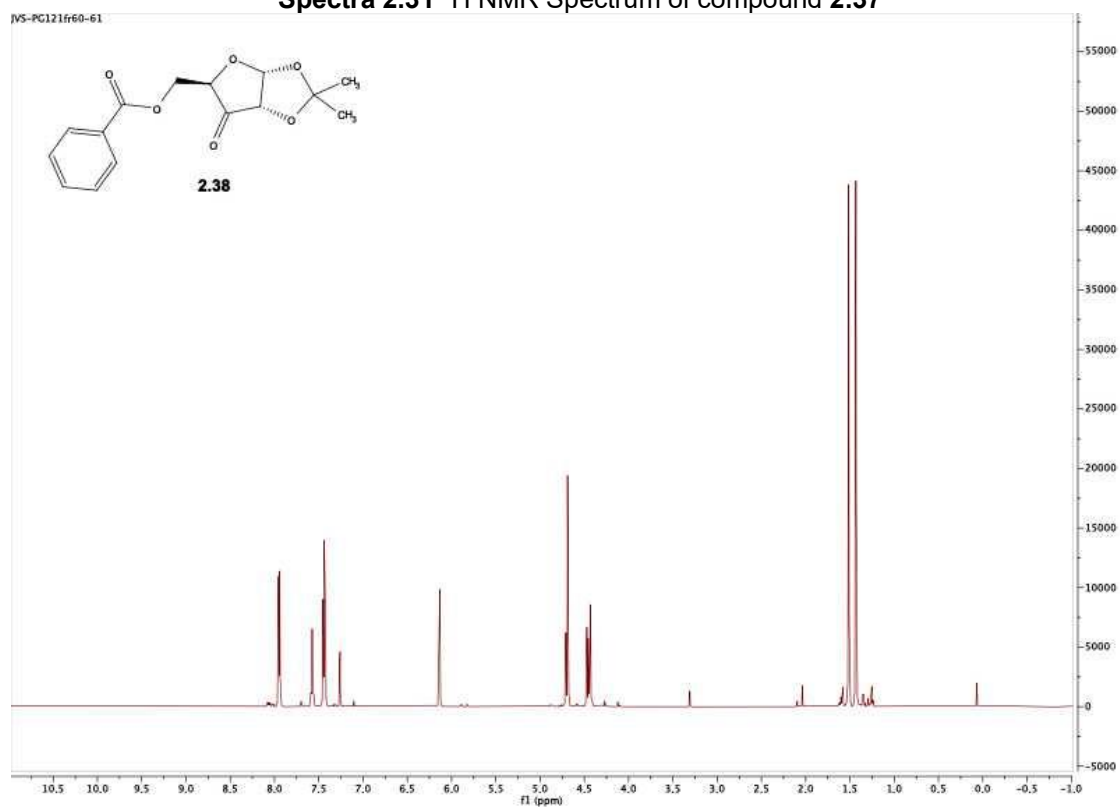
Spectra 2.29 ¹H NMR Spectrum of compound **2.35**



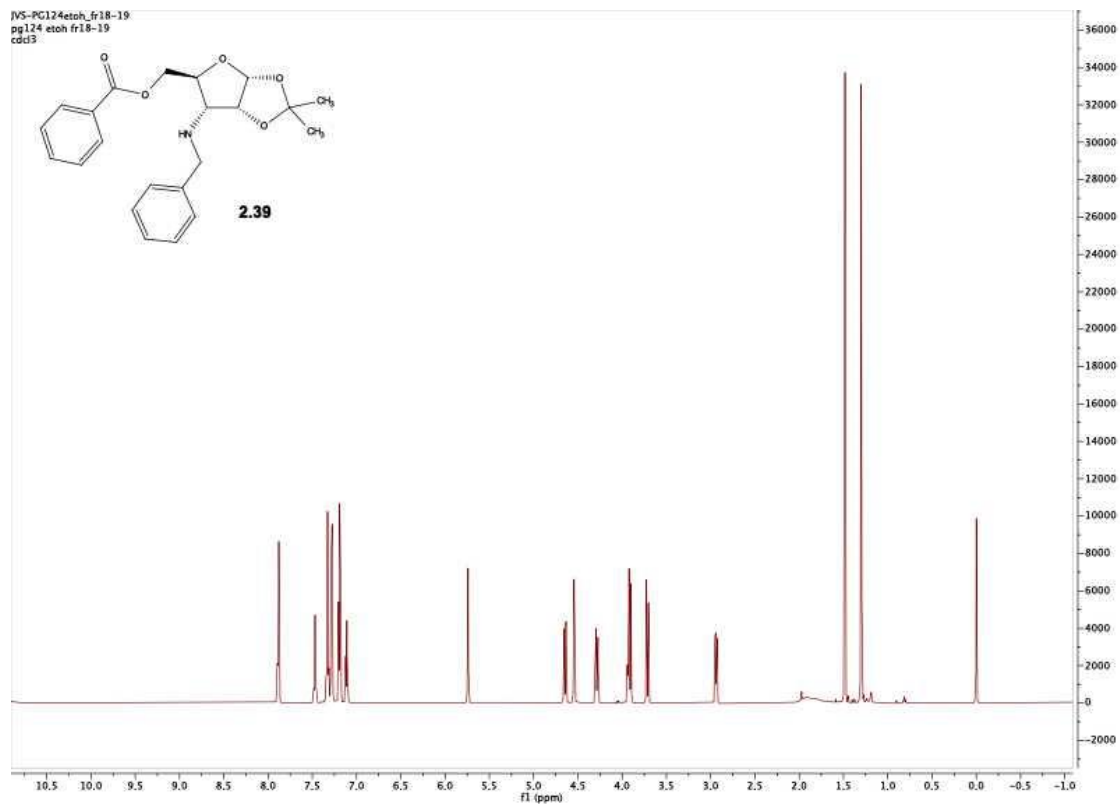
Spectra 2.30 ¹H NMR Spectrum of compound **2.36**



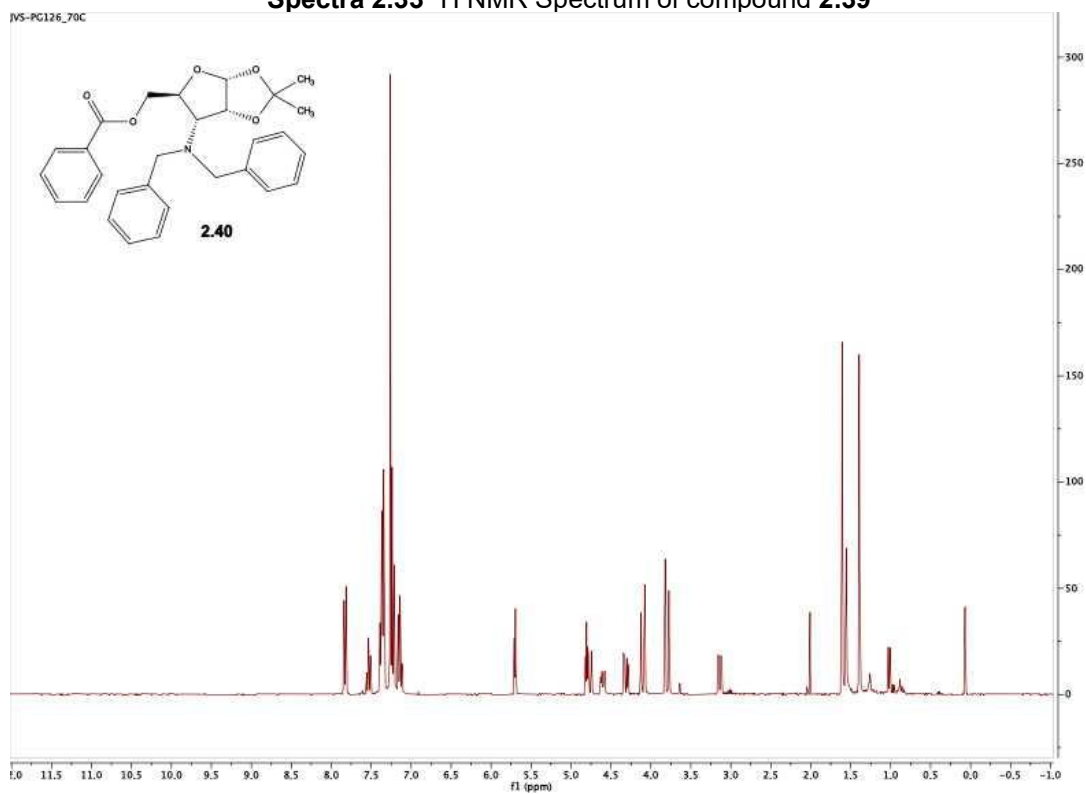
Spectra 2.31 ^1H NMR Spectrum of compound 2.37



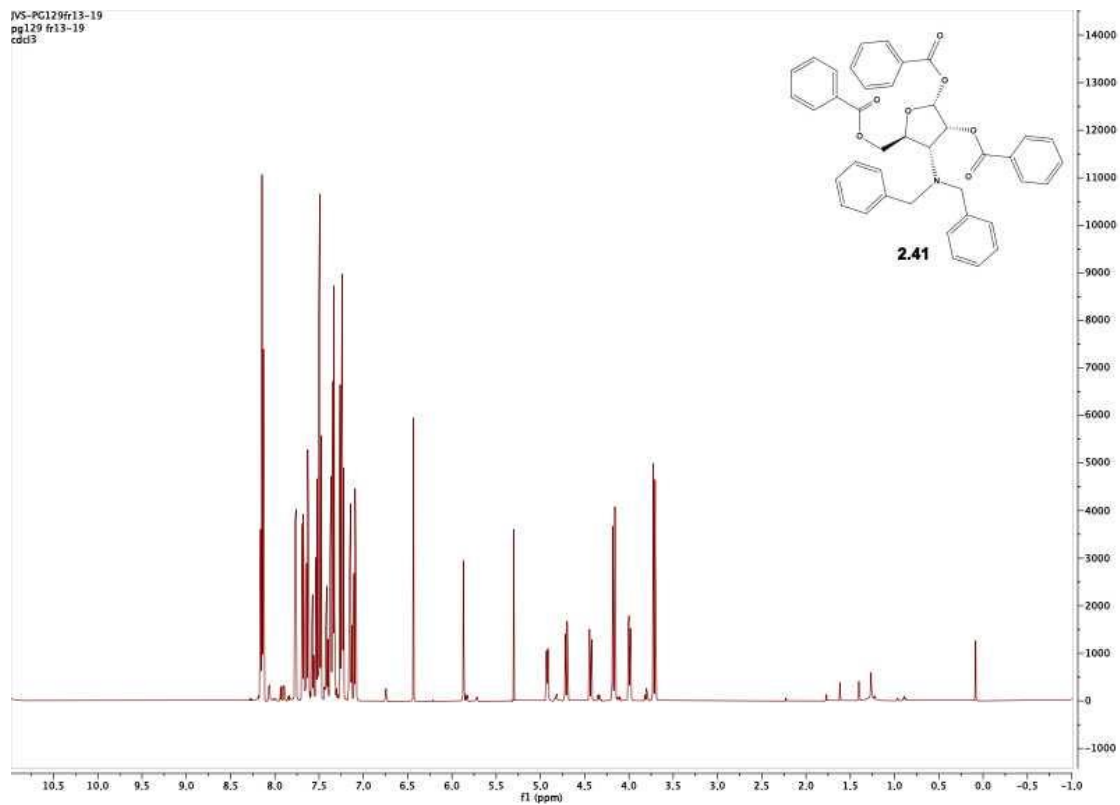
Spectra 2.32 ^1H NMR Spectrum of compound 2.38



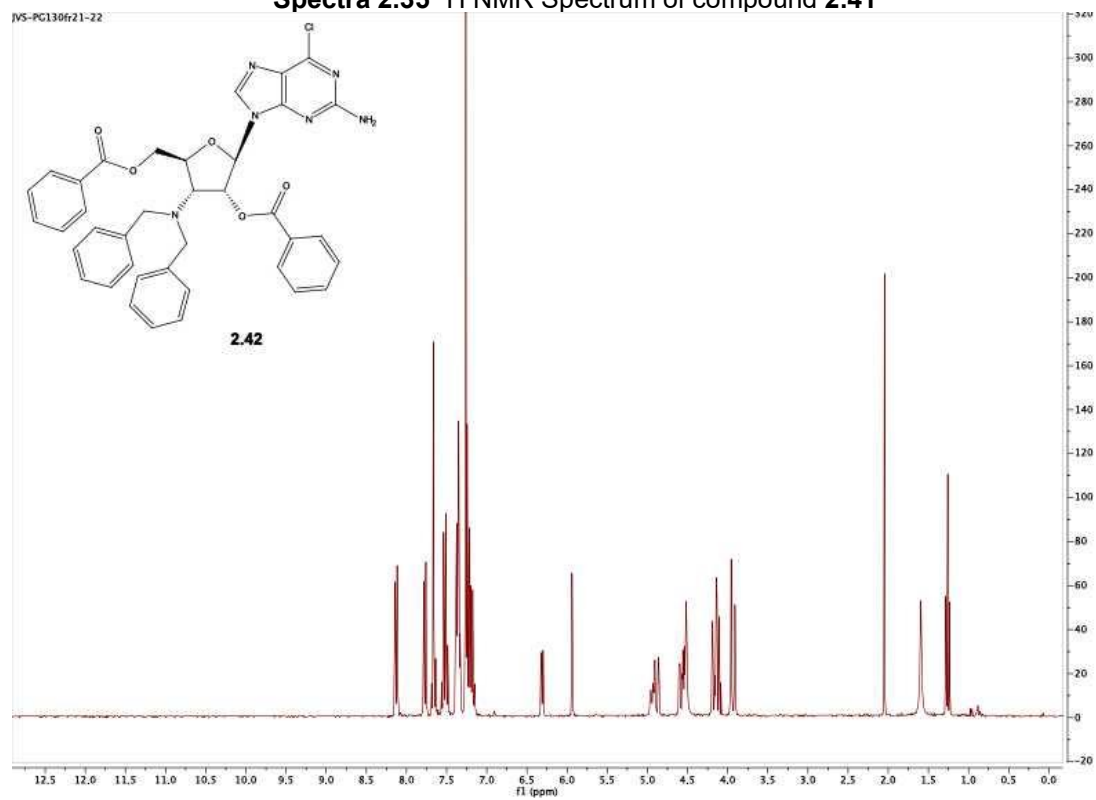
Spectra 2.33 ^1H NMR Spectrum of compound **2.39**



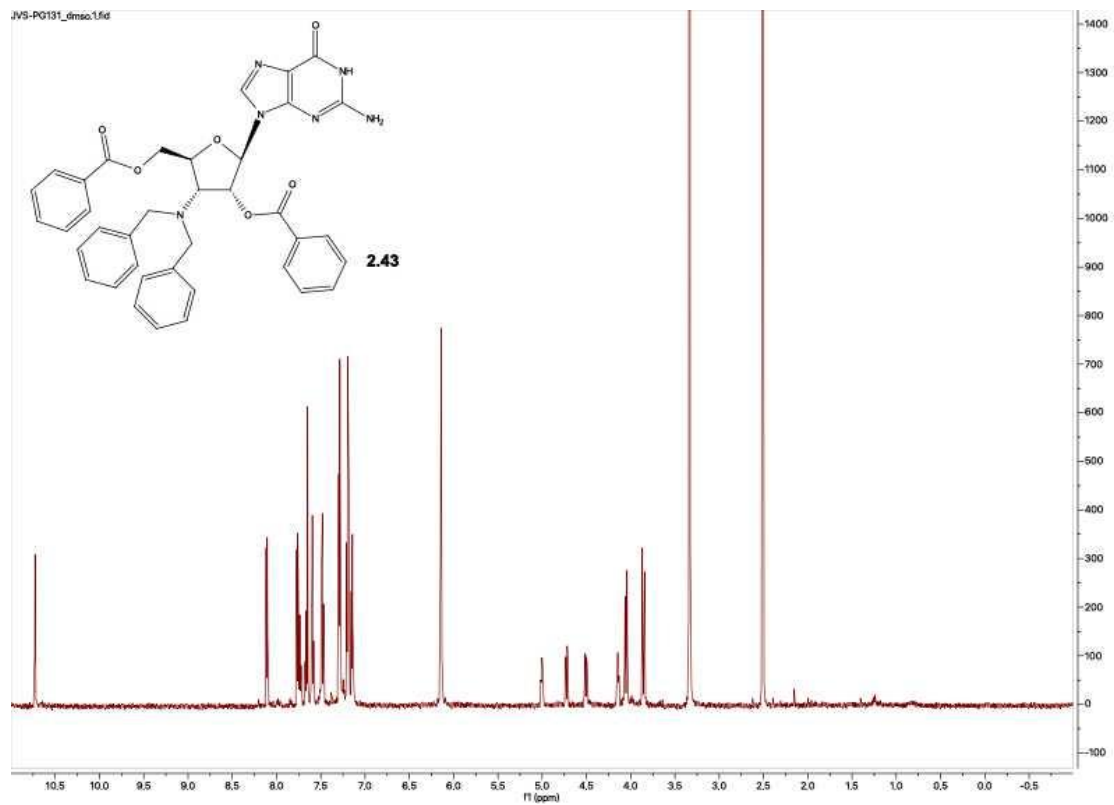
Spectra 2.34 ^1H NMR Spectrum of compound **2.40**



Spectra 2.35 ^1H NMR Spectrum of compound **2.41**



Spectra 2.36 ^1H NMR Spectrum of compound **2.42**



Spectra 2.37 ^1H NMR Spectrum of compound **2.43**

References

- 1) Davis W. Martin Peter A. Mayes, Victor W. Rodwell, Darlyn K. Granner, J. *Harper's Review of Biochemistry*, Twentieth.; Lange Medical Publications: Los Altos, California, 1985
- 2) Jordheim, L. P.; Durantel, D.; Zoulim, F.; Dumontet, C. Advances in the Development of Nucleoside and Nucleotide Analogues for Cancer and Viral Diseases. *Nat Rev Drug Discov* **2013**, 12 (6), 447–464. DOI: 10.1038/nrd4010.
- 3) Idzko, M.; Ferrari, D.; Eltzschig, H. K. Nucleotide Signaling during Inflammation. *Nature* **2014**, 509, 310. DOI: 10.1038/nature13085
<https://www.nature.com/articles/nature13085#supplementary-information>
- 4) Baldwin, S. A.; Mackey, J. R.; Cass, C. E.; Young, J. D. Nucleoside Transporters: Molecular Biology and Implications for Therapeutic Development. *Mol. Med. Today* **1999**, 5 (5), 216–224. DOI: 10.1016/S1357-4310(99)01459-8.
- 5) Shryock, J. C.; Belardinelli, L. Adenosine and Adenosine Receptors in the Cardiovascular System: Biochemistry, Physiology, and Pharmacology. *Am. J. Cardiol.* **1997**, 79(12), 2–10. DOI: 10.1016/S0002-9149(97)00256-7.
- 6) Luděk, E.; Markéta, Š.; Radim, N.; Jiří, N.; Tomáš, K.; Martin, P.; Erik, C.; Daniel, R.; Structure-activity relationships of nucleoside analogues for inhibition of tick-borne encephalitis virus. *Antiviral Research.* **2016**, 133, 119-129, DOI: 10.1016/j.antiviral.2016.07.018.
- 7) Kato, E. I. K. Sugar-Modified Nucleosides in Past 10 Years, A Review. *Curr. Med. Chem.* **2001**, 8 (4), 385–423. DOI: 10.2174/0929867013373471
- 8) Tsesmetzis, N.; Paulin, J.; Rudd, S.G.; Herold, N. Nucleobase and Nucleoside Analogues: Resistance and Re-Sensitisation at the Level of Pharmacokinetics, *Pharmacodynamics and Metabolism. Cancers (Basel).* **2018**, 10(7), 240. DOI: 10.3390/cancers10070240.
- 9) Kamzeeva, P.N.; Aralov, A.V.; Alferova, V.A.; Korshun, V.A. Recent Advances in Molecular Mechanisms of Nucleoside Antivirals. *Curr Issues Mol Biol.* **2023**, 45(8), 6851-6879. DOI: 10.3390/cimb45080433.
- 10) Moyle, G. Toxicity of antiretroviral nucleoside and nucleotide analogues: is mitochondrial toxicity the only mechanism? *Drug Saf.* **2000**, (6), 467-81. DOI: 10.2165/00002018-200023060-00001.
- 11) Cano-Soldado, P.; Pastor-Anglada, M. Transporters that translocate nucleosides and structural similar drugs: structural requirements for substrate recognition. *Med. Res. Rev.* **2011**, 32, 428–45.
- 12) Minuesa, G. Drug uptake transporters in antiretroviral therapy. *Pharmacol. Ther.* **2011**, 132, 268–279.
- 13) Arnér, E. S. J.; Eriksson, S. Mammalian Deoxyribonucleoside Kinases. *Pharmacol. Ther.* **1995**, 67 (2), 155–186. DOI: 10.1016/0163-7258(95)00015-9.

- 14) Rampazzo, C.; Gazzola, C.; Ferraro, P.; Gallinaro, L.; Johansson, M.; Reichard, P.; Bianchi, V. Human High-Km 5'-Nucleotidase Effects of Overexpression of the Cloned CDNA in Cultured Human Cells. *Eur J Biochem* **1999**, 261 (3), 689–697.
- 15) Ewald, B.; Sampath, D.; Plunkett, W. Nucleoside Analogs: Molecular Mechanisms Signaling Cell Death. *Oncogene* **2008**, 27 (50), 6522–6537. DOI: 10.1038/onc.2008.316.
- 16) Sampath, D.; Rao, V. A.; Plunkett, W. Mechanisms of Apoptosis Induction by Nucleoside Analogs. *Oncogene* **2003**, 22, 9063.
- 17) Zhu, C.; Johansson, M.; Permert, J.; Karlsson, A. Phosphorylation of Anticancer Nucleoside Analogs by Human Mitochondrial Deoxyguanosine Kinase. *Biochem. Pharmacol.* **1998**, 56 (8), 1035–1040. DOI: 10.1016/S0006-2952(98)00150-6
- 18) Berdis, A. Inhibiting DNA Polymerases as a Therapeutic Intervention against Cancer. *Front. Mol. Biosci.* **2017**, 4, 78. DOI: 10.3389/fmolb.2017.00078
- 19) Galmarini, C. M.; Mackey, J. R.; Dumontet, C. Nucleoside Analogues and Nucleobases in Cancer Treatment. *Lancet Oncol.* **2002**, 3 (7), 415–424. DOI: 10.1016/S1470-2045(02)00788-X.
- 20) Griffig, J.; Koob, R.; Blakley, R.L. Mechanisms of inhibition of DNA synthesis by 2-chlorodeoxyadenosine in human lymphoblastic cells *Cancer Res.* **1989**, 49, 6923–6928
- 21) Hentosh, P.; Koob, R.; Blakley, R.L. Incorporation of 2-halogeno-2'-deoxyadenosine 5-triphosphates into DNA during replication by human polymerases alpha and beta *J Biol Chem.* **1990**, 265, 4033–4040.
- 22) Brockman, R.W.; Schabel, F.M.; Montgomery, J.A. Biologic activity of 9-beta-D-arabinofuranosyl-2-fluoroadenine, a metabolically stable analog of 9-beta-D-arabinofuranosyladenine *Biochem Pharmacol.* **1977**, 26, 2193–2196.
- 23) Huang, P.; Chubb, S.; Plunkett, W. Termination of DNA synthesis by 9-beta-D-arabinofuranosyl-2-fluoroadenine. A mechanism for cytotoxicity *J Biol Chem.* **1990**, 265, 16617–16625.
- 24) Zhenchuk, A.; Lotfi, K.; Juliusson, G.; Albertioni, F. Mechanisms of Anti-Cancer Action and Pharmacology of Clofarabine. *Biochem. Pharmacol.* **2009**, 78 (11), 1351–1359. DOI: 10.1016/j.bcp.2009.06.094.
- 25) Cooper, T. Role of Nelarabine in the Treatment of T-Cell Acute Lymphoblastic Leukemia and T-Cell Lymphoblastic Lymphoma. *Ther. Clin. Risk Manag.* **2008**, 3, 1135–1141.
- 26) Johnston, J. B. Mechanism of Action of Pentostatin and Cladribine in Hairy Cell Leukemia. *Leuk. Lymphoma.* **2011**, 52 (2), 43–45. DOI: 10.3109/10428194.2011.570394.
- 27) G Rose, M.; P Farrell, M.; Schmitz, J. Thymidylate Synthase: A Critical Target for Cancer Chemotherapy; *Clinical Colorectal Cancer.* **2002**, 1(4), 220-229. DOI: 10.3816/CCC.2002.n.003.

- 28) Mini, E.; Nobili, S.; Caciagli, B.; Landini, I.; Mazzei, T. Cellular Pharmacology of Gemcitabine. *Ann. Oncol.* **2006**, 17(5), 7–12.
- 29) Jones, P.A.; Taylor, S.M. Cellular differentiation, cytidine analogs and DNA methylation. *Cell.* **1980**, 20, 85–93.
- 30) Stresemann, C.; Lyko, F. Modes of Action of the DNA Methyltransferase Inhibitors Azacytidine and Decitabine. *Int. J. Cancer.* **2008**, 123 (1), 8–13.
<https://doi.org/10.1002/ijc.23607>
- 31) Seley-Radtke, K.L.; Yates, M.K. The evolution of nucleoside analogue antivirals: A review for chemists and non-chemists. Part 1: Early structural modifications to the nucleoside scaffold. *Antiviral Res.* **2018**, 154, 66-86. DOI: 10.1016/j.antiviral.2018.04.004.
- 32) Ettmayer, P.; Amidon, G. L.; Clement, B.; Testa, B. Lessons Learned from Marketed and Investigational Prodrugs. *J Med Chem*, **2004**, 47 (10), 2393–2404. DOI: 10.1021/jm0303812.
- 33) Stefano, A. D.; Sozio, P.; Cerasa, L. S. Antiparkinson prodrugs. *Molecules*, **2008**, 13(1), 46-68.
- 34) Han, H.-K.; Amidon, G. L. Targeted Prodrug Design to Optimize Drug Delivery. *AAPS PharmSci*, **2000**, 2 (1), 48–58. DOI: 10.1208/ps020106.
- 35) Stella, V. J.; Himmelstein, K. J. Prodrugs and Site-Specific Drug Delivery. *J Med Chem.* **1980**, 23 (12), 1275–1282.
- 36) Ugo, P.; Ethel, C.; Garnier A.; Steven, C.; Franck, A.; Raymond, S. *Chemical Reviews* **2014** 114 (18), 9154-9218 DOI: 10.1021/cr5002035
- 37) Farquhar, D.; Srivastva, D. N.; Kuttesch, N. J.; Saunders, P. P. Biologically Reversible Phosphate-Protective Groups. *J. Pharm. Sci.* **1983**, 72 (3), 324–325. DOI: 10.1002/jps.2600720332.
- 38) Naesens, L.; Bischofberger, N.; Augustijns, P.; Annaert, P.; Van den Mooter, G.; Arimilli, M. N.; Kim, C. U.; De Clercq, E. Antiretroviral Efficacy and Pharmacokinetics of Oral Bis(Isopropylloxycarbonyloxymethyl)9-(2-Phosphonylmethoxypropyl)Adenine in Mice. *Antimicrob. Agents Chemother.* **1998**, 42 (7), 1568–1573.
- 39) Naesens, L.; Neyts, J.; Balzarini, J.; Bischofberger, N.; Clercq, E. De. In Vivo Antiretroviral Efficacy of Oral Bis(POM)-PMEA, the Bis(Pivaloyloxymethyl)Prodrug of 9-(2-Phosphonylmethoxyethyl) Adenine (PMEA). *Nucleosides and Nucleotides.* **1995**, 14 (3–5), 767– 770. DOI: 10.1080/15257779508012468
- 40) Pompon, A.; Lefebvre, I.; L. Imbach, J.; Kahn, S.; Farquhar, D. Decomposition Pathways of the Mono- and Bis(Pivaloyloxymethyl) Esters of Azidothymidine 5'-Monophosphate in Cell Extract and in Tissue Culture Medium: An Application of the “on-Line ISRP-Cleaning” HPLC technique. *Antivir. Chem. Chemother.* **1994**, 5, 91–98. DOI: 10.1177/095632029400500205.
- 41) Khan, S. R.; Nowak, B.; Plunkett, W.; Farquhar, D. Bis(Pivaloyloxymethyl) Thymidine 5'- Phosphate Is a Cell Membrane-Permeable Precursor of Thymidine

- 5'-Phosphate in Thymidine Kinase Deficient CCRF CEM Cells. *Biochem. Pharmacol.* **2005**, 69 (9), 1307–1313. DOI: 10.1016/j.bcp.2005.02.008.
- 42) Sastry, J. K.; Nehete, P. N.; Khan, S.; Nowak, B. J.; Plunkett, W.; Arlinghaus, R. B.; Farquhar, D. Membrane-Permeable Dideoxyuridine 5' Monophosphate Analogue Inhibits Human Immunodeficiency Virus Infection. *Mol. Pharmacol.* **1992**, 41 (3), 441-445.
- 43) Segovia, M. C.; Chacra, W.; Gordon, S. C. Adefovir Dipivoxil in Chronic Hepatitis B: History and Current Uses. *Expert Opin. Pharmacother.* **2012**, 13 (2), 245–254. DOI: 10.1517/14656566.2012.649727
- 44) Kearney, B. P.; Flaherty, J. F.; Shah, J. Tenofovir Disoproxil Fumarate. *Clin. Pharmacokinet.* **2004**, 43 (9), 595–612. DOI: 10.2165/00003088-200443090-00003.
- 45) Yuen, M.-F.; Han, K.-H.; Um, S.-H.; Yoon, S. K.; Kim, H.-R.; Kim, J.; Kim, C. R.; Lai, C.-L. Antiviral Activity and Safety of LB80380 in Hepatitis B e Antigen–Positive Chronic Hepatitis B Patients with Lamivudine-Resistant Disease. *Hepatology.* **2009**, 51 (3), 767–776. DOI: 10.1002/hep.23462.
- 46) Starrett, J. E., Jr.; Tortolani, D. R.; Russell, J.; Hitchcock, M. J. M.; Whiterock, V.; Martin, J. C.; Mansuri, M. M. *J. Med. Chem.* **1994**, 37, 1857.
- 47) Arimilli, M. N.; Kim, C. U.; Dougherty, J.; Mulato, A.; Oliyai, R.; Shaw, J. P.; Cundy, K. C.; Bischofberger, N. *Antiviral Chem. Chemother.* **1997**, 8, 557.
- 48) Hwang, Y.; Cole, P. A. *Org. Lett.* **2004**, 6, 1555.
- 49) McGuigan, C.; Pathirana, R. N.; Mahmood, N.; Devine, K. G.; Hay, A. J. Aryl Phosphate Derivatives of AZT Retain Activity against HIV1 in Cell Lines Which Are Resistant to the Action of AZT. *Antivir. Res.* **1992**, 17 (4), 311–321.
- 50) McGuigan, C.; Pathirana, R. N.; Mahmood, N.; Hay, A. J. Aryl Phosphate Derivates of AZT Inhibit HIV Replication in Cells Where the Nucleoside Is Poorly Active. *Bioorg. Med. Chem. Lett.* **1992**, 2 (7), 701–704. DOI: 10.1016/S0960-894X(00)80395-9.
- 51) Veeranjanyulu, G.; Bharath, V.; Sivakumar, R.; Chiao, K.; Chi-Huey, W.; Shang-Cheng, H. *The Journal of Organic Chemistry.* **2021**, 86 (7), 4977-4985 DOI: 10.1021/acs.joc.0c02888
- 52) Serpi, M.; Pertusati, F. An overview of ProTide technology and its implications to drug discovery, *Expert Opinion on Drug Discovery.* **2021**, 16(10), 1149-1161, DOI: 10.1080/17460441.2021.1922385
- 53) World Health Organization (WHO). <https://www.who.int/news-room/feature-stories/detail/who-recommends-against-the-use-of-remdesivir-in-covid-19-patients>.
- 54) Sofia, M.J.; Bao, D.; Chang, W. Discovery of a β -d-2'-Deoxy-2'- α -fluoro-2'- β -C-methyluridine nucleotide prodrug (PSI-7977) for the treatment of hepatitis C virus. *J Med Chem.* **2010**, 53(19), 7202–7218.

- 55) Saboulard, D.; Naesens, L.; Cahard, D.; Salgado, A.; Pathirana, R.; Velazquez, S.; McGuigan, C.; De Clercq, E.; Balzarini, J. Characterization of the Activation Pathway of Phosphoramidate Triester Prodrugs of Stavudine and Zidovudine. *Mol. Pharmacol.* **1999**, 56 (4), 693-704.
- 56) Siccardi, D.; Gumbleton, M.; Omid, Y.; McGuigan, C. Stereospecific Chemical and Enzymatic Stability of Phosphoramidate Triester Prodrugs of D4T in Vitro. *Eur. J. Pharm. Sci.* 2004, 22 (1), 25–31. DOI: 10.1016/j.ejps.2004.02.006.
- 57) Birkus, G.; Wang, R.; Liu, X.; Kutty, N.; MacArthur, H.; Cihlar, T.; Gibbs, C.; Swaminathan, S.; Lee, W.; McDermott, M. *Antimicrob. Agents Chemother.* **2007**, 51, 543.
- 58) Procházková E, Navrátil R, Janeba Z, et al. Reactive cyclic intermediates in the ProTide prodrugs activation: trapping the elusive pentavalent phosphorane. *Org Biom Chem.* **2019**, 17(2), 315–320.
- 59) Simmons, B.; Liu, Z.; Klapars, A. Mechanism-based solution to the ProTide synthesis problem: selective access to Sofosbuvir, Acelarin, and INX-08189. *Org Lett.* **2017**, 19(9), 2218–2221.
- 60) McGuigan, C.; Pathirana, R. N.; Mahmood, N.; Hay, A. J. *Bioorg. Med. Chem.* **1992**, 2, 701.
- 61) McGuigan, C.; Pathirana, R. N.; Balzarini, J.; De Clercq, E. *J. Med. Chem.* **1993**, 36, 1048.
- 62) Bordoni, C.; Cima, C.M.; Azzali, E. Microwave-assisted organic synthesis of nucleoside ProTide analogues. *RSC Adv.* **2019**, 9(35), 20113–20117.
- 63) Van Boom, J. H.; Burgers, P. M. J.; Crea, R.; Luyten, W. C. M. M.; Reese, C. B. *Tetrahedron* **1975**, 31, 2953.
- 64) Sofia, M. J.; Bao, D.; Chang, W.; Du, J.; Nagarathnam, D.; Rachakonda, S.; Reddy, P. G.; Ross, B. S.; Wang, P.; Zhang, H. R.; Bansal, S.; Espiritu, C.; Keilman, M.; Lam, A. M.; Steuer, H. M.; Niu, C.; Otto, M. J.; Furman, P. A. *J. Med. Chem.* **2010**, 53, 7202.
- 65) McGuigan, C.; Murziani, P.; Slusarczyk, M.; Gonczy, B.; Vande Voorde, J.; Liekens, S.; Balzarini, J. *J. Med. Chem.* **2011**, 54, 7247.
- 66) Quintiliani, M.; Persoons, L.; Solaroli, N.; Karlsson, A.; Andrei, G.; Snoeck, R.; Balzarini, J.; McGuigan, C. *Bioorg. Med. Chem.* **2011**, 19, 4338.
- 67) Qiu, Y.-L.; Ptak, R. G.; Breitenbach, J. M.; Lin, J.-S.; Cheng, Y.-C.; Drach, J. C.; Kern, E. R.; Zemlicka, J. *Antiviral Res.* **1999**, 43, 37.
- 68) McGuigan, C.; Harris, S. A.; Daluge, S. M.; Gudmundsson, K. S.; McLean, E. W.; Burnette, T. C.; Marr, H.; Hazen, R.; Condreay, L. D.; Johnson, L.; De Clercq, E.; Balzarini, J. *J. Med. Chem.* **2005**, 48, 3504.
- 69) McGuigan, C.; Slater, M. J.; Parry, N. R.; Perry, A.; Harris, S. *Bioorg. Med. Chem. Lett.* **2000**, 10, 645.

- 70) Ang, P.; Shen, J.P.; Hardy-Abeloos, C.J.; Huang, J.K.; Ross, J.S.; Miller, V.A.; Jacobs, M.T.; Chen, I.L.; Xu, D.; Ali, S.M. Genomic Landscape of Appendiceal Neoplasms. *JCO Precision Oncology*. **2018**, 2, 1-18.
- 71) Nomura, R.; Saito, T.; Mitomi, H.; Hidaka, Y.; Lee, S.Y.; Watanabe, S.; Yao, T. GNAS mutation as an alternative mechanism of activation of the Wnt/beta-catenin signaling pathway in gastric adenocarcinoma of the fundic gland type. *Hum Pathol*. **2014**, 45(12), 2488-2496.
- 72) Ideno, N.; Yamaguchi, H.; Ghosh, B.; Gupta, S.; Okumura, T.; Steffen, D.J.; Fisher, C.G.; Wood, L.D.; Singhi, A.D.; Nakamura, M.; Gutkind, J.S.; Maitra, A. GNAS(R201C) Induces Pancreatic Cystic Neoplasms in Mice That Express Activated KRAS by Inhibiting YAP1 Signaling. *Gastroenterology*. **2018**, 155(5), 1593-607 .
- 73) Fecteau, R.E.; Lutterbaugh, J.; Markowitz, S.D.; Willis, J.; Guda, K. GNAS mutations identify a set of right-sided, RAS mutant, villous colon cancers. *PLoS One*. **2014**; 9(1), 87966.
- 74) Alakus, H.; Babicky, M.L.; Ghosh, P.; Yost, S.; Jepsen, K.; Dai, Y.; Arias, A.; Samuels, M.L.; Mose, E.S.; Schwab, R.B. Genome-wide mutational landscape of mucinous carcinomatosis peritonei of appendiceal origin. *Genome medicine*. **2014**, 6(5), 4.3
- 75) Coles, G.L.; Cristea, S.; Webber, J.T.; Levin, R.S.; Moss, S.M.; He, A.; Sangodkar, J.; Hwang, Y.C.; Arand, J.; Drainas, A.P.; Mooney, N.A.; Demeter, J.; Spradlin, J.N.; Mauch, B.; Le, V.; Shue, Y.T.; Ko, J.H.; Lee, M.C.; Kong, C.; Nomura, D.K.; Ohlmeyer, M.; Swaney, D.L.; Krogan, N.J.; Jackson, P.K.; Narla, G.; Gordan, J.D.; Shokat, K.M.; Sage, J. Unbiased Proteomic Profiling Uncovers a Targetable GNAS/PKA/PP2A Axis in Small Cell Lung Cancer Stem Cells. *Cancer Cell*. **2020**, 38(1), 129-143.
- 76) O'Hayre, M.; Degese, M.S.; Gutkind, J.S. Novel insights into G protein and G protein-coupled receptor signaling in cancer. *Current opinion in cell biology*. **2014**, 27, 126-35.
- 77) Abagyan, R.A.; Totrov, M.M. Biased probability Monte Carlo as a powerful global energy optimization method for biomolecular structure prediction. *Pap Am Chem S*. **1996**, 211(35).
- 78) Abagyan, R.I.; Totrov, M.; Kuznetsov, D. Icm - a New Method for Protein Modeling and Design - Applications to Docking and Structure Prediction from the Distorted Native Conformation. *J Comput Chem*. **1994**, 15(5), 488-506.
- 79) Hu, Q.; Shokat, K.M. Disease-Causing Mutations in the G Protein Galphas Subvert the Roles of GDP and GTP. *Cell*. **2018**, 173(5), 1254-1264.
- 80) Robins, M.; Hansske, F.; Low, N. A mild conversion of vicinal diols to alkenes. Efficient transformation of ribonucleosids into 2'-ene and 2',3'-dideoxynucleosides, *Tetrahedron Letters*. **1984**, 25(4), 367-370.
- 81) Morris, R.; John, W.; Danuta, M.; Nicholas, L.; Fritz, H.; Stanislaw, W. *The Journal of Organic Chemistry*. **1995** 60 (24), 7902-7908 .

- 82) Morris, R.; Ruiming, Z.; Fritz, H.; Stanislaw, W. Synthesis of sugar-modified 2,6-diaminopurine and guanine nucleosides from guanosine via transformations of 2-aminoadenosine and enzymatic deamination with adenosine deaminase. *Canadian Journal of Chemistry*. **1997**, 75(6): 762-767.
- 83) Gong-Xin, H.; Norbert, B. A convenient preparation of protected 3'-deoxyguanosine from guanosine, *Tetrahedron Letters*, **1995**, 36(39), 6991-6994.
- 84) Michel, B.Y.; Krishnakumar, K.S.; Strazewski, P. Total synthesis of a xylo-Puromycin analog. *Nucleic Acids Symp Ser (Oxf)*. **2008**, 52, 575-576.
- 85) Greenberg, S.; Moffatt, J. *J. Am. Chem. Soc.* **1973**, 95, 4016.
- 86) Jain, C.; Jenkins, D.; Russell, F.; Verheyen, H. Moffatt G, *J. Org. Chem.* **1974**, 39, 30.
- 87) Russell, F.; Greenberg, S.; Moffatt, J. *J. Am. Chem. Soc.* **1973**, 95, 4025.
- 88) Zhang, L.; Cui, Z.; Zhang, B. (2003), An Efficient Synthesis of 3'-Amino-3'-deoxyguanosine from Guanosine. *HCA*, **1986**, 703-710.
- 89) Porcari, A.R.; Ptak, R.G.; Borysko, K.Z.; Breitenbach, J.M.; Vittori, S.; Wotring, L.L.; Drach, J.C.; Townsend, L.B. Deoxy sugar analogues of triciribine: correlation of antiviral and antiproliferative activity with intracellular phosphorylation. *J Med Chem*. **2000**, 43(12), 2438-2448.
- 90) Fan, Y.; Gaffney, B.L.; Jones, R.A. Transient silylation of the guanosine O6 and amino groups facilitates N-acylation. *Org Lett*. **2004**, 6(15), 2555-2557.
- 91) Aurélien, L.; Loic, S.; Manuel, L.; David, G.; Jana, N.; Marc, P.; David, M. *Journal of the American Chemical Society* **2014** 136 (35), 12406-12414.
- 92) Culver, W.; Ram, Z.; Walbridge, S.; Ishii, H.; Oldfield, E.J.; Blaese, M. *Science*, **1992**, 256, 1150-1152.
- 93) Kang, S. H.; Sinhabadu, A. K.; Cory, J. G.; Mitchell, B. S.; Thakker, D. R.; Cho, M. *J. Pharm. Res.* **1997**, 14, 706.
- 94) Kang, S. H.; Sinhabadu, A. K.; Cho, M. *J. Nucleosides Nucleotides* **1998**, 17, 1089.
- 95) Starrett, J. E., Jr.; Tortolani, D. R.; Russell, J.; Hitchcock, M. J. M.; Whiterock, V.; Martin, J. C.; Mansuri, M. M. *J. Med. Chem.* **1994**, 37, 1857.
- 96) Starrett, J. E.; Tortolani, D. R.; Hitchcock, M. J. M.; Martin, J. C.; Mansuri, M. M. *Antiviral Res.* **1992**, 19, 267.
- 97) Krecmerova, M.; Holy, A.; Pohl, R.; Masojidkova, M.; Andrei, G.; Naesens, L.; Neyts, J.; Balzarini, J.; De Clercq, E.; Snoeck, R. *J. Med. Chem.* **2007**, 50, 5765.
- 98) Tang, Y.-B.; Peng, Z.-G.; Liu, Z.-Y.; Li, Y.-P.; Jiang, J.-D.; Li, Z.-R. *Bioorg. Med. Chem. Lett.* **2007**, 17, 6350.
- 99) Kim, C. U.; Luh, B. Y.; Martin, J. C. *J. Org. Chem.* **1991**, 56, 2642.
- 100) Mackman, R. L.; Boojamra, C. G.; Prasad, V.; Zhang, L.; Lin, K.-Y.; Petrakovsky, O.; Babusis, D.; Chen, J.; Douglas, J.; Grant, D.; Hui, H. C.; Kim, C. U.;

- Markevitch, D. Y.; Vela, J.; Ray, A.; Cihlar, T. *Bioorg. Med. Chem. Lett.* **2007**, *17*, 6785.
- 101) Boojamra, C. G.; Mackman, R. L.; Markevitch, D. Y.; Prasad, V.; Ray, A. S.; Douglas, J.; Grant, D.; Kim, C. U.; Cihlar, T. *Bioorg. Med. Chem. Lett.* **2008**, *18*, 1120.
- 102) Mackman, R. L.; Ray, A. S.; Hui, H. C.; Zhang, L.; Birkus, G.; Boojamra, C. G.; Desai, M. C.; Douglas, J. L.; Gao, Y.; Grant, D.; Laflamme, G.; Lin, K.-Y.; Markevitch, D. Y.; Mishra, R.; McDermott, M.; Pakdaman, R.; Petrakovsky, O. V.; Vela, J. E.; Cihlar, T. *Bioorg. Med. Chem.* **2010**, *18*, 3606.
- 103) Liu. Efficient Synthesis of 9-(4-[¹⁸F]Fluoro-3-Hydroxymethylbutyl)Guanine ([¹⁸F]FHBG) and 9-[(3-[¹⁸F]Fluoro-1-Hydroxy-2-Propoxy)Methyl]Guanine ([¹⁸F]FHPG); *Journal of Fluorine Chemistry*, **2017**, *201*, 24.
- 104) Derudas. Virtual Screening of Acyclovir Derivatives as Potential Antiviral Agents: Design, Synthesis, and Biological Evaluation of New Acyclic Nucleoside ProTides. *Journal of medicinal chemistry* **2017**, *60* (18).
- 105) Wang. An Improved Total Synthesis of PET HSV-Tk Gene Expression Imaging Agent 9-[(3-[¹⁸F]Fluoro-1-Hydroxy-2-Propoxy)Methyl]Guanine ([¹⁸F]FHPG). *Synthetic communications*. **2004**, *34* (5).
- 106) Zheng. An Improved Total Synthesis of PET HSV-Tk Gene Reporter Probe [¹⁸F]FHPG. *Journal of labelled compounds & radiopharmaceuticals*. **2003**, *46*.
- 107) Dillon. Application of the "trimethyl Lock" to Ganciclovir, a pro-Prodrug with Increased Oral Bioavailability. *Bioorganic & medicinal chemistry letters*. **1996**, *6* (14)
- 108) Martin. Synthesis and Antiviral Activity of Various Esters of 9-[1,3-Dihydroxy-2-Propoxy)Methyl]Guanine. *Journal of pharmaceutical sciences : a publication of the American Pharmaceutical Association* **1987**, *76* (2)
- 109) Prisbe. Synthesis and Antiherpes Virus Activity of Phosphate and Phosphonate Derivatives of 9-((1,3-Dihydroxy-2-Propoxy)Methyl)guanine. *Journal of medicinal chemistry*. **1986**, *29* (5).